Imperial College London

Integration of Ionic Liquid Biorefinery with Constructed Wetland Remediation of Wastewater

Anton Edward Josef Firth

Supervised by Prof Jason P. Hallett and Prof Paul S. Fennell

Thesis submitted for the degree of Doctor of Philosophy (PhD)

Department of Chemical Engineering

Imperial College London

August 2021

Declaration of Originality and Copyright

The entirety of the work described in this thesis was carried out at Imperial College London between October 2017 and January 2021. Unless otherwise stated the work is my own and has not been submitted previously for a degree at this or another university.

Copyright

The copyright of this thesis rests with the author and is made available under a Creative Commons Attribution Non-Commercial No Derivatives licence. Researchers are free to copy, distribute or transmit the thesis on the condition that they attribute it, that they do not use it for commercial purposes and that they do not alter, transform or build upon it. For any reuse or redistribution, researchers must make clear to others the licence terms of this work.

Publications

The following publications are a result of my own PhD work or collaborative projects conducted during my PhD:

1. **Firth A.,** Mac Dowell N., Fennell P., Hallett J., 2020, Assessing the Economic Viability of Wetland Remediation of Wastewater, and the Potential for Parallel Biomass Valorisation, Environmental Science: Water Research & Technology, vol. 6, issue 8, pp. 2103-2121
2. Chen M., Malaret F., **Firth A.,** Verdia P, Abouelela A., Chen Y., Hallett J., 2020, Design of a Combined ionoSolv-Organolsolv Biomass Fractionation Process for Biofuel Production and High Value-Added Lignin Valorisation, Green Chemistry, vol. 22, issue 15, pp. 5161-5178
3. CJ Clarke, ND Richardson, **Firth A.**, JP Hallett, P Licence, 2020, Thermolysis of Organofluoroborate Ionic Liquids to NHC-Organofluoroborates, ACS Sustainable Chem. Eng, vol. 8, issue 44, pp. 16386-16390

Abstract

Constructed wetland remediation has significant potential as a low-cost and low-maintenance water treatment technology. The high growth rates and yields of wetland species mean that constructed wetlands can also serve as a source of lignocellulosic biomass, which can be fractionated and processed into a wide range of useful fuels, chemicals, and materials. The work presented in this thesis investigates the potential for the widespread adoption of constructed wetlands for wastewater remediation, and for the valorisation of the generated biomass through an ionic liquid biorefinery.

Firstly, this work investigates the effect of varying the degree of substitution of the cation in aqueous alkylammonium hydrogen sulfate ionic liquids. A decreasing degree of substitution was found to significantly enhance solution acidity in a way that differed from addition of excess sulfuric acid. The effects of this acidity were tested for the ionic liquid pretreatment of *Miscanthus*, through which a promising new pretreatment solvent was identified. Methylbutylammonium hydrogen sulfate produced pulps with purities of up to 94%, in two-thirds of the time of current benchmark ionic liquids.

Secondly, a desk study was carried out to quantify the economic potential for wetland remediation, for the removal of organic and nutrient contamination, and for the remediation of Acid Mine Drainage, relative to conventional technologies. Constructed wetlands were found to be comparatively economically favourable at a wide range of conditions, particularly those with lower flow rates and/or contamination. Valorisation of the wetland biomass was found to be able to offset a significant proportion of total costs, but may require mixing with other feedstocks due to areal requirements.

Valorisation of wetland feedstocks through ionic liquid pretreatment was then investigated experimentally. Feedstock independence was validated by pretreating 7 common wetland species. Large improvements in digestibility and pulp purity were observed (to around 80% and 70% respectively), with low variability between species. These feedstocks' high extractives content was found to increase the rate of pseudolignin formation, but this could be avoided through pre-extraction with ethanol and water. Recycling performance was found to decrease with each cycle, although this was offset to a certain degree through biomass pre-extraction and through addition of acid between cycles.

Finally, a novel fractionation process was suggested and developed using duckweed as a feedstock, allowing the full range of its promising features to be utilised. Ionic liquid interactions with pure starch were probed, allowing conditions amenable to starch processing to be determined. Pretreatment of duckweed with ionic liquids at mild conditions allowed near-quantitative sugar release to be achieved in 8 hours of hydrolysis, while a protein-enriched post-saccharification residue was also generated.

Acknowledgements

Throughout my PhD, I have been blessed with a fantastic group of friends, family, and colleagues. It has been a long and intense few years, but those around me have helped me stay focussed and thoroughly happy throughout its entirety. Tell you what though, feels pretty good to be done.

Firstly, I would like to thank my parents. Your love and support has always been unwavering, no matter what weird lab hours I was deciding to pull, and you have provided me with the nicest home I could wish to come back to every day. Next, I would like to thank Sophie, you have supported me at both my highest and my lowest, you have put up with my endless shenanigans and PhD chat, and you have been everything I could wish for in a girlfriend. You even taught me a trick or two in the lab…

I would like to thank the ICL ChemEngg PhD Shiitake group: Bretchen, Mrs. Chloë Amour, Seb, Em, Hannah, Nix, and Ol. I cannot understate how much our lunches, cafs, Nimmt, Hbar, Slug nights, weekends away, builders', and gym sessions all made this PhD infinitely more enjoyable and made me actively look forward to coming in every day, no matter how little duckweed I was managing to grow.

A special thank you to Jason and Paul. Firstly (along with Niall), you showed the utmost faith in me and helped secure me this PhD position. Since then, you have given me full freedom to pursue my research interests and helped me grow as a researcher, and I always enjoy our off-topic conversations. I have made some great friendships in the Hallett group. In particular Pedro, who taught me so much, from chemistry, to meditation, to team-building; Aida, who provided me with endless good ideas and advice, and has been the best possible co-founder at DyeRecycle; Amir, who has consistently offered his time to help me get unstuck in the lab and made me laugh with outrageous statements; Francisco (Papi) for all the laughs, Terra Mystica, and "short projects"; Louis for catharsis and HPLC tutelage; Raul for fixing absolutely everything and for beautiful Chilean meals; Samson for football chats; and Coby for being Coby. I would also like to thank Liem, Heather, Shirley, Angela, Amir II, Mo, Adam, and Victor, all of whom made the lab a fun and vibrant place to work. In addition, Sochi was a stellar student to supervise, got me crucial data, and was a pleasure to work with. The support staff in the department have also all massively helped me on a regular basis, in particular Patricia, Kaho, and Ben.

And to those outside Imperial: Victor, Rodolphe, Maxi (family in all but blood relation); Prav and Saz for making me stay up until 5 when I told you I need to be in at 8; Alex for your spicy memes, insults, and assists; Alex, Sam, and Henri for SoL sessions with endless fantastic arguments; Daniel and Alan for accepting my tardiness; the Kroos, who put up with my finishing; and Andrej, Granny, and Grandpa.

Lastly, I dedicate this thesis to Baka, Michael, Homaa, and Jasper. I wish I could celebrate this with you in person, but I am sure you are watching from somewhere.

Glossary

[BA]	butylammonium
[DMBA]	N,N-dimethylbutylammonium
[DMEtA]	N,N-dimethylethanolammonium
[HA]	hexylammonium
[Hmim]	1-methylimidazolium
[H*x*im]	monoalkylimidazolium cation substituted with alkyl group *x* at position 1 on the imidazolium ring. *x* is expressed in terms of its chain length with individual lower case letters (e.g. [Hbim] representing 1-butylimidazolium).
[MBA]	N-methylbutylamine
[MEA]	monoethanolammonium
[OAc]	acetate
[*xy*im]	dialkylimidazolium cation substituted with alkyl groups *x* and *y* at the 1 and 3 positions on the imidazolium ring. *x* and *y* are expressed in terms of their chain length with individual lower case letters (e.g. [emim] representing 1-ethyl-3-methylimidazolium).
AFEX	ammonia fibre expansion
AIL	acid insoluble lignin (Klason lignin)
AIR	acid insoluble residue
ALD	anoxic limestone drain
AMD	acid mine drainage
APIL	aprotic ionic liquid
ASL	acid soluble lignin
BOD	biochemical oxygen demand
CW	Constructed wetland
DA	dilute acid
DMSO	dimethyl sulfoxide
FTIR	Fourier transform infrared
FWS	free water surface
G	guaiacyl
GPC	gel permeation chromatography
H	*p*-hydroxyphenyl
H_0	Hammett acidity

HMF	5-hydroxymethylfurfural
HPLC	high performance liquid chromatography
HSQC	heteronuclear single quantum coherence
HSSF	horizontal sub-surface flow
ICP-MS	inductively coupled plasma – mass spectroscopy
IL	ionic liquid
LCC	lignin-carbohydrate complex
M_n	number-average molecular weight
M_w	weight-average molecular weight
NH_4-N	ammoniacal nitrogen
NREL	National Renewable Energy Laboratory
N_{TIS}	number of tanks in series
NMR	nuclear magnetic resonance
O&M	operation and maintenance
org-N	organic nitrogen
ox-N	oxidised nitrogen
PDI	polydispersity index
PIL	protic ionic liquid
ppm	parts per million
P_{TIS}	effective number of tanks in series
S	syringyl
SE	steam explosion
SRB	sulfate-reducing bacteria
T_{onset}	temperature of onset of thermal degradation
TGA	thermogravimetric analysis
TN	total nitrogen
UV-Vis	ultraviolet-visible
VF	vertical flow
wt%	weight percent
α	Kamlet-Taft acidity
β	Kamlet-Taft basicity
π*	Kamlet-Taft polarity

Table of Contents

Declaration of Originality 2
Copyright 2
Publications 2
Abstract 3
Acknowledgements 4
Glossary 5
List of Figures 11
List of Tables 16
Introduction 17
Chapter 1: Background 19
1.1 Ionic Liquids 19
1.1.1 General 19
1.1.2 Physicochemical Properties 20
1.1.3 Protic Ionic Liquids 23
1.1.4 Ecological Impact 25
1.1.5 Applications of Ionic Liquids 26
1.2 Biorefinery 28
1.2.1 General 28
1.2.2 Lignocellulose 31
1.2.3 Pretreatment 38
1.3 Ionic Liquid Pretreatment 43
1.3.1 Types of IL Pretreatment 43
1.3.2 ionoSolv Pretreatment 47
1.4 Constructed Wetland Remediation: AMD, BOD, and Nutrients 55
1.4.1 General 55
1.4.2 Acid Mine Drainage 57
1.4.3 Wetland Remediation of AMD 61
1.4.4 Wetland Remediation of BOD and Nutrient Contamination 72
1.5 Duckweed 75
1.5.1 Growth 75
1.5.2 BOD and Nutrient Remediation 77
1.5.3 Metal Remediation 79
1.5.4 Duckweed Composition 82

1.5.5 Duckweed Utilisation 84
Research Gap and Objectives 87
Thesis Structure 89
References 89
Chapter 2: Effects of Physical Structure of Alkylammonium Hydrogen Sulfate Ionic Liquids on Acidity and Pretreatment Efficacy 99
2.1 Introduction 99
2.2 Materials and Methods 103
2.2.1 General Equipment 103
2.2.2 Materials 103
2.2.3 IL Synthesis 103
2.2.4 IL Characterisation 104
2.2.5 Pretreatment 107
2.2.6 Biomass Characterisation 109
2.2.7 Lignin Characterisation 111
2.3 Results and Discussion 113
2.3.1 IL Characterisation 113
2.3.2 Pretreatment With Varying Cations 117
2.3.3 Excess Acid Pretreatments 122
2.3.4 Exploring Different Strategies to Avoid Saccharification Inhibition 125
2.3.5 Development of [MBA][HSO_4] as a promising pretreatment solvent 129
2.3.6 Lignin Analysis 133
2.4 Conclusions 139
References 141
Chapter 3: Assessing the Economic Viability of Wetland Remediation of Wastewater, and the Potential for Parallel Biomass Valorisation 143
3.1 Introduction 143
3.2 Materials and Methods 145
3.2.1 Wetland Design for BOD and Nutrient Removal 145
3.2.2 Wetland Design for AMD Remediation 148
3.2.3 Conventional Costs of AMD Remediation 149
3.3 Results and Discussion 150
3.3.1 BOD and Nutrient Removal 150
3.3.2 AMD Remediation 159
3.3.3 Biomass Valorisation 165
3.4 Conclusions 168

References 169
Chapter 4: Pretreatment of Wetland Species **173**
4.1 Introduction 173
4.2 Materials and Methods 174
4.2.1 General Equipment 174
4.2.2 IL Synthesis 174
4.2.3 Pretreatment 175
4.2.4 Pulp Characterisation 175
4.2.5 Liquor Analysis 176
4.2.6 Biomass Digestion and Metal Quantification 177
4.2.7 Lignin Characterisation 178
4.2.8 Statistical Analysis 178
4.3 Results and Discussion 179
4.3.1 IL Screening Using Virgin *Phragmites Australis* 179
4.3.2 Pretreatment of Multiple *Phragmites Australis* Batches 190
4.3.3 Pretreatment of Common Constructed Wetland Species 194
4.3.4 Mixed Feedstock Recycling Pretreatment 1 199
4.3.5 Pulp Mass Closure 207
4.3.6 Mixed Feedstock Recycling Pretreatment 2 209
4.3.7 Pretreatment of Metal-Contaminated Feedstocks 215
4.4 Conclusions 221
References 223
Chapter 5: Pretreatment of Duckweed **227**
5.1 Introduction 227
5.2 Materials and Methods 230
5.2.1 General Equipment 230
5.2.2 IL Synthesis 230
5.2.3 Pretreatment of Biomass 231
5.2.4 Pretreatment of Starch 231
5.2.5 Biomass Characterisation 232
5.2.6 Liquor Analysis 234
5.2.7 Biomass Digestion and Metal Quantification 235
5.2.8 Liquor Dialysis 235
5.2.9 Duckweed Sourcing and Metal Contamination 236
5.2.10 Statistical Analysis 237

5.3 Results and Discussion 238
5.3.1 Starch Pretreatment 238
5.3.2 Pretreatment of Virgin Duckweed 246
5.3.3 Pretreatment of Metal-Contaminated Duckweed 260
5.4 Conclusions 269
References 271
Conclusions **274**
Key Findings 274
Limitations and Further Work 277
Concluding Remarks 280
Appendix **281**

List of Figures

Figure 1.1: Commonly studied IL anions and cations 19

Figure 1.2: Scientific publications related to ionic liquids in different fields, according to the Institute for Scientific Information Web of Science 26

Figure 1.3: Required steps for production of first generation and second generation bio-ethanol 30

Figure 1.4: 3D structure of lignocellulose 32

Figure 1.5: Cellulose repeating unit, with glucose monomers linked by a β-1,4 glycosidic bond 32

Figure 1.6: Proposed mechanism for acid-catalysed formation of HMF and levulinic acid from hexose sugars 34

Figure 1.7: Proposed mechanism for the acid-catalysed dehydration of xylose to furfural 35

Figure 1.8: Main lignin sub-units 36

Figure 1.9: Different types of wetland cell design 56

Figure 2.1: Alkylammonium cations screened 102

Figure 2.2: Hammett acidity of alkylammonium hydrogen sulfate ILs with varying cations 114

Figure 2.3: Variation of the Hammett acidity of [BA][HSO_4] with excess base 115

Figure 2.4: Variation of the Hammett acidity of [DMBA][HSO_4] with excess sulfuric acid 115

Figure 2.5: Variation of the Hammett acidity of [DMBA][HSO_4] and water with free sulfuric acid ... 116

Figure 2.6: Variation of IL acidic proton concentration with temperature 117

Figure 2.7: Pretreatment performance of different ionic liquids 118

Figure 2.8: Digestibility and purity of pulps pretreated using varying ionic liquids 119

Figure 2.9: Digestibility and purity of pulps pretreated using varying ionic liquids 122

Figure 2.10: Pretreatment performance using [DMBA][HSO_4] with excess acid 123

Figure 2.11: Pretreatment performance at peak saccharification yield, using [BA][HSO_4] under several conditions 126

Figure 2.12: Variation of digestibility with glucan/lignin ratio, for pulps pretreated at different conditions and with differing ionic liquids 128

Figure 2.13: Pretreatment performance using [MBA][HSO_4] 130

Figure 2.14: Pulp purity and digestibility following pretreatment with [MBA][HSO_4] 131

Figure 2.15: Enzymatic hydrolysis timecourse, on pulps pretreated with [MBA][HSO_4] at 170 ^oC for 20 minutes, and on untreated *Miscanthus* 133

Figure 2.16: *Miscanthus* lignin sub-units and linkages 134

Figure 2.17: HSQC NMR signal intensities of lignin sub-units and linkages, from lignin recovered following pretreatment with varying ionic liquids 135

Figure 2.18: GPC analysis of recovered lignin following pretreatment with varying ionic liquids 137

Figure 3.1: Effect of varying the number of wetland cells on required overall area and treatment costs 152

Figure 3.2: Volumetric costs of BOD and nutrient removal using constructed wetlands , for a range of input and output conditions 154

Figure 3.3: Ratio of simulated wetland remediation costs to reported conventional remediation costs in literature, for BOD, phosphorous, and nitrogen removal 155

Figure 3.4: Effect of varying design parameters on simulated effluent concentrations in a Monte Carlo simulation, for secondary and tertiary treatment..... 158

Figure 3.5: Effect of varying economic parameters on simulated wetland treatment costs in a Monte Carlo simulation, for secondary treatment and tertiary treatment 159

Figure 3.6: Correlation between varied economic parameters and simulated wetland treatment costs in a Monte Carlo simulation, for secondary treatment and tertiary treatment of domestic wastewater 159

Figure 3.7: Ratio of wetland remediation costs to conventional remediation costs of low-pH AMD, for HSSF and VF designs with high and low acidity removal rates 161

Figure 3.8: Simulated wetland performance for overall-site low-pH AMD, for case study data found in literature 163

Figure 3.9: Ratio of wetland remediation costs to conventional remediation costs of circumneutral AMD, for FWS designs with high and low acidity removal rates 164

Figure 3.10: Required profits per unit dry mass of harvested wetland biomass, in order to offset 10% of total treatment costs 165

Figure 4.1: Pretreatment performance of different ionic liquids 180

Figure 4.2: Digestibility and purity of pulps pretreated using varying ionic liquids 181

Figure 4.3: Total hydrolysis sugar yield using varying ionic liquids..... 184

Figure 4.4: Molecular weight profiles of recovered lignin following pretreatment with varying ionic liquids..... 185

Figure 4.5: GPC analysis of recovered lignin following pretreatment with varying ionic liquids 186

Figure 4.6: Relative abundance of structural units of recovered lignin following pretreatment with varying ionic liquids, as determined by HSQC NMR spectroscopy 187

Figure 4.7: HSQC NMR spectra of recovered lignin following pretreatment with varying ionic liquids 189

Figure 4.8: Pretreatment performance of two *Phragmites australis* batches..... 190

Figure 4.9: Key pretreatment indicators of three *Phragmites australis* batches 191

Figure 4.10: GPC analysis of recovered lignin from three *Phragmites australis* batches following pretreatment with [DMBA][HSO_4] 193

Figure 4.11: Molecular weight profiles of recovered lignin from different *Phragmites australis* batches following pretreatment with [DMBA][HSO_4]..... 194

Figure 4.12: Key pretreatment indicators of 11 wetland feedstocks 195

Figure 4.13: Predicted vs. actual pretreatment indicators for a mixed wetland feedstock 200

Figure 4.14: Pretreatment performance with IL recycling for a mixed wetland feedstock..... 201

Figure 4.15: IL solution solute content with IL recycling before and after pretreatment of a mixed wetland feedstock..... 204

Figure 4.16: Total solute content of recovered IL solution following pretreatments with IL recycling 207
Figure 4.17: FTIR spectrum of water-soluble extractives removed from mixed wetland feedstock pulp, and of calcium sulfate dihydrate 208
Figure 4.18: Acid/Base ratio of IL liquor following pretreatment, over 3-4 cycles 210
Figure 4.19: Pretreatment performance with IL recycling for a mixed wetland feedstock, with varying acid addition between cycles 212
Figure 4.20: Pretreatment performance with IL recycling for a double-extracted mixed wetland feedstock, with acid addition after cycle 3 214
Figure 4.21: Metal removal from the pulp through IL pretreatment of mixed metal-contaminated wetland feedstock using varying ILs 216
Figure 4.22: Metal partitioning following IL pretreatment of mixed metal-contaminated feedstock using varying ILs 218
Figure 4.23: Pretreatment performance of different ionic liquids with a mixed metal-contaminated wetland feedstock 219
Figure 5.1: Structure of amylose and amylopectin 228
Figure 5.2: Harvested *Spirodela* Polyrhiza 236
Figure 5.3: Material flow diagram during IL pretreatment of starch 239
Figure 5.4: Fractionation of different starches following pretreatment with [DMBA][HSO_4] 240
Figure 5.5: Water-insoluble residue of starches following pretreatment with [DMEtA][HCOO] 242
Figure 5.6: Fractionation of different starches following pretreatment with [DMEtA][HCOO] 243
Figure 5.7: Fractionation of different starches following pretreatment with [MEA][OAc] 243
Figure 5.8: Fractionation of different starches following pretreatment with [Hmim]Cl 245
Figure 5.9: Protein material flow during compositional analysis 247
Figure 5.10: Starch recovery in *Spirodela polyrhiza* under several pretreatment conditions 248
Figure 5.11: Saccharification and digestibility kinetics of pulps pretreated using varying ionic liquids 251
Figure 5.12: Protein partitioning during IL pretreatment of *Spirodela polyrhiza* 256
Figure 5.13: Solid recovered following dialysis of IL liquors 258
Figure 5.14: Starch recovery in two duckweed species under two pretreatment conditions 262
Figure 5.15: Saccharification and digestibility kinetics of duckweed pulps pretreated using varying ionic liquids 263
Figure 5.16: Protein partitioning during IL pretreatment of two duckweed species 264
Figure 5.17: Metal partitioning during IL pretreatment of metal-contaminated *Lemna minor* 267
Figure A1-1: Proton NMR of [BA][HSO_4] 281
Figure A1-2: Carbon NMR of [BA][HSO_4] 282
Figure A1-3: Proton NMR of [HA][HSO_4] 282
Figure A1-4: Carbon NMR of [HA][HSO_4] 283

Figure A1-5: Proton NMR of [MBA][HSO_4] 283
Figure A1-6: Carbon NMR of [MBA][HSO_4] 284
Figure A1-7: Proton NMR of [DMBA][HSO_4] 284
Figure A1-8: Carbon NMR of [DMBA][HSO_4] 285
Figure A1-9: Proton NMR of [Hmim][Cl] 285
Figure A1-10: Carbon NMR of [Hmim][Cl] 286
Figure A1-11: Proton NMR of [DMEtA][HCOO] 286
Figure A1-12: Carbon NMR of [DMEtA][HCOO] 287
Figure A1-13: Proton NMR of [MEA][OAc] 287
Figure A1-14: Carbon NMR of [MEA][OAc] 288
Figure A2-1: Example UV-Vis spectrum, for varying concentrations of 4-nitroaniline in [DMBA][HSO_4] (20 wt% water) 289
Figure A2-2: Example graph of UV-Vis absorbance vs. (concentration*path length), for a solution of 4–nitroaniline in [DMBA][HSO_4] (20 wt% water) 290
Figure A2-3: Linear Sankey diagrams for H-bond donors and acceptors in aqueous IL systems 291
Figure A2-4: 1H NMR (400 MHz; DMSO-d_6) spectra of IL solutions before (red) and after (blue) thermal degradation testing for 72 hours at 170 ^oC 293
Figure A2-5: Saccharification yield of pulps pretreated using [BA][HSO_4] followed by varying pulp washing protocols 294
Figure A2-6: Saccharification yield of pulps pretreated using [HA][HSO_4] and of untreated *Miscanthus* 295
Figure A2-7: Pretreatment performance using [BA][HSO_4] with 100% excess base 295
Figure A2-8: Pretreatment performance using [MBA][HSO_4] with excess base 296
Figure A2-9: Degree of condensation and S/G ratio of lignin recovered following pretreatment with varying ionic liquids 297
Figure A2-10: HSQC NMR spectra of recovered lignin following pretreatment with varying ionic liquids 303
Figure A2-11: GPC analysis of recovered lignin following pretreatment with [MBA][HSO_4] with an acid/base ratio of 1.00 and with 5% excess base 304
Figure A3-1: Effect of varying the number of wetland cells on required overall area and treatment costs for nitrogen removal 308
Figure A3-2: Costs of nutrient removal using constructed wetlands per unit mass of contaminant removed, for a range of input and output conditions 309
Figure A3-3: Remediation costs and required wetland areas for BOD removal, varying with flow rate and influent concentration, for two different effluent concentrations 310
Figure A3-4: Remediation costs and required wetland areas for phosphorus removal, varying with flow rate and influent concentration, for two different effluent concentrations 311
Figure A3-5: Remediation costs and required wetland areas for nitrogen removal, varying with flow rate and influent concentration, for two different ammonia nitrogen effluent concentrations 312

Figure A4-1: HSQC NMR spectra of recovered lignin following pretreatment with varying ionic liquids 315
Figure A4-2: Two further pretreatment indicators of 11 wetland feedstocks 316
Figure A4-3: Accuracy of model predictions for 0.5 wt% [DMEtA][HCOO], with and without including Davies activity for charged species 321
Figure A4-4: Davies activity vs. acid/base ratio for 0.5 wt% [DMEtA][HCOO] 322
Figure A4-5: Accuracy of optimized model predictions for 0.5 wt% [DMEtA][HCOO] 323
Figure A4-6: Accuracy of model predictions for 0.5 wt% [Hmim][Cl], with and without including Davies activity for charged species 325
Figure A4-7: Accuracy of optimized model predictions for 0.5 wt% [Hmim][Cl] 327
Figure A5-1: Optical determination of duckweed growth rates 328
Figure A5-2: Harvested *Spirodela polyrhiza* 330
Figure A5-3: FTIR spectra of formic acid, dimethylethanolamine, and [DMEtA][HCOO] 330
Figure A5-4: Protein fractionation during pretreatment 331

List of Tables

Table 1.1: Typical composition ranges of different types of biomass 31

Table 1.2: Aboveground metal concentrations and translocation factors for common reeds and cattails 67

Table 3.1: Assumed wetland acidity and metal removal rate ranges 148

Table 3.2: Assumed wetland construction costs and operational costs 149

Table 3.3: Simulated low-pH AMD scenarios 160

Table 4.1: Feedstocks used for pretreatment 176

Table 4.2: Temperature profile used for biomass digestion 177

Table 4.3: Change in pretreatment metrics between cycles 1 and 3, recycling IL between cycles 213

Table 4.4: Metal content of untreated biomass (ppm) 215

Table 5.1: Effect of extra analysis on determined composition of *Spirodela polyrhiza* 247

Table 5.2: Composition of *Lemna minor* 261

Table 5.3: Metal contents of duckweed before and after growth in metal-contaminated water 266

Table A2-1: Varying pulp washing protocols 294

Table A3-1: Comparison of conventional nutrient removal costs from literature with calculated costs for wetland BOD and nutrient removal 306

Table A4-1: Composition of wetland species used for pretreatment 313

Table A4-2: Composition of untreated nut shells 316

Table A4-3: Pretreatment data of nut shells 316

Table A4-4: Composition of *Pistia stratiotes* before and after IL pretreatment 317

Table A5-1: Starch content determined according to different Megazyme protocols 328

Table A5-2: Duckweed pretreatment data 329

Table A5-3: Protein content of pulp and lignin from pretreated duckweed 329

Introduction

Global primary energy supply, as well as feedstocks in the chemical industry, are currently dominated by cheap and abundant fossil fuels.[1–3] There is an increasing awareness of the serious environmental impact of both the CO_2 emissions and of the extraction of these fuels, which may manifest itself through carbon taxes that raise their price. However, cost-effective alternatives to fossil fuels are also required for a societal shift. The main alternatives that are put forward (such as wind, solar, or nuclear) are generally focussed on carbon-neutral electricity generation. However, these technologies cannot directly solve the need for sustainable production of liquid fuels or platform chemicals, which require hydrocarbon inputs. These needs can only be feasibly met through biorefinery, the sustainable conversion of biomass to fuels and high-value chemicals.[4]

Biorefinery must be implemented carefully to ensure it is really sustainable. Biorefinery has historically focussed on feedstocks with high sugar, starch, or oil content (e.g. sugarcane, maize, or rapeseed), in so-called first-generation biorefinery.[5] However, such species tend to be used as food crops, leading to potential political, economic, and ethical issues around their use.[5] Additional drawbacks also include high levels of NO_x emissions due to high fertiliser use, and land change for cultivation reducing or even offsetting any reductions in CO_2 emissions relative to fossil fuel use.[6–8] Recently, efforts in biorefinery have focussed on lignocellulosic feedstocks, termed second-generation feedstocks. These feedstocks offer a range of advantages over first-generation feedstocks, such as lower fertiliser requirements, geographic availability, enhanced biodiversity, and the ability to be grown on marginal land. [6,9–11] The three main components of lignocellulose (cellulose, hemicellulose, and lignin) can all be valorised to meet the fuel, chemical, and material demands of modern society. In order to unlock this potential, however, the complex and recalcitrant structure of lignocellulose must be disrupted.

This disruption can be accomplished through the ionoSolv process, which was initially pioneered around 10 years ago at Imperial College London by Dr. Agniezska Brandt-Talbot, and has since been developed by Professor Jason Hallett's research group.[12–16] Ionic liquids are a novel class of compounds that exhibit a number of advantageous properties, and are more environmentally benign than most traditional solvents. The ionoSolv process uses low-cost ionic liquids (as cheap as \$0.78/kg [17]) to depolymerise and dissolve lignin, thus fractionating lignocellulosic biomass into a carbohydrate-rich stream and a recoverable lignin stream.[14] These streams can then be further processed into fuels, chemicals, and materials whose current production routes rely on fossil fuels.

Water scarcity is a serious additional problem facing society, and one which is worsened by the impacts of climate change.[18–22] Due to the combined effects of increasing demand, groundwater

depletion, and increasing levels of water pollution, water scarcity is set to increase substantially by 2050.[18,20–22] There is, therefore, a clear need for more widespread treatment and re-use of wastewater. However, many water-scarce areas are in economically developing regions, which means water remediation technologies also need to be low-cost and must not be energy- or resource-intensive, unlike conventional technologies such as the activated sludge process.[22–24]

Constructed wetland remediation fits this technology profile. Constructed wetlands are a passive water remediation technology, in which artificial wetlands are used to mimic the water treatment abilities of natural wetlands. Through a number of complex contaminant removal mechanisms that arise from the confluence of aquatic and terrestrial ecosystems, constructed wetlands are able to effectively remediate a wide range of contaminants and wastewaters.[25] Constructed wetland uptake is not well reported in most parts of the world, but there are tens of thousands in operation over Europe, North America, and China, ranging from small domestic systems to large systems covering thousands of hectares.[25–30] Due to their high performance but low maintenance requirements, very low energy input, and supposedly low cost, constructed wetlands are considered to be a suitable water remediation technology for developing countries.[31–38] Many wetland species also display very rapid growth, even compared to commonly studied energy crops such as *Miscanthus*.[39–41] Constructed wetland biomass is currently under-utilised, or even regarded as a waste product. The adoption of constructed wetlands thus provides an opportunity for substantial biomass utilisation, while wetland biomass valorisation would concomitantly improve the process economics of constructed wetland remediation.

The target of the work carried out in this thesis has therefore been to integrate ionic liquid biorefinery with constructed wetland remediation of wastewater, providing one holistic solution while also furthering the understanding of the underlying ionoSolv process.

Chapter 1: Background

1.1 Ionic Liquids

1.1.1 General

Ionic Liquids (ILs) are ionic compounds with relatively low melting points, often taken as being below 100 °C.[42] A subclass of these, commonly taken as those with melting points around 0 °C, are named Room Temperature Ionic Liquids (RTILs). Behaviour of ILs can be altered (and hopefully one day tailored) by selection and alteration of the constituent anion and cation, with a vast number of theoretically possible structures (at least 10^6 binary and 10^8 ternary combinations).[43] This has led to them being frequently described as 'designer solvents'. In practice, however, only a relatively small number of anionic and cationic structures have been commonly studied, shown in Fig. 1.1. Cations are typically organic, while anions can be either organic or inorganic. It can be seen that particular focus has been paid to alkylated nitrogenous cations (e.g. alkylimidazolium, alkylpyrridinium, or alkylammonium). The low melting point of ILs is primarily due to a combination of asymmetry and bulkiness of the constituent ions, as well as delocalisation of charge over more than one atom.[13,44]

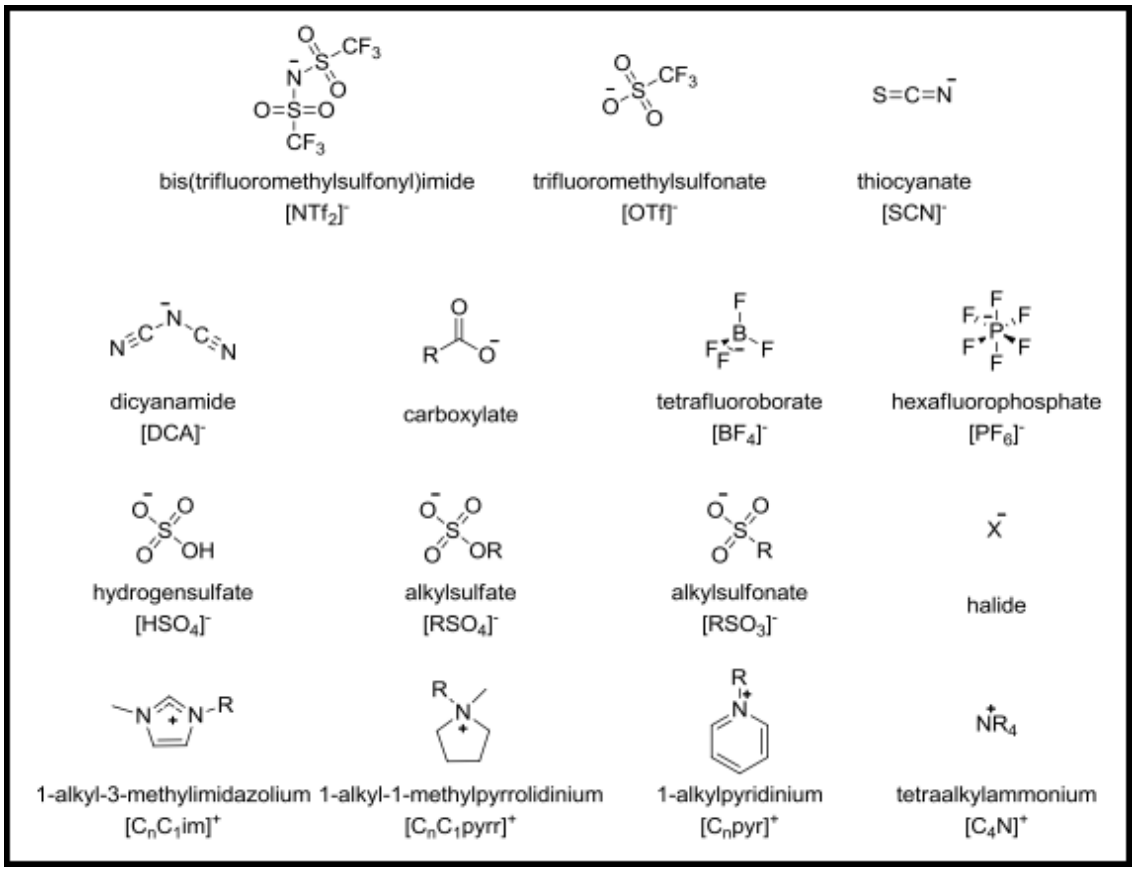


Figure 1.1: Commonly studied IL anions and cations.[45]

1.1.2 Physicochemical Properties

Poor reporting of IL parameters is fairly common in the literature, which may lead to problems in reproducibility.[46] As a result, the Royal Society of Chemistry recommend that any publications on ILs include NMR and MS analyses, water and halide content, and detail the synthesis procedure.[47]

The thermal behaviour of ILs has a major impact on their use in various applications. Of particular importance are their melting point (T_m) and glass transition temperature (T_g), for which lower values are desirable. The advantage of a lower glass transition temperature is that it leads to lower viscosity, which in turn eases handling, improves mass transport, and reduces energy costs of pumping. In addition, lower viscosity usually leads to higher conductivities in ILs, in close agreement with the Walden Rule, which may be desirable for certain applications.[46,48] The variables T_m and T_g may be reduced by decreasing the attractive forces and packing efficiency of the ions, i.e. by altering the structure of the anion or cation.[46] Through certain modifications, the constituent ions are therefore able to form amorphous solids and/or liquids at lower temperatures (in the case of T_g and T_m respectively). Incorporation of alkyl chains introduces rotational degrees of freedom at low temperatures and multiple alkyl chains of different lengths can also reduce symmetry, all contributing to a lower melting point (although increasing chain length can increase both viscosity and melting point).[13,49,50] Both T_m and T_g were found to be decreased by asymmetry of the starting amine in alkylammonium, alkylpyrrolidinium, and alkylimidazolium ILs.[51] Fluorination of the anion can also reduce the melting point of ILs (as well as improving IL stability), due to the electron-withdrawing nature of the fluorine atom, which reduces the hydrogen-bonding ability of the anion.[52] Delocalisation of ionic charge over several atoms can also reduce the IL melting point, and can be favoured by use of an aromatic cation and of a polyatomic anion (i.e. not a halide).[13,44] Although ionic structure can thus be modified to reduce IL viscosities, they generally remain high at room temperatures: from 10 mPa·s to well over 1000 mPa·s, compared to around 934 mPa·s for glycerol, 1 mPa·s for water and ethanol, or below 0.3 mPa·s for acetone.[53] IL viscosities reduce dramatically upon heating, however, sometimes reaching similar values to that of water.[54] IL viscosities can also be substantially reduced by addition of water or organic solvents (e.g. [bmim][BF_4] viscosity, high due to its symmetrical anion, was found to decrease by over 50% when 2 wt% of water was added).[53,55,56]

It is not just their low melting points, however, that has led to so much interest in the use of ILs. Their negligible volatility is cited as one of their key advantages, particularly when compared to organic compounds for use as solvents and leading to their description as “green solvents”.[57] Although the idea of ILs being “non-volatile” is outdated, ILs do possess a very low vapour pressure.[58,59] This property, along with their stability and liquid range extending to high temperatures, has several

advantages: ILs can be used at high temperatures in non-pressurised equipment, other volatile solvents can be removed by distillation without removing the IL, ILs have very low flammabilities, and volatile emissions associated with other organic solvents are eliminated (as well as the units required to dispose of them).[13,58,60–62]

ILs have also been reported to have a much wider electrochemical window than water (i.e. the range of potentials between those of cation reduction and anion oxidation, in which the IL is electrochemically inert), of up to 6 V, although this depends on the IL structure and is affected by impurities.[50,63,64] For comparison, the electrochemical window of water is 1.23 V.[65] Such electrochemical stability has led to the use of ILs in electrodeposition and battery applications.

Due to their distinctive combination of ionic, organic, and inorganic features, bonding in ionic liquids is very complex. Besides Coulombic interactions between the anion and cation, ILs can also exhibit hydrogen bonding (between hydrogen bond donor and acceptor sites), dipolarity forces (permanent and induced), and electron pair donor/acceptor interactions (forming Lewis acid-base complexes).[66] Predicting the bonding behaviour in the ionic liquid medium is therefore extremely challenging, and requires the use of sophisticated computational methods.[66] Such diverse bonding behaviour also means ILs have tremendous potential (and ability) as solvents, able to dissolve a range of both organic and inorganic materials.[42] Furthermore, as ILs are frequently made up of non-coordinating ions, they may be both polar and non-coordinating solvents.[42] Combined with their low volatility, ILs are thus well suited to replace harmful, volatile organic solvents. IL solvation properties are highly dependent upon the constituent ions, as well as on the presence of any co-solvents/impurities.[67] They are commonly quantified using the Kamlet-Taft polarity scales, in which solvents are numerically characterised by their polarizability (π^*), hydrogen bond acidity/donating ability (α), and hydrogen bond basicity/accepting ability (β).[68] These scales are empirical, and are determined by measuring the shift in UV wavelength of specific solvatochromic dye molecules, although Niedermeyer et al. have suggested multiple methods to calculate them, of varying accuracy and ease, in the hope that it may allow ILs to be designed with specific behaviour.[67–69] ILs were found to have generally high values of π^* regardless of structure, due to their inherent ionic nature.[68] Values were consistently around 1, very similar to DMSO and water. Much larger ion effects were found for α and β, with the former affected primarily by the cation, and the latter by the anion.[68]

The temperature behaviour of ILs is one point of concern. Many ILs have a decomposition temperature lower than their boiling point, and so this degradation temperature effectively provides an upper bound for their application.[58] Furthermore, IL costs are often a major portion of IL-based process OPEX, hence losses through degradation must be minimised. In addition, although ILs have been found

to have low flammabilities, IL thermal degradation compounds may be flammable as well as potentially toxic (such as alkylimidazoles, although identification of the breakdown products can be challenging[70,71]).[60–62] The decomposition behaviour of ILs is typically fairly high but can vary widely, with some decomposing at very high temperatures (e.g. [emim][PF_6] at 450 °C [50]), and others at more moderate ones (e.g. [$Bt_{1\ Bn}$][$N(CN)_2$] at 155 °C [50]). Thermogravimetric analysis (TGA) is a commonly used method for investigating the thermal behaviour of ILs: as temperature is increased constantly, mass loss is measured, and a graph of percentage remaining mass (or percentage mass loss) against temperature is typically produced. From these results, the onset temperature, T_{onset}, is defined by the point of intersection between the tangent of the temperature-mass loss curve during degradation, and the axis of 0 mass loss.[72] However, several issues exist with this methodology and the way in which it is often reported:

- Firstly, T_{onset} is typically a significant overestimate of the true temperature at which degradation begins (T_{start}), possibly due to the speed of temperature increase being too high (typically 10 or 20 °C/min).[58,73,74] For example, [bmim][BF_4] has an ostensibly high T_{onset} of 424 °C, but has a mass loss rate of 1.37%/h at 250 °C.[75] T_{onset} may, however, be used to compare the relative stability of ILs if carried out under the same conditions.[73]
- Secondly, the thermal behaviour during TGA may be affected by several factors such as heating rate, sample mass and geometry, presence of impurities (especially water, which decreases thermal stability), pan material, and possibly the atmosphere in which the test is carried out (e.g. inert vs air).[58] These may affect both heat transfer as well as the degradation pathway followed.
- Thirdly, evaporation of the IL itself (rather than due to degradation) can also affect results, and should be taken into account for a more rigorous mass loss calculation.[58,72]

Longer-term isothermal mass loss experiments have also been carried out to evaluate the long-term performance of ILs at one particular temperature, which may be relevant to particular applications. For example, the popular IL 1-ethyl,3-methylimidazolium acetate ([emim][OAc], used extensively in biomass pretreatment) was tested isothermally at temperatures between 105 °C and 170 °C (typical pretreatment temperatures) by Clough et al.[76] Despite a reported T_{onset} of 215 °C, 50% degradation had occurred after 3 hours at 170 °C, significant degradation was observed after a few hours as low as 120 °C, and 1% mass loss was found after 10 hours at just 105 °C, making this IL unsuitable for large-scale biomass processing.[76] The parameters of TGA should therefore be tailored to the expected application of the IL in order to generate meaningful results.[58] More sophisticated analysis techniques have also been developed, such as integrating mass spectroscopy to analyse degradation products and therefore learn more about the specific degradation pathways.[58] It has been shown that choice

of both anion and cation can affect the degradation behaviour of ILs, with some authors suggesting particular importance of the anion.[73] It has also been noted that, given a fixed cation, IL thermal stability may be seen to increase with the hydrophobicity of the anion.[77]

1.1.3 Protic Ionic Liquids

Protic Ionic Liquids (PILs) are a class of ILs formed from a Bronsted acid and a Bronsted base. The reaction involves the transfer of a proton from the acid to the base (as in Scheme S1.1), and as a result PILs are characterised by the presence of a proton available for hydrogen-bonding.[46] The reaction does not necessarily go to completion, and unreacted acid and base may therefore be present.[78] High ionicity is desired to minimise such impurities, as they can lead to the volatilisation of potentially hazardous acids and bases, leading to changes in composition (and thus behaviour[78]) as well as IL losses which increase OPEX.[78] However, distillation of some PILs is a simple and desirable recovery method, during which the proton transfer reaction is reversed.[79] This favours low proton-transfer energies, and thus low ionicity, in order to ensure the boiling temperature is lower than the decomposition temperature.[46,54] There is currently no standard way of measuring the ionicity of PILs, but several techniques have been used to qualify it (or even quantify it for certain systems), including NMR, ionic conductivity, and IR spectroscopy.[46,80] The difference in pKa between constituent acid and conjugate acid of the constituent base may also be used to semi-quantify the degree of proton transfer, with a larger difference indicating a higher ionicity. Yoshizawa et al. concluded that a difference in pKa greater than 10 led to complete proton transfer based on ionic conductivities.[81] However, a study by Stoimenovski et al. used ionic conductivities and a probe indicator acid to show that, despite very similar pKa differences (around 6), primary and tertiary alkylammonium acetate PILs showed contrasting ionicities.[82] The former showed signs of high ionicity, while the latter showed a low degree of proton transfer.

$$\mathrm{HA} + \mathrm{B} \rightleftharpoons \mathrm{BH}^+ + \mathrm{A}^- \qquad \text{(S1.1)}$$

Scheme S1.1: Formation of a Protic Ionic Liquid by reaction of a Bronsted acid (A) with a Bronsted base (B).

PILs display several advantages over Aprotic Ionic Liquids (APILs), which differ structurally from PILs as the proton is replaced by a substituent group such as an alkyl group.[83] The most significant benefit of PILs is their simple, one-step synthesis: PIL synthesis only involves a neutralisation reaction (without further purification), whereas those of APILs are significantly more complicated. For example, synthesis of the PIL triethylammonium hydrogen sulfate ([TEA][HSO_4]) from raw materials only requires seven synthetic steps, compared to over 20 for even a "simple" APIL such as 1-ethyl,3-methylimidazolium chloride [emim]Cl.[84] The exothermic nature of PIL synthesis also leads to negligible

energy costs, or even the opportunity for energy recovery due to the high heat of reaction between many acids and bases.[85] Furthermore, due to the large number of processing steps, APILs typically have a much lower atom economy during their synthesis and must be purified (and the resulting waste streams treated).[86] This simpler synthesis is complemented by the ability to use very cheap starting reagents for PIL synthesis, with bases such as alkylamines and mineral acids such as sulfuric acid. As a result, PILs are not just easier to synthesise but can also be produced at extremely low costs. This is particularly true of the alkylammonium hydrogen sulfate PILs: Baaqel et al. estimated a production cost of \$0.78/kg for [TEA][HSO_4], which lower than that of acetone (itself a byproduct of phenol production), and \$1.46/kg for 1-methylimidazolium hydrogen sulfate ([Hmim][HSO_4]).[17] These production costs are dominated by the material costs of the amines. Such costs are consistently said to compare very favourably to those of APILs,[45,87,88] although no bulk cost estimates of the latter have been determined in detail.

In general, PILs have been shown to display higher conductivities and lower viscosities than APILs, assumed to be due to the presence of the proton, with some PILs found to have similar conductivities to aqueous salt systems.[46,83] When comparing alkylammonium PILs and quaternary ammonium APILS (considered to be the most similar APIL with known data), Xu et al. found viscosities to be an order of magnitude lower.[83] However, such findings go against those of Zhao et al, who reported generally higher viscosities and lower conductivities in PILs compared to APILs.[89] The previously mentioned ability to distil certain PILs is also an advantage, offering a straightforward regeneration route not available to most APILs. In addition, by using differing ratios of acid and base (particularly in non-monoprotic ILs such as those based on sulfuric acid), IL properties can be further adjusted to specific applications.[78] There are a few drawbacks of PILs, relative to APILs, however. Firstly, as the constituent acid and base are in equilibrium with the IL, PILs have a higher volatility than APILs, giving them higher vapour pressures.[46] Secondly, although some classes of PILs (typically those that are fully ionised) display high thermal stability, some PILs can "decompose" at low temperatures due to volatile constituent acid and base boiling off, unintentionally leaving non-stoichiometric mixtures that may behave differently.[46] Thirdly, PILs tend to exhibit higher corrosiveness than APILs due to the presence of the proton, particularly for those based on polyprotic acids, such as the alkylimidazolium hydrogen sulfate ILs used extensively in this thesis.[90] Lastly, PILs have a narrower electrochemical window due to the presence of the proton.[91]

1.1.4 Ecological Impact

As previously mentioned, much of the interest surrounding ILs is because of their reputation as "green solvents". In order to cement such a status, the ecological impact of ILs must be investigated. Certain ILs have been shown to be highly toxic, while others have been found to be of low toxicity. However, it is hard to obtain high-level conclusions due to the wide variety of possible IL structures and chemical natures, and because toxicity findings for one type of cell/organism may not necessarily be applicable to others.[92,93] A large number of studies have, nonetheless, been carried out, and Egorova et al. have produced a comprehensive review of IL toxicity studies.[93] By collating such data, the following factors were found to affect IL toxicity:

- Length of cation alkyl chain (and thus hydrophobicity), with longer chains increasing toxicity due to an increased ability to interfere with the bi-lipid layer of cell membranes.[93–96]
- Functionalisation of the cation side chain, with incorporation of an oxygen-containing functional group (e.g. hydroxyl or methoxyl) generally reduced toxicity.[93]
- Anion moiety, with halide anions generally less toxic but fluoride-containing anions more toxic.[93]
- Cation moiety, although significant interdependence was found between the anion and cation regarding toxicity.[93] In general, phosphonium cations were found to be most toxic.[93] Aromatic cations (e.g. imidazolium or pyridinium, with imidazolium found to be the more toxic of the two[97]) were more toxic than non-aromatic (e.g. pyrrolidinium).[98] Alkylammonium ILs have also been found to be less toxic than pyrridinium and imidazolium counterparts.[99]

In addition to IL toxicity, there have been concerns over IL biodegradability and build-up in the environment, due to the stability of ILs.[100] As a result, there has been research directed towards creating biodegradable[101–109] and biocompatible[101–105,109] ILs, typically using bio-derived reagents such as amino acids (e.g. choline[101–105] or lysine[109]) and carboxylic acids (e.g. lactic acid[101,102] or levulinic acid[102,105]). However, such ILs typically demonstrate low thermal stability.[110] One IL based on biodegradable ions was not classed as readily biodegradable according to the OECD standards, showing that use of biodegradable components may not be sufficient to produce an IL that can be classified as biodegradable.[111] Furthermore, by-products from bacterial metabolism of ILs can themselves be damaging.[112] A different route towards improved ecological performance has also included designing ion structures in alkylimidazolium ILs that render the IL biodegradable. Gathergood et al. found that incorporating an ester group into the alkylimidazolium side chain, and use of the octyl sulfate anion both improved biodegradability of an otherwise poorly biodegradable class of ILs.[106–108]

PILs have been shown to have a lower toxicity and higher biodegradability compared to APILs. Peric et al. found a range of PILs to be potentially biodegradable in water, unlike the studied APILs.[92] Additionally, the PILs did not display any aquatic toxicity, and showed EC_{50} values orders of magnitude below those of the APILs. In addition, Reid et al. found 15 out of 16 tested PILs (containing carboxylate and chloride anions, with secondary and tertiary alkylammonium cations) to be neither carcinogenic, nor mutagenic.[113] However, Oliveira et al. found the biodegradability of four alkylammonium carboxylate PILs to all be low.[95]

In addition to toxicity and biodegradability, the environmental impact of IL production has been questioned, with many coming from petrochemical feedstocks.[114] Deetlefs et al. compared different IL synthesis routes on a lab-scale, with substantial differences in E-factor (mass of waste/ mass of product[115]) and atom economy depending on the protocol followed.[86] Baaqel et al. conducted a recent LCA comparing the overall impact of producing [TEA][HSO_4], [Hmim][HSO_4], glycerol, and acetone.[17] Overall costs were calculated based on both direct production costs, as well as indirect costs covering effects on human health, ecosystems, and resource damage. The effect of incorporating these indirect costs more than doubled total costs. [TEA][HSO_4] was found to have the lowest direct and total costs, followed by acetone, with both having similar indirect costs. However, incorporating indirect costs made glycerol's total costs higher than those of [Hmim][HSO_4], despite lower direct costs. This was due in large part to the huge land requirements for cultivation of rapeseed and soybean. This type of comprehensive environmental analysis for large-scale production should be encouraged for appropriate comparison and selection of sustainable chemicals.

1.1.5 Applications of Ionic Liquids

Due to their particular combination of properties, interest in IL has exploded over the last 20 years in a variety of fields (Fig 1.2), despite their first discovery in 1888 (the PIL ethanolammonium nitrate).[46]

The generally low vapour pressure, high polarity, and large liquid temperature range, has led to ILs being used as solvents, such as for reactions between reactants that are soluble in both organic and aqueous solvents.[117] One example of their use as a green solvent is in the cracking of dialkoxypropanes, which would otherwise require a volatile organic solvent and a toxic catalyst, or high pressure and temperature.[118] Due to their desirable properties as solvents, ILs have also been considered for use in chromatography,[119] Carbon Capture and Storage (CCS),[120] biomass fractionation,[14,121,122] and protein handling, purification, and modification.[123] ILs may also provide suitable acidity to be used as catalysts.[46,124] An example of their use as both a catalyst and solvent is

in esterification of acetic acid in the Fischer reaction, where ILs may form one phase with water, allowing easy separation of the separate ester phase.[125]

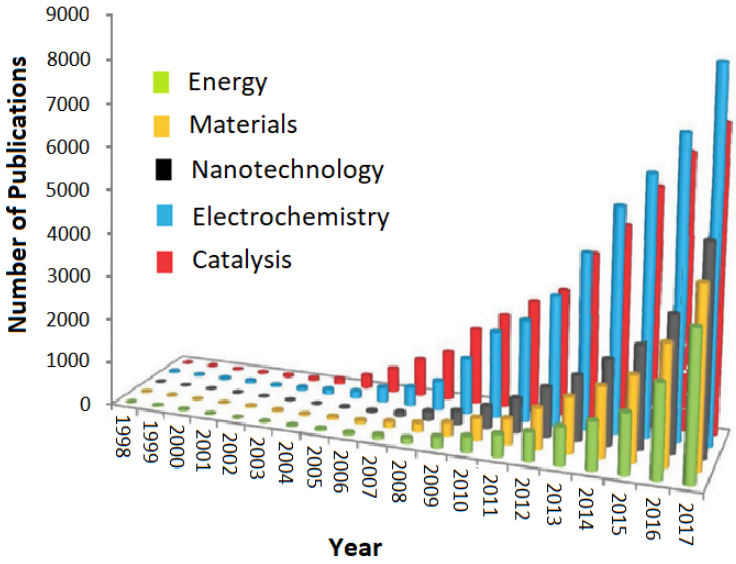


Figure 1.2: Scientific publications related to ionic liquids in different fields, according to the Institute for Scientific Information Web of Science. Adapted from Barzinjy et al.[116]

The wide electrochemical window of ILs relative to water has also led to interest in using them for electrodeposition of metals with negative reduction potentials (e.g. Al^{3+}/Al [91]), as these cannot be deposited from aqueous systems. Other favourable properties for this application include their relatively low vapour pressures and good thermal conductivity, and their tuneable properties by anion and cation selection.[91] Successful deposition of several common metals, including Ti, Cu, Fe, Zn, Ag, Al, and Pb has been carried out in APILs.[91] In addition, deposition of light metals (e.g. Na, Li), rare earth metals (e.g. La, Dy), and noble metals (e.g. Pt, Pd) has also been successful.[126] Despite their narrower window, PILs have been used to deposit Ag, Au, Cu, Co, As, Cr, Pb, and Zn.[45,91,122] This wide electrochemical window, high conductivity, and thermal stability has also led to interest in their use as electrolytes in electrochemical systems such batteries and fuel cells.[46,54,117,118]

It should be noted that one setback in the deployment of ILs is their high corrosiveness to many resistant metals under certain conditions. This property of ILs has, however, not been widely studied.[45,90] This is despite the clear need for material compatibility knowledge required for scaled-up IL-based processes. For example, BASF replaced [emim]Cl by [emim][OAc] in their CELLIONIC cellulose solutions due to the high corrosiveness issues of the former.[127] Recently, Malaret conducted an extensive corrosion study involving multiple metals and ILs (both PILs and APILs).[90] Although corrosion behaviour was found to be highly system-dependent, a number of high-level trends were extracted:

1. Metal corrosion rates in PILs tend to be higher than those in APILs, assumed to be due to the presence of protons that can be reduced to H_2 in the cathodic reaction
2. Temperature generally increases the rate of corrosion
3. Water generally acts as a corrosion promoter in IL systems

1.2 Biorefinery

1.2.1 General

According to the IEA, biorefinery refers to the "sustainable processing of biomass into a spectrum of marketable products […] and energy".[128] The aim of biorefinery is to therefore produce high-value chemicals and/or energy using biomass feedstocks. The ulterior motive for this is to move away from society's current reliance on unsustainable petrochemical feedstocks, and towards utilisation of this abundant and renewable resource. This would have the benefit of moving towards a carbon-neutral economy, thus reducing further global warming.

The production of biofuels is one of the main areas of interest in biorefinery. The two main types of biofuel produced are biodiesel and bioethanol. The main advantage of the latter is that bioethanol may be theoretically produced from any plant, whereas biodiesel requires specific high-oil species such as rapeseed. There are currently two established generations of biofuel, differing in the type of biomass used: first generation biofuels use crops with high sugar (e.g. sorghum plants like sugarcane), starch (e.g. maize), or oil contents (e.g. rapeseed or soybean);[5,129–132] the second generation use lignocellulosic biomass.[129] Some sources also describe a third generation of biofuel derived from algae.[133,134]

First-generation biofuels require much less biomass processing, due to their much less recalcitrant structure, containing high concentrations of easily hydrolysable starch, or high sugar and oil contents (see Fig. 1.3). However, they also suffer from a number of serious drawbacks. Firstly, their feedstocks tend to be food crops, which can lead to competition for land between fuel and food, which has associated political, economic and ethical issues (the infamous "food vs. fuel" debate").[5] For example, Elander and Putsche estimated that, for every 2.5 million tonnes of bioethanol produced from corn, the price of corn increased by up to $2/tonne.[135] However, there are other drawbacks including high levels of NO_x emissions due to high fertiliser use, biodiversity loss, water overconsumption, and the land change for cultivation reducing or even negating any reductions in CO_2 emissions relative to fossil fuel use.[6–8,129,131]

Second generation biofuels avoid many of these drawbacks. Their feedstock, lignocellulosic biomass (i.e. made up of lignocellulose, further explored in Section 1.2.2), encompasses a wide range of vegetation, including grasses, hardwoods, softwoods, and agricultural residues. Cellulose, one of its three main constituents, is the most abundant polymer on Earth.[5] As a result, feedstocks for second generation biorefinery are cheaper, are not geographically limited, include perennial crops, and avoid competition with food crops for land as they can be grown on marginal land.[9–11,135–137] Additional benefits include lower fertiliser requirements, perennial and/or rapid growth in certain species, and improvements in soil health.[8,45,138] However, lignocellulosic feedstocks are limited by higher processing costs due to their more complex structure.[139]

In their review article, Hou et al. identify two distinct routes for biorefinery of lignocellulose.[140] The first is direct pyrolysis in order to gasify or liquefy the lignocellulose, leading to a range of products such as syngas, bio-fuels, fertilizer, and heat. The second route is full or partial fractionation of the lignocellulose matrix, allowing individual constituents to be more easily processed. Production of lignocellulosic bioethanol generally corresponds to the latter, and is made up of three main steps (see Fig. 1.3).

1. Pretreament

   The goal is to release the glucose within the cellulose (as well as sugars within hemicellulose, to a lesser extent), which can then be fermented by various microorganisms into ethanol. However, lignocellulose is resistant to enzymatic and chemical attack, thus protecting the cellulose from being depolymerised. As a result, the structure of the biomass must altered in some way to render the cellulose more accessible to hydrolysis. This process is referred to as pretreatment, and has been described as the most important step in lignocellulosic biorefinery due to its effect on costs: it was found to be the second most expensive step in the production of second generation bioethanol after feedstock costs.[141,142] The current approaches to pretreatment are described in Section 1.2.3, and often involve biomass fractionation to some extent.

2. Hydrolysis/Saccharification

   Following pretreatment, the next step towards biofuel production is the depolymerisation of cellulose into glucose, and hemicellulose into its constituent sugars. This depolymerisation is carried out *via* hydrolysis (and may be termed saccharification). Hemicellulose is much more easily hydrolysed than cellulose (due to the highly crystalline nature of cellulose, explored further in Section 1.2.2).[143] There are two general ways in which this process is carried out: chemical hydrolysis using acid, or enzymatic hydrolysis using cellulase enzymes, with the latter

being the more common due to milder conditions (leading to less sugar degradation) and no corrosion issues, despite longer operating times.[135,143] During enzymatic hydrolysis, some cellulase irreversibly adsorbs to the cellulose, thereby reducing the activity of the enzyme. Addition of surfactants may minimise this irreversible adsorption.[135,144] As a result, a compromise must be reached in terms of enzymatic loadings, with higher loadings able to increase the rate and yield of the process but engendering higher costs.[135] Enzyme recycling may reduce costs, but it has been reported to reduce efficiency with each subsequent reuse.[135] The yield of glucose may be normalised to the theoretical maximum yield based on the cellulose in the original biomass (termed the saccharification yield) or based on the cellulose in the pre-treated solid (termed the digestibility).

3. Fermentation

Once sugars have been obtained, the final step is fermentation of the hexose sugars into ethanol, following which the ethanol may be removed by distillation, with any leftover lignocellulosic matter settling to the bottom of the distillation column.[143] This stage tends to focus on the use of hexose sugars as they are fermented by many microorganisms, but there may be a significant quantity of pentose sugars released during hydrolysis. As a result, utilisation of these sugars may prove key to rendering second generation bioethanol more economically competitive. The development of yeast strains able to convert xylose to ethanol may also be possible.[135] However, the strains that ferment pentose sugars are less common and present lower yields.[143,145] The possibility of combined hydrolysis and fermentation (termed Simultaneous Saccharification and Fermentation, SSF) has been investigated, as it offers the possibility to lower costs. However, it requires the use of genetically engineered microorganisms that can operate in the mixture, and renders process optimisation more complex than for two individual operations.[135,145]

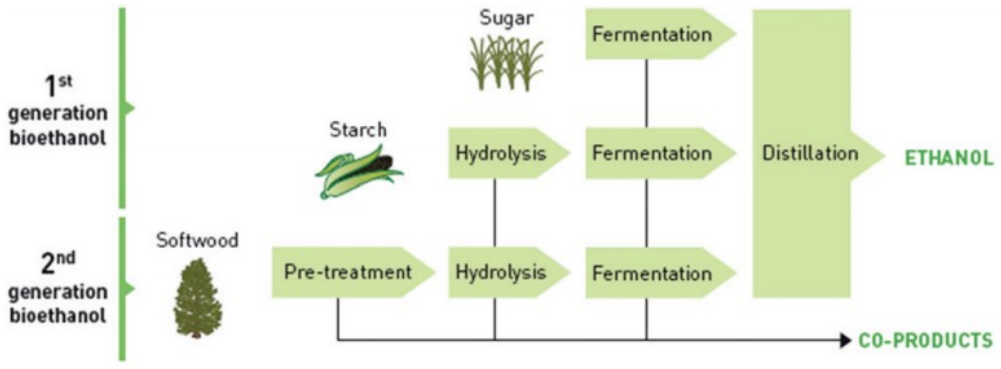


Figure 1.3: Required steps for production of first generation and second generation bio-ethanol.[73]

The economic feasibility of lignocellulosic biorefinery has been investigated several times. Results consistently showed that in order to be economically competitive, if not economically viable, the valorisation of the other components of lignocellulose is essential, in particular lignin which has several potential uses such as an emulsifier, binder, or dispersant.[73,146] However, production of other substances such as furfural (which may be generated by the dehydration of xylose) may also become important.[140,147] Reduction in the costs of enzymatic hydrolysis have also been suggested as a way of rendering the process of lignocellulosic biorefinery more economically viable, such as through genetic modification of feedstocks or cellulase-producing microorganisms.[135]

1.2.2 Lignocellulose

The drawback of lignocellulosic biomass relates to the structure of its cell walls. These are made of lignocellulose, a matrix of three polymers: cellulose, hemicellulose, and lignin. The ratio of these varies between species, but also within individual plants with time and environmental conditions.[143] Typical composition ranges for different types of lignocellulosic biomass are shown in Table 1.1. Lignocellulose typically accounts for around 90% of plant dry matter,[73] with the remainder including components such as ash, proteins, pectins, lipids, and phenolics.[148,149]

Table 1.1: Typical composition ranges of different types of biomass. [5,135,150]

Feedstock Type	Example	Cellulose (% dry wt.)	Hemicellulose (% dry wt.)	Lignin (% dry wt.)
Grasses and agro-residues	*Miscanthus*, corn stover	25-45	30-50	7-30
Hardwood	Willow	40-55	24-40	18-25
Softwood	Pine	45-50	25-35	25-35

While each of its three constituent polymers may be processed to yield useful products, the lignocellulosic matrix is extremely recalcitrant to fractionation, which has limited the economic viability of its products. It is believed that the three dimensional structure of lignocellulose is key to its chemical and enzymatic recalcitrance.[151] The rigid cellulose fibres are embedded in a matrix of amorphous hemicellulose, which may bind non-covalently to their surface.[73] In addition, the resistant lignin is covalently cross-linked to the hemicellulose, thereby acting as a sheath to the lignocellulose matrix.[73,152] As a result of this structure, the cellulose is not easily accessible (see Fig. 1.4). The ratio of the three polymers also impacts the recalcitrance of the biomass, with a rough assumption being that recalcitrance increases with lignin content.[23] In accordance with this, grasses and agricultural residues

typically exhibit the lowest recalcitrance and the lowest lignin content.[152] However, lignin content alone is not always sufficient to predict resistance to fractionation.[153]

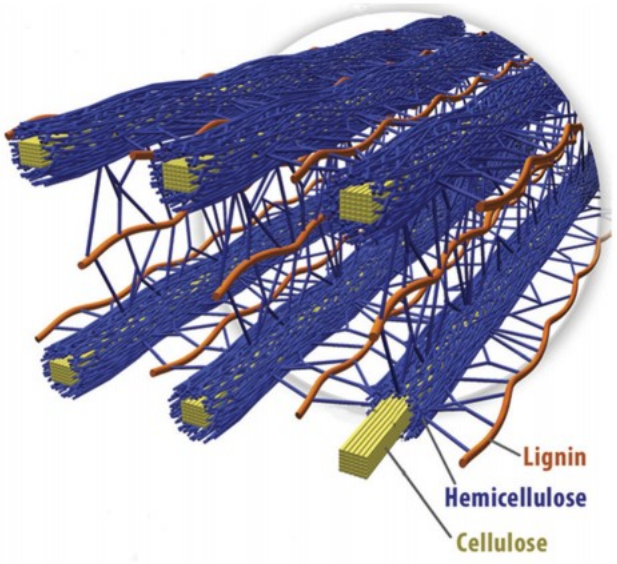


Figure 1.4: 3D structure of lignocellulose.[73]

Cellulose

Cellulose is a polymer made up of repeating glucose units, exhibiting the greatest degree of polymerisation in lignocellulose.[73,152] Glucose monomers are linked by β-1,4 glycosidic bonds (see Fig. 1.5), making cellulose a linear polymer that can form long, flat chains (with a degree of polymerisation of around 10,000-15,000).[154,155] The β-1,4 glycosidic bonds also lead to an extensive network of inter- and intra-molecular hydrogen bonding: each glucose monomer forms two intra-molecular hydrogen bonds, and one inter-molecular hydrogen bond with another chain.[154,156,157] Cross-linked cellulose chains are further held together by van der Waal forces, and thus aggregate together into elementary fibrils and then rigid microfibrils.[150,154,156,157] As a result, cellulose has a large, highly ordered, crystalline structure that makes it insoluble in water (despite solubility of its oligomers and monomers[73]) and a range of common solvents.[5,151]

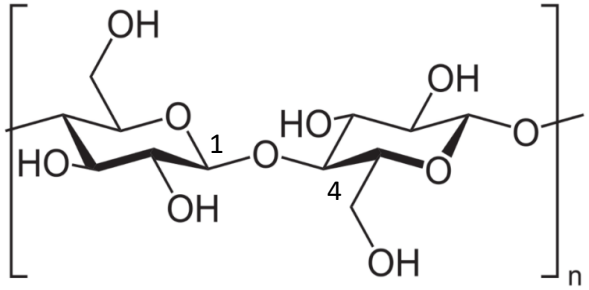


Figure 1.5: Cellulose Repeating unit, with glucose monomers linked by a β-1,4 glycosidic bond.

There exist six different polymorphs of cellulose: I, II, III_I, III_{II}, IV_I, and IV_{II}.[154,157] These differ in terms of their molecular orientations and thus the location of the inter-molecular hydrogen bonds. Cellulose-I (itself either I_α or I_β) is the metastable native form of cellulose found in biomass, while Cellulose-II is the most thermodynamically stable form of cellulose. The two differ based on whether the cellulose chains runs parallel or anti-parallel. Conversion between the different cellulose polymorphs is possible. Cellulose-I can be converted to cellulose-II by regeneration (dissolution and recrystallization) or mercerisation (alkali treatment). Cellulose-III_I and cellulose-III_{II} are formed by ammonia treatment of cellulose-I and cellulose-II respectively, and can be further converted to cellulose-IV_I and cellulose-IV_{II} by heat treatment.

Cellulose has historically been the most utilised fraction of lignocellulose because of its many material applications. The most ubiquitous use of cellulose is for paper and packaging (for which the fibre integrity and strength must be preserved), but a wide range of other applications exist. Dissolving pulp (high-purity, bleached cellulose that is dissolved to break down the fibre structure) is used to produce a range of different materials such as Viscose yarn (by far the major use), cellulose acetate, or cellophane.[158,159] Dissolving pulp is also used to produce microcrystalline cellulose, used in the pharmaceutical and food industries.[158,160] Nanocellulose is a relatively new route for cellulose utilisation, in which nano-scale fibres are extracted from cellulose (generally under 100 nm in diameter and several micrometers in length).[161] Nanocellulose displays a number of promising properties for materials applications, such as high tensile strength, transparency, and biocompatibility.[161,162] As a result, a number of possible applications have been suggested mainly focussing on medical use (e.g. drug delivery or tissue repair).[161,162]

As well as material applications, cellulose also offers potential for production of a range of useful chemicals and fuels, mostly through initial hydrolysis to glucose. Amongst others, cellulose can thus be used to produce ethanol, levulinic acid,[163] lactic acid,[164] and 5-hydroxymethylfurfural (HMF).[165] Lactic acid is used in the pharmaceutical and food industries, and as a monomer for the bioplastic polylactic acid (PLA).[166] The pathway for production of levulinic acid and HMF from glucose is shown in Fig. 1.6. Levulinic acid can be further processed to yield a number of specialty chemicals and fuels,[167] as shown by Serrano-Ruiz et al. who converted cellulose to jet fuel starting by acidic hydrolysis to levulinic acid.[168] HMF has attracted significant attention as a platform chemical as it can be converted to a large number of other chemicals, including 2,5-furandicarboxylic acid (FDCA, the monomer for a bioplastic aiming to replace PET) and 2,5-dimethylfuran (a potential biofuel with high energy content).[169,170]

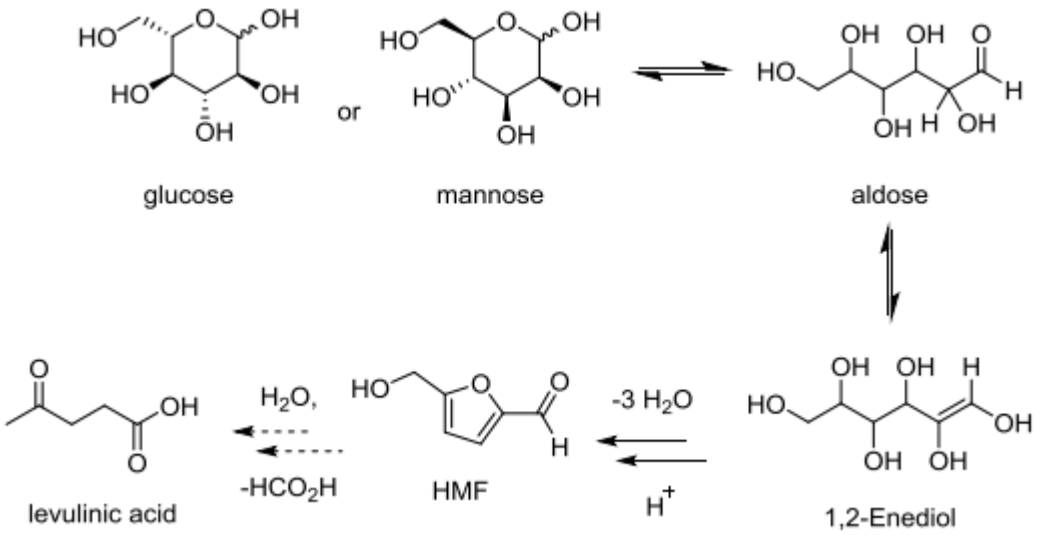


Figure 1.6: Proposed mechanism for acid-catalysed formation of HMF and levulinic acid from hexose sugars.[45]

Hemicellulose

Hemicellulose, unlike cellulose, is a heteropolymer made up of a mix of two pentose (xylose and arabinose) and three hexose sugars (glucose, galactose, and mannose).[73,151] Different "types" of hemicellulose exist, and are named according to their component sugars (e.g. xylan, glucomannan, xyloglucan, etc.). As different feedstock classes have different abundances of sugars, hemicelluloses can have very different compositions. For example, mannose is the most common hemicellulose sugar in softwoods, while xylose is the most common in hardwoods and grasses. [73,150,171,172] In addition to sugars, hemicellulose may contain functional groups such as acetyl and methyl groups, as well as sugar (uronic) acids.[73]

Hemicellulose is made up of a linear β-1,4 linked backbone, with a large number of short branches, making it much more amorphous than cellulose.[172,173] Its degree of polymerisation is much lower than that of cellulose (100-200).[174] Its lower molecular weight and low crystallinity mean that hemicellulose is much less resistant than cellulose, and may be depolymerised under milder conditions.

Hemicellulose material applications are not as widespread as those of cellulose (mainly focussing on hydrogels and membranes).[175,176] Efforts to valorise hemicellulose have instead mostly focussed on chemical valorisation. The hexose sugars in hemicellulose can be fermented into ethanol, or can be converted to HMF and levulinic acid in the same way as glucose.[177] However, as mentioned in previously, the large quantities of pentose sugars currently limit the usefulness of hemicellulose for

fermentation. One route for valorising pentose sugars is through their dehydration to furfural under acidic conditions (see Fig. 1.7), or using halide salts, or using trivalent cations in aqueous solutions.[178] Furfural is a valuable platform chemical similar to HMF, that can be used to produce a range of compounds, broadly classified by Li et al. into fuel components, C_4 chemicals, and C_5 chemicals.[179] Based on factors including raw material, processing cost, and market potential, it was ranked as a top 30 biomass-derived platform chemical by the U.S. Department of Energy.[180]

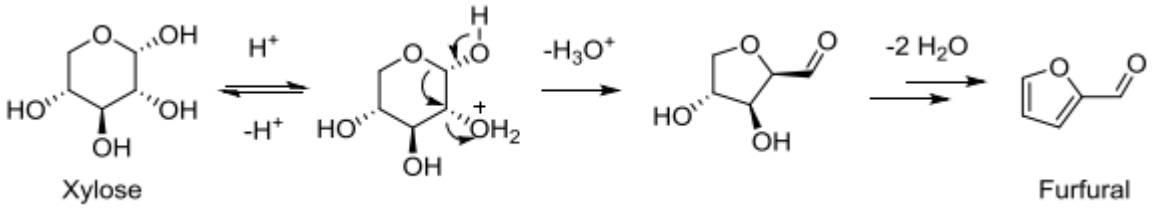
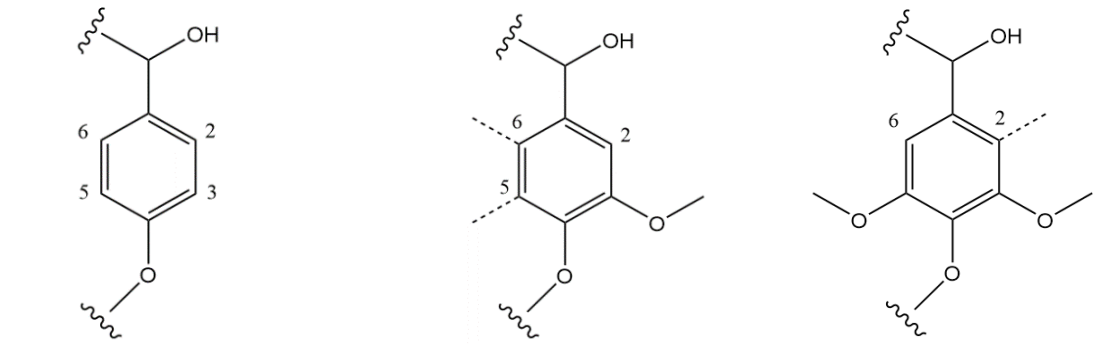


Figure 1.7: Proposed mechanism for the acid-catalysed dehydration of xylose to furfural.[45,181]

Lignin

Lignin is a three dimensional polyphenolic polymer that serves as a sheath around the cellulose and hemicellulose. It provides structural strength to the cell wall and resistance against enzymatic attack, and is impermeable.[5,145,182] Lignin is formed by the radical polymerisation of three hydroxycinnamyl alcohols (called monolignols): *p*-coumaryl, coniferyl, and sinapyl alcohol.[143] Once incorporated into the lignin structure, these are identified as the sub-units p-hydroxyphenyl (H), guaiacyl (G), and syringyl (S). These sub-units are primarily linked by β-*O*-4' ether bonds, but other linkages also exist (e.g. β-β', β-5', and β-1').[183] As seen in Fig. 1.8, the three monomers differ based on the methoxy group substitution at the C_3 and C_5 rings positions: H units have none, S units are substituted at both, while G units are only substituted at the C_3 position. As a result, the C_5 position on the G sub-unit aromatic ring is more reactive, and forms extensive 5-5' cross-linkages that are not easily hydrolysed.[73] Small quantities of other sub-units can be found in lignin, such as ferulates and *p*-coumarates.[184] In biomass processing, the structure of lignin is mainly characterised by Gel Permeation Chromatography (GPC) and 2D Heteronuclear Single Quantum Coherence NMR (2D HSQC NMR). The former is used to determine the molecular weight distribution of the lignin, while the latter is a sophisticated technique allowing the structure of the lignin to be semi-quantitatively evaluated.[184]



H *p*-hydroxyphenyl | **G** guaiacyl | **S** syringyl

Figure 1.8: Main lignin sub-units.

One of the obstacles to lignin valorisation is its poorly defined structure, due to the random radical polymerisation of the monolignols making lignin is a very heterogeneous polymer.[185] The structure of lignin can even vary within an individual plant based on tissue, growth conditions, and growth stage.[186–189] Lignin structure (expectedly) also varies significantly between feedstock types due to a different distribution of sub-units and linkages. Grasses contain all three types of sub-units, hardwoods contain a fairly even split of S and G sub-units, while softwoods are composed predominantly of G sub-units.[73,190] S-lignin typically contains a higher number of β-*O*-4' linkages, meaning grasses typically contain a higher proportion of these linkages (74-84%) than hardwoods (60-62%) or softwoods (45-50%).[191,192]

The presence of lignin is one of the main factors behind the recalcitrance of untreated lignocellulose. Lignin surrounds the lignocellulosic matrix, restricting the accessibility of the sugars within. However, lignin also irreversibly binds to hydrolase enzymes through hydrogen bonds and electrostatic interactions, leading to high enzyme requirements in processing of lignocellulose.[73,193] Lignin may also contain compounds such as vanillin that can inhibit fermentation and enzymatic hydrolysis. Removal of lignin is therefore one of the primary aims of pretreatment. This is discussed further in Section 1.2.3. As a result of their different lignin sub-unit and linkage compositions, different types of biomass exhibit different degrees of recalcitrance. Typically, digestibility decreases in the order grasses > hardwoods > softwoods, due to the increasing proportion of G sub-units and decreasing proportion of labile β-*O*-4' linkages.

Despite its unpredictable and resistant structure (often rendered even less reactive due to condensation reactions in pretreatment), there has been much interest around valorising lignin. A

major reason is because lignin is the only aromatic component of lignocellulose, but also because valorisation of such a major component substantially impacts the economic feasibility of second generation biorefinery.[194–196] In addition, the volumes of generated lignin are predicted to be very substantial: the U.S. DoE estimates 225 million tonnes of lignin to be generated annually in the USA by 2030.[197] In order to fully utilise lignin for its aromaticity, depolymerisation is required, such as through acid or base catalysis, oxidative depolymerisation by strong oxidising agents, or depolymerisation in ILs.[182,198] Another route for producing aromatic chemicals from lignin is through thermal methods, such as pyrolysis to form bio-oils.[87,199] A wide range of more direct applications for lignin (i.e. those requiring more minimal processing) have also been looked into, such as its use as a filler,[200,201] a flame retardant for biodegradable polymers,[202] in carbon fibres,[203,204] a UV filter in biodegradable films,[205] and as a heavy metal adsorbent.[206] However, for these types of applications several properties of the lignin polymer can be crucial, such as its molecular weight distribution or residual carbohydrate content.[207] Currently, 95% of industrial lignin is burned as a fuel due to its reasonable energetic content (HHV reported to be 23-25 MJ/kg for ionoSolv lignins[87]).[208]

Matrix Structure

Within the complex lignocellulosic matrix, cellulose fibres are embedded in amorphous hemicellulose. Due to the abundance of hydroxyl groups on both polymers, hydrogen bonding occurs between the bundles of cellulose fibres and hemicellulose chains.[209,210] This has been confirmed computationally to be important to the shear strength of lignocellulose at the cellulose-hemicellulose interface.[209] However, the exact mechanism through which hemicellulose binds cellulose fibres into a network is still not fully understood. A number of hypotheses have been proposed, such as hemicellulose strands directly “tethering” fibrils together by bonding to their surfaces, or indirectly tethering fibrils by linking them to pectins and other hemicellulose chains.[211]

Interactions between lignin and the carbohydrate fractions are less well understood and are not conclusively agreed on. There is, however, significant interest surrounding such interactions due to their reported effect of increasing biomass recalcitrance.[212,213] Debate centres around the existence of extensive covalent bonding between these fractions, making up so-called lignin carbohydrate complexes (LCCs). Early evidence for such complexes was based upon the residual lignin fraction in Kraft pulp. This was shown (by gel permeation chromatography and compositional analysis) to contain alkali-stable lignin-carbohydrate linkages, that could explain the low delignification rates during the final stages of the Kraft process.[214,215] Furthermore, in milled wood enzyme lignin, around 10% of carbohydrates are unable to be enzymatically hydrolysed and must be hydrolysed using acid, taken to

be a sign of bonding to lignin.[216] Particularly with the development of 2D HSQC NMR, isolation and analysis techniques have become increasingly sophisticated and allowed deeper probing of potential LCC structures. These techniques were comprehensively reviewed by Koshijima and Watanabe,[217] and more recently by Giummarella et al.[212] This has led to five proposed types of lignin-carbohydrate bond: benzyl ethers, benzyl esters, γ-esters, ferulate/coumarate esters and hemiacetal/acetal linkages.[212,218]

Although a large number of experimental studies on biomass isolates indirectly indicate the presence of LCCs, there is still some doubt over their existence.[219] This is due to the potential modification of native structures during their isolation, leading to the development of milder isolation techniques such as using enzymes.[212] Furthermore, there is also uncertainty in the analytical techniques employed (e.g. difficulties in conclusively characterising native NMR spectra using model compounds).[212,219] However, recent work by Nishimura et al. has provided clear evidence for the presence of benzyl ether bonds in woods using a range of NMR techniques.[218] Further studies demonstrating such conclusive evidence may soon close the debate over the existence of LCCs.

1.2.3 Pretreatment

While each of the three fractions of lignocellulose may be processed to yield useful products, the lignocellulosic matrix is extremely recalcitrant to chemical and enzymatic attack, and must therefore be modified to allow further processing.[147] This process is referred to as pretreatment. As most applications tend to focus on cellulose utilisation, the general aim of pretreatment is to improve the accessibility of the cellulose fibres within the biomass, either through disruption or fractionation of the lignocellulose matrix.

Non-pretreated biomass displays poor saccharification yields at reasonable enzymatic loadings.[145] Three main factors are responsible, and their examination allows the more detailed aims of pretreatment to be determined:

1. The relatively low accessibility of cellulose to cellulytic enzymes within the lignocellulosic matrix.[152,220,221]

   Increased surface area of the sample, both external and internal (the latter referred to as porosity), allows the enzymatic solution to permeate through the biomass, and may be enhanced through mechanical means.[220] However, Stone et al. emphasise the point that the enhanced internal surface area must be within pores large enough for cellulases to enter, which they find to be around 30 Å in diameter.[220] On a smaller scale, the structure of lignocellulose also contributes to a low accessibility of cellulose fibres: the cellulose is

embedded in a protective structure of hemicellulose and lignin, and as a result removal of the two latter polymers enhances cellulose accessibility and glucose yields.[221]

2. Deactivation of cellulolytic enzymes by lignin through irreversible binding.[152]
   In their investigation into the effects of lignin on softwood pre-treatment, Kumar et al. found lignin's effect on cellulose accessibility to be the dominant inhibitory effect, however. This was done by comparing saccharification yields of steam pretreated biomass with those of delignified steam pretreated biomass that had its extracted lignin added to the saccharification mixture.[221]

3. Higher crystallinity of cellulose,
   The ratio of crystalline to amorphous cellulose has also been postulated as having a significant impact on hydrolysis by decreasing accessibility of cellulose fibres and increasing the polymer's recalcitrance to hydrolysis.[145,146,222] One argument supporting this theory is that comminution of biomass improves hydrolysis yields substantially, despite only a small increase in accessible surface area due to the small aspect ratio of lignocellulose fibres.[152] However, the impact of crystallinity, or at least its relative importance, has been debated, with some studies showing significant improvements in hydrolysis yields despite increases in crystallinity.[152,220]

The aims of pretreatment targeting production of bioethanol and cellulosic materials are, therefore, to reduce the lignin content of biomass and/or improve the accessibility of the cellulose fibres, reduce cellulose crystallinity, and increase internal and external surface area, all while preserving cellulose yields and avoiding the formation of substances that are harmful to downstream processing. [143,152,222] However, depending on the intended application there may be other desired outcomes, e.g. removing or preserving the hemicellulose fraction, or recovering lignin as a separate fraction.[143,222–224] In practice, the success of pretreatment tends to be reported in terms of delignification and saccharification yields.

Types of Pretreatment

There exists a range of different pretreatment technologies, which act via different mechanisms and thus may achieve different pretreatment outcomes, and which have associated advantages and drawbacks. They may be broadly categorised into mechanical, physicochemical, chemical, and biological. The most common types of pretreatment are described below. This study focusses on chemical pretreatment using Ionic Liquids (ILs), which will be covered in the following section.

The most common physical pretreatment involves comminution of the biomass. This is often done through grinding or milling, which tend to produce particle sizes of around 0.2-2 mm.[152] This process leads to an increase in surface area and has been shown to reduce cellulose crystallinity.[143,225] As a result, saccharification yields may be significantly improved: in the work of da Silva et al, ball milling of sugarcane bagasse and straw for 60 minutes and 90 minutes respectively more than tripled glucose yields compared to native biomass.[225] However, the associated energy expenditure of significant comminution is considerable, and the ratio of initial to final biomass size has been found to be roughly proportional to the energy needed.[226,227] As an example, particle size reduction of air-dried willow chips and air-dried *Miscanthus* to under 1 mm was found to consume over 10% and 3.5% of the biomass energy content respectively. Furthermore, the energy required for this size reduction of *Miscanthus* doubled if the biomass had a moisture content of 15%.[226] In addition to the final and initial particle sizes, moisture content, and machinery used, the type of biomass input is also a crucial factor for energy requirement.[152,226] In the work of Miao et al, the hardwood willow was found to require significantly more energy than the three grasses tested.[226] Similarly, Cadoche et al. found hardwood (unnamed species) required much more energy for milling than straw or corn stover (both agricultural residues).[228] As a result of high energy costs, slight comminution of biomass is often used as a first step to enhance the performance of other pre-treatment methods.[152] It may also be used as a second step following a different pre-treatment, which can result in lower energy requirements: Brandt et al found that after brief ionic liquid soaking, grinding energy requirements of pine chips could be decreased by 50-70%, attributed to ILs' lubricating properties.[152,227] One advantage of comminution pretreatment is that hemicellulose is not removed and may be hydrolysed into potentially useful sugars such as xylose. In addition, comminution of biomass is a relatively environmentally friendly option which does not form harmful degradation products. Other, less common, physical pretreatment methods include irradiation, extrusion, freeze/thaw, and pyrolysis.[143]

Steam explosion (SE) is a common physicochemical pretreatment method. This process involves immersion in high-pressure steam (160-260 ^{o}C, at pressures of 10-50 bar[152]) followed by rapid pressure reduction. The high temperatures lead to the hydrolysis and removal of hemicellulose from the biomass, possibly due to the formation of acids during the process.[5,143] High temperatures also cause the lignin to melt, depolymerise and repolymerise, and thus be redeposited in droplets on the surface of cellulose fibres.[221,229,230] The sudden pressure drop leads to comminution of the sample, and therefore to an increase in surface area, although not necessarily to a decrease in crystallinity.[231] This comminution uses around 40% less energy than conventional methods, and thus affords significant savings on energy costs, while allowing chipped biomass to be used as feedstocks. The process can last from seconds to minutes, depending on the chosen temperature and intended severity of

pretreatment.[135,152] Increasing the severity leads to enhanced hemicellulose hydrolysis and increases digestibility of the pulp.[152] However, this can lead to the formation of degradation products (e.g. furfural, organic acids, and 5-hydroxymethyl-2-furfural)[5,142] which inhibit downstream biological processes and thus require the sample to be washed, leading to a loss of soluble sugars formed from the hydrolysis of hemicellulose and possibly of cellulose.[143,152,232] Enhanced digestibility through increased pretreatment severity may therefore be counterbalanced by increased loss of sugars.[152] The addition of acid (such as H_2SO_4) or SO_2 during steam hydrolysis has been shown to catalyse the process, allowing lower severities to be used, and to increase hemicellulose solubilisation while reducing degradation of sugars.[143,152] The low costs, environmental effects, and hazards of the chemicals involved, as well as the ease of potential scale-up, make steam explosion an attractive option for pretreatment.[5] However, there are several drawbacks, notably the loss of soluble sugars and the relatively low rates of lignin removal which leads to poor saccharification yields in feedstocks with elevated lignin contents. Other forms of hydrothermal pretreatment are also employed, with the simplest being Liquid Hot Water (LHW) pretreatment, which involves the application of high-temperature water under pressure (typically 130-240 ^{o}C).[233] This leads to a similar pretreatment mechanism as SE (minus the comminution), i.e. hydrolysis of hemicellulose due to the formation of weak organic acids, and redistribution of lignin.[234] pH can be controlled in the aqueous phase to minimise formation of degradation products and improve hemicellulose removal.[235] However, LHW suffers from a high energy expenditure, and the same limited lignin removal as SE.[233]

Another common physicochemical pretreatment method is Ammonia Fibre Expansion (AFEX). This process is similar to steam explosion and involves liquid ammonia being applied to pre-wetted biomass (around 1-2 kg of ammonia/kg dry biomass)[5,143] under pressure, followed by rapid pressure release.[152] The conditions involved in AFEX, however, are generally milder than steam explosion: temperatures used are around 60-150 ^{o}C, and pressures around 10-15 bar, although residence times tend to be longer (from minutes to an hour).[152] Liquid ammonia's viscosity and surface tension are significantly lower than water's, facilitating penetration into the biomass, and thus not requiring as significant particle size reduction beforehand. The process leads to hemicellulose hydrolysis, redistribution of lignin through depolymerisation and repolymerisation (catalysed by the basicity of ammonia), possible reduction in cellulose crystallinity, as well as an increase in surface area through fragmentation following pressure release.[234] One of the benefits of AFEX is that hemicellulose is mostly redistributed rather than solubilised, as it is hydrolysed to insoluble oligomers (insolubility may be due to deacetylation).[143] Therefore, the process increases accessibility of cellulose, while allowing the hemicellulose to be partly converted to sugars during enzymatic hydrolysis.[234] Furthermore, the ease of recovery of ammonia and the lack of degradation occurring during the process mean that washing

is not required after pretreatment: it is a "dry-to-dry" process.[234] The relative ease of ammonia recovery also aids scale-up: AFEX scale-up has already taken place, being used in a pilot plant. Similarly to steam explosion, AFEX pretreatment has been shown to be less effective on feedstocks with higher lignin contents due to lignin being mainly redistributed rather than removed.[152,236] As a result, AFEX has shown significant improvements in saccharification of grasses, but less so for softwoods and hardwoods.

Supercritical CO_2 explosion has been suggested as an alternative to steam explosion and AFEX. The size of CO_2 molecules is similar to that of water and ammonia, allowing it to enter pores as easily. The formation of carbonic acid through the dissolution of CO_2 in water has been postulated to increase the hydrolysis of hemicellulose.[143] Furthermore, supercritical CO_2 explosion is thought to be capable of operating at lower temperatures than steam explosion (as low as 35 ^oC although pressures are higher[237]), thus inhibiting the formation of degradation products and providing an advantage over steam explosion.[143] One study has suggested supercritical CO_2 explosion to be more cost-effective than AFEX.[237] However, sugar yields have been found to be worse than both AFEX and steam explosion.[238]

Dilute Acid (DA) pretreatment is a fairly straightforward and very common chemical pretreatment process, and is similar to the first stage of steam explosion. Biomass samples are added to hot dilute acid (0.6-3.0 wt%), resulting in hemicellulose removal and lignin redistribution through melting and de/repolymerisation (low solubility of lignin in the aqueous solution leading to droplets depositing on the biomass surface[239–241]).[242] Temperatures are around 120-220 ^oC, at pressures of 3-15 bar, with pretreatment times of up to around 90 minutes.[233,236] Similarly to SE, formation of degradation products and loss of soluble sugars through washing is a considerable drawback, as is the required downstream neutralisation of the acid.[232,233] DA pretreatment is successful with grasses and agricultural residues due to the increased surface area and porosity and thus cellulose accessibility, but has limited success with hardwoods and softwoods due to the limited lignin removal.[242]

Alkaline pretreatment of biomass, for example using lime, ammonia, or sodium hydroxide, can also be effective. This method mainly operates through lignin solubilisation, typically at lower temperatures and pressures, and with longer residence times than acid pretreatment (85-150 ^oC for 3-13 hours, or even ambient conditions for up to several days), causing lower sugar degradation.[143,152] Cleavage of lignin ether bonds leads to its depolymerisation and dissolution into the alkali solution.[192,233] Swelling of the biomass also leads to enhanced surface area and decreased cellulose crystallinity.[220,233] However, alkali pretreatment appears to be more suitable for low lignin content

feedstocks such as agricultural residues (e.g. dilute NaOH pretreatment was found not to have any effect on softwoods with a lignin content above 26%).[143]

Biological pretreatment methods are attractive due to their environmental friendliness and low energy requirements.[5] They tend to be focussed around the use of brown-, white-, and soft-rot fungi, with particular focus on white-rot which are able to produce lignin-degrading enzymes.[135] The main disadvantage of these methods is their low rate: pretreatment takes weeks rather than minutes or hours.[143] However, other issues exist such as the consumption of sugars by the biological organisms themselves and the degradation (and therefore loss) of potentially valuable/useful lignin.

The organosolv process is a chemical method that involves fractionating the lignocellulose matrix by pretreating biomass with organic solvents (such as ethanol, acetone, or ethylene glycol, with up to 70 wt% water) at high temperatures and pressures (100-200 ^{o}C, 30-150 minutes).[243,244] This is typically done in the presence of a small amount (up to around 2%) of an acid or base catalyst.[143,243] Lignin is dissolved into the organic solvent, while hemicelluloses are either hydrolysed (in the case of an acidic catalyst) or preserved (in the case of a base catalyst).[232,245] This leaves a polysaccharide-rich solid fraction that is easily hydrolysed, while a separate lignin stream can be recovered from the organic solvent. One of the distinguishing features of the organosolv process is the high quality of the obtained lignin, which has a low sulfur and carbohydrate content, narrow range of low molecular weights, and potentially low degree of condensation.[246,247] However, despite promising results with a range of feedstocks, drawbacks involve the costs and safety risks associated with the required high-pressure equipment, as well as the costs of the organic solvents.[232,244]

1.3 Ionic Liquid Pretreatment

1.3.1 Types of IL pretreatment

IL pretreatment involves heating biomass in IL to fractionate/disrupt the lignocellulosic matrix. IL pretreatment can be divided into two distinct approaches: the Dissolution process and the ionoSolv process.[73]

The Dissolution process involves dissolution of the entire lignocellulosic matrix within the IL, by heating at 90-160 ^{o}C for 3-16 hours.[73] This is followed by addition of an antisolvent (e.g. water, or water/acetone in order to retain more lignin in solution), precipitating a more easily hydrolysable, often carbohydrate-enriched solid.[248,249] This solid is then thoroughly washed in order to remove any residues of IL or antisolvent which may inhibit hydrolysis or fermentation.[73] Further antisolvent

addition to the liquor allows any dissolved lignin and hemicellulose to be precipitated and then removed.[73] Hydrolysis yields are improved primarily *via* decreased crystallinity of the regenerated cellulose caused by the breaking of the cellulose's hydrogen bond network during dissolution, as well as by lignin removal and by the disruption of the lignocellulosic matrix structure.[73,250] Most of the hemicellulose is also regenerated with the pulp, thus allowing enhanced recovery of its constituent sugars.[73]

The ionoSolv process involves dissolution of only the lignin (and possibly hemicellulose) in the IL, thus leaving a cellulose-rich pulp which is removed and thoroughly washed. Lignin is then precipitated from the IL by adding water, leaving a liquor containing hemicellulose remnants dissolved in IL. Removal of lignin from the cellulose pulp improves saccharification yields, while crystallinity of the cellulose has been shown to be largely unaffected, or even to increase significantly, and most of the hemicellulose is often degraded and dissolved into the IL.[73,88]

The main difference between both processes is thus the dissolution of the highly crystalline cellulose fraction, which requires disruption of its extensive hydrogen bonding network. As a result, cellulose dissolution requires a solvent with a high hydrogen-bond basicity (β), as measured using the empirical Kamlet-Taft solvent parameters.[73] It has been estimated that a β value above 0.8 is required in order to dissolve the cellulose fraction,[251,252] whereas a β value above 0.4 is needed for lignin dissolution.[253] More recently, however, this concept has been extended to involve the net hydrogen bond basicity of the solvent, the difference between hydrogen bond acidity and basicity, which was found to be required to be over 0.35 in order to dissolve cellulose.[252] The choice of IL, therefore, primarily affects which process takes place. The pretreatment solvent properties of the IL tend to be dominated by the anion,[69,254,255] leading to a relatively low number of different anions being used for each process. However, Janesko modelled the interactions between [emim]Cl, cellulose, and lignin, and found lignin to interact equally strongly with the imidazolium cation as the chloride anion due to the pi-stacking interactions of the imidazolium aromatic ring (although cellulose dissolution was found to be more dependent on the anion). This may not only explain the success and propensity of imidazolium-based ILs in biomass pretreatment, but also demonstrates that cation selection can also be of importance for successful pretreatment.[256]

The choice of IL, however, is not always sufficient to determine which process has taken place. Water has a low β of 0.14,[257] and thus dilution of the IL leads to a decreasing hydrogen bond basicity.[141] The Dissolution process, therefore, requires close to anhydrous conditions in order to optimally dissolve the entire biomass structure.[73] As a result, certain ILs such as [Hmim]Cl have been reported as being Dissolution or ionoSolv ILs depending on their degree of dilution.[122,248] Additional factors, such as the

temperature and biomass loadings used in pretreatment can also affect the process selected due to solubility limits. The hydrophilicity of an IL has also been found to increase with β[12], suggesting that development of an IL able to dissolve cellulose at reasonable water concentrations may not be possible.[73]

ILs containing dialkylimidazolium cations and chloride and acetate anions have been shown to have high β values (i.e. over 1).[141,254]As a result, the most common Dissolution pretreatment ILs are aprotic ILs with these two ion classes, such as [emim][OAc] and [bmim]Cl which have been studied at length. Although protic ILs (PILs) tend not to be have sufficient hydrogen bond basicity to dissolve cellulose even when dry,[73] there are a number of exceptions. Among these are a small number of carboxylate and chloride PILs, such as $[NH_3(CH_2)_2OH][HCOO]$ and [Heim]Cl.[258]

The most common ILs for ionoSolv pretreatments may be broadly divided into two categories: acidic and basic, and tend to be PILs due to their easy synthesis, lower cost, and lower hydrogen bond basicity allowing cellulose to remain undissolved. Acidic ILs dissolve and hydrolyse both the lignin and the hemicellulose, leading to a cellulose-rich pulp. High-purity cellulose can be achieved, opening pathways for cellulosic materials applications, but valorisation of hemicellulose and its constituent sugars is not possible due to their rapid hydrolysis and degradation in solution. The most common acidic ILs tend to involve the $[HSO_4]^-$ anion, although others have been used such as Cl^- and $[MeSO_4]^-$.[12] Due to the low basicity of the anion,[259] these ILs are not able to solubilise the cellulose even with dialkylimidazolium-based cations (such as [bmim][HSO_4] and [emim][HSO_4])[12,253] and under anhydrous conditions.[253] There have been a large number of studies focussing on the use of $[HSO_4]^-$ ILs, which have gradually moved away from alkylimidazolium-based cations (e.g. $[Hbim]^+$)[78] to cheaper alkylammonium cations (e.g. $[TEA]^+$ and dimethylbutylammonium $[DMBA]^+$).[260–262] Regarding acidic PILs using a chloride anion, 1-methylimidazolium chloride ([Hmim]Cl) has been used most commonly. Although it has been shown to dissolve cellulose and lignocellulose when dry (as has [Heim]Cl),[248,249,258,263] it has been used in the ionoSolv process when diluted with 20 wt% water, in particular due to its ability to extract metals from metal-contaminated biomass (explored later).[45,264]

More recently, there has also been a number of studies focussing on the use of basic PILs for ionoSolv pretreatment. Basic PILs still dissolve and depolymerise lignin due to their alkaline conditions, while broadly preserving the hemicellulose fraction in the pulp. These PILs have tended to focus on carboxylate anions combined with alkylammonium,[193,223,259,265,266] pyridinium,[267] or pyrrolidinium[193,267] cations. Although these anions tend to be cellulose-dissolving, the protic nature of the IL reduces its basicity sufficiently that they have been found not to dissolve cellulose or lignocellulose when dry. Additionally, a number of studies have added water to the pretreatment mixture in order to reduce

viscosity, thus reducing the β of the solvent.[223,266] Protic alkylimidazolium acetate and formate ILs (e.g. [Hmim][OAc] and [Heim][HCOO]) have not been substantially studied in terms of their pretreatment efficacy but generally been reported as not dissolving lignocellulose or cellulose when dry,[249,267] although one study has reported [Hmim][OAc] as being able to dissolve up to 4 wt% of cellulose and lignocellulose at 115 °C.[268].

There have also been several studies on bio-compatible, basic PILs containing a cholinium cation ($[Cho]^+$). A wide range of anions have been screened, typically with amino acid anions (so-called [Cho][AA] ILs, e.g. using lysinate, taurinate, serinate, and glycinate anions)[258,269–273] or others such as acetate or arginate.[258,271] There is, however, some degree of uncertainty in the literature on the process these ILs employ. [Cho][OAc], [Cho][Lys], and [Cho][Ser] have been reported as able to dissolve up to 4 wt% of cellulose, pine, and eucalyptus after 24 hours at 150 °C.[258] In addition, a study on [Cho][OAc] and [Cho][Lys] pretreatment reports on the use of an antisolvent to precipitate regenerated, highly digestible solid, consistent with a Dissolution approach, although with a particularly high degree of lignin removal.[274] This is attributed to a high (>1) β value, calculated computationally. However, a series of studies on [Cho][AA] ILs present them clearly as ionoSolv ILs, explicitly stating the lack of required cellulose anti-solvent and the selective removal of lignin as the pretreatment mechanism.[272,273] In addition, other studies on this class of ILs have mentioned dilution following pretreatment, but no precipitation of a regenerated solid fraction, and with a similar lignin-specific removal mechanism.[270,271]

Analysis of the literature has revealed that the vast majority of studies do not explicitly state which approach is taken. As previously stated, naming of the IL is not always sufficient, as other parameters such as water content, temperature and biomass loading can affect the pretreatment process. In many studies, the pretreatment process is ambiguous from the methodology, which simply says which solvent/anti-solvent is added following pretreatment, which occurs in both processes. In the case of the ionoSolv process, the aim is to wash any residual IL and dissolved lignin from the pulp, as well as to aid removal from the reaction vessel as the pretreatment slurry is viscous. In the Dissolution process, the anti-solvent is used to precipitate the solid fraction. The Dissolution process is typically said to lead to significant reductions in cellulose crystallinity in the biomass, while the ionoSolv process often leads to an increase in cellulose crystallinity due to removal of amorphous lignin and hemicellulose, as well as amorphous cellulose regions.[275] However, a change in crystallinity index of the biomass is not always sufficient evidence to determine which process has taken place in studies. Certain cellulose-dissolving ILs have been found not to significantly change the crystallinity index of regenerated cellulose.[276] Additionally, the regenerated solid using certain Dissolution process ILs and conditions contains a significantly lower hemicellulose and lignin content, which could offset

reductions in cellulose crystallinity. Therefore, it is imperative that the process be stated explicitly, particularly in the case of ILs that may behave as either Dissolution or ionoSolv ILs, or in the case of new pretreatment ILs.

Results from these two processes have both been promising across a wide range of feedstocks. However, there are several factors which render the ionoSolv process favourable:

1. The ionoSolv process has been found to tolerate, and even require, water within the IL, [12,78,277] whereas the Dissolution process is designed to operate under anhydrous conditions in order to preserve the solubility of cellulose. Since biomass samples often have a moisture content around 50%, and 5-10% when air-dried, anhydrous requirements add complexity to the pretreatment process as well as significant extra cost and energy expenditure in removing water from the system.[73,278]
2. Very cheap $[HSO_4]^-$ ILs (as low as \$0.78/kg) have been found to perform well in the ionoSolv process, whereas the Dissolution process currently uses relatively expensive ILs.[17] As shown by Marcuschamer et al, a high IL price (in their scenario \$50/kg) renders an industrial IL pretreatment process economically infeasible, and is the largest sole contributor to cost.[279] A cheaper IL (in their analysis \$2.5/kg) allows a competitive ethanol price to be reached, with some flexibility in solids loading and IL recycle and recovery rate.
3. The cheap ILs used in the ionoSolv process have a number of favourable properties relative to those used in the Dissolution process. They are PILs, allowing distillation to be used to easily purify the IL, whereas the APILs used in the Dissolution process would degrade before boiling. Moreover, common ionoSolv ILs have been shown to have high thermal stabilities at biomass pretreatment conditions,[87,88,223,258] whereas common dissolution ILs have been shown to have relatively low thermal stability at these conditions.[76] This would thus require a higher IL make-up stream, which would be especially damaging to process economics due to the higher IL costs. As IL stability has been shown to decrease with increasing β,[73] this stability issue may not be easily avoided by IL modification.
4. The ionoSolv process involves one less processing step (i.e. precipitating the cellulose).

1.3.2 ionoSolv pretreatment

Pretreatment Mechanisms

As previously described, the ionoSolv process involves the fractionation of the lignocellulosic matrix, by dissolution of the lignin fraction and generally of the hemicellulose fraction. This leaves a highly

digestible pulp, while a separate lignin stream is recovered by addition of water to the liquor. A number of studies have been carried out to elucidate the mechanisms occurring during this process.

The majority of ionoSolv pretreatments use acidic ILs with a Cl^- or $[HSO_4]^-$ anion. As a result, extensive hemicellulose removal is observed, often approaching near-quantitative removal at optimal conditions for enzymatic saccharification and pulp purity.[260,280] The glycosidic bonds within the amorphous hemicellulose polymer are hydrolysed in the acidic medium, and hemicellulose oligomers are then dissolved into the IL.[147] Once within the IL liquor, the fate of the dissolved hemicellulose may be tracked by HPLC analysis. The hemicellulose oligomers have been found to undergo further depolymerisation, eventually to monomeric sugars, which may dehydrate to form small quantities of breakdown products such as furfural or HMF.[147] There is also a relatively high amount of acetic acid present in the liquor (compared to sugar breakdown products), due to the removal of acetyl groups within the hemicellulose.[147,281] In the case of basic ILs, very little hemicellulose removal is found to occur at acid/base ratios of 1 or below, as hemicellulose has been found to be more stable in alkaline solutions.[266]

Lignin removal is the hallmark of the ionoSolv process, common to both the acidic and basic variants of the process. Similarly to hemicellulose, lignin removal proceeds by depolymerisation followed by dissolution into the IL. Depolymerisation of the lignin in acidic ILs has been found to proceed *via* hydrolysis of the labile β-*O*-4' linkage, as confirmed by 2D HSQC NMR.[14,122,260,262,280] The resulting lower molecular weight fragments dissolve more easily into the IL. While decreases in signal intensities are observed for C-C linkages such as β-β' and β-5', these are thought to be more likely modified than broken.[147] The mechanism for lignin removal in basic ILs has not been studied as extensively, but would appear to also be due to cleavage of the β-*O*-4' linkage, susceptible to hydrolysis in alkaline as well as acidic conditions.[266]

Unlike hemicellulose, however, dissolved lignin is not just broken down into successively smaller fragments in the IL. Firstly, lignin fragments can undergo reactions between S and G aromatic sub-units, forming larger fragments in so-called "condensation reactions".[14,122,260,282,283] These fragments can then re-deposit onto the biomass surface, as seen by decreasing delignification rates at longer pretreatment durations.[147,260] Condensed lignin can be identified by 2D HSQC NMR. An additional problem is the condensation reactions of dissolved lignin fragments with dissolved carbohydrates and sugar breakdown products. These substances can react together to form high molecular weight humin-like organic structures that have been termed pseudolignin (common to acidic pretreatments such as Dilute Acid[284]) that can also redeposit onto the pulp.[14,78,260] These reactions are found to occur more readily at increasing pretreatment severity (i.e. time, duration, and increasing acid/base

ratio).[78,280,283] When redeposited onto the biomass surface, pseudolignin has been found to be more very inhibiting to enzymatic saccharification, more so than native lignin.[285] Differentiating between lignin and pseudolignin is very challenging due to the poorly defined structure of both materials. However, pseudolignin formation can be easily determined by precipitated lignin yields being larger than lignin removal rates (although a lack of this indicator cannot rule out the possibility of pseudo-lignin formation). The lack of hemicellulose removal in basic ionoSolv ILs would appear to limit the degree of pseudolignin formation.[266] Washing of the cellulose pulp with DMSO in order to dissolve the reprecipitated lignin was carried out by Chambon.[87] Saccharification yields in *Miscanthus* were found to increase by a factor of 1.1 to 1.5, with DMSO darkening and pulp lightening in colour (taken to be a sign of lignin dissolution). However, it was judged that the drawbacks of such an extra step in an industrial context would likely outweigh the benefits.

Based on GPC and 2D HSQC NMR measurements, a four-stage mechanism has been proposed by Gschwend et al. for the removal of lignin in acidic ILs[260]:

1. Cleavage of ether bonds and dissolution of uncondensed lignin fragments. Precipitated lignin yields are low due to limited extraction, with lignin fragments relatively large (still containing large numbers of cleavable ether bonds) and of relatively uniform molecular weight.
2. Continued extraction of lignin fragments, along with further hydrolysis of the lignin fragments that are already dissolved, leading to a disperse range of molecular weights. Precipitated lignin yields are fairly low due to small fragments not precipitating from the IL upon water addition.
3. Limited further lignin extraction, and lignin fragments in solution have now been hydrolysed to small fragments, with a narrow range of molecular weights. These fragments are beginning to condense rapidly, leading to a rapid increase in precipitated lignin yield.
4. Cessation of lignin hydrolysis and extraction, with dissolved lignin fragments undergoing condensation reaction and possible pseudolignin formation, with re-precipitation onto the pulp occurring. Some small unreactive fragments are also prevalent, leading to a large range of molecular weights.

As covered in Section 1.2.2, cellulose's extensive hydrogen bonding and resulting highly crystalline structure makes it much more resistant to hydrolysis than hemicellulose. During acidic ionoSolv pretreatment, glucan recovery (taken to be representative of cellulose recovery) has been shown to decrease slowly (much more slowly than hemicellulose removal), only substantially reducing at extended durations at high temperatures or with excess acid present.[14,260,283] A small amount of glucan is sometimes rapidly lost during IL pretreatment (5-10%), which is attributed to small regions of amorphous cellulose and/or glucan within the hemicellulose structure.[280,283] Until recently, the

cellulose from the ionoSolv process was generally only characterised by saccharification yield (and to a certain extent by its purity). George et al. observed crystallinity to increase during ionoSolv pretreatment, thought to be due to the removal of hemicellulose and lignin.[88] There has been only one full characterisation study carried out recently by Tu et al. on pulps obtained by pretreating *Miscanthus* with [TEA][HSO_4].[286] The obtained cellulose was found to still contain the native cellulose-I structure and maintain a high degree of crystallinity, but the average degree of polymerisation was substantially reduced due to depolymerisation of longer chains. It was thus concluded that increased cellulose accessibility was the main factor responsible for enzymatic hydrolysis improvements, and that the recovered cellulose was suitable for materials applications.

Factors Affecting IL Pretreatment

The effect of time and temperature has been shown to be a critical factor in the ionoSolv process. This is best exemplified by the studies of Gschwend et al, who varied the pretreatment temperature between 120 ^oC and 180 ^oC when pretreating *Miscanthus* with [TEA][HSO_4].[14,15] Several competing effects become apparent. Firstly, increasing pretreatment temperature, as expected, increases pretreatment kinetics: hemicellulose removal and glucan degradation proceed much more rapidly, while delignification (initially) increases more rapidly. However, previously mentioned lignin and pseudolignin condensation reactions (and subsequent re-deposition onto the pulp) also rapidly accelerate at higher temperatures. This leads to a peak for delignification and saccharification yield (that typically coincide). As temperature increases, this peak gets increasingly sharp and occurs increasingly rapidly: peak saccharification in *Miscanthus* occurs after 15 minutes at 180 ^oC using [TEA][HSO_4], compared to 8 hours at 120 ^oC. It is also worth noting that basic PILs do not appear to suffer as acutely from such condensation reactions. However, pretreatments using these ILs also have slower kinetics as a result of their basicity, with optimal pretreatment of sugarcane bagasse (an agricultural residue) using monoethanolammonium acetate ([MEA][OAc]) taking 2 hours at 150 ^oC, compared to 45 minutes for *Miscanthus* using [TEA][HSO_4].[15,266] Furthermore, such ILs are typically less thermally stable and so their kinetics cannot be feasibly increased by operating at higher temperatures.[223]

The effect of the water content of the IL solution on pretreatment effectiveness has also been investigated for the ionoSolv process. Verdíá et al. compared [Hbim][HSO_4] with 0 (dry) and 20 wt% water content when pretreating *Miscanthus* at a single condition, finding saccharification yields to consistently be substantially lower in dry IL.[78] This was accompanied by higher pulp yields and lignin contents, as well as significant pseudolignin formation. Similar findings have also been reported by

Gschwend and Brandt, comparing the pretreatment performance of [emim][HSO_4] and [bmim][HSO_4] on poplar and *Miscanthus* (respectively) at varying water contents.[287,288] Both studies found saccharification yield to exhibit a general plateau around 10-40 wt% of water. The requirement for water is a positive finding, as increased water content has the dual benefit of decreasing the viscosity of the IL (facilitating handling and reducing pumping energy), while also reducing the energy demand for IL dehydration after anti-solvent addition.[87] However, Rafat investigated the effect of water content on different feedstocks pretreated using [DMBA][HSO_4].[277] Although *Miscanthus* exhibited the aforementioned plateau in performance between around 10-40 wt%, softwoods showed maximum efficacy at 10 wt%, with performance decreasing substantially at higher contents due to decreasing delignification. Water content was also found to vary the Hammett acidity (further explored in Chapter 2) of the IL solution in an interesting manner. Highest Hammett acidity values (meaning least acidic, as with pH) were found at 20-30 wt% with Hammett acidity values decreasing below 20 wt% and from 30-50 wt%.

Rafat then demonstrated synergy between time, temperature, and water content during pretreatment of softwood, using a Box-Behnken experimental design.[277] It was shown that these three factors all affect pretreatment severity, and can to a certain extent be traded off against each other to maintain high efficacy. These three parameters were also incorporated into a single severity factor (as used in other pretreatment technologies), which was however found to be a relatively poor predictor of IL pretreatment performance.

The effect of acid/base ratio of ILs on pretreatment efficacy has also been explored in several studies using protic $[HSO_4]^-$ ILs. [14,78,262] Best delignification and saccharification results tended to be obtained with approximately stoichiometric acid/base ratios. Variations in acid/base ratio were found to strongly affect pretreatment performance. Increasing acid content increases severity in a manner analogous to increasing temperature: a small increase (1-2%) leads to improved lignin and hemicellulose removal kinetics, a medium excess (9%) begins to inhibit saccharification due to lignin and pseudolignin condensation and redeposition, while a large excess (50%) essentially suppresses all saccharification. Excess base has been found to reduce delignification and hemicellulose removal kinetics. Despite this, however, pulps pretreated with excess base display similar saccharification yields to stoichiometric IL solutions, even when using up to 20% excess base, and do not display as sharp an operating point as stoichiometric or excess acid pretreatments. This is assumed to be due to a decrease in lignin redeposition and pseudolignin formation. Changing the amount of acid or base can therefore be used to improve pretreatment behaviour, either by improving kinetics or by improving the range of suitable operating times without over-treating the biomass. In practice, however, shorter incubation times are likely to be preferred in an industrial context.

The acid/base ratio has also been varied in a basic ionoSolv pretreatment by Nakasu et al, using [MEA][OAc] to pretreat sugarcane bagasse at a single timepoint.[266] In this case, increasing base was found to increase saccharification yields, even down to pure base. This was attributed to the high solubility of hydrolysed lignin in the basic monoethanolamine and the lack of acidity leading to no pseudolignin formation. Due to the monoprotic nature of this IL, direct comparisons with $[HSO_4]^-$ IL results are not possible: in the latter excess base (up to 100%) is still protonated by the proton on the $[HSO_4]^-$ anion, while in the former any excess base is present as free base in solution.

The effectiveness of the ionoSolv pretreatment has been confirmed for a range of feedstocks, covering all major groups (grasses, agricultural residue, hardwoods, and softwoods). All have shown high delignification and improvements in saccharification yields with a range of acidic ILs, typically acidic alkylammonium $[HSO_4]^-$, alkylimidazolium $[HSO_4]^-$ and alkylimidazolium chloride.[78,260,262,280,289] Even the particularly recalcitrant softwoods have been successfully pretreated, with Gschwend et al. reporting quantitative sugar release from pine.[261] However, differences between feedstocks type are still reflected in the pretreatment conditions required for successful pretreatment: softwoods require much more severe pretreatment conditions than grasses, with hardwoods generally requiring intermediate severity. As an example, using [DMBA][HSO_4] at 170 °C, *Miscanthus* pretreatment has been found to be optimal after 30 minutes using [DMBA][HSO_4], whereas pine requires durations of 45 minutes using [Hbim][HSO_4].[260,280]

IL recycling has been shown to be important to process economics, and has been investigated in several studies.[73,122,279] [TEA][HSO_4] and [Hmim]Cl have shown near-quantitative recovery of the IL following pretreatment, although this has not taken the mass of dissolved solutes into account. So far, studies on IL recycling in ionoSolv pretreatment have shown fairly consistent performance in terms of saccharification yield, delignification, and characteristics of recovered lignin across up to 6 cycles. Following cycle 1 or 2, lignin yields remain elevated, showing that a steady-state is reached and residual dissolved lignin does not continue accumulating in the IL. However, both Tu and Brandt et al. reported a decrease in acid/base ratio between cycles, although this was not accurately quantified.[14,290] This is further explored in Chapter 4.

Solids loading (i.e. the ratio of biomass to IL used) is another important consideration in IL pretreatment. An increase in loading can lower equipment and processing costs, but may lead to a decrease in pretreatment performance. Most ionoSolv studies typically use a biomass loading of 10-20% wt/wt. However, a number of studies have investigated the effect of an increased solids loading, which would allow for reduced IL consumption and/or smaller reactor volumes, and thus improve process economics.[280,291,292] In general, performance decreases with solids loading, with suggested

reasons being either insufficient wetting of the biomass by the IL, or increased lignin reprecipitation onto the pulp. This represents another process parameter in which a compromise may be required.

Chambon et al. carried out a study focussing on scale-up considerations.[291] Size distribution of the raw biomass particles was found to affect pretreatment performance. *Miscanthus* and pine particles were ground to three different size distributions, termed "coarse" (10-12 mm), "medium" (1-3 mm), and "fine" (0.18-0.85 mm, typical of bench-scale studies) before being pretreated with [TEA][HSO_4] at 120 ^oC for 6 hours. A medium particle size was determined to be most suitable for both feedstocks, with similar or improved saccharification and delignification compared to fine particles, thus reducing grinding energy requirements. Fine particles were found to lead to higher hemicellulose removal but lowered delignification due to enhanced lignin redeposition as a result of the increased surface area. In addition, the ionoSolv process was found to reduce particle size of the biomass, to a much higher extent than dilute acid pretreatment, presumed to be due to the lack of lignin removal in the latter. In addition, scaling up pretreatment 100-fold to a 1 L reactor improved pretreatment performance relative to bench-scale, due to an improvement in heat and mass transfer from stirring reducing lignin condensation and redeposition.

Applications of ionoSolv

As can be seen, there has been a fairly exhaustive study of the mechanisms behind the ionoSolv process and of the factors affecting its efficacy. In recent years, research has begun moving expanding more on its real-life applications, with work in this direction so far being driven by Dr Aida Rafat.

Pretreatment of metal-contaminated biomass has been investigated as a way to dispose of waste materials and improve process economics (negative value feedstock) and is the subject of a patent.[293] During pre-treatment of copper-treated construction wood (Cu contents almost 3000 ppm, with similarly high levels of Cr and As), Gschwend et al. found that the PIL [Hmim]Cl was able to extract metals from within the biomass while maintaining reasonable saccharification yields, with a significant proportion of metals being left in the IL liquor following pretreatment.[122] Over 90% of Cu was extracted, as well as 75-80% of As, and around 60% of Cr, with consistent performance using recycled IL over 6 pretreatment cycles. Furthermore, preliminary attempts to deposit these metals out of a 50 µL drop of the recycled IL were promising: after 10 minutes of applying a -0.7 V potential, 8-15% of the metals were removed from the solution. The pretreated and thus decontaminated pulps displayed relatively high digestibility, and were subsequently readily fermented to ethanol.

This work was built upon by Rafat et al, who studied the pretreatment of postconsumer waste wood.[16] This highly heterogeneous sample was found to contain elevated levels of 10 metals, particularly Fe, Pb, Zn, Cr, Cu, and Ti, with metals particularly concentrated in the paint fraction of the feedstock. [Hmim]Cl consistently displayed elevated (usually highest) metal extraction, due to the ability of the cation and anion to chelate with the heavy metals. Other ILs (mainly containing the $[HSO_4]^-$ anion) were found to have more variable performance, occasionally matching that of [Hmim]Cl and occasionally being far inferior. [Hmim][HSO_4], however, was found to have superior extraction performance to alkylammonium $[HSO_4]^-$ ILs. Only V and Ti were found to have low extractability from the biomass, with a maximum of around 50-60% by [Hmim]Cl. Increasing the solids loading from 10-50% wt/wt using [Hmim]Cl was found to decrease metal extraction by around 5-20%, although relatively high performance was still achieved across all metals, with 74-95% extraction even at the highest loading. Increasing the mass loading did, however, lead to a substantial increase in the metal content of the lignin stream. This was found to be problematic for lignin utilisation, and electrodeposition before lignin precipitation was suggested as a possible solution. Lastly, electrodeposition of Pb from the IL solution was demonstrated at low overpotentials.

Rafat and Hallett also investigated the use of the ionoSolv process for the decontamination of toxic creosote-treated timber.[294] High pretreatment severity (170 ^oC for 45 minutes) was required to delignify this feedstock and produce a highly digestible pulp (20 times more so than the untreated biomass). The creosote-treated timber was found to contain a number of polyaromatic hydrocarbon (PAH) compounds such as naphthalene, anthracene, and dibenzofuran. Complete removal of PAH compounds from the pulp was achieved, with these compounds either remaining in the liquor or mainly co-precipitating with the lignin (due to their hydrophobicity). It was proposed that the contaminated lignin stream could then be used as a fuel in a compliant waste boiler.

Rafat also investigated valorisation of pretreated *Miscanthus* pulp through one-step alkaline H_2O_2 oxidation without bleaching of the pulp.[277] The one-hour alkaline oxidation further enhanced pulp purity beyond that of commercially available dissolving pulp by removal of residual lignin and hemicellulose, but was more effective at removing pseudolignin than native lignin. In addition, the alkaline medium was found to lead to significant depolymerisation of the cellulose. In the process, the suspension obtained during the oxidation was found to contain cellulose nanocrystals (CNCs), a high-value and useful material, which were recovered by dialysis and freeze-drying. This is a simple process for CNC production compared to the usual multi-step processes that require pulp bleaching and produce a large amount of waste, require very long reaction times, or require large reactor volumes due to very low solids loadings.[295–297]

1.4 Constructed Wetland Remediation: AMD, BOD, and Nutrients

1.4.1 General

Constructed Wetlands (CWs) are a form of passive water remediation technology that aim to replicate the water filtration abilities of natural wetlands (known as "the Earth's kidneys"). While exact definitions of wetlands vary, they may generally be described as areas where the soil is usually saturated with water or submerged. Wetland design has been extensively studied, and varying designs exist based on flow patterns, types of plants, and types of substrate.[25] These can thus be tailored to maximise treatment efficacy and efficiency for different wastewater input types, and several cells of different designs may be cascaded together. The effects of wetland design and hydrology are covered in more depth in Chapter 3. However, a general classification of wetland types would be as follows (see Fig. 1.9):

- Free Water Surface (FWS) wetlands contain areas of open water, and resemble natural wetlands most closely. These types of CW are the simplest and most common, and are better able to deal with variable flow rates.
- Sub-Surface Flow wetlands, either Horizontal Sub-Surface Flow (HSSF) or Vertical Flow (VF) usually use a gravel bed with vegetation planted underneath, with water flow kept below the surface of the bed. These types of CW are typically more expensive but better able to remove high levels of contamination.

The complex interactions within wetlands derive from their confluence between terrestrial and aquatic ecosystems, and this allows them to play an important role in water remediation. Contaminant removal takes place *via* a range of mechanisms, including physical processes (e.g. sedimentation), sorption processes (e.g. adsorption to soil or complexing with organic substances), phytoremediation (e.g. rhizofiltration, phytoextraction, or phytodegradation), redox processes (e.g. nitrification and denitrification), and bacterial metabolism.[25,298–301] The most important factors will be analysed in more depth in the following sections. These processes may be significantly affected by a number of site-specific factors including water depth, temperature, pH, redox potential, and hydrology.[25] As a result, prediction of wetland performance is challenging, and wetland design is based on empirical design rules (further explored in Chapter 3).

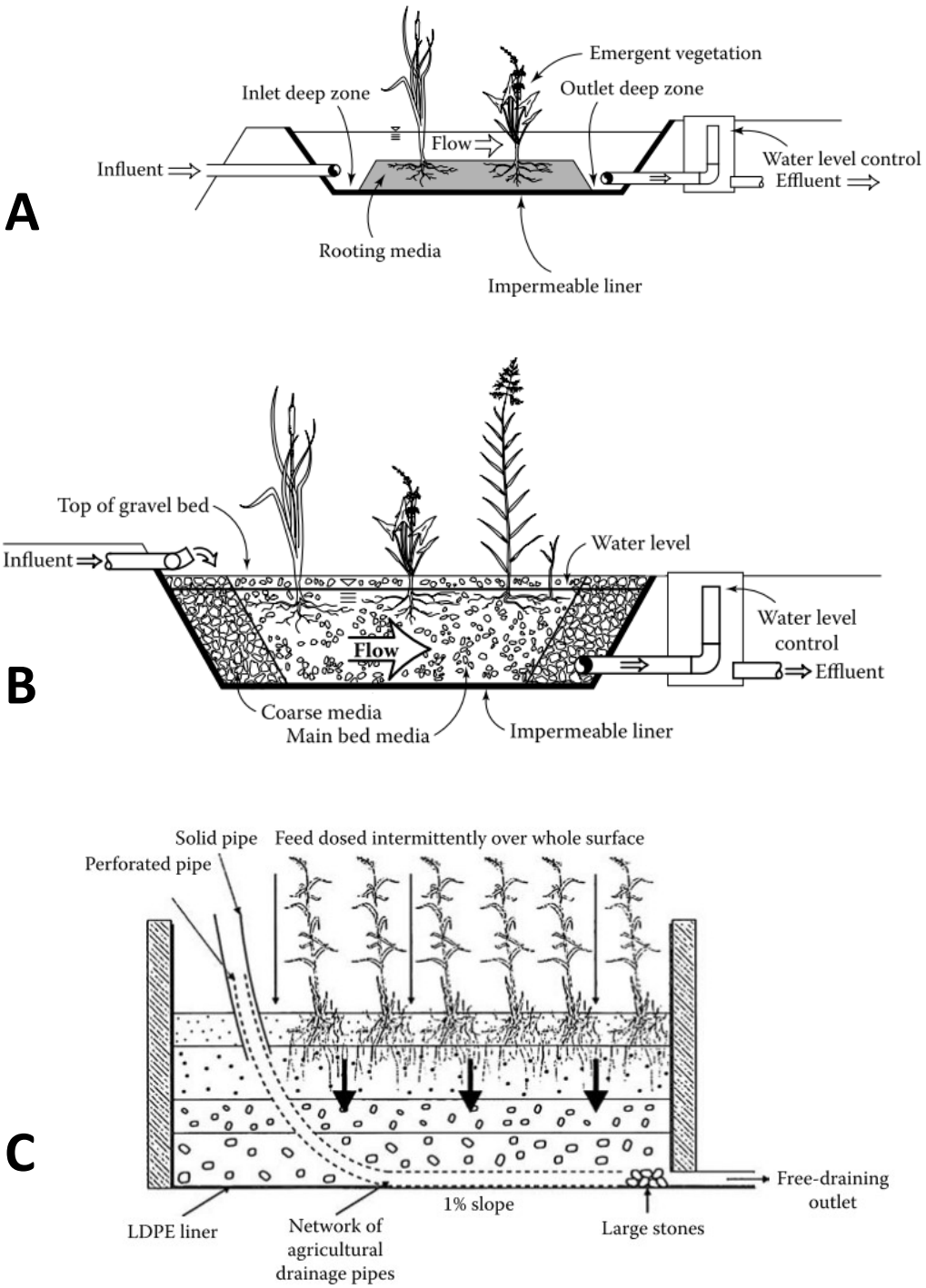


Figure 1.9: Different types of wetland cell design.[25] Plots are A: Free Water Surface, B: Horizontal Sub-Surface Flow, C: Vertical Flow.

Since their initial development in the 1950s, CWs have evolved into a viable and (surprisingly) widely used water remediation technology.[302] Three major attractions are consistently stated for CWs:

1. Extremely low energy requirements (only for pumping), which have been reported as below 0.1 kWh/m^3 of treated water,[303] far lower than even conventionally low-energy technologies such as trickling filters (0.61 kWh/m^3).[25]
2. Lower costs compared to other traditional remediation technologies. This blanket statement, however, has not been proven beyond anecdotal evidence or a small number of individual case studies, and is further explored in Chapter 3.
3. The ability to remediate multiple contaminants in parallel, compared to traditional remediation technologies that require separate stages for different contaminants.[304–307]

CWs have been shown to be effective at removing a wide range of contaminants, including Biochemical Oxygen Demand (BOD), nutrients, pharmaceuticals, metals, pathogens, and pesticides.[25,298,308–310] As a result, they have been shown to effectively treat a wide range of different wastewaters, such as domestic, animal (e.g. dairies, piggeries), industrial, and urban stormwater.[25] This study has focussed on the use of wetlands for treatment of two distinct types of wastewater: BOD- and nutrient-contaminated wastewaters, and Acid Mine Drainage (AMD). Particular focus has been paid to the latter, which has to date mainly been the subject of academic research despite being a problem of major scale and significance. In addition to wastewater remediation, CWs have been shown to offer a number of advantages such as promoting ecological and social benefits, and a lower carbon footprint than traditional treatment.[311–313]

1.4.2 Acid Mine Drainage

Acid Mine Drainage (AMD) is water emanating from operational or non-operational mining sites, often with low pH and containing high concentrations of dissolved metals.

Causes

The source of AMD's acidity is the dissolution and oxidation of ferrous sulfide minerals.[314] This process occurs commonly with pyrite, FeS_2, and can be represented by a simplified reaction pathway. Iron(III), termed ferric iron, is able to oxidise pyrite rapidly, with this reaction being about an order of magnitude faster than the oxidation of pyrite by oxygen.[315] Ferric iron is not typically present in the system, and is generated by the oxidation of iron(II) (termed ferrous iron) by oxygen[316], with this reaction being identified as the rate-determining step in the formation of AMD from pyrite. [317] These reactions are displayed in Eqs. 1.1 and 1.2, with Eq. 1.3 representing the overall reaction.

$$FeS_2 + 14\ Fe^{3+} + 8\ H_2O \rightarrow 15\ Fe^{2+} + 2\ SO_4^{2-} + 2\ H^+ \quad (1.1)$$

$$Fe^{2+} + 0.25\ O_2 + H^+ \rightarrow Fe^{3+} + 0.5\ H_2O \quad (1.2)$$

$$FeS_2 + 3.5\ O_2 + H_2O \rightarrow Fe^{2+} + 2\ SO_4^{2-} + 2H^+ \quad (1.3)$$

Another important reaction which may take place is the precipitation of iron(III) hydroxide (termed "yellow boy" due to the yellow precipitation on river beds), see Eq. 1.4. However, this precipitation only occurs at pH above 3.5, and thus serves as a buffer to keep the pH low[318].

$$Fe^{3+} + 3\ H_2O \rightarrow Fe(OH)_{3\,(s)} + 3\ H^+ \quad (1.4)$$

It can thus be seen that the oxidation of pyrite leads to the liberation of protons, and so to a potentially significant lowering of the local pH: values are frequently reported in the range of 2-4, and negative pHs have been reported at the Iron Mountain site in California (although the difficulty of measuring such low values of pH should be noted).[319–322] However, this is just one simplified pathway. Many physicochemical factors affect the formation of AMD, such as pH, temperature, oxygen content of the gas or liquid phase, permeability of the rocks, exposed surface area, or redox potential.[323] Depending on these, other reactions such as the formation of elemental sulfur[316] may occur, not all of which lead to further acidification. These physicochemical factors also influence important biological factors: the formation of AMD from pyrite and other sulfides is accelerated by various aerobic and anaerobic microorganisms such as *Thiobacillus ferrooxidans* and *Desulfovibrio desulfuricans*.[324] Such biological oxidation may be significantly faster than chemical oxidation, especially at low pH.[325,326] Another important factor affecting acidity is the local mineralogy: the presence of neutralising carbonate minerals such as dolomite may buffer any generated acidity to some extent.[323,324] This can even lead to the formation of alkaline drainage, which is less damaging and may revert to being acidic following future oxidation of any leftover ferrous iron.[323] Taking into account all the above factors, the rate of generation of AMD can be seen to be very site-specific.

The acidity of AMD leads to its second main characteristic: elevated dissolved metal concentrations. Metal solubilities tend to increase with decreasing pH,[327,328] and as a result AMD is able to dissolve salts and thus mobilise metals as it flows through the mining sites. Many of these metals are classified as heavy metals, such as Fe, Mn, Cu, Ni, Zn, Pb, As, or U.[321] The relative abundance of each metal will depend on local mineralogy and hydrogeology, this is another site-specific factor which renders AMD hard to generalise.[320,324] However, the concentrations of the most abundant metal contaminants (e.g. Fe, Al, Mn) often reaches the order of hundreds of mg/L, and occasionally the order of g/L.[316,318,320,321,329–331]

While formation of AMD can occur naturally, its rate is slow and its environmental impact is therefore minimal.[324] Human mining activity significantly increases this rate by increasing the exposure of sulfide-containing rocks to air and water. This may occur deep within the mine itself, upon contact with groundwater. This is often the case following mine closure, when water pumping ceases and a subsequent rise in groundwater level is observed.[332] However, a more important source is the generation of large volumes of mining waste such as tailings and spoil heaps, through which surface water may flow.[298] In this case, minerals are much more disaggregated, with the increased surface area leading to faster-forming and more severe AMD.[332]

Effects

As previously mentioned, the quantity and composition of AMD can exhibit significant spatial variation. In addition, temporal variation may exist due to seasonal changes in climate, especially in terms of wetting cycles which push contaminants through the system.[324,333] For example, samples taken in the Witwatersrand basin in South Africa were found to have higher conductivity and lower pH at the end of the wet season than those taken in summer, hypothesised to be due to a rise in the water table increasing seepage of contaminants.[318] As a result of this spatial and temporal variation, prediction of site-specific effects of AMD is difficult, and there is no standard practice for doing so.[323,333] General effects, however, can be described and show AMD to pose a serious environmental problem with long-lasting effects, as its generation may continue for decades or centuries.[298]

The environmental impacts of AMD can be distinguished between those of its acidity and those of its metal content, with the latter being considered more important.[324,334] While some heavy metals are essential nutrients for growth, the elevated levels typical in AMD can be toxic to aquatic and terrestrial life.[298,335] This can be seen through the Substance Priority List published by the US Agency for Toxic Substances and Disease Registry, in which 4 of the top 10 are heavy metals, including the top 3 (As, Pb, and Hg).[336] Heavy metal pollution can lead to a damaging decrease in biodiversity through its toxicity, salinization of the environment, and effects on sedimentation processes.[323,333] Furthermore, build-up of these substances in the food chain may eventually pose a risk to humans. While less damaging, the acidity of AMD may also pose an ecological threat if the pH of waterways is significantly lowered.[337,338] The combination of these different impacts and their multiple pathways can lead to a damaging loss in biodiversity which disrupts the food chain and may therefore lead to ecological collapse.[333]

In theory, AMD may be generated at any mining site containing pyrite, and is therefore likely to be a global issue. As a result, local studies on AMD are fairly geographically wide-ranging. However, quantification of its prevalence on a large scale is relatively rare. In 1993, the US Forest Service

estimated that up to 16,000 km of streams were being affected by AMD in the Western US alone, originating from 20,000-50,000 mines.[324] Estimates for the cost of cleanup in the years 1993 and 1996 ranged up to $72 billion.[339] In 1994, the Canadian Mine Environmental Neutral Drainage (MEND) program estimated the cost of liability associated with AMD in Canada at $2-5 billion.[340] Also in 1994, the National Rivers Authority estimated that around 600 km of waters had been affected by abandoned coal and metal mines in England and Wales.[341] In 2002, Younger et al. estimated that 4,500 km of European waters were contaminated.[342]

Conventional Treatment

There are two approaches to AMD management: containment and remediation, sometimes called source control and migration control.[332] The former involves limiting the exposure of the AMD-causing sulfides to oxygen and water in order to prevent further generation, while the latter involves treating AMD once it has been formed. [332] While these approaches are not necessarily in opposition, this study is concerned with the remediation of existing AMD, and so containment methods will not be considered. The aims of AMD remediation are to neutralise the acidity of the water and to reduce its heavy metal content. Current methods may be classified into chemical or biological, and active or passive.[332] Active approaches involve continuous input of energy or material into the system, while passive approaches involve limited inputs once in place.

The most common approach would thus be classified and chemical and active, and involves the addition of alkaline substances such as lime or calcium carbonate to increase the pH of AMD waters.[332,343] This has the benefit of stimulating the oxidation of some metals, such as iron(II) and manganese(II), and the precipitation of dissolved metals under the form of hydroxides (although this may buffer any pH changes).[330,332] While this method has low material costs, it has relatively high operating costs (e.g. due to the use of precipitators or agitated reactors[329]), and metal precipitation leads to the formation of a sludge which must then be suitably disposed of.[332,344] Following the addition of calcium-based alkaline substances, levels of Ca^{2+} and SO_4^{2-} (from the original oxidation of pyrite) may be elevated. Ion exchange resins may then be used to reduce salinity to appropriate levels, such as in the GYP-CIX process.[345]

One of the most common passive remediation processes is the use of Anoxic Limestone Drains (ALDs). In these systems, AMD is forced though a drain containing limestone, which is covered by an impermeable plastic liner and embedded in clay, and is thus kept anoxic.[332] As the limestone in these trenches dissolves, alkalinity is introduced into the system and the pH subsequently rises. However, precipitation of iron(III) hydroxide and aluminium hydroxide (‘armouring’) reduces permeability and

severely inhibits performance.[329,332] This may be avoided by maintaining anoxic conditions to prevent oxidation of iron(II), typically by capping with soil and covering with plastic, but means that ALDs are not suitable for waters with high concentration of ferric iron and aluminium.[329,332] ALDs may also be used in conjunction with other remediation methods in order to raise pH in a first stage: they have been seen to significantly improve the performance of constructed wetlands.[329,332] Other methods of note include the use of membranes and bioreactors.[323,332,346] The principal drawbacks with the conventional methods outlined are cost and the need for long-term maintenance, with the later especially important when considering the long lifetime of AMD.[329]

1.4.3 Wetland Remediation of AMD

Mechanisms

Wetlands offer an alternative to AMD remediation, corresponding to both passive biological and passive chemical methods. The main action of wetlands is reduction of heavy metal concentrations, which occurs through a number of mechanisms.

The simplest remediation mechanism is dilution: being often positioned in low-lying areas, wetlands may receive clean as well as contaminated influent streams.[323] This has the dual benefit of reducing heavy metal concentrations to less harmful levels and raising the pH of the contaminated water, but does not remove contaminants from the system. However, the contribution of dilution in wetland remediation has been questioned.[347]

Oxidative and reductive processes play a large part in determining the distribution of metals in wetlands. Wetlands are typically observed to have both aerobic and anaerobic regions. The aerobic regions are shallower, with oxygen introduced via dissolution into the water at a free surface and therefore present in the water column, and exudation by plant roots into the shallow soil.[332] If the soil is not submerged, aerobic conditions exist anywhere above the water level.[348] Deeper into the soil, conditions tend to be anaerobic. Within the aerobic region, oxidation and hydrolysis of metals occurs, which can lead to the formation of insoluble oxides, hydroxides, and oxyhydroxides.[298] However, such processes may be strongly pH-dependent, such as for iron and manganese, where they are inhibited by lower pH and are thus more dependent on the activity of oxidising bacteria (e.g. *Ferrobacillus ferrooxidans*) which may not necessarily be acidophilic.[329,330] Since the hydrolysis of ferric iron releases protons, such oxidation and subsequent hydrolysis of ferrous iron may be essentially inhibiting itself and other oxidation reactions if no pH buffering is implemented.[329] Within the anaerobic regions, reductive processes occur. The primary reaction is the reduction of sulfur, which is strongly enhanced

by the activity of sulfate-reducing bacteria such as *Desulfovibrio*. Sulfate is reduced to sulfide, leading to the precipitation of many highly insoluble metal sulfides and increasing the pH by generating net alkalinity.[322,332,348] If the reaction is bacterially-mediated, sulfate may be used to oxidise organic material, leading to the formation of bicarbonate and thus the precipitation of insoluble metal carbonates.[298,348] Hydrogen sulfide may also be generated as part of these reductive processes.[321,343] Bacterial activity may lead to other reduction reactions such as methanogenesis.[332] While some sulfate-reducing bacteria may be able to withstand highly acidic conditions, their performance may be inhibited at low pH.[329] There are conflicting reports as to the relative importance of oxidative versus reductive processes. Some studies report that sulfate reduction plays the major role in wetland remediation, whereas others argue that the majority of metal immobilisation is in oxidised forms. In the work of Fennessy et al, oxidative processes were found to be more important for iron removal in the constructed wetland investigated, whereas in the natural wetland it is reductive processes which dominated.[343] In practice, local conditions and the design of the wetland are likely to determine the relative importance, with no general rule applicable.

Sorption processes have been thought to form an important part of wetland remediation of AMD. This may take place via adsorption of metals onto ion exchange sites in the soil (due to electrostatic attraction), such as when binding to clay.[349] This property of the soil may be quantified through the Cation Exchange Capacity.[350] Another possible sorption process is complexing with organic substances such as humic and fulvic acid.[300] Iron and manganese hydroxide precipitates have also been shown to act as adsorption sites for certain metals such as copper or nickel.[298] Adsorption to microorganisms may also take place.[300] The low flow velocities of wetlands allow sedimentation of particulates containing adsorbed metals, thus leading to metal immobilisation in sediment.[343] Machemer and Wildeman found that, in laboratory experiments, competition between metals for adsorption sites on wetland substrate is important at high metal concentrations, with Fe and Cu being preferentially adsorbed over Mn and Zn (similar findings about preferential metal adsorption has been noted elsewhere[298]).[351] This conclusion was corroborated by field data from an operational wetland. In addition, it was found that the contribution of adsorption processes to this wetland's remediation was only significant during the first 4 months of operation, after which it was assumed that adsorption sites were filled with the preferentially adsorbed metals. After this point, the establishment of sulfate-reducing bacteria led to sulfide precipitation becoming the dominant process in remediation. It should be noted that the environmental conditions such as pH will affect adsorption processes, and may also change the speciation of adsorbed metals.[298,329]

The last main mechanism is phytoremediation. Wetland plants are typically macrophytes (aquatic plants), but may also include algae. Their role in AMD remediation is multifaceted, but may be broadly

classed into direct effects and indirect effects.[322] Direct effects are explored later, but relate to the uptake of metals by the plant itself, stored either in the belowground section (i.e. the roots) or aboveground (flowers, shoots and leaves). In order to effectively remove metals from the system, the resulting biomass must then be harvested, otherwise it will eventually decay and reintroduce the heavy metals into the system.[330] The indirect effects of wetland plants lead to enhanced performance of other wetland remediation mechanisms, and are mainly related to the effects of plants' rhizospheres (the area of soil affected by the activity of the roots). Firstly, as previously mentioned, plants may excrete oxygen through their roots, leading to oxidative conditions in the rhizosphere that may cause metals to precipitate out of the soil solution. In addition, the roots provide increased surface area for the precipitation of metallic compounds.[332] The combination of these two effects can be seen through the formation of (mainly iron) plaques on the root surfaces of certain species, which may then engender co-precipitation and adsorption of other metals.[352] Plant roots may exude chelating compounds which complex with metals, reducing mobility.[300] Decaying plant material provides organic material for the wetland, and roots may also fix nutrients into the soil, encouraging microbial growth and activity.[298,329] Plant roots bind soil together, leading to lower erosion and lower loss of contaminated material during periods of low water level.[300,329] Furthermore, the roots also affect the hydrology of wetlands by slowing down and increasing the homogeneity of the flow.[332] This enhances sedimentation and increases retention time, thought to be an important parameter in wetland remediation performance.[300]

The number of mechanisms in wetlands and their integration makes individual contributions hard to analyse. This complexity is further increased by the fact that many, if not all, of these processes may be interrelated to a certain degree, and are also dependent on local conditions.[329] For example, plants' rhizospheres affect microbial activity and redox potential. Redox processes themselves affect pH, which is an important factor for sorption processes (which are evidently also dependent on the type and composition of soil present at the site) and microbial activity. In addition, the redox potential affects the oxidation state of metals, and thus their mobility.[350] Such complexity is compounded by varying inputs to the system due to variability in AMD formation. Site-specific characteristics such as soil composition, depth, and composition, water level, or local ecology, will also affect wetland remediation mechanisms.[298,323] As a result, while wetlands represent potentially useful methods to remediate AMD, it is very challenging to quantitatively predict their remediation performance.[298,323]

Phytoremediation Mechanisms

The term phytoremediation refers to the use of plants to remove contaminants from soil, water, or air. Depending on species, a wide range of substances may be removed, degraded, or immobilised. The main advantages of phytoremediation are its low energy cost for the removal of relatively low concentration contaminants, its renewability, and its limited environmental disruption.[353] However, these come at the cost of slow and possibly variable performance. There are a variety of mechanisms by which plants may reduce contamination. These may be broadly classed as: phytoextraction, rhizofiltration, phytostabilisation, phytovolatilisation, phytodegradation, and rhizodegradation.[298]

Phytoextraction refers to the uptake of a substance by the plant, and its subsequent storage within the plant's above-ground structure, namely the shoots and leaves. While the process can apply to both organic and inorganic species, it is typically referred to as pertaining to heavy metals. Depending on plant species, the concentration of stored heavy metals can exceed typically toxic levels by orders of magnitude. Species may be classed as hyperaccumulators if these concentrations are significantly higher than those in non-accumulating species grown at the same location, often taken to mean by over a factor of 100.[350,353] The mechanisms behind such uptake and storage have been investigated, but are still not fully understood.[298] Metal uptake first takes place via plant roots. Root uptake from soil is strongly affected by the bioavailability of the heavy metals: generally for uptake, metals must be in soil solution as ions or soluble complexes, or adsorbed to soil at ion exchange sites.[350,353] While this is affected by many factors, two can be considered particularly relevant to wetland phytoremediation of AMD. Firstly, higher soil moisture enhances phytoextraction by increasing the amount of soil solution, as well as enhancing biomass production and thus total extraction of metals.[350] Secondly, decreasing pH enhances phytoextraction by increasing metal mobility and by more H^+ ions competing with metal cations for adsorption at soil binding sites.[350,353] Once at the roots, metal ions may be adsorbed to sites on the root cell wall due to electrostatic attraction, thereby preventing their translocation to the plant shoots.[298,353] Entry into the cells is controlled by transport proteins in the cell membrane, called transporters, which can be modelled as having varying kinetic parameters, some of which are ion-specific.[353] Ions may then pass through root cells into the root vascular system, termed the xylem, but may be immobilised in transit.[353] Translocation from root to shoot in the xylem is then driven by the root pressure, and transpiration from leaves.[353] Once in the aerial part of the plant, metals may be stored via precipitation in the form of insoluble compounds, typically sulfates, carbonates, or phosphates.[354] In addition, metals may be stored via compartmentalisation, specifically in the vacuole of plant cells.[355] This process is aided by the chelation of metals by organic acids (e.g. citrate) or phytochelators.[354,356] Metal storage can be classed as

apoplastic (extracellular) and symplastic (intracellular).[354] Phytoextraction may be artificially enhanced by adding chelators into the soil in order to increase the mobility of metals.[355]

Phytostabilisation, also referred to as rhizostabilisation, is a broad term which encompasses several mechanisms. It refers to the reduction of contaminant bioavailability and mobility.[357] This may be through a reduction in soil erosion or dust.[353] It may also be through rhizofiltration: the removal of contaminants by plant roots from aqueous solution in the rhizosphere, either through adsorption to roots or uptake into the plant (which may lead to phytoextraction).[356] Lastly, phytostabilisation may take place through the sorption of metals or enhanced precipitation of insoluble metal compounds in the rhizosphere.[355] The latter may be as a result of microorganisms in the rhizosphere, whose activity and population numbers are enhanced by the plant, or via the secretion of organic compounds from plant roots.[353,355]

Phytovolatilisation refers to the transpiration of volatile compounds through plant leaves following uptake. This mechanism primarily applies to organic contaminants, but does occur for some volatile inorganic compounds, as well as to Hg.[355] One issue with phytovolatilisation as a remediation technique is that any removed contaminants may re-enter the system through precipitation.[355]

Phytodegradation involves the breakdown of contaminants by plants. This process is only applicable to organic substances, which may be metabolised within the plant or broken down by enzymes secreted out of the plant.[355] Rhizodegradation, although slower, similarly involves the breakdown of organic contaminants, but in this case by microorganisms present in the rhizosphere.[355]

Phytoextraction Feasibility

A phytoremediation mechanism of high interest is phytoextraction (and by extension rhizofiltration). Periodic harvesting of contaminated biomass allows complete removal of heavy metals from the ecosystem, and can lead to recovery of valuable metals, a process termed ‘phytomining’.

Phytoextraction requires the presence of species which accumulate metals in their above-ground tissues, termed metal accumulators. The degree of translocation of metals from roots to shoots (stems, leaves, and flowers[330]) is expressed using the translocation factor: the ratio of metal concentration in shoots to that in roots. A translocation factor greater than 1 indicates preferential storage in shoots and may be used to define accumulator status.[358] As a result, this is often considered a requisite for a species to be considered for phytoextraction.[330] Desired properties in plants used for phytoextraction and phytomining are: tolerance to high levels of metals, high metal accumulation in shoots and leaves, fast-growing, and a deep root system.[354] Unfortunately, hyperaccumulators species

tend to only have accumulating capabilities for a small number of elements, whereas AMD often contains a mix of several different metal contaminants.[350] Furthermore, hyperaccumulators are often slow-growing, which limits their use in terms of phytomining.[353] As a result, use of metal-tolerating non-hyperaccumulating species with high biomass growth rates may represent a more effective source for phytoextraction and phytomining, even if metal recovery is harder due to lower concentrations.[353] Particular focus has been paid to common reeds (*Phragmites australis*) and cattails (*Typha latifolia, Typha domingensis, Typha angustifolia*), which have high growth rates, grow commonly on AMD contaminated wetlands and outcompete other species, and are indigenous to many parts of the world.[322,346,359–361] These species are examples of emergent plants (i.e. with below-water roots, but with shoots extending above the surface). While submerged and floating species have been shown to display higher metal accumulation (see Section 1.5.3), the harsh nature of AMD means such plants are typically not hardy enough to grow.[320,348] However, in practice even wetlands treating wastewaters for BOD and nutrient removal typically use a fairly narrow range of biomass, focussing on emergent plants such as reeds, sedges, and cattails.[362]

Studies have been carried out on the use of emergent wetland plants as phytoextractors. Unfortunately, findings have not been promising. Metals tend to accumulate preferentially in roots, with a variety of wetland plants consistently demonstrating translocation factors below 1 for almost all metals studied.[363] For the same species, variation in reported translocation factors is expected between studies, as site-specific factors such as pH, salinity and redox conditions may affect the translocation behaviour of plants. Low translocation factors may explain the metal tolerance of such species: by preventing significant metal uptake into plant tissue, wetland plants may grow on heavily contaminated soil without suffering adverse effects.[346] While the translocation factor allows quick identification of accumulating plant species, an arguably more important metric in evaluating the feasibility of phytomining is the concentration of metals in aerial tissues. As with the translocation factor, this is heavily influenced by local conditions as well as the metal content of the input water: several studies have shown correlation between local metal concentration and concentrations in aboveground tissues.[359,360] Such variation makes generalisation of metal concentrations difficult, and so a range of values for reeds and cattails has been provided in Table 1.2, but this list is far from exhaustive. It should be noted that the last entry in Table 1.2 appeared to find common reeds and cattails to both be accumulators for several common species and found very high metal concentrations, and is viewed sceptically.

As a result of low translocation factors and relatively low metal concentrations, several studies have cast doubt upon the feasibility of using wetland plants for phytomining.[358] However, the use of ionic liquids to pretreat wetland species for biofuel production, with metal recovery as a possible secondary

value stream, may render phytomining economically viable. For such a use, fast-growing, non-accumulating species such as reeds or cattails may still be able to extract significant quantities of metals at low concentrations, with these metals later being concentrated in the liquor during the pretreatment process.[298]

Table 1.2: Aboveground metal concentrations and translocation factors for common reeds and cattails. Translocation factor is defined as the ratio of metal concentration in shoots to that in roots.

Source	Species	Metal	Max concentration in aboveground tissue (ppm)	Translocation Factor (<1/>1)
[361]	*Typha latifolia*	Fe	270	< 1
		Mn	2400	> 1
		Co	0.76	< 1
		Ni	2.4	< 1
[359]	*Phragmites australis*	Fe	5.0	< 1
		Mn	0.16	< 1
		Al	2.1	> 1
[360]	*Phragmites australis*	Zn	51.6	< 1
		Cu	7.9	< 1
		Cd	0.19	< 1
		Pb	0.42	< 1
	Typha angustifolia	Zn	48	< 1
		Cu	9.3	< 1
		Cd	0.21	< 1
		Pb	0.25	< 1
[320]	*Phragmites australis*	Fe	1500	< 1
		Zn	150	< 1
		Cu	34	< 1
		Cd	0.49	< 1
[330]	*Phragmites australis*	Al	3400	> 1
		Mg	1800	> 1
		Mn	2500	> 1
		Fe	6700	> 1
	Typha latifolia	Al	1100	> 1
		Mg	3200	> 1
		Mn	2600	> 1
		Fe	1800	< 1

Importance of Phytoremediation in AMD Wetlands

Phytoextraction of metals in living macrophytes has been estimated to account for under 1% of the annual loading of many metals from AMD in wetlands.[320,361] However, the other phytoremediation mechanisms have been shown to play a significant role in the overall function of wetlands.

Ye et al. estimated that around 30% of Fe removal in a wetland cell was due precipitation in the oxygenated rhizosphere of cattails.[361] Woulds et al. found that increased biomass production led to increased iron removal in a constructed wetland.[322] The wetland was populated by cattails, which have been found to reduce the redox potential of sediments[343], favouring reduction processes (although there have also been reports of increased populations of oxidising bacteria in their rhizospheres[347]). In the study of Nyquist et al, several wetlands were constructed with and without plants present.[320] The authors concluded that the presence of plants led to increased pH, reduced redox potential, and increased metal sedimentation (1.5 times higher in the case of Cu).

A mesocosm-scale study by Rodriguez et al. investigated the effects of growing of two macrophytes (common reed and reed canarygrass, *Phalaris arundinaecea*) with certain apparently complementary properties such as growth season, root depth, and density.[364] While overall remediation was better than either monoculture, no synergistic effects were noted, with remediation of individual contaminants never exceeding that of either species.

Lastly, the presence of vegetation introduces organic substrate into the wetland, which is used by the microorganisms within the ecosystem and is therefore crucial to wetlands' low maintenance traits.[322]

A small number of drawbacks of wetland phytoremediation have been noted in the literature. The most commonly noted drawback relates to the disposal of metal-contaminated plant material if not suitable for phytomining.[346,355] However, the use of ionic liquids would at least partially remove this issue by concentrating metals into an ionic liquid liquor (see Section 1.3.2). The other main drawbacks mentioned are species-dependent: spatial (both between geographical regions and within specific sites) and seasonal variations in plant growth may lead to inconsistent performance (especially concerning uptake),[352] and the possible uncontrolled spread of some invasive species such as water hyacinths.[346] The high water content of macrophytes has also been mentioned as a drawback, presumably due to the increased weight for transportation or time and energy requirements for drying.[300,356]

AMD Remediation in Practice

Natural wetlands have been observed to grow commonly near certain AMD generation sites in South Africa.[318,321] However, they may also be constructed artificially, allowing conditions to be more carefully controlled. One of the biggest design decisions is whether the wetland is to remove metals principally by oxidative or by reductive processes, and therefore whether it should be designed to operate aerobically or anaerobically. In aerobic wetlands, which are more effective for the treatment of alkaline waters due to the enhanced abiotic oxidation of many metals at neutral pH, the flow of water is designed to be relatively shallow and slow.[329] In anaerobic wetlands, which are more suitable for acidic influent, a substrate of organic matter (such as mushroom compost) is often used, such that any oxygen present is used by microorganisms to oxidise and break down this organic matter, maintaining the anaerobic conditions required by sulfate-reducing bacteria. In this case, the flow of water must be more carefully directed to ensure it passes through the anaerobic substrate, rather than relying on slow diffusive processes.[329,348] This may be done through the use of vertical-flow wetlands (VF), which transmit over 10 times more water through the anaerobic zone than a horizontal sub-surface flow system (HSSF) of similar size. However, decreasing hydrological conductivity of the system will lead to increasing flow pressure requirements over time.[348] Furthermore, such wetlands require a minimum hydraulic head of around 1.5 m to operate, which may not be naturally available (thus requiring installation of pumps, and rendering the process less 'passive').[365] Moreover, there have been some reports of poor long-term performance in certain VF designs, with the system failing after around 1-2 years.[347]

Many studies have been conducted on the efficacy of wetlands for AMD remediation, with results showing significant variation. Performance is often evaluated in terms of iron removal, as this is typically the major contaminant.[329] However, depending on the site other metals such as manganese or nickel may also be one of the key removal targets. Some studies are described here, and may give a reflection of the range of removal efficiencies seen.

Woulds et al. found the efficiency of metal removal at a five year old Scottish wetland remediating AMD to be around 20%, ranging from 8% for Ca to 25% for Fe.[322] Performance was said to have deteriorated significantly over time, attributed to the particularly low pH, relatively high metal loadings, drying out of much of the wetland, death of most of the original cattails, and channelization of the flow leading to lower retention times. However, this conclusion may have been based on an unfair comparison. Average 2002 removal rates for summer and winter were compared with maximum and minimum removal rates in 1997, when the wetland was new. Relative to the maximum removal rates in 1997, 2002 performance was found to be around 2-3 times lower. However, 2002

rates were significantly higher than the minimum removal rates in 1997. It is unclear whether the minimum removal rates when new might have been due to a lag period during which bacterial communities and redox conditions were still being established.

In a paper on wetland remediation of AMD, Eger et al. report removal rates of 90% of trace metals (Co, Ni, Cu, Zn) and increases in pH from 5.2 to around 7 for a "pilot scale sulfate reduction system" in Minnesota.[348] However, metal loadings were relatively low (1.4-25 mg/L), and details on the system itself are not given besides the effects of varying substrate.[348] In the same work, an aerobic wetland was found to remove up to 87% of input Ni, the major local contaminant, but also mildly decreased the pH (by around 0.1-0.2 pH units). Interestingly, Ni removal was only said to be a result of sorptive interactions with the peat substrate, and the decrease in pH was therefore linked to the exchange of protons for metal ions at exchange sites in the peat. Performance of the aerobic wetland was found to decrease with increasing water depth.

In the work of Ye et al, leachate from coal combustion containing elevated metal concentrations at circumneutral pH was partly treated by four wetland cells populated mainly by *Typha latifolia* (which outcompeted other species originally planted).[361] Removal of most trace metals (e.g. Al, Cu, Zn) was described as "poor" due to the low retention time of 5 hours, but removal of Fe, Mn, Co, and Ni was found to be relatively successful: in the second year of operation, 94% of Fe, 98% of Mn, 95% of Co, and 63% of Ni were removed by the wetland, showing significant improvement over the first year. However, this may partly be due to the circumneutral pH of around 7.

The Wheal Jane mine is one of the best-known case studies of sudden AMD release, occurring due to groundwater rising following closure of the mine (and thus cessation of pumping to lower the water table). Following the incident, a passive treatment plant with three different treatment schemes was set up.[331] All schemes contained aerobic wetland cells populated by reeds, anaerobic cells (underground chambers full of organic substrate and without vegetation, and which should therefore not be considered as wetlands according to Johnson et al.[332]), and an aerobic rock filter. Two of these treatment schemes combined wetland and conventional remediation by integrating either a lime addition or an ALD step, in order to raise the influent pH before the wetland cells, but not to engender precipitation. Interestingly, the anaerobic cell only began to function as designed following a long shutdown period, over the course of which the number of sulfate-reducing bacteria increased by a factor of 100 for an unexplained reason. The ALD system consistently performed the best, followed by the lime addition system, and finally the lime-free system. Metal removal rates were for determined for Fe (95-100%), Cd (53-98%), Al (35-90%), Cu (42-95%), Mn (45-60%), K (-2-41%), Mg (26-41%), Na (20-33%), and Zn (47-73%). A larger active treatment plant is also present at the Wheal

Jane site, using conventional chemical methods to remediate the AMD. However, performance of the two systems was not compared. Attempts have also been made to implement similar schemes before vertical flow anaerobic wetlands, but long-term performance has been disappointing due to limestone depletion and iron accumulation in compost.

Fennessy et al. compared the performance of a constructed and a natural wetland receiving AMD with a relatively high pH averaging 6.4 (thought to be due to local limestone bedrock providing buffering).[343] The natural wetland exhibited higher iron removal (89% compared to 53%), with reductive processes being more important, whereas in the constructed wetland oxidative processes dominated. The improved performance of the natural wetland was thought to be due to lower flow per unit area leading to higher retention times and permeation of the flow to anaerobic reduction zones.

Temporal variation of wetland performance has also been investigated. A study on remediation of landfill leachate at a site in France using a constructed wetland populated by reeds and cattails showed significant variation in metal removal for many metals, with generally higher removal rates in spring.[358] However, comparison of removal rates between summer and winter at a constructed wetland in Scotland with almost no remaining plant growth showed only small differences.[322] The slight improvement in metal removal in summer for some metals was postulated to be due to precipitation and sulfate reduction rates increasing with temperature, and lower rainfall increasing retention times. Ye et al. observed no seasonal variation in metal removal from coal combustion leachate.[361] On a smaller scale, diurnal variation in metal removal has also been observed, attributed to increased levels of dissolved oxygen and higher pH during the day.[300]

An example of the unsuccessful use of wetland remediation of AMD is in the work of Nyquist et al.[348] In this study, four wetlands were constructed. One wetland contained a substrate of sand above a substrate of peat and sewage sludge, was populated with macrophytes, and received AMD. In this wetland, only Cu removal was notable (around 57%), with low Zn removal (8%) and almost no Fe or Cd removal. This was blamed on the severity of the AMD (pH of 2.65, Fe content of 265 mg/L). However, this explanation is not particularly thorough. Two possible reasons for such poor performance could be a lack of sulfate-reducing bacteria (which itself might be due to the severity of conditions) or poor design of the wetlands such that insufficient flow passed through the anaerobic zone: there was almost no reduction in sulfate concentrations. The latter suggestion is corroborated by the fact that pH in the sediment did noticeably increase despite the lack of sulfate reduction, suggesting that there was little flow through the sediment. As a result, the wetland depended on aerobic processes to treat very acidic AMD, despite the fact that rates of abiotic oxidation for many

metals are low in such acidic environments. In addition, the reported removal rates were slightly surprising for several reasons. Firstly, they were very low considering the relatively high concentrations of metals accumulated in the sediment (up to around 300 mg/g dry weight for Fe) and in plant shoots (up to 1.5 mg/g dry weight for Fe). Secondly, increased sedimentation of metals in the presence of plants tended to lead to lower removal rates from the AMD, which appears counterintuitive. An interesting conclusion from the study, however, was that the use of unoxidised mine tailings as a secondary substrate above a primary substrate of peat and sewage sludge (used in the other three wetlands constructed for the study) could inhibit much of the formation of AMD in terms of metal release, even if the pH of input water was lowered from around 5.94 to around 4.04.[320]

Wetland sizing is thought to be important to successful function, and is further explored in Chapter 3. The impact of sizing may be evaluated through three metrics: retention time, and hydraulic and metal loadings per unit area per unit time. Increased retention time and decreased metal and hydraulic loading in wetlands have been shown to lead to increased metal removal, and all must be taken into account during wetland design in order to size the system correctly.[300,348] Meanwhile, higher hydraulic loadings can increase the size of aerobic regions and reduce penetration to anaerobic regions, compromising the effectiveness of reductive processes.[343] Unfortunately, these metrics are rarely reported in AMD constructed wetland studies, even though their effects on performance may be significant. This renders comparison between studies difficult, and may explain some of the variation in performance.

1.4.4 Wetland Remediation of BOD and Nutrient Contamination

When well-designed (see Chapter 3), CWs have been found to exhibit high removal of BOD and nutrients. As a result, the use of CWs to remediate BOD- and nutrient-contamination is fairly well established at both small- and large-scale, particularly compared to their use for AMD remediation. There were estimated to be over 1,200 constructed wetlands in the UK in 2008, and there are thousands in operation in North America, primarily treating wastewater for BOD and nutrient contamination.[25–27] These range from 4,000 single-home horizontal flow designs in Kentucky, to a 6,000 ha wetland in Florida removing phosphorus from stormwater runoff for flows of up to 8,000,000 m^3/d.[25,30] A number of different mechanisms take place in CWs to remove these contaminants.

BOD

Organic matter is a major contaminant for a wide range of effluents. It is usually expressed in terms of the Biochemical Oxygen Demand (BOD), which represents the amount of oxygen required by

microorganisms to oxidise the organic matter. The BOD is measured by the oxygen consumption in an airtight container over 5 days.[25] BOD contamination damages aquatic ecosystems precisely due to this oxygen demand: as microorganisms consume oxygen to break down organic matter, the dissolved oxygen levels within waterways are depleted.[366] Depending on its severity, the effects of such oxygen stress can lead to the collapse of an aquatic ecosystem.

BOD removal occurs primarily *via* microbial breakdown, either anaerobically or aerobically.[367–369] These microorganisms can be found either in the soil medium itself, or in the biofilms within plant rhizomes.[367] A number of different pathways may be followed depending on the conditions and wetland regions in which they can place: respiration, fermentation (to lactic acid or ethanol), nitrate/iron/sulfate reduction, and methanogenesis.[25,368] Aerobic processes are more rapid than anaerobic processes, but are obviously dependent on suitable oxygen transfer into the system, either from plant roots or by diffusion from the air.[310,370] The secondary mechanism for BOD removal is through sedimentation of particles of organic matter.[368,369] Direct uptake into macrophytes has overall been found to be negligible compared to bacterial degradation,[368,369] but phytovolatilisation can be a significant factor for removal of certain hydrophilic compounds such as phenol, acetone, or THF.[367,371,372] It is worth noting that pathogens are often associated with organic contamination, and that high pathogen removal has been reported in CWs, such as up to 99% removal of faecal coliforms by Neralla et al.[25,373,374] Pathogen removal would appear to be mainly due to sedimentation and rhizofiltration, but other factors have been suggested including UV radiation, excretion of biocides by certain plants, predation by certain organisms (e.g. nematodes and zooplankton), and attack by microorganisms.[25,367,368,370,375]

Nutrients

Nutrient contamination typically refers to elevated levels of either nitrogen or phosphorus. Both of these nutrients are crucial for improving plant growth, and are thus used in fertilisers. However, nitrogen and phosphorus levels are both limiting factors for algal growth in fresh waters.[366] Therefore, when released into waterways they can lead to rapid and uncontrolled algal growth, which has a number of damaging consequences:

1. Some types of algae (e.g. cyanobacteria, known as blue-green algae) can produce compounds toxic to livestock and humans.[366,376,377]
2. Large algal blooms cause large swings in dissolved oxygen (high during the day from photosynthesis, and low at night due to respiration), which also affects water pH (damaging to certain organisms).[366,376]

3. Large algal blooms also filter out a substantial amount of light, which can have negative effects on both aquatic flora and fauna.[366,376,378]
4. When these blooms eventually die, their decomposition introduces a large BOD that causes depletion of oxygen levels [366,376]

This entire process is known as eutrophication, and is one of the most common and damaging forms of aquatic pollution. Globally, the number of "dead zones" due to eutrophication is doubling approximately every 10 years, affecting over 245,000 km^2.[379] Eutrophication has an estimated annual cost of $2.2 bn in the U.S.A alone.[380]

Phosphorus is present in wetland systems as inorganic phosphate ions (termed orthophosphate), and as part of organic material. Moreover, these forms may all be present in different physical forms: dissolved, particulate, or soluble reactive (forms readily hydrolysed by soil enzymes).[25,301,370,381] Phosphorus discharge limits are generally given for total phosphorus. Within the CW, all these forms are inter-converted, and eventually the final sink is one of the solid compartments.[25] Phosphorus can precipitate as a number of minerals such as apatite ($Ca_5(Cl,F)(PO_4)_3$) and hydroxyl-apatite ($Ca_5(Cl,F)(PO_4)_3$), and can co-precipitate with metal oxyhydroxides and carbonates (with Fe and Al in acidic soils, with Ca and Mg in alkaline soils).[382] Adsorption onto the substrate is another major removal mechanism, that is dependent on the soil redox potential, pH, metal content (typically Fe, Al, Ca, and Mg), and amount of native soil phosphorous.[368] Phosphorous is adsorbed onto minerals of the same metals with which it co-precipitates. Displacement of water or hydroxyls from Fe and Al oxyhydroxides has been reported as an important immobilisation mechanism.[368] Sedimentation of particulate phosphate is a more minor removal mechanism.[368] Lastly, the impact of plant uptake is twofold. Phosphorous makes up around 0.1-1.1% of a wetland plant's dry mass,[383] and plant uptake may thus account for significant removal during the growth season, but upon decay the plants release the phosphorous back into the system. Harvesting would, however, allow for phosphorous removal from the system.[368] Microbial phosphorus accounts for 15-25% of total CW ecosystem,[384] but has been reported as simply leading to rapid cycling of phosphorus states, ultimately ending up removed in a solid compartment.[25]

Similarly to phosphorus, nitrogen exists in several forms within CWs (organic nitrogen, nitrites and nitrates, and ammoniacal). Unlike phosphorus, however, these forms tend to have individual discharge limits, and can also be fully removed from the CW system through a number of microbial processes that depend on factors such as temperature, pH, redox potential, and C/N ratio[385,386]:

- Ammonification is the conversion of organic nitrogen to ammoniacal nitrogen by microorganisms. This process is most rapid when performed aerobically.[368]

- Nitrification is the biological oxidation of ammoniacal nitrogen to nitrates, and is carried out in two steps by different bacteria, with nitrites as the intermediate species.[368,386]
- Denitrification is the final step in the microbial removal of nitrogen, and is the reduction of nitrate to nitrogen gas, usually requiring organic compounds to be the electron donating substrate.[386] This process requires anoxic conditions,[386] and accounts for 60-95% of nitrogen removal in CWs.[387]
- Anaerobic Ammonia Oxidation (Anammox) has also more recently been found to occur in constructed wetlands,[388] a process in which nitrite and ammonia are converted to nitrogen gas and water. This process is advantageous as it requires no organic carbon and has a low oxygen requirement (provided by the nitrite).[25]

Ammoniacal nitrogen can also be removed by volatilisation of ammonia, although this requires an elevated pH (above at least 8.0) otherwise ammoniacal nitrogen will mainly be dissociated as ammonium ions.[385] Lastly, plant uptake of nitrogen is similar to phosphorus: while nitrogen is needed for growth (0.3-2.1% dry weight in wetland plants[383]), upon plant decay it is buried and thus immobilised, but regular harvesting represents an option for removal from the system.[25,368]

1.5 Duckweed

The term "duckweed" refers to members of the *Lemnaceae* family, comprising around 40 species of small, floating macrophytes across 5 genera: *Lemna*, *Spirodela*, *Landoltia*, *Wolffia*, and *Wolfiella*.[389–391] Duckweed are characterised by a floating, leaflike body called a frond, with different species having one or several roots. In addition, they may produce flowers depending on species and growth conditions.[392] While duckweed has typically been included in lists of CW species, its growth and metal uptake characteristics and its composition vary substantially from the most common CW species.

1.5.1 Growth

One of the major attractions of duckweed as a feedstock is its high growth rate when properly managed: doubling times of around 24-72 hours are frequently claimed under optimum conditions.[392,393] Duckweed growth (global except for polar areas[389,392]) displays a senescence-rejuvenation cycle, in which fronds produce a decreasing number of daughter fronds of smaller size and shorter lifespan, until a critical point is reached and the number, size, and lifespan of daughter fronds begins to increase again.[389] Such cycles can last up to around a month, and are accelerated by higher temperatures.[389]

There have been many reports attempting to quantify possible harvest rates on a larger scale. However, there is significant variation in the values quoted, ranging from 5-104 t/ha/y (dry basis).[389,392,394–398] Many of the higher quoted figures are extrapolations from small-scale studies under favourable or optimal conditions, which would not be representative of large-scale aquaculture or of wastewater remediation.[390] At higher plant densities, and at non-ideal conditions (e.g. temperature, nutrients, light intensity), growth rates can be substantially lower.[399,400] Xu et al. warn of predicting field system performance on laboratory results in this way.[392] Under proper management, realistic large-scale growth rates of around 30 t/ha/y seem to be a reasonable assumption.[389,390,401,402] This compares favourably with other second-generation energy crops such as *Miscanthus* or switchgrass, which produce around 10-20 and 12-16 t/ha/y respectively.[403] For small-scale experiments, growth rates are often reported in terms of the Relative Growth Rate, used in Eq. 1.5.

$$W_1 = W_0 e^{RGR*t} \quad (1.5)$$

where W_0 is the initial mass, W_1 is the final mass, t is the time interval for growth, and RGR is the Relative Growth Rate

While duckweed may be able to survive in a relatively large range of temperatures, nutrient loadings, Total Dissolved Solids, and pH, these must all be kept within fairly narrow limits for duckweed to exhibit maximal growth rates.[390,394,404] Acceptable temperature ranges are 7-33 ^oC, with maximal growth between 25-31 ^oC.[389,390] Acceptable pH ranges are 5-9, with an optimum between 6.5 and 7.5.[389,392] Depth of water is thought not to play an important role, but may lead to big temperature fluctuations or drying out during hot weather if too low.[389,390] Duckweed should be grown on relatively flat land, in slow-moving or still water (under 0.1-0.3 m/s unless protected by rooted macrophytes such as *Phragmites australis*[390,394]), and without significant wind, in order to ensure a consistent coverage of the water surface.[389,390,404] The reason for this is twofold: full coverage prevents the growth of algae which can inhibit duckweed growth, and secondly to prevent the plants being blown into the banks, leading to overcrowding and an associated reduction in growth.[404] Polyethylene wind protection grids may be employed to overcome wind issues.[390]

Due to the large number of species comprised, and their wide geographic distribution, there may be large differences between duckweed strains. Xu et al. state that some of the differences between strains (both geographic and species) include growth rates, nutrient tolerance and uptake rates, and the adaptability to different wastewaters.[392] Edwards et al. compared the growth of *Spirodela polyrhiza*, *Lemna perpusilla*, and *Wolffia arrhiza*, cultivated on septage (septic tank effluent) in 200 m^2 earthen ponds.[405] Yields decreased in the order *S. polyrhiza* > *L. perpusilla* > *W. arrhiza*, the same

order as decreasing frond size, with *S. polyrhiza* producing almost twice as much biomass as *L. perpusilla*. However, the protein content of the latter was 4% higher. Vermaat and Hanif compared the growth of five different species on domestic sewage and artificial wastewater.[406] *Lemna gibba* and *Spirodela polyrhiza* were found to be have the highest growth rates on domestic wastewater (2-3.5 times higher than other species tested), and thus concluded to be the most appropriate species for growth on such a medium. Bergmann et al. performed a screening test on 41 duckweed strains, using geographic isolates of 12 species covering all 5 genera, to determine the most suitable species and strain for growth on swine lagoon wastewater.[407] Using total protein production over 11 days as the performance indicator, all 41 species were ranked, with *Landoltia punctata 7776, Lemna gibba 8678,* and *Lemna minor 7501* ranked as the three top species. Variation at a geographic level was found to be very significant, e.g. *L. minor* rankings ranged from 3rd to 30th and *L. gibba* from 2nd to 18th. Ziegler et al. investigated the growth rates of various species and geographic strains of duckweed under ideal conditions, and found significant variation, with doubling times ranging from 1.34 days to 4.54 days.[393] The authors concluded that differences in growth rate exhibit more variation with geographic strain than by species or genus.

1.5.2 BOD and Nutrient Remediation

Duckweeds are effective sinks for nutrients such as potassium and phosphorus (P).[404] Duckweed is an efficient P sink, and can accumulate it up to 1.5% of its mass (dry basis), with ortho-PO_4 being its preferred form.[389,390] It has a higher tolerance for NH_4^+ than other species, but high concentrations are still toxic by depolarising the cell membrane. Furthermore, unionised ammonia is significantly more toxic (it is soluble in lipids so crosses cell membrane and affects metabolism), and higher NH_4^+ concentrations have associated higher ammonia levels due to dissociation unless the pH decreases.[389,392] Absolute ranges of nutrient ranges for duckweed growth are provided by Iqbal.[390] Due to its ability to grow rapidly on waters containing high levels of nitrogen (N) and P, removal of these nutrients by duckweed has been investigated in several studies. N uptake rates range from 0.15-1.67 g/m^2/d and P uptake rates from 0.01-0.22 g/m^2/day, as compiled from literature by Iqbal and in agreement with reported values from several other studies.[390,398,408]

Due to its high growth rate and uptake of nutrients (particularly phosphate, nitrate, and potassium), duckweed-based wastewater treatment systems for N, P and BOD removal have been studied and built, with particular focus on domestic and agricultural wastewaters.[389,390,409] In addition to nutrient removal, the inhibition of algal growth by complete surface coverage leads to effluent with low Total Suspended Solids (TSS).[390,409] The design and operation of such duckweed wastewater treatment

systems is covered in detail by Iqbal.[390] It should be noted that organic carbon is not used for growth, but instead broken down by bacteria associated with duckweed. As a result, duckweed treatment can be used after anaerobic digestion, with the former reducing carbon content and the latter reducing N, P, and nutrient content.[390] Additionally, such duckweed remediation systems have been shown to sequester three times more carbon than they emit, highlighting their sustainability.[410]

Vermaat and Hanif reported 77% P removal and 93% N-removal in 12 days from domestic sewage using *Lemna gibba*.[406] The major removal mechanism for P (56% of input) was found to be duckweed uptake. However, 50% of N input was found to be removed by nitrification (and thus volatilised and removed from the system), with duckweed uptake accounting for 34%. Other studies have, however, reported a higher proportion of N removal being attributable to uptake, at 75-80%.[397,411] Over 10 days, Krishna and Polprasert reported N removal of 58% from domestic wastewater by *Lemna gibba*.[408] El-Shafai et al. treated anaerobically-digested domestic wastewater by *Lemna minor*, in three ponds with a total retention time of 15 days and volume of 1.44 m^3.[397] 80% and 78% removal of N and P were reported in summer, as well as almost quantitative removal of faecal coliform, with 80% of N removal by plant uptake. However, in winter the system was deficient at removing nutrients (45% for N, 40% for P) and faecal coliforms, due to the lower growth rates at lower temperatures (13-20 ^oC). Removal of residual (mostly removed by anaerobic digestion) COD, BOD, and TSS, however, remained unchanged over winter, at 64-72%, 73-75%, and 43-63% respectively.

Oron et al. used *Lemna gibba* to treat sewage supernatant in mini-ponds of 0.4 m^2 of varying retention time.[396] A retention time of 5 days was found to reduce BOD, and NH_3 concentrations to levels suitable for agricultural re-use, with 4-8 days said to be the optimal retention time. An economic analysis of a duckweed sewage treatment plant was also conducted, for a population of 150,000 people. The costs of such a system ($0.05/$m^3$ wastewater treated, in 1994 USD) were found to be in line with those of conventional oxidation ponds.

There is very little data on the performance of full-scale systems.[390] One of the largest duckweed treatment plants is that built by the PRISM foundation in Mirzapur, Bangladesh. The 0.6 ha system treated 125 m^3/day of wastewater from hospitals, schools, and residences, for a total of 2,000-3,000 people. Levels P, BOD, NH_3, and turbidity were reduced by over 95%, to below those required for drinking water in the USA.[389,390,412] Additionally, levels of N were found to reduced by 74-77%.[398] The system's retention time was of 20.4 days, although 80-90% of BOD removal, and 90% of nutrient uptake occurred within the first 7.5 days suggesting it was oversized for these nutrients.[390]

Leng et al. suggest duckweed may be used for a large range of effluents (e.g. dairies, piggeries, alcohol production, tanneries) and agricultural run-offs (e.g. beef and sheep grazing, sugar industry).[389]

However, it is suggested that the best use would be for removal of P from human sewage, as the large amounts of P currently being discharged into the ocean are making it a deficient nutrient (classed as a critical raw material by the European Commission[413]). The author further estimates that up to 100 duckweed sewage treatment facilities existed at the time of writing (1999). Iqbal reports that by 1998 the Lemna Corporation, had constructed over 125 duckweed systems for tertiary treatment of lagoon effluents with flows of up to 7,000 m^3/day.[390]

1.5.3 Metal Remediation

Many studies have been carried out on the uptake of heavy metals from metal-contaminated solutions by different duckweed species. Results relating to metal uptake are typically characterised by two quantities: the concentration of the metal in duckweed tissue (dry basis), and the bioconcentration factor (BCF): (ppm of metal in tissue)/(ppm of metal in solution). The advantage of phytoremediation for metal removal is due to the relatively high costs and sludge disposal issues of other technologies (e.g. chemical repcipitation, ion exchange, coagulation-flotation).[414,415]

Zayed et al. investigated the accumulation rates of Cd, Cr, Cu, Pb, Ni, and Se in *Lemna minor.*[416] The plants were kept in nutrient solutions containing 0.1-10 mg/L for each each metal for a duration of 8 days, with the solution being replaced every 2 days. Results showed significant uptake levels, said to be similar to hyperaccumulating species. Cd was accumulated to the greatest extent, reaching 13,300 ppm and with a BCF between 550 and 1333. Tissue concentrations of Se, Cu, and Cr reached around 3,000-4,000 ppm, those of Ni 1,790 ppm, and those of Pb 630 ppm. In all species, tissue metal content increased with solution concentration, but no such consistent trends in BCF were observed. BCFs for all metals reached maxima in the range 400-800 except Cd (1333) and Ni (179). The effect on growth was also quantified for duckweed grown on 10 mg/L solutions, with growth reduction relative to controls ranging from 8.3% to 35.1%

Jain et al. compared the accumulation performance of *Lemna minor* and water velvet from nutrient solutions enriched with 2-8 mg/L of Fe and/or Cu.[417] The study lasted 14 days, with the solutions being replaced every 2 days. Over each two day interval, decreasing amounts of each metal were accumulated by the duckweed, showing that at first they were used for growth but the plants eventually became saturated. Plant tissue concentrations increased with solution concentration, reaching maxima around 6,800 ppm after 14 days in the most concentrated solution. Individual Fe concentrations up to 4 mg/L, individual Cu concentrations up to 1 mg/L, and mixed concentrations up to 2 mg/L for each metal did not inhibit growth. BCFs of around 50-70 were observed for both metals individually, with lower values for mixed metal solutions. However, these are based on the plant wet

mass, and so would be around 450-630 assuming 90% moisture content, which is consistent with the findings of Zayed et al.[416]

Sharma et al. measured the accumulation of Zn, Pb, and Ni in *Spirodela polyrhiza* over 4 days, using nutrient solutions with 10 mg/L of each metal.[418] Tissue concentrations at the end of the study were 27,000, 10,000, and 5,000 ppm of Zn, Ni, and Pb respectively, with corresponding BCFs of 2700, 1000, and 550. The majority of uptake occurred in the first 24 hours, particularly for Ni and Pb, suggested to be due to passive uptake before metabolic control leads to a plateau. The use of duckweed as a "mini-ore" for Zn phytomining is suggested. A decrease in chlorophyll content was found to occur, with Zn causing the biggest decrease, attributed to inhibition of chlorophyll synthesis.

Sekomo et al. investigated the use of *Lemna minor* for polishing textile wastewater.[414] Synthetic post-anaerobic digestion wastewater was produced by initially adding 0.05, 1.5, 0.1, 0.25, and 1.25 mg/L of Cd, Cr, Pb, and Zn respectively to nutrient solution, with these quantities later doubled. Emphasis was placed on the removal of metals from solution rather than the biomass uptake. Over 7 days, removal rates ranged from 25% for Cd to 95% for Cr, although significant quantities were deposited as "sediment". Increasing illumination of the system from 16 hours per day to 24 hours had no effect on removal. It was concluded that duckweed may be used as a polishing step, for Cr and Zn in particular, but that for high metal loads a pretreatment step may be required.

Mo et al. investigated the removal of Al, Pb, Cu, and a mix of all three metals by duckweed (species not given) from aqueous solutions over 10 days. Concentrations were varied between 1-10 mg/L for each metal and the pH between 4 and 5.[419] Removal rates for individual metal solutions tended to increase with metal concentration and pH, ranging from 77-93% for Al, 6-33% for Cu, 35-65% for Pb at pH 5. In mixed solutions, removal rates tended to be lower, particularly at higher concentrations of each metal. There was significant change in colour of the duckweed in 5 and 10 mg/L solutions of all metals, highlighting the toxicity of the metals at such concentrations. Additionally, it was noticed that duckweed metal content was consistently lower than the quantity removed from solution. This was taken to imply that some metal is weakly adsorbed to the duckweed and was being washed out by EDTA or DI water after harvesting.

Bokhari et al. investigated the uptake of Cd, Cu, Pb, and Ni from raw municipal effluent and sewage mixed industrial effluent over 31 days, using *Lemna minor*.[420] High removal rates (above 80%) were observed for all metals, with a maximum of 99% for Ni. BCFs were found to vary between 210 and 558, with the highest observed being 558 and 523 for Cu and Pb. However, the effect on growth rate was not reported.

Rai et al. grew *Spirodela polyrhiza* on metal-contaminated pond water, with relatively low concentrations of Cu, Cr, Mn, and Cd (0.08-0.25 mg/L) and slightly higher concentrations of Pb and Fe (1.61-4.18 mg/L).[421] After 15 days, tissue concentrations of 150-440 ppm were observed for Mn, Cr, and Cu, and with slightly higher concentrations for Pb and Fe (1,700 and 5,600 ppm respectively). Cd accumulation was found to be the lowest, at 20 ppm. Growth rates were positive, although no control appeared to be carried out. Additionally, extremely high BCFs were reported, from 2,500 to 36,500 despite an apparently identical definition.

Several studies have been carried out on As uptake. Alvarado et al. grew *Lemna minor* under a concentration of 0.15 mg/L. Removal rate was found to be 140 mg As/ha/d, with a plant tissue concentration of 2 ppm (assumed to be on a dry basis although not explicitly stated).[422] However, the climatic conditions were acknowledged to be unfavourable for duckweed growth, with even the control fronds decreasing in total mass. Rahman et al. investigated the difference in uptake mechanism between arsenate and arsenite.[423] Arsenate was found to be accumulated via the phosphate uptake pathway, possible due to the similarity between the two ions, as well as adsorbed onto Fe plaques. However, it was determined that arsenite uptake was via a different mechanism. In solutions containing 0.3 mg/L of arsenic, maximum tissue concentrations (at minimum phosphate concentrations due to competition in uptake) were found to be 26 ppm. The study concluded that duckweed would be a suitable candidate for As phytoremediation.

Leblebici observed extremely high uptake of Pb in both *Spirodela polyrhiza* and *Lemna minor*, with a maximum tissue concentration of 561,000 ppm in *L. minor* and 330,000 ppm in *S. polyrhiza* from 50 mg/L Pb solutions.[424] Such high metal concentrations (half a plant's mass being lead) are viewed skeptically. However, these were accompanied by significant decreases in growth. The effect of nutrient enrichment on metal uptake and growth reduction was also observed above 5 mg/L of Pb. Nutrient enrichment was found to abate both the accumulation of metals and the reduction in growth, allowing the plants to grow in higher metal concentrations. Comparison of total metal uptake with and without nutrient enrichment (i.e. allowing comparison of the effects of increased growth rate at the expense of reduced metal concentrations) was not carried out.

It is, therefore, clear that duckweed has the ability to uptake metals to very high levels. However, for effective phytoremediation, a balance between growth rate and uptake is required. Most of the aforementioned studies have not reported the effect on growth rates, with those that have generally showing a decrease in growth, or a change in colouration. Other studies focussing on the physiological responses of duckweed to heavy metals (rather than focussing on uptake/removal) over the same concentration ranges have shown negative impacts such as decreased photosynthetic pigments and

decreased protein contents.[425–429] It is worth noting, however, that for some metals conflicting findings have been reported on metal toxicity limits, likely due to differences in tolerance between strains. Therefore, further work should be done to establish clearer limits for the application of duckweed for metal removal. This should focus on whether duckweed can be used for high levels of metal contamination (i.e. several mg/L), or whether it should only be used for "polishing" applications with low metal concentrations. Further studies could involve the use of different configurations (e.g. a low-concentration "pool" for duckweed growth, before transplantation to a high-concentration "pool" for rapid accumulation before harvesting), or genetic modification of duckweed for heavy metal tolerance (with genetic modification already of interest due to duckweed's relative biological simplicity[430]).

1.5.4 Duckweed Composition

Duckweed is primarily composed of cellulose (10-13%), starch (3-75%), protein (7-45%), lipids (2-10%), lignin (2-9%), extractives (13%, only one value reported) and ash (12-28%)[395,396,401,409,431–433]. It can be seen that there is significant quantitative variation between studies, particularly with regards to starch and protein content. Starch serves as the storage medium for glucose produced during photosynthesis, and is stored under the form of semicrystalline granules inside the chloroplast. During the night, when no photosynthesis is occurring, the starch is broken down and used for metabolic purposes.[434] Starch contents of up to 75% have been reported. This upper bound, in the work of Reid et al, was under phosphorus deficiency and with glucose in the growth medium.[435] If glucose was removed from the growth medium, starch content reached 30% of dry mass. At their highest, starch levels are thus comparable with those of first-generation biofuel crops such as corn and wheat (60-75%).[436] Factors affecting starch and protein content are further explored later in this section.

Zhao et al. performed a thorough investigation of the carbohydrate composition of *Lemna minor*, with a focus on the composition of the cell wall material. Carbohydrates were found to account for 51% of total dry mass, of which 20% was found to be starch. Analysis of monosaccharides showed glucose to account for 33% of total dry mass, followed by uronic acid (10%) and xylose (5%). The significant quantities of uronic acid and relatively low quantities of xylose were taken to show high pectin and low hemicellulose content respectively. The high ash content of duckweed has been attributed to significant quantities of crystalline calcium oxalate.[390,431] Duckweed's high protein content has led to its use as animal feed in parts of the world, especially in south-east Asian countries such as Vietnam.[389]

The starch content of duckweed can be increased by manipulation of several environmental parameters. Over 30 days, Reid et al. observed significant increases in starch accumulation in *Spirodela oligorhiza* in response to phosphorus deficiency, accompanied by a cessation of growth but little

change in protein content. Starch content increased from around 20% to 75% and 30% in media with and without glucose respectively.[435] Similar results were observed by Sree and Appenroth, with starch contents increasing from around 5% to 45% in phosphorus-deficient nutrient medium.[437] In the work of White, starch concentration is observed to increase with decreasing potassium concentrations, although quantitative results are not provided.[438] By transferring *Spirodela polyrhiza* fronds to tap water for 5 days, Cheng et al. achieved starch contents of 46%, although the original starch content of the fronds is not reported.[433] In another study, Kesaano reported an average increase in starch content from 10% to 19% when transferred from sewage lagoon wastewater to nutrient deficient river water, for a mixed culture of *Lemna minor* and *Wolffia* spp.[439] Cui et al. investigated the effect of temperature, light, and nutrient starvation on starch accumulation.[440] An increase in starch content was found with nutrient starvation (being placed in well water with very low levels of nutrients), increasing light intensity, and decreasing temperature. Over 8 days, the maximum increase in starch content observed was from 15% to 27%, at the highest light intensity and lowest temperature (5 ^{o}C). All increases in starch content were accompanied by decreases in protein content, from around 30% to 20%. Cui et al. reported continuous starch accumulation during illuminated hours, and a decrease during dark hours.[434] A lower temperature during dark hours was found to increase starch content, although a lower daytime temperature produced little effect. Li et al. also found increasing light intensity, decreasing temperature, and nutrient starvation to increase starch content in a range of different monocultures and polycultures.[400] In addition, although most polycultures showed no synergies, certain polycultures were found to promote starch accumulation.

Presence of heavy metals has also been shown to affect starch accumulation in several studies. Appenroth et al. observed a transient increase in starch contents of *Spirodela polyrhiza* grown on solutions containing 2.5-5 mg/L of Cr, although this was then followed by a decrease after 2 days.[441] The increase was hypothesised to be due to inhibition of starch export from the plastid, and the decrease due to inhibition of photosynthesis. In a later study, Appenroth et al. also observed increases in starch contents of *Lemna minor* and *Spirodela polyrhiza* grown on solutions containing up to 6 mg/L of Ni.[442] Over 7 days, the maximum increase in starch content was from around 2% to 10% and 7% for *S. polyrhiza* and *L. minor* respectively (fresh weight basis), when grown in 2 mg/L solutions. Sree and Appenroth reported increases in starch contents from around 5% to 50% for *Lemna minor* grown in Cd solutions of up to 6 mg/L, with the maximum content at 1 mg/L.[437]

When under stress, duckweed produce large quantities of Absisic Acid (ABA), with levels falling once the stress is relieved. ABA is thought to inhibit growth but increase starch accumulation, and addition of external ABA to growth medium has been show to produce these effects.[434] Certain species of

duckweed are also known to form special high-starch fronds termed turions when under environmental stress.[434] Those of *Spirodela polyrhiza* are reported to contain around 70% starch.[392]

The protein content may also be manipulated. White noted increasing protein concentration with potassium concentration.[438] Oron et al. reported decreasing protein content with increasing retention time for *Lemna gibba* treating sewage supernatant, going from 32% to 20% as retention time increased from 3-10 days.[396] Li et al. found protein contents were maximised at 25 °C (in the investigated range of 20-30°C) and increased with increasing light intensity.[400] Additionally, nutrient starvation was found to lower protein content (a finding corroborating that of Leng et al, that increasing N content of the growth medium promotes protein accumulation[389]), and synergistic effects in terms of protein accumulation were found among certain polycultures investigated. Gupta et al. suggest a tradeoff between carbohydrate content, and protein content and growth rate, with the latter two increasing at the expense of the former, when grown on high-nutrient water.[409]

1.5.5 Duckweed Utilisation

Fresh duckweed has been reported to have a moisture content of 80-97%.[392,404,421,431] There are contradictory reports on the drying of duckweed biomass. Skillicorn et al. claimed that fresh duckweed storage for longer than 2 or 3 days above 20 °C was not possible.[412] However, they also reported storage of duckweed meal for over 5 years without deterioration, if dried to below 10% moisture and kept away from sunlight and humidity.[412] There has also been reports of storage durations of up to 13 years, in either sundried or pelleted form.[409] Due to its high water content, the difficulty of efficiently drying duckweed on a large-scale has been mentioned as a potential barrier to its widespread use.[390,412] However, certain more recent sources claim duckweed may be sun dried relatively easily, with Gupta et al. stating 24-48 hours in summer and 4-6 days in winter.[392,409] This is corroborated by the laboratory experience in Chapter 5 of this study.

Currently, duckweed tends to be used as animal feed due to its high protein content, or as fertiliser due to its high water and nitrogen contents.[389,390] However, its high growth rate and high proportion of starch make duckweed a suitable candidate for bioethanol.[392] Zhao et al. state that the use of duckweed as a biorefining feedstock is held back by a lack of information on duckweed composition.[431] Several studies have, nevertheless, been carried out on its use for production of bioethanol.

A number of studies have investigated the enzymatic digestibility of non-thermophysically pretreated duckweed. These studies do, however, involve a different form of pretreatment (often not recognised as such): grinding of the duckweed to a fine powder, i.e. mechanical pretreatment. This is also typically accompanied by liquefaction of the powdered duckweed by incubation at 80-100 °C (or by autoclaving

at 121 °C), either with or without thermostable amylase enzymes. Xu et al. milled and liquefied *Spirodela polyrhiza* that had been enriched in starch in an aforementioned study, before performing enzymatic hydrolysis and then fermentation in a 14 litre CSTR.[443,444] 97% of starch was hydrolysed, leading to an overall ethanol yield of 95% (relative to starch only). Extrapolation of the study's results led to a theoretical ethanol production of around 6.4 m^3/ha/y. Similarly, Ge et al. milled and liquefied *Lemna minor* that had been enriched in starch through nutrient starvation. 79-96% glucose release was observed following hydrolysis at different mass loadings (50, 60, and 290 mg/mL of powder input), with 95% subsequent fermentation efficiency. A number of other studies involving milling and liquefaction of duckweed have reported similarly high glucose and ethanol yields.[445–448]

In addition to higher growth rates, the low degree of lignification of duckweed means lower enzyme costs are required compared to other bioethanol crops, which is said to lead to a lower production cost for ethanol than using wheat straw.[449] However, Xu et al. suggest that pretreatment may still be required to increase the enzymatic digestibility and thus reduce enzyme costs and energy inputs for grinding.[392] The most thorough set of studies have been performed by Zhao et al. In their 2012 study, the enzymatic digestibility of non-thermophysically pretreated duckweed was investigated.[450] However, it should be noted that the material hydrolysed was Water-Insoluble and Alcohol-Insoluble Residue (WIAIR), produced by grinding the biomass with a pestle and mortar, two extractions in ethanol, one in acetone, and finally a sodium acetate washing step. The WIAIR was determined to contain very little lignin due to the lack of staining with phloroglucinol-HCl. Different enzymes mixtures were tested, with maximum glucose release of 90.7% and reducing sugar yield of 85.2% after 8 hours using an excess mixture of cellulase and beta-glucosidase. Yields were defined relative to the composition of the WIAIR, rather than the untreated biomass. A subsequent reduction in enzyme loading led to a glucose yield of 80% after 24 hours. In a follow-up to their 2011 work, in 2014 Zhao et al. performed steam explosion pretreatment and saccharification on *Lemna minor*.[432] 100% reducing sugar release was achieved after 8 hours of saccharification, following 10 minute pretreatments at 210 °C and 230 °C, with yields decreasing with lower temperatures. However, their definition of yield is based on "taking unhydrolysed carbohydrate to be 100%", seemingly suggesting that their "yield" is equivalent to our protocol's definition of digestibility (i.e. normalised to the sugar content of the pretreated material rather than the untreated biomass). This is corroborated by the reducing sugar yield approaching 100% for the highest temperature pretreatment (230 °C), at which significant sugar degradation and losses would be expected. A five-fold reduction in enzyme loadings (using cellulase and beta-glucosidase) led to glucose yields of 80% after 24 hours, following steam explosion at 210°C. This was around 8 times higher than that of the untreated duckweed. In 2015, Zhao et al. performed simultaneous saccharification and fermentation of *Lemna minor* pretreated by steam explosion, using

the same low-enzyme conditions from their 2014 work.[432,449] Although high ethanol yields were achieved (78.5% of the theoretical maximum based on glucan in the steam-exploded slurry), substrate concentration was only 1% wt/vol, leading to an ethanol concentration of 0.25%. This is far below the 4% needed for distillation in second generation biorefining according to the authors (a possible underestimate since distillation still requires around 30% of the energy content of the ethanol at this concentration[451]). By increasing the initial quantity of yeast (10% wt/vol) fourfold, and pre-culturing the yeast on steam-exploded liquor (to adapt to inhibiting by-products), ethanol yields of 70% were achieved at 20% wt/vol substrate loadings, leading to 3.5% wt/wt of ethanol.

A small number of other studies have also involved more 'explicit' forms of pretreatment, such as the work of Souto et al, who performed hydrothermal pretreatment of *Landoltia punctata*, followed by simultaneous saccharification and fermentation (SSF).[452] Optimal pretreatment conditions (200 ^{o}C for 10 minutes) were found to maximise ethanol yield, reaching 89% of the theoretical maximum, compared to 26% in untreated biomass. No saccharification yields were provided, however. Takai et al. performed alkaline/oxidative pretreatment of *Wolfia arhiza* (fronds and turions) for 24 hours at room temperature and ground the "pulp" into a powder, followed by either separate hydrolysis and fermentration or SSF.[453] 79-80% ethanol yield was acheievd by SSF, which outperformed SHF in both yield and kinetics. No comparison with untreated material was performed, nor any saccharification yields provided, however. Chen et al. ground and liquefied *L. punctata* using amylase enzymes, before carrying out pectinase pretreatment and then starch saccharification (upon addition of amyloglucosidase enzymes).[401] The exact pretreatment sequence carried out is poorly described, however. Optimisation of the pectinase loading, time, and temperature led to a glucose release of 56% after only 2 hours of saccharification (compared to 24% in biomass that had not been pretreated with pectinase but had been liquified), with a subsequent fermentation efficiency of 90%. By extrapolating these lab-scale results, a theoretical ethanol yield of 5.9 m^3/ha/y was found to be achievable, 1.5 times higher than that of corn stover and twice that of corn, and in line with the findings of Xu et al.[402]

Other biorefinery products other than ethanol have also been targeted from duckweed. Duckweed has been used for production of biogas,[448,454,455] biochemicals (such as levulinic acid, lactic acid, or acetone),[434,445,456,457] bio-oil,[455] or fermentation to other fuels such as butanol.[434] Interestingly, Calicioglu found that upstream fermentation of duckweed into ethanol (and removal of the ethanol) improved biomethane yields by 51% relative to directly digesting raw duckweed.[448]

Research Gap and Objectives

As has been explored in this literature review, there has been significant research focussing on the transition to a more bio-based economy, from energy provision to materials and chemicals. One of the key reasons hindering this transition is the current lack of a large-scale biomass pretreatment technology to unlock the potential benefits of lignocellulosic biomass. Most existing technologies suffer from drawbacks, typically the inability to deal with all types of feedstocks and the lack of a separate lignin stream for subsequent valorisation.

The ionoSolv process has been developed over the last ten years or so and offers the possibility of filling this current gap through the use of low-cost ILs, production of a highly pure cellulose, effective pretreatment of all types of lignocellulosic feedstocks, and the recovery of lignin. The parameters affecting the efficacy of the ionoSolv process have been studied fairly extensively, but there remain gaps to be filled. In particular, the effect of alkylammonium cation structure has not been sufficiently examined and offers the possibility for both enhanced performance and decreased costs, in line with the "designer solvent" tag of ILs. In addition, thorough study of acidity within the ionoSolv process has not been carried out to date, either being combined into general severity, or not being accurately quantified (i.e. without using Hammett acidity). Acidity underpins the ionoSolv process when using its flagship low-cost ILs, and can offer both improvements in kinetics but can also ruin pretreatment performance in excess.

Wetland remediation has been extensively studied and proven to work when well designed and applied. Its low maintenance requirements and low costs have frequently been lauded, without justification of the latter beyond anecdotal evidence and individual case studies. Therefore, while this technology has been rolled out fairly widely, it is still on a scale dwarfed by conventional remediation technologies. In order to provide further credibility, a high-level analysis is required to explore both the economic advantages of wetland remediation, and the conditions where these advantages are not as pronounced.

The use of constructed wetlands also leads to the production of high-yielding biomass that is effectively being grown on marginal land, exemplifying the advantages of second-generation biorefinery. This biomass has the potential to both boost the process economics of wetland remediation, and play a significant part in widespread biorefinery should constructed wetlands increase their share of the (ubiquitous, and growing) water remediation sector. To date, there has been little study of pretreatment of wetland species, and none with ionic liquids. The pretreatment studies that have been carried out have also not concerned samples containing metals, or considered

future implementation aspects such as feedstock independence. A coherent, holistic approach to wetland remediation would include proper study of utilisation of wetland biomass.

Lastly, while the growth, starch/protein accumulation, nutrient remediation, and metal uptake capabilities of duckweed have been comprehensively studied, its utilisation has not been. Pretreatment studies have only focussed on bioethanol or bioenergy yields, with no attempts at fractionation or metal removal, and no studies have employed ionic liquids. Moreover, despite being used on a wide array of lignocellulosic feedstocks, the ionoSolv process have not been used for extraction of protein from any biomass, nor has its interaction with starch been investigated.

The objectives of this thesis were therefore to:

- Investigate the pretreatment efficacy of primary and secondary alkylammonium $[HSO_4]^-$ ionic liquids, aiming to improve kinetics without impairing performance
- Explore the effect of different degrees and sources of acidity on pretreatment efficacy (saccharification yields, pulp purity, and lignin characteristics), using the Hammett acidity function for quantification
- Evaluate the economic performance of constructed wetlands for remediating BOD, nutrient, and AMD contamination, compared to conventional remediation technologies for a wide range of input conditions and for different wetland designs
- Investigate the effect of biomass valorisation on the overall process economics of wetland remediation
- Demonstrate the efficacy of the ionoSolv process on a range of typical wetland species, including those from different wetland applications, thus showing feedstock independence
- Identify a suitable operating condition for an ionoSolv process treating a range of different species
- Investigate the recycling performance of the ionoSolv process when treating wetland species, with a focus on the impacts of recycling on the IL acid/base ratio
- Study the stability of different types of starches at elevated temperatures in a range of common ionoSolv ionic liquids
- Explore the fractionation of duckweed using the ionoSolv process, aiming to separate carbohydrates and protein into different recoverable fractions
- Investigate the metal extraction abilities of the ionoSolv process at optimal conditions for duckweed fractionation

1.7 Thesis Structure

This thesis is structured into 5 chapters, outlined as follows:

- Chapter 1 has aimed to provide an overview of the main technologies and research underpinning the work in this thesis, in particular ionic liquid pretreatment of biomass and wetland remediation of wastewater.
- Chapter 2 investigates the effect of cation structure and acidity on the efficacy of the ionoSolv pretreatment process, using *Miscanthus* as a feedstock throughout.
- Chapter 3 investigates the economic viability of wetland remediation of wastewater, in the form of a high-level economic analysis compared to conventional treatment technologies, with an additional study of the potential for biomass valorisation.
- Chapter 4 investigates the effectiveness of the ionoSolv process for the fractionation of wetland species, with an aim towards developing a feedstock-independent process for utilisation of constructed wetland biomass.
- Chapter 5 explores the ionoSolv pretreatment of duckweed, focussing on the triple-goal of starch recovery, protein extraction, and metal removal.

Chapters 2-5 are all results chapters, with the most relevant previous works and the methods used covered within each.

References

1 BP plc, *BP Statistical Review of World Energy 2019*, 2019.
2 International Energy Agency, IEA Sankey Diagram, https://www.iea.org/sankey/#?c=World&s=Final consumption, (accessed 25 March 2020).
3 P. G. Levi and J. M. Cullen, *Environ. Sci. Technol.*, 2018, **52**, 1725–1734.
4 M. Aresta, A. Dibenedetto and F. Dumeignil, *Biorefinery: from biomass to chemicals and fuels*, De Gruyter, 2012, vol. 2.
5 Y. H. Oh, I. Y. Eom, J. C. Joo, J. H. Yu, B. K. Song, S. H. Lee, S. H. Hong and S. J. Park, *Korean J. Chem. Eng.*, 2015, **32**, 1945–1959.
6 G. P. Hammond, S. Kallu and M. C. McManus, *Appl. Energy*, 2008, **85**, 506–515.
7 T. Searchinger, R. Heimlich, R. A. Houghton, F. Dong, A. Elobeid, J. Fabiosa, S. Tokgoz, D. Hayes and T. H. Yu, *Science*, 2008, **319**, 1238–1240.
8 F. Cherubini, N. D. Bird, A. Cowie, G. Jungmeier, B. Schlamadinger and S. Woess-Gallasch, *Resour. Conserv. Recycl.*, 2009, **53**, 434–447.
9 F. Pancaldi and L. M. Trindade, *Front. Plant Sci.*, 2020, **11**, 227.
10 S. Fahd, G. Fiorentino, S. Mellino and S. Ulgiati, *Energy*, 2012, **37**, 79–93.
11 M. A. Mehmood, M. Ibrahim, U. Rashid, M. Nawaz, S. Ali, A. Hussain and M. Gull, *Sustain. Prod. Consum.*, 2017, **9**, 3–21.
12 A. Brandt, M. J. Ray, T. Q. To, D. J. Leak, R. J. Murphy and T. Welton, *Green Chem.*, 2011, **13**, 2489.
13 A. Brandt, PhD Thesis, Imperial College London, 2012.
14 A. Brandt-Talbot, F. J. V. Gschwend, P. S. Fennell, T. M. Lammens, B. Tan, J. Weale and J. P. Hallett, *Green Chem.*, 2017, **19**, 3078–3102.
15 F. J. V. Gschwend, F. Malaret, S. Shinde, A. Brandt-Talbot and J. P. Hallett, *Green Chem.*, 2018, **20**, 3486–3498.
16 A. R. Abouelela, S. Tan, G. H. Kelsall and J. P. Hallett, *ACS Sustain. Chem. Eng.*, 2020, **8**, 14441–14461.

17 H. Baaqel, I. Díaz, V. Tulus, B. Chachuat, G. Guillén-Gosálbez and J. P. Hallett, *Green Chem.*, 2020, **22**, 3132–3140.
18 United Nations, *International Initiative on Water Quality, SC/HYD/WQ/2015/5/En*, Paris, 2015.
19 United Nations, *TRANSFORMING OUR WORLD: THE 2030 AGENDA FOR SUSTAINABLE DEVELOPMENT, A/RES/70/1*, 2015.
20 E. Corcoran, C. Nellemann, E. Baker, R. Bos, D. Osborn and H. Savelli, *Sick Water? the central role of wastewater management in sustainable development. A rapid response assessment*, Birkeland Trykkeri AS, Norway, 2010.
21 M.-S. Javier, S. M. Zadeh and H. Turral, *More people, more food, worse water? a global review of water pollution from agriculture*, Food and Agriculture Organization of the United Nations, Rome, 2018.
22 WWAP (United Nations World Water Assessment Programme), *The United Nations World Water Development Report 2015: Water for a Sustainable World*, United Nations Educational, Scientific and Cultural Organization, Paris, 2015.
23 R. P. Schwarzenbach, T. Egli, T. B. Hofstetter, U. von Gunten and B. Wehrli, *Annu. Rev. Environ. Resour.*, 2010, **35**, 109–136.
24 M. Libhaber, Appropriate Technologies for Wastewater Treatment and Effluent Reuse for Irrigation, http://siteresources.worldbank.org/EXTWAT/Resources/4602122-1213366294492/5106220-1234469721549/27.2_WWT_Carbon_Footprint.pdf, (accessed 31 July 2019).
25 R. H. Kadlec and S. D. Wallace, *Treatment wetlands*, CRC Press, Boca Raton, 2nd edn., 2009.
26 P. Cooper, in *Wastewater Treatment, Plant Dynamics and Management in Constructed and Natural Wetlands*, ed. J. Vymazal, Springer, Dordrecht, 2008, pp. 149–160.
27 J. Vymazal, *Water*, 2010, **25**, 353–369.
28 T. Zhang, D. Xu, F. He, Y. Zhang and Z. Wu, *Ecol. Eng.*, 2012, **47**, 189–197.
29 D. Zhang, R. M. Gersberg and T. S. Keat, *Ecol. Eng.*, 2009, **35**, 1367–1378.
30 Brown & Caldwell, *Stormwater Treatment Area 2 Operation Plan, CN040935-WO34*, 2011.
31 Lavdim Osmanaj, Agon Haxhikadrija, Pierre-Henri Dodane and Astrit Vokshi, *J. Hydraul. Eng.*, 2015, **1**, 27–34.
32 A. S. Juwarkar, B. Oke, A. Juwarkar and S. M. Patnaik, *Wat. Sci. Tech.*, 1995, **32**, 291–294.
33 V. M. Lakay, MSc Thesis, University of Cape Town, 2012.
34 O. Alagbe and G. M. Alalade, *Univers. J. Environ. Res. Technol.*, 2013, **5**, 597–606.
35 M. L. Solano, P. Soriano and M. P. Ciria, *Biosyst. Eng.*, 2004, **87**, 109–118.
36 A. K. Kivaisi, *Ecol. Eng.*, 2001, **16**, 545–560.
37 P. Denny, *Water Sci. Technol.*, 1997, **35**, 27–34.
38 D. Q. Zhang, K. B. S. N. Jinadasa, R. M. Gersberg, Y. Liu, W. J. Ng and S. K. Tan, *J. Environ. Manage.*, 2014, **141**, 116–131.
39 J. F. Köbbing, N. Thevs and S. Zerbe, *Mires Peat*, 2013, **13**, 1–14.
40 J. Vymazal, L. Kröpfelová, J. Švehla, V. Chrastný and J. Štíchová, *Ecol. Eng.*, 2009, **35**, 303–309.
41 M. Scholz and B. H. Lee, *Int. J. Environ. Stud.*, 2005, **62**, 421–447.
42 T. Welton, *Chem. Rev.*, 1999, **99**, 2071–2083.
43 R. D. Rogers and K. R. Seddon, *Science*, 2003, **302**, 792–793.
44 P. A. Hunt, B. Kirchner and T. Welton, *Chem. - A Eur. J.*, 2006, **12**, 6762–6775.
45 F. Gschwend, PhD Thesis, Imperial College London, 2017.
46 T. L. Greaves and C. J. Drummond, *Chem. Rev.*, 2008, **108**, 206–237.
47 N. V. Plechkova and K. R. Seddon, *Chem. Soc. Rev.*, 2008, **37**, 123–150.
48 C. Schreiner, S. Zugmann, R. Hartl and H. J. Gores, *J. Chem. Eng. Data*, 2010, **55**, 1784–1788.
49 H. Niedermeyer, M. A. Ab Rani, P. D. Lickiss, J. P. Hallett, T. Welton, A. J. P. White and P. A. Hunt, *Phys. Chem. Chem. Phys.*, 2010, **12**, 2018–2029.
50 S. Zhang, N. Sun, X. He, X. Lu and X. Zhang, *J. Phys. Chem. Ref. Data*, 2006, **35**, 1475–1517.
51 M. Hirao, H. Sugimoto and H. Ohno, *J. Electrochem. Soc.*, 2000, **147**, 4168.
52 J. M. Pringle, J. Golding, K. Baranyai, C. M. Forsyth, G. B. Deacon, J. L. Scott and D. R. MacFarlane, *New J. Chem.*, 2003, **27**, 1504–1510.
53 P. Wasserscheid and T. Welton, *Ionic Liquids in Synthesis*, Wiley, Darmstadt, 2nd edn., 2007.
54 J.-P. Belieres and C. A. Angell, *J. Phys. Chem. B*, 2007, **111**, 4926–4937.
55 C. Comminges, R. Barhdadi, M. Laurent and M. Troupel, *J. Chem. Eng. Data*, 2006, **51**, 680–685.
56 K. R. Seddon, A. Stark and M. J. Torres, *Pure Appl. Chem.*, 2000, **72**, 2275–2287.
57 M. J. Earle and K. R. Seddon, *Pure Appl. Chem.*, 2000, **72**, 1391–1398.
58 C. Maton, N. De Vos and C. V. Stevens, *Chem. Soc. Rev.*, 2013, **42**, 5963.
59 M. J. Earle, J. M. S. S. Esperança, M. A. Gilea, J. N. C. Lopes, L. P. N. Rebelo, J. W. Magee, K. R. Seddon and J. A. Widegren, *Nature*, 2006, **439**, 831–834.
60 D. M. Fox, W. H. Awad, J. W. Gilman, P. H. Maupin, H. C. De Long and P. C. Trulove, *Green Chem.*, 2003, **5**, 724–727.
61 M. Smiglak, W. M. Reichert, J. D. Holbrey, J. S. Wilkes, L. Sun, J. S. Thrasher, K. Kirichenko, S. Singh, A. R. Katritzky and R. D. Rogers, *Chem. Commun.*, 2006, 2554–2556.
62 H. J. Liaw, C. C. Chen, Y. C. Chen, J. R. Chen, S. K. Huang and S. N. Liu, *Green Chem.*, 2012, **14**, 2001–2008.
63 M. Hayyan, F. S. Mjalli, M. A. Hashim, I. M. AlNashef and T. X. Mei, *J. Ind. Eng. Chem.*, 2013, **19**, 106–112.
64 A. M. O'Mahony, D. S. Silvester, L. Aldous, C. Hardacre and R. G. Compton, *J. Chem. Eng. Data*, 2008, **53**, 2884–

2891.
65 H. Tomiyasu, H. Shikata, K. Takao, N. Asanuma, S. Taruta and Y. Y. Park, *Sci. Rep.*, 2017, **7**, 1–12.
66 R. Hayes, G. G. Warr and R. Atkin, *Chem. Rev.*, 2015, **13**, 6357–6426.
67 A. M. Filipa Clá udio, L. Swift, J. P. Hallett, T. Welton, J. A. P Coutinho and M. G. Freire, *Phys. Chem. Chem. Phys*, 2014, **16**, 6593.
68 M. A. Ab Rani, A. Brant, L. Crowhurst, A. Dolan, M. Lui, N. H. Hassan, J. P. Hallett, P. A. Hunt, H. Niedermeyer, J. M. Perez-Arlandis, M. Schrems, T. Welton and R. Wilding, *Phys. Chem. Chem. Phys.*, 2011, **13**, 16831–16840.
69 H. Niedermeyer, C. Ashworth, A. Brandt, T. Welton and P. A. Hunt, *Phys. Chem. Chem. Phys.*, 2013, **15**, 11566–11578.
70 R. E. Del Sesto, T. M. McCleskey, C. Macomber, K. C. Ott, A. T. Koppisch, G. A. Baker and A. K. Burrell, *Thermochim. Acta*, 2009, **491**, 118–120.
71 V. Kamavaram and R. G. Reddy, *Int. J. Therm. Sci.*, 2008, **47**, 773–777.
72 A. Seeberger, A.-K. Andresen and A. Jess, *Phys. Chem. Chem. Phys.*, 2009, **11**, 9375–9381.
73 A. Brandt, J. Gräsvik, J. P. Hallett and T. Welton, *Green Chem.*, 2013, **15**, 550–583.
74 J. M. Crosthwaite, M. J. Muldoon, J. K. Dixon, J. L. Anderson and J. F. Brennecke, *J. Chem. Thermodyn.*, 2005, **37**, 559–568.
75 M. E. V. Valkenburg, R. L. Vaughn, M. Williams and J. S. Wilkes, *Thermochim. Acta*, 2005, **425**, 181–188.
76 M. T. Clough, K. Geyer, P. A. Hunt, J. Mertes and T. Welton, *Phys. Chem. Chem. Phys.*, 2013, **15**, 20480–20495.
77 J. G. Huddleston, A. E. Visser, W. M. Reichert, H. D. Willauer, G. A. Broker and R. D. Rogers, *Green Chem.*, 2001, **3**, 156–164.
78 P. Verdía, A. Brandt, J. P. Hallett, M. J. Ray and T. Welton, *Green Chem.*, 2014, **16**, 1617–1627.
79 J. P. Belieres and C. A. Angell, *J. Phys. Chem. B*, 2007, **111**, 4926–4937.
80 M. Shen, Y. Zhang, K. Chen, S. Che, J. Yao and H. Li, *J. Phys. Chem. B*, 2017, **121**, 1372–1376.
81 M. Yoshizawa, W. Xu and C. A. Angell, *J. Am. Chem. Soc.*, 2003, **50**, 15411–15419.
82 J. Stoimenovski, E. I. Izgorodina and D. R. MacFarlane, *Phys. Chem. Chem. Phys.*, 2010, **12**, 10341–10347.
83 W. Xu, *Science*, 2003, **302**, 422–425.
84 L. Chen, M. Sharifzadeh, N. Mac Dowell, T. Welton, N. Shah and J. P. Hallett, *Green Chem.*, 2014, **16**, 3098–3106.
85 C. Chiappe, A. Mezzetta, C. S. Pomelli, G. Iaquaniello, A. Gentile and B. Masciocchi, *Green Chem.*, 2016, **18**, 4982–4989.
86 M. Deetlefs and K. R. Seddon, *Green Chem.*, 2010, **12**, 17–30.
87 C. Chambon, PhD Thesis, Imperial College London, 2017.
88 A. George, A. Brandt, K. Tran, S. M. S. N. S. Zahari, D. Klein-Marcuschamer, N. Sun, N. Sathitsuksanoh, J. Shi, V. Stavila, R. Parthasarathi, S. Singh, B. M. Holmes, T. Welton, B. A. Simmons and J. P. Hallett, *Green Chem.*, 2015, **17**, 1728–1734.
89 C. Zhao, G. Burrell, A. A. J. Torriero, F. Separovic, N. F. Dunlop, D. R. Macfarlane and A. M. Bond, *J. Phys. Chem. B*, 2008, **23**, 6923–6936.
90 F. Malaret, PhD Thesis, Imperial College London, 2021.
91 Q. Zhang, Q. Wang, S. Zhang, X. Lu and X. Zhang, *ChemPhysChem*, 2016, **17**, 335–351.
92 B. Peric, J. Sierra, E. Martí, R. Cruañas, M. A. Garau, J. Arning, U. Bottin-Weber and S. Stolte, *J. Hazard. Mater.*, 2013, **261**, 99–105.
93 K. S. Egorova and V. P. Ananikov, *ChemSusChem*, 2014, **7**, 336–360.
94 S. Stolte, M. Matzke, J. Arning, A. Böschen, W.-R. Pitner, U. Welz-Biermann, B. Jastorff and J. Ranke, *Green Chem.*, 2007, **9**, 1170–1179.
95 M. V. Oliveira, B. T. Vidal, C. M. Melo, R. C. de de Miranda, C. M. Soares, ao A. Coutinho, P. Sonia Ventura, S. Mattedi and A. S. Lima, *Chemo*, 2016, **147**, 460–466.
96 B. Yoo, B. Jing, S. E. Jones, G. A. Lamberti, Y. Zhu, J. K. Shah and E. J. Maginn, *Sci. Rep.*, 2016, **6**, 1–7.
97 M. H. Fatemi and P. Izadiyan, *Chemosphere*, 2011, **84**, 553–563.
98 S. P. M. Ventura, A. M. M. Gonçalves, T. Sintra, J. L. Pereira, F. Gonçalves and J. A. P. Coutinho, *Ecotoxicology*, 2013, **22**, 1–12.
99 X. Wang, C. A. Ohlin, Q. Lu, Z. Fei, J. Hu and P. J. Dyson, *Green Chem.*, 2007, **9**, 1191–1197.
100 S. Stolte, S. Steudte, A. Igartua and P. Stepnowski, *Curr. Org. Chem.*, 2012, **15**, 1946–1973.
101 R. M. Vrikkis, K. J. Fraser, K. Fujita, D. R. MacFarlane and G. D. Elliott, *J. Biomech. Eng.*, 2009, **131**, 1–31.
102 A. Mühlbauer, PhD Thesis, University of Lille, 2014.
103 M. Petkovic, J. L. Ferguson, H. Q. N. Gunaratne, R. Ferreira, M. C. Leitão, K. R. Seddon, L. P. N. Rebelo and C. S. Pereira, *Green Chem.*, 2010, **12**, 643–64.
104 H. Garcia, R. Ferreira, M. Petkovic, J. L. Ferguson, M. C. Leitão, H. Q. N. Gunaratne, K. R. Seddon, L. P. N. Rebelo and C. Silva Pereira, *Green Chem.*, 2010, **12**, 367–36.
105 M. Markiewicz, J. Maszkowska, V. Nardello-Rataj and S. Stolte, *RSC Adv.*, 2016, **6**, 87325–87331.
106 N. Gathergood, M. T. Garcia and P. J. Scammells, *Green Chem.*, 2004, **6**, 166–175.
107 N. Gathergood, P. J. Scammells and M. T. Garcia, *Green Chem.*, 2006, **8**, 156–160.
108 M. T. Garcia, N. Gathergood and P. J. Scammells, *Green Chem.*, 2005, **7**, 9–14.
109 L. Liu, Y. Hu, P. Wen, N. Li, M. Zong, B. Ou-Yang and H. Wu, *Biotechnol. Biofuels*, 2015, **8**, 119–128.
110 Y. Cao and T. Mu, *Ind. Eng. Chem. Res.*, 2014, **53**, 8651–8664.

111 A. Haiß, A. Jordan, J. Westphal, E. Logunova, N. Gathergood and K. Kümmerer, *Green Chem.*, 2016, **18**, 4361–4373.
112 Y. Deng, I. Beadham, M. Ghavre, M. F. Costa Gomes, N. Gathergood, P. Husson, B. Légeret, B. Quilty, M. Sancelme and P. Besse-Hoggan, *Green Chem.*, 2015, **17**, 1479–1491.
113 J. E. S. J. Reid, N. Sullivan, L. Swift, G. A. Hembury, S. Shimizu and A. J. Walker, *Sustain. Chem. Process.*, 2015, **3**, 17–28.
114 J. Hulsbosch, D. E. De Vos, K. Binnemans and R. Ameloot, *ACS Sustain. Chem. Eng.*, 2016, **4**, 2917–2931.
115 R. A. Sheldon, *Green Chem.*, 2017, **19**, 18–43.
116 A. A. Barzinjy, S. M. Hamad and A. F. Arkawazi, *Jordan J. Phys.*, 2019, **12**, 45–62.
117 M. Caillon-caravanier, C. Le Floch and D. Lemordant, *J. Phys. Chem. B*, 2008, **112**, 9406–9411.
118 C. Wang, L. Guo, H. Li, Y. Wang, J. Weng and L. Wu, *Green Chem.*, 2006, **8**, 603–607.
119 M. P. Marszałł and R. Kaliszan, *Crit. Rev. Anal. Chem.*, 2007, **37**, 127–140.
120 M. Ramdin, T. W. De Loos and T. J. H. Vlugt, *Ind. Eng. Chem. Res.*, 2012, **51**, 8149–8177.
121 R. P. Swatloski, S. K. Spear, J. D. Holbrey and R. D. Rogers, *J. Am. Chem. Soc.*, 2002, **124**, 4974–4975.
122 F. J. V. Gschwend, L. M. Hennequin, A. Brandt-Talbot, F. Bedoya-Lora, G. H. Kelsall, K. Polizzi, P. S. Fennell and J. P. Hallett, *Green Chem.*, 2020, **22**, 5032–5041.
123 A. Schindl, M. L. Hagen, S. Muzammal, H. A. D. Gunasekera and A. K. Croft, *Front. Chem.*, 2019, **7**, 1–31.
124 T. Welton, *Coord. Chem. Rev.*, 2004, **248**, 2459–2477.
125 P. A. Ganeshpure, G. George and J. Das, *J. Mol. Catal. A Chem.*, 2008, **279**, 182–186.
126 F. Liu, Y. Deng, X. Han, W. Hu and C. Zhong, *J. Alloys Compd.*, 2016, **654**, 163–170.
127 N. Sun, H. Rodríguez, M. Rahman and R. D. Rogers, *Chem. Commun.*, 2011, **47**, 1405–1421.
128 A. Sonnenberg, J. Baars and P. Hendrickx, *IEA Bioenergy Task 42 Biorefinery*, 2013.
129 A. Mohr and S. Raman, *Energy Policy*, 2013, **63**, 114–122.
130 C. E. Vlachos, N. A. Mariolis and G. N. Skaracis, *J. Agric. Sci.*, 2015, **153**, 853–861.
131 A. Gasparatos, P. Stromberg and K. Takeuchi, *Anim. Front.*, 2013, **3**, 12–26.
132 A. V. Umakanth, H. A. Bhargavi, L. Keerthi and V. A. Tonapi, in *Sorghum in the 21st Century: Food – Fodder – Feed – Fuel for a Rapidly Changing World*, eds. V. A. Tonapi, H. S. Talwar, A. K. Are, B. V. Bhat, C. R. Reddy and T. J. Dalton, Springer, Singapore, 2020, pp. 705–721.
133 A. Singh, S. I. Olsen and P. S. Nigam, *J. Chem. Technol. Biotechnol.*, 2011, **86**, 1349–1353.
134 J. P. Maity, J. Bundschuh, C. Y. Chen and P. Bhattacharya, *Energy*, 2014, **78**, 104–113.
135 Y. Sun and J. Cheng, *Bioresour. Technol.*, 2002, **83**, 1–11.
136 J. Shi, J. M. Gladden, N. Sathitsuksanoh, P. Kambam, L. Sandoval, D. Mitra, S. Zhang, A. George, S. W. Singer, B. A. Simmons and S. Singh, *Green Chem.*, 2013, **15**, 2579.
137 A. Singh, B. M. Smyth and J. D. Murphy, *Renew. Sustain. Energy Rev.*, 2010, **14**, 277–288.
138 A. J. Haughton, A. J. Bond, A. A. Lovett, T. Dockerty, G. Sünnenberg, S. J. Clark, D. A. Bohan, R. B. Sage, M. D. Mallott, V. E. Mallott, M. D. Cunningham, A. B. Riche, I. F. Shield, J. W. Finch, M. M. Turner and A. Karp, *J. Appl. Ecol.*, 2009, **46**, 315–322.
139 N. Sathitsuksanoh, Z. Zhu, N. Templeton, J. A. Rollin, S. P. Harvey and Y. H. P. Zhang, *Ind. Eng. Chem. Res.*, 2009, **48**, 6441–6447.
140 Q. Hou, M. Ju, W. Li, L. Liu, Y. Chen, Q. Yang and H. Zhao, *Molecules*, 2017, **22**, 1–24.
141 T. V. Doherty, M. Mora-Pale, S. E. Foley, R. J. Linhardt and J. S. Dordick, *Green Chem.*, 2010, **12**, 1967–1975.
142 P. Alvira, E. Tomás-Pejó, M. Ballesteros and M. J. Negro, *Bioresour. Technol.*, 2010, **101**, 4851–4861.
143 P. Kumar, P. Kumar, D. M. Barrett, D. M. Barrett, M. J. Delwiche, M. J. Delwiche, P. Stroeve and P. Stroeve, *Ind. Eng. Chem. (Analytical Ed.*, 2009, **48**, 3713–3729.
144 D. Menegol, A. L. Scholl, R. C. Fontana, A. J. P. Dillon and M. Camassola, *Energy Convers. Manag.*, 2014, **88**, 1252–1256.
145 N. Mosier, C. Wyman, B. Dale, R. Elander, Y. Y. Lee, M. Holtzapple and M. Ladisch, *Bioresour. Technol.*, 2005, **96**, 673–686.
146 S. H. Lee, T. V. Doherty, R. J. Linhardt and J. S. Dordick, *Biotechnol. Bioeng.*, 2009, **102**, 1368–1376.
147 A. Brandt-Talbot, F. J. V. Gschwend, P. S. Fennell, T. M. Lammens, B. Tan, J. Weale and J. P. Hallett, *Green Chem.*, 2017, **19**, 3078–3102.
148 K. Houston, M. R. Tucker, J. Chowdhury, N. Shirley and A. Little, *Front. Plant Sci.*, 2016, **7**, 1–18.
149 A. Heredia, A. Jiménez and R. Guillén, *Z. Lebensm. Unters. Forsch.*, 1995, **200**, 24–31.
150 H. Zabed, J. N. Sahu, A. Suely, A. N. Boyce and G. Faruq, *Renew. Sustain. Energy Rev.*, 2017, **71**, 475–501.
151 M. Zavrel, D. Bross, M. Funke, J. Büchs and A. C. Spiess, *Bioresour. Technol.*, 2009, **100**, 2580–2587.
152 J. D. McMillan, in *Enzymatic Conversion of Biomass for Fuels Production*, eds. M. E. Himmel, J. O. Baker and R. Overend, American Chemical Society, Washington, 1994, pp. 292–324.
153 C. Li, L. Sun, B. A. Simmons and S. Singh, *Bioenergy Res.*, 2013, **6**, 14–23.
154 A. C. O'Sullivan, *Cellulose*, 1997, **4**, 173–207.
155 R. C. Pettersen, in *The Chemistry of Solid Wood*, ed. R. Rowell, American Chemical Society, Washington, 1984, pp. 57–126.
156 K. H. Gardner and J. Blackwell, *Biopolymers*, 1974, **13**, 1975–2001.
157 R. J. Moon, A. Martini, J. Nairn, J. Simonsen and J. Youngblood, *Chem. Soc. Rev.*, 2011, **40**, 3941–3994.
158 C. Chen, C. Duan, J. Li, Y. Liu, X. Ma, L. Zheng, J. Stavik and Y. Ni, *BioResources*, 2016, **11**, 5553–5564.

159 L. P. Christov, M. Akhtar and B. A. Prior, *Enzyme Microb. Technol.*, 1998, **23**, 70–74.
160 D. Trache, M. H. Hussin, C. T. Hui Chuin, S. Sabar, M. R. N. Fazita, O. F. A. Taiwo, T. M. Hassan and M. K. M. Haafiz, *Int. J. Biol. Macromol.*, 2016, **93**, 789–804.
161 P. Phanthong, P. Reubroycharoen, X. Hao, G. Xu, A. Abudula and G. Guan, *Carbon Resour. Convers.*, 2018, **1**, 32–43.
162 M. T. Islam, M. M. Alam, A. Patrucco, A. Montarsolo and M. Zoccola, *AATCC J. Res.*, 2014, **1**, 17–23.
163 L. Peng, L. Lin, J. Zhang, J. Zhuang, B. Zhang and Y. Gong, *Molecules*, 2010, **15**, 5258–5272.
164 M. Dusselier and B. F. Sels, *Top. Curr. Chem.*, 2014, **353**, 85–126.
165 S. Xiao, B. Liu, Y. Wang, Z. Fang and Z. Zhang, *Bioresour. Technol.*, 2014, **151**, 361–366.
166 F. A. Castillo Martinez, E. M. Balciunas, J. M. Salgado, J. M. Domínguez González, A. Converti and R. P. de S. Oliveira, *Trends Food Sci. Technol.*, 2013, **30**, 70–83.
167 K. Yan, C. Jarvis, J. Gu and Y. Yan, *Renew. Sustain. Energy Rev.*, 2015, **51**, 986–997.
168 J. C. Serrano-Ruiz, D. J. Braden, R. M. West and J. A. Dumesic, *Appl. Catal. B Environ.*, 2010, **100**, 184–189.
169 R. J. Van Putten, J. C. Van Der Waal, E. De Jong, C. B. Rasrendra, H. J. Heeres and J. G. De Vries, *Chem. Rev.*, 2013, **113**, 1499–1597.
170 A. Al Ghatta, J. D. E. T. Wilton-Ely and J. P. Hallett, *ACS Sustain. Chem. Eng.*, 2019, **7**, 16483–16492.
171 T. E. Timell, *Wood Sci. Technol.*, 1967, **1**, 45–70.
172 P. Bajpai, *Wood and Fiber Fundamentals*, Elsevier, 3rd edn., 2018.
173 H. V. Scheller and P. Ulvskov, *Annu. Rev. Plant Biol.*, 2010, **61**, 263–289.
174 O. Benaimeche, N. T. Seghir, Ł. Sadowski and M. Mellas, in *Encyclopedia of Renewable and Sustainable Materials*, eds. S. Hashmi and I. Choudhury, Elsevier, 2020, pp. 649–662.
175 X. Liu, Q. Lin, Y. Yan, F. Peng, R. Sun and J. Ren, *Curr. Med. Chem.*, 2018, **26**, 2430–2455.
176 L. Hu, M. Du and J. Zhang, *Open J. For.*, 2018, **08**, 15–28.
177 J. B. Binder, A. V. Cefali, J. J. Blank and R. T. Raines, *Energy Environ. Sci.*, 2010, **3**, 765–771.
178 B. Danon, G. Marcotullio and W. De Jong, *Green Chem.*, 2014, **16**, 39–54.
179 X. Li, P. Jia and T. Wang, *ACS Catal.*, 2016, **6**, 7621–7640.
180 T. Werpy and G. Petersen, *Top value added chemicals from biomass Volume I—Results of screening for potential candidates from sugars and synthesis gas energy efficiency and renewable energy, National Renewable Energy Laboratory, DOE/GO-102004-1992*, 2004.
181 J. B. Binder, J. J. Blank, A. V. Cefali and R. T. Raines, *ChemSusChem*, 2010, **3**, 1268–1272.
182 C. Xu, R. A. D. Arancon, J. Labidi and R. Luque, *Chem. Soc. Rev.*, 2014, **43**, 7485–7500.
183 R. Parthasarathi, R. A. Romero, A. Redondo and S. Gnanakaran, *J. Phys. Chem. Lett.*, 2011, **2**, 2660–2666.
184 J. L. Wen, S. L. Sun, B. L. Xue and R. C. Sun, *Materials (Basel).*, 2013, **6**, 359–391.
185 I. Kögel-Knabner and W. Amelung, in *Treatise on Geochemistry: Second Edition*, eds. H. Holland and K. Turekian, Elsevier, 2nd edn., 2013, vol. 12, pp. 157–215.
186 E. Windeisen and G. Wegener, in *Polymer Science: A Comprehensive Reference*, eds. K. Matyjaszewski and M. Möller, Elsevier B.V., 2012, vol. 10, pp. 255–265.
187 R. B. Santos, E. A. Capanema, M. Y. Balakshin, H. M. Chang and H. Jameel, *J. Agric. Food Chem.*, 2012, **60**, 4923–4930.
188 J. Rencoret, A. Gutiérrez, L. Nieto, J. Jiménez-Barbero, C. B. Faulds, H. Kim, J. Ralph, A. ´ Ngel, T. Martínez, J. C. Del Río and (J Rencoret, *Plant Physiol. Ò*, 2011, **155**, 667–682.
189 M. M. Campbell and R. R. Sederoff, *Plant Physiol.*, **110**, 3–13.
190 O. Y. Abdelaziz, D. P. Brink, J. Prothmann, K. Ravi, M. Sun, J. García-Hidalgo, M. Sandahl, C. P. Hulteberg, C. Turner, G. Lidén and M. F. Gorwa-Grauslund, *Biotechnol. Adv.*, 2016, **34**, 1318–1346.
191 M. Li, Y. Pu and A. J. Ragauskas, *Front. Chem.*, 2016, **4**, 1–8.
192 R. Rinaldi, R. Jastrzebski, M. T. Clough, J. Ralph, M. Kennema, P. C. A. Bruijnincx and B. M. Weckhuysen, *Angew. Chemie - Int. Ed.*, 2016, **55**, 8164–8215.
193 E. G. A. Rocha, T. C. Pin, S. C. Rabelo and A. C. Costa, *Fuel*, 2017, **206**, 145–154.
194 R. Ma, Y. Xu and X. Zhang, *ChemSusChem*, 2015, **8**, 24–51.
195 Y. H. P. Zhang, *J. Ind. Microbiol. Biotechnol.*, 2008, **35**, 367–375.
196 R. H. Narron, H. Kim, H. M. Chang, H. Jameel and S. Park, *Curr. Opin. Biotechnol.*, 2016, **38**, 39–46.
197 J. E. Holladay, J. F. White, J. J. Bozell and D. Johnson, *Top Value-Added Chemicals from Biomass Volume II — Results of Screening for Potential Candidates from Biorefinery Lignin, Pacific Northwest National Lab, PNNL-16983*, Richland, 2007, vol. II.
198 M. P. Pandey and C. S. Kim, *Chem. Eng. Technol.*, 2011, **34**, 29–41.
199 W. Mu, H. Ben, A. Ragauskas and Y. Deng, *Bioenergy Res.*, 2013, **6**, 1183–1204.
200 D. Kai, M. J. Tan, P. L. Chee, Y. K. Chua, Y. L. Yap and X. J. Loh, *Green Chem.*, 2016, **18**, 1175–1200.
201 B. Košíková, A. Gregorová, A. Osvald and J. Krajčovičová, *J. Appl. Polym. Sci.*, 2007, **103**, 1226–1231.
202 L. Liu, G. Huang, P. Song, Y. Yu and S. Fu, *ACS Sustain. Chem. Eng.*, 2016, **4**, 4732–4742.
203 J. F. Kadla, S. Kubo, R. A. Venditti, R. D. Gilbert, A. L. Compere and W. Griffith, *Carbon N. Y.*, 2002, **40**, 2913–2920.
204 W. Fang, S. Yang, X.-L. Wang, T.-Q. Yuan and R.-C. Sun, *Green Chem.*, 2017, **19**, 1794–1827.
205 H. Sadeghifar, R. Venditti, J. Jur, R. E. Gorga and J. J. Pawlak, *ACS Sustain. Chem. Eng.*, 2017, **5**, 625–631.
206 Y. Ge and Z. Li, *ACS Sustain. Chem. Eng.*, 2018, **6**, 7181–7192.

207 R. Abejón, H. Pérez-Acebo and L. Clavijo, *Processes*, 2018, **6**, 1–50.
208 R. C. Sun, *ChemSusChem*, 2020, **13**, 4385–4393.
209 N. Zhang, S. Li, L. Xiong, Y. Hong and Y. Chen, *Model. Simul. Mater. Sci. Eng.*, 2015, **23**, 85010.
210 J. P. Joseleau, N. Cartier, G. Chambat, A. Faik and K. Ruel, *Biochimie*, 1992, **74**, 81–88.
211 D. J. Cosgrove, *Nat. Rev. Mol. Cell Biol.*, 2005, **6**, 850–861.
212 N. Giummarella, Y. Pu, A. J. Ragauskas and M. Lawoko, *Green Chem.*, 2019, **21**, 1573–1595.
213 J. H. Grabber, *Crop Sci.*, 2005, **45**, 820–831.
214 A. Isogai, A. Ishizu and J. Nakano, *J. Wood Chem. Technol.*, 1987, **7**, 463–483.
215 A. Isogai, A. Ishizu and J. Nakano, *J. Wood Chem. Technol.*, 1987, **7**, 311–324.
216 J. Obst, *Tappi*, 1982, **65**, 109–12.
217 T. Koshijima and T. Watanabe, *Association between Lignin and Carbohydrates in Wood and other Plant Tissues*, Springer, Heidelberg, 2003.
218 H. Nishimura, A. Kamiya, T. Nagata, M. Katahira and T. Watanabe, *Sci. Rep.*, 2018, **8**, 1–11.
219 L. Kyllönen, A. Parviainen, S. Deb, M. Lawoko, M. Gorlov, I. Kilpeläinen and A. W. T. King, *Green Chem.*, 2013, **15**, 2374–2378.
220 J. E. Stone, A. M. Scallan, E. Donefer and E. Ahlgren, *Adv. Chem. Ser.*, 1969, **95**, 219–241.
221 L. Kumar, V. Arantes, R. Chandra and J. Saddler, *Bioresour. Technol.*, 2012, **103**, 201–208.
222 J. A. Perez-Pimienta, M. G. Lopez-Ortega, P. Varanasi, V. Stavila, G. Cheng, S. Singh and B. A. Simmons, *Bioresour. Technol.*, 2013, **127**, 18–24.
223 T. C. Pin, P. Y. S. Nakasu, S. Mattedi, S. C. Rabelo and A. C. Costa, *Fuel*, 2019, **235**, 1506–1514.
224 B. Yang and C. E. Wyman, *Biofuels, Bioprod. Biorefining*, 2008, **2**, 26–40.
225 A. S. A. Da Silva, H. Inoue, T. Endo, S. Yano and E. P. S. Bon, *Bioresour. Technol.*, 2010, **101**, 7402–7409.
226 Z. Miao, T. E. Grift, A. C. Hansen and K. C. Ting, *Ind. Crops Prod.*, 2011, **33**, 504–513.
227 A. Brandt, J. K. Erickson, J. P. Hallett, R. J. Murphy, A. Potthast, M. J. Ray, T. Rosenau, M. Schrems and T. Welton, *Green Chem.*, 2012, **14**, 1079–1085.
228 L. Cadoche and G. D. López, *Biol. Wastes*, 1989, **30**, 153–157.
229 J. Li, G. Henriksson and G. Gellerstedt, *Bioresour. Technol.*, 2007, **98**, 3061–3068.
230 L. A. Donaldson, K. K. Y. Wong and K. L. Mackie, *Wood Sci. Technol.*, 1988, **22**, 103–114.
231 H. Peng, L. Gao, M. Li, Y. Shen, Q. Qian and X. Li, *RSC Adv.*, 2014, **4**, 36603–36614.
232 A. D. Moreno, E. Tomás-Pejó, M. Ballesteros and M. J. Negro, in *Biofuels: Alternative Feedstocks and Conversion Processes for the Production of Liquid and Gaseous Biofuels*, eds. A. Pandey, C. Larroche, C.-G. Dussap, E. Gnansounou, S. K. Khanal and S. Ricke, Elsevier, 2nd edn., 2019, pp. 379–399.
233 J. Zhang, H. Zhou, D. Liu and X. Zhao, in *Lignocellulosic Biomass to Liquid Biofuels*, eds. A. Yousuf, F. Sannino and D. Pirozzi, Elsevier, 2019, pp. 17–65.
234 J. A. Perez-Pimienta, C. A. Flores-Gómez, H. A. Ruiz, N. Sathitsuksanoh, V. Balan, L. da Costa Sousa, B. E. Dale, S. Singh and B. A. Simmons, *Bioresour. Technol.*, 2016, **211**, 216–223.
235 N. S. Mosier, R. Hendrickson, M. Brewer, N. Ho, M. Sedlak, R. Dreshel, G. Welch, B. S. Dien, A. Aden and M. R. Ladisch, *Appl. Biochem. Biotechnol. - Part A Enzym. Eng. Biotechnol.*, 2005, **125**, 77–97.
236 C. E. Wyman, B. E. Dale, R. T. Elander, M. Holtzapple, M. R. Ladisch and Y. Y. Lee, *Bioresour. Technol.*, 2005, **96**, 1959–1966.
237 Y. Zheng, H. M. Lin and G. T. Tsao, *Biotechnol. Prog.*, 1998, **14**, 890–896.
238 A. R. C. Morais, A. M. Da, C. Lopes and R. Bogel-Łukasik, *Chem. Rev.*, 2015, **115**, 3–27.
239 B. S. Donohoe, S. R. Decker, M. P. Tucker, M. E. Himmel and T. B. Vinzant, *Biotechnol. Bioeng.*, 2008, **101**, 913–925.
240 S. V. Pingali, V. S. Urban, W. T. Heller, J. McGaughey, H. ONeill, M. Foston, D. A. Myles, A. Ragauskas and B. R. Evans, *Biomacromolecules*, 2010, **11**, 2329–2335.
241 Y. Pu, F. Hu, F. Huang, B. H. Davison and A. J. Ragauskas, *Biotechnol. Biofuels*, 2013, **6**, 1–13.
242 P. Bajpai, in *Pretreatment of Lignocellulosic Biomass for Biofuel Production*, ed. P. Bajpai, Springer, Singapore, 2016, pp. 17–70.
243 D. Wei Kit Chin, S. Lim, Y. L. Pang and M. K. Lam, *Biofuels, Bioprod. Biorefining*, 2020, **14**, 808–829.
244 X. Zhao, K. Cheng and D. Liu, *Appl. Microbiol. Biotechnol.*, 2009, **82**, 815–827.
245 C. Tang, Y. Chen, J. Liu, T. Shen, Z. Cao, J. Shan, C. Zhu and H. Ying, *Ind. Crops Prod.*, 2017, **95**, 383–392.
246 T. Li and S. Takkellapati, *Biofuels, Bioprod. Biorefining*, 2018, **12**, 756–787.
247 S. Bauer, H. Sorek, V. D. Mitchell, A. B. Ibáñez and D. E. Wemmer, *J. Agric. Food Chem.*, 2012, **60**, 8203–8212.
248 A. Ovejero-Pérez, V. Rigual, J. C. Domínguez, M. V. Alonso, M. Oliet and F. Rodriguez, *Int. J. Biol. Macromol.*, 2020, **157**, 461–469.
249 M. M. Hossain, A. Rawal and L. Aldous, *ACS Sustain. Chem. Eng.*, 2019, **7**, 11928–11936.
250 S. H. Lee, T. V. Doherty, R. J. Linhardt and J. S. Dordick, *Biotechnol. Bioeng.*, 2009, **102**, 1368–1376.
251 K. Kuroda, H. Kunimura, Y. Fukaya and H. Ohno, *Cellulose*, 2014, **21**, 2199–2206.
252 L. K. J. Hauru, M. Hummel, A. W. T. King, I. Kilpeläinen and H. Sixta, *Biomacromolecules*, 2012, **13**, 2896–2905.
253 F. J. V. Gschwend, J. P. Hallett and A. Brandt-Talbot, *Molecules*, 2020, **25**, 2318.
254 M. A. Ab Rani, A. Brant, L. Crowhurst, A. Dolan, M. Lui, N. H. Hassan, J. P. Hallett, P. A. Hunt, H. Niedermeyer, J. M. Perez-Arlandis, M. Schrems, T. Welton and R. Wilding, *Phys. Chem. Chem. Phys.*, 2011, **13**, 16831–16840.
255 G. F. De Gregorio, C. C. Weber, J. Gräsvik, T. Welton, A. Brandt and J. P. Hallett, *Green Chem.*, 2016, **18**, 5456–

5465.
256 B. G. Janesko, *Phys. Chem. Chem. Phys.*, 2011, **13**, 11393–11401.
257 M. J. Kamlet and R. W. Taft, *J. Am. Chem. Soc.*, 1976, **98**, 377–383.
258 V. Rigual, A. Ovejero-Pérez, S. Rivas, J. C. Domínguez, M. V. Alonso, M. Oliet and F. Rodriguez, *ACS Sustain. Chem. Eng.*, 2020, **8**, 1362–1370.
259 J. Sun, N. V. S. N. M. Konda, R. Parthasarathi, T. Dutta, M. Valiev, F. Xu, B. A. Simmons and S. Singh, *Green Chem.*, 2017, **19**, 3152–3163.
260 F. J. V. Gschwend, F. Malaret, S. Shinde, A. Brandt-Talbot and J. P. Hallett, *Green Chem.*, 2018, **20**, 3486–3498.
261 F. J. V. Gschwend, C. L. Chambon, M. Biedka, A. Brandt-Talbot, P. S. Fennell and J. P. Hallett, *Green Chem.*, 2019, **21**, 692–703.
262 L. Weigand, S. Mostame, A. Brandt-Talbot, T. Welton and J. P. Hallett, *Faraday Discuss.*, 2017, **202**, 331–349.
263 B. J. Cox and J. G. Ekerdt, *Bioresour. Technol.*, 2013, **134**, 59–65.
264 F. J. Gschwend, L. M. Hennequin, A. Brandt, F. E. Bedoya-Lora, G. H. Kelsall, K. Polizzi, P. Fennell and J. Hallett, *Green Chem.*, 2020, **22**, 5032–5041.
265 R. de C.M. Miranda, J. V. Neta, L. F. Romanholo Ferreira, W. A. Gomes, C. S. do Nascimento, E. de B. Gomes, S. Mattedi, C. M. F. Soares and Á. S. Lima, *Carbohydr. Polym.*, 2019, **206**, 302–308.
266 P. Y. S. Nakasu, C. J. Clarke, S. C. Rabelo, A. C. Costa, A. Brandt-Talbot and J. P. Hallett, *ACS Sustain. Chem. Eng.*, 2020, **8**, 7952–7961.
267 E. C. Achinivu, R. M. Howard, G. Li, H. Gracz and W. A. Henderson, *Green Chem.*, 2014, **16**, 1114–1119.
268 S. Xia, G. A. Baker, H. Li, S. Ravula and H. Zhao, *RSC Adv.*, 2014, **4**, 10586–10596.
269 H. Ren, M. H. Zong, H. Wu and N. Li, *Ind. Eng. Chem. Res.*, 2016, **55**, 1788–1795.
270 T. Dutta, G. Papa, E. Wang, J. Sun, N. G. Isern, J. R. Cort, B. A. Simmons and S. Singh, *ACS Sustain. Chem. Eng.*, 2018, **6**, 3079–3090.
271 Y. X. An, M. H. Zong, H. Wu and N. Li, *Bioresour. Technol.*, 2015, **192**, 165–171.
272 X.-D. Hou, T. J. Smith, N. Li and M.-H. Zong, *Biotechnol. Bioeng.*, 2012, **109**, 2484–2493.
273 X. D. Hou, N. Li and M. H. Zong, *ACS Sustain. Chem. Eng.*, 2013, **1**, 519–526.
274 N. Sun, R. Parthasarathi, A. M. Socha, J. Shi, S. Zhang, V. Stavila, K. L. Sale, B. A. Simmons and S. Singh, *Green Chem.*, 2014, **16**, 2546–2557.
275 A. George, A. Brandt, K. Tran, S. M. S. N. S. Zahari, D. Klein-Marcuschamer, N. Sun, N. Sathitsuksanoh, J. Shi, V. Stavila, R. Parthasarathi, S. Singh, B. M. Holmes, T. Welton, B. A. Simmons and J. P. Hallett, *Green Chem.*, 2015, **17**, 1728–1734.
276 E. Husson, S. Buchoux, C. Avondo, D. Cailleu, K. Djellab, I. Gosselin, O. Wattraint and C. Sarazin, *Bioresour. Technol.*, 2011, **102**, 7335–7342.
277 A. R. Abouelela, PhD Thesis, Imperial College London, 2021.
278 P. Mäki-Arvela, I. Anugwom, P. Virtanen, R. Sjöholm and J. P. Mikkola, *Ind. Crops Prod.*, 2010, **32**, 175–201.
279 D. Klein-Marcuschamer, B. A. Simmons and H. W. Blanch, *Biofuels, Bioprod. Biorefining*, 2011, **5**, 562–569.
280 F. J. V. Gschwend, C. L. Chambon, M. Biedka, A. Brandt-Talbot, P. S. Fennell and J. P. Hallett, *Green Chem.*, 2019, **21**, 692–703.
281 L. V. Kozlova, P. V. Mikshina and T. A. Gorshkova, *Biochem.*, 2012, **77**, 395–403.
282 K. Shimada, S. Hosoya and T. Ikeda, *J. Wood Chem. Technol.*, 1997, **17**, 57–72.
283 L. Weigand, S. Mostame, A. Brandt-Talbot, T. Welton and J. P. Hallett, *Faraday Discuss.*, 2017, **202**, 331–349.
284 F. Hu and A. Ragauskas, *RSC Adv.*, 2014, **4**, 4317–4323.
285 F. Hu, S. Jung and A. Ragauskas, *ACS Sustain. Chem. Eng.*, 2013, **1**, 62–65.
286 W. C. Tu, L. Weigand, M. Hummel, H. Sixta, A. Brandt-Talbot and J. P. Hallett, *Cellulose*, 2020, **27**, 4745–4761.
287 F. J. V. Gschwend, J. P. Hallett and A. Brandt-Talbot, *Molecules*, 2020, **25**, 1–10.
288 A. Brandt, M. J. Ray, T. Q. To, D. J. Leak, R. J. Murphy and T. Welton, *Green Chem.*, 2011, **13**, 2489–2499.
289 C. L. Chambon, M. Chen, P. S. Fennell and J. P. Hallett, *Front. Chem.*, 2019, **7**, 1–13.
290 W. Tu, PhD Thesis, Imperial College London, 2018.
291 C. L. Chambon, P. Verdía and J. Hallett, *Sci. Reports, Pre-Print*, 2021, 1–29.
292 A. R. Abouelela, S. Tan, G. H. Kelsall and J. P. Hallett, *ACS Sustain. Chem. Eng.*, 2020, **8**, 14441–14461.
293 US20190241679A1, 2019.
294 A. R. Abouelela and J. P. Hallett, *ACS Sustain. Chem. Eng.*, 2021, **9**, 704–716.
295 R. Koshani, T. G. M. Van De Ven and A. Madadlou, *J. Agric. Food Chem.*, 2018, **66**, 7692–7700.
296 T. Isogai, T. Saito and A. Isogai, *Cellulose*, 2011, **18**, 421–431.
297 L. Chen, J. Y. Zhu, C. Baez, P. Kitin and T. Elder, *Green Chem.*, 2016, **18**, 3835–3843.
298 A. S. Sheoran and V. Sheoran, *Miner. Eng.*, 2006, **19**, 105–116.
299 C. Lee, T. D. Fletcher and G. Sun, *Eng. Life Sci.*, 2009, **9**, 11–22.
300 J. S. Dunbabin and K. H. Bowmer, *Sci. Total Environ.*, 1992, **111**, 151–168.
301 J. Vymazal, H. Brix, P. Cooper, R. Haberl, R. Perfler and J. Laber, *Removal mechanisms and types of constructed wetlands*, Backhuys, 1998.
302 J. Vymazal, *Environ. Sci. Technol.*, 2011, **45**, 61–69.
303 H. Brix, *Water Sci. Technol.*, 1999, **40**, 45–50.
304 H. I. Mustapha, PhD Thesis, Wageningen University, 2018.

305 Z. Zhao, C. Xu, X. Zhang and X. Song, *Environ. Sci. Pollut. Res.*, 2019, **26**, 11988–11997.
306 C. Kazner, T. Wintgens and P. Dillon, *Water Reclamation Technologies for Safe Managed Aquifer Recharge*, IWA Publishing, 2012, vol. 11.
307 M. J. Pardue, J. W. Castle, J. H. Rodgers and G. M. Huddleston, *Chemosphere*, 2014, **103**, 67–73.
308 J. Vymazal, *Ecol. Eng.*, 2014, **73**, 724–751.
309 J. Vymazal and T. Březinová, *Environ. Int.*, 2015, **75**, 11–20.
310 J. Vymazal, *Ecol. Eng.*, 2009, **35**, 1–17.
311 T. Pan, X. D. Zhu and Y. P. Ye, *Ecol. Eng.*, 2011, **37**, 248–254.
312 R. L. Knight, *Water Sci. Technol.*, 1997, **35**, 35–43.
313 C. Liquete, A. Udias, G. Conte, B. Grizzetti and F. Masi, *Ecosyst. Serv.*, 2016, **22**, 392–401.
314 P. T. Bobrowsky and B. Marker, Eds., *Encyclopedia of Engineering Geology*, Springer International Publishing, Cham, 2017.
315 G. W. Luther, *Geochim. Cosmochim. Acta*, 1987, **51**, 3193–3199.
316 G. K. Druschel, B. J. Baker, T. M. Gihring and J. F. Banfield, *Geochem. Trans.*, 2004, **5**, 13–32.
317 P. C. Singer and W. Stumm, *Science*, 1970, **167**, 1121–1123.
318 H. Tutu, T. S. McCarthy and E. Cukrowska, *Appl. Geochemistry*, 2008, **23**, 3666–3684.
319 D. K. Nordstrom and C. N. Alpers, *Proc. Natl. Acad. Sci. U. S. A.*, 1999, **96**, 3455–3462.
320 J. Nyquist and M. Greger, *Ecol. Eng.*, 2009, **35**, 630–642.
321 M. S. Humphries, T. S. McCarthy and L. Pillay, *S. Afr. J. Sci.*, 2017, **113**, 63–71.
322 C. Woulds and B. T. Ngwenya, *Appl. Geochemistry*, 2004, **19**, 1773–1783.
323 A. Akcil and S. Koldas, *J. Clean. Prod.*, 2006, **14**, 1139–1145.
324 US Environmental Protection Agency, *Acid Mine Drainage Prediction, EPA 530-R-94-036*, 1994.
325 S. Douglas and T. J. Beveridge, *FEMS Microbiol. Ecol.*, 1998, **26**, 79–88.
326 D. Fortin, B. Davis and T. J. Beveridge, *FEMS Microbiol. Ecol.*, 1996, **21**, 11–24.
327 F. M. Tack, O. W. J. J. Callewaert and M. G. Verloo, *Environ. Pollut.*, 1996, **91**, 199–208.
328 M. C. Chuan, G. Y. Shu and J. C. Liu, *Water. Air. Soil Pollut.*, 1996, **90**, 543–556.
329 B. Gazea, K. Adam and A. Kontopoulos, *Miner. Eng.*, 1996, **9**, 23–42.
330 T. J. Cutright, J. Senko, S. Sivaram and M. York, *Soil Sediment Contam.*, 2012, **21**, 970–984.
331 P. G. Whitehead, G. Hall, C. Neal and H. Prior, *Sci. Total Environ.*, 2005, **338**, 41–51.
332 D. B. Johnson and K. B. Hallberg, *Sci. Total Environ.*, 2005, **338**, 3–14.
333 N. F. Gray, *Environ. Geol.*, 1997, **30**, 62–71.
334 M. J. Brodie, L. M. Broughton and A. Robertson, in *Second international conference on the abatement of acidic drainage*, 1991.
335 G. J. Atchison ', M. G. Henry and M. B. Sandheinrich ', *Environ. Biol. Fishes*, 1987, **18**, 11–25.
336 ATSDR, ATSDR 2011 Subst. Prior. List, https://www.atsdr.cdc.gov/spl/index.html#modalIdString_myTable2017, (accessed 25 October 2017).
337 R. W. Warner, *Ohio J. Sci.*, 1971, **71**, 202–215.
338 J. L. Lackey, *Public Health Rep.*, 1938, **53**, 1499–1507.
339 US Environmental Protection Agency, *Hardrock Mining Framework - Appendix A*, Washington DC, 1997.
340 Mine Environment Neutral Drainage Programme, *Report of Results of a Workshop on Mine Reclamation, MEND REPORT 5.8e*, Ontario, 1994.
341 National Rivers Authority, *Abandoned Mines A Report of the National Rivers Authority*, HMSO Publications, Bristol, 1994.
342 P. L. Younger, S. Banwart and R. S. Hedin, *Mine Water: Hydrology, Pollution, Remediation*, Springer Netherlands, Dordrecht, 2002.
343 M. S. Fennessy, W. J. Mitsch, M. S. Fennessy and W. J. Mitsch, *Water Environ. Fed.*, 1989, **61**, 1691–1701.
344 B. Aubé and J. Zinck, in *Brazil-Canada Seminar on Mine Rehabilitation*, Florianópolis, 2003, pp. 1–12.
345 D. Everett, J. Du Plessis and H. Gussman, in *International Mine Water Association Symposium Zambia*, 1993.
346 P. K. Rai, *Int. J. Phytoremediation*, 2008, **10**, 133–160.
347 F. J. Brenner, *Water Sci. Technol.*, 2001, **44**, 449–454.
348 P. Eger, *Wat. Sci. Tech.*, 1994, **29**, 249–256.
349 S. E. Bailey, T. J. Olin, R. M. Bricka and D. D. Adrain, *Water Res.*, 1999, **33**, 2469–2479.
350 V. Sheoran, A. S. Sheoran and P. Poonia, *Pedosphere*, 2016, **26**, 148–166.
351 S. D. Machemer and T. R. Wildeman, *J. Contam. Hydrol.*, 1992, **9**, 115–131.
352 L. Guo and T. J. Cutright, *Environ. Technol. (United Kingdom)*, 2016, **37**, 1821–1828.
353 M. M. Lasat, *J. Hazard. Subst. Res.*, 2003, **2**, 5–25.
354 C. Garbisu and I. Alkorta, *Bioresour. Technol.*, 2001, **77**, 229–236.
355 M. Ghosh and S. P. Singh, *As. J. Energy Env*, 2005, **6**, 214–231.
356 V. Dushenkov, P. B. A. Nanda Kumar, H. Motto and I. Raskin, *Environ. Sci. Technol.*, 1995, **29**, 1239–1245.
357 C. Pérez-Sirvent, C. Hernández-Pérez, M. J. Martínez-Sánchez, M. L. García-Lorenzo and J. Bech, *J. Soils Sediments*, 2017, **17**, 1384–1393.
358 E. Grisey, X. Laffray, O. Contoz, E. Cavalli, J. Mudry and L. Aleya, *Water. Air. Soil Pollut.*, 2012, **223**, 1723–1741.
359 L. Guo and T. J. Cutright, *Int. J. Phytoremediation*, 2017, **19**, 254–261.

360 A. Aksoy, F. Duman and G. Sezen, *J. Freshw. Ecol.*, 2005, **20**, 783–785.
361 Z. H. Ye, S. N. Whiting, Z.-Q. Lin, C. M. Lytle, N. H. Qian and N. Terry, *J. Environ. Qual.*, 2001, **30**, 1464–1473.
362 H. Wu, J. Zhang, H. H. Ngo, W. Guo, Z. Hu, S. Liang, J. Fan and H. Liu, *Bioresour. Technol.*, 2015, **175**, 594–601.
363 J. H. Qian, A. Zayed, Y. L. Zhu, M. Yu and N. Terry, *J. Environ. Qual.*, 1999, **28**, 1448–1455.
364 M. Rodriguez and J. Brisson, *Ecol. Eng.*, 2016, **91**, 302–309.
365 Piramid Consortium, *ENGINEERING GUIDELINES FOR THE PASSIVE REMEDIATION OF ACIDIC AND / OR METALLIFEROUS MINE DRAINAGE AND SIMILAR WATERS, EVK1-CT-1999-000021*, 2003.
366 F. M. Wilhelm, in *Encyclopedia of Inland Waters*, ed. G. E. Likens, Elsevier Inc., 2009, pp. 110–119.
367 A. K. Choudhary, S. Kumar and C. Sharma, *Pollution*, 2011, **37**, 3666–3672.
368 J. Vymazal, H. Brix, P. Cooper, R. Haberl, R. Perfler and J. Laber, *Removal mechanisms and types of constructed wetlands*, Backhuys, 2006.
369 J. Watson, S. Reed, Robert H. Kadlec, R. L. Knight and A. Whitehouse, in *Constructed Wetlands for Wastewater Treatment: Municipal, Industrial and Agricultural*, ed. D. A. Hammer, 1989, pp. 221–238.
370 S. Norton, Removal Mechanisms in Constructed Wastewater Wetlands, http://home.eng.iastate.edu/~tge/ce421-521/stephen.pdf, (accessed 15 February 2021).
371 J. K. Grove and O. R. Stein, *Water Res.*, 2005, **39**, 4040–4050.
372 C. Polprasert, N. P. Dan and N. Thayalakumaran, *Water Sci. Technol.*, 1996, **34**, 165–171.
373 S. Neralla, R. W. Weaver, B. J. Lesikar and R. A. Persyn, *Bioresour. Technol.*, 2000, **75**, 19–25.
374 R. H. Kadlec and R. L. Knight, *Treatment Wetlands*, CRC Press, Boca Raton, 1996.
375 V. Ottová, J. Balcarová and J. Vymazal, *Water Sci. Technol.*, 1997, **35**, 117–123.
376 M. Chislock and E. Doster, *Nat. Educ.*, 2013, **4**, 1–8.
377 I. Chrous and J. Bartram, *Toxic Cyanobacteria in Water: A guide to their public health consequences, monitoring and management*, E & FN Spon, London, 1999.
378 M. Lehtiniemi, J. Engström-Öst and M. Viitasalo, *Environ. Biol. Fishes*, 2005, **73**, 1–8.
379 R. J. Diaz and R. Rosenberg, *Science*, 2008, **321**, 926–929.
380 W. K. Dodds, W. W. Bouska, J. L. Eitzmann, T. J. Pilger, K. L. Pitts, A. J. Riley, J. T. Schloesser and D. J. Thornbrugh, *Environ. Sci. Technol.*, 2009, **43**, 12–19.
381 R. Kadlec, *Water*, 2016, **8**, 243–278.
382 K. R. Reddy and E. M. D'Angelo, *Glob. Wetl.*, 1994, **23**, 309–324.
383 C. L. McJannet, P. A. Keddy and F. R. Pick, *Funct. Ecol.*, 1995, **9**, 231–238.
384 K. R. Reddy, J. R. White and Y. Wang, *STABILITY AND BIOAVAILABILITY OF RECENTLY ACCRETED PHOSPHORUS IN STORMWATER TREATMENT AREAS Final Report December 2002*, 2002.
385 K. R. Reddy and W. H. Patrick, *C R C Crit. Rev. Environ. Control*, 1984, **13**, 273–309.
386 R. D. Hauck, in *The Natural Environment and the Biogeochemical Cycles*, ed. O. Hutzinger, Springer Verlag, 1984, vol. 1, pp. 105–125.
387 D. J. Spieles and W. J. Mitsch, *Ecol. Eng.*, 1999, **14**, 77–91.
388 O. Shipin, T. Koottatep, N. T. T. Khanh and C. Polprasert, *Water Sci. Technol.*, 2005, **51**, 299–306.
389 R. A. Leng, *Duckweed: A tiny aquatic plant with enormous potential for agriculture and environment*, FAO, 1999.
390 S. Iqbal, *Duckweed Aquaculture. Potentials, Possibilities and Limitations for Combined Wastewater Treatment and Animal Feed Production in Developing Countries, SANDEC Report No. 6/99*, 1999.
391 Identification of Duckweed, https://www2.palomar.edu/users/warmstrong/1wayindx.htm, (accessed 10 October 2018).
392 J. Xu, H. Zhao, A. M. Stomp and J. J. Cheng, *Biofuels*, 2012, **3**, 589–601.
393 P. Ziegler, K. Adelmann, S. Zimmer, C. Schmidt and K. Appenroth, 2015, **17**, 33–41.
394 R. A. Leng, J. H. Stambolie and R. Bell, Duckweed - A Potential High-Protein Feed Resource for Domestic Animals and Fish, http://www.fao.org/ag/aga/agap/frg/lrrd/lrrd7/1/3.htm, (accessed 4 October 2018).
395 D. D. Culley, E. Rejmánková, J. Květ and J. B. Frye, *J. World Maric. Soc.*, 2009, **12**, 27–49.
396 G. Oron, *Agric. Water Manag.*, 1994, **26**, 27–40.
397 S. A. El-Shafai, F. A. El-Gohary, F. A. Nasr, N. Peter van der Steen and H. J. Gijzen, *Bioresour. Technol.*, 2007, **98**, 798–807.
398 G. J. Alaerts, M. D. Rahman Mahbubar and P. Kelderman, *Water Res.*, 1996, **30**, 843–852.
399 K. R. Reddy and W. F. DeBusk, *Econ. Bot.*, 1985, **39**, 200–208.
400 Y. Li, F. Zhang, M. Daroch and J. Tang, *Biosci. Rep.*, 2016, **36**, 1–8.
401 Q. Chen, Y. Jin, G. Zhang, Y. Fang, Y. Xiao and H. Zhao, *Energies*, 2012, **5**, 3019–3032.
402 J. Xu, W. Cui, J. J. Cheng and A. Stomp, *Biosyst. Eng.*, 2011, **110**, 67–72.
403 Worldwatch Institute, *Biofuels for Transport: Global Potential and Implications for Sustainable Energy and Agriculture*, Earthscan, 2007.
404 Growing Duckweed, http://bioponica.net/growing-duckweed/, (accessed 1 September 2018).
405 E. Edwards, M. S. Hassan, C. H. Chao and C. Pacharaprakiti, 1992, **40**, 109–117.
406 J. E. Vermaat and M. Khalid Hanif, *Water Res.*, 1998, **32**, 2569–2576.
407 B. A. Bergmann, J. Cheng, J. Classen and A. M. Stomp, *Bioresour. Technol.*, 2000, **73**, 13–20.
408 K. C. Bal Krishna and C. Polprasert, *Ecol. Eng.*, 2008, **34**, 243–250.
409 C. Gupta and D. Prakash, *Toxicol. Environ. Chem.*, 2014, **95**, 1256–1266.

410 R. A. Mohedano, G. Tonon, R. H. R. Costa, C. Pelissari and P. Belli Filho, *Sci. Total Environ.*, 2019, **691**, 1043–1050.
411 S. Körner and J. E. Vermaat, *Water Res.*, 1998, **32**, 3651–3661.
412 P. Skillicorn, W. Journey and W. Spira, *Duckweed Aquaculture: A New Aquatic Farming System for Developping Countries*, World Bank, Washington DC, 1993.
413 European Commission Report, Critical Raw Materials Resilience: Charting a Path towards greater Security and Sustainability, Communication from the commission to the european parliament COM, 474 final, Brussels, Belgium, http://info.worldbank.org/governance/wgi/., (accessed 12 March 2021).
414 C. B. Sekomo, D. P. L. Rousseau, S. A. Saleh and P. N. L. Lens, *Ecol. Eng.*, 2012, **44**, 102–110.
415 P. Ahmad and M. N. V. Prasad, Eds., *Abiotic Stress Responses in Plants*, Springer, New York, 2012.
416 Z. A., G. S. and T. N., *J. Environ. Qual.*, 1998, **27**, 715–721.
417 S. K. Jain, P. Vasudevan and N. K. Jha, *Biol. Wastes*, 1989, **28**, 115–126.
418 S. S. Sharma and J. P. Gaur, *Ecol. Eng.*, 1994, **4**, 37–43.
419 S. C. Mo, D. S. Choi and J. W. Robinson, *J. Environ. Sci. Heal. . Part A Environ. Sci. Eng.*, 1988, **23**, 139–156.
420 S. H. Bokhari, I. Ahmad and M. Mahmood-ul-hassan, *Int. J. Phytoremediation*, 2016, **18**, 25–32.
421 U. N. Rai, S. Sinha, R. D. Tripathi and P. Chandra, *Ecol. Eng.*, 1995, **5**, 5–12.
422 S. Alvarado, M. Guédez, M. P. Lué-Merú, G. Nelson, A. Alvaro, A. C. Jesús and Z. Gyula, *Bioresour. Technol.*, 2008, **99**, 8436–8440.
423 M. A. Rahman, H. Hasegawa, K. Ueda, T. Maki, C. Okumura and M. M. Rahman, *Chemosphere*, 2007, **69**, 493–499.
424 Z. Leblebici and A. Aksoy, *Water. Air. Soil Pollut.*, 2011, **214**, 175–184.
425 W. Hou, X. Chen, G. Song, Q. Wang and C. Chi Chang, *Plant Physiol. Biochem.*, 2007, **45**, 62–69.
426 Y. UYSAL and F. TANER, *Ekoloji*, 2007, **16**, 9–15.
427 K. N. Velichkova, I. N. Sirakov and D. T. Slavcheva-Sirakova, *Planta Daninha*, 2019, **37**, 19194452.
428 M. A. Jayasri and K. Suthindhiran, *Appl. Water Sci.*, 2017, **7**, 1247–1253.
429 N. Khellaf and M. Zerdaoui, *Iran. J. Environ. Heal. Sci. Eng.*, 2009, **6**, 161–166.
430 Y. Liu, Y. Wang, S. Xu, X. Tang, J. Zhao, C. Yu, G. He, H. Xu, S. Wang, Y. Tang, C. Fu, Y. Ma and G. Zhou, *Plant Biotechnol. J.*, 2019, **17**, 2143–2152.
431 X. Zhao, G. K. Moates, N. Wellner, S. R. A. Collins, M. J. Coleman and K. W. Waldron, *Carbohydr. Polym.*, 2014, **111**, 410–418.
432 X. Zhao, G. K. Moates, D. R. Wilson, R. J. Ghogare, M. J. Coleman and K. W. Waldron, *Biomass and Bioenergy*, 2014, **72**, 206–215.
433 J. J. Cheng and A. M. Stomp, *Clean - Soil, Air, Water*, 2009, **37**, 17–26.
434 W. Cui and J. J. Cheng, *Plant Biol.*, 2015, **17**, 16–23.
435 M. S. Reid and R. L. Bieleski, *Plant Physiol.*, 1970, **46**, 609–613.
436 Y. Lin and S. Tanaka, *Appl. Microbiol. Biotechnol.*, 2006, **69**, 627–642.
437 K. S. Sree and K. Appenroth, *Albanian J. Agric. Sci.*, 2014, 11–14.
438 H. L. White, *Ann. Bot.*, 1928, **3**, 771–782.
439 M. Kesaano, MSC Thesis, Utah State University, 2011.
440 W. Cui, J. Xu, J. J. Cheng and A. M. Stomp, *Biol. Eng.*, 2011, **3**, 187–197.
441 K. J. Appenroth, Á. Keresztes, É. Sárvári, A. Jaglarz and W. Fischer, *Plant Biol.*, 2003, **5**, 315–323.
442 K. Appenroth, K. Krech, Á. Keresztes, W. Fischer and H. Koloczek, *Chemosphere*, 2010, **78**, 216–223.
443 W. Cui, J. Xu and J. J. Cheng, in *American Society of Agricultural and Biological Engineers Annual International Meeting*, Louisville, 2011, vol. 7, pp. 5820–5834.
444 J. Xu, W. Cui, J. J. Cheng and A. M. Stomp, *Biosyst. Eng.*, 2011, **110**, 67–72.
445 S. Soda, T. Ohchi, J. Piradee, Y. Takai and M. Ike, *Biomass and Bioenergy*, 2015, **81**, 364–368.
446 A. Faizal, A. A. Sembada and N. Priharto, *Saudi J. Biol. Sci.*, 2021, **28**, 294–301.
447 D. Pagliuso, A. Grandis, E. Lam and M. S. Buckeridge, *Bioenergy Res.*, 2020, 1–11.
448 O. Calicioglu and R. A. Brennan, *Bioresour. Technol.*, 2018, **257**, 344–348.
449 X. Zhao, G. K. Moates, A. Elliston, D. R. Wilson, M. J. Coleman and K. W. Waldron, *Bioresour. Technol.*, 2015, **194**, 263–269.
450 X. Zhao, A. Elliston, S. R. A. Collins, G. K. Moates, M. J. Coleman and K. W. Waldron, *Biomass and Bioenergy*, 2012, **47**, 354–361.
451 W. D. Huang and Y. H. Percival Zhang, *Energy Environ. Sci.*, 2011, **4**, 784–792.
452 L. R. F. Souto, I. F. da Silva, J. L. Ninow, S. R. A. Collins, A. Elliston and K. W. Waldron, *Biomass and Bioenergy*, 2019, **127**, 1–7.
453 S. Soda, T. Ohchi, J. Piradee, Y. Takai and M. Ike, *Biomass and Bioenergy*, 2015, **81**, 364–368.
454 D. Yadav, L. Barbora, D. Bora, S. Mitra, L. Rangan and P. Mahanta, *Int. Biodeterior. Biodegrad.*, 2017, **119**, 253–259.
455 P. Duan, Z. Chang, Y. Xu, X. Bai, F. Wang and L. Zhang, *Bioresour. Technol.*, 2013, **135**, 710–719.
456 C. Liu, Q. Feng, J. Yang and X. Qi, *Bioresour. Technol.*, 2018, **255**, 50–57.
457 F. Lai, Y. Jin, L. Tan, K. He, L. Guo, X. Tian, J. Li, A. Du, Y. Huang, H. Zhao and Y. Fang, *Biomass Convers. Biorefinery*, 2021, 1–12.

Chapter 2: Effects of Physical Structure of Alkylammonium Hydrogen Sulfate Ionic Liquids on Acidity and Pretreatment Efficacy

2.1 Introduction

Due to their solvation capabilities and high chemical activity, ionic liquids (ILs) have attracted interest for use in acid catalysis. Part of this interest has focussed on the use of ILs as reaction media, which are subsequently acidified by addition of a Lewis or Bronsted acid.[1–7] ILs have been shown to enhance the acidity of dissolved acids in certain systems,[1,8,9] and have also been shown to play an active role in catalysing certain reactions beyond their role as a solvent.[1,10] Of particular interest has been the dialkylimidazolium chloride-aluminium chloride system, in which the relative amount of $AlCl_3$ determines whether the system is acidic or basic.[4,5,9] There has also been a number of studies in which the ILs themselves have introduced acidity into the system, serving as solvent-catalysts. This involves ILs with an acidic proton on either the anion or cation (e.g. $[HSO_4]^-$ and $[H_2PO_4]^-$, $[Hmim]^+$, or the slightly acidic C_2 proton in disubstituted imidazolium cations),[9,11–14] as well as by incorporating acidic functional groups (e.g. -COOH or $-SO_3H$) in so-called Bronsted functionalised ILs.[9,15–19] A comprehensive review of the theory and applications of ionic liquids in acid catalysis can be found in the work of Johnson et al,[9] with a more recent review of applications in the works of Vekariya and Vafaeezadeh.[17,19] However, acidity in ionic liquids is challenging to predict using aqueous acid-base theory, due to complex ionic and hydrogen bond interactions in the non-aqueous environment.[20–23] The acidity of such non-aqueous systems is typically expressed using the Hammett acidity function (H_0). Analogous to pH, H_0 is a logarithmic scale for expressing acidity of liquids. The use of the H_0 function allows the acidity of a medium to be measured directly, thus avoiding any solvent levelling effects and allowing comparison between solvents. H_0 has typically been determined by measuring the degree of protonation of UV probe molecules, although a method of determination by NMR has also been developed to overcome certain limitations of the spectrophotometric method.[24,25]

Lignocellulose is a matrix of three polymers: cellulose, hemicellulose, and lignin. While each of these polymers may be processed to yield useful products, the lignocellulosic matrix is extremely recalcitrant to chemical and enzymatic attack, and must therefore be modified to allow further processing; this process is referred to as pretreatment. There exists a large number of pretreatment technologies that act via different mechanisms and thus may achieve different pretreatment outcomes (detailed further

in Chapter 1). Among these, several of the most prominent use acid catalysis, notably dilute acid (DA), acid-catalysed organosolv, and ionoSolv pretreatment. In all of these pretreatment processes, glycosidic linkages in the hemicellulose polymer are hydrolysed, with the resulting oligomers and monomers dissolved into the liquid phase, while the lignin β-*O*-4' ether linkages are hydrolysed.[26–32] However, there are some differences regarding the effects on the lignin fraction. During ionoSolv and acid-catalysed organosolv pretreatment, the ether bond cleavage allows dissolution of the lower molecular weight lignin fragments.[26,28,30–33] In DA pretreatment, however, there is limited lignin removal due to the low solubility of lignin in the aqueous solution.[29] The lignin instead redistributes by coalescing before redepositing onto the cell wall as spherical droplets.[29,34,35]

Studies on the ionoSolv process have mostly focussed on protic ILs with $[HSO_4]^-$ and Cl^- anions. The effect of acidity on the ionoSolv process has been investigated in a number of studies using these anions. Jia et al. compared the abilities of 3 ILs to catalytically hydrolyse the β-*O*-4' linkage in lignin model compounds: 1-methyl-imidazolium chloride ([Hmim]Cl), 1-butyl-3-methyl-imidazolium chloride ([bmim]Cl), and 1-butyl-2,3-dimethyl-imidazolium chloride ([bmmim]Cl).[36] [Hmim]Cl was found to substantially outperform both other ILs, achieving 71% conversion compared to under 5%. This trend was attributed to the presence of H^+ ions in solution and thus increased acidity using the $[Hmim]^+$ cation, compared to the slight acidity of the $[bmim]^+$ cation and lack of acidity of the $[bdmim]^+$ cation. In a follow-up study, Cox et al. investigated the ability of 5 different ILs to cleave the β-*O*-4' linkage in lignin model compounds.[30] In addition to [bmim][HSO_4], the remaining four ILs contained the $[Hmim]^+$ cation paired with the Cl^-, $[HSO_4]^-$, $[BF_4]^-$, and Br^- anions. All ILs were found to be acidic (H_0 between 1.48 and 2.08), but the rates of hydrolysis did not correlate with the relative acidities, indicating an anion interaction effect.

A number of studies have also investigated the effect of modifying the acid-base ratio of $[HSO_4]^-$ ILs. Verdía et al. investigated the effect of varying the acid/base ratio of 1-butyl-imidazolium hydrogen sulfate ([Hbim][HSO_4]) on its pretreatment effectiveness, using mostly excess base conditions in the pretreatment of *Miscanthus*.[37] Addition of excess acid led to accelerated kinetics, leading to higher hemicellulose removal for a given duration. A similar trend was observed for delignification (as well as precipitated lignin yields), except for high quantities of excess acid, at which lignin and pseudolignin redeposition occurred. As a result, pulp cellulose content increased with increasing acidity up to 1% excess acid, and was tracked by pulp digestibility. Despite this, saccharification yields were found to be fairly constant between 20% excess base and 1% excess acid, due to increased glucan degradation and lignin/pseudolignin redeposition with increasing acid. This study, therefore, showed that the acid/base ratio of the IL may be tuned in order to improve reaction kinetics. The lack of acid/base data points between 1% excess acid and 50% excess acid and the relatively small number of timepoints,

however, limit the conclusions that may be drawn about excess acid pretreatments from this study. Brandt-Talbot et al. compared the pretreatment of *Miscanthus* with stoichiometric [TEA][HSO_4] and [TEA][HSO_4] with 9% excess acid.[26] Once again, increasing the acid/base ratio was found to lead to accelerated hemicellulose and lignin removal, reducing the time required to reach the optimum saccharification yield, although this maximum was below that achieved by the stoichiometric IL. 2D HSQC NMR and GPC analysis of the precipitated lignin revealed that both lignin ether bond cleavage and condensation were also accelerated, consistent with the more rapid delignification and pseudolignin formation. Weigand et al. varied the acid/base ratio of [DMBA][HSO_4] between 0.98 and 1.02 at multiple temperatures in the pretreatment of willow.[38] There was found to be an interplay between acid/base ratio and temperature, with increases in both leading to increased pretreatment severity and thus accelerating the process.

There have been a range of studies into different ionoSolv process parameters: varying pretreatment temperature and duration[38–40], water content[37,41], biomass loading[42,43], biomass particle size[43], and variations in acid/base ratio.[26,37,38] Its effectiveness on a wide range of feedstock types has also been confirmed.[26,38,39,44–46] However, despite ILs being called 'designer solvents' due to their inherent tunability, there has been relatively little work done on the effect of IL structure in the ionoSolv process. Currently, two tertiary alkylammonium cations and two alkylimidazolium cations dominate ionoSolv studies: $[TEA]^+$, dimethylbutylammonium ($[DMBA]^+$), 1-methylimidazolium ($[Hmim]^+$), and 1-butylimidazolium ($[Hbim]^+$). IL cost has been shown to play a significant role in overall process economics and is dominated by the cost of the amine in alkylammonium $[HSO_4]^-$ ILs.[47,48] Due to the extremely low cost of sulfuric acid and their one-step synthesis, this class of ILs can be produced as cheaply as \$0.78/kg.[49] However, the use of a simpler alkylamine reagent would allow further savings to be made. George et al. varied alkylammonium cation structure in ILs containing the $[HSO_4]^-$ IL when pretreating switchgrass.[47] One pretreatment temperature and duration (120 °C, 180 minutes) was used for all ILs, with saccharification yield used to evaluate performance. However, this single pretreatment condition was not optimised for all ILs. Decreasing degree of substitution of the cation, from triethylammonium ($[TEA]^+$) to monoethylammonium, was found to lead to significantly decreasing saccharification yields. Unlike other ILs tested, lignin recoveries using monoethylammonium were indicative of pseudolignin formation, typical of excessively severe pretreatment conditions.[26,38,40] Gschwend et al. screened three different cations with the $[HSO_4]^-$ anion in the pretreatment of pine: $[TEA]^+$, $[DMBA]^+$, and $[Hbim]^+$.[39] Once again, a single pretreatment condition was used to compare the three ILs, using the optimised conditions for [Hbim][HSO_4] (170 °C, 30 minutes). The choice of cation was found to have a significant effect on pretreatment efficacy, with

[DMBA][HSO_4] and [Hbim][HSO_4] having saccharification yields around twice as high as [TEA][HSO_4] as well as more extensive β-*O*-4' bond cleavage.

In this chapter, timecourse pretreatments were carried out using alkylammonium [HSO_4] ILs with different degrees of cation substitution (shown in Fig. 2.1), Hammett acidities, and acid/base ratios. Thus, it aims to further investigate both the effect of acidity and cation structure on pretreatment performance. Unlike the study of George et al, timecourse experiments allow different ILs to be compared at more optimal conditions, leading to a fairer comparison.[47] *Miscanthus x giganteus* has been used as the pretreatment feedstock for this study. It is a high-yielding energy crop which holds significant potential for future bioenergy use, and has also been well studied in the ionoSolv process using alkylammonium [HSO_4]$^-$ ILs, making results more easily comparable to previous work.[40,43,50]

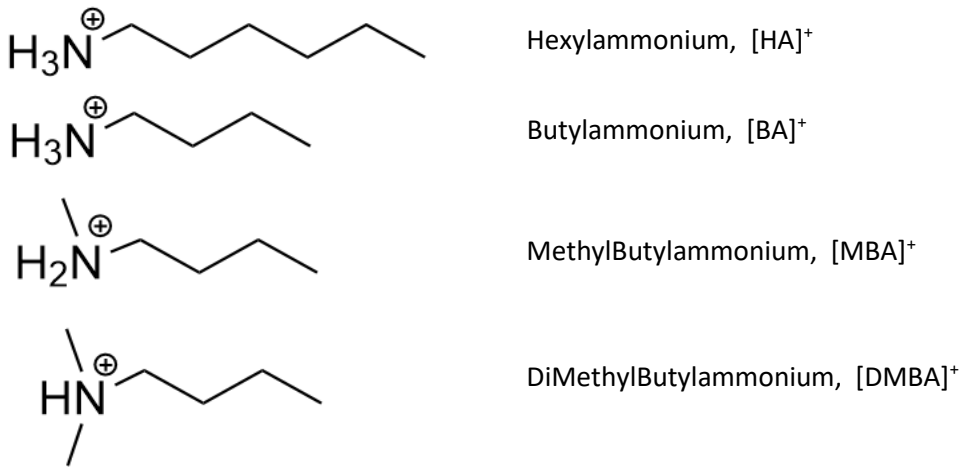


Figure 2.1: Alkylammonium cations screened.

2.2 Materials and Methods

2.2.1 General Equipment

All masses were determined using one of the following balances: AND GH-252 (resolution: 0.00001 g), VWR LA 214i (resolution: 0.0001 g), or VWR LA 254i (resolution: 0.0001 g). The centrifuge used was a VWR Centri Star 3.0. All rotary evaporation was performed using either a Buchi R-300 or a Buchi R-210. All UV-Vis measurements were performed using a Perkin Elmer Lambda 650.

Sugar contents were quantified using a Shimadzu HPLC system with an Aminex HPX-97P column from Bio-rad (300 x 7.8 mm), using purified water as a mobile phase at 0.6 mL/min, and operating at a column temperature of 85 ^{o}C. All samples used filtered through a 0.2 µm PTFE syringe filter. Calibration was carried out for each set of runs, using standards of 0.1, 1, 2, and 4 mg/mL of glucose, xylose, mannose, galactose, and arabinose, as well as 8 mg/mL of glucose. A least squares linear regression fit was used to create a calibration curve.

2.2.2 Materials

N-Methyl-*N*-butylamine (>98.1%) and 5M sulfuric acid were purchased from VWR. *N*-Butylamine (>99.5%), *N*-hexylamine (>99.0%), 4-nitroaniline (>99%), anhydrous dichloromethane (>99.8%), potassium hydrogen phthalate (>99.95%), and Cellic Ctec2 enzymes were purchased from Sigma Aldrich. *N*,*N*-Dimethyl-n-butylamine (>98.0%) was purchased from Tokyo Chemicals Industry. All the above were used as received. The biomass used was *Miscanthus x giganteus*, sourced from Silwood Park campus (Imperial College London), ground and sieved to obtain a particle size of 180-850 µm. Its composition was determined as detailed in Section 2.2.6 and is provided in the Appendix.

2.2.3 IL Synthesis

Using a dropping funnel, sulfuric acid was added dropwise to a round bottomed flask containing the corresponding amine, magnetically stirred and chilled to 0 ^{o}C using an ice bath. IL water content was reduced to below 20% by rotary evaporation as measured using a V20 Volumetric Karl-Fischer Titrator (Mettler-Toledo), standardised using Hydranal water standards. Acid-base ratios were determined by titration by 0.1M NaOH, using a G20S Compact Titrator (Mettler-Toledo), standardised using potassium hydrogen phthalate. Further details are provided in the Appendix. Acid-base ratios are expressed on a molar basis. NMR signals are provided below, with NMR spectra provided in the Appendix.

ButylAmmonium Hydrogen Sulfate [BA][HSO_4] (Figs. A1-1 and A1-2):

^{1}H NMR: δ_H (400 MHz, DMSO-d_6)/ppm: 7.68 (s, 3H, N-*H*$_3$), 4.45 (s, br, *H*$_2$O, *H*SO_4), 2.77 (m, 2H, N-C*H*$_2$), 1.52 (m, 2H, N-CH_2-C*H*$_2$), 1.32 (m, 2H, N-CH_2-CH_2-C*H*$_2$), 0.88 (t, J = 7.3, 3H, N-CH_2-CH_2-CH_2-C*H*$_3$).

^{13}C NMR δ_C (101 MHz, DMSO-d_6)/ppm: 39.12 (N-*C*H_2), 29.43 (N-CH_2-*C*H_2), 19.53 (N-CH_2-CH_2-*C*H_2), 13.94 (N-CH_2-CH_2-CH_2-*C*H_3).

HexylAmmonium Hydrogen Sulfate [HA][HSO_4] (Figs. A1-3 and A1-4):

^{1}H NMR: δ_H (400 MHz, DMSO-d_6)/ppm: 7.67 (s, 3H, N-*H*$_3$), 4.19 (s, br, *H*$_2$O, *H*SO_4), 2.75 (m, 2H, N-C*H*$_2$), 1.51 (m, 2H, N-CH_2-CH_2-CH_2-CH_2-C*H*$_2$), 1.27 (m, 6H, N-CH_2-C*H*$_2$-C*H*$_2$ -C*H*$_2$), 0.86 (m, 3H, N-CH_2-CH_2-CH_2-CH_2-C*H*$_3$).

^{13}C NMR δ_C (101 MHz, DMSO-d_6)/ppm: 39.41 (N-*C*H_2), 31.17 (N-CH_2-*C*H_2), 27.33 (N-CH_2-CH_2-*C*H_2), 25.90 (N-CH_2-CH_2-CH_2-*C*H_2), 22.33 (N-CH_2-CH_2-CH_2-CH_2-*C*H_2), 14.31 (N-CH_2-CH_2-CH_2-CH_2-CH_2-*C*H_3).

MethylButylAmmonium Hydrogen Sulfate [MBA][HSO_4] (Figs. A1-5 and A1-6):

^{1}H NMR: δ_H (400 MHz, DMSO-d_6)/ppm: 8.31 (s, 2H, N-*H*$_2$), 6.41 (s, br, *H*$_2$O, *H*SO_4), 2.98 (m, 2H, N-C*H*$_2$), 2.55 (t, J = 5.5, 3H, N-C*H*$_3$), 1.54 (m, 2H, N-CH_2-C*H*$_2$), 1.31 (h, J = 7.4, 2H, N-CH_2-CH_2-C*H*$_2$), 0.89 (t, J = 7.4, 3H, N-CH_2-CH_2-CH_2-C*H*$_3$).

^{13}C NMR δ_C (101 MHz, DMSO-d_6)/ppm: 48.64 (N-*C*H_3), 33.05 (N-*C*H_2), 27.81 (N-CH_2-*C*H_2), 19.63 (N-CH_2-CH_2-*C*H_2), 13.96 (N-CH_2-CH_2-CH_2-*C*H_3).

DiMethylButylAmmonium Hydrogen Sulfate [DMBA][HSO_4] (Figs. A1-7 and A1-8):

^{1}H NMR: δ_H (400 MHz, DMSO-d_6)/ppm: 9.23 (s, 1H, N-*H*), 5.65 (s, br, *H*$_2$O, *H*SO_4), 2.98 (t, J = 8.4, 2H, N-C*H*$_2$), 2.72 (s, 6H, N-(C*H*$_3$)$_2$), 1.54 (q, J = 7.6, 2H, N-CH_2-C*H*$_2$), 1.25 (m, 2H, N-CH_2-CH_2-C*H*$_2$), 0.85 (t, J = 7.8, 3H, N-CH_2-CH_2-CH_2-C*H*$_3$).

^{13}C NMR δ_C (101 MHz, DMSO-d_6)/ppm: 57.00 (N-(*C*H_3)$_2$), 42.76 (N-*C*H_2), 26.23 (N-CH_2-*C*H_2), 19.72 (N-CH_2-CH_2-*C*H_2), 14.01 (N-CH_2-CH_2-CH_2-*C*H_3).

2.2.4 IL Characterisation

Hammett Acidity Measurements

IL Hammett acidity was measured using Ultraviolet-Visible (UV-Vis) spectroscopy, combining the Beer-Lambert law (Eq. 2.1) and a modified form of the Henderson-Hasselbalch equation (Eq. 2.2) as in the work of Grasvik et al.[25]

$$A = \varepsilon \times c \times l \quad (2.1)$$

where *A* is absorbance, ε is absorptivity, *c* is concentration, *l* is path length.

$$H_0 = pK_{BH^+} - log\left(\frac{\varepsilon_0 - \varepsilon}{\varepsilon}\right) \quad (2.2)$$

where H_0 is Hammett acidity, $pK_{BH^+}$is the basicity constant of the Hammett base, ε_0 is the absorptivity of the fully un-protonated Hammett base, and ε is the absorptivity of the partially protonated Hammett base. Full derivation of Eq. 2.2 is provided in the Appendix.

In this method, the Hammett base is a molecule that is partially protonated by the acidic solution, and has 2 different UV peaks for its protonated and un-protonated forms. The un-protonated peak is referred to as λ_{max}. Solutions of the Hammett base are prepared in the IL, with different Hammett base concentrations. The UV-Vis absorbance of these solutions is measured at λ_{max}, with a fixed path length. A graph is then plotted of *A* vs. (*c x l)*, and the gradient is determined, providing ε in accordance with Eq. 2.1. From this, Eq. 2.2. may be used to determine H_0.

The Hammett base used was 4-nitroaniline. A suitable base must be partially protonated by the acidic solution (neither fully protonated or un-protonated), and must have an un-protonated absorbance peak that does not overlap with that of the acidic solution. 4-nitroaniline has been reported to be suitable for the range of Hammett acidities investigated, and was found not to overlap with the absorbance peaks of the ILs investigated.[51]

Although available in the literature, ε_0 was determined in order to validate the experimental method used, by comparison with literature values. Eq. 2.1 is used to determine ε_0, by measuring the UV-Vis absorbance of varying concentrations of 4-nitroaniline in a non-acidic solvent at λ_{max} (380 nm), using a fixed path length. The solvent used must be non-acidic in order to prevent any protonation of the 4-nitroaniline. Approximately 25 mg of 4-nitroaniline were accurately weighed into a 50 mL glass jar, using a funnel to ensure particles did not stick to the walls of the container. The jar was then sealed with a rubber sleeve stopper to keep it airtight. The jar was then purged with nitrogen by blanketing with a nitrogen balloon and slowly syringing out the gas inside the jar several times. This was to remove any air and water vapour, as the presence of water would slightly protonate the 4-nitroaniline. A 12 mL screw syringe was used to transfer approximately 66 g of anhydrous dichloromethane (weighed accurately) into the glass jar, while blanketing with a nitrogen balloon in order to maintain atmospheric pressure. The jar was magnetically stirred for at least 30 minutes, or until the dye was completely dissolved. This solution was termed the “stock solution”, with a target concentration of 2 mM. Due to possible water ingress or dye degradation during long-term storage, stock solutions were not kept for more than 24 hours. This stock solution was then diluted in anhydrous DCM, in order to obtain a range of concentrations of 4-nitroaniline in DCM. This was done by purging a 20 mL sealed glass jar with nitrogen (as described above), adding a measured mass of anhydrous DCM while

blanketing with a nitrogen balloon, and adding a measured mass of stock solution while blanketing with a nitrogen balloon, and magnetically stirring for at least 30 minutes. In this way, five different concentrations of 4-nitroaniline in DCM were prepared. These were then transferred into sealed UV-clear quartz cuvettes with a path length of 0.5 cm, and the UV absorbance was measured. The absorptivity of fully unprotonated 4-nitroaniline (ε_0) was thus determined to be 16,600 M^{-1} cm^{-1}, around 10% higher than the value of 15,500 M^{-1} cm^{-1} reported by Grasvik et al.[25] The higher value determined in this study is thought to be due to the more rigorous anhydrous conditions employed (e.g. near-constant blanketing with nitrogen balloons). This would lead to lower water ingress from air and thus less protonation of the Hammett base during measurements, and thus a more accurate and higher value of ε_0.

H_0 was determined by preparing solutions of 4-nitroaniline in the IL solutions, with varying concentrations. Due to the low concentrations required, large volumes of ILs would have been required for each set of measurements. Additionally, performing serial dilutions using the ILs (as with the DCM) was unfeasible due to their high viscosity. Instead, a 2 mM stock solution of 4-nitroaniline in DCM was prepared and diluted to required levels, as when measuring ε_0. 1 mL of each diluted solution was then transferred into a 3 mL glass vial using an Eppendorf pipette, and the DCM was removed by rotary evaporation, leaving a small amount of 4-nitroaniline in the vial. 2 mL of IL solution were then transferred into the jar using a non-pyrogenic serological 10 mL pipette and *Powerpette Plus* pipette controller. Vials were then wrapped in foil (to prevent photodegradation of the 4-nitroaniline), and shaken overnight to ensure complete mixing and reaction between the 4-nitroaniline and IL solutions. The next day, the UV absorbance of all 5 solutions were measured as before. ε was then determined by measuring the gradient of the *A* vs. *cl* graph. Using Eq. 2.2, H_0 was then calculated, using a pK_{BH+} value of 1.00 for 4-nitroaniline, obtained from literature.[25,52] All Hammett acidity measurements were repeated twice, i.e. preparing new stock solutions of 4-nitroaniline in DCM and ionic liquid which were then diluted to the desired concentrations. Example graphs of *A* vs. *cl*, and example UV-Vis spectra can be found in the Appendix.

Thermal Stability

Ionic liquid thermal stability was investigated by using transferring approximately 10 g of IL solution into a sealed ACEX pressure tube, and heating to 170 °C for 72 hours in a Thermo Scientific Heratherm convection oven. ^1H and ^{13}C NMR spectroscopy in DMSO-d_6 were carried out on IL solutions before and after thermal treatment, in order to observe any changes in peaks, which would indicate the presence of degradation products above 1 mol%.

Density Measurements

IL solution densities were measured using a Mettler-Toledo DM40 density meter, between 0 °C and 50 °C. Solutions were sonicated for 20 minutes before measurements to remove any bubbles and dissolved air. The cell condition was verified before each use by measuring the density of purified water at 20 °C (0.99821 g/cm^3), and ensuring it was within the tolerance (0.00008 g/cm^3).

2.2.5 Pretreatment

All pretreatment experiments were carried out in triplicates, and in accordance with the Hallett Group's Standard Operating Procedure, with standard deviations of triplicates displayed as error bars. Several terms were used when describing pretreatment parameters, defined in Eqs. 2.3 and 2.4:

$$Water\ Content\ (\%) = \frac{m_{IL} \times wc_{IL} + m_{biomass} \times mc_{biomass} + m_{water}}{m_{IL} + m_{water}} \times 100 \quad (2.3)$$

$$Biomass\ Loading\ (\%) = \frac{m_{biomass} \times (1 - mc_{biomass})}{m_{biomass} \times mc_{biomass} + m_{IL} + m_{water}} \times 100 \quad (2.4)$$

where *m* is the mass of substance *x* added or recovered, *mc* is the moisture content of a solid on an air-dry basis, *wc* is the water content of a solution. Subscript *IL* refers to the IL solution used for pretreatment, subscript *water* refers to any water added, and subscript *biomass* refers to the untreated biomass used for pretreatment.

The moisture content of the untreated feedstock was first determined as detailed in Section 2.2.6. Approximately 1 g of biomass on an oven-dried basis was measured on a piece of tared aluminium foil and transferred into a 15 mL ACE pressure tube, with the air-dried mass recorded. The required amount of IL and water were then added in order to reach the target biomass loading and water content. The former was added by mass (which was recorded), and the latter by volume using an Eppendorf pipette. Following this, the pressure tubes were sealed using a Teflon cap with a silicone O-ring, and vortexed for at least one minute, or until a visually homogeneous mixture was obtained.

Pressure tubes were placed in a Thermo Scientific Heratherm oven at the specified temperature (typically 120-170 °C) for the specified duration, after which they were removed and allowed to air-cool. Once cool enough to handle, 40 mL of ethanol were added, and the resulting slurry was transferred from the pressure tubes into 50 mL Falcon centrifuge tubes. The falcon tubes were vortexed and left to stand for one hour, before being manually shaken and then centrifuged at 3000

rpm for 50 minutes. The supernatant was decanted manually into a round-bottom flask (RBF). Three more such ethanol washes were carried out, following which the resulting pulp was transferred into a cellulose thimble and washed by Soxhlet extraction using 150 mL of ethanol for 20-24 hours. Following this, thimbles were left to dry in a fume hood overnight, and the remaining ethanol was added to that from the earlier ethanol washes.

The following day, the air-dried pulps were transferred from the cellulose thimble onto a piece of tared aluminium foil, with their masses recorded before being transferred to glass sample vials. A sample of this pulp was then used to quantify the moisture content, using the method detailed in Section 2.2.6. From this, the pulp yield was obtained using Eq. 2.5.

$$Pulp\ Yield\ (\%) = \frac{m_{pulp}\ \times\ (1 - mc_{pulp})}{m_{biomass}\ \times\ (1 - mc_{biomass})} \times 100 \tag{2.5}$$

where *m* is the mass of substance *x* added or recovered, and *mc* is the moisture content of a solid on an air-dry basis. The subscript *biomass* refers to the untreated biomass used for pretreatment, and subscript *pulp* refers to the pretreated biomass.

The ethanol collected throughout the pretreatment was evaporated under reduced pressure (40-70 mbar) at 40 °C. The resulting solution remaining in the round-bottomed flask was a mixture of IL and lignin. Following this, the lignin was precipitated by addition of 30 mL of water, and the resulting mixture transferred into a 50 mL Falcon centrifuge tube. The Falcon tube was then vortexed and left to stand for an hour before being centrifuged at 3000 rpm for 40 minutes, with the supernatant then disposed of in the relevant chemical waste. Two more such washes with water were carried out. The Falcon tube was then capped with tissue paper (held in place with Parafilm) and partially immersed in liquid nitrogen for several minutes, before being placed in a freeze-dryer for 48 hours. The resulting dry lignin was then transferred onto a piece of tared aluminium foil, had its mass recorded, and was transferred into a glass sample vial. The lignin yield was then obtained using Eq. 2.6.

$$Lignin\ Yield\ (\%) = \frac{m_{lignin}}{m_{biomass}\ \times\ (1 - mc_{biomass})\ \times\ Lignin_{biomass}} \times 100 \tag{2.6}$$

where m_{lignin} is the mass of recovered lignin, and $mc_{biomass}$ is the moisture content of the untreated biomass used for pretreatment, and $Lignin_{biomass}$ is the lignin content of the untreated biomass.

2.2.6 Biomass Characterisation

Moisture Content

Biomass moisture content was determined using the National Renewable Energy Laboratory protocol 'Determination of Total Solids in Biomass and Total Dissolved Solids in Liquid Process Samples'.[53] When measuring the moisture content of untreated biomass and pretreated pulps, measurements were made in triplicate for the former and only once for the latter. The mass of a piece of aluminium foil was recorded. Approximately 50 mg of sample were transferred onto the foil, and the total mass recorded. The foil was folded into a packet and placed in a VWR Venti-Line convection oven at 105 °C overnight. The following day, the packet was placed in a desiccator for 15 minutes, and then had its mass recorded. The moisture content was then calculated on an air-dried basis according to the Eq. 2.7:

$$\%\ \text{Moisture}_{\text{air-dried basis}} = \frac{m_{\text{air-dried}} - m_{\text{oven-dried}}}{m_{\text{air-dried}} - m_{\text{foil}}} \times 100 \qquad (2.7)$$

where $m_{\text{air-dried}}$ is the air-dry mass of the foil and biomass packet, $m_{\text{oven-dried}}$ is the mass of the packet after it has been removed from the oven and placed in the desiccator, and m_{foil} is the mass of the foil packet.

Enzymatic Hydrolysis (Saccharification)

Enzymatic hydrolysis assays were carried out on pretreated pulps and untreated biomass, as well as on blank controls. The protocol used the Hallett Group's Standard Operating Procedure, a modified version of the National Renewable Energy Laboratory protocol 'Low Solids Enzymatic Saccharification of Lignocellulosic Biomass'.[54]

The moisture content of the samples used was first determined, as detailed in Section 2.3.6. 100 ± 10 mg of biomass on an oven-dry basis were measured on a piece of tared aluminium foil, with the air-dry mass recorded, and then transferred into a Sterilin tube. For blank samples (used as controls for sugars in the enzyme solutions), 0.1 mL of purified water were added instead. The enzyme solution was prepared using the following quantities of reagent per sample: 5 mL of 0.1M sodium citrate buffer of pH 4.8, 40 μL of tetracycline hydrochloride antibiotic solution (10 mg/mL in 70% ethanol), 30 μL of cycloheximide antibiotic solution (10 mg/mL in purified water), 4.81 mL of purified water, and 20 μL of Ctec2 enzymes. 9.9 mL of solution was transferred to each tube, using a serological pipette. The tubes were then closed and incubated at 50 °C and 250 rpm for 7 days in an Innova 42 incubator shaker

(New Brunswick Scientific). Following incubation, samples were filtered and run through the HPLC, as described in Section 2.2.1.

Eqs. 2.8 and 2.9 were used to calculate saccharification yield and digestibility:

$$Saccharification\ Yield\ (\%) = \frac{(c_{sample} - c_{blank}) \times V_{sample} \times corr_{anhydro} \times Pulp\ Yield}{m_{sample} \times (1 - mc_{sample}) \times Glucan_{untreeated}} \times 100 \quad (2.8)$$

$$Digestibility\ (\%) = \frac{Saccharification\ Yield \times Glucan_{untreeated}}{Pulp\ Yield \times Glucan_{pulp}} \times 100 \quad (2.9)$$

where c_{sample} is the glucose concentration of the hydrolysis sample as determined by HPLC, c_{blank} is the glucose concentration of the blank control as determined by HPLC , V_{sample} is the volume of the hydrolysis sample (10 mL), $corr_{anhydrous}$ is a correction factor accounting for the increase in mass of sugars during hydrolysis (0.9 for glucose), *Pulp Yield* is as defined in Eq. 5, m_{sample} is the mass of sample hydrolysed, mc_{sample} is the moisture content of the sample hydrolysed, $Glucan_{untreated}$ is the glucan content of the untreated biomass, and $Glucan_{untreated}$ is the glucan content of the pulp.

Compositional Analysis

Compositional Analysis was used to determine the composition of both the untreated biomass and pretreated pulps, in terms of glucan, xylan, galactan, mannan, arabinan, acid-soluble lignin, acid-insoluble lignin, ash and extractives. The compositional analysis protocol followed was that of the National Renewable Energy Laboratory 'Determination of Structural Carbohydrates and Lignin in Biomass'.[55] All measurements were performed in triplicate on untreated biomass and once for each pulp.

If performing this test on untreated biomass, the extractives content was first measured (as extractives were removed from the pulps by Soxhlet extraction during the pretreatment process). This was done by weighing out a known amount of air-dried biomass of known moisture content onto a tared piece of aluminium foil, and transferring this into a cellulose thimble. From the air-dried mass added and the moisture content, the oven-dried mass was determined. Samples were then Soxhlet extracted with 150 mL of ethanol for 24 hours. The biomass and thimble were left to dry in a fume hood overnight. Following this, the ethanol used for the extraction was evaporated under reduced pressure. The mass of the flask and remaining residue (i.e. extractives) was then recorded, from which the extractives mass was determined. The remaining solid biomass had its moisture content determined as described in Section 2.3.6 and was stored in a sample vial.

Several terms were used when describing results, defined as in Eqs. 2.10-2.12:

$$Glucan\ Recovery\ (\%) = \frac{Glucan_{pulp} \times\ Pulp\ Yield}{Glucan_{untreated}} \times 100 \quad (2.10)$$

$$Hemicellulose\ Removal\ (\%) = \ 100 - \frac{Hemicellulose_{pulp} \times\ Pulp\ Yield}{Hemicellulose_{untreated}} \times 100 \quad (2.11)$$

$$Delignification\ (\%) = 100 - \frac{Lignin_{pulp} \times\ Pulp\ Yield}{Lignin_{untreated}} \times 100 \quad (2.12)$$

where *Glucan* is the proportion of glucan in the sample, *Hemicellulose* is the proportion of hemicellulose in the sample (assumed to be all sugars except glucan), *Lignin* is the proportion of lignin in the sample (the sum of acid-soluble and acid-insoluble lignin), and *Pulp Yield* is defined as in Eq. 2.5. Subscript *pulp* refers to the pretreated biomass, while the subscript *untreated* refers to the untreated biomass.

2.2.7 Lignin Characterisation

Gel Permeation Chromatography (GPC)

20 mg of lignin was dissolved in 1 mL of DMSO containing 0.1 wt% LiBr and left to dissolve for 2 days, before being filtered through a 0.2 µm PTFE syringe filter. GPC was performed using an Agilent 1260 Infinity, using an AGuard guard column, followed by an A6000M and A3000 column (all from Viscotek), with HPLC-grade DMSO containing 0.1 wt% LiBr as a mobile phase at 0.4 mL/min and operating at a column temperature of 60 °C. Detection was carried out using the Agilent 1260 Infinity RI detector. Calibration was carried out using a set of 10 pullulan polysaccharide standards from Agilent, ranging from 180 to 780,000 g/mol.

^{1}H-^{13}C HSQC NMR Spectroscopy

HSQC NMR was performed on selected lignin samples. Samples were prepared by dissolving 40 mg of lignin in 0.5 mL of DMSO-d_6, and then transferring the solution into an NMR spectroscopy tube. Measurements were carried out using a Bruker 600 MHz spectrometer (pulse sequence hsqcetgpsi2, spectral width of 10 ppm in F2 (1H) with 2048 data points and 160 ppm in F1 (13C) with 256 data

points, 16 scans and 1 s interscan delay). Spectra were analysed using MestReNova 5.3.0. Integral areas were assigned as in the work of Brandt-Talbot et al.[26,32] All spectra were selected when integrating areas, in order to ensure the same integral areas. For ether linkages, the C-H_α-signals were integrated, for PCA and H the 2,6-signals were integrated. All integrals were normalised to the sum of the G_2 + $G_{2\,cond}$ volume integrals. The S/G ratio of recovered lignin was determined as in Eq. 11:

$$S/G = \frac{0.5 * S_{2,6} + S_{cond}}{G_2 + G_{2\,cond}} \quad (11)$$

where *S* is the volume integral of the relevant syringyl sub-unit, and *G* is the volume integral of the relevant guaiacyl sub-unit. Subscripts *2* and *6* refer to the position of the protons on the aromatic ring of the measured sub-unit, and subscript *cond* refers to condensed sub-units.

2.3 Results and Discussion

2.3.1 IL Characterisation

Thermal Stability

Thermal degradation tests were carried out on all four ILs in order to ensure their thermal stability at the pretreatment temperatures used. ILs were heated at 170 °C for 72 hours, with the solutions analysed by ^{1}H NMR before and after. ^{1}H NMR spectra are provided in the Appendix, with no significant differences in peak shifts or integrals, indicating a lack of breakdown products above 1% mol. This is consistent with the findings of Pin et al., who reported the degradation onset temperature of [BA][HSO_4] to be 290 °C.[56] Similarly, no degradation of [TEA][HSO_4] was observed by Chambon after 100 hours at 150 °C.[43] All four ILs are thus suitable high temperature pretreatment solvents, with negligible degradation over the course of the pretreatments.

Hammett Acidity and Density

IL Hammett acidity measurements were performed by MSc student Sochi Amako, under my supervision and using a protocol developed myself. All molecular dynamics simulations were carried out by Dr Richard Matthews at my request, and only a high-level summary of those results is presented here.

Hammett acidity measurements for ILs with an acid-base ratio of 1.00 are presented in Fig. 2.2, with all solutions containing 20 wt% water. It must be emphasised that a lower H_0 value corresponds to a higher tendency for the solution to donate protons, and thus a "higher" solution acidity (H_0 is analogous to pH, as the two scales converge in aqueous solutions). A clear trend is observed: as the degree of substitution of the alkylammonium cation is increased, H_0 of the IL solution increases. This behaviour is not predicted by aqueous acidity theory, as the pK_as of the constituent amines' conjugate acids in water are all similar (between 10.02 and 10.56[57–60]) and do not follow the same trend. The trend of increasing H_0 with increasing degree of cation substitution was investigated by carrying out molecular dynamics (MD) simulations of the system (see Appendix). It was revealed that as the degree of substitution decreased, the strength of anion-cation and anion-anion interactions increased due to increased hydrogen-bonding. This effect led to reduced water intercalation into the ionic network, leaving larger free water clusters and ion clusters in the solution. Under lower solvation, the proton activity of sulfuric acid has been shown to increase non-linearly, due to a significantly reduced proton

solvation energy.[61,62] Therefore, the increased acidity of primary and secondary ammonium cations may be due to enhanced proton activity arising in pockets of clustered ions in the solution. Further computational and experimental work should be carried out in order to confirm this hypothesis.

The H_0 value of the least acidic IL in this study, [DMBA][HSO_4], was found to be lower than those of 1-methyl imidazolium hydrogen sulfate ([Hmim][HSO_4]) and 1-butyl-3-methyl-imidazolium hydrogen sulfate ([bmim][HSO_4]) reported by Cox et al.[30] When dry, [Hmim][HSO_4] and [bmim][HSO_4] were found to have H_0 values of 1.99 and 2.08 respectively, compared to an H_0 of 1.62 for [DMBA][HSO_4] with 20 wt% water in this study. When diluted in DMSO the H_0 of the alkylimidazolium $[HSO_4]^-$ ILs was found to increase logarithmically.[30] It would therefore appear that either alkylammonium $[HSO_4]^-$ ILs are significantly more acidic (due to the cation itself or due to the cation enhancing the acidity of the anion), or that the presence of water is contributing to the greater acidity of the alkylammonium IL solutions. The value determined for [DMBA][HSO_4] in this study is almost identical to that reported by Rafat at the same water content.[63]

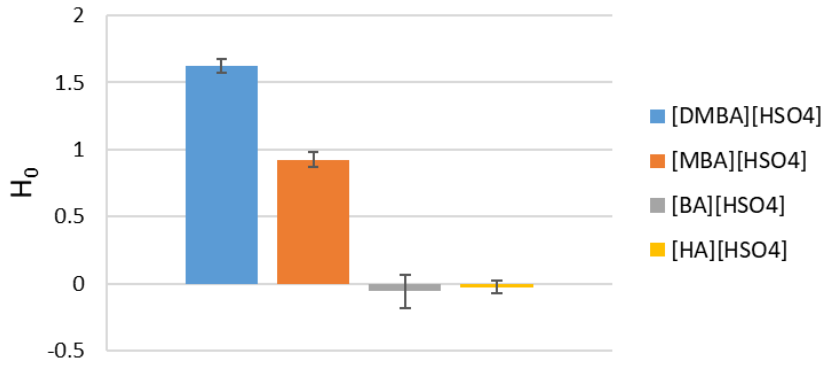


Figure 2.2: Hammett acidity of alkylammonium hydrogen sulfate ILs with varying cations. All ILs contained 20 wt% water.

H_0 of [BA][HSO_4] was measured at different acid-base ratios: 1.00, 0.95, 0.91, and 0.87 (corresponding to 0%, 5%, 11%, and 17% excess base). Results are shown in Fig. 2.3. H_0 is seen to increase as excess base is added. This is expected, as the excess base is protonated by the $[HSO_4]^-$ anions up to 100% excess base, leading to a mixture of $[HSO_4]^-$ and $[SO_4]^{2-}$ anions and thus reducing solution acidity. This supports the hypothesis that the more acidic behaviour of primary alkylammonium $[HSO_4]^-$ ILs is due to the anion acidity being enhanced, rather than originating from the cation.

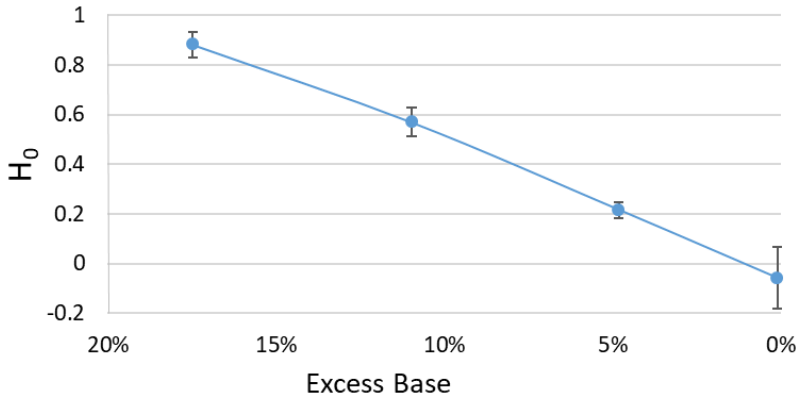


Figure 2.3: Variation of the Hammett acidity of [BA][HSO_4] with excess base. All measurements were conducted using 20 wt% water. Excess base is measured on a molar basis.

H_0 of [DMBA][HSO_4] was measured at different acid base ratios between 1.00 and 1.40, with 20 wt% water in all cases. Results are shown in Fig. 2.4. Unlike the addition of excess base, excess acid does not react with either species in the IL, instead forming a mixture of the IL and sulfuric acid. As expected, H_0 decreases with increasing acid-base ratio. The effect of cation substitution on H_0 is seen to be very significant: H_0 of [HA][HSO_4], [BA][HSO_4], and [MBA][HSO_4] correspond to that of [DMBA][HSO_4] containing 31%, 32%, and 11% excess sulfuric acid respectively.

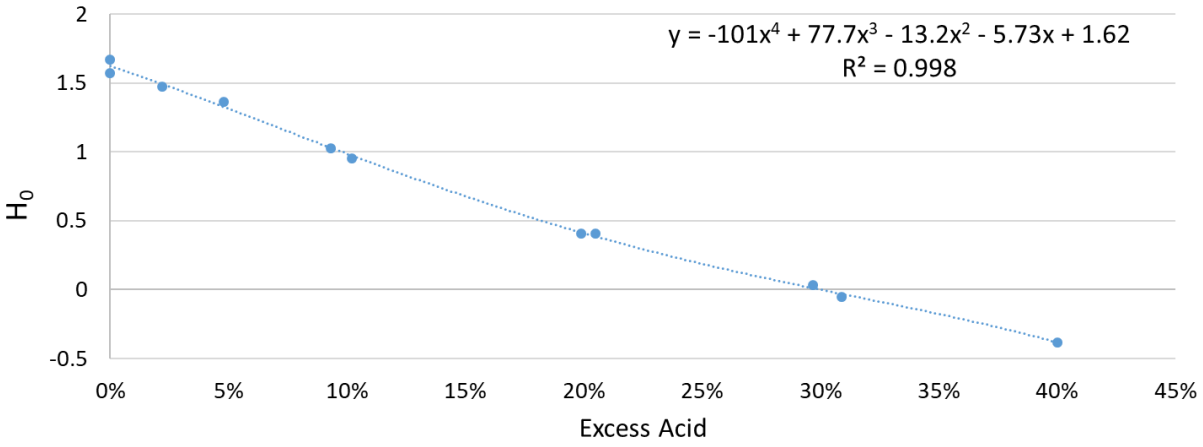


Figure 2.4: Variation of the Hammett acidity of [DMBA][HSO_4] with excess sulfuric acid. All measurements were conducted using 20 wt% water. Excess acid is measured on a molar basis. The regression equation displayed is used in Section 2.3.3 to interpolate the required amount of excess acid to reach a desired H_0 value.

Fig. 2.5 compares H_0 of aqueous sulfuric acid (from the work of Hammett and Deyrup[51]) with that of [DMBA][HSO_4] containing excess sulfuric acid. Results are plotted as a function of "free" sulfuric acid, representing either the sulfuric acid content of the aqueous solutions, or the excess acid in the IL solutions. Interestingly, values of H_0 are very similar at low quantities of free sulfuric acid despite the presence of the $[HSO_4]^-$ anions already present in the IL. This could be due to association between the anion and cation hindering dissociation of the anion's proton. The decrease in H_0 when adding excess sulfuric acid to [DMBA][HSO_4] is close to linear, whereas the curve for aqueous sulfuric acid solutions is clearly non-linear due to the solvent levelling effects of the water.[25] Grasvik et al. reported a similar observation when adding excess sulfuric acid to water and to dry [bmim][HSO_4].[25]

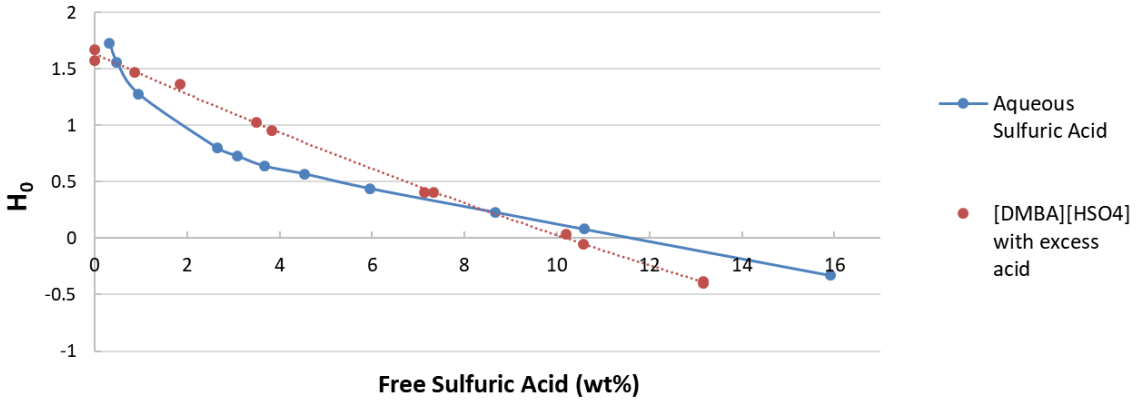


Figure 2.5: Variation of the Hammett acidity of [DMBA][HSO_4] and water with free sulfuric acid. All IL measurements were conducted using 20 wt% water. Free sulfuric acid is measured on a weight basis. Hammett acidity data for free sulfuric acid was taken from the work of Hammett and Deyrup.[51]

The effect of IL molar density on the observed Hammett acidity trends was investigated by considering the number of acidic protons in solution per unit volume of IL. In this analysis, the term 'acidic proton' refers to any proton from an H_2SO_4 molecule or $[HSO_4]^-$ anion. From density measurements, the concentration of acidic protons was determined for the four different ILs with 1:1 acid-base ratio, as well as for [DMBA][HSO_4] with 11% and 31% excess acid. Results are shown in Fig. 2.6. There is one apparent trend for ILs with 1:1 acid-base ratio: as molecular weight increases, the acidic proton concentration decreases. However, the concentrations of acidic protons do not follow the same trends as the relative Hammett Acidities of the different ILs. It can thus be concluded that density differences do not play a significant role in the observed acidity trends.

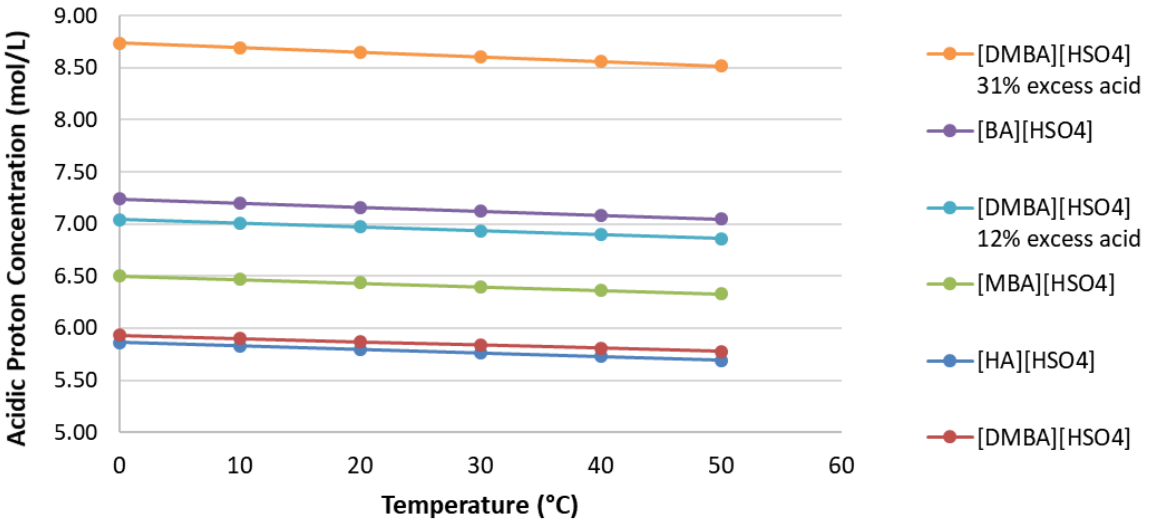


Figure 2.6: Variation of IL acidic proton concentration with temperature. All IL measurements were conducted using 20 wt% water. Excess sulfuric acid is measured on a molar basis.

2.3.2 Pretreatment With Varying Cations

Pretreatments were performed on *Miscanthus x giganteus*, initially using [DMBA][HSO_4], [MBA][HSO_4], and [HA][HSO_4] with acid-base ratios of 1.00 and using [BA][HSO_4] with an acid-base ratio of 0.97. These were all carried out at 150 °C, ranging from 15 minutes to up to 90 minutes. Compositional analysis was carried out on the obtained pulps. Pretreatment and compositional analysis results are shown in Figs. 2. 7 and 2.8.

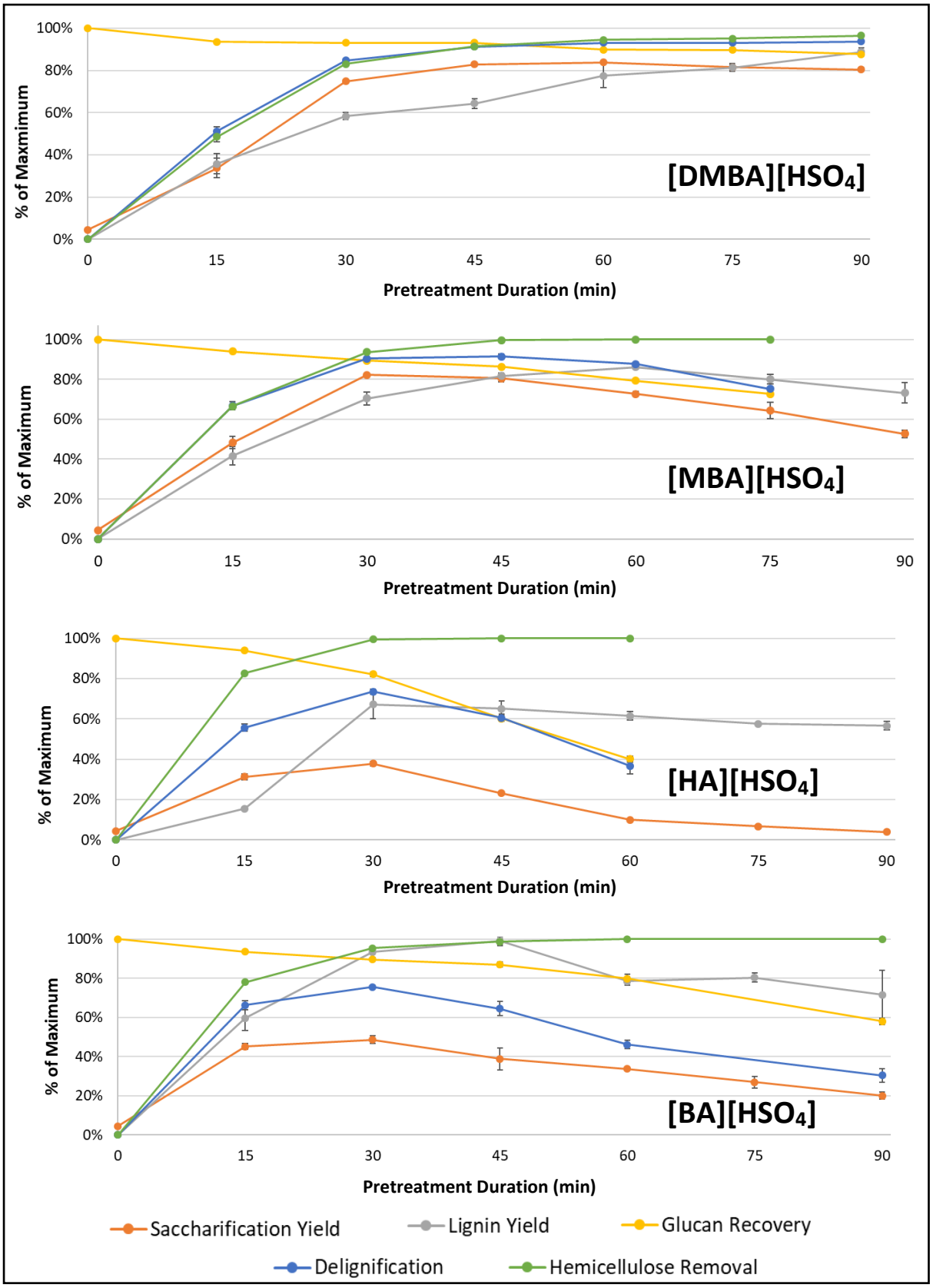


Figure 2.7: Pretreatment performance of different ionic liquids. The ionic liquids used is indicated on each plot. All pretreatments were carried out on *Miscanthus* at 150 °C, with 20 wt% water, and at a biomass loading of 10% wt/wt.

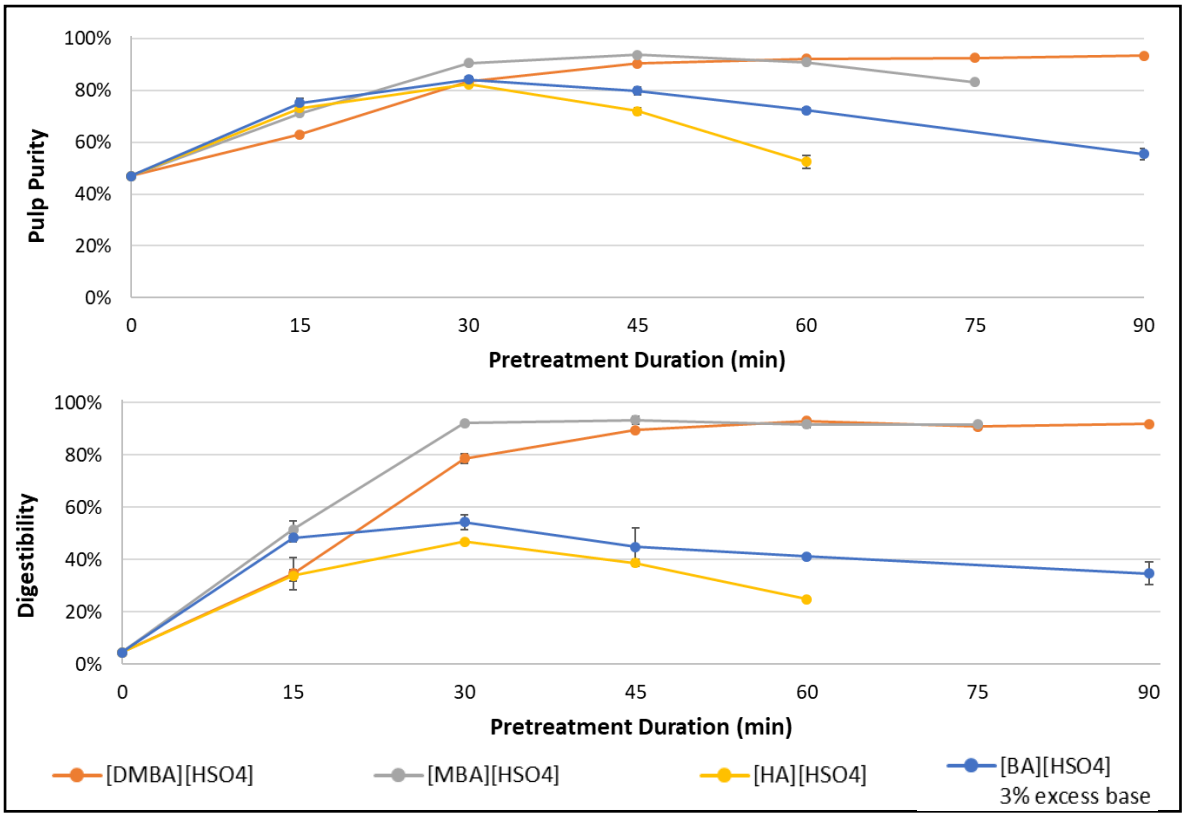


Figure 2.8: Digestibility and purity of pulps pretreated using varying ionic liquids. All pretreatments were carried out on *Miscanthus* at 150 °C, with 20 wt% water, and at a biomass loading of 10% wt/wt.

[DMBA][HSO_4] displays similar pretreatment behaviour to that of triethylammonium hydrogen sulfate ([TEA][HSO_4]), another tertiary alkylammonium hydrogen sulfate IL used to pretreat *Miscanthus* in the work of Gschwend et al.[40] Delignification increases until 60 minutes of pretreatment, at which point lignin removal plateaus around 93%. Similarly, hemicellulose removal rapidly increases to around 94% after 60 minutes, before the rate of increase begins to slow down significantly. Combined with consistently high glucan recoveries (88% after 90 minutes), this leads to pulp glucan contents consistently above 90% from 45-90 minutes. Pulp digestibility is observed to track delignification and hemicellulose removal (and thus pulp purity) and remains above 90% from 45 minutes onwards. Due to the high purity of the pulp, saccharification yields peak at 84% after one hour, before slowly decreasing as a result of gradual glucan degradation. Delignification and hemicellulose removal using [DMBA][HSO_4] were significantly higher than those reported by Gschwend et al. using [TEA][HSO_4].[40] This resulted in higher pulp purities (93% vs 81% after 90 minutes) and consistently higher saccharification yields (peaks of 84% vs 75%). However, glucan recoveries using [TEA][HSO_4] were reported to be almost quantitative, whereas those of [DMBA][HSO_4] decreased from 94% to 88%

between 15 and 90 minutes of pretreatment. These results would appear to indicate that [DMBA][HSO_4] is a more acidic solvent than [TEA][HSO_4], despite both having tertiary alkylammonium cations and being isomers. This is consistent with [DMBA][HSO_4] showing a substantially higher rate of β-*O*-4' bond cleavage in lignin model compounds in the work of De Gregorio et al,[64] as well as in softwood lignin in the work of Gschwend et al.[39] In the latter study, [DMBA][HSO_4] was also found to generate significantly higher saccharification yields than [TEA][HSO_4] at the same conditions. Therefore, the improved performance of [DMBA][HSO_4] in terms of pulp purity and saccharification yield from grass biomass, further show it to be a more promising pretreatment solvent.

The effect of increased acidity of primary and secondary ammonium cations is clearly observed through accelerated pretreatment performance. Both classes of IL display maxima in lignin removal, after 30 and 45 minutes for primary and secondary ammonium cations respectively. These peaks are 74% and 75% for [HA][HSO_4] and [BA][HSO_4] respectively, and 92% for [MBA][HSO_4]. This maximum in lignin removal is due to depolymerisation and dissolution of lignin into the IL being counterbalanced by the redeposition of lignin and pseudolignin onto the pulp. This process has been shown to be accelerated for more severe (i.e. acidic or high-temperature) pretreatment.[26,38,40] The effect of acidity is thus displayed through the sharper and lower delignification peak for the more acidic primary alkylammonium cations, in which the redeposition begins occurring more rapidly. While no such peak was observed at the times investigated in this study using [DMBA][HSO_4], Gschwend et al. observed a broad peak in lignin removal using [TEA][HSO_4] after 90-120 minutes pretreatment at 150 °C.[40] It is assumed that [DMBA][HSO_4] would display similar behaviour at extended pretreatment durations. Hemicellulose removal was also accelerated using primary and secondary alkylammonium ILs, reaching 100% in all cases, and in as low as 30 minutes for [HA][HSO_4]. The effect of increased acidity is also observed through the increased glucan degradation. All ILs display an initial drop in glucan recovery of around 7%, presumed to be due to degradation of more easily-hydrolysable amorphous cellulose or of glucan contained in hemicellulose.[65] However, the rate of further degradation is far higher in primary and secondary alkylammonium ILs, reaching 60%, 20%, and 20% for [HA][HSO_4], [BA][HSO_4], and [MBA][HSO_4] respectively after 60 minutes, compared to only 10% for [DMBA][HSO_4]. Cellulose degradation proceeds by endwise hydrolysis at mild conditions, but rapidly increases once a certain severity threshold is reached and the crystalline structure is disrupted.[65] The marked increase in degradation, particularly in primary alkylammonium cations, is thus likely due to disruption of the crystalline structure of the cellulose with primary and secondary alkylammonium cations at 150 °C.

Following peak lignin removal in primary and secondary alkylammonium ILs, hemicellulose removal continues increasing to 100% and glucan recoveries consistently decrease. Overall, the increasing hemicellulose removal is outweighed by decreasing lignin removal and glucan recovery, and this

results in peaks in pulp purity occurring at the same point as peaks in lignin removal. Due to its lower acidity, lignin redeposition is less rapid in [MBA][HSO_4], and thus does not counterbalance lignin removal as much as in the primary alkylammonium ILs. As a result, delignification reaches a much higher peak, and the pulp purity peak is significantly higher and broader: 94% after 45 minutes in [MBA][HSO_4], compared to 84% and 82% after 30 minutes in [BA][HSO_4] and [HA][HSO_4] respectively. Despite higher pulp purities than those achieved by Gschwend et al. using [TEA][HSO_4],[40] saccharification yields of primary alkylammonium ILs are very low, peaking at just 49% and 38% for [BA][HSO_4] and [HA][HSO_4] respectively. While this may partly be attributed to increased glucan degradation, pulp digestibilities are also significantly lower: 47% and 54% compared to 74% for [TEA][HSO_4]. Pulp digestibility is typically linked to pulp purity and particularly delignification, due to lignin blocking the access of enzymes to the cellulose fibres, as well as deactivating the enzymes by irreversibly binding to them through hydrogen bonds and electrostatic interactions.[66–69] Pseudolignin has been found to inhibit enzymatic hydrolysis more than native lignin, which may explain the low digestibilities at longer pretreatment durations.[70] Reasons for the poor digestibilities using primary alkylammonium ILs are further explored in Section 2.3.4. This effect is not observed in pretreatments with [MBA][HSO_4], where digestibilities are expectedly high, peaking at 93% at the same time as pulp purity. In the work of George et al, it was concluded that higher degree of substitution on the alkylammonium cation increased saccharification yield.[47] This was found by comparing the performance of mono-, di-, and tri-ethylammonium hydrogen sulfate for pretreatment of switchgrass at 120 ^oC for 180 minutes. The poor performance of the primary and secondary alkylammonium hydrogen sulfate ILs in that study may now be partly attributed to an overly long pretreatment duration for this class of ILs.

There are several differences in pretreatment behaviour among the primary and secondary alkylammonium ILs which do not directly follow the expected acidity trend. H_0 of [BA][HSO_4] with 3% excess base is estimated to be 0.13, by interpolating the data in Fig. 2.3. This value is similar to that of stoichiometric [HA][HSO_4] (-0.03), and far lower than that of stoichiometric [MBA][HSO_4] (0.93). The behaviour of slightly basic [BA][HSO_4] was therefore expected to resemble that of [HA][HSO_4], but in practice is significantly closer to that of [MBA][HSO_4] in several metrics. Hemicellulose removal is slightly slower than [MBA][HSO_4] and significantly slower than [HA][HSO_4], reaching 100% after 60 minutes, compared to 45 and 30 minutes respectively. As previously mentioned, glucan recoveries are almost identical to those of [MBA][HSO_4], and far higher than those of [HA][HSO_4]. Lignin removal behaviour matches that of [HA][HSO_4] much more closely both quantitatively and qualitatively: peak removal is around 75% after 30 minutes, before then rapidly decreasing with time. Lignin removal is thought to be due to cleavage of the β-*O*-4' bonds by the $[HSO_4]^-$ anion facilitating dissolution, with

the rate of cleavage increased in ILs with stronger anion-cation association.[64] Therefore, the unexpected trends in glucan recovery and hemicellulose removal may suggest a significant cation effect beyond its association with the anion, whereby the butylammonium cation interacts less significantly with the polysaccharide fraction of the biomass than the other cations tested.

Unlike for [DMBA][HSO_4], lignin recovery yields of primary and secondary ammonium cations eventually exceed delignification for all three ILs, indicating the formation of pseudolignin, again due to the more acidic conditions.[41] Lignin recovery yields are always higher than delignification for [BA][HSO_4] with 3% excess base. Similar behaviour is observed for [MBA][HSO_4] with 2% and 5% excess base (see Section 2.3.5) but not at 1.00 acid-base ratio. This indicates increased solubilisation of lignin and pseudolignin in the IL solution due to the increased concentration of alkylammonium cation. Lignin yields in [MBA][HSO_4], [HA][HSO_4], and [BA][HSO_4] all exhibit a maximum value, unlike those of [DMBA][HSO_4], which may be explained by the accelerated condensation and redeposition of lignin and pseudolignin onto the pulp due to the more acidic conditions.

2.3.3 Excess Acid Pretreatments

In order to further investigate the effect of acidity and cation structure on pretreatment efficacy, pretreatments were carried out using two solutions of [DMBA][HSO_4], with 11% and 31% excess sulfuric acid. The acid-base ratios were selected to match the Hammett acidities of [HA][HSO_4] and [MBA][HSO_4], using the regression equation displayed in Fig. 2.4. Pretreatment and compositional analysis data are displayed in Figs. 2.9 and 2.10. Both pretreatments and saccharification assay with excess acid were performed by Sochi Amako under my supervision, while the corresponding compositional analyses were performed myself.

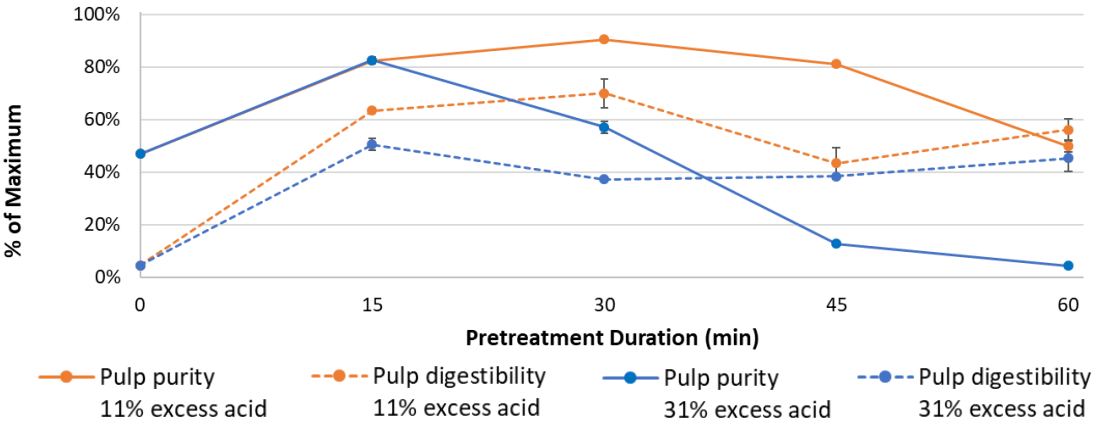


Figure 2.9: Digestibility and purity of pulps pretreated using varying ionic liquids. All pretreatments were carried out on *Miscanthus* at 150 °C, with 20 wt% water, and at a biomass loading of 10% wt/wt.

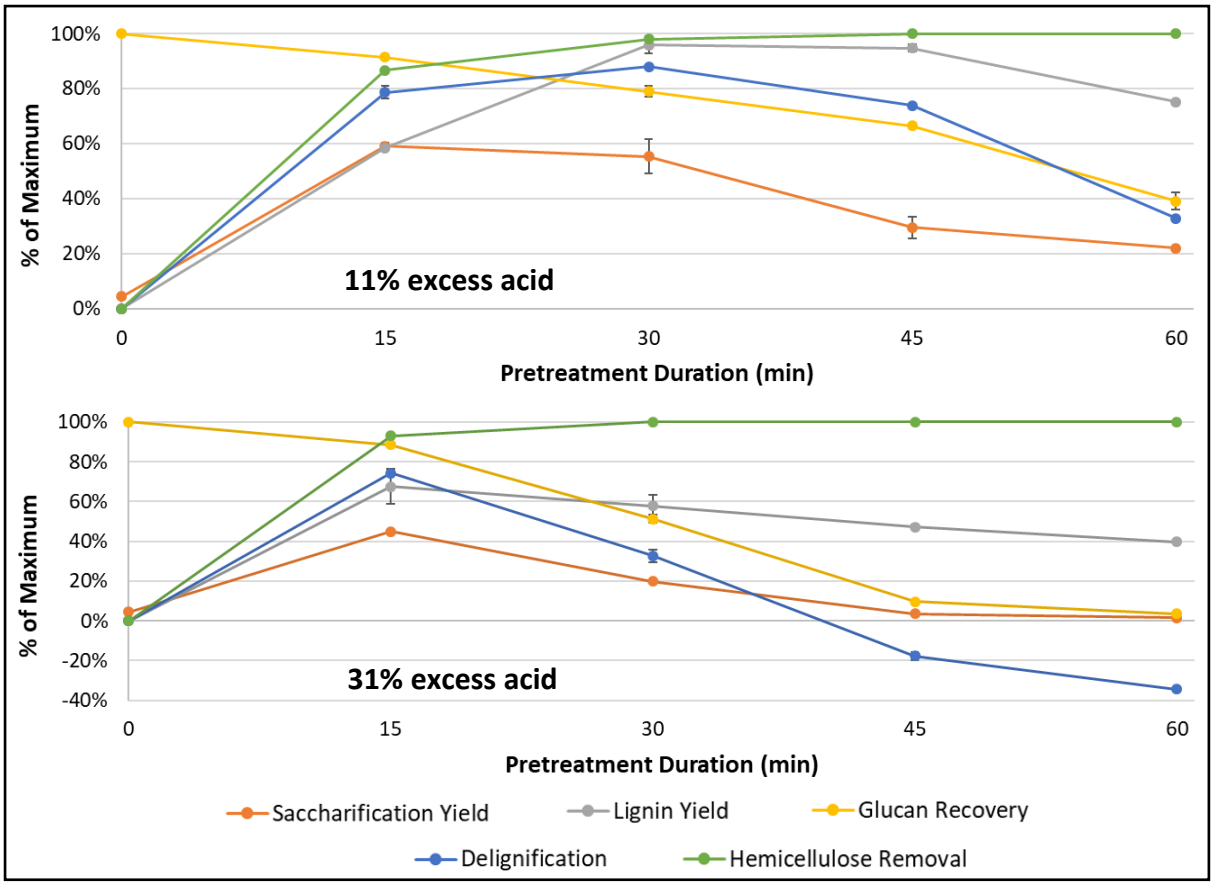


Figure 2.10: Pretreatment performance using [DMBA][HSO_4] with excess acid. Amounts of excess acid are indicated in the plots. All pretreatments were carried out on *Miscanthus* at 150 °C, with 20 wt% water, and at a biomass loading of 10% wt/wt.

The effects of increased acidity on [DMBA][HSO_4] pretreatment are apparent across all metrics. Glucan recovery is severely reduced with excess acid, reaching 39% and 3% after 60 minutes for acid-base ratios of 1.11 and 1.31, compared to 90% using an acid-base ratio of 1.00. Due to the limited loss of glucan at 150 °C using tertiary alkylammonium hydrogen sulfate ionic liquids with 1.00 acid-base ratios, decreasing glucan recovery would appear to be the most evident indicator of excess acid within the IL solution. Delignification is observed to peak with 11% excess acid, reaching 88% after 30 minutes, a similar value to the 1.00 acid-base pretreatment. However, no such peak is observed with 31% excess acid, in which delignification begins at 74% after 15 minutes before continuously decreasing due to redeposition of lignin and pseudolignin. The presence of pseudolignin can be confirmed by lignin recovery yields far exceeding lignin removal, as well as delignification becoming negative (i.e. more lignin on the pulp than contained in the starting biomass). Similar to the pretreatments in Section 2.3.2, trends in pulp purity tend to track those of delignification. 11% excess acid displays a relatively sharp peak in purity of 90% after 30 minutes, whereas 31% excess acid begins

with a pulp purity of 83% after 15 minutes. Saccharification yields are low for both solutions, with the highest values being after 15 minutes in both ILs, due to the high glucan losses and lignin and pseudolignin redeposition with increasing pretreatment duration. Similar to primary alkylammonium HSO_4 ILs, digestibilities are low despite reasonably high peak pulp purities: peak digestibilities are 69% and 52% for acid-base ratios of 1.11 and 1.31, in both cases coinciding with maximum pulp purity. These findings corroborate the previous findings that IL pretreatment with low H_0 inhibits saccharification despite apparently successful pretreatment performance (i.e. production of high-purity cellulose pulps).

Comparison of these pretreatments with those of [HA][HSO_4] and [MBA][HSO_4] provides further insight into the effect of cation structure and solution acidity on pretreatment performance. Despite equal Hammett acidities, pretreatment with excess sulfuric acid appears to be more severe than using a less substituted alkylammonium cation. This is most clearly evidenced by much lower glucan recoveries in solutions of excess acid after 60 minutes of pretreatment: 40% vs 3% ([HA][HSO_4] vs 31% excess acid), and 73% vs 39% ([MBA][HSO_4] vs 11% excess acid). Other pretreatment indicators also suggest more severe pretreatments, through accelerated behaviour. Delignification peaks at a similar value in both cases, but 15 minutes earlier using excess acid. However, there is a far sharper peak using excess acid compared to [MBA][HSO_4], while compared to [HA][HSO_4] excess acid leads to delignification rapidly decreasing after 15 minutes rather than peaking after 30 minutes. Quantitative hemicellulose removal is achieved at around the same time for both sets of solutions, but values before that are consistently higher using excess acid. Maximum pulp purity values are approximately equal between solutions of equal Hammett acidity, but differences in trends are observed, similarly to delignification. 11% excess acid has a much sharper peak than [MBA][HSO_4], and 31% excess acid displays rapidly decreasing pulp purity beyond 15 minutes of pretreatment while [HA][HSO_4] pulp purity peaks after 30 minutes and decreases more slowly.

Saccharification yields using 11% excess acid appear accelerated relative to those using [MBA][HSO_4], decreasing consistently after 15 minutes rather than a broad peak after 30 minutes. Peak saccharification yields of [MBA][HSO_4] are far higher than those using 11% excess acid, peaking at 82% compared to 59%. It interesting to note the significantly lower digestibility of pulps using 11% excess acid, compared to those obtained using [MBA][HSO_4], despite similar pulp purities. This discrepancy suggests an acidity "limit" around an H_0 value of 0.93, below which saccharification begins to be strongly inhibited. Saccharification yields using 31% excess acid also appear accelerated relative to those using [HA][HSO_4], with a maximum after 15 minutes compared to 30 minutes. Peak saccharification is higher using excess acid, at 46% compared to 38%. However, this may be partly due to the higher glucan recoveries with excess acid after 15 minutes (88%) than with [HA][HSO_4] after 30

minutes (82%). Peak pulp digestibility is also slightly higher using excess acid: 52% vs 47%. This may also be due to the shorter pretreatment duration, leading to less saccharification inhibition.

Significant differences in pretreatment behaviour are observed between excess acid solutions, and solutions with primary and secondary alkylammonium cations despite equal Hammett acidities. These differences show that, at fixed temperature, the Hammett acidity of the IL solution is not the only factor predicting pretreatment performance and thus cannot be used by itself as a severity factor. Addition of excess sulfuric acid to [DMBA][HSO_4] at fixed water contents decreases H_0, due to higher concentrations of the $[HSO_4]^-$ anion, and thus a higher concentration of dissociated protons. The observed differences in pretreatment severity suggest different sources of acidity between the two types of solutions, which cannot be distinguished using the Hammett acidity parameter. Therefore, these findings add credence to the theory that the acidity of the primary and secondary alkylammonium ILs is due to the increased activity of protons from lower solvation of the $[HSO_4]^-$ anions, rather than increased proton dissociation in solution.

2.3.4 Exploring Different Strategies To Avoid Saccharification Inhibition

Further investigation into the poor saccharification yields of primary alkylammonium $[HSO_4]^-$ ILs was carried out by performing multiple pretreatments using [BA][HSO_4]. The thermal stability of this class of ILs had already been confirmed, eliminating IL degradation products as a possible cause of saccharification inhibition.

Using [BA][HSO_4], a number of different process parameters were individually altered in a bid to reduce pretreatment severity and improve pulp digestibility and saccharification yield. Pretreatment timecourses were performed at a lower temperature (120 ^oC), with a higher water content (40 wt%), and using up to 20% excess base. Pretreatment and compositional analysis results at peak saccharification yield are displayed in Fig. 2.11, with full timecourse results provided in Appendix A. For comparison, previously analysed data using [BA][HSO_4] with 3% excess base at 150 ^oC has been included in Fig. 2.11. Increasing excess base from 3% to 6% and 20% appears to make the pretreatment less severe, as evidenced by decreasing hemicellulose removal and lignin yields after 30 minutes of pretreatment. However, as excess base increases from 3% to 6%, delignification remains almost identical. This is thought to be due to increased lignin redeposition in 3% excess base due to its higher acidity, which counterbalances increased lignin removal.

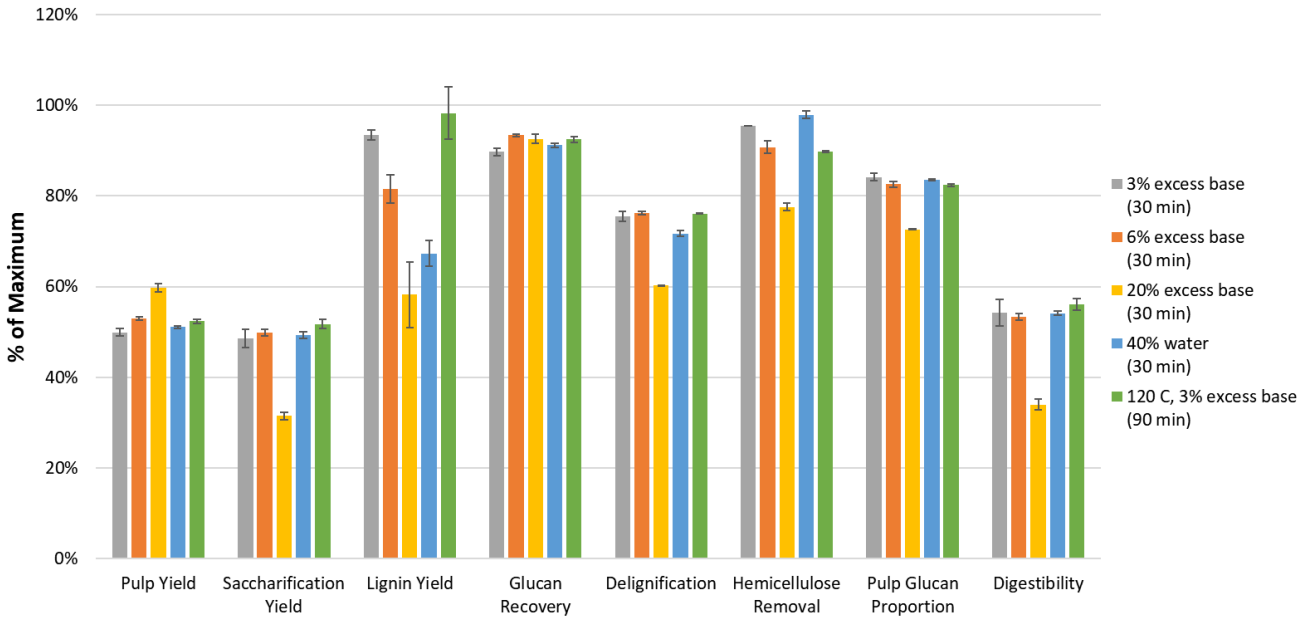


Figure 2.11: Pretreatment performance at peak saccharification yield, using [BA][HSO_4] under several conditions. Except where specified otherwise, pretreatments were carried out on *Miscanthus* at 150 °C, with 20 wt% water, an acid/base ratio of 1.00, and at a biomass loading of 10% wt/wt.

Doubling the solution water content to 40 wt% at a 1.00 acid-base ratio did not appear to significantly reduce pretreatment severity, relative to using 3% excess base with 20 wt% of water. Although lignin removal decreased by 4%, hemicellulose removal remained near-quantitative, somewhat expectedly as hemicellulose is removed by hydrolysis of glycosidic linkages.[37] Additionally, the maximum saccharification yield was still reached after 30 minutes of pretreatment, as with a water content of 20 wt%. Lignin yields decreased substantially, from 93% to 67%, which may be due to the decreased solubility of lignin in the more aqueous solution leading to more rapid redeposition and precipitation, rather than staying in solution and reacting with hemicellulose breakdown products to form pseudolignin. Rafat found the H_0 of [DMBA][HSO_4] to in fact decrease as water was added from 20 wt% to 40 wt% (from around 1.6 to 1.4). While this finding cannot be confidently applied to [BA][HSO_4] without measurements due to its different solvation behaviour, quantitative hemicellulose removal would appear to suggest a similar trend.

Reducing the pretreatment temperature from 150 °C to 120 °C, while still using 3% excess base, expectedly retarded reaction kinetics, reaching peak saccharification in 90 minutes. However, this is still strongly accelerated when compared to the behaviour of [TEA][HSO_4] at 120 °C in the work of Brandt et al, who report peak saccharification yields after 8 hours of pretreatment.[40] Pretreatment performance at peak saccharification was found to be very similar to that at 150 °C, with the largest difference being a 6% reduction in hemicellulose removal. The similarly high lignin yields, in both cases

around 20% higher than delignification, indicate substantial pseudolignin formation even at this lower temperature.

Pulp purities remained high, ranging from 82-84%, except when using 20% excess base which generated a purity of 73%. However, all conditions displayed poor saccharification, with digestibilities remaining below 60%. Except when using 20% excess base, digestibilities remained within 2% of that obtained using 3% excess base at 150 °C. Pretreatment with 20% excess base displayed the lowest digestibility, at 34%. A pulp of similar purity produced by [MBA][HSO_4] at similar conditions (71% purity after 15 minutes at 150 °C) displayed a digestibility of 50%. Thus, even when accounting for lower pulp purity, there is still a significant saccharification inhibition when using excess base.

Significantly altering pretreatment conditions with [BA][HSO_4] was therefore found not to lead to large improvements in saccharification yields or digestibility. Further experiments were carried out on pulps displaying saccharification inhibition, in a bid to improve digestibility and determine the reason for inhibition. Pretreatments were carried out using [BA][HSO_4] with an acid-base ratio of 1.00, for 30 minutes at 150 °C, and with four different pulp-washing protocols post-pretreatment, detailed in the Appendix. These protocols were designed to avoid hornification of the biomass (shown to significantly reduce saccharification yields in certain feedstocks),[39,71] remove any water-soluble saccharification-inhibiting compounds or residual IL, and remove any lignin that had re-precipitated onto the pulp surface. No significant differences in saccharification yield were observed between any of the washing protocols, with all yields between 54-57%.

The effect of enzyme loading on saccharification yield was investigated, by doubling from 0.2 to 0.4 $mL_{enzyme}/g_{biomass}$ (24 to 48 $FPU/g_{biomass}$), for pulps pretreated using [HA][HSO_4] at 150 °C for 30 minutes. Under the higher loading, saccharification yield after 7 days increased by a factor of 1.6, from 38% to 59% (see Appendix). In the work of Gschwend et al. using [TEA][HSO_4], Chambon using [DMBA][HSO_4], and in this work using [MBA][HSO_4] (see Fig. 2.18) saccharification yield has stopped increasing by 7 days.[40,43] Additionally, in the work of Sathitsuksanoh et al, cellulase enzyme loading (between 5-15 $FPU/g_{biomass}$) was found to have relatively little effect on saccharification yield from COSLIF-pretreated *Phragmites Australis* after 24 hours.[72] Similarly, in the work of Baker et al. on dilute acid-pretreated poplar, enzyme loading was only found to affect the hydrolysis kinetics.[73] Cellulase enzyme loadings of 7-42 $FPU/g_{biomass}$ gave the same 7-day saccharification yield, with similar values at 5 $FPU/g_{biomass}$, with a lower maximum only observed at 3 $FPU/g_{biomass}$. From their findings, is it may be inferred that cellulose accessibility is typically the limiting kinetic factor for enzymatic sugar release from pretreated biomass at the enzyme loadings considered in this study. This is corroborated in this study by doubling the enzyme loading for saccharification of raw *Miscanthus*, which only marginally increases

saccharification from 4.46% to 5.41%. From this study's substantial observed increase in saccharification yields in pretreated biomass, it was hypothesised that the saccharification inhibition in primary alkylammonium hydrogen sulfate ILs is due to increased enzyme deactivation, rather than due to low cellulose accessibility in the pulp.

Analysis of pretreatment and compositional data from all ILs across a number pretreatment indicators revealed digestibility to be most strongly correlated with the ratio of glucan to lignin in the pretreated pulp ($r = 0.85$, $p < 0.01$). This was closely followed by the correlation with delignification ($r = 0.78$, $p < 0.01$) and pulp purity ($r = 0.72$, $p < 0.01$), with a much weaker correlation with hemicellulose removal ($r = 0.60$, $p < 0.01$). The relationship between digestibility and glucan/lignin ratio is shown in Fig. 2.12. Primary alkylammonium ILs clearly display lower glucan/lignin ratios which appear to limit their digestibility. Although displaying high pulp purities, these result from the rapid and extensive removal of hemicellulose, which may mask their less significant lignin removal. It may therefore be concluded that lignin removal is the dominant factor controlling pretreatment efficacy when targeting sugar release. Hemicellulose removal would appear to be of limited importance, if any, contrary to reports in several studies.[74–77] The medium correlation of digestibility with hemicellulose removal may be due to the associated lignin removal (which cannot be decoupled in such acidic solvents) or general cell wall disruption, an aspect also considered by Yang et al.[77] The limited importance of hemicellulose removal is consistent with studies pretreating biomass with alkylammonium carboxylate ILs, which selectively delignify biomass while retaining the hemicellulose fraction.[78,79] Primary alkylammonium ILs may, however, still be suitable for pretreatments targeting higher-purity cellulose production for subsequent bleaching, due to their extensive and rapid hemicellulose removal.

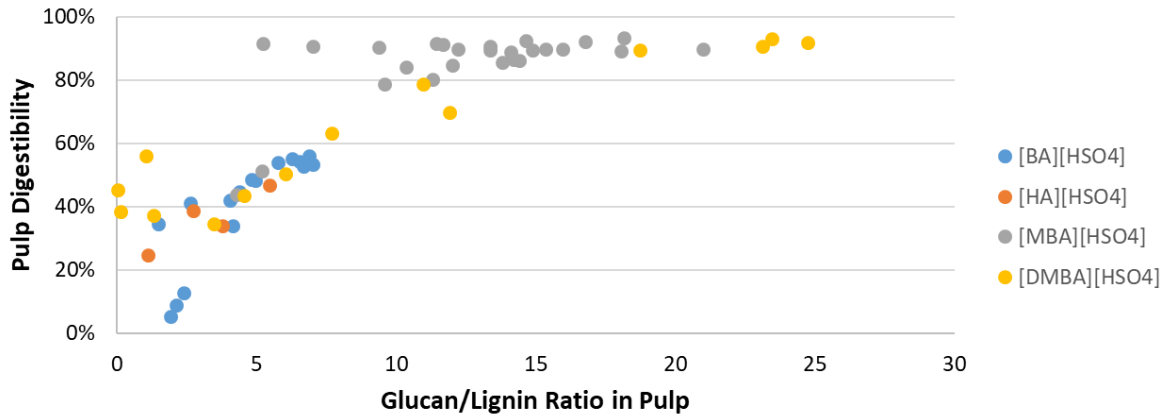


Figure 2.12: Variation of digestibility with glucan/lignin ratio, for pulps pretreated at different conditions and with differing ionic liquids. Pretreatments were carried out on *Miscanthus* at 120-170 °C, with a water content of 20-40 wt%, and at a biomass loading of 10% wt/wt.

In addition to the above experiments, a pretreatment timecourse was carried out using [BA][HSO_4] with 100% excess base, with data displayed in the Appendix. Assuming that all excess base is fully protonated by the [HSO_4]$^-$ anions (reasonable considering the large pK_a difference of 8.7 between butylamine and the [HSO_4]$^-$ anion[57,80]), the IL used is effectively [BA]$_2$[SO_4] as all [HSO_4]$^-$ anions have been deprotonated. The lack of acidic protons in the IL solution leads to a mild pretreatment, with limited lignin and hemicellulose removal after 3 hours (33% for both). Mildness of pretreatment is also evidenced by lignin yields closely matching lignin removal at all points, implying a lack of pseudolignin formation even at long pretreatment durations. Lignin and hemicellulose removal and glucan losses, without the [HSO_4]$^-$ anion, may be due to the water present in the solution, thus resembling a hydrothermal pretreatment. Similarly to the hydrothermal pretreatment of switchgrass at 150 ^oC for 20 minutes by Kumar et al, lignin removal exceeds hemicellulose removal, which is not observed in pretreatment using [HSO_4]$^-$ ILs.[81] Due to the low extent of lignin removal, saccharification yields and digestibilities remain low, reaching only 12% and 14% after 3 hours. The mildness of this pretreatment implies a low acidity of this IL solution, containing a high abundance of butylammonium cations. These results further corroborate the theory that primary and secondary alkylammonium cations enhance the acidity of alkylammonium [HSO_4]$^-$ solutions due to interactions with the [HSO_4]$^-$ anions, rather than by the cations being the direct source of acidity. Similarly, Cox et al. reported the H_0 of [Hmim]Cl to be lower than that of [Hmim][HSO_4].[30] This is unexpected, as both ILs contain the same cation but the former lacks an acidic proton on the anion, and has a circumneutral pH in dilute solutions. Therefore, the apparently enhanced acidity of [Hmim]Cl would appear to originate from interactions between ions in the non-aqueous environment, similarly to the behaviour of primary and secondary alkylammonium [HSO_4]$^-$ ILs in this study. Such non-aqueous ionic interactions could be due to the higher hydrogen bond basicity of the Cl^- anion.[82]

2.3.5 Development of [MBA][HSO_4] as a promising pretreatment solvent

In Section 2.3.2 pretreatment of *Miscanthus* using [MBA][HSO_4] was found to generate pulps with comparable maximum pulp purity and saccharification yield to those generated using [DMBA][HSO_4], at significantly shorter pretreatment durations. The pretreatment behaviour of [MBA][HSO_4] was therefore further investigated under several different conditions.

Pretreatment was carried out at two additional temperatures, 120 ^oC and 170 ^oC, with results displayed in Fig. 2.13. Pretreatment at 170 ^oC was generally similar to 150 ^oC, but with significantly accelerated kinetics: a slightly lower peak saccharification yield of 78% was achieved after 15 minutes, while maximum pulp purity of 94% was reached after 20 minutes. Maximum pulp purity was equal to

that at 150 °C, as slightly higher delignification at 170 °C was offset by a similar decrease in glucan recovery. While remaining high, pulp digestibility at peak saccharification (86%) was 6% lower than at 150 °C, and 3% lower at peak pulp purity (90%). Peak lignin removal above 100% after 20 minutes is a clear sign of pseudolignin formation.

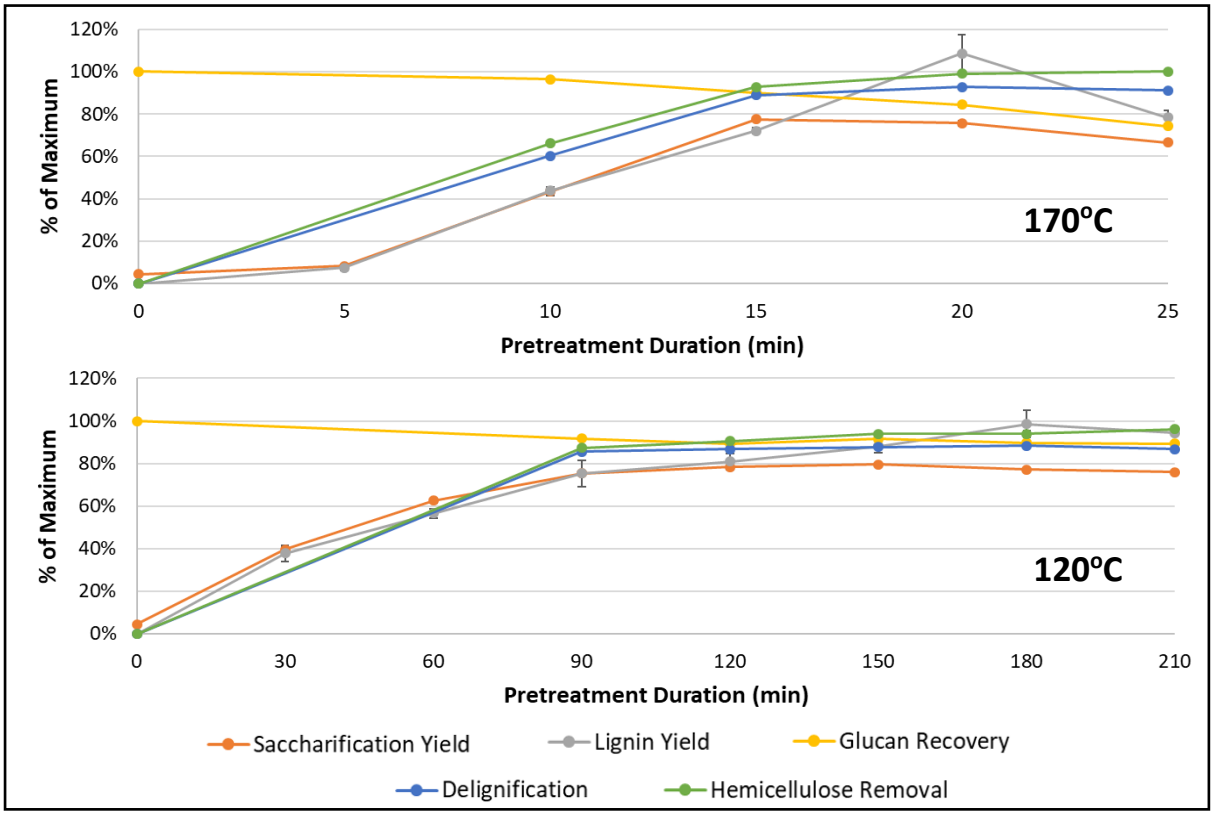


Figure 2.13: Pretreatment performance using [MBA][HSO_4]. Pretreatment temperatures are indicated on the plots. All pretreatments were carried out on *Miscanthus*, with 20 wt% water, an acid/base ratio of 1.00, and at a biomass loading of 10% wt/wt.

In addition to slower kinetics, pretreatment at 120 °C displayed differences in behaviour to 150 °C. An initial glucan loss of 10% was observed, similarly to previous pretreatments and attributed to hydrolysis of amorphous cellulose. However, at these conditions this initial loss did not significantly increase with pretreatment duration. Additionally, maxima in saccharification yield and pulp purity were significantly broader. A maximum saccharification yield of 80% was achieved after 150 minutes, with values plateauing between 120 and 180 minutes. Similarly, pulp purity was found to continually increase, reaching 89% after 150 minutes and only subsequently increasing to 90% after 210 minutes. Such broad maxima in both indicators is likely due to the absence of net lignin redeposition at these milder conditions: delignification remained between 86% and 88% between 90 and 210 minutes. This was despite lignin yields increasing in this period, and surpassing delignification above 180 minutes

(indicating pseudolignin formation). Increasing lignin yields above 90 minutes with constant delignification could be attributed to two mechanisms, possibly acting in parallel. Firstly, small, water-soluble dissolved lignin fragments may condense into larger, water-insoluble fragments, possibly while also incorporating hemicellulose breakdown products. Secondly, further lignin removal may be counterbalanced by lignin redeposition onto the pulp. In addition to lower redeposition, much higher lignin yields were reached at 120 °C compared to 150 °C (99% vs. 86%), indicating improved solubility of dissolved lignin and pseudolignin in the IL liquor. Pulp digestibilities at 120 °C remained high but were lower than at 150 °C at peak saccharification (90% vs 92%) and at peak pulp purity (85% vs 93%).

Pretreatments were also carried out using excess base at 150 °C (2% and 5% excess) and 170 °C (2% excess), in an attempt to increase pulp purity by reducing glucan degradation. Pulp purity and digestibility results are displayed in Fig. 2.14 and compared to those with no excess base, with full pretreatment and compositional analysis results provided in the Appendix.

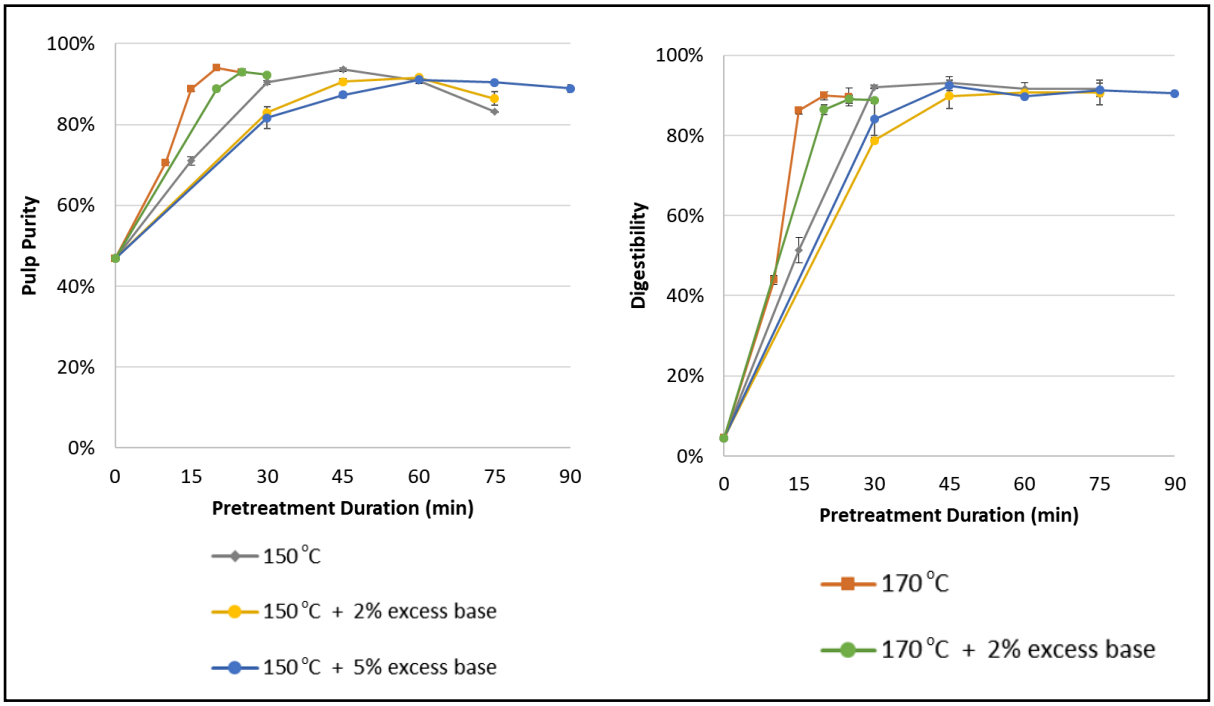


Figure 2.14: Pulp purity and digestibility following pretreatment with [MBA][HSO_4] at different conditions. All pretreatments were carried out on *Miscanthus*, with 20 wt% water, and at a biomass loading of 10% wt./wt.

In all cases, addition of excess base did not significantly affect maximum pulp purity, changing from 94% to 92% and 91% at 150 °C (using 2% and 5% excess respectively), and from 94% to 93% at 170 °C. Several reasons for this have been identified:

- Delignification and hemicellulose removal were both slower using excess base. This led to longer pretreatments being required to reach maximum pulp purity. Addition of 2% and 5% excess base increased pretreatment duration at 150 °C from 45 minutes to 60 minutes. Similarly, at 170 °C optimal pretreatment duration increased from 20 to 25 minutes. As a result of longer required pretreatments, the reduction in glucan degradation was partially offset.
- Reduction in pretreatment severity led to lower peak delignification values, as well as lower hemicellulose removal at peak pulp purity. The combination of these factors was sufficient to counteract the reductions in glucan degradation, leading to slightly lower maximum pulp purities.

Peak saccharification yields were not significantly impacted by addition of excess base. At 150 °C, peak yield was 80% with 2% excess base and 83% with 5% excess base, compared to 82% with no excess base. At 170 °C, peak yields were 79% using 2% excess base and 78% without excess base. At both temperatures, the required pretreatment duration for maximum saccharification yield was increased (to 45 and 25 minutes at 150 °C and 170 °C respectively). Similarly, pulp digestibilities were only slightly reduced by the addition of excess base, remaining above 90% at peak saccharification and pulp purity. The robustness of [MBA][HSO_4] to excess base is promising for IL recycling, during which the acid/base ratio is observed to decrease (determined from increases in pH between cycles using *Miscanthus* in previous studies, and determined by titration using wetland feedstocks in Chapter 4).[83,84]

The high purity of the obtained pulps was expected to lead to more rapid hydrolysis, due to more accessible cellulose and lower enzyme inhibition by lignin. An enzymatic hydrolysis timecourse was carried out on the highest purity pulps obtained using [MBA][HSO_4], pretreated at 170 °C for 20 minutes. Results are displayed in Fig. 2.15. Hydrolysis kinetics mirror those reported by Chambon for pretreatment of *Miscanthus* using [TEA][HSO_4] at 120 °C at the same enzyme loading, with maximum sugar release reached after 3 days of hydrolysis.[43] This suggests that the limiting kinetic factor for sugar release in high-purity pretreated pulps is the rate of the hydrolysis itself, rather than cellulose accessibility and deactivation of cellulase enzymes by residual lignin.

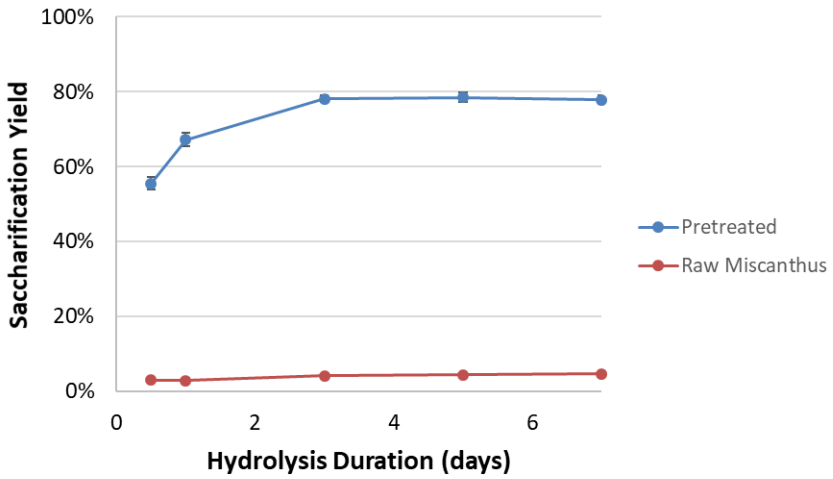


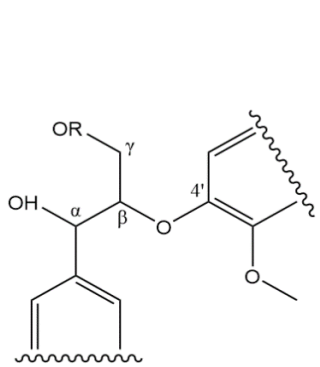
Figure 2.15: Enzymatic hydrolysis timecourse, on pulps pretreated with [MBA][HSO_4] at 170 °C for 20 minutes, and on untreated *Miscanthus*.

2.3.6 Lignin Analysis

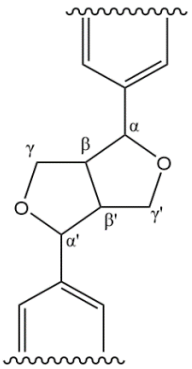
HSQC 2D NMR analysis was performed to investigate the effect of solution acidity on the structure of the recovered lignin. A study conducted by Cox et al. looked at the cleavage of lignin model compounds using four ionic liquids with the 1-methylimidazolium cation and different anions as well as two hydrogen sulfate ILs and tried to relate the obtained monomer yields to the Hammett acidity of the different protic ILs.[30] While the most acidic IL in the study, 1-methylimidazolium chloride ([Hmim]Cl), resulted in the highest monomer yields from the model compounds, the other ionic liquids did not follow a specific trend attributable to their acidity. A study looking at *Miscanthus* pretreatment with [TEA][HSO_4] showed that ether cleavage and condensation reactions in the lignin were accelerated when the IL contained 9% excess acid.[84] Similarly, when 2% excess acid and 2% excess base in the fractionation of willow with [TEA][HSO_4] were compared, the excess acid IL resulted in more cleaved β-*O*-4' linkages, especially at temperatures of 150 °C and above.[38]

Here, analysis was carried out on lignin obtained using [DMBA][HSO_4] with acid-base ratios of 1.00, 1.11, and 1.31, [BA][HSO_4] with an acid-base ratio of 0.97, and [HA][HSO_4] and [MBA][HSO_4] with acid-base ratios of 1.00, all for 60 minutes of pretreatment at 150 °C. Fig. 2.16 displays the most important lignin subunits and linkages found in *Miscanthus* lignin. Native *Miscanthus* lignin has been found to contain primarily syringyl (S), guaiacyl (G), and hydroxyphenyl (H) subunits, typical for grass lignin, as well as lower quantities of *p*-coumaric acid (PCA) and ferulic acid (FA).[26,85] These are most commonly linked by β-β', β-*O*-4', and β-5' ether bond linkages.[46] Volume integrals were calculated for major side chain (β-β', β-*O*-4', and β-5') and subunit (guaiacyl G_2, G_6 and $G_{2,cond}$, syringyl $S_{2,6}$ and $S_{cond.}$, *p*-coumaric

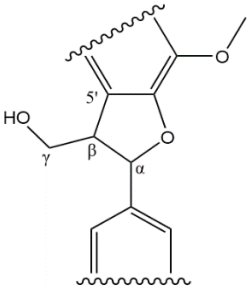
acid $PCA_{2,6}$ and *p*-hydroxyphenyl units $H_{2,6}$) signals. Other signals had to be omitted from the semi-quantitative analysis due to overlap with other signals. Results are displayed in Fig. 2.17, and are presented relative to the sum of the G_2 and $G_{2,\ condensed}$ signals, which has been shown by Gschwend et al. to be constant in IL pretreatment of *Miscanthus*.[26,46] HSQC spectra are provided in the Appendix.



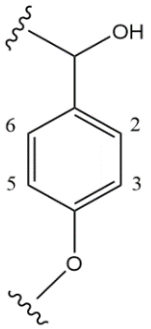
β-O-4'
β-aryl ether



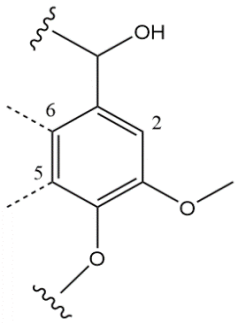
β-β'
resinol



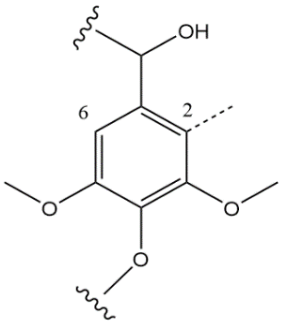
β-5'
phenylcoumaran



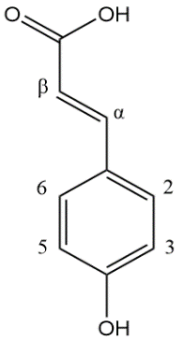
H
p-hydroxyphenyl



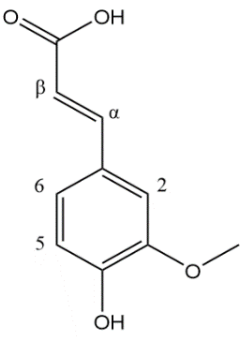
G
guaiacyl



S
syringyl



PCA
p-coumaric acid



FA
ferulic acid

Figure 2.16: *Miscanthus* lignin sub-units and linkages. Adapted from Brandt-Talbot et al.[26]

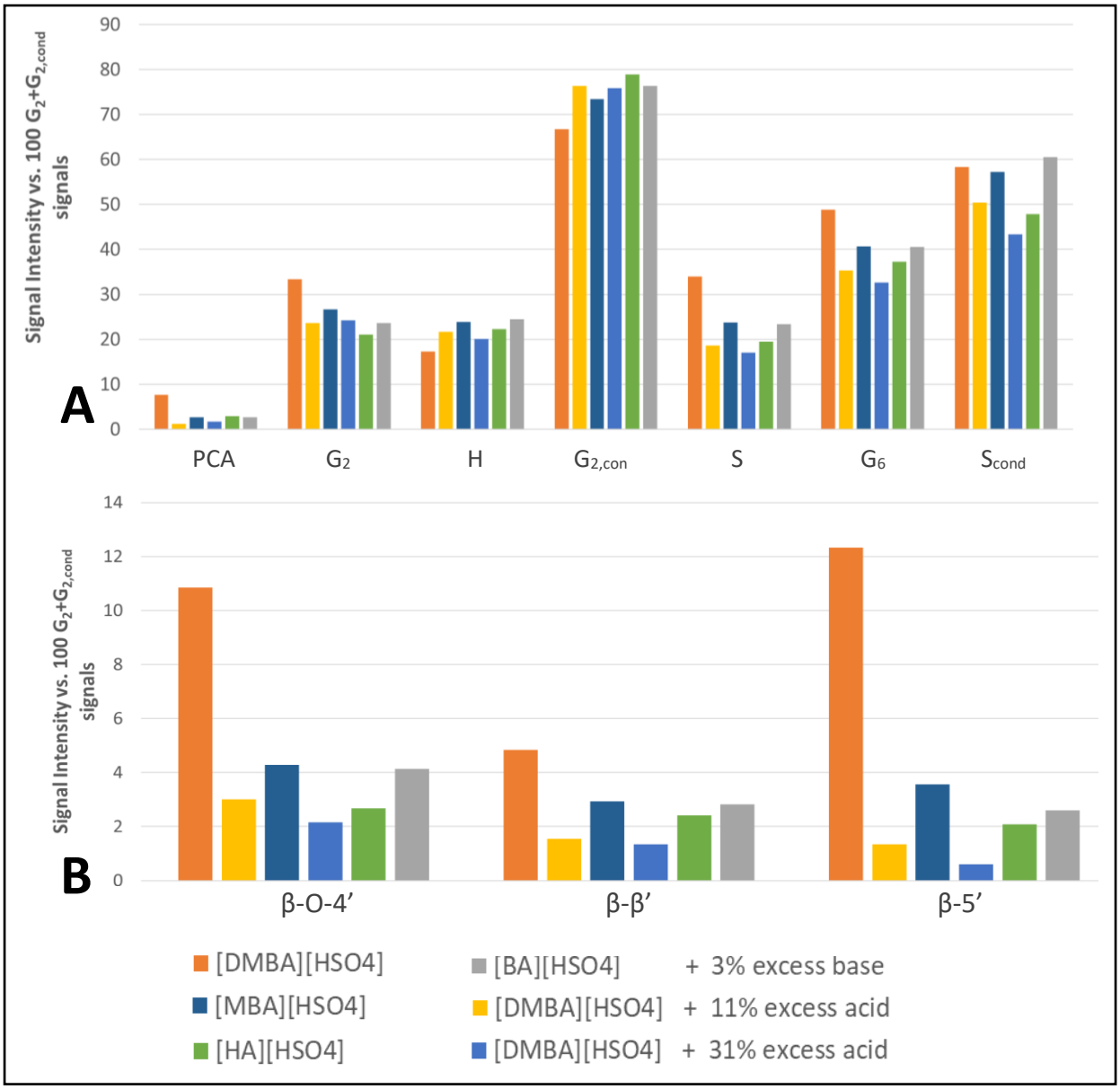


Figure 2.17: HSQC NMR signal intensities of lignin sub-units and linkages, from lignin recovered following pretreatment with varying ionic liquids. Plots are A: Major lignin subunits, B: major lignin linkages. All pretreatments were carried out on *Miscanthus* at 150 °C for 60 minutes, with 20 wt% water, and at a biomass loading of 10% wt/wt.

Several expected high-level trends are observed with the increasing severity resulting from excess acid added to [DMBA][HSO_4]: a reduction in signal intensity for ether linkages, indicating a cleavage or modification of the linkage, increasing condensation on both the S and G units, as evidenced by an increase in $S_{cond.}$ and $G_{2,cond.}$, and a decrease in G_6, with respect to total S and G signals, respectively, and the disappearance of PCA signals as H signals increase, indicating a transformation of PCA to H, all of which has been reported in the past for *Miscanthus* lignin isolated with the isomer [TEA][HSO_4].[40,84]

The S/G ratio is observed to decrease from 0.9 to 0.6 with the addition of 31% excess acid. A decrease in S/G ratio has previously been reported for Eucalyptus lignin extracted with [TEA][HSO_4] over a time course at 150 °C, and was ascribed to the fact that S-derived condensation products are less stable and their degradation results in a more G-rich lignin.[86]

Comparing the HSQC results of the lignin isolated with the secondary and primary ammonium ILs no clear trends are distinguished. With exception of the lignin isolated with [DMBA][HSO_4] without excess acid, in all lignin samples the PCA seems to have been converted to H and the vast majority of ether linkages have been broken or modified over the duration of the extraction. Also, the level of condensation on the S unit seems roughly constant between these five lignins with a proportion of condensation of 71-73%. Small differences are observed with respect to condensation on the G unit where a larger loss of G_6 signals is observed by adding acid to [DMBA][HSO_4] than for the secondary and primary ammonium ILs despite a roughly similar ratio of G_2 to $G_{2,cond.}$ (proportion of $G_{2,cond.}$ is 73-79% with respect to G_2+$G_{2,cond.}$for all five lignins). It should be noted that a change in G_5 cannot be quantified in grass lignins using 2D HSQC NMR due to overlap with $H_{3,5}$ and $PCA_{3,5}$ signals. In summary, while there is a significant difference between [DMBA][HSO_4] and all other solutions, the differences between lignins isolated under high acidity observed using HSQC NMR are small.

GPC analysis was also carried out to investigate the effect of solution acidity on the molecular weight of precipitated lignin, with results shown in Fig. 2.18. Analysis was carried out on lignin recovered from [DMBA][HSO_4] with acid-base ratios of 1.00, 1.11, and 1.31, and using [HA][HSO_4] and [MBA][HSO_4] with an acid-base ratio of 1.00, for 30 and 60 minutes of pretreatment.

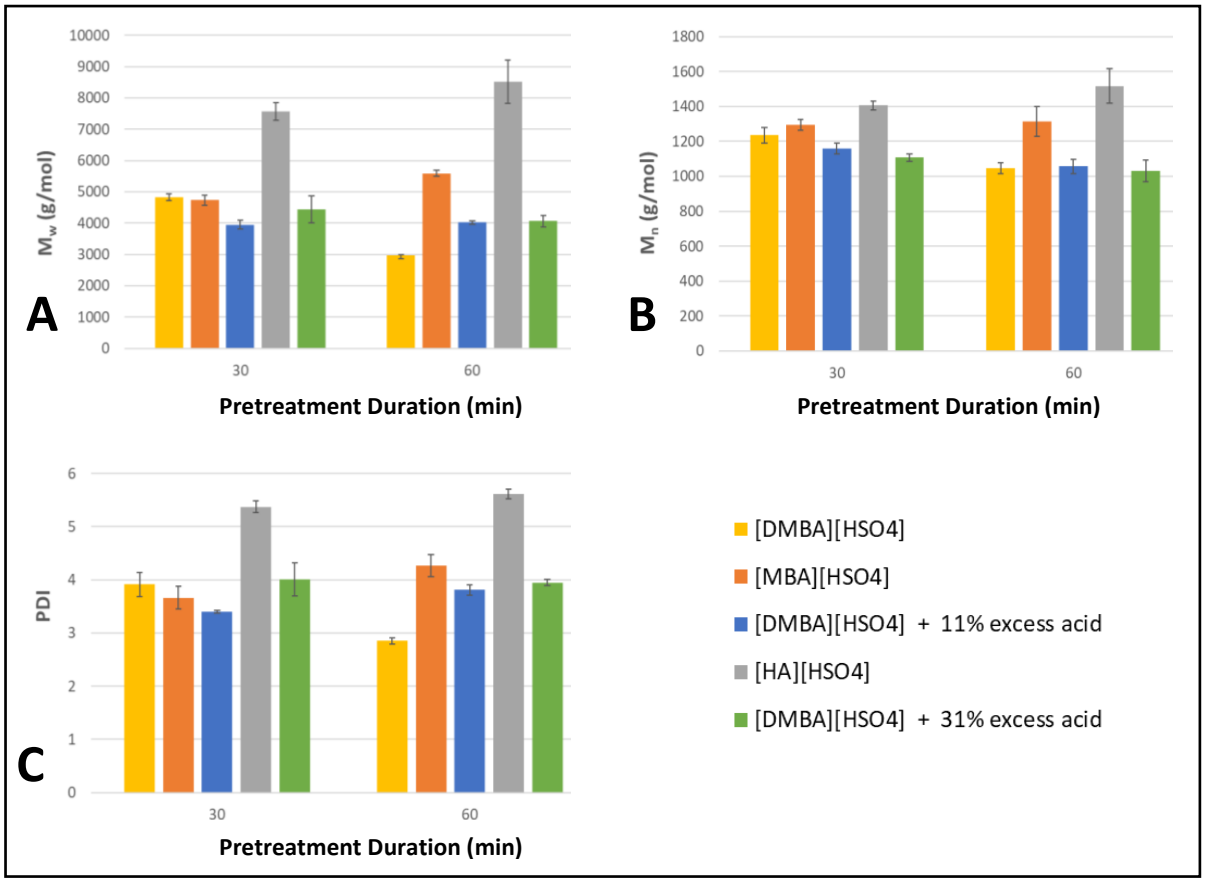


Figure 2.18: GPC analysis of recovered lignin following pretreatment with varying ionic liquids. Plots are A: Weight-averaged molecular mass, B: number-averaged molecular mass, C: Polydispersity Index (PDI). All pretreatments were carried out on *Miscanthus* at 150 °C, with 20 wt% water, and at a biomass loading of 10% wt/wt.

The lowest M_w of ca. 3000 Da is reached with [DMBA][HSO_4] without excess acid after 60 min. Surprisingly, the difference between 11 and 31% excess acid does not seem to make a large difference in terms of lignin molecular weight, despite substantial differences in acidity. Both result in a M_w of ca. 4000 Da after 60 min. Furthermore [DMBA][HSO_4] with and without excess acid results in a lignin M_n of just over 1000 Da after 60 min. The results further show that lignin molecular weight tends to increase as the degree of substitution of the alkylammonium cation decreases, with this trend getting more pronounced at longer pretreatment durations, with the highest M_w being reached after 60 min with [HA][HSO_4]. However, there is no clear trend between Hammett acidity of the IL solution, and lignin molecular weight characteristics. This is evidenced when comparing [HA][HSO_4] with [DMBA][HSO_4] (31% excess acid), and [MBA][HSO_4] with [DMBA][HSO_4] (11% excess acid). In both cases, lignin extracted using primary and secondary alkylammonium hydrogen sulfate ILs displayed significantly higher molecular weight (both weight-averaged and number-averaged) than their excess

acid [DMBA][HSO_4] counterparts, despite equal solution Hammett acidities. Additionally, the primary and secondary alkylammonium hydrogen sulfate ILs show increasing molecular weight from 30 to 60 minutes, whereas those with [DMBA][HSO_4] (both with and without excess acid) show decreasing or very similar molecular weight over this time interval. The difference in molecular weight trends between primary and secondary alkylammonium hydrogen sulfate ILs and [DMBA][HSO_4] with excess acid is unexpected and indicates that a cation effect rather than an acidity effect is responsible for the observations. Large differences in pine lignin characteristics isolated with [TEA][HSO_4] and [DMBA][HSO_4] under otherwise identical conditions have previously been reported.[39] Additionally, GPC analysis was carried out on lignins extracted using [MBA][HSO_4] with 5% excess base, for 30-90 minutes at 150 ^oC. Results are compared to those using [MBA][HSO_4] (acid-base ratio 1.00) and can be found in the Appendix. Addition of excess base reduces both M_w and M_n, presumably due to less condensation as a result of lower severity. The trends in molecular weight when adding 5% base to [MBA][HSO_4] do not mirror those of adding 11% excess acid to [DMBA][HSO_4]. In the case of [DMBA][HSO_4], increasing solution H_0 (from 11% excess acid to no excess) led to a higher M_w at 30 minutes and a lower M_w at 60 minutes, while M_n remained relatively similar. In the case of [MBA][HSO_4], increasing solution H_0 (by adding 5% excess base) led to substantially lower M_w and M_n at 30 and 60 minutes, with a bigger difference at the longer duration. Although the H_0 values of the less acidic solutions were likely not matched, these results demonstrate that, while solution acidity has a significant effect on molecular weight distribution, the way it affects these distributions may vary with IL. Addition of excess base to more acidic IL solutions is thus not analogous to addition of excess acid to less acidic IL solutions.

ionoSolv lignins from various feedstocks have previously been studied using HSQC 2D NMR and GPC and have been proposed to go through four stages during extraction.[40,86] In stage I, extraction of lignin from the biomass matrix results in isolated lignins with some intact ether bonds, low levels of condensation and high molecular weights (both M_w and M_n) and low PDI. In stage II, extraction continues while the already extracted lignin undergoes ether hydrolysis and condensation but freshly extracted lignin still looking roughly intact, results in highly polydisperse lignin with a low M_n but high M_w. Once lignin extraction is complete, stage III is reached. At this point, the polydispersity is lower again with both M_n and M_w lowered due to most of the ether bonds having been cleaved without excessive condensation. In stage IV, condensation reactions are predominant, resulting in high M_w lignins while the M_n does not show significant changes. Consequently, the PDI increases again during stage IV.

While the NMR data suggests consistency of condensation of S and G units between the lignins isolated under strongly acidic conditions, the GPC data shows significant differences in molecular weights. This suggests that the NMR data is not a good indicator of the size of high molecular weight lignin. The findings indeed indicate that these two methods are highly complementary, as evidenced by the differences and similarities seen between the studied lignins.

2.4 Conclusions

In this chapter, the acidity of four alkylammonium $[HSO_4]^-$ protic ionic liquids with different cation structures were compared. Unexpectedly, a lower degree of substitution of the cation was found to enhance the IL solution acidity (containing 20 wt% water), as measured by the Hammett acidity function. The acidity of [MBA][HSO_4] was found to be equivalent to that of [DMBA][HSO_4] with 11% excess acid, while those of [HA][HSO_4] and [BA][HSO_4] were found to be equivalent to that of [DMBA][HSO_4] with 31% and 32% excess acid respectively. This was attributed to increased anion-cation and anion-anion interactions in of primary and secondary alkylammonium ILs, reducing the intercalation of water into the ionic network, and thus reducing the solvation of the $[HSO_4]^-$ anions, increasing their proton activity. Density effects were shown to not play a significant role. Although addition of up to 20% excess base to [BA][HSO_4] was found to make the IL solution less acidic, its H_0 was still substantially lower than that of [DMBA][HSO_4], as well as lower than that of [MBA][HSO_4].

The pretreatment performance of all four ILs was compared through timecourse experiments at 150 ^oC, using *Miscanthus* as a feedstock. Expectedly, more acidic IL solutions displayed accelerated pretreatment behaviour, achieving peak pulp purity and saccharification at shorter pretreatment durations. Additional hallmarks of severe pretreatments were also observed, such as significant lignin redeposition on the pulp, higher glucan degradation, and pseudolignin formation. Primary alkylammonium cations were found to produce pulps of reasonable purity (>80%), but with low digestibilities. The reason for the low pulp digestibilities was found to be highly correlated to a lower glucan/lignin ratio in the pulps from these ILs, with the more extensive hemicellulose removal found not to significantly improve saccharification yields. Saccharification was shown to be inhibited by increased enzyme deactivation rather than low cellulose accessibility, with this inhibition observed for a range of conditions using [BA][HSO_4]. These included including milder pretreatments at lower temperature, using up to 20% excess base, or significantly reducing the IL concentration.

11% and 31% excess acid was added to [DMBA][HSO_4], with resulting solution acidities equal to those of [MBA][HSO_4] and [HA][HSO_4]. These excess acid solutions were then used for pretreatment timecourses at 150 ^oC and compared to those using the primary and secondary alkylammonium

cations. Pretreatments using excess acid were significantly more severe, displaying much lower glucan recoveries, and earlier and sharper delignification peaks. Both also displayed saccharification inhibition, with low digestibilities observed throughout the timecourse, including at high pulp purities. These results were taken as evidence of different types of acidity existing between solutions of primary and secondary alkylammonium $[HSO_4]^-$ ILs, and solutions containing excess acid. These different types of acidity are thus not distinguishable using the Hammett acidity function. Additionally, the Hammett acidity function does not appear to be appropriate for use as part of a severity factor for IL pretreatment, at least when changing the IL structure.

[MBA][HSO_4] was found to be a viable alternative to [DMBA][HSO_4], a current benchmark for IL pretreatment. At 150 °C, very similar maximum saccharification yields (>80%) and pulp purities (> 90%) were observed, with [MBA][HSO_4] achieving these in around two thirds the pretreatment time. The pretreatment performance of [MBA][HSO_4] was found to be relatively insensitive to a range of parameters, such as increases and decreases in pretreatment temperature, and addition of up to 5% excess base (important for IL recycling considerations). A thermal degradation test revealed [MBA][HSO_4] displayed the same thermal stability as [DMBA][HSO_4], with no degradation products visible by NMR after 72 hours at 170 °C.

HSQC spectroscopy was performed on the lignin recovered from pretreatments using [DMBA][HSO_4], [MBA][HSO_4], [BA][HSO_4], and [HA][HSO_4], as well as those using [DMBA][HSO_4] with 11% and 31% excess acid. Expectedly, ether bond cleavage was found to increase in more acidic solutions, with this effect more pronounced using excess acid than ILs with primary and secondary alkylammonium cations. Relative to [DMBA][HSO_4], lignin condensation also increased with increased acidity, but was relatively similar between the more acidic solutions. In general, increasing acidity was found to decrease the S/G ratio of recovered lignin. Trends among the more acidic solutions were not always consistent, implying significant factors beyond Hammett acidity. GPC analysis revealed that lignin molecular weight tended to increase over time in primary and secondary alkylammonium HSO_4 ILs but decreased in solutions of [DMBA][HSO_4] with excess acid.

Overall, this study has provided further insight into the behaviour of alkylammonium $[HSO_4]^-$ ILs in the ionoSolv process, as well as the effects of increased acidity on pretreatment efficacy. The development of [MBA][HSO_4] as a promising pretreatment solvent highlights the tunability of ionic liquids, and the importance of thorough screening to improve performance. It is hoped that the results obtained will provide a basis for further probing and optimisation of the ionoSolv process, as part of a movement towards a more bio-based economy.

References

1 A. C. Pinto, A. A. M. Lapis, B. V. da Silva, R. S. Bastos, J. Dupont and B. A. D. Neto, *Tetrahedron Lett.*, 2008, **49**, 5639–5641.
2 N. Brausch, A. Metlen and P. Wasserscheid, *Chem. Commun.*, 2004, **4**, 1552–1553.
3 Y. Chauvin, A. Hirschauer and H. Olivier, *J. Mol. Catal.*, 1994, **92**, 155–165.
4 T. Welton, *Coord. Chem. Rev.*, 2004, **248**, 2459–2477.
5 J. Dupont, R. F. De Souza and P. A. Z. Suarez, *Chem. Rev.*, 2002, **102**, 3667–3692.
6 A. A. M. Lapis, B. A. DaSilveira Neto, J. D. Scholten, F. M. Nachtigall, M. N. Eberlin and J. Dupont, *Tetrahedron Lett.*, 2006, **47**, 6775–6779.
7 R. Rinaldi, R. Palkovits and F. Schüth, *Angew. Chemie*, 2008, **120**, 8167–8170.
8 G. P. Smith, A. S. Dworkin, R. M. Pagni, S. P. Zingg, T. E. Adv Phys Org Chem, S. Prakash, J. Superacids and J. L. Inorg, *J. Am. Chem. Soc.*, 1989, **111**, 1491.
9 K. E. Johnson, R. M. Pagni and J. Bartmess, *Monatshefte für Chemie*, 2007, **138**, 1077–1101.
10 J. Augé and G. Sizun, *Green Chem.*, 2009, **11**, 1179–1183.
11 L. S. Santos, B. A. DaSilveira Neto, C. S. Consorti, C. H. Pavam, W. P. Almeida, F. Coelho, J. Dupont and M. N. Eberlin, *J. Phys. Org. Chem.*, 2006, **19**, 731–736.
12 A. Sarkar, S. R. Roy, N. Parikh and A. K. Chakraborti, *J. Org. Chem.*, 2011, **76**, 7132–7140.
13 Z. Duan, Y. Gu, J. Zhang, L. Zhu and Y. Deng, *J. Mol. Catal. A Chem.*, 2006, **250**, 163–168.
14 C. Chiappe, E. Leandri and M. Tebano, *Green Chem.*, 2006, **8**, 742–74.
15 Z. Fei, D. Zhao, T. J. Geldbach, R. Scopelliti and P. J. Dyson, *Chem. - A Eur. J.*, 2004, **10**, 4886–4893.
16 A. C. Cole, J. L. Jensen, I. Ntai, K. T. Loan Tran, K. J. Weaver, D. C. Forbes and J. H. Davis, *J. AM. CHEM. SOC*, 2002, **124**, 5962–5963.
17 R. L. Vekariya, *J. Mol. Liq.*, 2017, **227**, 44–60.
18 Y. Zhao, J. Long, F. Deng, X. Liu, Z. Li, C. Xia and J. Peng, *Catal. Commun.*, 2009, **10**, 732–736.
19 M. Vafaeezadeh and H. Alinezhad, *J. Mol. Liq.*, 2016, **218**, 95–105.
20 M. Addicoat, R. Atkin, J. N. Canongia Lopes, M. Costa Gomes, M. Firestone, R. Gardas, S. Halstead, C. Hardacre, L. J. Hardwick, J. Holbrey, P. Hunt, V. Ivaništšev, J. Jacquemin, R. Jones, B. Kirchner, R. Lynden-Bell, D. Macfarlane, G. Marlair, H. Medhi, M. Mezger, A. Pádua, I. Pantenburg, S. Perkin, J. E. S. J. Reid, M. Rutland, S. Saha, K. Shimizu, J. M. Slattery, M. Swadźba-Kwaśny, S. Tiwari, S. Tsuzuki, B. Uralcan, A. Van Den Bruinhorst, M. Watanabe and J. Wishart, *Faraday Discuss.*, 2018, 206, 291–337.
21 P. A. Hunt, *Top. Curr. Chem.*, 2017, 375.
22 R. P. Matthews, T. Welton and P. A. Hunt, *Phys. Chem. Chem. Phys*, 2015, **17**, 14437.
23 K. Fumino, A. Wulf and R. Ludwig, *Phys. Chem. Chem. Phys.*, 2009, **11**, 8790–8794.
24 D. Fărcaşiu, A. Ghenciu and G. Miller, *J. Catal.*, 1992, **134**, 118–125.
25 J. Grasvik, J. P. Hallett, T. Q. To and T. Welton, *Chem. Commun.*, 2014, **50**, 7258–7261.
26 A. Brandt-Talbot, F. J. V. Gschwend, P. S. Fennell, T. M. Lammens, B. Tan, J. Weale and J. P. Hallett, *Green Chem.*, 2017, **19**, 3078–3102.
27 Y. L. Loow, T. Y. Wu, J. M. Jahim, A. W. Mohammad and W. H. Teoh, *Cellulose*, 2016, **23**, 1491–1520.
28 Z. Zhang, M. D. Harrison, D. W. Rackemann, W. O. S. Doherty and I. M. O'Hara, *Green Chem.*, 2016, **18**, 360–381.
29 Y. Pu, F. Hu, F. Huang, B. H. Davison and A. J. Ragauskas, *Biotechnol. Biofuels*, 2013, **6**, 1–13.
30 B. J. Cox, S. Jia, Z. C. Zhang and J. G. Ekerdt, *Polym. Degrad. Stab.*, 2011, **96**, 426–431.
31 B. J. Cox and J. G. Ekerdt, *Bioresour. Technol.*, 2012, **118**, 584–588.
32 A. Brandt, L. Chen, B. E. Van Dongen, T. Welton and J. P. Hallett, *Green Chem.*, 2015, **17**, 5019–5034.
33 X. Pan, D. Xie, R. W. Yu and J. N. Saddler, *Biotechnol. Bioeng.*, 2008, **101**, 39–48.
34 B. S. Donohoe, S. R. Decker, M. P. Tucker, M. E. Himmel and T. B. Vinzant, *Biotechnol. Bioeng.*, 2008, **101**, 913–925.
35 S. V. Pingali, V. S. Urban, W. T. Heller, J. McGaughey, H. ONeill, M. Foston, D. A. Myles, A. Ragauskas and B. R. Evans, *Biomacromolecules*, 2010, **11**, 2329–2335.
36 S. Jia, B. J. Cox, X. Guo, Z. C. Zhang and J. G. Ekerdt, *ChemSusChem*, 2010, **3**, 1078–1084.
37 P. Verdía, A. Brandt, J. P. Hallett, M. J. Ray and T. Welton, *Green Chem.*, 2014, **16**, 1617–1627.
38 L. Weigand, S. Mostame, A. Brandt-Talbot, T. Welton and J. P. Hallett, *Faraday Discuss.*, 2017, **202**, 331–349.
39 F. J. V. Gschwend, C. L. Chambon, M. Biedka, A. Brandt-Talbot, P. S. Fennell and J. P. Hallett, *Green Chem.*, 2019, **21**, 692–703.
40 F. J. V. Gschwend, F. Malaret, S. Shinde, A. Brandt-Talbot and J. P. Hallett, *Green Chem.*, 2018, **20**, 3486–3498.
41 A. Brandt, M. J. Ray, T. Q. To, D. J. Leak, R. J. Murphy and T. Welton, *Green Chem.*, 2011, **13**, 2489.
42 A. Brandt, J. P. Hallett, D. J. Leak, R. J. Murphy and T. Welton, *Green Chem.*, 2010, **12**, 672.
43 C. Chambon, PhD Thesis, Imperial College London, 2017.
44 C. L. Chambon, T. Y. Mkhize, P. Reddy, A. Brandt-Talbot, N. Deenadayalu, P. S. Fennell and J. P. Hallett, *Biotechnol. Biofuels*, 2018, **11**, 247.
45 C. L. Chambon, M. Chen, P. S. Fennell and J. P. Hallett, *Front. Chem.*, 2019, **7**, 1–13.
46 F. Gschwend, PhD Thesis, Imperial College London, 2017.
47 A. George, A. Brandt, K. Tran, S. M. S. N. S. Zahari, D. Klein-Marcuschamer, N. Sun, N. Sathitsuksanoh, J. Shi, V.

Stavila, R. Parthasarathi, S. Singh, B. M. Holmes, T. Welton, B. A. Simmons and J. P. Hallett, *Green Chem.*, 2015, **17**, 1728–1734.
48 L. Chen, M. Sharifzadeh, N. Mac Dowell, T. Welton, N. Shah and J. P. Hallett, *Green Chem.*, 2014, **16**, 3098–3106.
49 H. Baaqel, I. Díaz, V. Tulus, B. Chachuat, G. Guillén-Gosálbez and J. P. Hallett, *Green Chem.*, 2020, **22**, 3132–3140.
50 A. J. Haughton, A. J. Bond, A. A. Lovett, T. Dockerty, G. Sünnenberg, S. J. Clark, D. A. Bohan, R. B. Sage, M. D. Mallott, V. E. Mallott, M. D. Cunningham, A. B. Riche, I. F. Shield, J. W. Finch, M. M. Turner and A. Karp, *J. Appl. Ecol.*, 2009, **46**, 315–322.
51 L. Hammett and A. Deyrup, *J. Am. Chem. Soc.*, , DOI:10.1021/ja01346a015.
52 R. Stewart and D. Dolman, *A comparison of the acidity and basicity of aromatic amines*, 1967, vol. 45.
53 A. Sluiter, B. Hames, D. Hyman, C. Payne, R. Ruiz, C. Scarlata, J. Sluiter, D. Templeton and J. Wolfe, *Determination of Total Solids in Biomass and Total Dissolved Solids in Liquid Process Samples, NREL/TP-510-42621*, 2008.
54 M. G. Resch, J. O. Baker and S. R. Decker, *Low Solids Enzymatic Saccharification of Lignocellulosic Biomass: Laboratory Analytical Procedure (LAP), Issue Date: February 4, 2015*, 2015.
55 A. Sluiter, B. Hames, R. O. Ruiz, C. Scarlata, J. Sluiter and D. Templeton, *Determination of Structural Carbohydrates and Lignin in Biomass, NREL/TP-510-42618*, 2008.
56 T. C. Pin, P. Y. S. Nakasu, S. Mattedi, S. C. Rabelo and A. C. Costa, *Fuel*, 2019, **235**, 1506–1514.
57 H. K. Hall, *J. Am. Chem. Soc.*, 1957, **79**, 5441–5444.
58 pKas of Organic Acids and Bases, https://labs.chem.ucsb.edu/zhang/liming/pdf/pKas_of_Organic_Acids_and_Bases.pdf, (accessed 3 June 2019).
59 pKa Compilation, https://www.chem.wisc.edu/areas/reich/pkatable/pKa_compilation-1-Williams.pdf, (accessed 20 June 2019).
60 D. R. Lide, *CRC Handbook of Chemistry and Physics*, CRC Press, Boca Raton, 84th edn., 2004.
61 M. A. Paul and F. A. Long, *Chem. Rev.*, 1957, **57**, 1–45.
62 V. Kazansky and V. Solkan, *Phys. Chem. Chem. Phys.*, 2003, **5**, 31–35.
63 A. R. Abouelela, PhD Thesis, Imperial College London, 2021.
64 G. F. De Gregorio, C. C. Weber, J. Gräsvik, T. Welton, A. Brandt and J. P. Hallett, *Green Chem.*, 2016, **18**, 5456–5465.
65 Q. Xiang, J. S. Kim and Y. Y. Lee, *Appl. Biochem. Biotechnol. - Part A Enzym. Eng. Biotechnol.*, 2003, **106**, 337–352.
66 E. G. A. Rocha, T. C. Pin, S. C. Rabelo and A. C. Costa, *Fuel*, 2017, **206**, 145–154.
67 N. Pareek, T. Gillgren and L. J. Jönsson, *Bioresour. Technol.*, 2013, **148**, 70–77.
68 J. D. McMillan, in *Enzymatic Conversion of Biomass for Fuels Production*, eds. M. E. Himmel, J. O. Baker and R. Overend, American Chemical Society, Washington, 1994, pp. 292–324.
69 A. Brandt, J. Gräsvik, J. P. Hallett and T. Welton, *Green Chem.*, 2013, **15**, 550–583.
70 F. Hu, S. Jung and A. Ragauskas, *ACS Sustain. Chem. Eng.*, 2013, **1**, 62–65.
71 X. L. Luo, J. Y. Zhu, R. Gleisner and H. Y. Zhan, *Cellulose*, 2011, **18**, 1055–1062.
72 N. Sathitsuksanoh, Z. Zhu, N. Templeton, J. A. Rollin, S. P. Harvey and Y. H. P. Zhang, *Ind. Eng. Chem. Res.*, 2009, **48**, 6441–6447.
73 J. O. Baker, M. R. King, W. S. Adney, S. R. Decker, T. B. Vinzant, S. E. Lantz, R. E. Nieves, S. R. Thomas, L. C. Li, D. J. Cosgrove and M. E. Himmel, *Appl. Biochem. Biotechnol. - Part A Enzym. Eng. Biotechnol.*, 2000, **84–86**, 217–223.
74 T. Jeoh, C. I. Ishizawa, M. F. Davis, M. E. Himmel, W. S. Adney and D. K. Johnson, *Biotechnol. Bioeng.*, 2007, **98**, 112–122.
75 A. Várnai, M. Siika-aho and L. Viikari, *Enzyme Microb. Technol.*, 2010, **46**, 185–193.
76 V. T. de O. Santos, G. Siqueira, A. M. F. Milagres and A. Ferraz, *Ind. Crops Prod.*, 2018, **111**, 722–730.
77 B. Yang and C. E. Wyman, *Biotechnol. Bioeng.*, 2004, **86**, 88–98.
78 P. Y. S. Nakasu, C. J. Clarke, S. C. Rabelo, A. C. Costa, A. Brandt-Talbot and J. P. Hallett, *ACS Sustain. Chem. Eng.*, 2020, **8**, 7952–7961.
79 J. Sun, N. V. S. N. M. Konda, R. Parthasarathi, T. Dutta, M. Valiev, F. Xu, B. A. Simmons and S. Singh, *Green Chem.*, 2017, **19**, 3152–3163.
80 Ka and pKa for Polyprotic Acids, http://www2.ucdsb.on.ca/tiss/stretton/Database/polyprotic_acids.htm, (accessed 25 March 2020).
81 S. Kumar, U. Kothari, L. Kong, Y. Y. Lee and R. B. Gupta, *Biomass and Bioenergy*, 2011, **35**, 956–968.
82 A. Oehlke, K. Hofmann and S. Spange, *New J. Chem.*, 2006, **30**, 533–536.
83 W. Tu, PhD Thesis, Imperial College London, 2018.
84 A. Brandt-Talbot, F. J. V. Gschwend, P. S. Fennell, T. M. Lammens, B. Tan, J. Weale and J. P. Hallett, *Green Chem.*, 2017, **19**, 3078–3102.
85 Q. Sun, Y. Pu, X. Meng, T. Wells and A. J. Ragauskas, *ACS Sustain. Chem. Eng.*, 2015, **3**, 2203–2210.
86 F. Malaret, F. J. V. Gschwend, J. M. Lopes, W.-C. Tu and J. P. Hallett, *RSC Adv.*, 2020, **10**, 16050–16060.

Chapter 3: Assessing the Economic Viability of Wetland Remediation of Wastewater, and the Potential for Parallel Biomass Valorisation

3.1 Introduction

Pollution of global waters has been highlighted as one of the major problems facing society.[1–4] The increasing contamination of waterways has wide-ranging damaging impacts, from local ecology to human health.[1,3–5] In addition, such contamination has a severe economic impact, with the World Bank estimating that countries need to spend $150 bn a year in order to meet sustainability targets.[6] Additionally, by 2050 the OECD projects that water demand will have increase by 55% relative to 2000, and climate change is expected to increase water stress globally.[3,7,8] There is therefore significant pressure for economic and effective treatment and re-use of wastewater.

Three of the major global pollutants are organic wastes (characterised by the Biochemical Oxygen Demand, BOD), and the nutrients nitrogen and phosphorus.[9] Increased BOD and nutrient concentrations in waterways can lead to unsustainable algal growth, forming algal blooms which deplete oxygen levels, consume dissolved inorganic carbon, and may both increase the pH of surface waters and cause ocean acidification.[10–12] This is further explored in Chapter 1. The result is possibly irreversible damage to local ecosystems, and the services which they provide.[10,13] Anthropogenic activity has been shown to have a significant impact on BOD and nutrient concentrations in surface waters, mainly from agriculture, industry, and urban activity.[13–16] 80% of global municipal wastewater, and 90% of the sewage from developing countries, is discharged without treatment, contributing to the 2 million tonnes of effluent entering worldwide waterways each day.[1,8] Following physical separation of larger particles, BOD and nitrogen removal from wastewater is often performed using biological systems such as activated sludge, trickling filters, and oxidation ponds.[17,18] Phosphorus removal may be accomplished *via* a variant of the activated sludge process, or via chemical precipitation of metallo-phosphorus compounds.[17,19,20] These technologies, while effective in economically developed countries, may be considered too expensive and energy- and resource-intensive for many developing countries in which wastewater treatment is not a priority investment.[5,8,21]

Acid Mine Drainage (AMD) is an acidic discharge with typically elevated metal content, generated during and following mining activity and which may last for decades or centuries.[22] Formation of AMD

is naturally slow and has limited environmental impact, but human mining activity significantly accelerates its generation by increasing the exposure of sulfide-containing rocks to air and water.[23] This is further explored in Chapter 1. Several localised studies have been carried out to quantify the prevalence of AMD-polluted waterways, estimating that up to 16,000 km, 4,500 km, and 600 km of U.S, European, and British waterways are being affected respectively.[23–25] The costs of clean-up for the U.S and Canada have been estimated at up to $72bn and $5bn respectively.[26,27] The most common remediation technology is the addition of alkaline substances such as lime or calcium carbonate to increase the pH of AMD waters.[28,29] The principal drawbacks with the conventional remediation methods are cost and the need for long-term maintenance, with the latter especially important when considering the long lifetime of AMD.[30]

Wetland remediation involves using man-made constructed wetlands (CWs) to treat contaminated wastewater, simulating the "biological filter" effect of natural wetlands. Details on the remediation mechanisms and applications of constructed wetlands can be found in Chapter 1. CWs have been repeatedly highlighted as suitable wastewater treatment technologies for smaller communities in developing countries.[31–38] This is due to their lower resource requirements relative to wastewater treatment plants, and to the generally warmer tropical and subtropical climates in such countries, shown to improve constructed wetland performance.[37,39–42] However studies on wetland remediation in developing countries tend to either analyse the possible advantages of this technology, or focus on the promising performance of individual wetland systems to promote their use. There is thus a lack of studies reviewing their use over a large region, making quantifying the uptake of CW systems in developing countries challenging, although several studies have qualitatively suggested that uptake may be fairly limited.[36,37,43] The most notable exception is in China, where multiple comprehensive reviews have studied the deployment and performance of constructed wetlands.[40,44,45] In China, the ratio of CW capacity to wastewater treatment plant capacity increased from 0.06% in 2003 to 0.83% in 2010, with this ratio showing a continually increasing trend.[40,45] These systems were found to treat a wide range of different effluents, with the most common being domestic sewage, and were found to be most used in regions with more tropical climates.[40]

Wetland remediation is often reported as being a low-maintenance and low-cost alternative to conventional remediation of several types of wastewater. While the former claim is relatively self-evident, the latter tends not to be substantiated. Comparative economic studies do exist, but are generally case-specific and thus do not provide a general overview of the economic viability of wetland remediation.[46–48] In this chapter, the costs of wetland treatment of wastewater for BOD and nutrient removal (BOD, phosphorus, and nitrogen) are determined for a range of influent and effluent conditions. These are compared to those of conventional treatment found in the literature to identify

the most economically favourable range of conditions for wetland remediation. The effect of uncertainty in the sizing and costing parameters are investigated semi-quantitatively. In addition, the relative costs of wetland and conventional remediation are presented for remediation of both circumneutral and low-pH Acid Mine Drainage (AMD), under different contaminant removal rates and wetland designs. The economic impact and feasibility of biomass harvesting and utilisation are discussed, with the aim of improving the process economics of wetland remediation. It should be noted that the results from this chapter have been published in the RSC journal Environmental Science: Water Research & Technology.[49] Much of that manuscript has been re-used in this chapter, in accordance with the RSC guidelines.

3.2 Materials and Methods

3.2.1 Wetland Design for BOD and Nutrient Removal

For BOD and nutrient (nitrogen and phosphorus) removal, the methodology of Kadlec and Wallace, based upon the *P-k-C** model, was used to size wetlands to achieve effluent targets.[50] Free Water Surface (FWS) wetland designs were used in this study, due to the higher availability of data. In the BOD and nutrient removal *P-k-C** model, a given wetland is designed and constructed as one or more cells, operating in series. Each wetland cell behaves hydraulically as a number, *N*, of tanks in series (TIS), termed the N_{TIS}. A higher N_{TIS} value corresponds to a well-designed wetland with a narrower range of residence times, and thus a closer approximation to ideal plug flow, with lower output concentrations. A low N_{TIS} value corresponds to a poorly-designed wetland with channelling and/or poor mixing, leading to a larger range of outputs, with a generally higher mean output concentrations. The value of N_{TIS} is determined in practice using tracer measurements through the wetland. To reflect the weathering of a particular contaminant as it flows through the cell and the subsequent change in removal rates, a value termed the P_{TIS} is used as an effective value for N_{TIS}, thus accounting for both hydraulics and contaminant removal. Kadlec and Wallace provide a methodology for estimating P_{TIS} for a given wetland cell.[50]

Within each wetland cell, a water balance is applied to each tank in series, to account for changes due to precipitation, evapotranspiration, and infiltration, as shown in Eq. 3.1. However, infiltration, evapotranspiration, and precipitation were set to 0 in all analysis except Monte Carlo simulations.

$$\mathrm{Q_o} = \mathrm{Q_i} - \mathrm{A} \cdot (\mathrm{I} + \mathrm{Et} - \mathrm{P}) \tag{3.1}$$

where *Q* is the volumetric flow rate, *A* is the wetland area, *I* is infiltration per unit area, *Et* is evapotranspiration per unit area, and *P* is precipitation per unit area.

Within each tank, the model assumes a first-order areal removal rate for each contaminant, with a fixed background concentration. The mass balance for contaminant removal, assuming no contaminant concentration in precipitation, is shown in Eq. 3.2. Eqs. 3.1 and 3.2 are thus sequentially applied to each of the P_{TIS} for all contaminants, and a minimum wetland area which meets effluent targets for all contaminants may be determined. Values for *k* and *C** for different contaminants in FWS wetlands were taken from the compiled data in the work of Kadlec and Wallace, using median values in the reported frequency distributions for phosphorus and nitrogen removal.[50] No precipitation, evapotranspiration, infiltration or transpiration were included when generating results, making these conservative estimates (i.e. without contaminant removal through transpiration and infiltration, or dilution of contaminants through precipitation).

$$Q_o \cdot C_o = Q_i \cdot C_i - A \cdot (I \cdot C_o - \alpha \cdot Et \cdot C_o - k \cdot (C_o - C^*)) \quad (3.2)$$

where *C* is pollutant concentration, *α* is the transpiration fraction of evapotranspiration, *k* is the first-order areal removal rate of the contaminant, C^* is the background concentration of the contaminant. Subscripts *i* and *o* represent input and output values respectively. *Q*, *Et*, *I*, and *A* are defined as in Eq.3.1.

When sizing wetlands for given effluent standards, exceedance multipliers were used to account for intra-system variability in performance. These values represent the frequency of deviation from the calculated effluent concentration, and were compiled for different pollutants in the work of Kadlec and Wallace.[50] They are applied as shown in Eq. 3.3. 90% multipliers were used for this study, meaning that the output concentrations are expected to be at or below the target output concentration 90% of the time.

$$C_{design} = \frac{C_{target}}{\Psi} \quad (3.3)$$

where C_{design} is the output concentration used to design the wetland, C_{target} is the actual output concentration target, and Ψ is the exceedance multiplier for a given frequency.

BOD Removal

In the case of BOD removal, background concentrations are significantly higher than for other pollutants, due to the growth and decay of the wetland biomass, and wetlands receiving higher levels of input are reported to have higher background concentrations.[50] A '4-tier' system is implemented in

the data classifications of Kadlec and Wallace: “super” (BOD input > 200 mg/L), “primary” (100 < BOD input < 200 mg/L), “secondary” (30 < BOD input < 100 mg/L), and “tertiary” (BOD input < 30 mg/L). Each class is calculated to have its own *k*-value and background concentration *C**. For the purpose of this study the system was altered: each class was assumed to have the same *k*-value of 37 m/yr (the mean of the medians given for primary, secondary, and tertiary classes). The background BOD concentration was linearly scaled with the BOD input concentration for input BOD concentrations above 15 mg/L, using Eq. 3.4. For input BOD concentrations below 15 mg/L, *C** was set to 2 mg/L, the background concentration given by Kadlec and Wallace for treatment wetlands with the lowest BOD input.[50] This is because some level of residual BOD is unavoidable in wetland systems due to their biological nature.[50]

$$C^* = 0.0593 \cdot \left(BOD_{input} - 15\right) + 2 \tag{3.4}$$

where BOD_{input} is the BOD concentration at the input to the tank.

Nitrogen Removal

Wetland sizing for nitrogen removal accounts for the different possible forms of nitrogen in the wetland system: organic nitrogen (org-N), ammonia nitrogen (NH_4-N), and oxidised nitrogen (NO_x-N). The sum of these three components is Total Nitrogen (TN). Following the guidance of Kadlec and Wallace[50], it is assumed that sequential conversion between the three species and ultimate removal occurs as in Eq. 3.5.

Org-N -> NH_4-N -> NO_x-N -> removal (3.5)

Eq. 3.2 was thus modified to take into account such sequential conversion, as shown in Eqs. 3.6-3.8.

$$Q_{o,org} \cdot C_{o,org} = Q_{i.org} \cdot C_{i,org} - A \cdot (I \cdot C_{o.org} - \alpha \cdot Et \cdot C_{o,org} - k_{org} \cdot (C_{o,org} - C^*_{org})) \tag{3.6}$$

$$Q_{o,a} \cdot C_{o,a} = Q_{i.a} \cdot C_{i,a} - A \cdot (I \cdot C_{o.a} - \alpha \cdot Et \cdot C_{o,a} - k_a \cdot (C_{o,a} - C^*_a) + k_{org} \cdot (C_{o,org} - C^*_{org})) \tag{3.7}$$

$$Q_{o,ox} \cdot C_{o,ox} = Q_{i.ox} \cdot C_{i,ox} - A \cdot (I \cdot C_{o.ox} - \alpha \cdot Et \cdot C_{o,ox} - k_{ox} \cdot (C_{o,ox} - C^*_{ox}) + k_a \cdot (C_{o,a} - C^*_a)) \tag{3.8}$$

where subscripts *org*, *a*, and *ox* refer to organic nitrogen, ammonia nitrogen, and oxidised nitrogen respectively.

3.2.2 Wetland Design for AMD Remediation

A low-pH buffering effect is observed in AMD: as the pH is increased, dissolved metals are oxidised and precipitated in the form of hydroxides leading to the release of protons. Metal content can therefore be considered to contribute to total acidity. While AMD total acidity should be measured experimentally, it may be approximated by Eq. 3.9, originally given by Watzlaf et al. and adapted by Kirby and Cravotta.[51,52] Only Fe, Al, and Mn are included in this formula, as they tend to dominate metal content, but it may be extended to include other metals. Assuming negligible alkalinity under pH 5, Eq. 3.9 can be considered to give the net acidity for low-pH drainage.[51] For higher-pH drainage, acidity is of less concern and so Eq. 3.8 is not used. Instead, such waters are primarily characterised by their metal content, in particular Fe and Mn.

$$\text{Total Acidity (mg } CaCO_3\text{/L)} = 50 \cdot \left(10^{(3\text{-pH})} + 2 \cdot \frac{C_{Fe}}{55.8} + 2 \cdot \frac{C_{Mn}}{54.9} + 3 \cdot \frac{C_{Al}}{27.0}\right) \quad (3.9)$$

where *Total Acidity* is expressed in units of (mg $CaCO_3$/mL), and C_x corresponds to the total dissolved concentration of element *x*, expressed in mg/L.

The wetland designs investigated for AMD remediation were aerobic FWS wetlands and two types of anaerobic wetlands: horizontal sub-surface flow (HSSF) and vertical flow (VF). Following guidance from literature, FWS wetlands were used for circumneutral AMD, and HSSF and VF designs were used for low-pH wetlands.[53–55] Typical ranges for zero-order areal removal rates for acidity and metal content were sourced from literature and (see Table 3.1). [51,53–58] These high-level design models are appropriate for a high-level study looking at overall trends. However, it should be noted that due to the varied nature of AMD, and its complex and interacting removal mechanisms in constructed wetlands, more detailed models should be used for individual case studies.

Table 3.1: Assumed wetland acidity and metal removal rate ranges.

Wetland Type	Removal Rate (g/m^2/day)	Sources
FWS	Fe: 10-20 Mn: 0.5-2	[53–56]
HSSF	Acidity: 3.5-10	[54,55,58]
VF	Acidity: 15-30	[51,55,57,58]

Land pricing data was sourced from literature, with values given in Table 3.2. Capital costs for HSSF and FWS wetlands were taken from Kadlec and Wallace's manual on wetland design, the only source which took economies of scale into account.[50] The relationships given are empirically fitted to the costs of wetlands built in the U.S. These values were compared to those of Brix et al. and Demchak et

al. (both given as a flat rate per unit area), and found to be relatively consistent.[57,59] The capital costs of VF wetlands were roughly estimated as being twice as high as those of an anaerobic HSSF wetland of the same area. This was based on the relative pricing used in AMDTreat software and in the work of Demchak et al.[57,60] Review of several literature sources revealed a range of reported operating costs, ranging from around $2,400-12,800/ha/y, and so a mid-range value of $7,000 was assumed.[50,61–66]

Additionally, the construction cost formula given by Kadlec and Wallace was collated from literature, and it was acknowledged that such reported costs often do not include land costs or engineering costs. As a result, an additional land cost of $20,000/ha (covering most U.S. pastureland [67]) was added in addition to the construction cost for wetlands for BOD and nutrient removal only, and a 50% indirect cost for all wetlands (e.g. for contingency and engineering costs). Land costs were not considered for wetlands treating mine drainage as it was assumed such land would be considered severely contaminated and therefore of little, if any, value.

Table 3.2: Assumed wetland construction costs and operational costs. All prices are in 2018 USD, adjusted for inflation.

Wetland Type	Construction cost ($1,000/ha)	Operational cost ($/ha/y)
FWS	$242 \cdot A^{0.690}$	7,000
HSSF	$812 \cdot A^{0.704}$	
VF	$1{,}624 \cdot A^{0.704}$	

3.3.3 Conventional Costs of AMD Remediation

Chemical neutralisation of AMD represents the benchmark remediation technology, and so a relevant comparison for wetland remediation costs. Capital and operating cost curves for conventional neutralisation were taken from a report by the Canadian Centre for Mineral and Energy Technology.[68] These curves varied with influent acidity concentration and flow rate, and linear interpolation and limited linear extrapolation were used between given values in order to estimate costs for a given system. Values were converted to from 1994 CAD to 1994 USD using historical exchange rates, and from 1994 USD to 2018 USD by using the Chemical Engineering Plant Cost Index (CEPCI).

3.3 Results and Discussion

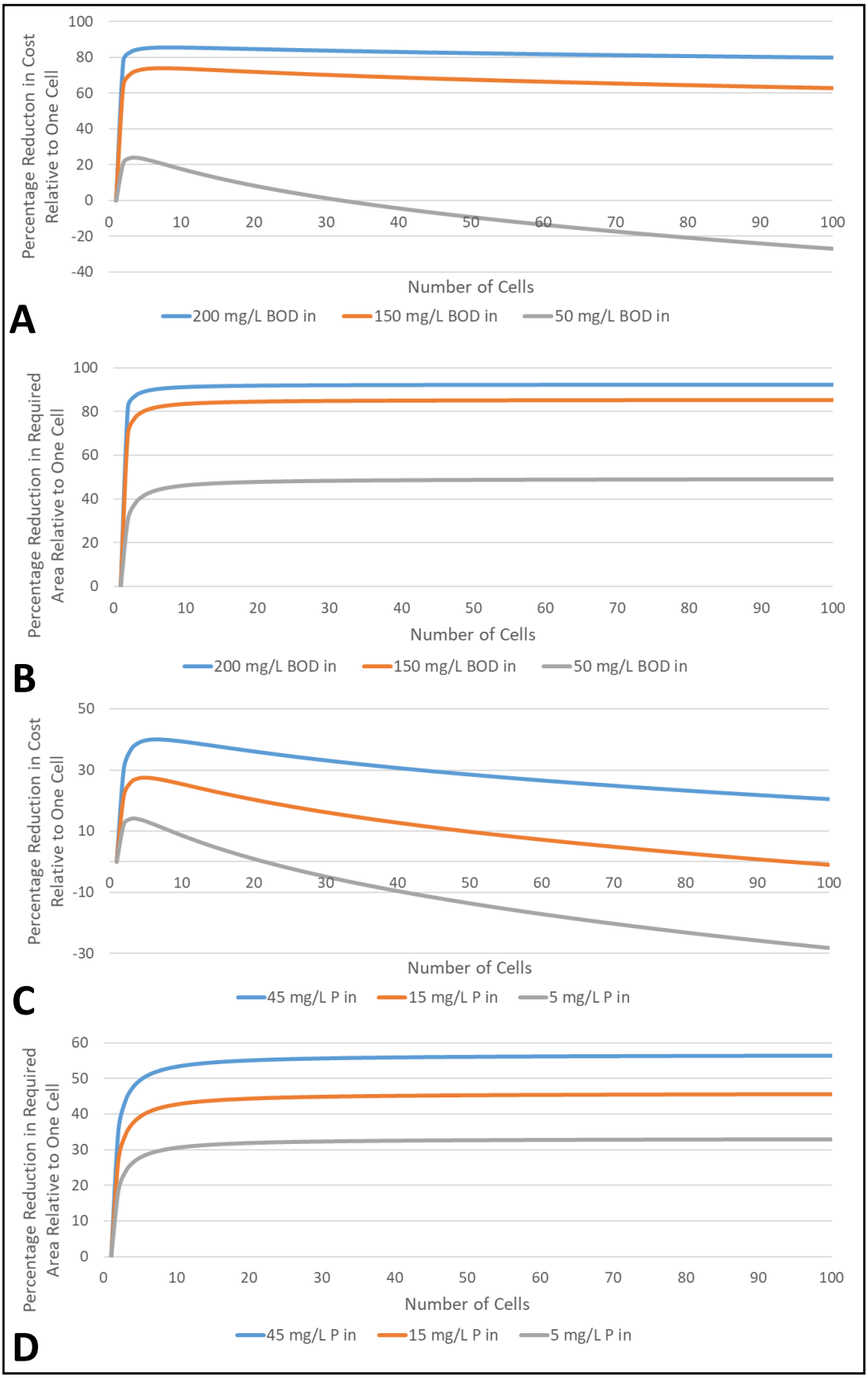
3.3.1 BOD and Nutrient Removal

Number of Cells

Constructed wetlands are generally built as a number of cells, through which the water flows sequentially. Inlet and outlet structures ensure mixing of the water between cells, thus improving the hydraulic performance of the system. A wetland designed with more cells therefore has a narrower distribution of residence times, leading to lower required areas. In terms of overall costs, multiple lower-area cells do not benefit as much from economies of scale for construction (see Table 3.2), with this counterbalanced to a certain extent by reduced operational costs and a reduced total area.

Fig. 3.1 shows the effect of varying the number of cells on overall costs and areas, for varying input concentrations and fixed output concentrations of BOD, phosphorus and nitrogen, at a flow rate of 5,000 m^3/d. The *k* values reported by Kadlec and Wallace were determined from given wetland data, based on an assumed or measured P_{TIS} value for each wetland cell. For BOD removal, a P_{TIS} value of 1 was used for each cell, whereas for org-N, NH_4-N, ox-N, and phosphorus (P) a value of 3 was used. The contaminant removal model detailed in Section 3.2 was applied to each wetland cell in series, with perfect mixing assumed to occur between cells. For a given wetland, all cells were set to be of equal size.

Results show that optimisation of the cell number can lead to significant reductions in cost and area, for the three contaminants. In all cases, total area rapidly decreases with increasing cell number, before reaching a plateau. This trend is to be expected: there is assumed perfect mixing between cells, and thus as the number of cells increases towards infinity the system approaches perfect plug flow. However, as the number of cells increases and required total area decreases, individual cell size decreases and thus the cost per unit area increases. These two competing effects lead to an optimum cell number at which costs are minimised. Possible area savings tend to be significantly larger for BOD removal than P and nitrogen (N) removal, and increase more rapidly with input pollutant concentration. This is due to the much higher background concentrations in BOD removal wetlands, which have also been assumed to increase with input concentration (as detailed in the Methodology). While such reductions in area with increasing wetland cells may appear surprisingly large, they are in line with trends reported by Kadlec and Wallace, who do not investigate the effect on process economics.[50] For all pollutants, area and cost savings relative to one single cell were found to be far more dependent on pollutant input and output concentrations than on flow rate.


A
Percentage Reducton in Cost Relative to One Cell
100
80
60
40
20
0
-20
-40
0 10 20 30 40 50 60 70 80 90 100
Number of Cells
200 mg/L BOD in
150 mg/L BOD in
50 mg/L BOD in
B
Percentage Reduction in Required Area Relative to One Cell
100
80
60
40
20
0
0 10 20 30 40 50 60 70 80 90 100
Number of Cells
200 mg/L BOD in
150 mg/L BOD in
50 mg/L BOD in
C
Percentage Reduction in Cost Relative to One Cell
50
30
10
-10
-30
0 10 20 30 40 50 60 70 80 90 100
Number of Cells
45 mg/L P in
15 mg/L P in
5 mg/L P in
D
Percentage Reduction in Required Area Relative to One Cell
60
50
40
30
20
10
0
0 10 20 30 40 50 60 70 80 90 100
Number of Cells
45 mg/L P in
15 mg/L P in
5 mg/L P in

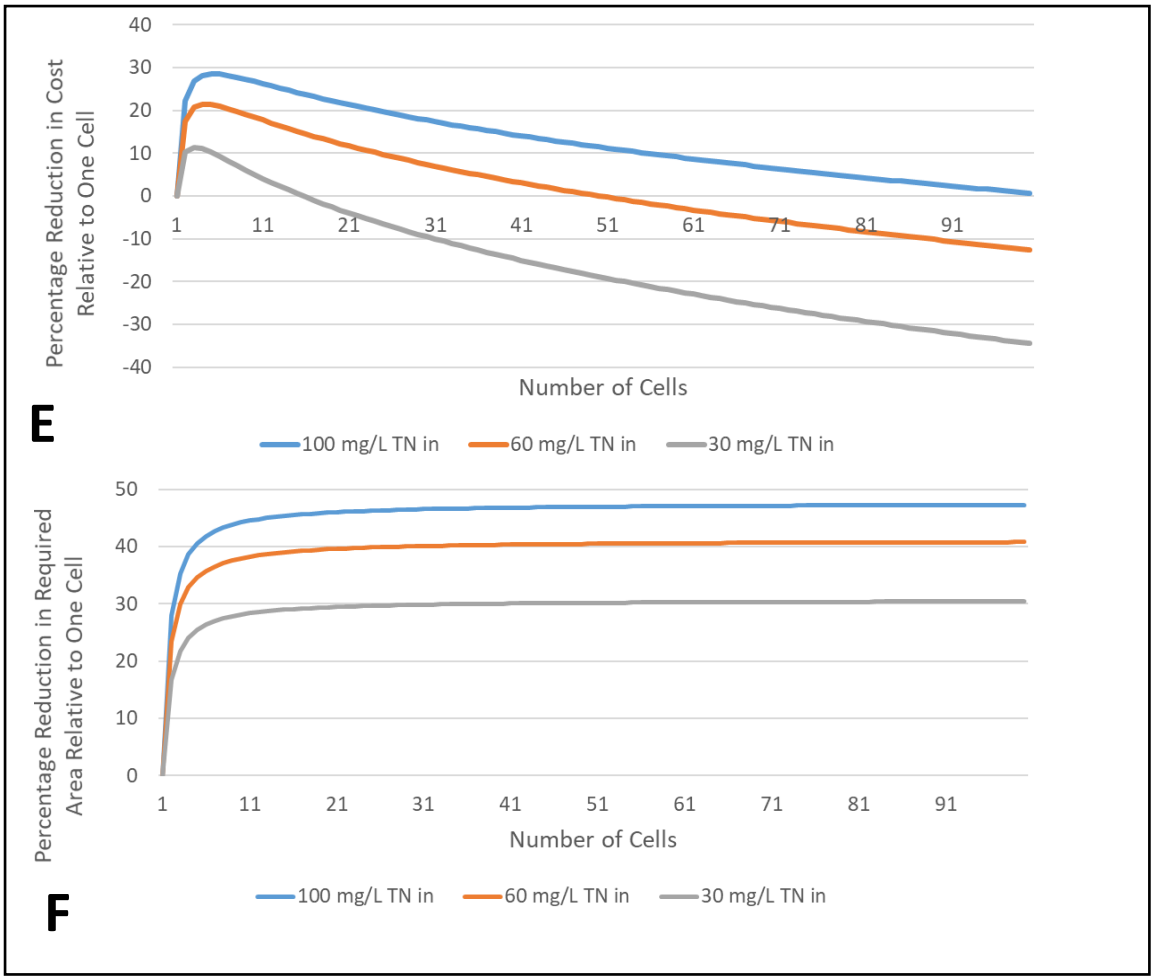


Figure 3.1: Effect of varying the number of wetland cells on required overall area and treatment costs. All reductions are relative to using one single cell. All biochemical oxygen demand (BOD) plots are for 5,000 m^3/d influent of varying concentration, with an output concentration of 30 mg/L. All phosphorus (P) plots are for 5,000 m^3/d influent of varying concentration, with an output concentration of 1 mg/L. All total nitrogen (TN) plots are for 5,000 m^3/d of varying TN input concentrations, with an output concentration of 5 mg/L. Plots are A: Reduction in total cost for BOD removal, B: Reduction in required area for BOD removal, C: reduction in total cost for phosphorus removal, D: Reduction in required area for phosphorus removal, E: Reduction in total cost for TN removal, F: Reduction in required area for TN removal.

BOD and Nutrient Removal Costs

Full contour plots for the costs of BOD and nutrient removal with input concentration and flow rate are provided in the Appendix.

Fig. 3.2 shows the cost of remediation for each contaminant, for a range of input and effluent conditions. For removal of all contaminants (BOD, P, TN), economies of scale are initially significant, with an exponent of around 0.8 and as a result volumetric treatment costs at 10,000 m^3/d are around half of those at 50 m^3/d. However, as size increases the exponent increases to around 0.9, and volumetric costs tend to plateau, leading to relatively little change above 5000 m^3/d. In the ranges investigated, the volumetric costs for BOD removal tend to be significantly lower than those for P and N removal, and economies of scale tend to decrease more slowly with flow rate. This is due to higher BOD removal rates, leading to generally lower required areas. When designing for simultaneous removal of multiple contaminants in a wetland system, it is common for one contaminant to act as a "bottleneck" and dictate required size and cost. From this range of results it can be concluded that tertiary treatment (i.e. P and N removal) will tend to significantly increase costs relative to secondary treatment (only BOD removal), particularly P removal. For all contaminants, particularly N and BOD, volumetric costs are more sensitive to changes in effluent concentrations than influent concentrations. This is due to the first-order removal rate model, which leads to lower removal rates approaching the background concentration.

No general method for estimating the costs of conventional remediation was found, which typically takes place through a form of activated sludge process, possibly followed by further treatment. A direct comparison of costs for wetland remediation and conventional remediation would involve process design considerations for each input condition due to the case-specific nature of wastewater treatment, beyond the scope of this study. Calculated costs of constructed wetland remediation were therefore compared with literature values for conventional secondary and tertiary wastewater treatment,[19,46,69–78] with results displayed in Fig. 3.3. All sources were for countries with similar level of economic development to the U.S.A. All conventional costs were adjusted to 2018 USD by first converting currencies using historical exchange rates, and then applying the CEPCI for the relevant years.

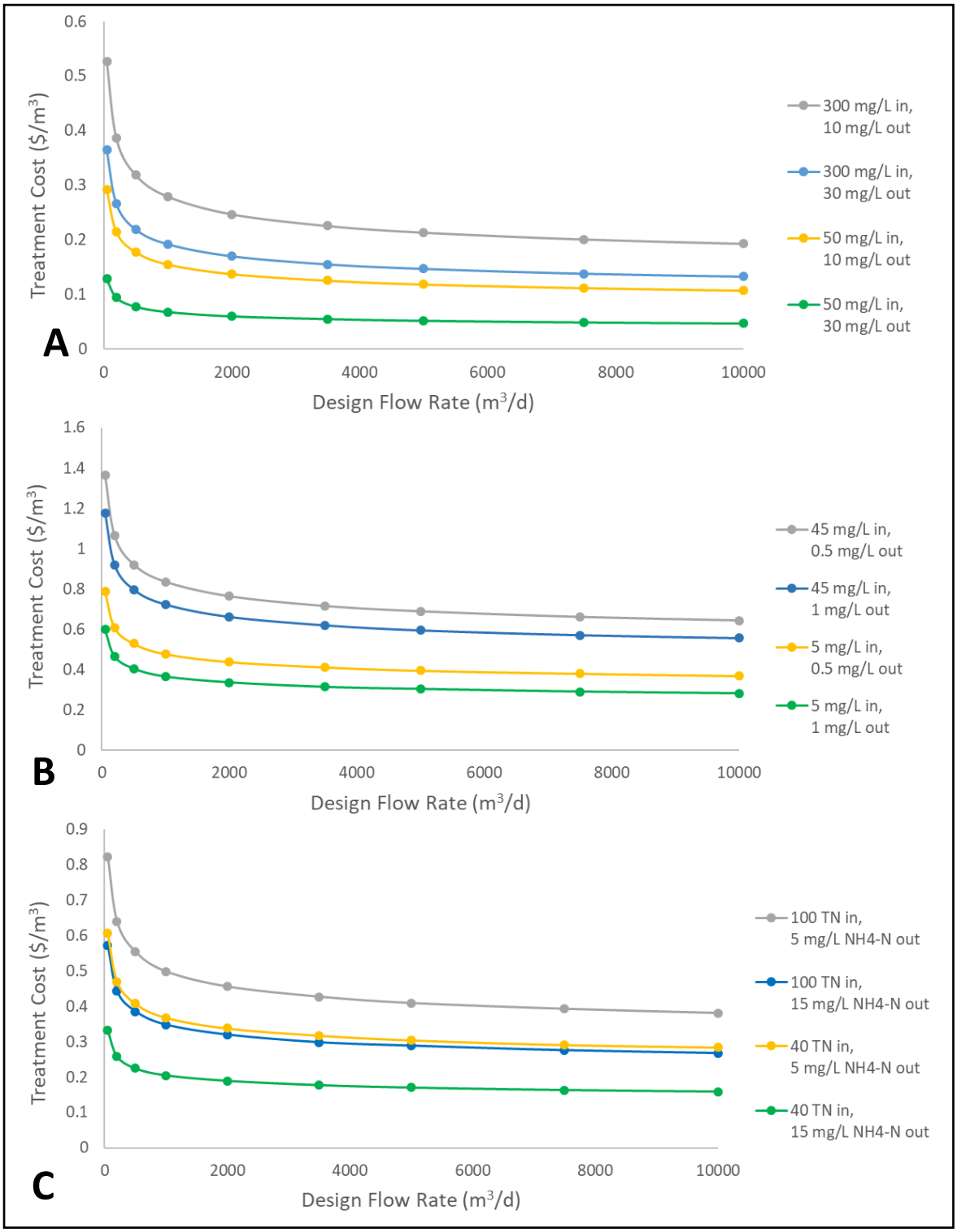


Figure 3.2: Volumetric costs of BOD and nutrient removal using constructed wetlands, for a range of input and output conditions. Plots are A: biochemical oxygen demand (BOD) removal, B: phosphorus (P) removal, C: total nitrogen (TN) removal, assuming input nitrogen made up of 50% organic nitrogen and 50% ammonia nitrogen (NH_4-N). Equivalent plots showing the gravimetric costs of BOD and nutrient removal can be found in the Appendix. It should be noted that the size of the designed wetland varies with based on required flow rate and degree of contaminant removal.

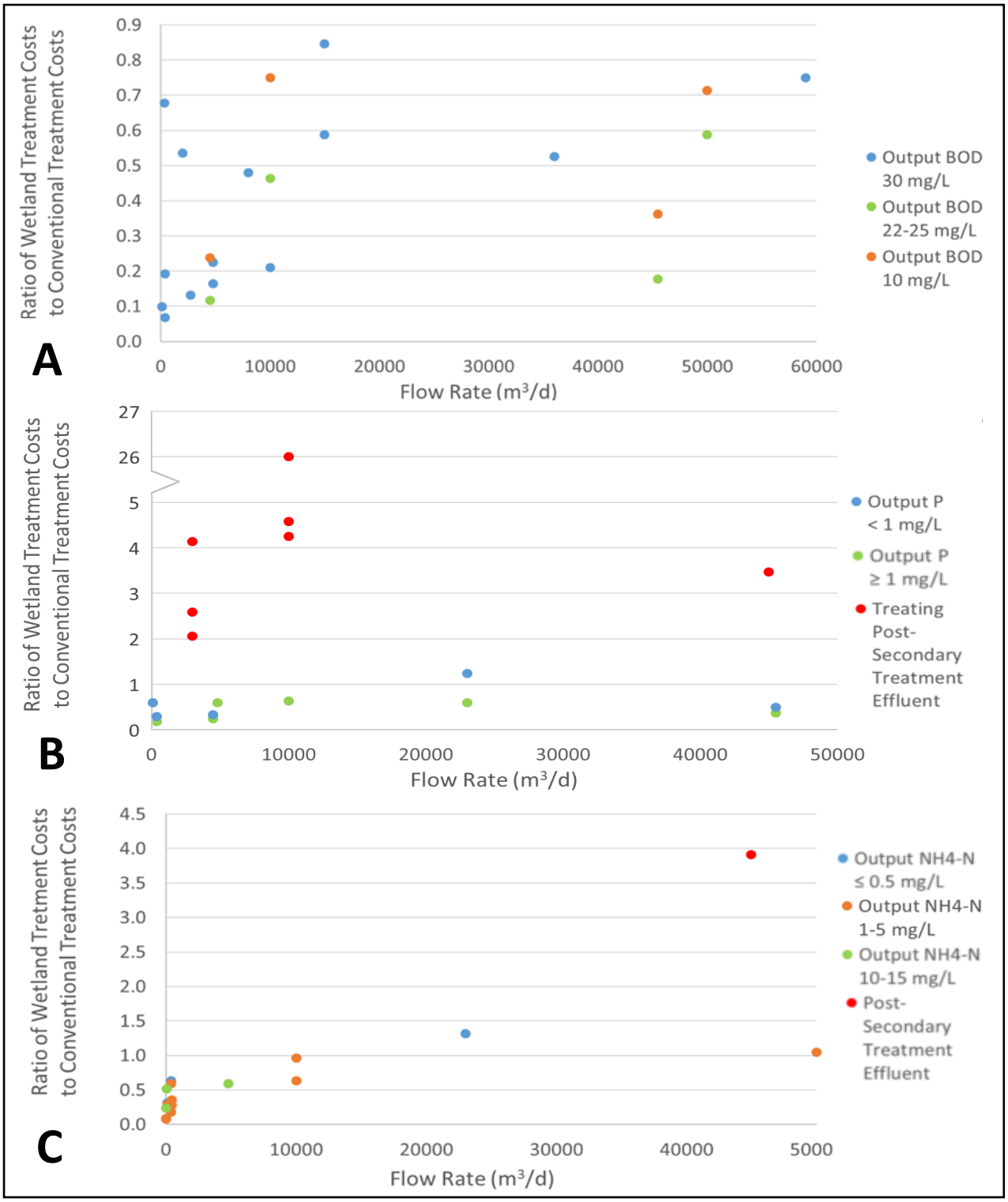


Figure 3.3: Ratio of simulated wetland remediation costs to reported conventional remediation costs in literature, for BOD, phosphorus, and nitrogen removal. Plots are A: biochemical oxygen demand (BOD) removal, B: phosphorus (P) removal, C: nitrogen removal. NH_4-N corresponds to the concentration of ammonia nitrogen. The data sets used to make these plots may be found in the Appendix.

By comparing reported costs from various studies with the equivalent costs calculated using this study's methodology, high-level conclusions may be drawn. The following conditions are identified as most economically competitive for constructed wetland remediation:

- Treatment to secondary treatment standards, i.e. BOD removal. Cost estimates for this category of wetland were found to be over 25% cheaper than 86% of reported data. Costs appeared to generally become more similar at higher flow rates, e.g. above 30,000 m^3/d. This is expected due to economies of scale, although there are few high-flow data points.
- Integrated secondary and tertiary treatment for P and N removal, found to be over 25% cheaper than 91% and 81% of reported data respectively. Removal of P appears to be significantly cheaper than conventional remediation to levels around 0.5 mg/L, with fairly little data available below this threshold. Removal of N appears economically favourable to outputs around 1 mg/L NH_4-N. Wetland costs may be considered to be generally cheaper up to around 10,000 m^3/d for removal of both contaminants. Above this threshold limited data was found, but appeared to favour conventional remediation for N removal, and varied for P removal.
- Integrated second and tertiary treatment for small flow rates (below around 500 m^3/d), even for relatively stringent discharge conditions such as phosphorus and ammonia concentrations below 0.5 mg/L. Under these conditions, wetland remediation was found to be 36-91% cheaper.

Small flow rates are found to be the condition where constructed wetlands are most economically competitive, as well as least land intensive. The application of wetland wastewater treatment in smaller communities is thus most promising, and there is likely the most available land near such communities. Wetland remediation of wastewater was found to be least economically viable for tertiary treatment of secondary-treated wastewater, with costs significantly higher than conventional alternatives (2-26 times higher). However, this is primarily attributed to the studies considering upgrading existing secondary treatment facilities, thus avoiding significant costs. It may also be attributed to the assumed first-order removal kinetics, leading to low removal rates at low concentrations and thus large area requirements in order to reach strict discharge limits.

The optimum number of cells was investigated for flow rates between 10 and 50,000 m^3/d. BOD inputs ranged from 50-300 mg/L, P inputs from 5-45 mg/L, and total nitrogen from 30-100 mg/L (assuming half organic nitrogen and half ammonia nitrogen). Output concentrations were taken as 30 mg/L BOD, 1 mg/L P, and 5 mg/L ammonia nitrogen. The optimum number of cells for BOD removal ranged from 2 to 18 with maximum area of 10 ha, with both the size and number of cells increasing with flow rate and input concentration. Phosphorus and nitrogen removal were found to require a similar number

of cells, 2-16 and 1-13 cells respectively. However, cell sizes were much larger, with a maximum size of 55 ha and 54 ha for P and N removal respectively.

Uncertainty

There is a degree of uncertainty with several parameters used in the wetland sizing and costing approach used in this study. Two sets of Monte Carlo simulations were carried out to investigate the variability of results:

1. The variation of design parameters on output concentrations. Wetlands were sized using the methodology currently outlined for secondary and tertiary treatment of municipal wastewater. Contaminant removal rates were then varied based upon the frequency distribution given in the work of Kadlec and Wallace.[50] Additionally, precipitation and evapotranspiration factors were varied randomly between 0-2 cm/d and 0-1 cm/d respectively. All output concentrations were multiplied by the 90% exceedance multiplier to give the target output concentration rather than the design output concentration. As sizing parameters were varied, a range of output effluent concentrations was obtained. The proportion of this range below the target concentration was determined. Correlation coefficients were also calculated, using all output values and the corresponding varied input factors. Results are displayed in Fig. 3.4.
2. The effect of parameter variation on overall cost, for secondary and tertiary treatment of domestic wastewater. Land costs were varied between 0 and 200,000 $/ha, construction costs were varied between 50% and 150% of the cost function used, operating costs were varied between $2000/ha/y and $12,000/ha/y, and indirect costs were varied between 0% and 100% of total capital costs. The parameters varied in the first Monte Carlo simulation were kept constant. The range of calculated costs are displayed in Fig. 3.5, as a mean with error bars representing standard deviation.

Simulation 1 consistently shows that for secondary treatment, around 50% of simulations give output effluents below the design target. When investigating the parameters used in each run, there is a clear correlation between the output concentration and 1/k, with this effect far exceeding that of precipitation and evapotranspiration. Median k-values, as reported by Kadlec and Wallace34, were used in this study, explaining the proportion of simulations reaching the effluent target being around 50%. For tertiary treatment, phosphorus removal is the limiting factor in wetland sizing, thus displaying the lowest proportion of simulations with output concentrations below the discharge limit, around 45%. As a result, there is therefore a strong correlation with the 1/k value. Determination of the k-factor for the limiting contaminant(s) at a specific site can therefore be identified as the most

important aim for real-life wetland design. For BOD and N removal, the wetland is larger than required to reach discharge limits, leading to a much higher proportion of simulations achieving the effluent target. In addition, as concentrations approach background concentrations, they exhibit decreasing removal due to the first-order removal rates, and the correlation with 1/k decreases significantly. The proportion of simulations achieving target BOD effluents increases with flow rate, likely due to the higher number of cells used, with decreasing BOD background concentrations in each cell.

Simulation 2 demonstrates that costs are moderately sensitive to the assumed cost parameters, with the standard deviation of overall cost equal to between one third and one quarter of the mean value. However, considering the large cost ranges investigated, these standard deviations are small enough to maintain the high-level conclusions drawn from comparison with literature. Investigation of correlations are shown in Fig. 3.6. For smaller areas, construction costs appear to have the highest influence on overall costs. However, as the required wetland size increases, Operation and Maintenance (O&M) costs eventually dominate as economies of scale reduce the relative impact of construction costs and indirect costs. The impact of varying land costs from 0 to $200,000/ha is seen to have a very weak correlation to overall remediation costs, offering flexibility in terms of location.

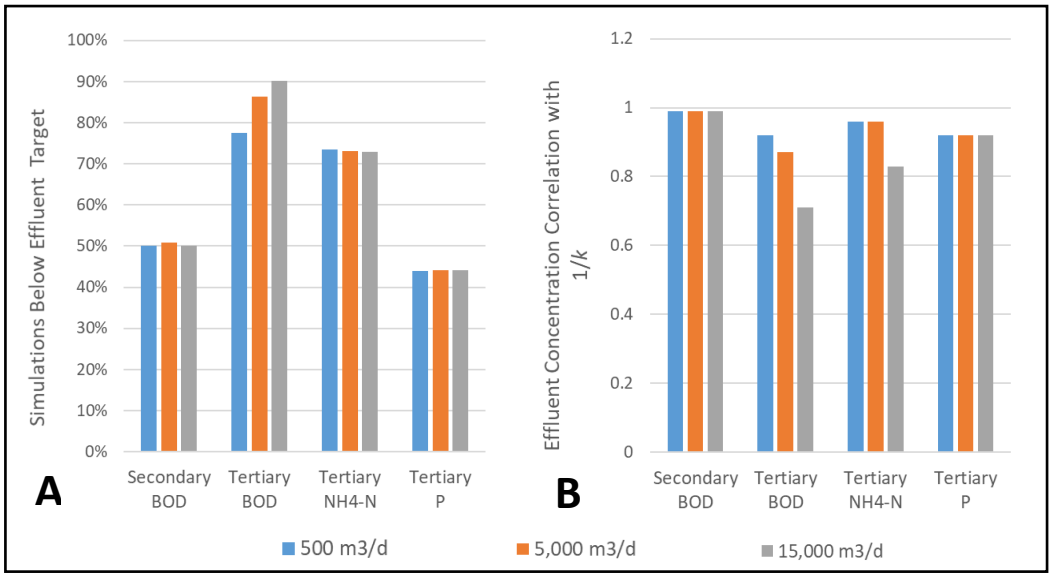


Figure 3.4: Effect of varying design parameters on simulated effluent concentrations in a Monte Carlo simulation, for secondary treatment and tertiary treatment. Plots are A: Proportion of simulations achieving output concentrations below targets concentrations; B: Correlation of effluent output concentrations with removal rate constant. BOD refers to biochemical oxygen demand, P refers to phosphorus, NH_4-N refers to ammonia nitrogen, and *k* corresponds to the first-order removal rate constant of each contaminant. Values in plot A refer to a proportion of the full range of simulated results, coefficients in plot B were calculated using all simulated inputs and outputs; there are therefore no error bars.

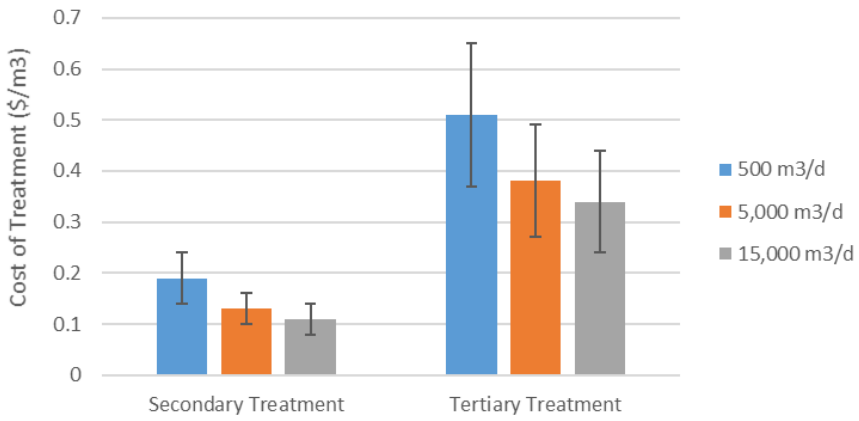


Figure 3.5: Effect of varying economic parameters on simulated wetland treatment costs in a Monte Carlo simulation, for secondary treatment and tertiary treatment. Error bars represent one standard deviation in the range of simulated results.

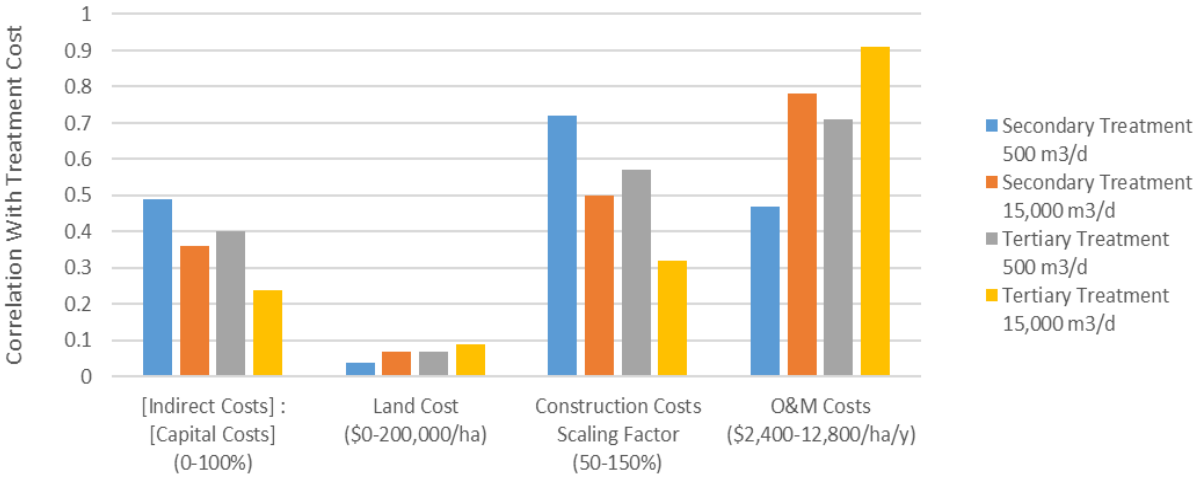


Figure 3.6: Correlation between varied economic parameters and simulated wetland treatment costs in a Monte Carlo simulation, for secondary treatment and tertiary treatment of domestic wastewater. Correlation coefficients were calculated using the full range of simulated results, and there are therefore no error bars.

3.3.2 AMD Remediation

Low-pH Drainage

The costs of anaerobic HSSF and VF wetland remediation relative to chemical remediation were calculated for low-pH AMD, using input acidity concentration and flow rate as independent variables, for both maximum and minimum acidity removal rate. Results are displayed in Fig. 3.7. In addition, nine different AMD scenarios were simulated to compare the costs of wetland remediation and chemical neutralisation, based on the conditions simulated by Skousen when comparing the costs of

different chemical remediation schemes.[79] Their details are shown in Table 3.3, and are plotted in Fig 3.7. In the following analysis, economically favourable conditions are considered to be those where wetland remediation is found to be over 25% cheaper than conventional remediation and economically competitive where wetland remediation is found to be within 25% of the costs of conventional remediation.

Table 3.3: Simulated low-pH AMD scenarios. Cells highlighted in green represent cases where wetland remediation is economically favourable, orange for economically competitive, and red for economically unfavourable. High Rate and Low Rate refer to the assumed acidity removal rate.

Scenario Number	Flow Rate (m^3/s)	Acidity (mg/L)	Ratio VF High Rate	Ratio VF Low Rate	Ratio HSSF High Rate	Ratio HSSF Low Rate
1	0.004	100	0.10	0.16	0.10	0.21
2		500	0.26	0.44	0.27	0.60
3		2500	0.65	1.07	0.70	1.60
4	0.04	100	0.37	0.61	0.39	0.87
5		500	0.80	1.34	0.91	2.09
6		1500	1.60	2.71	1.99	4.77
7	0.08	100	0.46	0.77	0.50	1.13
8		500	0.98	1.64	1.15	2.69
9		2500	1.69	2.87	2.20	5.35

Fig. 3.7 shows there is a range of conditions under which wetland remediation of AMD appears to be economically competitive or favourable relative to chemical remediation. This is particularly true at low flow rates and/or acidities, where the capital costs of building a chemical plant become prohibitive. However, this may also be partly due to the zero-order removal rate assumption, which may become less accurate at low acidity inputs. For cases with flow rates under around 0.02 m^3/s and acidities under around 300 mg/L, wetland remediation is economically competitive regardless of acidity removal rate. However, results tend to be very sensitive to the assumed acidity removal rate, which varies significantly in literature. When a high acidity removal rate is assumed, wetland remediation is found to be economically competitive for a range of input acidities up to around 500 mg/L above 0.04 m^3/s. However, in the case of a low removal rate, only acidities up to around 180 mg/L are competitive for such flows. Additionally, as acidities increase to high levels (above around 1500 mg/L), the cost effectiveness of wetland remediation is very sensitive to the flow rate. As such, careful design and preparatory studies would be required for wetland remediation at these conditions.

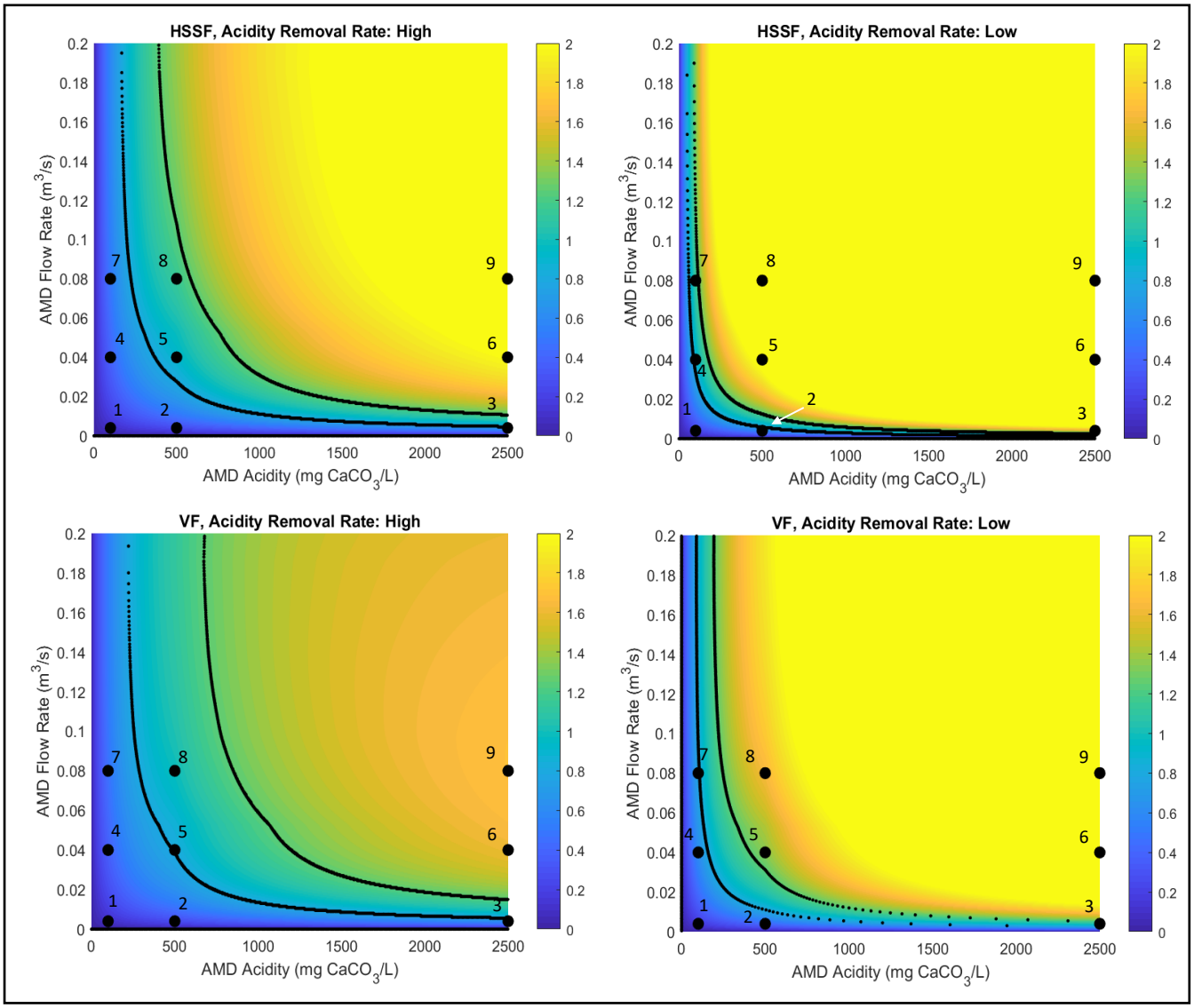


Figure 3.7: Ratio of wetland remediation costs to conventional remediation costs of low-pH AMD, for HSSF and VF designs with high and low acidity removal rates. The 9 numbered points plotted are scenarios 1-9, as described in Table 3.3. The area to the left of the black lines represents the economically favourable zone, the middle area between the lines represents the economically competitive zone, and the area to the right of the black lines represents the economically unfavourable zone.

As the economically favourable conditions are at low flows and/or acidities, the associated areas tend to be of moderate size. For HSSF designs, the required areas in these regions are under 26 ha and 22 ha for high and low acidity removal rates respectively. For VF designs, the required areas are under 9 ha for both assumed removal rates. As wetland remediation of AMD has yet to be implemented on a

very large scale, the low areas required at the most economically viable conditions may encourage implementation of this technology. Should the technology thus establish itself, a subsequent decrease in capital costs may increase the range of economically viable conditions to eventually include large wetlands handling large and/or highly acidic flows.

The least economically viable are those with high flows and acidity: flows with acidity above 1000 mg/L and flows above 0.06 m^3/s are economically unviable in all scenarios. However, in the range of representative scenarios, the majority are not within this region, and are either within or closer to the economically viable zone:

- Scenarios 1 and 2 are always economically favourable, regardless of acidity removal rate or wetland design. These are the scenarios with the lowest flow rates and acidities under 500 mg/L.
- Scenario 3 is economically favourable for HSSF and VF designs with high removal rates, economically competitive for a low-rate VF design, and economically unfavourable for low-rate HSSF designs. This demonstrates that acidity can still be a determining factor in technology selection at low flow rates.
- Scenario 4 is economically favourable under all conditions except for an HSSF design with a low removal rate, for which it is still economically competitive.
- Scenario 7 is economically favourable under high removal rate and competitive for low removal rates.
- Scenarios 5 and 8 are economically competitive for high-rate designs, and economically unfavourable for low-rate designs.
- Only scenarios 6 and 9 are clearly economically unviable under all configurations.

Costs for VF and HSSF designs were compared for their maximum and minimum acidity removal rates, and mid-range rates. At minimum removal rates, HSSF designs were found to be around 17-48% more expensive for economically favourable and competitive cases. At maximum removal rates for economically competitive and favourable conditions, HSSF designs range from 10% cheaper at the lowest flow rates and acidities, to 22% more expensive than VF designs. Lastly, costs were compared for an HSSF design operating at maximum removal rate, and a VF design at mid-range removal rate. Under these assumptions, VF designs were found to be 2-35% more expensive, with this figure decreasing with acidity and flow rate. Due to the significant effect of varying the removal rate within the reported ranges, it would appear that neither design offers a clear advantage in terms of costs. The main advantage of a VF design over an HSSF design is thus the lower area requirement for a generally similar cost.

Overall-site low-pH AMD data was sourced from literature, in order to estimate the economic favourability and required size of remediation wetlands for reported AMD cases. Influent metal concentrations, pH, and flow rate were all required for wetland sizing. The former two parameters were relatively well-reported, but flow rates were less common. Furthermore, many of the studies reporting flow rates were for individual output streams at a given site, and not for overall sites. As a result, data was sourced from a relatively small number of studies[80–83], with the vast majority of figures sourced from two studies: one on Pennsylvanian coal mines, and the other on mines in the Iberian Pyrite Belt.[84,85] Results are presented in Fig. 3.8.

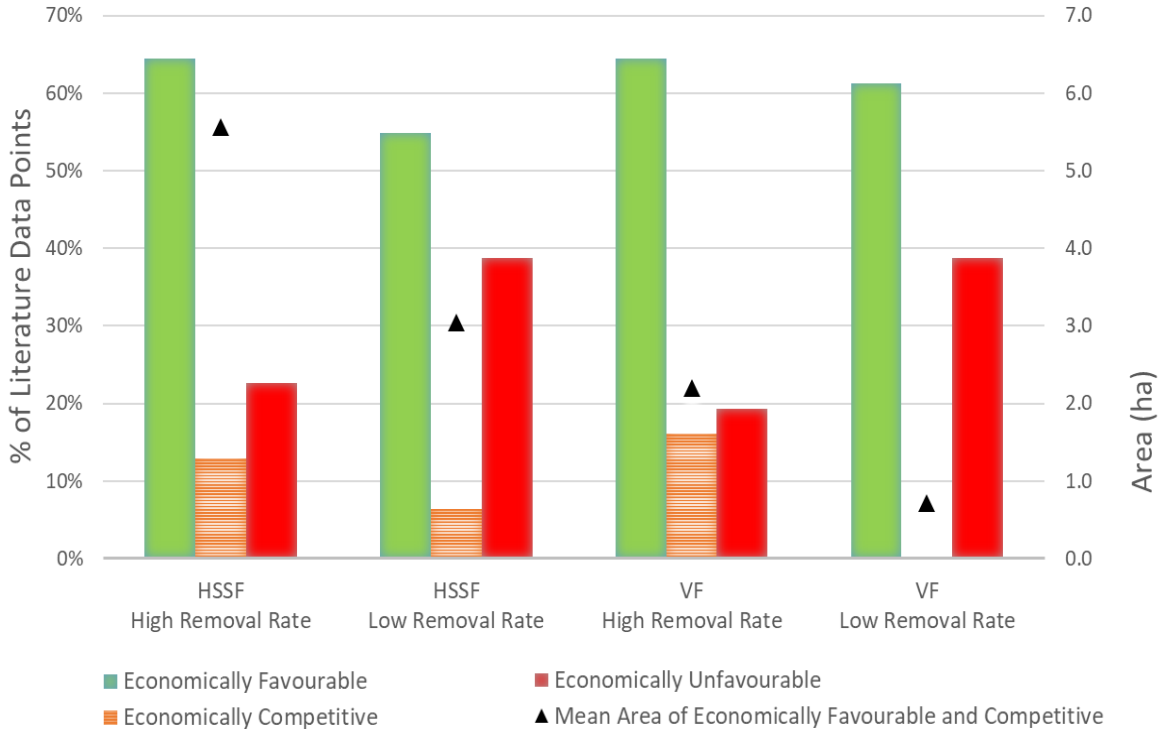


Figure 3.8: Simulated wetland performance for overall-site low-pH AMD, for case study data found in literature.

For all wetland designs and removal rates, over half (55-65%) of the simulated conditions were found to be economically favourable for wetland remediation, 0-16% were found to be economically competitive, and 19-39% were found to be economically unfavourable. When looking at the economically favourable and competitive conditions, the mean wetland area for HSSF designs is 3.05-5.57 ha for low and high removal rates respectively, with the corresponding ranges for VF wetlands being 0.71-2.20 ha. Wetlands with high removal rates have higher mean areas due to the higher areas required for more severe inputs, under which the low removal rate designs are not economically competitive. Thus, under this set of literature data, wetland remediation would appear to be able to

play a significant role in remediation of AMD, without requiring impractically large areas. However, although 26 of the 31 data points had acidities within the range of the examples provided by Skousen[79], only 8 had flow rates within that range (with most being below 0.004 m^3/s), and only 7 had both acidity and flow rates within the range of example conditions. This may be interpreted as either the sample size or the example conditions not being widely representative.

Circumneutral-pH Drainage

Similarly, the costs of aerobic FWS wetland remediation relative to chemical remediation were calculated for circumneutral AMD, using input Fe concentration and flow rate as independent variables, for both maximum and minimum acidity removal rate. In this study, circumneutral was used to refer to AMD with a pH above 5 for which dissolved metal content was the main target for remediation. Results are displayed in Fig. 3.9. Overall trends are similar to those of low-pH AMD remediation: the most economically favourable conditions are those of low flow rate and/or input Fe. However, in this case all generated conditions were found to be economically favourable, for both high and low Fe removal rates and for higher flow rates. It should be noted that even for large required wetland areas (e.g. over 100 ha), costs are still significantly lower than those for conventional treatment, suggesting that practicality issues are likely to constrain wetland remediation of large flows and metal inputs rather than economic ones.

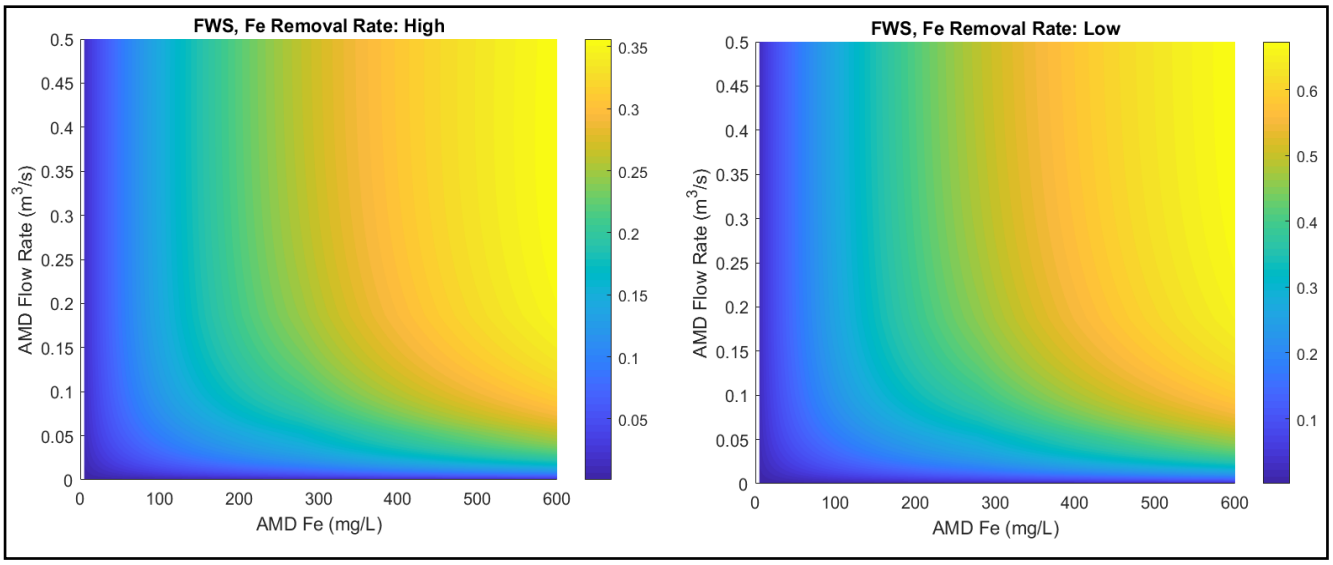


Figure 3.9: Ratio of wetland remediation costs to conventional remediation costs of circumneutral AMD, for FWS designs with high and low acidity removal rates.

3.3.3 Biomass Valorisation

The economic impact of constructed wetland biomass was also investigated as part of this study. This was done by determining the required profit per tonne of biomass generated to offset 10% of total remediation costs, under the previously stated assumption of 20 tonnes/ha/y. Wetlands treating low-pH and circumneutral AMD were investigated, as well as wetlands treating municipal wastewater to secondary and tertiary levels. This analysis was carried out for wetlands greater than 0.5 ha in size, as the required profit quickly escalates to infeasible quantities at low areas. Results are presented in Fig. 3.10, and are directly proportional to the assumed biomass yield per area.

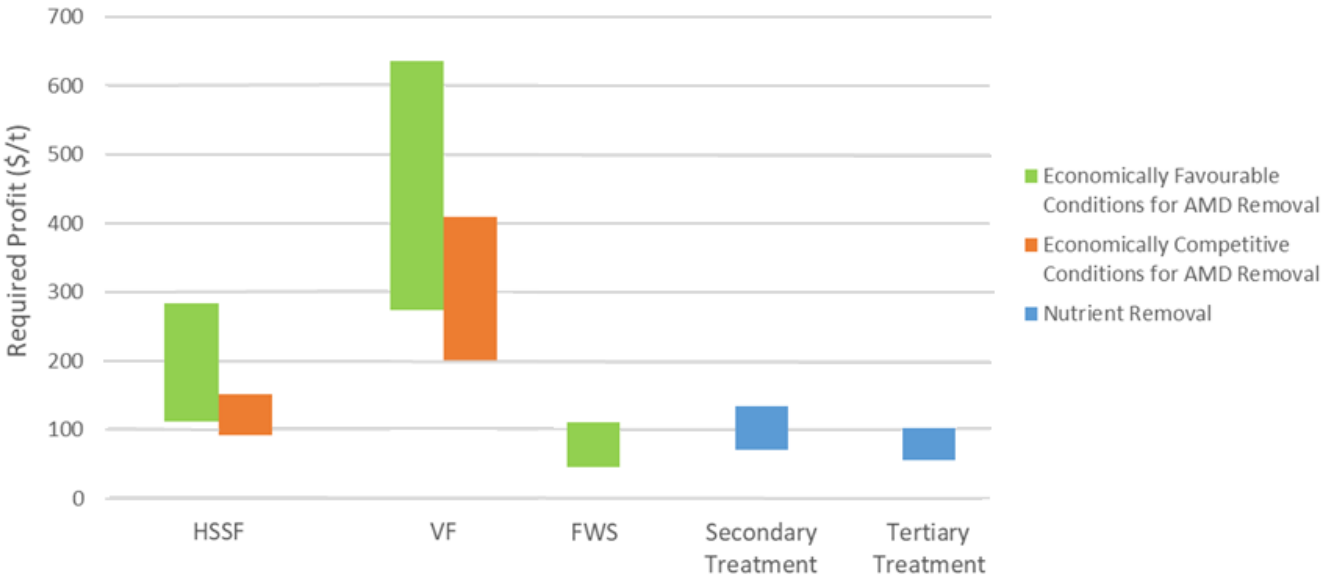


Figure 3.10: Required profit per unit dry mass of harvested wetland biomass, in order to offset 10% of total treatment costs. HSSF and VF represent treatment of low-pH AMD using an HSSF and VF wetland design respectively. FWS represents treatment of circumneutral-pH AMD using a FWS wetland design. Secondary Treatment and Tertiary Treatment represent treatment of domestic wastewater using a FWS wetland design.

There is significant variation between required profits depending on the wastewater type, for a 10% reduction in overall costs. Wetlands treating circumneutral-pH AMD and municipal wastewater require profits of the order of $50-100/tonne of dry biomass. HSSF wetlands treating low-pH AMD require around $110-280/tonne, while VF wetlands treating low-pH AMD require around $270-630/tonne. The significantly lower costs for a given flow rate explain the lower required profits for FWS wetlands treating circumneutral-pH AMD and municipal wastewater. For wetlands treating low-

pH AMD, VF wetlands require a lower area, which may explain the significantly higher required profits relative to HSSF designs. The similarity between low-removal-rate and high-removal-rate wetlands can be explained: those with low removal rates have higher costs to offset, but this is counterbalanced by the larger areas from which to harvest. However, for all wastewater types, the lowest required profits were for the largest wetlands, which may already be considered to have technical limitations due to their size.

Four possible revenue sources have been considered for comparative purposes: directly selling reeds ($70/t)[86,87], biorefinery for bioethanol production ($420 - 1,000/t bioethanol)[87,88], biorefinery for cellulose pulp production ($450 - 900/t pulp)[87,89], and production of reed pellets for fuel use ($140/t).[86,90] All revenue options are heavily dependent on the achievable profit margin, which will vary with the scale of operation. As a result, thorough analysis into the process economics of each route and market size is required, which has been considered beyond the scope of this study. However, some preliminary analysis on the feasibility of several options has been carried out by Croon in a 2014 study, which considers the utilisation of reed biomass purchased at $70/t.[87] While technologically feasible, the major obstacles to reed utilisation are identified as the costs of harvest and transport to processing plants, and the large scales needed for economical production. Integration of wetland remediation with reed processing may allow harvest and transport costs to be essentially absorbed into wetland O&M costs: Croon's study concerns harvesting of natural reed beds which have no such costs. Furthermore, harvest and transport costs are reported to be in the range of $600/ha, corresponding to 9% of the O&M costs assumed in this study, and significantly smaller than the uncertainty in O&M costs based on review of literature.[91]

The major practical drawback would thus appear to be required areas for minimum economic production. Croon gives minimum economic productions of 50,000 t/y, 150,000 t/y, and 60,000 t/y for bioethanol, pulp, and pellets respectively. However, in 2016 26% of pulp mills in Europe operated at under 100,000 t/y, and 6% under 25,000 t/y, with this latter figure instead being used as the minimum economic production.[92] The required areas for bioethanol, pulp, and pellet production are thus calculated to be 19,400 ha, 3,600 ha, and 3,000 ha. It should be noted that these figures assume 35% cellulose content, no cellulose degradation, 80% sugar release yield, and 90% ethanol yield, and are therefore different to those calculated by Croon. Required areas are clearly substantial and would need to be distributed among a number of large wetland sites, which tend to be least economically favourable. Therefore, this is only likely to be feasible if wetland remediation were to become more established.

In the case of bioethanol production, it may be possible to blend wetland biomass with different feedstocks in a general pretreatment process. In the NREL's technoeconomic analysis of a lignocellulosic bioethanol plant producing 218,000 t/y of bioethanol from corn stover, feedstock costs (including handling) were found to account for 34% of total bioethanol production costs.[93] Therefore, the blending of wetland biomass could still allow substantial cost reductions while reducing the required wetland area. Additionally, the magnitude of possible savings could reduce the required minimum economic production capacity of smaller bioethanol plants using only wetland biomass, thus reducing area requirements.

Anaerobic digestion (AD) to produce biogas may represent a more appropriate option for smaller-scale, more disaggregated implementation of constructed wetlands. Development of small-scale anaerobic digesters for localised biogas production has been considered a promising route for energy and fertiliser provision in small communities in developing countries.[94,95] In addition to wetland biomass, a range of feedstocks can be used in AD such as other types of biomass or animal waste.[96] Small-scale AD may thus allow the combination of wetland remediation of agricultural and domestic wastewater with localised energy production. AD can also be seasonal in operation, which would be beneficial for communities relying on a small number of wetlands' biomass outputs. Although digestion on a small scale for local use may not significantly affect overall economics of wetland remediation, its advantages could prove particularly attractive to small communities in developing countries, and thus help instigate more widespread adoption of CWs.

The effect of possible metal recovery was also investigated for wetlands treating AMD, possible for instance through ionic liquid pretreatment of metal-contaminated feedstocks.[97] The theoretical maximum metal recovery was found to be extremely low, even with the optimistic assumed biomass metal uptake: around 2 kg/ha/y of Fe and Al, 1 kg/ha/y of Mn and 100 g/ha/y of trace metals, providing negligible economic impact. Uncertainty in the values for biomass growth rate and metal uptake are very unlikely to affect this conclusion. The reason for such low uptake is that the main metal removal mechanisms in wetlands involve immobilisation in the sediment. Additionally, the wetland species typically used are metal-tolerant or moderately metal-accumulating rather than hyper-accumulating. While hyper-accumulating species may allow more significant metal recovery, growth rates of such species tend to be low, and their accumulating capacities tend to only apply to a small number of metals per species. However, despite the lack of economic benefit, the possibility of utilising metal-contaminated wetland biomass would solve the disposal issue from AMD wetlands.[98,99] Additionally, should metal concentrations in wetland sediment reach high levels that require end-of-life disposal, the feasibility of treating the generated metal-concentrated sludge for metal recovery may be investigated.

3.4 Conclusions

In this chapter, it has been demonstrated that constructed wetlands offer an economically viable method for remediation of wastewater under a wide range of conditions, for both BOD and nutrient removal and remediation of low-pH and circumneutral Acid Mine Drainage. The *P-k-C** model was used to size FWS wetlands for removal of BOD, phosphorus, and nitrogen, which incorporates a first-order areal removal model with a background concentration. A wide range of input contaminant concentrations and flow rates were simulated, and the costs calculated for remediation to various effluent standards. These costs were found by using a construction cost function from literature, to which provisions for land costs and indirect costs were explicitly added, and mid-range O&M costs based on examination of literature.

Wetlands used for BOD and nutrient removal were found to have an optimum number of cells, at which decreased area requirements from improved hydraulic performance counterbalance the increased cost of each smaller cell. By optimising cell number, economic savings of up to 86% and 42% were found for BOD and P removal over the ranges investigated. When compared to literature values, wetland remediation was found to be most suitable for secondary treatment of municipal wastewater, both at low and high flow rates. When considering tertiary treatment of wastewater, wetland remediation was found to be economically competitive for integrated secondary and tertiary to stringent standards (around 0.5 mg/L phosphorus and 1 mg/L ammonia nitrogen), also particularly at low flow rates but remaining competitive above 10,000 m^3/d. For tertiary treatment of post-secondary treatment wastewater, wetland remediation was significantly more expensive than conventional treatment methods. The uncertainty of the sizing and costing estimates were investigated using two separate Monte Carlo simulations. The first found a strong correlation ($r > 0.9$, $p < 0.01$) between the wetland size and the reciprocal of the contaminant removal rate, for the “bottleneck” contaminant, with no significant correlation for precipitation and evapotranspiration rates. The second found costs to be most sensitive to variations in capital costs for small wetlands, and to O&M costs with increasing size. Land costs were found to have little impact on overall costs.

Wetland remediation of circumneutral AMD was found to be economically favourable relative to chemical dosing under all conditions investigated, and particularly at low flow rates and Fe concentrations. For low-pH AMD, wetland remediation was found to be economically competitive at a fairly limited range of flow rates and acidities, with this range particularly sensitive to the assumed acidity removal rate. However, a significant proportion of simulated realistic AMD conditions were found to fall within the economically favourable and competitive zones, as well as a majority of overall-site literature data. No clear economic advantage which could be ascertained between VF and HSSF

designs due to the large ranges of removal rates from literature. However, the VF design tended to require a lower area requirement for similar costs.

The possibility of utilising the wetland biomass to offset costs was explored, for direct biomass sale, production of pellets, digestion to biogas, and biorefinery to bioethanol, and pulp. While it was not possible to quantitatively determine the most suitable product, practicality barriers were identified, particularly regarding the required wetland area. A biorefinery with metal recovery was found to have a negligible economic impact but did, however, present a method to utilise contaminated biomass which may otherwise be regarded as a waste product of wetland AMD remediation. The valorisation of wetland biomass *via* an IL biorefinery is further explored in Chapters 4 and 5.

There remain several areas for future work with regards to high-level modelling of wetland remediation. The first, as highlighted by the Monte Carlo analysis, is increased removal rate data, with an aim to reduce the uncertainty introduced by the wide range of removal rate estimates or to gain a better understanding of high-level parameters affecting the removal rate. Additionally, there remains scope for development of high-level wetland remediation models. The P-*k*-*C** model has been shown to be the most suitable for SSF wetlands in a review by Rousseau et al, and represents an improvement upon the first-order *k*-*C** model. [100] However, several of the limitations of the first-order *k*-*C** model outlined by Kadlec may still be improved upon.[101] Multiple studies have tested a first-order removal rate model for certain metals, but the use of such a model for general wetland design would require additional studies with well-reported design properties in order to more confidently estimate the relevant removal rates, background concentrations and P_{TIS} values.[24,102,103] While sophisticated packages do exist for constructed wetland performance, they are intended for detailed design of individual wetlands, and may thus be considered too detailed for this type of high-level estimate. Such models are included in Meyer et al.'s review into the modelling of constructed wetlands, who also emphasise the need for increased data collection and availability.[104]

References

1 United Nations, *International Initiative on Water Quality, SC/HYD/WQ/2015/5/En*, Paris, 2015.

2 United Nations, *TRANSFORMING OUR WORLD: THE 2030 AGENDA FOR SUSTAINABLE DEVELOPMENT, A/RES/70/1*, 2015.

3 E. Corcoran, C. Nellemann, E. Baker, R. Bos, D. Osborn and H. Savelli, *Sick Water? the central role of wastewater management in sustainable development. A rapid response assessment*, Birkeland Trykkeri AS, Norway, 2010.

4 M.-S. Javier, S. M. Zadeh and H. Turral, *More people, more food, worse water? a global review of water pollution from agriculture*, Food and Agriculture Organization of the United Nations, Rome, 2018.

5 R. P. Schwarzenbach, T. Egli, T. B. Hofstetter, U. von Gunten and B. Wehrli, *Annu. Rev. Environ. Resour.*, 2010, **35**, 109–136.

6 World Bank, *Reducing Inequalities in Water Supply, Sanitation, and Hygiene in the Era of the Sustainable Development Goals*, Washington DC, 2017.

7 OECD (Organisation for Economic Co-operation and Development), *Environmental Outlook to 2050: Key Findings*

on Water, 2012.
8 WWAP (United Nations World Water Assessment Programme), *The United Nations World Water Development Report 2015: Water for a Sustainable World*, United Nations Educational, Scientific and Cultural Organization, Paris, 2015.
9 T. A. Larsen, M. Maurer, K. M. Udert and J. Lienert, *Water Sci. Technol.*, 2007, **56**, 229–237.
10 V. H. Smith, *Environ. Sci. Pollut. Res.*, 2003, **10**, 126–139.
11 M. F. Chislock, E. Doster, R. A. Zitomer and A. E. Wilson, *Nat. Educ. Knowl.*, 2013, **4**, 1–8.
12 R. Howarth, F. Chan, D. J. Conley, J. Garnier, S. C. Doney, R. Marino and G. Billen, *Front. Ecol. Environ.*, 2011, **9**, 18–26.
13 S. R. Carpenter, F. Caraco, N, D. L. Correll, R. W. Howarth, A. N. Sharpley and V. H. Smith, *Ecol. Appl.*, 1998, **8**, 559–568.
14 N. N. Rabalais, *AMBIO A J. Hum. Environ.*, 2002, **31**, 102–112.
15 S. Nixon, *Ophelia*, 1995, **45**, 199–219.
16 E. M. BENNETT, S. R. CARPENTER and N. F. CARACO, *Bioscience*, 2006, **51**, 227.
17 J. Peirce, R. Weiner and P. Vesilind, in *Environmental Pollution and Control*, Butterworth-Heinemann, 4th edn., 1998, pp. 105–123.
18 M. Samer, *Biological and Chemical Wastewater Treatment Processes*, InTech, Rijeka, 2015, vol. i.
19 F. Jiang, M. Beck, R. Cummings and K. Rowles, *Estimation of costs of phosphorus removal in wastewater treatment facilities: construction de novo, Water Policy Working Paper #2004-010*, 2004.
20 S. Yeoman, T. Stephenson, J. N. Lester and R. Perry, *Environ. Pollut.*, 1988, **49**, 183–233.
21 M. Libhaber, Appropriate Technologies for Wastewater Treatment and Effluent Reuse for Irrigation, http://siteresources.worldbank.org/EXTWAT/Resources/4602122-1213366294492/5106220-1234469721549/27.2_WWT_Carbon_Footprint.pdf, (accessed 31 July 2019).
22 A. S. Sheoran and V. Sheoran, *Miner. Eng.*, 2006, **19**, 105–116.
23 US Environmental Protection Agency, *Acid Mine Drainage Prediction, EPA 530-R-94-036*, 1994.
24 P. L. Younger, S. Banwart and R. S. Hedin, *Mine Water: Hydrology, Pollution, Remediation*, Springer Netherlands, Dordrecht, 2002.
25 National Rivers Authority, *Abandoned Mines A Report of the National Rivers Authority*, HMSO Publications, Bristol, 1994.
26 US Environmental Protection Agency, *Hardrock Mining Framework - Appendix A*, Washington DC, 1997.
27 Mine Environment Neutral Drainage Programme, *Report of Results of a Workshop on Mine Reclamation*, Ontario, 1994.
28 D. B. Johnson and K. B. Hallberg, *Sci. Total Environ.*, 2005, **338**, 3–14.
29 M. S. Fennessy, W. J. Mitsch, M. S. Fennessy and W. J. Mitsch, *Water Environ. Fed.*, 1989, **61**, 1691–1701.
30 B. Gazea, K. Adam and A. Kontopoulos, *Miner. Eng.*, 1996, **9**, 23–42.
31 Lavdim Osmanaj, Agon Haxhikadrija, Pierre-Henri Dodane and Astrit Vokshi, *J. Hydraul. Eng.*, 2015, **1**, 27–34.
32 A. S. Juwarkar, B. Oke, A. Juwarkar and S. M. Patnaik, *Wat. Sci. Tech.*, 1995, **32**, 291–294.
33 V. M. Lakay, MSc Thesis, University of Cape Town, 2012.
34 O. Alagbe and G. M. Alalade, *Univers. J. Environ. Res. Technol.*, 2013, **5**, 597–606.
35 M. L. Solano, P. Soriano and M. P. Ciria, *Biosyst. Eng.*, 2004, **87**, 109–118.
36 A. K. Kivaisi, *Ecol. Eng.*, 2001, **16**, 545–560.
37 P. Denny, *Water Sci. Technol.*, 1997, **35**, 27–34.
38 D. Q. Zhang, K. B. S. N. Jinadasa, R. M. Gersberg, Y. Liu, W. J. Ng and S. K. Tan, *J. Environ. Manage.*, 2014, **141**, 116–131.
39 S. A. W. Diemont, *Environ. Int.*, 2006, **32**, 332–341.
40 T. Zhang, D. Xu, F. He, Y. Zhang and Z. Wu, *Ecol. Eng.*, 2012, **47**, 189–197.
41 J. L. Faulwetter, V. Gagnon, C. Sundberg, F. Chazarenc, M. D. Burr, J. Brisson, A. K. Camper and O. R. Stein, *Ecol. Eng.*, 2009, **35**, 987–1004.
42 A. M. Nahlik and W. J. Mitsch, *Ecol. Eng.*, 2006, **28**, 246–257.
43 B. Gopal, *Water Sci. Technol.*, 1999, **40**, 27–35.
44 D. Liu, Y. Ge, J. Chang, C. Peng, B. Gu, G. Y. S. Chan and X. Wu, *Front. Ecol. Environ.*, 2009, **7**, 261–268.
45 D. Zhang, R. M. Gersberg and T. S. Keat, *Ecol. Eng.*, 2009, **35**, 1367–1378.
46 G. McNamara, PhD Thesis, Dublin City University, 2018.
47 L. Cardoch, J. W. Day, J. M. Rybczyk and G. P. Kemp, *Ecol. Econ.*, 2000, **33**, 93–101.
48 I. Mannino, D. Franco, E. Piccioni, L. Favero, E. Mattiuzzo and G. Zanetto, *Environ. Manage.*, 2008, **41**, 118–129.
49 A. E. J. Firth, N. Mac Dowell, P. S. Fennell and J. P. Hallett, *Environ. Sci. Water Res. Technol.*, 2020, **6**, 2103–2121.
50 R. H. Kadlec and S. D. Wallace, *Treatment wetlands*, CRC Press, Boca Raton, 2nd edn., 2009.
51 G. R. Watzlaf, K. T. Schroeder, R. L. P. Kleinmann, C. L. Kairies, R. W. Nairn and W. B. Street, *The Passive Treatment of Coal Mine Drainage, DOE/NETL-2004/1202*, 2004.
52 C. A. Cravotta III and C. S. Kirby, in *America Society of Mining and Reclamation*, Morgantown, 2004, pp. 334–365.
53 R. Hedin, R. Narin and R. Kleinmann, *Passive Treatment of Coal Mine Drainage, Information Circular 9389*, 1994.
54 K. L. Ford, *Passive Treatment Systems for Acid Mine Drainage, Technical Note 409*, 2003.
55 J. Skousen and P. Ziemkiewicz, in *National Meeting of the American Society of Mining and Reclamation*, ASMR,

Breckenridge, 2005, pp. 1100–1133.
56 Kepler D.A., in *Mining and Reclamation Conference and Exhibition,* Charleston, 1990.
57 J. Demchak, T. Morrow and J. Skousen, *Geochemistry Explor. Environ. Anal.*, 2001, **1**, 71–80.
58 C. Zipper, J. Skousen and C. Jage, *Passive Treatment of Acid-Mine Drainage*, 2011.
59 H. Brix, R. H. Kadlec, R. L. Knight, J. Vymazal, P. Cooper and R. Haberl, *Constructed wetlands for pollution control: process, performance, design and operation*, IWA Publishing, London, 2000.
60 AMDTreat Software, https://amd.osmre.gov/, (accessed 20 June 2018).
61 D. B. George, *Development of guidelines and design equations for subsurface flow constructed wetlands treating municipal wastewater*, Cincinnati, 2000.
62 N. Mburu, PhD Thesis, IHE Delft.
63 T. Noack and Alan Plummer Associates, *Costs and Other Considerations for Constructed Wetlands*, Constructed Wetlands Workshop, Caesar KleburgWildlife Center, 2018.
64 J. Vymazal and L. Kropfelova, *Wastewater Treatment in Constructed Wetlands with Horizontal Sub-Surface Flow*, Springer, Dordrecht, 2008.
65 United States Environmental Protection Agency, *Wastewater Technology Fact Sheet Wetlands: Subsurface Flow, EPA 832-F-00-023*, Washington DC, 2000.
66 United States Environmental Protection Agency, *Wastewater Technology Fact Sheet Wetlands: Free Water Surface, EPA 832-F-00-024*, Washington DC, 2000.
67 US Department of Agriculture National Agricultural Statistics Service, *Land Values 2017 Summary, ISSN: 1949-1867*, 2017.
68 Mine Environment Neutral Drainage Program and Canadian Centre for Mineral and Energy Technology, *ACID MINE DRAINAGE - STATUS OF CHEMICAL TREATMENT AND SLUDGE MANAGEMENT PRACTICES*, 1994.
69 R. Bashar, K. Gungor, K. G. Karthikeyan and P. Barak, *Chemosphere*, 2018, **197**, 280–290.
70 United States Environmental Protection Agency, *Biological nutrient removal processes and costs, EPA-823-R-07-002*, Washington DC, 2007.
71 B. Papadopoulos, K. P. Tsagarakis and A. Yannopoulos, *J. Environ. Eng.*, 2007, **133**, 581–586.
72 S. Jafarinejad, *Appl. Water Sci.*, 2017, **7**, 2513–2521.
73 E. Friedler and E. Pisanty, *Water Res.*, 2006, **40**, 3751–3758.
74 T. Dogot, Y. Xanthoulis, N. Fonder and D. Xanthoulis, *Water Sci. Technol.*, 2010, **62**, 640–648.
75 R. Nogueira, A. G. Brito, A. P. Machado, P. Janknecht, J. J. Salas, L. Vera and G. Martel, *Desalin. Water Treat.*, 2009, **4**, 16–21.
76 M. Molinos-Senante, F. Hernández-Sancho, M. Mocholí-Arce and R. Sala-Garrido, *Resour. Energy Econ.*, 2014, **38**, 125–140.
77 Bolton & Menk Inc, *Ultra-Low Phosphorus Removal Pilot Study City of Mankato, Minnesota, Project No. M24.109541*, 2016.
78 US Environmental Protection Agency, *Economic Analysis of Final Water Quality Standards for Nutrients for Lakes and Flowing Waters in Florida*, Washington DC, 2010.
79 J. Skousen, in *Acid Mine Drainage, Rock Drainage, and Acid Sulfate Soils: Causes, Assessment, Prediction, Prevention, and Remediation*, eds. J. Jacobs, J. H. Lehr and S. M. Testa, Wiley, 2014, pp. 325–337.
80 H. Davies, P. Weber, P. Lindsay, D. Craw and J. Pope, *Sci. Total Environ.*, 2011, **409**, 2971–2980.
81 N. F. Gray, *Water Res.*, 1998, **32**, 2122–2134.
82 M. Olías, J. M. Nieto, A. M. Sarmiento, J. C. Cerón and C. R. Cánovas, *Sci. Total Environ.*, 2004, **333**, 267–281.
83 C. A. Johnson and I. Thornton, *Water Res.*, 1987, **21**, 359–365.
84 J. S. España, E. L. Pamo, E. Santofimia, O. Aduvire, J. Reyes and D. Barettino, *Appl. Geochemistry*, 2005, **20**, 1320–1356.
85 T. Ridge and J. Self, *Coal Mine Drainage Prediction and Pollution Prevention in Pennsylvania*, Pensylvania Department of Environmental Protection, 1998.
86 P. Icka, R. Damo and E. Icka, *Ann. "Valahia" Univ. Targoviste - Agric.*, 2017, **11**, 1–5.
87 F. W. Croon, *Mires Peat*, 2014, **13**, 1–13.
88 Ethanol Commodity Price, markets.ft.com/data/commodities/tearsheet/summary?c=Ethanol, (accessed 10 October 2019).
89 Wood Pulp Commodity Price, https://www.indexmundi.com/commodities/?commodity=wood-pulp&months=360, (accessed 10 October 2010).
90 G. Duke and P. Goriup, *Innovation for reed bed biomass fuel and biodiversity by FIELDFARE – ANALYSIS OF THE OPPORTUNITY, EU Business and Biodiversity Platform*, 2015.
91 UK Department for Energy and Climate Change, *Wetland Biomass to Bioenergy Gasification and anaerobic digestion of sustainably - sourced wetland biomass Phase 1 report, URN 13D/003*, 2013.
92 Confederation of European Paper Industries (CEPI), *Key Statistics 2016 European Pulp and Paper Industry*, Brussels, 2017.
93 D. Humbird, R. Davis, L. Tao, C. Kinchin, D. Hsu, A. Aden, P. Schoen, J. Lukas, B. Olthof, M. Worley, D. Sexton and D. Dudgeon, *Process Design and Economics for Biochemical Conversion of Lignocellulosic Biomass to Ethanol: Dilute-Acid Pretreatment and Enzymatic Hydrolysis of Corn Stover, NREL/TP-5100-47764*, 2002.
94 J. U. Smith, K. Yongabi, H. Black, E. Casson, K. Glenk, S. Langan, R. Matthews, J. Mugisha and P. Smith, *The*

Potential of Small-Scale Biogas Digesters to Alleviate Poverty and Improve Long Term Sustainability of Ecosystem Services in Sub-Saharan Africa, DFID NET-RC A06502, Heifer International, 2011.
95 J. Mwirigi, B. B. Balana, J. Mugisha, P. Walekhwa, R. Melamu, S. Nakami and P. Makenzi, *Biomass and Bioenergy*, 2014, **70**, 17–25.
96 S. Roj-Rojewski, A. Wysocka-Czubaszek, R. Czubaszek, A. Kamocki and P. Banaszuk, *Biomass and Bioenergy*, 2019, **122**, 126–132.
97 F. Gschwend, PhD Thesis, Imperial College London, 2017.
98 P. K. Rai, *Int. J. Phytoremediation*, 2008, **10**, 133–160.
99 M. Ghosh and S. P. Singh, *As. J. Energy Env*, 2005, **6**, 214–231.
100 D. P. L. Rousseau, P. A. Vanrolleghem and N. De Pauw, *Water Res.*, 2004, **38**, 1484–1493.
101 Robert H. Kadlec, *Ecol. Eng.*, 2000, **15**, 105–119.
102 R. R. Goulet, F. R. Pick and R. L. Droste, *Ecol. Eng.*, 2001, **17**, 357–371.
103 W. J. Tarutis, L. R. Stark and F. M. Williams, *Ecol. Eng.*, 1999, **12**, 353–372.
104 D. Meyer, F. Chazarenc, D. Claveau-Mallet, U. Dittmer, N. Forquet, P. Molle, A. Morvannou, T. Pálfy, A. Petitjean, A. Rizzo, R. Samsó Campà, M. Scholz, A. Soric and G. Langergraber, *Ecol. Eng.*, 2015, **80**, 205–213.

Chapter 4: Pretreatment of Wetland Species

4.1 Introduction

Many wetland species are high-yielding, with the most common, *Phragmites australis*, generally estimated to yield between around 10 and 30 tonnes/ha/y (dry basis).[1–3] Other common species such as *Typha latifolia* or *Typha angustifolia* are estimated to yield around 10-20 tonnes/ha/y.[4–7] These growth rates are comparable to those of dedicated energy crops such as *Miscanthus* or switchgrass.[8–10] Currently, harvested CW crops can represent a disposal issue with associated costs, particularly when treating metal-contaminated water due to elevated metal content.[11–13] In Chapter 3, it was shown that valorisation of wetland biomass has the potential to offset a reasonable proportion of CW costs if widely implemented.[14] Additionally, an LCA study by Liu et al. found that production of biofuels from CWs offers a greater reduction in greenhouse gases than current biofuel production systems (including cellulosic and algal fuels).[15] Despite showing promise for biofuel production there has, however, only been a small number of studies on pretreatment of wetland species. Peng et al. performed both steam explosion (SE), and SE followed by Dissolution pretreatment on *Phragmites australis* and *Thalia dealbata*, and subsequent anaerobic fermentation to H_2.[16] Low quantities of lignin and significant quantities of hemicellulose (76%) were removed during SE, with resulting low saccharification yields of 39%. There was little subsequent change in composition after IL pretreatment (with a final cellulose purity of 73%) but a large increase in saccharification yield (89%). Sathitsuksanoh et al. reported high sugar release (88%) from *Phragmites australis* using COSLIF pretreatment despite relatively low lignin removal[17], while Zhang et al reported reasonable saccharification yields (78%) from *Typha latifolia* following hot-water pretreatment.[18] The most detailed study found was conducted by He et al, who performed alkaline pretreatment on 14 wetland species but found large variations in saccharification yields (24-87%).[19] All of these studies only targeted sugar release (and subsequent ethanol yield) rather than the production of high-purity pulps, while also not mixing species, considering metal-contaminated feedstocks, or having a separate lignin recovery stream.

The work in this Chapter aims to comprehensively study the suitability of the ionoSolv process for large-scale valorisation of biomass harvested from constructed wetlands. Using timecourse pretreatments at 150 °C, the pretreatment performance of three different ILs was tested using *Phragmites australis*, the most common wetland species. Performance was evaluated in terms of saccharification yield, digestibility, and cellulose purity. Additionally, generated lignin was

characterised by GPC and HSQC spectroscopy. The pretreatment performance of three batches of *Phragmites australis* from different applications was then compared, and two optimal operating points identified. A further 8 feedstocks, covering 7 species, were pretreated at these operating points. The performance of two ILs was then tested when reused up to 4 times in the pretreatment of a mixed wetland feedstock. The ability of three different IL systems to remove metals from a metal-contaminated mixed wetland feedstock, while maintaining pretreatment performance, was also evaluated.

4.2 Materials and Methods

4.2.1 General equipment

Unless stated otherwise, all general equipment used was the same as in Chapter 2.

4.2.2 IL Synthesis

Reagents for [DMBA][HSO_4] and [MBA][HSO_4] were obtained as in Chapter 2. *N,N*-Dimethylethanolamine (>99.5%) and formic acid (>98.0%) were purchased from Sigma Aldrich, 1-methylimidazole (>99.0%) was purchased from VWR, and 1 mole ampoules of HCl were purchased from Fisher Scientific. All the above were used as received for IL synthesis. ILs were synthesised as in Chapter 2. Acid-base ratios of monoprotic ILs were determined by pH (see Appendix). Acid-base ratios are expressed on a molar basis. The acid/base ratio of recycled ILs was determined as described in Chapter 2, but accounting for the mass of dissolved solutes (determined as in Liquor Analysis). NMR signals are provided below, with NMR spectra provided in the Appendix.

1-MethylImidazolium Chloride [Hmim]Cl (Figs. A1-9 and A1-10):

^{1}H NMR: δ_H (400 MHz, D_2O)/ppm: 8.31 (s, 2H, N-*H*$_2$), 7.45 (t, J=1.9 2H, H-4/5), 7.43 (t, J=1.9 2H, H-4/5), 4.66 (s, br, *H*$_2$O), 3.91 (s, 3H, N-C*H*$_3$).

^{13}C NMR δ_C (101 MHz, D_2O)/ppm: 135.18 (*C*-2), 123.25 (*C*-4/5), 119.67 (*C*-4/5), 35.91 (N-*C*H_3).

DiMethylEthanolAmmonium Formate [DMEtA][HCOO] (Figs. A1-11 and A1-12):

^{1}H NMR: δ_H (400 MHz, DMSO-d_6)/ppm: 9.18 (s, br, N-*H*, N-CH_2-CH_2-O*H*), 8.34 (s, 1H, *H*-COO^-), 3.60, (m, 2H, H-*CH*$_2$), *2*.84 (m, 2H, N-CH_2-C*H*$_2$), 2.53 (m, 6H, N-(C*H*$_3$)$_2$).

^{13}C NMR δ_C (101 MHz, DMSO-d_6)/ppm: 167.15 (H-*C*OO^-), 59.65 (N-*C*H_2), 56.77 (N-(*C*H_3)$_2$), 43.51 (N-CH_2-*C*H_2OH).

4.2.3 Pretreatment

The pretreatment protocol of the Hallett group laboratory was followed, as described in Chapter 2.

During pretreatment experiments incorporating IL recycling, the IL was recovered by removing water under reduced pressure following lignin precipitation. Water was removed from the IL solution in a pre-weighted round-bottomed flask, which was then weighed following water removal to determine the total mass of recovered IL solution. IL recovery was then quantified using Eq. 4.1:

$$IL\ Recovery\ (\%) = \frac{m_{rec} \times (1 - wc_{rec} - sc_{rec}) + m_{liq} \times (1 - wc_{liq} - sc_{liq})}{m_{in} \times (1 - wc_{in} - sc_{in})} \times 100 \quad (4.1)$$

where *m* is the mass of IL solution, *wc* is the water content of the IL solution, and *sc* is the solute content of the IL solution (as determined in Liquor Analysis). Subscript *rec* refers to the recovered IL solution following the pretreatment cycle, *liq* refers to the aliquot of liquor taken following pretreatment for liquor analysis, and *in* refers to the IL solution input to the pretreatment.

All species used, as well as their harvest dates and source, are shown in Table 4.1.

4.2.4 Pulp Characterisation

Enzymatic Hydrolysis

Enzymatic hydrolysis assays were carried out on pretreated pulps and untreated biomass, as well as on blank controls. The enzymatic hydrolysis protocol of the Hallett group laboratory was followed, as described in Chapter 2.

Compositional Analysis

The compositional analysis protocol followed was that of the National Renewable Energy Laboratory 'Determination of Structural Carbohydrates and Lignin in Biomass', as described in Chapter 2.[20] Unless specified, only ethanol Soxhlet extraction was performed on the pulp beforehand (as part of the pretreatment protocol), while both water and ethanol Soxhlet extraction were performed on the untreated biomass. All measurements were performed in triplicates on untreated biomass and once for each pulp. In addition to the ash content obtained through the compositional analysis procedure, the ash content of certain samples was verified by directly ashing the samples, using the same heating profile.

Table 4.1: Feedstocks used for pretreatment.

Species	Common Name	Abbreviation	Harvest Month	Source
Phragmites australis (batch 1)	Common Reed	PA 1	July	Commercial Grower
Phragmites australis (batch 2)		PA 2	July	Constructed Wetland Treating Domestic Wastewater
Phragmites australis (batch 3)		PA 3	March	Constructed Wetland Treating Acid Mine Drainage
Typha latifolia (batch 1)	Common Bulrush/ Broadleaf Cattail	TL 1	October	Commercial Growers
Typha latifolia (batch 2)		TL 2	May	
Typha angustifolia	Lesser Bulrush/ Narrowleaf Cattail	TA	October	
Cyperus alternifolius	Umbrella Sedge	CA	October	
Carex pendula	Pendulous Sedge	CP	October	
Scirpus lacustris	Lakeshore Bulrush	SL	October	
Pistia stratiotes	Water Lettuce	PS	October	
Juncus effusus (batch 1)	Common Rush	JE	May	
Juncus effusus (batch 2)	Common Rush	JE 2	November	Natural Wetland Receiving Acid Mine Drainage
Sphagnum spp.	Sphagnum Moss	SS		
Ulex europaeus	Gorse	UE		
Betula pendula	Silver Birch	BP		
Molinia caerulea	Molinia	MC		

4.2.5 Liquor Analysis

The solute content of selected IL solutions was determined before and immediately after pretreatment, analysing for sugars and their degradation products. Approximately 200 mg of solution were weighed into a 1.5 mL microcentrifuge tube using a syringe. Approximately 700 mg of distilled

water were then added, the mixture was mixed using a vortex shaker, and was then centrifuged at 13.3 G for 20 minutes at 4 °C. The supernatant was decanted using an Eppendorf pipette and transferred to an HPLC vial, and analysed by HPLC. The HPLC used was a Shimadzu Prominance preparatory HPLC with both RI and UV detectors, and used an Aminex HPX-87H column (Biorad, 300 x 7.8 mm) with 0.005M H_2SO_4 as a mobile phase (0.6 mL/min). The column temperature was 55 °C, with a run time of 45 minutes. All samples used were filtered through a 0.2 µm PTFE syringe filter. Calibration was carried out for each set of runs, using standards of 0.01, 0.02, 0.1, 0.4, and 1 mg/mL of furfural, 5-HMF, levulinic acid, glacial acetic acid, and formic acid, and 0.2, 1, 2, and 4 mg/mL of glucose, xylose, and arabinose. A least squares linear regression fit was used to create a calibration curve. The mass fraction of each solute in the IL solution was determined using Eq. 4.2.

$$m_{solute} = \frac{c_{HPLC} \times \left(m_{liquor} + m_{water}\right) \times \rho_{sample}}{m_{liquor}} \quad (4.2)$$

where m_{solute} is the mass fraction of each solute, c_{HPLC} is the concentration of the solute in the sample as determined by HPLC, m_{liquor} is the mass of liquor sampled, m_{water} is the mass of water added to the sample, and ρ_{sample} is the density of the sample (taken as 1.04).

4.2.6 Biomass Digestion and Metal Quantification

Digestions were performed in triplicate for each species and pretreatment condition investigated, and during each experiment a set of blank digestions were also carried out in triplicate as a control. A known quantity of air-dried biomass (approximately 200 mg) was transferred into a MARS 6 Easyprep microwave digestion vessel. 9 mL of 69% trace-metal grade HNO_3 and 3 mL of 37% trace-metal grade HCl were then added to each digestion vessel (including blanks) using an Eppendorf pipette. The vessels were sealed closed, and samples were then digested in a MARS 6 microwave digester using the method shown in Table 4.2:

Table 4.2: Temperature profile used for biomass digestion.

Stage	Ramp (min)	Hold Time (min)	Temperature (°C)	Power (W)
1	2:00	1:00	105	1800
2	5:00	10:00	180	1800

Samples were left to cool for at least 3 hours in order to allow vapours to condense. The digestion liquor was transferred from the vessel into a 100 mL volumetric flask. The vessel was then washed out with a solution of 2% HNO_3 and 0.5% HCl, with the washings added to the volumetric flask until a total

volume of 100 mL was reached. Any samples with concentrations above 1 ppm were further diluted to below 1 ppm. An aliquot of this solution was then taken and filtered through a 0.2 µm syringe filter, and transferred into a 15 mL centrifuge tube, before further analysis. Metal contents of the solutions were later quantified by Inductively Coupled Plasma Mass Spectrometry (ICP-MS), using an Agilent ICP-MS 7900. All results were baselined to the metal contents of the blank digestions, and of the diluent for samples that were further diluted. Standards of 5, 50, 100, 500, and 1000 µg/L for Al, Ca, Cd, Cu, Fe, K, Mn, Ni, Pb, and Zn were prepared using Aristar 23 element ICP Calibration Standard (IV) purchased from VWR, diluted in 2% HNO_3.

Metal recovery in the pulp, lignin, and IL fractions were determined using Eqs. 4.3-5:

$$M_{pulp}(\%) = \frac{c_{M,pulp} \times Pulp\ Yield}{c_{M,untreated}} \times 100 \quad (4.3)$$

$$M_{lignin}(\%) = \frac{c_{M,lignin} \times Lignin\ Yield \times Lignin_{untreated}}{c_{M,untreated}} \times 100 \quad (4.4)$$

$$M_{IL}(\%) = \frac{c_{M,IL} \times m_{IL}}{c_{M,untreated} \times m_{untreated}} \times 100 \quad (4.5)$$

where *c* is the concentration of metal M in the sample (determined by ICP-MS), *Lignin* is the proportion of lignin in the sample (the sum of acid-soluble and acid-insoluble lignin), *Pulp Yield* is defined as Chapter 2, *Lignin Yield* is the yield of recovered lignin (relative to the theoretical maximum), and *m* is the mass of a specified fraction. Subscript *pulp* refers to the pretreated biomass, *untreated* refers to the untreated biomass, *IL* refers to the recovered ionic liquid, and *lignin* refers to the recovered lignin. Metal removal from the pulp was then calculated as 100 – M_{pulp} *(%)*.

4.2.7 Lignin Characterisation

Gel Permeation Chromatography (GPC) and HSQC NMR were performed on selected lignin samples as described in Chapter 2. HSQC NMR integral areas were assigned following previous studies using similar feedstocks.[21–29]

4.2.8 Statistical Analysis

Statistical analysis was performed using the Student's *t*-test for comparison of 2 data points, and using two-tailed ANOVA for comparison of three or more data points. Correlations were determined using Pearson's correlation coefficient. The significance level used was 0.05, corresponding to a 5% risk of falsely concluding statistical difference exists.

4.3 Results and Discussion

4.3.1 IL Screening Using Virgin *Phragmites Australis*

There are a large number of different wetland species. *Phragmites australis* (common reed), the most common of these, is abundant across the globe and has been extensively used in constructed wetland remediation studies. It was therefore decided to initially investigate the performance of the ionoSolv process using *Phragmites australis*, as any scaled-up process would need to be compatible with this common feedstock.

The ILs used were [DMBA][HSO_4], [MBA][HSO_4], and dimethylethanolammonium formate ([DMEtA][HCOO]). [DMBA][HSO_4] was selected as it is an established low-cost pretreatment IL, while [MBA][HSO_4] was tested in order to further probe its promising pretreatment effectiveness (while also being low-cost). [DMEtA][HCOO] was selected in order to probe the behaviour of a non-acidic IL. Additionally, it was used in order to determine whether the hemicellulose-preserving pretreatment behaviour of [MEA][OAc] is common to other alkylammonium carboxylate ILs. Several studies have focussed on the use of monoethanolammonium acetate ([MEA][OAc]), a protic IL, for biomass pretreatment. [MEA][OAc] has been shown to selectively extract lignin while preserving hemicellulose sugars due to its more basic nature, leading to high saccharification yields.[30,31] However, a tertiary alkylammonium cation was used instead of a primary or secondary alkylammonium cation, in order to avoid formylation of the non-ionised alkylamine into a formamide. The analogous acetylation reaction has been shown to occur during pretreatment using [MEA][OAc], with the resulting acetamide inhibiting sugar release.[31] Monoethanolammonium formate ([MEA][HCOO]) has previously been tested as a pretreatment solvent, showing a mild increase in digestibility of cotton stalks.[32] However, the pretreatment duration was far too short (30 minutes for 130 ^{o}C) and for a single timepoint, and lack of compositional analysis of the resulting pulp means hemicellulose preservation could not be inferred.

The performance of the three ILs was compared, for the pretreatment of Batch 1 of *Phragmites australis* (purchased from a commercial grower), with results shown in Figs. 4.1 and 4.2.

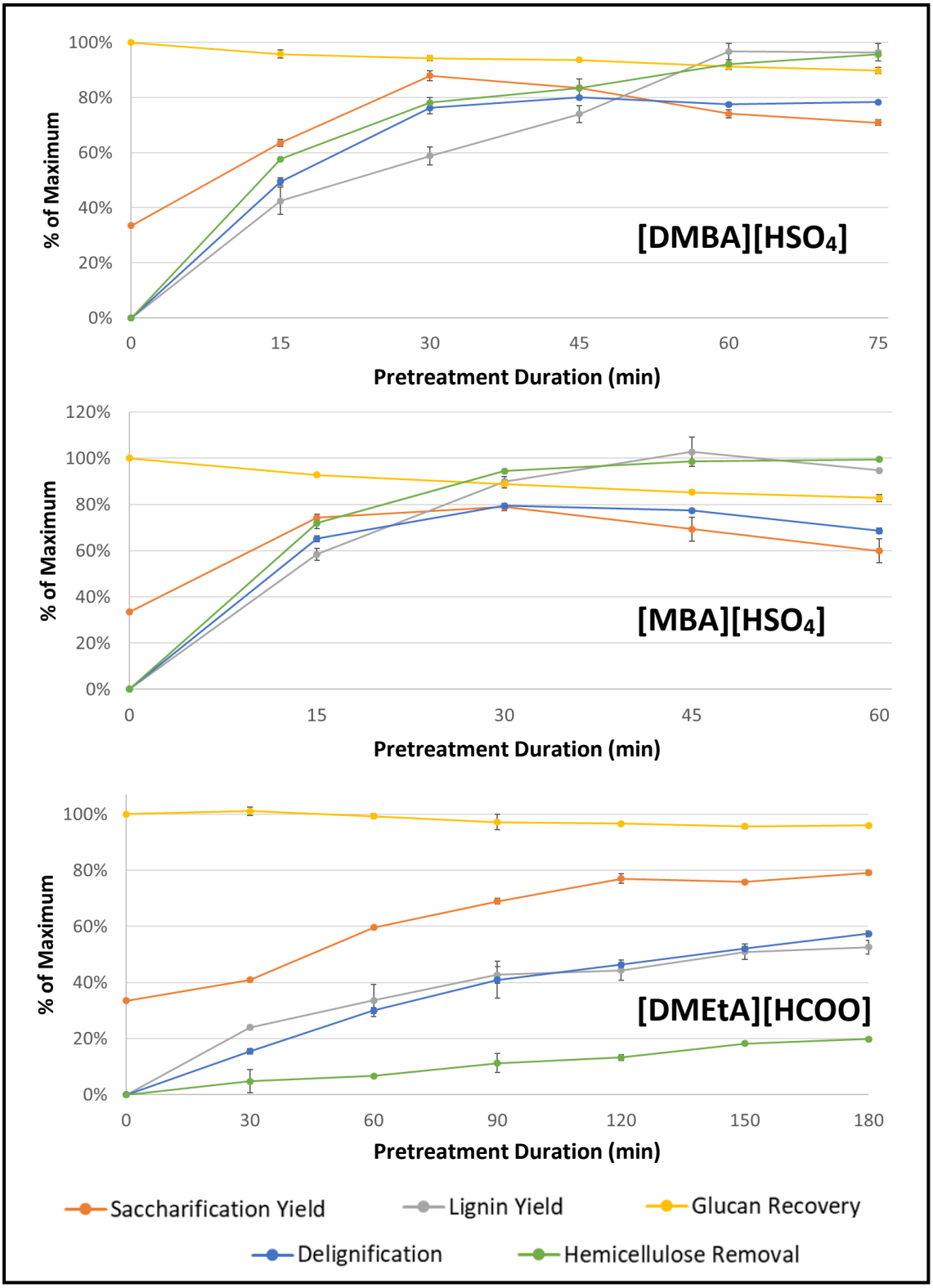


Figure 4.1: Pretreatment performance of different ionic liquids. ILs used are indicated on each plot. All pretreatments were carried out on Batch 1 of *Phragmites australis* (as defined in Table 1) at 150 °C, with 20 wt% water, and at a biomass loading of 10% wt/wt.

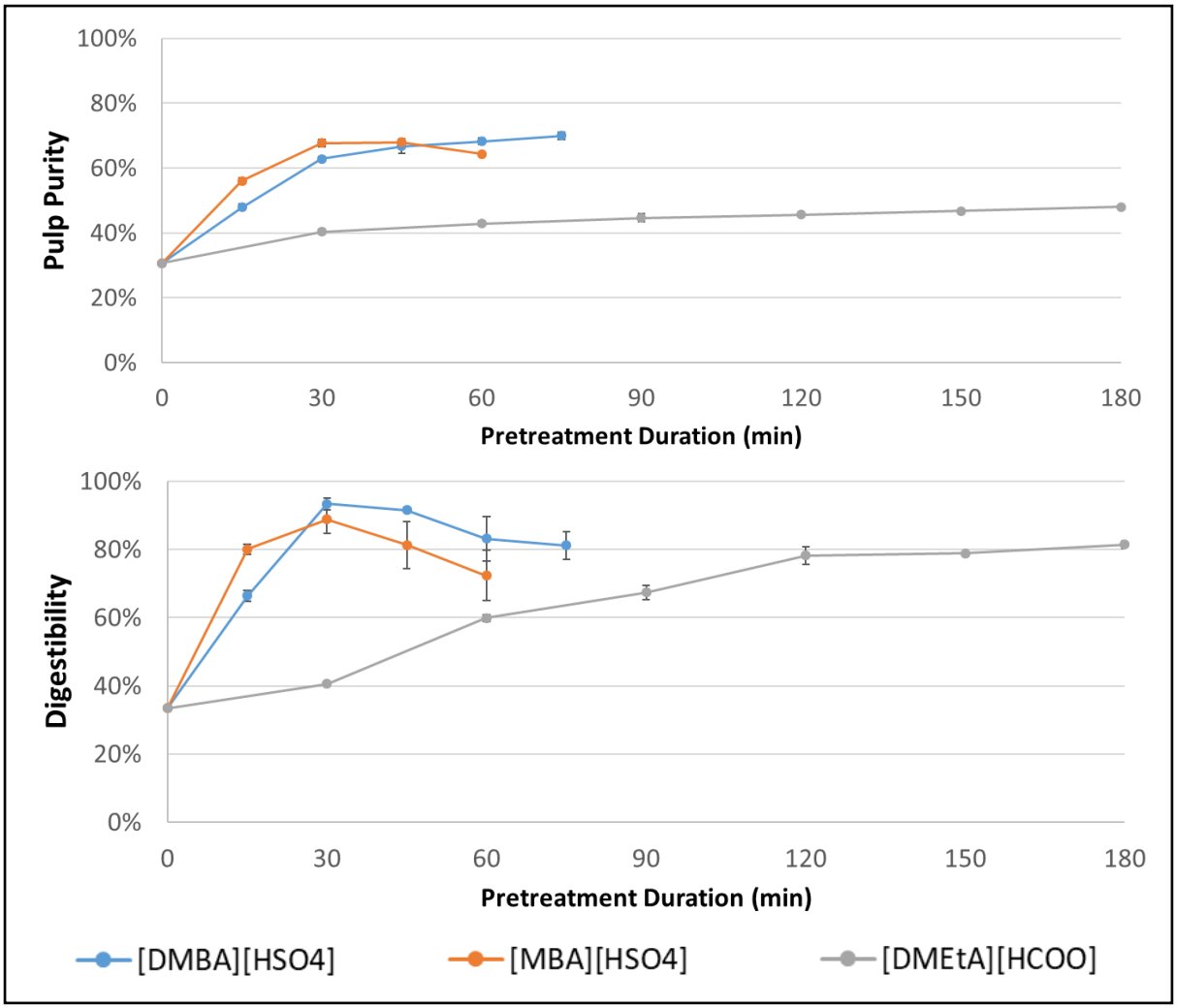


Figure 4.2: Digestibility and purity of pulps pretreated using varying ionic liquids. All pretreatments were carried out on Batch 1 of *Phragmites australis* (as defined in Table 4.1) at 150 °C, with 20 wt% water, and at a biomass loading of 10% wt/wt.

The pretreatment behaviours of [MBA][HSO_4] and [DMBA][HSO_4] are generally similar, with the former expectedly showing signs of higher severity due to its lower Hammett acidity value (see Chapter 2). Many of these trends are similar to those in Chapter 2 using *Miscanthus* as a feedstock. Relative to [DMBA][HSO_4], [MBA][HSO_4] displays higher glucan losses, reaching 17% after 60 minutes of pretreatment compared to 9% using [DMBA][HSO_4]. [DMBA][HSO_4] shows a large initial drop of around 4% after 15 minutes followed by a slower increase of 1-2% every 15 minutes. In contrast, glucan losses in [MBA][HSO_4] display a large initial drop of 7% followed by increases of around 3% every 15 minutes. The initial larger rise in glucan losses (during the early stages of pretreatment when temperatures are still increasing) is attributed to hydrolysis of amorphous cellulose and glucan contained in hemicellulose.[33] The subsequent slower increases can be explained by the crystalline cellulose being slowly hydrolysed endwise, as well as the crystalline structure of the cellulose possibly

being disrupted in the case of [MBA][HSO_4].[33] Another indicator of higher severity are the near-quantitative hemicellulose removal observed in [MBA][HSO_4], significantly higher than using [DMBA][HSO_4] (99.5% vs. 92.2% after 60 minutes). Additionally, delignification in [MBA][HSO_4] shows a clear peak at 30 minutes, beyond which redeposition of condensed lignin and pseudolignin outweigh further removal due to the more acidic conditions.[34] Clear evidence of redeposition is seen above 45 minutes, as both recovered lignin yields and delignification values both decrease. However, delignification using [DMBA][HSO_4] plateaus after 45 minutes, either due to the cessation of lignin removal, or due to further lignin removal being counterbalanced by lignin and pseudolignin redeposition. The latter hypothesis is thought to be more likely due to decreasing pulp digestibility, as pseudolignin inhibits saccharification enzymes more than native lignin[35], and redeposited lignin on the pulp surface can block access to cellulose pores.

There are, however, several differences between the pretreatment behaviour displayed here and that observed using *Miscanthus* in Chapter 2. Lignin yields using both ILs are significantly higher, despite lower feedstock lignin content (19.9% vs 26.2%), exceeding 100% of the lignin originally present in the biomass. Lignin yields above 100%, as well as lignin yields higher than delignification, are both clear signs of pseudolignin formation. This is thought to be due to the significantly higher extractives content found in Batch 1 of *Phragmites australis* than in *Miscanthus* (21.3% vs 2.7%), which may be reacting with dissolved lignin and hemicellulose degradation products and being incorporated into pseudolignin. Extractives are non-structural components of the biomass that can be extracted using various solvents (in this case ethanol and water), encompassing hundreds of possible compounds within individual biomass samples, and are more abundant in grasses.[36,37] They may broadly be classified into phenolic compounds, terpenes, proteins, non-structural carbohydrates, fatty compounds (e.g. fatty acids, waxes, triglycerides), nitrogenous compounds (e.g. alkaloids), and inorganics.[36,38]

This theory of extractives incorporating into pseudolignin was corroborated by pretreating the extractive-free biomass (i.e. pre-extracted with water and ethanol) for 30 and 60 minutes using [DMBA][HSO_4], leading to significantly reduced lignin yields (42% vs. 59%, and 59% vs 97%). This is further supported by reported higher acid-insoluble lignin contents during compositional analysis of grassy feedstocks without prior extraction.[39] The high degree of redeposition onto the pulp leads to maximum delignification values of around 80% in both ILs, approximately 10% lower than seen using *Miscanthus*. There is further evidence of delignification being limited by pseudolignin formation and redeposition, as at low pretreatment durations (under 30 minutes), delignification rates are very similar to those using *Miscanthus*.

The effect of pseudolignin redeposition is seen through trends in saccharification yields and pulp digestibilities. Using both acidic ILs, there are sharp peaks in saccharification and digestibility after 30 minutes (79% and 89% using [MBA][HSO_4], 88% and 93% using [DMBA][HSO_4]), despite pulp purities remaining fairly constant around 70%. The significantly lower peak saccharification using [MBA][HSO_4] than [DMBA][HSO_4] is due to both the significant glucan losses, as well as the more rapid pseudolignin formation arising from more acidic conditions. Digestibility trends are again very different to those using *Miscanthus*, for which values remain consistently high at long pretreatment durations.

Very different trends in pretreament performance are observed using [DMEtA][HCOO]. The reduced IL solution acidity, due to the lack of acidic proton on the ionised species, leads to much lower levels of polysaccharide hydrolysis. From 150 minutes onwards, glucan losses remain at 4%, while the more easily hydrolysed hemicellulose is only 20% removed after 3 hours of pretreatment. Instead, as previously reported with similar ILs, there is selective delignification of the biomass with hemicellulose sugars largely preserved.[30,31] Delignification proceeds much more slowly, reaching 60% after 3 hours, although still showing an increasing trend. Due to the less severe nature of the pretreatment, there is no clear sign of pseudolignin formation, with lignin yields closely tracking delignification. As a result, saccharification yields and digestibility continually increase over time, roughly tracking delignification. After three hours of pretreatment, pulp digestibility is 81% and still slowly increasing, despite low pulp purity of only 48%. These results show that the pretreatment behaviour of [MEA][OAc] is shared by [DMEtA][HCOO] and may be common to a number of alkylammonium carboxylate ILs.

Preservation of hemicellulose sugars allows fuller valorisation of the biomass, as it accounts for 22% of the feedstock. Total sugar yields for all three ILs, accounting for glucose, xylose, galactose, arabinose, and mannose, are shown in Fig. 4.3. Pulps pretreated with [DMEtA][HCOO] display a much higher total sugar yield, remaining between 67% and 70% above 2 hours, compared to peaks of 58% after 30 minutes and 46% after 15 minutes using [DMBA][HSO_4] and [MBA][HSO_4]. Future developments in utilisation of hemicellulose sugars may significantly improve the economic viability of such hemicellulose-preserving pretreatments, outweighing the longer residence times and more expensive ILs. The use of a hemicellulose-preserving or –removing pretreatment will depend on desired product application, however: certain pulp products such as dissolving pulp require extensive hemicellulose removal.

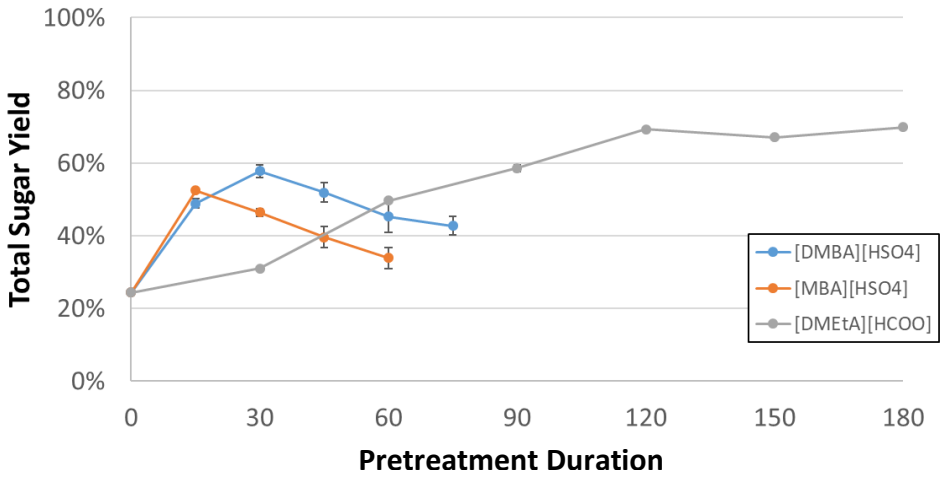


Figure 4.3: Total hydrolysis sugar yield using varying ionic liquids. All pretreatments were carried out on Batch 1 of *Phragmites australis* (as defined in Table 1) at 150 °C, with 20 wt% water, and at a biomass loading of 10% wt/wt.

The lignin recovered from all three ILs was characterised by GPC, with data shown in Figs. 4.4 and 4.5. At peak saccharification yield, recovered lignin using [DMEtA][HCOO] has a lower molecular weight, consistent with the lower rate of condensation reactions and pseudolignin formation. [MBA][HSO_4] lignin has higher M_n and M_w values than [DMBA][HSO_4] after 30 minutes of pretreatment, also consistent with more rapid pseudolignin formation due to more severe conditions. There are also substantial differences in the molecular weight profiles of the three ILs. All ILs show a relatively sharp peak in in molecular weight at around 700 g/mol, a broader peak at around 2000-4000 g/mol, and a small peak at around 400 g/mol. In the $[HSO_4]^-$ ILs, the sharp peak at 750 g/mol decreases as the pretreatment duration increases, while the broad peak shifts to higher molecular weights. This is thought to be due to smaller lignin fragments reacting thus combining into larger fragments (so-called condensation reactions, see Section 1.3.2), and formation of pseudolignin. In lignin from [DMEtA][HCOO], while the broad peak increases in intensity with duration, a sharp peak at 700 g/mol is still maintained even at long pretreatment durations, showing that small lignin fragments remain more stable in this neutral IL (i.e. do not condense extensively as in the acidic $[HSO_4]^-$ ILs). Additionally, the broad peak (at around 2000 g/mol) does not significantly shift to higher molecular weights and decreases in dispersity. The increase in broad peak relative intensity may be explained by some degree of condensation reactions of dissolved lignin fragments, while the decrease in its dispersity may provide further evidence for the lack of pseudolignin formation. The more native structure of the lignin produced using [DMEtA][HCOO] may make it more suitable for further chemical processing.[40]

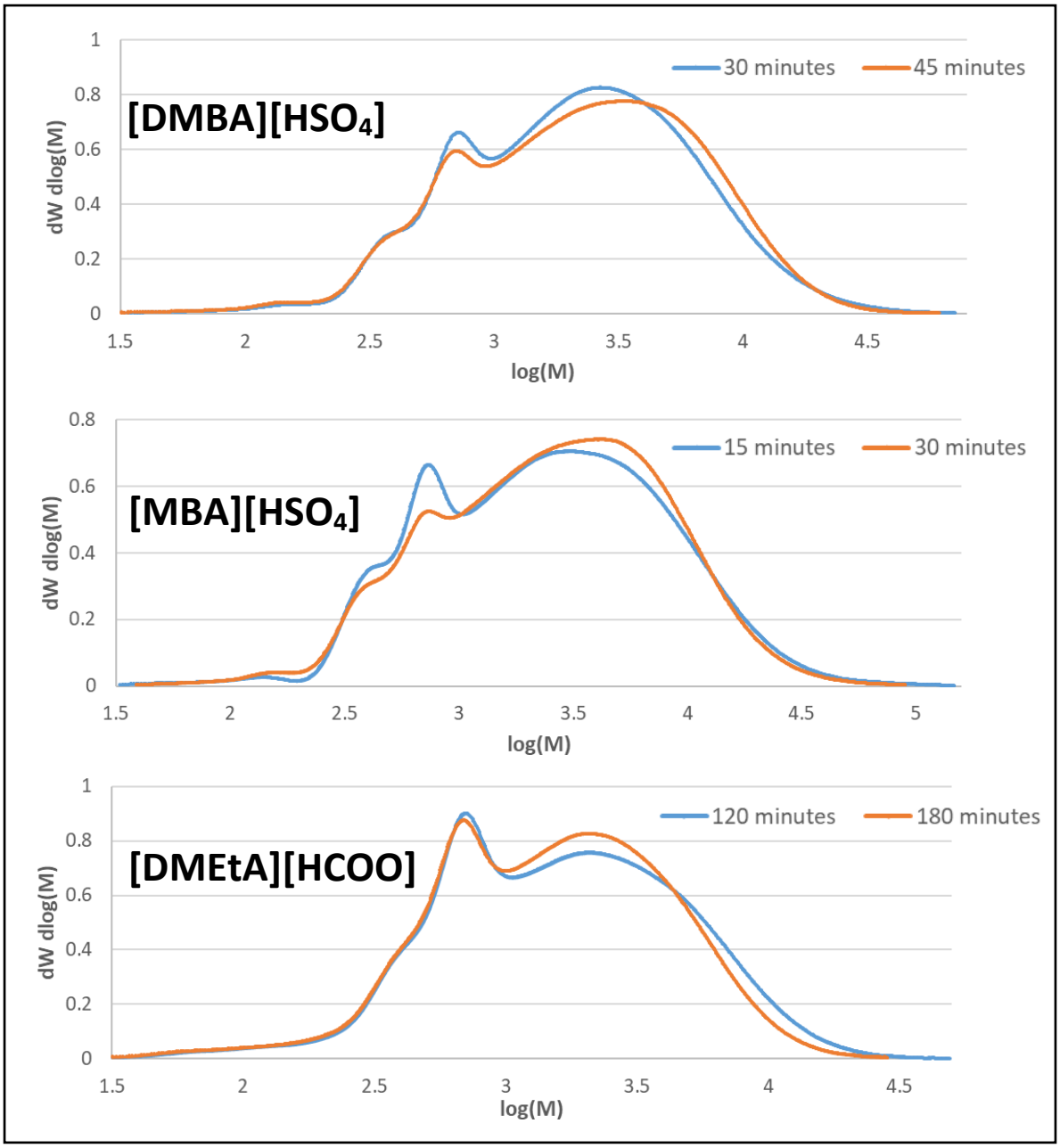


Figure 4.4: Molecular weight profiles of recovered lignin following pretreatment with varying ionic liquids. ILs used are indicated on each plot. All pretreatments were carried out on Batch 1 of *Phragmites australis* (as defined in Table 4.1) at 150 °C, with 20 wt% water, and at a biomass loading of 10% wt/wt.

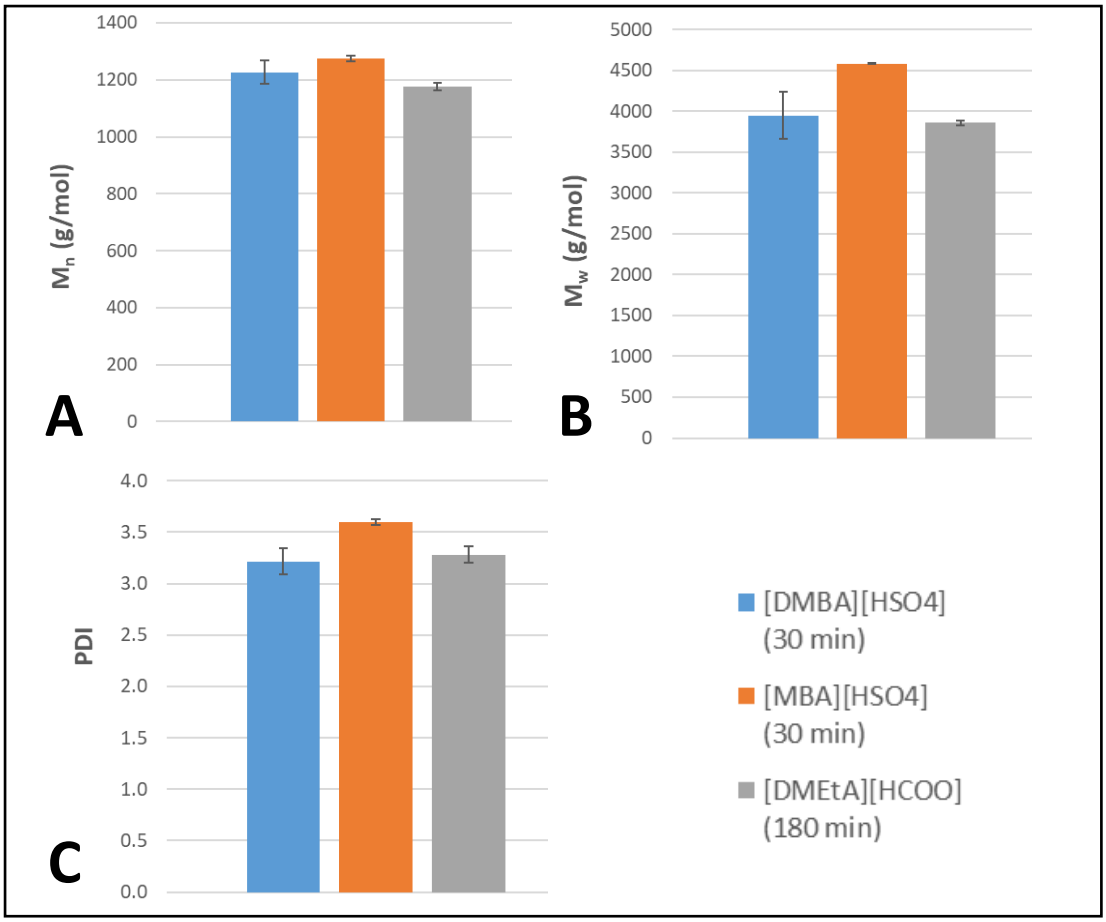


Figure 4.5: GPC analysis of recovered lignin following pretreatment with varying ionic liquids. Plots are A: Number-averaged molecular mass, B: Weight-averaged molecular mass, C: Polydispersity Index (PDI). All pretreatments were carried out on Batch 1 of *Phragmites australis* (as defined in Table 4.1) at 150 °C, with 20 wt% water, and at a biomass loading of 10% wt/wt.

2D HSQC NMR was performed on recovered lignin from pretreatments with [MBA][HSO_4] and [DMEtA][HCOO] for 60 minutes, with integration data and side-chain spectra shown in Figs. 4.6 and 4.7. The aromatic region spectrum is provided in the Appendix. Volume integrals were normalised to the sum of the G_2 and $G_{2\ cond}$ signals, which has been shown to remain fairly constant during pretreatment of *Miscanthus*, another grassy biomass.[21] The main subunits identified in the side-chain region were β-*O*-4' ether (A), β-β' resinol (B), and β-5' phenylcoumaran (C). In the aromatic region, these were uncondensed and condensed syringyl ($S_{2,6}$ and S_{cond}), oxidised syringyl ($S'_{2,6}$), uncondensed and condensed guaiacyl (G_2, G_5, G_6, $G_{2\ cond}$), *p*-coumaric acid ($PCA_{2,6}$, PCA_β), ferulate (FA_8, FA_6, FA_β), *p*-hydroxyphenyl ($H_{2,6}$), and tricin ($T'_{2,6}$, T_3, T_6, T_8). Using [MBA] [HSO_4], signals at 7.7/128, 7.7/131, and 4.1/67 were assigned to leaching of the plasticiser DEHP from pressure tube seals and labelled as "PL", as in previous work.[34] No such peaks were observed using [DMEtA][HCOO], presumed to be due to its lower acidity.

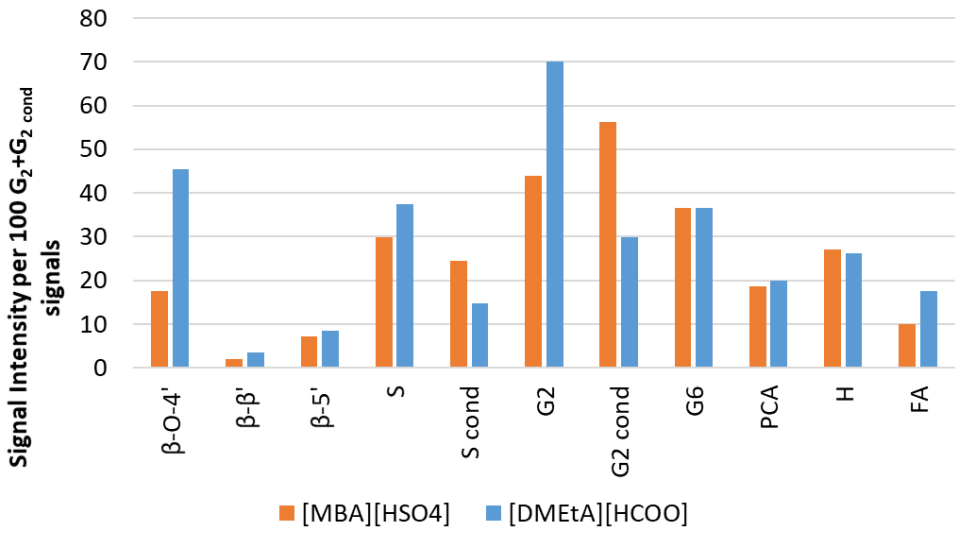


Figure 4.6: Relative abundance of structural units of recovered lignin following pretreatment with varying ionic liquids, as determined by HSQC NMR spectroscopy. Pretreatments were carried out on Batch 1 of *Phragmites australis* (as defined in Table 4.1) at 150 °C for 60 minutes, with 20 wt% water, and at a biomass loading of 10% wt/wt.

There is a large number of peaks using [DMEtA][HCOO] that are thought to correspond to carbohydrate material based on the literature (marked Ara_5 and $Xyl_{2\text{-}5}$, but which have not been exactly assigned due to the large number of unknown peaks).[21,25,26] These carbohydrate peaks are much more abundant in lignin recovered using [DMEtA][HCOO] than [MBA][HSO_4], implying a more significant carbohydrate content that would require removal for further lignin utilisation. Lignin recovered using [DMEtA][HCOO] also has a substantially larger number of β-*O*-4' linkages still present compared to that using [MBA][HSO_4]. The relative abundance of β-β' and β-5' linkages, however, is only slightly higher in [DMEtA][HCOO]. Using $[HSO_4]^-$ ILs, the ionoSolv process has been shown to remove lignin by extensively cleaving β-*O*-4' linkages, with much lower decreases in β-β' and β-5' linkages.[21,41] In the work of Weigand et al, after 60 minutes of pretreatment at 150 °C using [TEA][HSO_4] with 2% excess acid, the β-*O*-4' bond integral had decreased by around a factor of 2.5 relative to a more native-like lignin from a much milder pretreatment (30 minutes at 120 °C).[41] Lignin extracted from *Miscanthus* after 60 minutes of pretreatment at 150 °C was shown to have a β-*O*-4' bond integral around 2.5 times smaller when using [MBA][HSO_4] than [DMBA][HSO_4] (see Chapter 2). [MBA][HSO_4] is significantly more acidic than [TEA][HSO_4], which has a similar acidity to [DMBA][HSO_4]. It is thus likely that there has still been substantial β-*O*-4' bond cleavage using [DMEtA][HCOO], as its β-*O*-4' integral is also around 2.5 times higher than that of [MBA][HSO_4]. However, comparison with more native lignin (i.e. milled wood lignin) should be carried out to better

quantify the degree of β-*O*-4' bond cleavage using [DMEtA][HCOO], and thus determine more conclusively whether the same removal mechanism is involved for this class of ILs.

In the aromatic region (i.e. signals in the region (6.0-8.0)/(90-140), where the signals from the aromatic lignin sub-units are found), further differences are noted between both ILs, with spectra shown in Fig A4-1 in the Appendix. Pretreatment using [MBA][HSO_4] produces lignin with a substantially higher degree of condensation, as seen through integrals of $G_{2\ cond}$ and S_{cond}. The degree of condensation of G and S units was found to be 56% and 45% using [MBA][HSO_4], and 29% and 28% using [DMEtA][HCOO]. The lower degree of condensation using [DMEtA][HCOO], in addition to the lower degree of β-*O*-4' bond cleavage, further points towards the recovery of a more native-like lignin. The degree of condensation of lignins isolated using [DMEtA][HCOO] is still substantially higher than in lignins extracted using organosolv (wich can be below 10% [42]), but is comparable to that obtained using a hybrid ionosolv-organosolv pretreatment by Chen et al.[43] There were similar degrees of polymerisation of PCA units to H units in both ILs, which has been shown to occur using $[HSO_4]^-$ ILs in previous studies.[34,44] The S/G ratio of the extracted lignins was very similar: 0.54 and 0.52 using [MBA][HSO_4] and [DMEtA][HCOO] respectively, showing that both ILs are equally selective in their extraction. Ferulate signals were substantially higher in lignin extracted using [DMEtA][HCOO]. As ferulates are mostly attached to polysaccharides, this is consistent with observations from the side chain region.[25]

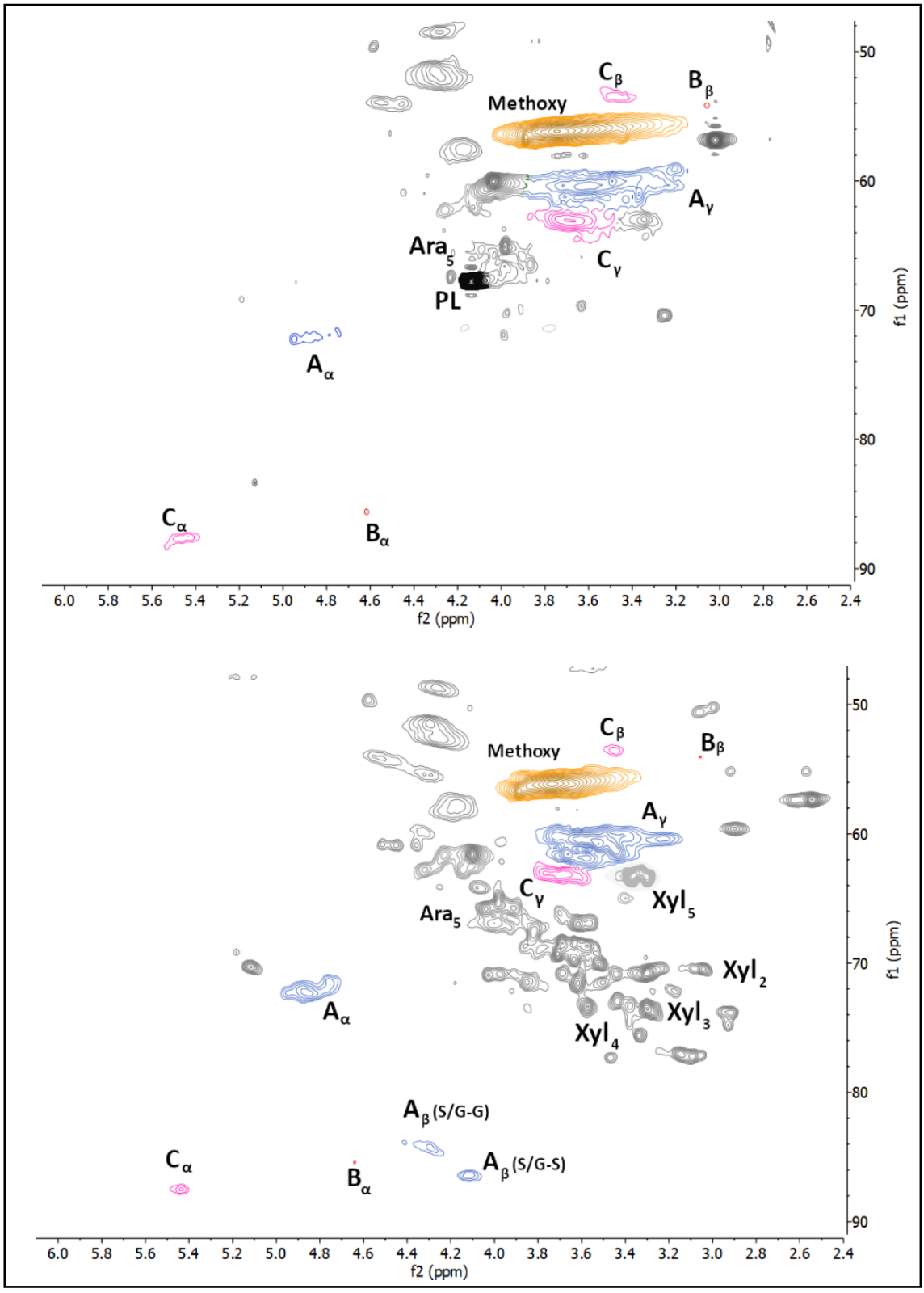


Figure 4.7: HSQC NMR spectra of recovered lignin following pretreatment with varying ionic liquids. Plots are Top: Using [MBA][HSO_4], Bottom: Using [DMEtA][HCOO]. Pretreatments were carried out on Batch 1 of *Phragmites australis* (as defined in Table 4.1) at 150 °C for 60 minutes, with 20 wt% water, and at a biomass loading of 10% wt/wt.

4.3.2 Pretreatment of Multiple *Phragmites Australis* Batches

Feedstock independence is a major consideration for a scaled-up biorefinery process. Before investigating different species, it was decided to use batches of *Phragmites australis* from wetlands treating different effluents, to determine whether the wetland application had any effect on performance. Batches 2 and 3 of *Phragmites australis* were pretreated at 150 °C using [DMBA][HSO_4]. As shown in Table 4.1, these batches originated from different applications: batch 2 from a constructed wetland treating domestic wastewater, and batch 3 from a constructed wetland treating Acid Mine Drainage (AMD). Pretreatment results are shown in Fig. 4.8, while Fig. 4.9 compares several important pretreatment indicators for all three batches.

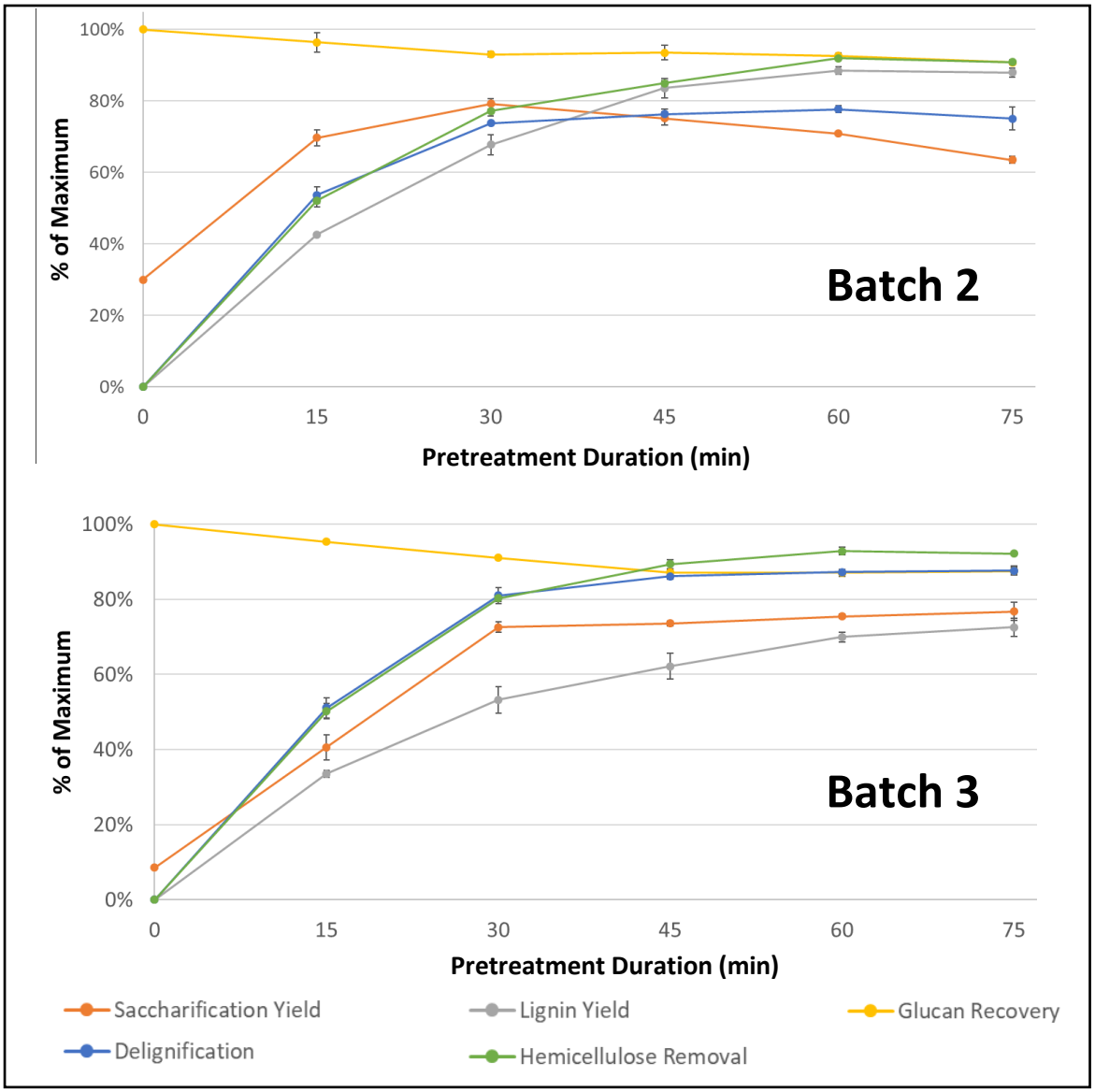


Figure 4.8: Pretreatment performance of two *Phragmites australis* batches. Batches are indicated on each plot, as defined in Table 4.1. All pretreatments were carried out using [DMBA][HSO_4] at 150 °C, with 20 wt% water, and at a biomass loading of 10% wt/wt.

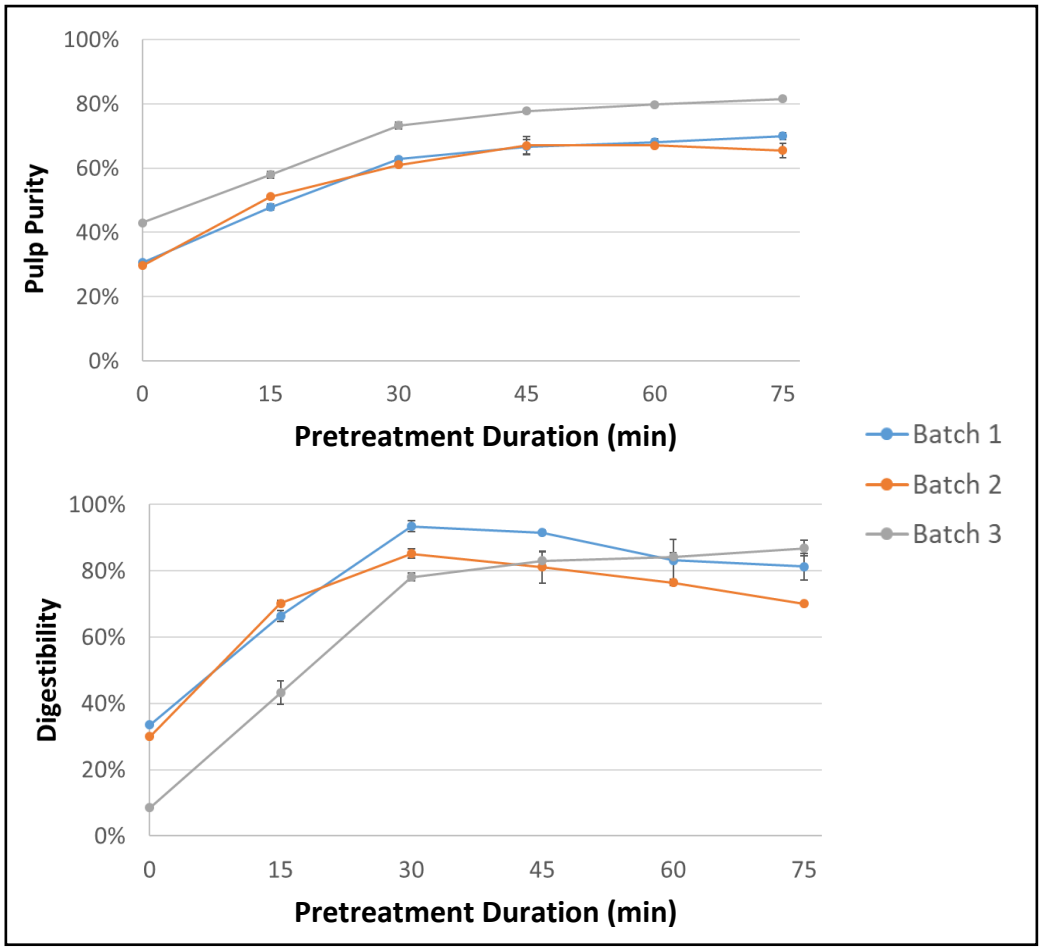


Figure 4.9: Key pretreatment indicators of three *Phragmites australis* batches. Batches are defined in Table 4.1. All pretreatments were carried out using [DMBA][HSO_4] at 150 °C, with 20 wt water, and at a biomass loading of 10% wt/wt.

Batch and batch 1 were being harvested from different locations treating different types of effluent, but show similar pretreatment behaviour. This is somewhat expected, as both batches were harvested at a similar time (see Table 1), contained significant amounts of green leaf material, and had a similar chemical composition (see Appendix). Both batches display high lignin yields which exceed delignification, along with a reduction in saccharification yields and plateauing delignification after 30 minutes, implying redeposition of lignin and pseudolignin. Additionally, more general signs of pretreatment with tertiary alkylammonium $[HSO_4]^-$ ILs can be seen, such as slowly increasing glucan losses, and high levels of hemicellulose removal. Batch 3 was harvested significantly later, during the senescence period, and was composed of mainly shoot material, with the little visible leaf material showing complete discolouration. Its composition is also very different (see Appendix), with a significantly higher glucan content and lower extractives content, as well as a slightly higher lignin

content. This composition is more similar to that of *Miscanthus* (see Appendix), as is its pretreatment behaviour (see Chapter 2). In particular, saccharification yields remain fairly constant above 30 minutes, while lignin yields do not exceed delignification. Additionally, peak delignification (88%) is significantly higher than in batches 1 and 2. These differences in behaviour may be due to a lack of substantial pseudolignin formation, as a result of the much lower extractives content (7.7%). Batches 1 and 2 show much higher digestibility of untreated biomass (30% and 33%) compared to batch 3 (9%) and to other feedstocks such as *Miscanthus* (4%) or sugarcane bagasse (13%).[45] This may be due to the significant leaf material in these feedstocks, which has been shown to be more easily hydrolysable than shoot material in switchgrass after hydrothermal pretreatment.[46] Batch 3 pulps also show higher pulp purities than batches 2 and 3. This may be due to a significant non-lignocellulosic fraction present in pulps from batches 1 and 2, which is further explored in Section 4.3.5.

Overall, it would appear that differences in pretreatment between all 3 batches are primarily due to differences in composition arising from harvest date, rather than from differences in application. Possibly due to its harvest during the senescence period, batch 3 showed a much lower extractives content, with higher glucan and lignin contents, leading to lower pseudolignin formation. However, it can be concluded that the ionoSolv process can successfully pretreat different *Phragmites australis* feedstocks, with large improvements in pulp purity, digestibility, and saccharification yields. While significantly lower than using *Miscanthus*, cellulose purity of around 70-80% is similar to that achieved in the ionoSolv process using other feedstocks such as pine or willow[47,48], as well as to that achieved through Kraft pulping.[49–51] This purity could be enhanced through further processing (e.g. water extraction as in Section 4.3.5, or bleaching). Pretreatment durations of 30 and 45 minutes were identified as promising conditions for achieving high pulp purity, saccharification, and digestibility at short durations.

The lignin recovered from batches 2 and 3 was analysed by GPC, with results shown in Figs. 4.10 and 4.11. Batches 1 and 2 show similar values of M_w, M_n, and PDI at 30 and 45 minutes. While there are small differences in apparent trends for M_n and PDI between 30 and 45 minutes, these were found to not be statistically significant. More significant differences are seen in the molecular weight profiles. At 30 minutes, batches 1 and 2 both have three similar molecular weight peaks: around 400 g/mol, 750 g/mol, and 3200-3800 g/mol. However, unlike batch 1, batch 2 also includes a fourth low-molecular weight peak around 120 g/mol. Between 30 and 45 minutes, the profiles change and become more similar: the peak at 750 g/mol flattens out slightly in both batches, and the lowest molecular weight peak in batch 2 reduces substantially in size. Batch 3 has higher molecular weight lignin, particularly after 30 minutes, and has a very different molecular weight distribution to both other batches, with a single broad peak around 2500 g/mol. Between 30 and 45 minutes, this peak

shifts slightly to lower molecular weights, with M_w remaining high while M_n decreases substantially and PDI increases. This is in close agreement with stage 2 of Gschwend et al's proposed 4-stage model of lignin removal in *Miscanthus*, in which dissolved lignin fragments are further depolymerised by the ionic liquid.[44] These results show a feedstock dependence of the recovered lignin's molecular weight distribution, even within a single species, which could have implications for potential applications.

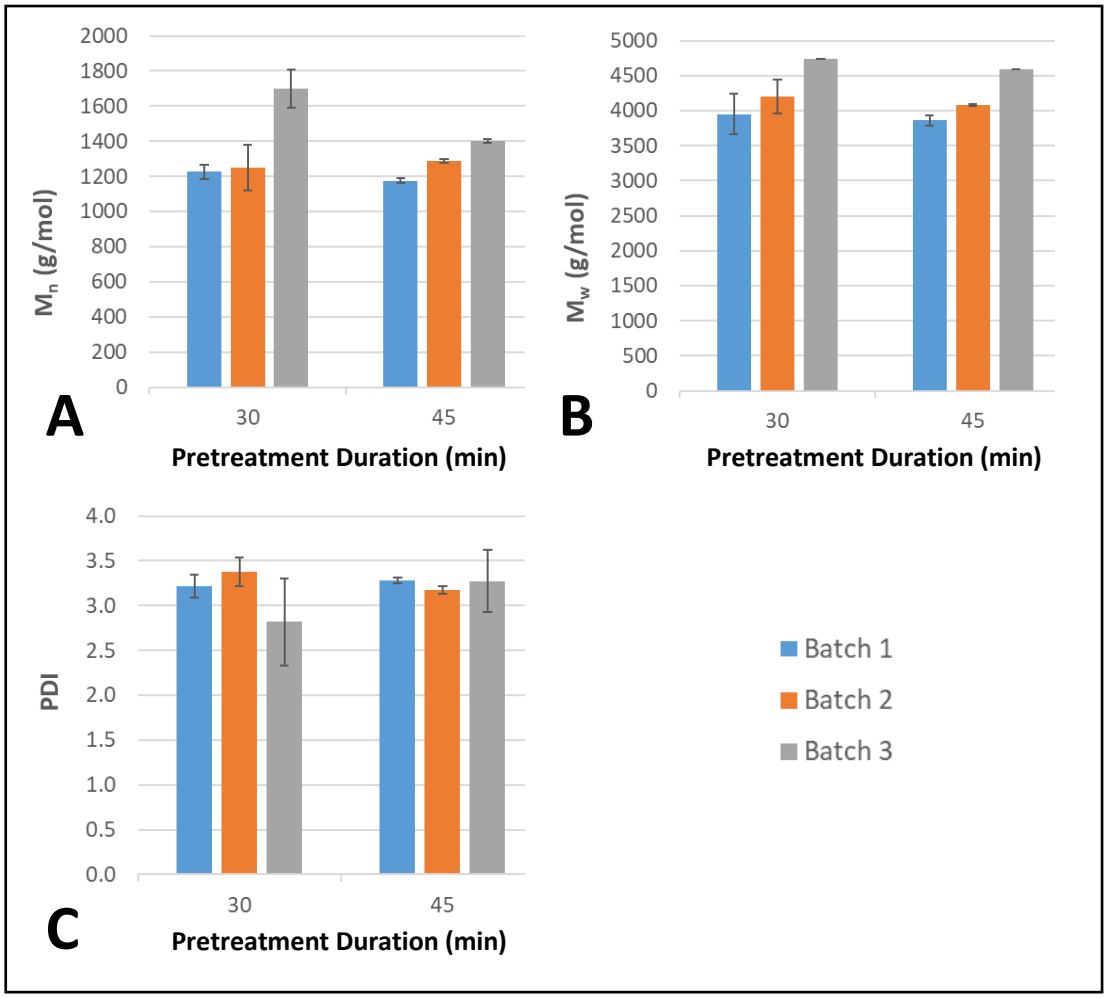


Figure 4.10: GPC analysis of recovered lignin from three *Phragmites australis* batches following pretreatment with [DMBA][HSO_4]. Plots are A: Number-averaged molecular mass, B: Weight-averaged molecular mass, C: Polydispersity Index (PDI). Batches are defined in Table 4.1. All pretreatments were carried out at 150 °C, with 20 wt% water, and at a biomass loading of 10% wt/wt.

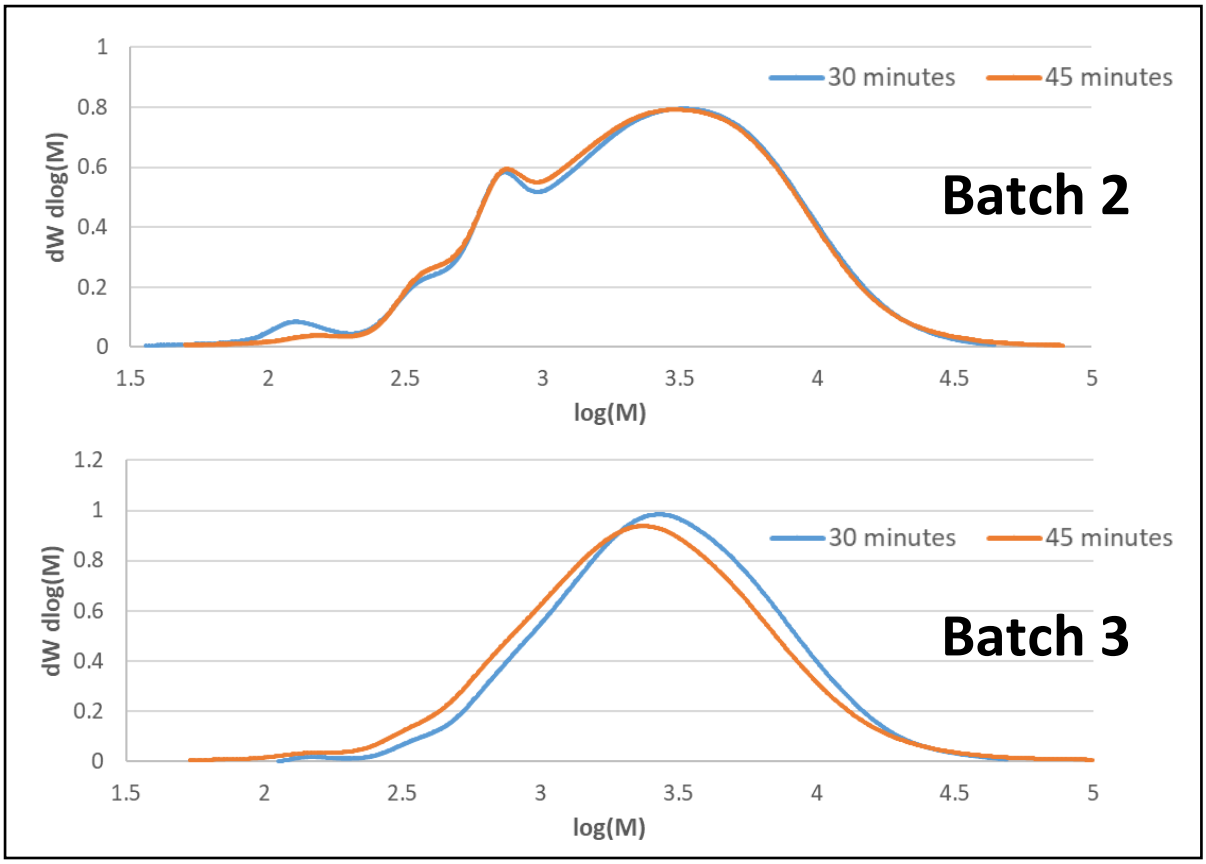


Figure 4.11: Molecular weight profiles of recovered lignin from different *Phragmites australis* batches following pretreatment with [DMBA][HSO_4]. Batches are indicated on each plot, as defined in Table 4.1. All pretreatments were carried out at 150 °C, with 20 wt% water, and at a biomass loading of 10% wt/wt.

4.3.3 Pretreatment of Common Constructed Wetland Species

Phragmites australis is a high-yielding, widely available species which is the focus of the majority of wetland remediation studies. However, feedstock independence is a key aspect for a process aiming to utilise constructed wetland biomass on a large scale. There are a large number of other common wetland species that have been used as part of constructed wetland remediation studies, and which may naturally populate constructed wetlands. For example, in CWs in China over 70 different species were found to have been used.[52] Following the identification of operating points for *Phragmites australis*, 8 other feedstocks (covering 7 species) were investigated for use in the ionoSolv process. They are listed in Table 4.1, with their composition data provided in the Appendix. These species were pretreated using [DMBA][HSO_4] for 30 and 45 minutes. Several indicators of pretreatment efficacy are displayed in Fig. 4.12, with further indicators included in the Appendix.

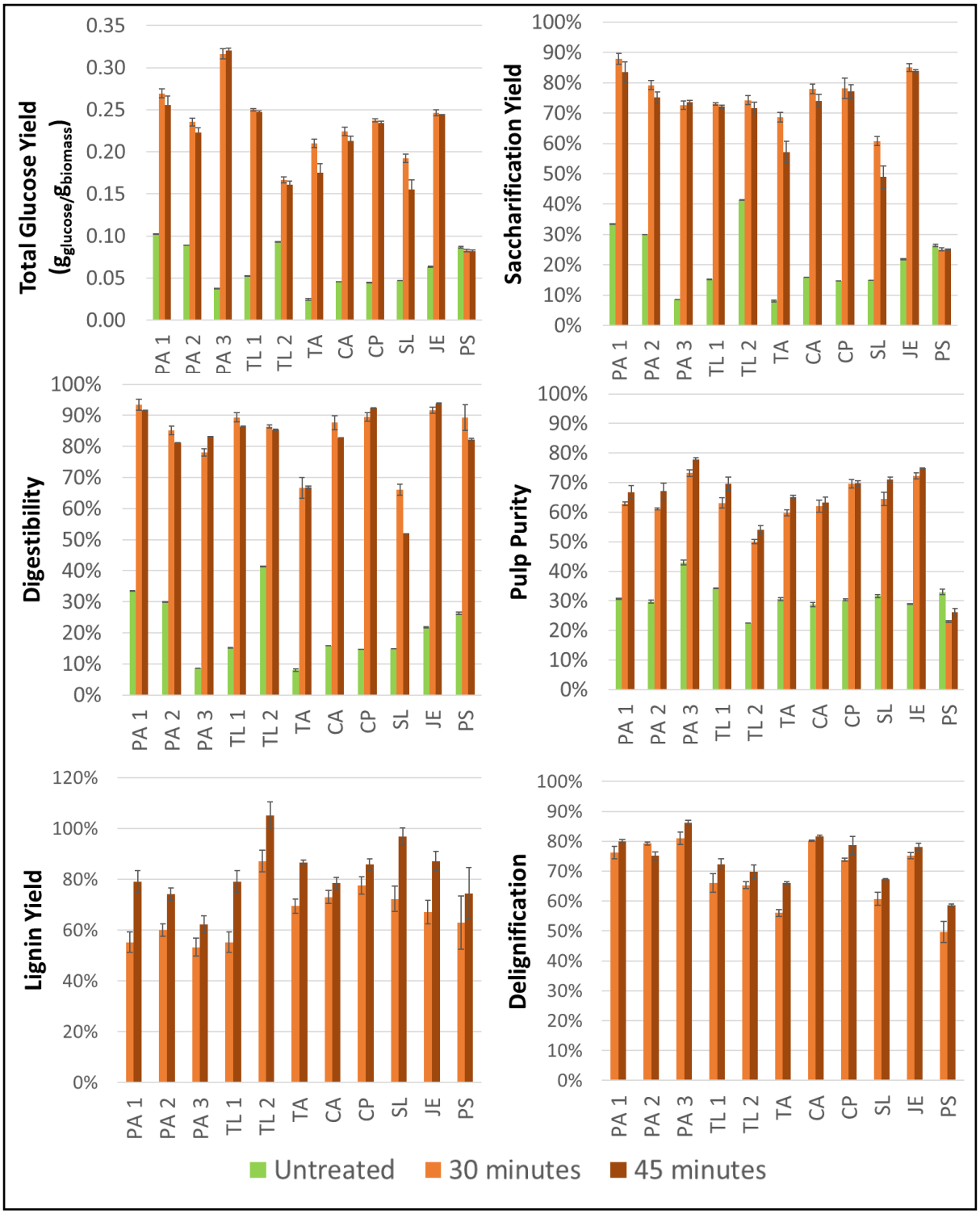


Figure 4.12: Key pretreatment indicators of 11 wetland feedstocks. Species abbreviations are provided in Table 4.1. All pretreatments were carried out using [DMBA][HSO_4] at 150 °C, with 20 wt% water, and at a biomass loading of 10% wt/wt.

The composition of the wetland feedstocks was found to be fairly similar, with most glucan contents ranging from 25-35%, hemicellulose contents from 19-25%, lignin contents from 17-22%, and extractives contents from 18-26%. Full composition data is provided in the Appendix. Both lignin and glucan contents are slightly lower than feedstocks previously studied in the ionoSolv process (which contained around 35-45% glucan and 20-30% lignin), while extractives contents are significantly higher (compared to around 5-10%).[45,47,48] There were substantial differences in pretreatment results among the different feedstocks for several indicators. However, for all species except *Pistia stratiotes*, pretreatment using [DMBA][HSO_4] significantly improved pulp digestibility, pulp purity, and saccharification yield relative to the untreated biomass.

Excluding *Pistia stratiotes*, glucan degradation ranged from 6-19% after 45 minutes (data not shown), with the majority below 13%. Although some of these values are larger than typically observed during the ionoSolv process, the rate of increase between 30 and 45 minutes is fairly low (degradation values at 30 minutes ranges from 5-19%). This implies rapid early hydrolysis of amorphous cellulose, glucan in hemicellulose, and possibly of starch, during the pretreatment, followed by slow hydrolysis of the more stable crystalline cellulose. Expectedly, high hemicellulose removal rates were seen across all feedstocks, ranging from 83-94% after 45 minutes excluding *Pistia stratiotes* (data shown in the Appendix). Larger variations were seen in lignin yield and delignification rates. After 45 minutes, lignin yields ranged from 62-105% while delignification ranged from 66-86% (excluding *Pistia straiotes* at 59%). The large variation in lignin yields may again be explained by the rapid formation of pseudolignin due to a high extractives content. A strong correlation was found between the untreated biomass extractive content and lignin yield ($r = 0.84$, $p < 0.01$), as well as between the original extractive content and the ratio of lignin yield to delignification ($r = 0.70$, $p < 0.05$). No statistically significant correlations, however, were found explaining the variation in delignification rates. These could be due to different physical characteristics of the biomass (e.g. pore volume), or chemical characteristics of the lignin (e.g. S/G ratio).

Digestibility in untreated material was generally around 10-20%, higher than most lignocellulosic feedstocks, and attributed to the relatively low lignin contents. For untreated material, digestibility was found to be strongly inversely correlated to lignin content ($r = -0.73$, $p < 0.01$), with no significant correlation to the ratio of glucan to lignin. Following pretreatment, digestibility increased to over 80% for the majority of feedstocks, leading to saccharification yields generally above 70%. However, the correlation between lignin content and digestibility became significantly weaker following pretreatment ($r = -0.47$, $p < 0.05$), possibly implying the presence of smaller amounts of more saccharification-inhibiting redeposited lignin and pseudolignin. For most species, pulp digestibility and saccharification yield decreased between 30 and 45 minutes, with only *Carex pendula* and *Phragmites*

australis batch 3 showing an increase in both values. A pretreatment time of 30 minutes therefore seems the most suitable operating point for pretreatment of wetland feedstocks targeting sugar release for bioethanol production. At this duration, only *Pistia stratiotes* and *Scirpus lacustris* had saccharification yields far below 70%. When considering feedstock independence, consistent total glucose release from a range of feedstocks is also critical. As seen in Fig. 12, the majority of feedstocks released around 20-25 wt% of glucose following pretreatment, relative to the starting biomass.

Pulp purity increased in all species between 30 and 45 minutes, with 45 minutes thus taken to be a suitable operating point for a pretreatment targeting pulp purity over glucan release. At this duration, the majority of pulp purities range from 63% to 75%, with only *Pistia stratiotes* and batch 2 of *Typha latifolia* below this. While significantly higher than glucan contents in the untreated biomass, pulp purities are not as high as those obtained in the ionoSolv process using other feedstocks (more typically 70-80%). This may be due to the substantial fraction of unaccounted, non-lignocellulosic material in the pulps (later explored in Section 4.3.5), which ranged from 0% in batch 3 of *Phragmites australis* to 29% in batch 2 of *Typha Latifolia*. The unaccounted proportion of the pulp was found to be highly correlated with the extractives content of the untreated biomass ($r = 0.84$, $p < 0.01$), and highly inversely correlated with the pulp purity ($r = -0.91$, $p < 0.01$). Additionally, the extractives content of the untreated biomass was found to be strongly inversely correlated with pulp purity ($r = -0.78$, $p < 0.01$). As seen in Section 4.3.5 when pretreating mixed wetland feedstocks, this unaccounted fraction was found to be removed by water Soxhlet extraction of the pulp. Assuming the unaccounted fraction of each species would similarly be removed by hot water extraction following pretreatment, pulp purities would be raised to 72-83% (excluding *Pistia stratiotes* but including batch 2 of *Typha latifolia*), when normalised to the unaccounted-free mass fraction.

There is a significant difference in composition between batches 1 and 2 of *Typha latifolia*, which were harvested at different stages of growth. Batch 1 contained large quantities of more woody shoot material as it was harvested towards the end of its growth cycle (in October), whereas batch 2 was herbaceous as it was harvested several months earlier in the growing period (May). As a result, batch 1 had a much higher glucan content (34% vs. 23%) as well as higher hemicellulose and lignin contents (26% vs 20%, and 19% vs 14% respectively). Batch 2, however, had a much higher extractives content (37% vs. 19%), the highest of all feedstocks investigated. The poor pulp purity of *Typha latifolia* batch 2 is thus due to the high extractives content in the pulp, due in turn to the very high extractives content of the untreated biomass. However, when normalised to the extractive-free content, both batches yield pulps of similar purity (80% and 76% for batches 1 and 2 respectively). In addition, both batches perform similarly in saccharification and digestibility metrics. The largest difference arises in the total glucose release per unit mass of biomass, due to the much lower glucan content in the untreated

biomass of batch 2. Similar results are observed with batches 1-3 of *Phragmites australis*. When normalised to an extractive-free basis, pulp purities are comparable (72%, 74%, and 78%), while total glucose release is significantly higher in batch 3, which was harvested latest and has the highest glucan content. However, compared to *Typha latifolia*, saccharification yields between batches show relatively large differences, even between batches 1 and 2.

The effect of different annual harvest frequencies in wetlands has been investigated in several studies.[53–59] Regarding total achievable biomass yield, conflicting results have been reported, suggested to be due to different locations and climates.[54–56] In general, however, it would appear that total biomass yields do not increase substantially through several harvests. Biomass harvested later in the growing cycle (i.e. from a single late harvest) also contains a higher proportion of fibrous stem material, which is more suitable for biofuel and cellulose production, as seen in this study.[54,55,57,60] Furthermore, multiple harvests lead to additional cost and can damage crop health if not properly managed.[1,54,56,58,61] Therefore, unless wetland feedstock extractives are valorised, single annual harvests would appear to be optimal for both wetland health and for feedstock quality. Further work should be carried out, however, to more conclusively ascertain whether wetland biomass yields can be improved through multiple harvests, and whether this benefit would be counterbalanced by a reduction in feedstock quality.[60]

Pistia stratiotes was the only species to show significantly different behaviour across several of the pretreatment metrics. As well as low saccharification yields, pulps had very low purities (around 25%) and glucan recoveries (around 30%), but with high digestibilities (> 80%). These results are not typical of the ionoSolv process, as exemplified by the other feedstocks in this study. This feedstock is herbaceous and has a very low lignin content (11%) compared to better studied feedstocks such as *Miscanthus*, sugarcane bagasse, pine, and even compared to the low-lignin wetland feedstocks in this study. Untreated *Pistia stratiotes* showed atypically large mass losses during the standard NREL compositional analysis protocol (see Appendix). These mass losses imply that there is a significant component that cannot be detected during the compositional analysis, in addition to the very high extractives content (32%) which is removed beforehand. These components are thus not soluble in water and ethanol, but are soluble in aqueous acid as they are not contained in the acid-insoluble residue. These could be acid-soluble proteins or inorganic compounds, among others. This mass loss, in conjunction with the very high extractives content, implies the overall structure of *Pistia stratiotes* may thus be substantially different to that of lignocellulose, explaining the difference in behaviour. The low glucan recoveries may be explained by a high content of amorphous cellulose or starch, which are easily hydrolysable during saccharification but degraded by the acidic $[HSO_4]^-$ ILs. This is corroborated by the fact that, while high, there is very little change in glucan degradation between 30

and 45 minutes, implying that all easily hydrolysable material has already been degraded. There has only been one study into the chemical composition of *Pistia stratiotes*, which gave a starch content of 6.4% and a cellulose content of 16.5%.[62] However, starch content may be sensitive to growth conditions, as in *Lemna* species, a genus of floating aquatic plants for which starch contents of 3-75% have been reported.[63–67] Pulp digestibility increases considerably following pretreatment, despite no substantial change in glucan or lignin content. This shows that a pretreatment step is still required to disrupt the structure of *Pistia stratiotes* and efficiently recover sugars. Further work should therefore be carried out on a milder IL pretreatment of this species, as it remains a promising species for water remediation due to its high growth rate and nutrient and metal uptake capabilities.[68–71] A pretreatment using a hemicellulose-preserving IL, such as [DMEtA][HCOO] or [MEA][OAc], may be appropriate for this feedstock.

4.3.4 Mixed Feedstock Recycling Pretreatment 1

A mixed wetland feedstock was prepared by mixing 9 of the tested feedstocks (all except *Pistia stratiotes* and batch 2 of *Typha latifolia*), encompassing 7 species. The content of each feedstock ranged from 5-13 wt%, with the mixed feedstock composition provided in the Appendix. This mixed feedstock was pretreated at 150 °C for 30 minutes using [MBA][HSO_4], and for 30 and 45 minutes using [DMBA][HSO_4] in a recycling experiment with 5 cycles. Pretreatment using [DMBA][HSO_4] for 30 and 45 minutes are referred to as [DMBA][HSO_4]$_{30\ min}$ and [DMBA][HSO_4]$_{45\ min}$ respectively. After each pretreatment, following lignin precipitation, water was removed from the IL under reduced pressure, and the IL was recovered and reused in the following cycle. After the 4th cycle, the acid/base ratio of the liquor was determined, and the amount of acid required to restore the ratio to 1.00 was calculated and added before the 5th cycle. Pretreatment results are shown in Fig. 4.14.

Cycle 1 was performed using fresh ILs. When using [DMBA][HSO_4], results of the mixed feedstock were compared to the arithmetic mean of the constituent species, as shown in Fig. 4.13. Differences between obtained and predicted values were found to be fairly small, showing no significant synergy or anti-synergy by mixing species. Across most indicators, mixed feedstock results matched predicted values within one standard deviation, and generally to within 2%. Only delignification rates were more than one standard deviation from the predicted value, being 4% and 2% lower after 30 and 45 minutes of pretreatment respectively.

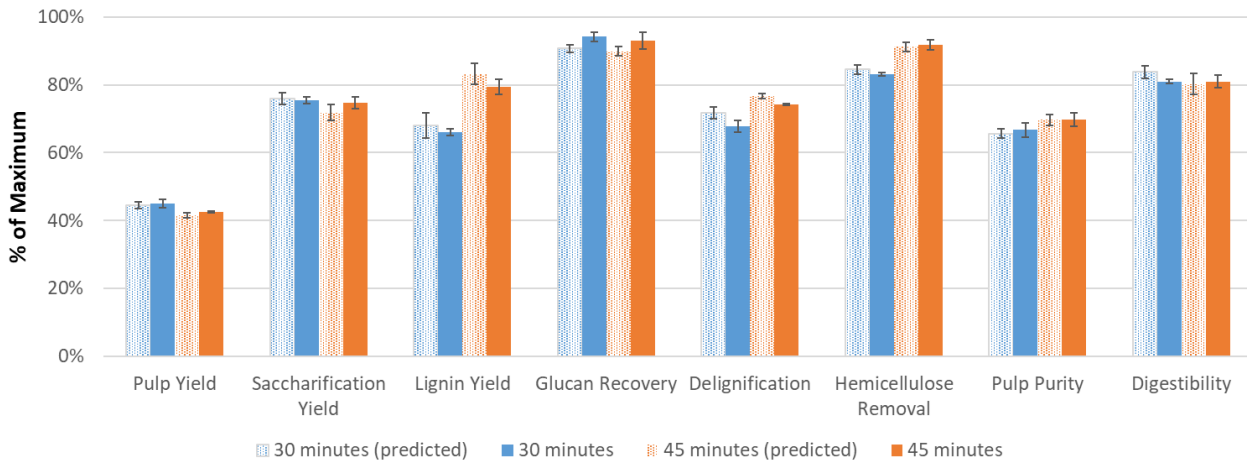


Figure 4.13: Predicted vs. actual pretreatment indicators for a mixed wetland feedstock. Pretreatments were carried out using [DMBA][HSO_4] at 150 °C, with 20 wt% water, and at a biomass loading of 10% wt/wt.

Ionic liquid recovery was calculated on a dry IL basis, and taking into account the mass fraction of the dissolved sugars and sugar degradation products. IL recovery trends were the same for all three conditions, beginning at 102% in cycle 1, and then remaining between 99% and 100% with no statistically significant trends. These values are similarly high to those of Brandt-Talbot et al. when conducting recycling experiments, using [TEA][HSO_4] to pretreat *Miscanthus*.[34] This is promising, considering Baral et al. estimated 97% as a minimum target for IL biorefinery using ILs of similar costs to alkylammonium [HSO_4]$^-$ ILs.[72] Recoveries after the first cycle were 102%, with the increase in mass attributed to lignin and extractives that remained dissolved in solution following lignin precipitation. This is corroborated by trends in lignin yields. These increase substantially to above 100% after cycle 1, presumed to be due to lignin condensation reactions and formation of pseudolignin, accelerated by the higher level of dissolved lignin fragments, carbohydrate breakdown products, and extractives. Lignin yields remain between 120-140% using [DMBA][HSO_4]$_{45\ min}$ and [MBA][HSO_4]. At this point there appears to be a steady state, with no further accumulation of dissolved lignin or extractives: these are assumed to removed in the precipitated lignin phase due to condensation reactions with pre-dissolved material. Similar behaviour was observed in in the work of Brandt-Talbot et al. when recycling [TEA][HSO_4] in the pretreatment of *Miscanthus*, with the IL said to be "self-cleaning" (although lignin yields plateaued around 100% in their study, due to the low extractives content).[34] Lignin yields remained around 140% despite addition of acid in cycle 5, possibly due to solubility limits in the IL. Using [DMBA][HSO_4]$_{30\ min}$, lignin yields generally continued increasing between cycles 1 and 4. This slower increase in lignin yields relative to both other timepoints may be due to the less severe

pretreatment conditions, leading to less lignin condensation and pseudolignin formation. This would also lead to the dissolved material being of lower molecular weight and thus more liable to accumulate in solution more. Addition of acid between cycles 4 and 5 increased the severity of conditions, explaining the large increase in lignin yields (from 118% to 151%).

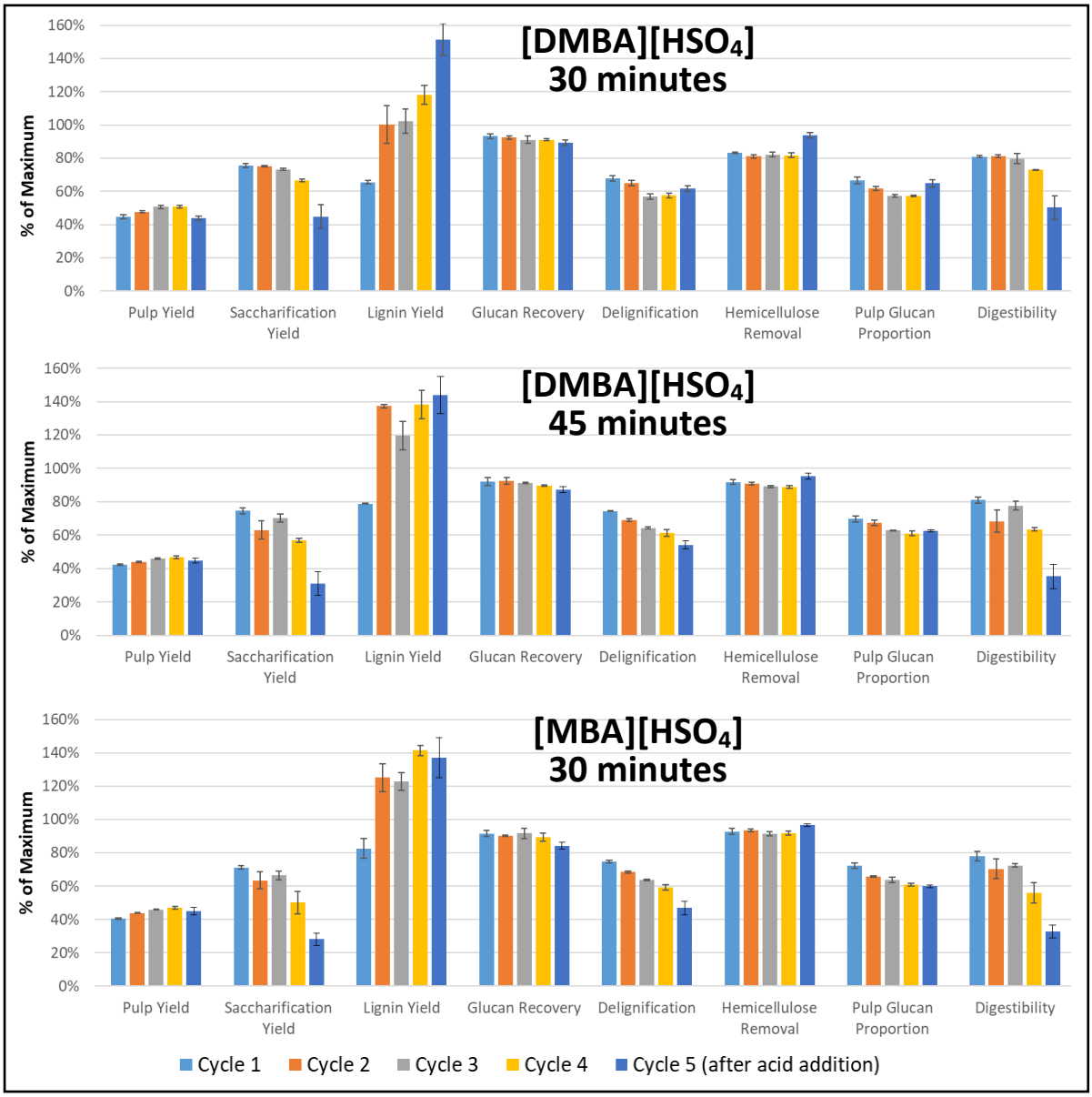


Figure 4.14: Pretreatment performance with IL recycling for a mixed wetland feedstock. Pretreament IL and duration are indicated on each plot. Pretreatments were carried out at 150 °C, with 20 wt% water, and at a biomass loading of 10% wt/wt.

Pretreatment performance was seen to decrease with each cycle between cycles 1 and 4. Pulp purity decreased by 9-11% for all three conditions, while saccharification yields dropped by 9-21% and

digestibility by 8-22%. Interestingly, decreases in pulp purity were fairly consistent across all three conditions, whereas decreases in digestibility were substantially lower using $[DMBA][HSO_4]_{30\ min}$, the least severe condition. This may indicate the formation of degradation products in solution at the more severe conditions, possibly due to dissolved lignin or extractives. The major factor affecting pulp purity was a drop in delignification. Between cycles 1 and 4, delignification decreased by 10% and 13% using $[DMBA][HSO_4]_{30\ min}$ and $[DMBA][HSO_4]_{45\ min}$, and by 16% using $[MBA][HSO_4]$ for 30 minutes. Although there were also minor overall decreases in glucan recovery (2%) and hemicellulose removal (1-3%), trends were found to not be statistically significant.

The pH of recycled IL (in a 1 wt% solution) has been found to increase with cycles, particularly at higher biomass loadings, implying that some acid reacts with the biomass during the pretreatment.[73] However, the mass of dissolved polysaccharide breakdown products was not taken into account in that analysis. Therefore, following cycle 4 the acid/base ratio of the recovered IL was measured. In order to accurately determine the acid/base ratio, the "pure IL" fraction of the recovered solution must be determined. It was assumed that the solution was comprised of water, dissolved polysaccharide breakdown products, and dissolved lignin, which were measured as detailed in the Section 4.2.5. Dissolved polysaccharide breakdown products were found to account for 2-4% of solution dry mass, while dissolved lignin was found to be below detectable levels. Under these assumptions, the ILs were determined to contain around 6% excess base at all three conditions. The mass of dissolved extractives was not accounted for due to a lack of quantitative analytical techniques, making this a maximum bound for excess base content. However, it was determined that a dissolved extractives content of 7.5-9.0% of solution dry mass would be required to account for all the apparent excess base. This would be equal to 81–96% of total extractive content from the biomass pretreated across all 4 cycles. While a certain proportion is expected to remain dissolved in solution, such levels of dissolved extractive material appear unlikely due to the high lignin yields observed, as well as the near-quantitative IL recoveries.

Excess base has been shown to significantly reduce delignification in previous studies, although not to the extent observed in this study. Using $[MBA][HSO_4]$ with 5% excess base to pretreat *Miscanthus* at 150 ^{o}C in Chapter 2, a 6% drop in delignification after 30 minutes of pretreatment was observed. However, in that study hemicellulose removal was also found to decrease by 11%, while glucan recovery increased by 2%. In order to restore pretreatment effectiveness, the required quantity of acid was added to increase the acid/base ratio back to 1.00 after cycle 4. From the results of cycle 5 it appears that this led to an excess of acid in the solution, implying that the determined acid/base ratio overestimated the quantity of excess base due to some level of dissolved extractives. The clearest sign of excess acid is the sharp increase in hemicellulose removal, reaching near-quantitative levels at all

conditions, and exceeding that of the first cycle by 4-11%. Another indicator of excess acid is a slight decrease in glucan recovery, dropping by 4-7% relative to the first cycle. Due to the excess acid, pretreatment performance was not restored to that of the first cycle. Using [DMBA][HSO_4]$_{45\ min}$ and [MBA][HSO_4], delignification reduced substantially, offsetting increases in hemicellulose removal. In the case of the former this led to a small increase in pulp purity, while for the latter pulp purity decreased further. Decreases in delignification were presumed to be due to the more severe conditions leading to more rapid pseudolignin formation and lignin condensation. Using [DMBA][HSO_4]$_{30\ min}$ led to improved performance relative to cycle 4. At the shorter pretreatment duration with this IL, an increase in severity increased delignification, although not to the levels of cycle 1. Although pulp purity increased close to that of cycle 1, it is evident that pretreatment performance was not restored as intended.

The pretreatment effectiveness of [MBA][HSO_4] at 30 minutes was very similar to that of [DMBA][HSO_4] for 45 minutes, as when pretreating batch 1 of *Phragmites australis*. [MBA][HSO_4] has previously been identified as a promising IL for the ionoSolv process, for which [DMBA][HSO_4] is a current gold standard, showing equally high performance at shorter reaction durations. This is as a result of its higher acidity, proposed to be due to the stronger ion interaction (see Chapter 2), leaving the $[HSO_4]^-$ anion less solvated and thus increasing its proton activity. The enhanced proton activity of the $[HSO_4]^-$ anion may explain why the effect of excess acid in cycle 5 appeared much more pronounced using [MBA][HSO_4] than [DMBA][HSO_4]$_{45\ min}$. Delignification decreased by 12% compared to 4% between cycles 4 and 5, while glucan recovery decreased by 5% compared to 2%.

The solute content of the IL was determined by HPLC both before and immediately after each pretreatment cycle. The solutes analysed for were polysaccharide degradation products, namely: glucose, xylose, arabinose, formic acid, acetic acid, levulinic acid, 5-hydroxymethylfurfural (HMF), and furfural. Results are shown in Figs. 4.15 and 4.16.

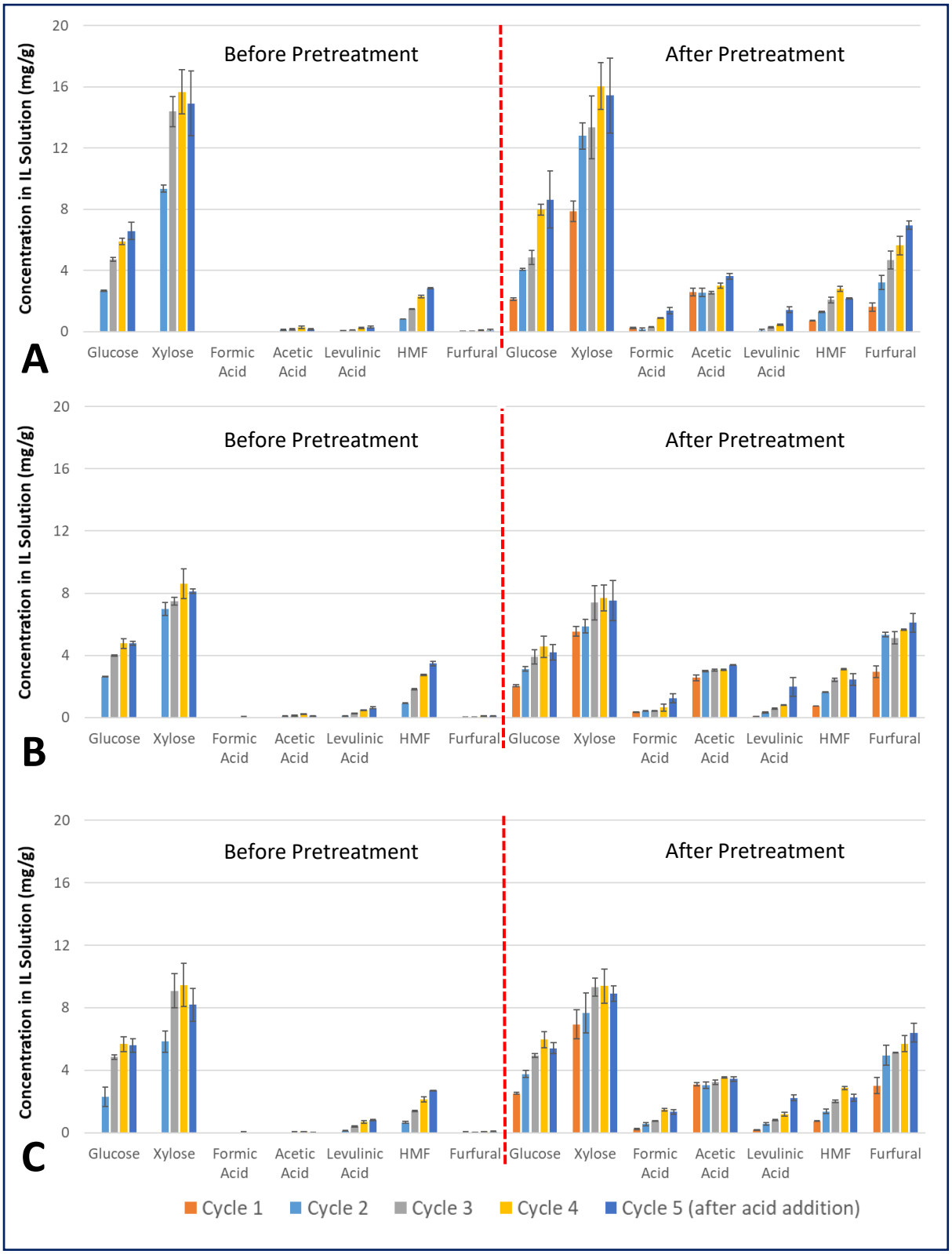


Figure 4.15: IL solution solute content with IL recycling before and after pretreatments of a mixed wetland feedstock. Plots are A: Using [DMBA][HSO_4] for 30 minutes, B: Using [DMBA][HSO_4] for 45 minutes, C: Using [MBA][HSO_4] for 30 minutes. IL solution contains 20 wt% water. Pretreatments were carried out at 150 ^oC, and at a biomass loading of 10% wt/wt.

Xylose is the most significant solute in the IL both before and after pretreatment due to the depolymerisation of hemicellulose. Under all three conditions, xylose concentrations in the IL increase quickly in the first two cycles before stabilising in the third cycle. This is presumably as the rate of degradation begins to approach the rate of solubilisation from the biomass during pretreatment. The xylose content after addition of acid remains relatively constant, despite higher solubilisation of hemicellulose sugars, implying a higher degradation rate. Glucose also accumulates in the IL solution, although at much lower levels. Glucose levels in $[DMBA][HSO_4]_{45\ min}$ and $[MBA][HSO_4]$ are similar and stabilise after cycle 3, whereas levels in $[DMBA][HSO_4]_{30\ min}$ are higher and carry on increasing over all 5 cycles (albeit at a decreasing rate). The reasons for this behaviour are assumed to be the same as for xylose: glucose levels will continue to increase until the rate of sugar degradation equals the rate of solubilisation. Glucose appeared more stable in solution than xylose. In the first pretreatment cycle it was found that, of the xylose removed from the biomass, 40% had degraded in solution during pretreatment using $[DMBA][HSO_4]_{30\ min}$, 64% using $[DMBA][HSO_4]_{45\ min}$, and 59% using $[MBA][HSO_4]$. Correspondingly, of the glucose removed from the biomass, 10% had degraded in solution during pretreatment using $[DMBA][HSO_4]_{30\ min}$, 26% using $[DMBA][HSO_4]_{45\ min}$, and 16% using $[MBA][HSO_4]$. This may, however, be due to the more rapid depolymerisation of hemicellulose meaning that xylose had a longer residence time in the IL solution than glucose. Both glucose and xylose concentrations remain fairly stable following pretreatment, indicating that there is no significant degradation of sugars in the IL at room temperature or at reduced pressure.

Furfural, formic acid, and acetic are all found in the IL following pretreatment. They do not accumulate in the IL, however, as they are volatile compounds and are mostly removed during the low-pressure evaporation of both water and ethanol. Formic acid and furfural are formed by the dehydration of sugars. Therefore, as sugars accumulate in the ILs, formic acid and furfural concentrations generally increase. Levels of both compounds are significantly higher in $[DMBA][HSO_4]_{45\ min}$ and $[MBA][HSO_4]$ than in $[DMBA][HSO_4]_{30\ min}$ during earlier cycles, as the more severe conditions degrade sugars faster. However, around cycle 4, similar levels of formic acid and furfural are seen in $[DMBA][HSO_4]_{30\ min}$ as sugars accumulate to higher concentrations. The increase in severity following addition of acid in cycle 5 generally leads to a notable increase in both compounds following pretreatment. The high levels of furfural, which must be removed during IL regeneration, may represent a valuable pretreatment by-product. However, furfural was also found by Tu to be important in the formation of pseudolignin when pretreating *Miscanthus*.[73] Acetic acid is released during hydrolysis of acetyl groups within the biomass hemicellulose. These acetyl groups account for 3.1% of the untreated biomass, and are fully removed from the biomass during pretreatment, as confirmed by compositional analysis on the pulps, and account for almost all the acetic acid present. The slight increase with cycle number may be due

to incomplete removal during low-pressure evaporation or the presence of non-hydrolysed acetyl groups remaining on hemicellulose oligomers. Trends for levulinic acid, another sugar degradation product, are very similar to those of furfural and formic acid. The main difference is that levulinic acid is a much less volatile compound, and therefore accumulates fairly consistently in the IL. In addition, the increase in levulinic acid arising from acid addition is much more marked, increasing by 87-216% from cycle 4 to cycle 5.

HMF is formed in solution by dehydration of glucose. Due to its low volatility, it is not removed under low-pressure, but can also degrade further, into levulinic acid and formic acid. Between cycles 1 and 4, HMF formation outweighs degradation, and concentrations increase relatively evenly under all three conditions. However, addition of acid appears to catalyse the HMF degradation, with levels decreasing substantially in the last cycle. HMF is a high-value chemical that has attracted attention as a possible bio-renewable platform chemical. Further studies should be carried out to determine the maximum accumulation level, and to thus determine whether it may be valorised in the ionoSolv process.

Total solute content (shown in Fig. 4.16) in the recovered IL increases between cycles 1 and 3, and appears to start levelling off between cycles 3 and 4. This may be due to an equilibrium arising, whereby new solutes dissolving into solution during pretreatment are counterbalanced by solute degradation and incorporation into pseudolignin during pretreatment. Total solute content of [MBA][HSO_4] and [DMBA][HSO_4]$_{45\ min}$ is fairly similar. This is somewhat expected due to their comparable degrees of hemicellulose removal and glucan degradation, implying similar degrees of severity. [DMBA][HSO_4]$_{30\ min}$, however, displayed significantly higher total solute content despite lower levels of glucan degradation and hemicellulose removal. This is thought to be due to a lower rate of solute degradation and incorporation into pseudolignin, due to the lower pretreatment severity. Following addition of acid, there appears to be a decrease in solute concentration in both [MBA][HSO_4] and [DMBA][HSO_4]$_{45\ min}$, and an increase in [DMBA][HSO_4]$_{30\ min}$. These could be explained by the increased rate of solute degradation and solubilisation respectively, due to the increase in pretreatment severity. However, the trends between cycles 4 and 5 were found not to be statistically significant.

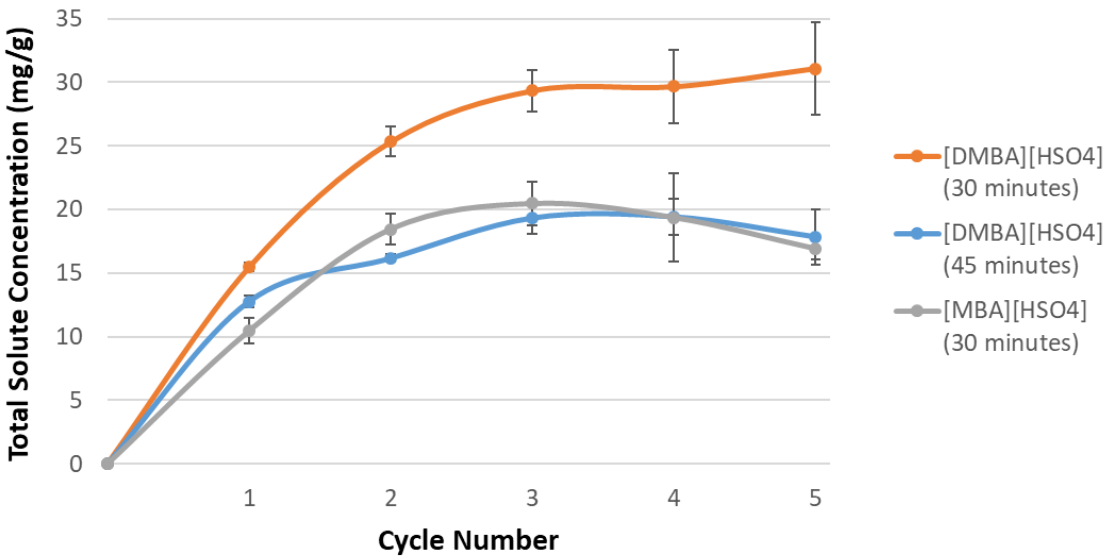


Figure 4.16: Total solute content of recovered IL solution following pretreatments with IL recycling. IL solution contains 20 wt% water.

4.3.5 Pulp Mass Balance Closure

As previously stated, the vast majority of pretreated pulps from wetland species contained a significant undetectable mass fraction during compositional analysis, with the size of this fraction strongly correlated with the untreated biomass extractive content. The NREL compositional analysis protocol recommends performing both ethanol and water Soxhlet extractions before analysis, to remove any non-lignocellulosic material. Although pulps are washed with ethanol using a Soxhlet extractor during the bench-scale ionoSolv process, this is to remove residual IL and dissolved lignin. It normally is assumed than any organic-extractable and water-extractable material is solubilised into the IL during pretreatment. This is corroborated by quantitative mass closures during compositional analysis of pretreated pulps. In this study, only two sets of pulps were found to have 100% mass closures following pretreatment: all pulps from batch 3 of *Phragmites australis* (which had a significantly lower extractives content than other feedstocks), and pulps from batch 1 of *Phragmites australis* when pretreated with [DMEtA][HCOO].

An unaccounted fraction of 12-16% was observed using the mixed wetland feedstock during the first recycling experiment, across all five cycles and under all three conditions. The first cycle was repeated, using [DMBA][HSO_4] for 45 minutes, with a water Soxhlet extraction following the ethanol Soxhlet extraction. The water extraction was found to remove 16% of pulp mass, with the ensuing compositional analysis having a quantitative mass closure. This had the added benefit of effectively raising pulp purity from 70% to 80%. Water was removed under reduced pressure from the liquid

fraction following hot water Soxhlet extraction, and the resulting grey solid was analysed by FTIR. The FTIR spectrum of the solid was found to closely match that of calcium sulfate dihydrate (see Fig. 4.17). The calcium and potassium contents of the pulps before and after water Soxhlet extraction were then determined. Before the water Soxhlet (and following the ethanol Soxhlet), the pulp contained 77% and 104% of the potassium and calcium contained in the raw biomass. These were reduced to 0% and 13% respectively by the water Soxhlet step. If all calcium and potassium were present in the pulp in the form of calcium sulfate dihydrate and potassium sulfate, this would equate to around 15% of pulp mass being removed by water Soxhlet extraction. This would account for almost all water-extractable mass, while sulfate salts of other common inorganic elements such as Na may account for the remaining 1%.

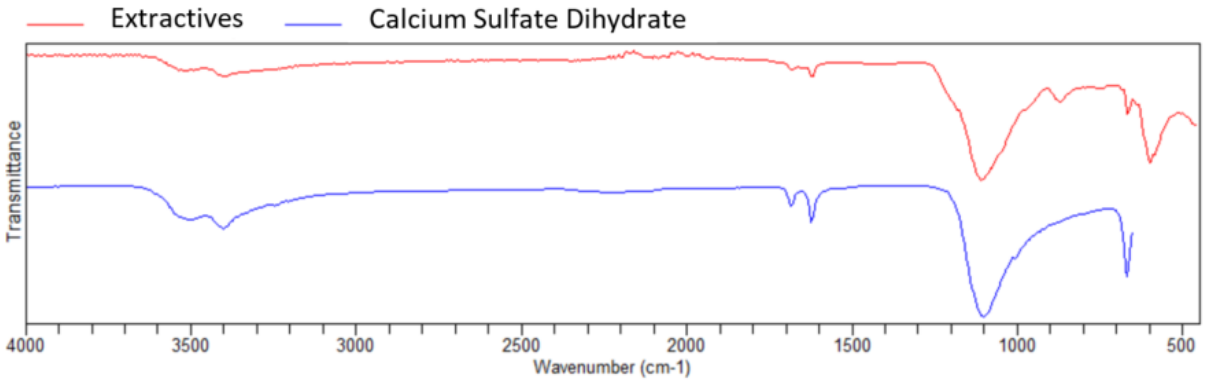


Figure 4.17: FTIR spectra of water-soluble extractives removed from mixed wetland feedstock pulp, and of calcium sulfate dihydrate. Pretreatments were carried out using [DMBA][HSO_4] at 150 °C for 45 minutes, with 20 wt% water, and at a biomass loading of 10% wt/wt.

The calcium and potassium contents of all three *Phragmites australis* batches, and of the mixed wetland feedstock, were determined. Batches 1 and 2 of *Phragmites australis* and the mixed feedstock were found to have a relatively high calcium and potassium content (1.9%, 2.5%, 1.6% respectively in the untreated biomass), while that of batch 3 was substantially lower (0.2%). Therefore, it appears that the high inorganic content of wetland feedstocks reacts with the $[HSO_4]^-$ anion to form IL-insoluble sulfate salts that deposit onto the pulp and must be removed by washing with water. Although calcium sulfate is considered insoluble in water, the low mass loadings during the water Soxhlet would lead to its gradual dissolution and removal. Similarly, during compositional analysis these deposits would dissolve due to the low mass loading and low pH (300 mg biomass in 84 g of water with 3 mL of H_2SO_4) and not be contained within the solid residue, thus not appearing as ash. This theory was corroborated by directly ashing the pulps and untreated mixed feedstock, which revealed a much higher ash content than that obtained through compositional analysis (14.5% vs 3.2%, and 3.4% vs. 1.2%).

Pretreatment was also performed on the mixed feedstock that had been Soxhlet extracted with ethanol and water beforehand. Pulps displayed an improved mass closure, but were found to still contain an elevated ash content by direct ashing compared to compositional analysis (9.9% vs 1.9%), effectively completing the mass balance. This shows that the calcium and potassium are partially removed by water extraction before pretreatment, but fully removed by water extraction after pretreatment. In a larger-scale process targeting cellulose production, a water extraction must be performed either before or after pretreatment in order to remove this inorganic material from the pulp, and in doing so significantly improve pulp purity. The benefit of performing the wash before pretreatment is that there would be less IL loss through reactions with the biomass Ca and K content, and removal of extractives would tend to minimise pseudolignin formation. However, this option would also significantly raise the input biomass moisture content, thus requiring a pre-input biomass drying stage or more extensive IL drying before use.

4.3.6 Mixed Feedstock Recycling Pretreatment 2

A modified recycling pretreatment was also carried out, with three cycles, for 45 minutes at 150 ^{o}C using [DMBA][HSO_4]. Pretreated pulps were additionally washed with hot water by Soxhlet, and the IL was filtered before rotary evaporation in order to remove any precipitated lignin that was not removed by centrifugation. After the first cycle, the acid/base ratio of the recovered IL was tested as before, and the amount of acid required to restore the acid/base ratio to 1.00 was calculated. However, this time varying amounts of acid were added to regenerate the IL: no acid, one third of the calculated required acid, or two thirds of the required acid were added. A fourth condition was also used: pretreating pre-extracted material, at the same conditions, without a water soxhlet on the pulp. This was to investigate the effect of the extractives upon the recycling performance. In this fourth condition, one half of the required acid needed to restore the acid-base ratio was added after the third cycle. The acid-base ratios of all four conditions are plotted in Fig. 4.18, with pretreatment results shown in Figs. 4.19 and 4.20. Trends between cycle 1 and cycle 3 are displayed in Table 4.3.

Following the first cycle, the excess base was measured to be 2% in both the non-extracted material and in the pre-extracted material. As previously stated, this value represents an upper bound, with any non-detectable material making the base excess appear higher. In the first recycling experiment, the amount of acid required to restore the acid/base ratio to 1.00 was added. However, this was found to lead to an excess of acid, implying the true acid/base ratio was higher than calculated. In this recycling experiment, three different quantities were added: no acid (to observe the effect of IL filtration between cycles), one third of the calculated amount, or two thirds of the calculated amount.

When no acid was added to the non-extracted material, the acid-base ratio of the IL carried on decreasing, reaching 4.5% excess base after the third cycle. However, the rate of increase of the excess base dropped after cycle 1, to around 1% per cycle. This may be an indication that after cycle 1, there is a maximum amount of non-detectable material dissolved in the IL (presumed to be extractives, lignin, and carbohydrate oligomers), and the remaining decrease is due to reactions with the biomass. This hypothesis is in line with the relatively stable lignin yields after cycle 1. If so, the 1% increase in excess base per cycle may provide a more accurate estimate of the amount of acid consumed per cycle. This estimate is corroborated by the acid-base trends when adding acid between cycles. Addition of 1/3 or 2/3 of the required acid (i.e. 0.67% and 1.33%) led to slightly decreasing and slightly increasing acid-base ratios after cycle 1, respectively, again suggesting an acid addition of around 1/2 the calculated amount (in this case 1% per cycle) to achieve steady state.

In the case of the extractive-free material, the acid-base ratio was found to decrease by around 2% per cycle for the first two cycles but did not change significantly after the third cycle. In this case, although lignin yields appear to carry on increasing between cycles 2 and 3, this increase is not statistically significant. Therefore, the apparent levelling off of the acid-base ratio between cycles 2 and 3 could be primarily due to a steady-state of non-detectable dissolved material in the IL liquor. Although the biomass does not contain extractives, it has a higher proportion of hemicellulose and lignin as a result, and these may remain dissolved.

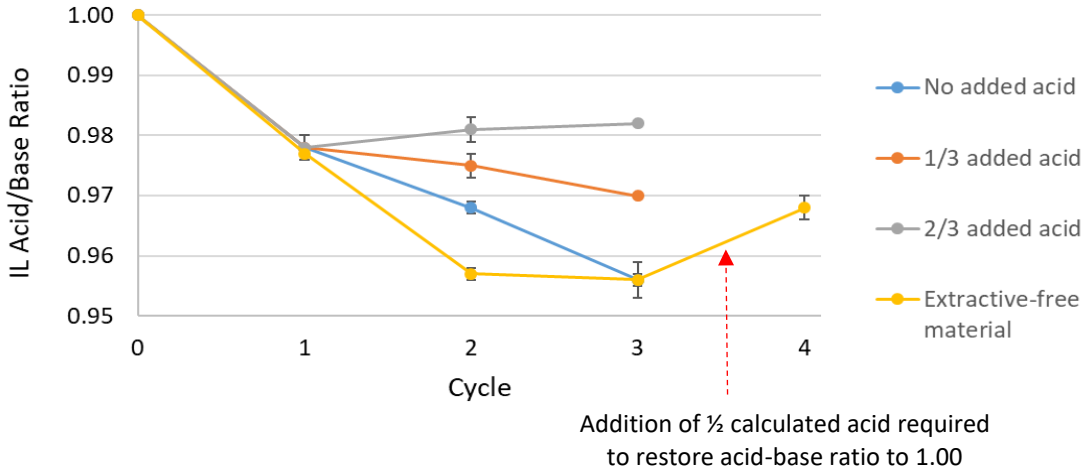


Figure 4.18: Acid/Base ratio of IL liquor following pretreatment, over 3-4 cycles. Cycle 0 corresponds to the acid-base ratio of the starting IL. When using extractive-free material, no acid was added between cycles 1 and 3, and half of the calculated amount of acid required to restore the acid-base ratio to 1.00 was added between cycles 3 and 4.

Part of the acid consumption can be explained by the reaction of the anion with calcium and potassium, producing sulfate salts, as observed in the direct ashing data (see Section 4.3.5). These results show that:

1. Pulps that are not subject to a water Soxhlet, from non-extracted biomass, contain 14.5% ash
2. Pulps that are not subject to a water Soxhlet, from extractive-free biomass, contain 9.9% ash
3. Pulps that are subject to a water Soxhlet contain 3.6% ash

If we assume that the ash content removed by a water Soxhlet is all $CaSO_4$, then these reactions are found to account for an acid consumption of 0.8% in non-extracted biomass, and 0.5% in extractive-free biomass.

Similarly to the first recycling experiment, pretreatment performance without acid addition worsened across key metrics: pulp purity and digestibility. The drop in pulp purity was primarily as a result of a drop in delignification. However, relative to the first recycling experiment this drop was reduced (4% vs. 11%), presumed to be due to the IL filtration between cycles. The presence of small quantities of residual lignin, not removed by centrifugation and decantation, would thus appear to have a significant impact. However, despite a smaller drop in pulp purity and delignification, the decrease in digestibility was far larger relative to the first recycling experiment (15% vs. 3%). This observation is particularly surprising considering the elevated pulp purities in the second recycling experiment, and the improved digestibility in the first cycle attributed to the elevated pulp purities. However, in later cycles the high-temperature water Soxhlet may be forming inhibitory compounds on the surface of the pulps, or redistributing lignin fragments and reducing the cellulose accessibility. This large drop in digestibility is also seen in pretreatments of non-extracted biomass with acid addition between cycles, corroborating the theory that inhibition is caused by the water Soxhlet extraction step. It is worth noting, however, that the water Soxhlet led to substantially improved digestibility of pulps in cycle 1, and that digestibility values in cycle 3 are similar to, or higher than, those in the first recycling experiment.

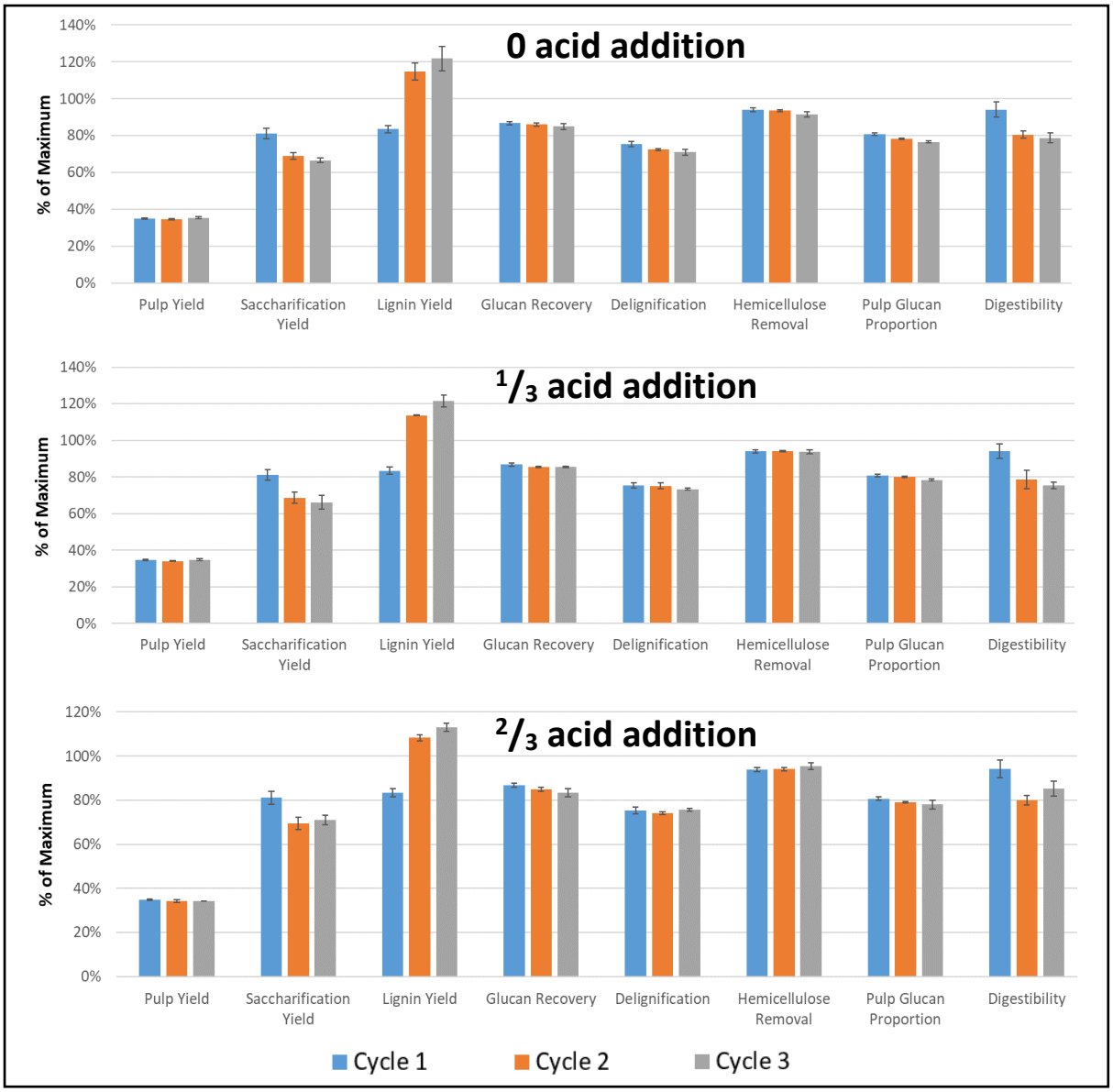


Figure 4.19: Pretreatment performance with IL recycling for a mixed wetland feedstock, with varying acid addition between cycles. Acid addition between cycles is indicated on each plot, as a proportion of the measured base excess after cycle 1. Pretreatments were carried out using [DMBA][HSO_4] for 45 minutes at 150 °C, with 20 wt% water, and at a biomass loading of 10% wt/wt. The aqueous IL was filtered between each cycle to remove suspended solids before water removal.

In terms of other pretreatment metrics, however, acid addition appeared to maintain pretreatment consistency across cycles. When adding $^1/_3$ or $^2/_3$ acid, there was no statistically significant drop in delignification or hemicellulose removal across all three cycles. The slight decrease in pulp purity when adding $^1/_3$ acid is not seen when adding $^2/_3$. Conversely, when adding $^2/_3$ there is a slight drop in glucan recovery not seen when adding $^1/_3$, suggesting a slight increase in solution acidity. These results therefore appear in agreement with the acid-base ratio measurements, suggesting that the "correct" amount of acid required lies between these two values, possibly around $^1/_2$ acid.

Table 4.3: Change in pretreatment metrics between cycles 1 and 3, recycling IL between cycles. Figures in red are those shown to be statistically significant.

Feedstock	Acid Added After Each Cycle	Delignification	Hemicellulose Removal	Glucan Recovery	Pulp Purity	Digestibility
Non-Extracted	0	**-4%**	-2%	-2%	**-4%**	**-15%**
	$^1/_3$	-2%	0%	-1%	**-2%**	**-19%**
	$^2/_3$	0%	+1%	**-3%**	-3%	**-9%**
Extractive-Free	0	**-6%**	**-6%**	+1%	**-5%**	-1%

Certain similarities were noted in the recycling performance of the extractive-free biomass, and of the non-extracted biomass without acid addition. There was a comparable drop in pulp purity (5%) over the three cycles, partially due to a drop in delignification (6%). However, in the case of the extractive-free material this was also accompanied by a significant drop in hemicellulose removal (6%). Despite a decrease in pulp purity, however, the digestibility of the pulps remained constant over all three cycles. The lack of a major drop in digestibility can be attributed to the absence of the water Soxhlet step. However, the lack of even a small drop in digestibility is thought to be due to the prior removal of extractives, and the avoidance of pseudolignin formation and redeposition. As previously shown (Section 4.3.1), in high-extractives feedstocks, the extractives combine with lignin to form pseudolignin, substantially increasing lignin yields. The same observation is noted here. Although lignin yields increase over cycles 1-3 (presumably due to a build-up of dissolved lignin in the liquor), they do not surpass delignification values in extractive-free biomass. In non-extracted biomass, however, lignin yields are always higher than delignification and reach over 100% from cycle 2 onwards, signs of pseudolignin formation. Pulp yields using extractive-free biomass were around 14% higher than non-extracted biomass over each cycle, due to the effectively higher lignin and cellulose contents of the feedstock.

The decrease in acid/base ratio manifests itself more clearly for extractive-free biomass than for non-extracted biomass (without acid addition). Three of the most typical signs of small amounts of excess base are a decrease in kinetics of delignification, hemicellulose removal, and glucan degradation.[41,74] Across the first 3 cycles, the extractive-free biomass displayed significant drops in both delignification and hemicellulose removal; non-extracted biomass only displayed a significant drop in delignification. In addition, the glucan recovery values of the non-extracted biomass were significantly lower in each cycle, by 4-7%. These observations suggest that pretreatments containing non-extracted biomass are

more acidic, even during cycle 1. One possible explanation is that the extractives contain fatty organic acids (e.g. oleic acid, stearic acid)[36,75], and that are removed following pretreatment when removing ethanol and/or water from the IL liquor under reduced pressure (approximately 30 mbar) and slightly elevated temperature (40-60 °C). These acids would thus add acidity to the pretreatment solution but would not contribute to the measured acid-base ratio of the liquor.

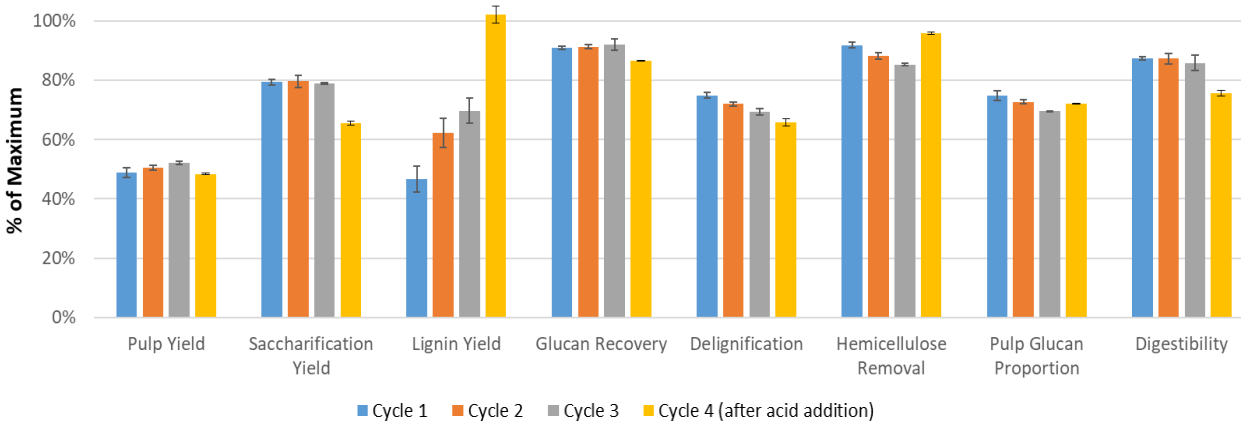


Figure 4.20: Pretreatment performance with IL recycling for a double-extracted mixed wetland feedstock, with acid addition after cycle 3. Pretreatments were carried out using [DMBA][HSO_4] for 45 minutes at 150 °C, with 20 wt% water, and at a biomass loading of 10% wt/wt. The aqueous IL was filtered between each cycle to remove suspended solids before water removal. $^1/_2$ the required acid to reach an acid-base ratio of 1.00 was added after cycle 3.

Due to the measured drop in acid-base ratio, and the characteristic signs of excess base pretreatment observed, it was decided to conduct a fourth cycle using extractive-free biomass, adding ½ the calculated acid required to reach a stoichiometric acid-base ratio. This was equivalent to adding 2.2% acid to the solution. The resulting pretreatment data shows clear signs of excess acid. Between cycles 3 and 4, hemicellulose removal increased by 11% (4% higher than in cycle 1), glucan recovery decreased by 5% (4% lower than cycle 1), and the lignin yield increased by 32% (increasing beyond delignification and over 100%). Delignification also decreased by 4%, taken to be a sign of lignin and pseudolignin redeposition. Overall, pulp purity increased by 3% due to the high increase in hemicellulose removal, but the effect of pseudolignin redeposition was seen in the 10% drop in digestibility of the pulps. Although the performance trends of the previous 3 cycles would suggest a clear increase in excess base, addition of ½ acid is clearly an overshoot. This is, therefore, likely due to significant quantities of non-detectable material in the liquor. This would have two consequences:

1. There was less IL in the liquor than thought. As pretreatments were operating at a low biomass loading of 10%, any realistic increases in biomass loading would not have a

significant impact on pretreatment efficacy over the three cycles. However, the quantity of acid added would have been larger than 2.2%.

2. The calculated 4.4% excess of base was an overestimate.

As a result of the two effects combined, the true acid-base ratio of the pretreatment solution would have likely been above 1.00. It is still unclear whether pretreatment performance can be kept consistent by replenishing any lost acid. Further experiments should aim to determine the required amount of acid to be added, as well as a reliable method for determining the "true" acid-base ratio of recycled liquors.

4.3.7 Pretreatment of Metal-Contaminated Feedstocks

The ability of IL pretreatment to extract metal from contaminated biomass is crucial for utilising biomass from AMD treatment wetlands, with the metal then able to be recovered from the IL liquor by electrodeposition.[76] A metal-contaminated mixed wetland feedstock was prepared by mixing 6 different species obtained from wetlands receiving AMD (PA 3, JE 2, SS, UE, BP, MC according to Table 1). This feedstock was pretreated at 150 ^{o}C for 30 minutes using [MBA][HSO_4], and for 45 minutes using [DMBA][HSO_4] and [Hmim]Cl. In previous studies, [Hmim]Cl has been found to be more effective for metal removal than alkylammonium [HSO_4]$^-$ ILs.[21,77] However, due to the higher cost of its constituent acid and base, it is more expensive than alkylammonium [HSO_4]$^-$ ILs.[78] The metal content of the untreated feedstock is shown in Table 4.4. AMD is generated from the oxidation of ferrous sulfide materials and is thus typically most abundant in Fe, reflected in the biomass content.[79] Mn and Al are also typical elements associated with AMD, while other elements present in high levels such as Zn may be due to the local mineralogy.[80–82]

Table 4.4: Metal content of untreated biomass (ppm).

Fe	Zn	Mn	Al	Pb	Cd
773 ±13	244 ±14	126 ±2	72 ±13	19 ±1	1 ±0

Metal removal from the pulp is displayed in Fig. 4.21. The performance of both [MBA][HSO_4] and [DMBA][HSO_4] are very similar across all elements, with [MBA][HSO_4] generally having a slightly higher performance. This similarity is to be expected as both belong to the same class of ILs, despite possessing different acidities. High extraction rates were obtained across all elements (75-90%) except Pb, for which no extraction was noted. The extraction rates of each element showed no correlation with its relative abundance in the untreated biomass. [Hmim]Cl substantially outperformed both alkylammonium ILs in the extraction of Mn, Zn, Pb, and Cd, achieving near-quantitative removal for

the former three elements. The largest difference in behaviour was for Pb, for which [Hmim]Cl displayed a strong affinity whereas [DMBA][HSO_4] and [MBA][HSO_4] displayed no extraction. However, [Hmim]Cl also displayed slightly worse removal of Al and Fe compared to the alkylammonium [HSO_4]$^-$ ILs. In general, it can be concluded that [Hmim]Cl achieved better metal removal from the pulp. This mirrors the overall findings of Rafat et al, and of Gschwend, who attributed this trend to the high coordination ability of [Hmim]Cl.[21,77] Rafat et al. compared the metal extraction performance of six ILs pretreating metal-contaminated wastewood, including the three tested in this study. In their study, much more severe conditions were used due to the softwood nature of the feedstock (170 °C, 45 minutes), and a larger number of metals were present. There were, however, similar levels of Zn and Cd, and much higher levels of Pb (484 ppm) in the feedstock. While overall trends were similar between these studies (i.e. performance in the order [Hmim]Cl > [MBA][HSO_4] > [DMBA][HSO_4]), there were a number of differences in the metal extraction performance of Zn and Pb using both [HSO_4]$^-$ ILs. Rafat et al. reported Pb extraction of 30-40% using both ILs, far higher than in this study, although much lower than the near-quantitative removal by [Hmim]Cl in both cases. The higher Pb extraction in Rafat et al's work is likely due to the heterogeneity of their wastewood samples, in which a paint fraction contained almost 2,000 ppm of Pb, whereas the wood fraction contained 46 ppm. Furthermore, the Pb contained within the paint fractions would have been on the surface of the material, unlike in the biomass. The more severe conditions may also have contributed to the higher removal. Zn removal was higher in this study, however, by around 30-50%. This may partially be due to the lower biomass loading employed (10% vs. 20% wt/wt), as well as to differences in the nature of the feedstocks: recently harvested grassy species, compared to old, metal-treated softwood.

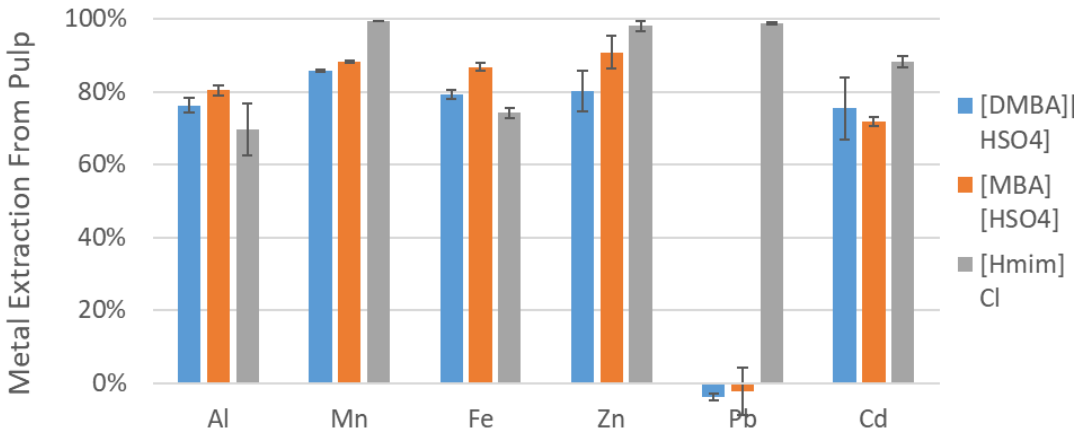


Figure 4.21: Metal removal from the pulp through IL pretreatment of mixed metal-contaminated wetland feedstock using varying ILs. Pretreatments were carried out at 150 °C, with 20 wt% water, and at a biomass loading of 10% wt/wt. Pretreatment duration was 45 minutes using [DMBA][HSO_4] and [Hmim]Cl, and 30 minutes using [MBA][HSO_4].

Fig. 4.22 shows the partitioning of the metals following pretreatment. Most elements were found to accumulate predominantly in the IL fraction, with generally low accumulation into the lignin fraction. Accumulation into the IL is important for the utilisation of contaminated biomass in pretreatment, as it may then be removed by electrodeposition[77,83], thus disposing of contaminants rather than simply concentrating them in a different fraction. Mass closures were found to often be above 100%, assumed to be due to contamination over the course of the pretreatment and non-homogeneity of the biomass. However, the partitioning trends of the elements still yield insight into the metal extraction behaviour of the IL. Results for Al are not shown due to widely varying results in the IL fraction, assumed to be due to more significant contamination over the course of the pretreatment. However, Al still appears to accumulate preferentially in the IL fraction, as the Al contents of the lignin were found to be relatively low: 4%, 5%, and 15% for [DMBA][HSO_4], [MBA][HSO_4], and [Hmim]Cl. For the elements shown, behaviour of both alkylammonium [HSO_4]$^-$ ILs were very similar. Metal affinity for the IL fraction over the lignin fraction followed the trend Mn > Fe > Cd > Zn >> Pb. Using [Hmim]Cl, the corresponding trend was Mn > Pb > Cd > Zn > Fe. As expected from the metal removal data, the biggest difference in partitioning behaviour was for Pb, in which almost all the metal was found in either the IL with [Hmim]Cl and in the pulp using [HSO_4]$^-$ ILs. One other substantial difference in behaviour was for Fe, of which a large fraction (28%) remained in the lignin using [Hmim]Cl, compared to 2-4% using the [HSO_4]$^-$ ILs. However, excluding Pb, the general partitioning performance of all three ILs can be considered broadly similar.

Due to the poor Pb removal using both [HSO_4]$^-$ ILs, as well as to its generally higher extraction performance, [Hmim]Cl would appear to be a “safer” choice for metal extraction from metal-contaminated biomass. However, for feedstocks in which Pb content is known not to be an issue, the [HSO_4]$^-$ ILs could represent a cheaper and viable alternative for metal extraction from AMD treatment wetland biomass. Furthermore, the process conditions used may be further optimised to maximise both metal extraction and pretreatment performance.

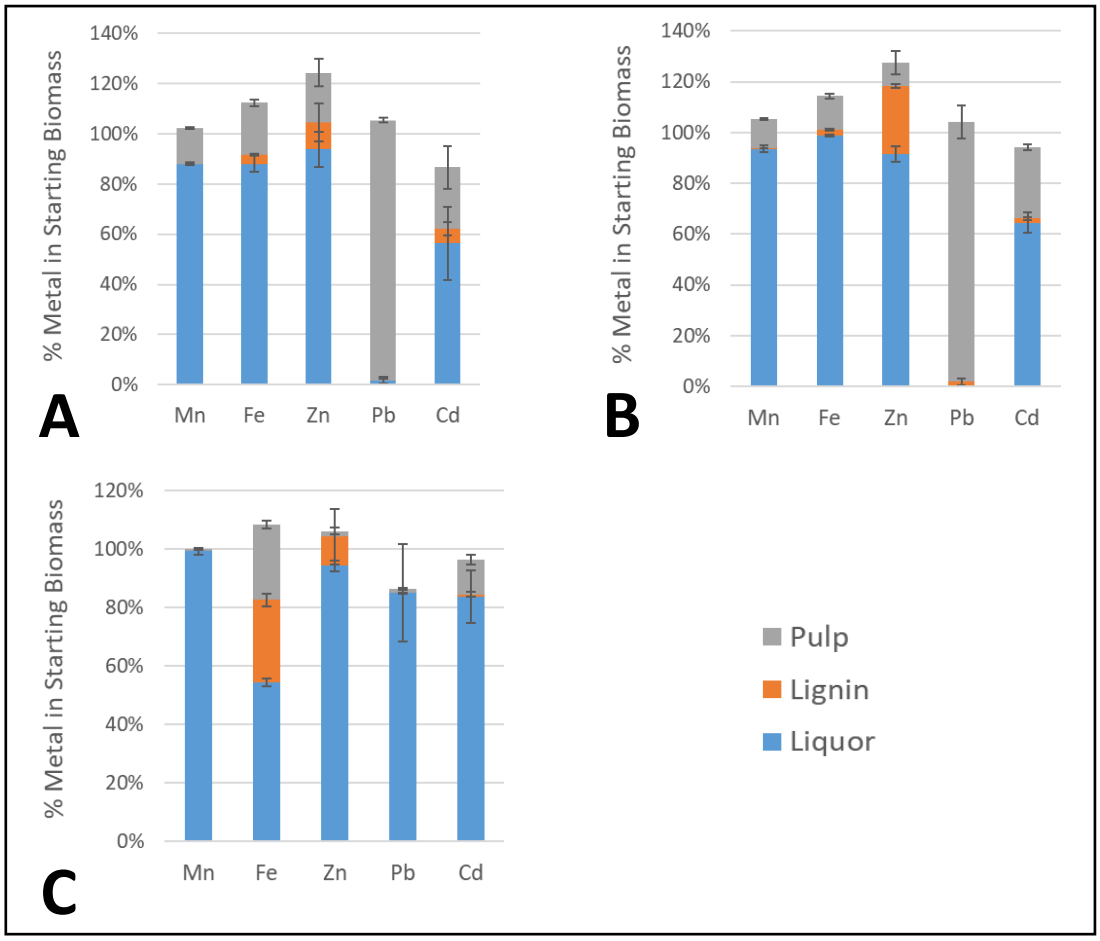


Figure 4.22: Metal partitioning following IL pretreatment of mixed metal-contaminated wetland feedstock using varying ILs. Plots are A: Using [DMBA][HSO_4] for 45 minutes, B: Using [MBA][HSO_4] for 30 minutes, C: Using [Hmim]Cl for 45 minutes. IL solution contains 20 wt% water. Pretreatments were carried out at 150 °C, and at a biomass loading of 10% wt/wt.

The pretreatment performance of all three ILs is shown in Fig. 4.23, while the composition of the mixed metal-contaminated feedstock is provided in the Appendix. The ILs were found to have very similar performance across all metrics. The largest discrepancy was in terms of the lignin yield. Both $[HSO_4]^-$ ILs displayed lignin yields 8-10% greater than delignification, indicating the formation of pseudolignin, whereas for [Hmim]Cl lignin yields were 3% lower than delignification, and the two values were not statistically different. Formation of pseudolignin in both $[HSO_4]^-$ ILs is unsurprising, given their higher acidity and the large extractive content of the feedstock (15%). The apparent lack of pseudolignin formation in [Hmim]Cl could be due to higher solubility of extractives and/or lignin in the IL rather than due to differing pretreatment severity, with both ILs having similar acidity (as measured by the Hammett acidity function).[84] The aromatic nature of the $[Hmim]^+$ cation would favour the solubility of

aromatic compounds such as lignin and many of the phenolic compounds in the extractives fraction. This is consistent with the results of Rafat et al, who reported delignification and lignin yields to remain relatively constant even for extended periods at 170 °C.[77] This may be taken as further evidence for Hammett acidity alone being a poor predictor of pretreatment efficacy, as demonstrated in Chapter 2.

A notable feature of the pretreatment was the low obtained pulp purities (56-58%). These were due to the low delignification extents (46-50%), as well as the relatively high glucan losses (14-16%). Hemicellulose removal remained high for all ILs (93-94%). However, despite the low lignin removal from the pulp, high digestibilities were observed (88-91%), substantially higher than the untreated biomass (14%). This is surprising in light of the results of Section 4.3.3, in which it was shown that there is a strong correlation between pulp digestibility and lignin content. The only feedstock with comparable results for delignification and digestibility was *Pistia stratiotes*, for which the biomass structure was concluded to be non-lignocellulosic, with a large undetected fraction and very low lignin content. In the case of the mixed metal-contaminated feedstock, however, mass closures are quantitative and the lignin content was found to be 30%.

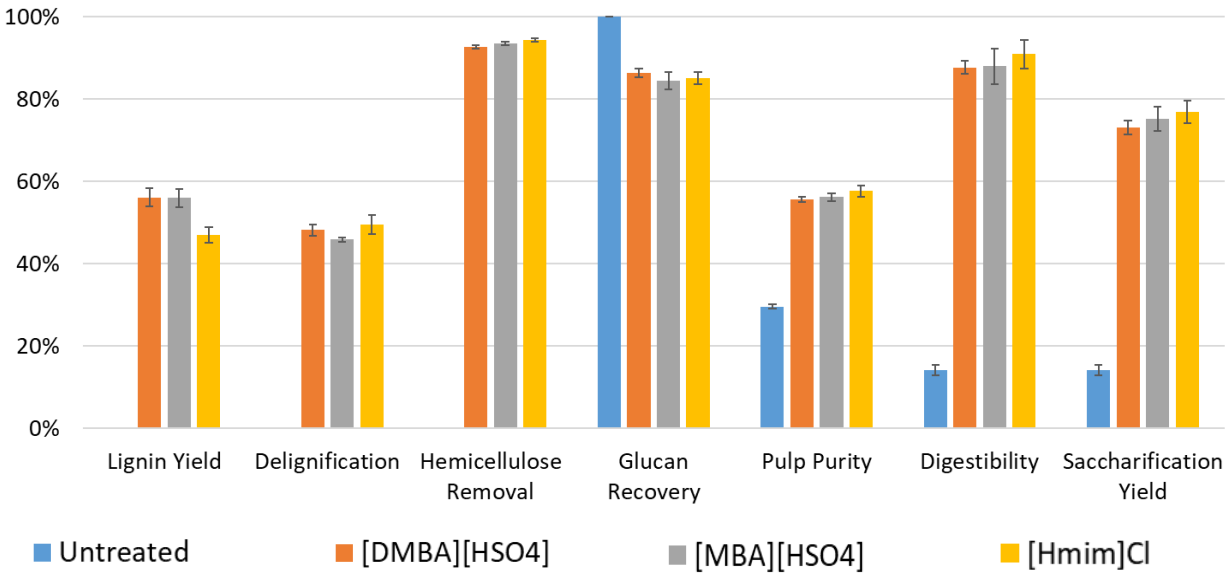


Figure 4.23: Pretreatment performance of different ionic liquids with a mixed metal-contaminated wetland feedstock. Pretreatments were carried out at 150 °C, with 20 wt% water, and at a biomass loading of 10% wt/wt. Pretreatment duration was 45 minutes using [DMBA][HSO_4] and [Hmim]Cl, and 30 minutes using [MBA][HSO_4].

Results in Section 4.3.4, and in a previous study by Gschwend,[21] have shown no significant synergy effects when mixing feedstocks. Pretreatment performance of the individual species would therefore presumably identify the reason for this elevated digestibility. However, only one of the constituent

feedstocks (*Phragmites australis* batch 3) was pretreated (Section 4.3.1). Additionally, a different batch of *Juncus effusus* was pretreated in Section 4.3.3. While both feedstocks displayed high digestibility (83-94%), this was accompanied by relatively high delignification (78-86%). It may therefore be supposed that the cause of the low delignification and high digestibility phenomenon is due to one of the four remaining constituent feedstocks. Of the six constituent feedstock species, available data (from this study or from the literature[85–89]) shows that all predominantly made up of lignocellulose except *Sphagnum spp.* Furthermore, all species were reported to have, or found to have, lignin contents below that of the mixed feedstock average. It may, therefore, be suggested that the lignin content of the mixed feedstock is artificially elevated due to acid-insoluble material from the *Sphagnum spp.* fraction being incorrectly labelled as lignin.

Although there is a consensus on the presence of phenolic polymers in Sphagnum mosses, there is significant debate over the structure of these polymers and whether they correspond to lignin.[90–96] A number of studies assert they are indeed lignin, but are unusually made up of primarily *p*-hydroxyphenyl units, with a very low methoxyl content.[91,92,96] However, Wilson et al. have reported the "lignin" to in fact be tannin or hydroxybenzofuran polymers, while others suggest it is made up of a range of different phenolics including sphagnum acid.[93,95–97] However, the reported quantities of these phenolic compounds are below 10% of dry weight.[91,93] This "lignin" fraction may also contain polysaccharides that are enzymatically hydrolysed, thus increasing the apparent digestibility as well as lignin content. A similar effect was observed during the compositional analysis of nut shells (see Appendix), due to the concentrated acid not being able to fully penetrate the hard, dense particles. In this case, however, the cause would be due to polysaccharides being incorporated into the "lignin" structure and not being hydrolysed during the compositional analysis. This idea is supported by certain studies. Kratzl and Eibl suggested that the acid-insoluble lignin was in fact methoxylated carbohydrates forming humin-like substances.[92] Farmer et al. reported that Sphagnum "lignin" is attached to carbohydrate oligosaccharides, but that they are liberated by acid hydrolysis.[94] Furthermore, the polysaccharide composition of Sphagnum species differs from those of other species in this mixed feedstock. As well as cellulose and hemicellulose, there is a significant fraction of sphagnan, a pectin-like polymer made up of monomeric sugars and uronic acids that is covalently linked to other polysaccharides.[97–100] Additionally, Sphagnum cell wall polysaccharides have been found to be coated by lipid substances, which could affect their behaviour during pretreatment and compositionnal analysis.[97] This explanation for the atypical pretreatment behaviour of the mixed feedstock is acknowledged to be very tentative. Due to the atypical composition of *Sphagnum spp.*, further work should target pretreatment of these species in order to better understand their pretreatment behaviour.

When compared to the results of Rafat et al, several differences are apparent.[77] In their study, [DMBA][HSO_4] displayed lignin yields much lower than delignification, and similar values for both using [MBA][HSO_4]. However, both ILs gave pulps with much lower saccharification yields compared to [Hmim]Cl (80% vs 50%), as well as much higher glucan losses (up to 40% using [MBA][HSO_4]) and hemicellulose removal. It appeared that the pretreatments using $[HSO_4]^-$ ILs were causing lignin redeposition, as well as possible pseudolignin redeposition, inhibiting saccharification. HSQC was used to show much lower lignin condensation in the case of [Hmim]Cl. This may partly have been due to the severe pretreatment conditions employed in that study. More severe conditions are generally required for pretreatment of softwood feedstocks, which are more recalcitrant than hardwoods or grasses. Therefore, while combination of contaminated and virgin wetland feedstocks and other grassy biomass appears viable, integration of other types of contaminated feedstocks may not be as feasible, and would require careful selection of process parameters to avoid under-treating or over-treating different biomass fractions.

4.4 Conclusions

In this chapter, the first major inroads have been made towards developing an IL pretreatment process tailored towards wetland species. Process conditions were first chosen by pretreating *Phragmites australis* with [MBA][HSO_4], [DMBA][HSO_4], and [DMEtA][HCOO]. Both $[HSO_4]^-$ ILs successfully pretreated this feedstock, reaching peak pulp purities of around 70% and peak digestibilities of around 90%, with [MBA][HSO_4] offering faster kinetics. However, both ILs displayed substantial pseudolignin formation, attributed to the incorporation of extractives into the precipitated "lignin". [DMEtA][HCOO] displayed more targeted lignin removal relative to hemicellulose removal leading to higher overall sugar release, and produced more native-like lignin, but had much slower kinetics.

Feedstock independence was confirmed by treating a total of 11 wetland feedstocks (covering 8 common species) using [DMBA][HSO_4]. Pretreatment using [DMBA][HSO_4] significantly improved digestibility and pulp purity of all feedstocks, except *Pistia stratiotes* (attributed to substantial non-lignocellulosic material, including high starch content). The majority of pretreated feedstocks displayed digestibilities above 80%, with total glucose release found to be fairly consistent, at around 20-25 wt% for the majority of species. Pulp purities ranged from 63-75%, but this range is predicted to increase to 72-83% with the addition of a water Soxhlet step (pre- or post- pretreatment) to remove a significant inorganic fraction arising from the reactions of the $[HSO_4]^-$ anion with Ca and K in the biomass. All feedstocks displayed pseudolignin formation except one feedstock with a significantly lower extractives content, with lignin yields strongly correlated to extractives content.

A mixed wetland feedstock was made, comprised of 9 different feedstocks, encompassing 7 species. This was pretreated using [DMBA][HSO_4] and [MBA][HSO_4], in the first of two recycling experiments. In total, 5 cycles were performed. Pretreatment performance was found to substantially worsen over the first four cycles, with digestibility decreasing by 8-12% and pulp purity by 9-11%. This decrease was driven by a 10% drop in delignification. After cycle 4, the recycled liquor was found to have a 6% excess of base, which was corrected by acid addition before cycle 5, in the hope of restoring performance. However, the resulting pretreatments displayed clear signs of excess acid addition, implying the 6% excess was an overestimate.

In the second recycling experiment, four conditions were employed using the mixed wetland feedstock, all using [DMBA][HSO_4] for 45 minutes, with an added filtration step between cycles. One condition employed pre-extracted material, while the others involved addition of no acid, $^1/_3$ acid, or $^2/_3$ acid to non-extracted material (relative to the amount calculated to restore the acid/base ratio to 1.00). The conditions using non-extracted biomass had an added water Soxhlet step at the end of the pretreatment process to remove the inorganic fraction. The acid-base ratio of all liquors was again found to decrease in solutions without acid addition, reaching 4.5% excess base after cycle 3. It was determined that addition of $^1/_2$ acid between cycles would appear to stabilise the acid-base ratio between cycles for non-extracted material. Acid addition and filtration between cycles reduced drops in delignification, leading to relatively consistent pulp purity over cycles 1-3. Despite this, however, pulps from non-extracted feedstocks displayed a much larger drop in digestibility over the first three cycles compared to the first recycling experiment. This was attributed to the water Soxhlet stage producing saccharification-inhibiting material on the surface of the pulps. The pre-extracted material showed larger drops in delignification and hemicellulose removal, and thus pulp purity, over the first three cycles. However, this was not accompanied by any significant drop in digestibility, attributed to the lack of dissolved extractives and water Soxhlet. However, addition of $^1/_2$ acid after cycle 3 led to clear signs of excess acid and a significant drop in digestibility.

Lastly, the metal extraction performance of IL pretreatment was tested on a mixed metal-contaminated wetland feedstock, made up of 6 species harvested from wetlands treating AMD. This mixed feedstock was found to contain elevated levels of Fe, Zn, Mn, Al, Pb, and Cd. Three ILs were tested: [DMBA][HSO_4], [Hmim]Cl, and [MBA][HSO_4]. Metal removal from the pulp was found to be generally highest using [Hmim]Cl, which achieved near-quantitative removal of Zn, Mn, and Pb. [HSO_4]$^-$ ILs achieved removal rates of 75-90% across all elements, except Pb, for which no significant removal was measured. [MBA][HSO_4] was found to slightly outperform [DMBA][HSO_4] across most elements. Metals removed from the pulp were found to preferentially accumulate in the IL fraction rather than the lignin fraction, an important feature for any metal removal pretreatment. The pretreatment

performance of the three ILs was very similar across all metrics, except lignin yield. [Hmim]Cl was the only IL not to demonstrate pseudolignin formation, thought to be due to the higher solubility of lignin and extractives as a result of the aromatic cation. Despite limited delignification (46-50%) and resulting pulp purities (56-58%), digestibilities were very high, around 90%, thought to be due to significant lignin-like material that was not true lignin.

In this chapter, several promising process conditions have been identified for the pretreatment of wetland feedstocks, particularly those that are most commonly used in wetland remediation. These conditions are similar to those used in pretreatment of *Miscanthus*, and presumably other grassy energy crops. Utilisation of the resulting pulps for both cellulose applications and bioethanol production both appear promising, with pulp purities above 70% and digestibilities above 80% readily achievable. Feedstock independence, including metal-contaminated feedstocks, is an important practical consideration that has been conclusively demonstrated. However, further work remains to be carried out on the recycling performance of ILs for pretreatment. In particular, work needs to target the "true" acid-base ratio and how it changes during pretreatment, as well as whether it can be restored. Removal of extractives would appear necessary as part of a scaled-up pretreatment process for this class of feedstocks, with pre-extraction more attractive than post-extraction based on these results. Therefore, further work should also look at identification and valorisation of the highest-value compounds in wetland species, as several works have already posited and investigated in other feedstocks.[101–104]

References

1 J. F. Köbbing, N. Thevs and S. Zerbe, *Mires Peat*, 2013, **13**, 1–14.
2 J. Vymazal, L. Kröpfelová, J. Švehla, V. Chrastný and J. Štíchová, *Ecol. Eng.*, 2009, **35**, 303–309.
3 M. Scholz and B. H. Lee, *Int. J. Environ. Stud.*, 2005, **62**, 421–447.
4 S. J. McNaughton, *Ecol. Monogr.*, 1966, **36**, 297–325.
5 B. H. Hill, *Aquat. Bot.*, 1987, **27**, 385–394.
6 R. E. Grosshans, PhD Thesis, University of Manitoba, 2014.
7 K. Suda, A. Shahbazi and Y. Li, in *Proceedings of the 2007 National Conference on Science and Technology*, ed. N. E, Springer, New York, 2007, pp. 9–15.
8 D. Bransby, S. Sladden and M. Downing, in *7th National Bioenergy Conference*, Nashville, 1996.
9 S. Collura, B. Azambre, G. Finqueneisel, T. Zimney and J. Weber, *Env. Chem Lett*, 2006, **4**, 75–78.
10 M. Khanna, B. Dhungana and J. Clifton-Brown, *Biomass and Bioenergy*, 2008, **32**, 482–493.
11 P. K. Rai, *Int. J. Phytoremediation*, 2008, **10**, 133–160.
12 M. Ghosh and S. P. Singh, *As. J. Energy Env*, 2005, **6**, 214–231.
13 R. H. Kadlec and S. D. Wallace, *Treatment wetlands*, CRC Press, Boca Raton, 2nd edn., 2009.
14 A. E. J. Firth, N. Mac Dowell, P. S. Fennell and J. P. Hallett, *Environ. Sci. Water Res. Technol.*, 2020, **6**, 2103–2121.
15 D. Liu, X. Wu, J. Chang, B. Gu, Y. Min, Y. Ge, Y. Shi, H. Xue, C. Peng and J. Wu, *Nat. Clim. Chang.*, 2012, **2**, 190–194.
16 H. Peng, L. Gao, M. Li, Y. Shen, Q. Qian and X. Li, *RSC Adv.*, 2014, **4**, 36603–36614.

17 N. Sathitsuksanoh, Z. Zhu, N. Templeton, J. A. Rollin, S. P. Harvey and Y. H. P. Zhang, *Ind. Eng. Chem. Res.*, 2009, **48**, 6441–6447.
18 B. Zhang, A. Shahbazi, L. Wang, O. Diallo and A. Whitmore, *J. Ind. Microbiol. Biotechnol.*, 2011, **38**, 819–824.
19 M. He, Q. Hu, Q. Zhu, K. Pan and Q. Li, *Environ. Prog. Sustain. Energy*, 2015, **34**, 276–281.
20 A. Sluiter, B. Hames, R. O. Ruiz, C. Scarlata, J. Sluiter and D. Templeton, *Determination of Structural Carbohydrates and Lignin in Biomass, NREL/TP-510-42618*, 2008.
21 F. Gschwend, PhD Thesis, Imperial College London, 2017.
22 J. L. Wen, S. L. Sun, B. L. Xue and R. C. Sun, *Materials (Basel).*, 2013, **6**, 359–391.
23 D. J. Yelle, P. Kaparaju, C. G. Hunt, K. Hirth, H. Kim, J. Ralph and C. Felby, *Bioenergy Res.*, 2013, **6**, 211–221.
24 J. C. Del Río, P. Prinsen, J. Rencoret, L. Nieto, J. Jiménez-Barbero, J. Ralph, Á. T. Martínez and A. Gutiérrez, *J. Agric. Food Chem.*, 2012, **60**, 3619–3634.
25 J. C. Del Río, J. Rencoret, P. Prinsen, Á. T. Martínez, J. Ralph and A. Gutiérrez, *J. Agric. Food Chem.*, 2012, **60**, 5922–5935.
26 X. Liu, Y. Li, C. M. Ewulonu, J. Ralph, F. Xu, Q. Zhang, M. Wu and Y. Huang, *ACS Sustain. Chem. Eng.*, 2019, **7**, 14135–14142.
27 H. Zhou, R. Zhang, W. Zhan, L. Wang, L. Guo and Y. Liu, *Green Chem.*, 2016, **18**, 6108–6114.
28 D. Savy, P. Mazzei, R. Roque, A. Nuzzo, S. Bowra and R. Santos, *Fuel Process. Technol.*, 2015, **138**, 637–644.
29 D. Savy, A. Nebbioso, P. Mazzei, M. Drosos and A. Piccolo, *Fuel Process. Technol.*, 2015, **131**, 175–181.
30 J. Sun, N. V. S. N. M. Konda, R. Parthasarathi, T. Dutta, M. Valiev, F. Xu, B. A. Simmons and S. Singh, *Green Chem.*, 2017, **19**, 3152–3163.
31 P. Y. S. Nakasu, C. J. Clarke, S. C. Rabelo, A. C. Costa, A. Brandt-Talbot and J. P. Hallett, *ACS Sustain. Chem. Eng.*, 2020, **8**, 7952–7961.
32 N. I. Haykir, E. Bahcegul, N. Bicak and U. Bakir, *Ind. Crops Prod.*, 2013, **41**, 430–436.
33 Q. Xiang, J. S. Kim and Y. Y. Lee, *Appl. Biochem. Biotechnol. - Part A Enzym. Eng. Biotechnol.*, 2003, **106**, 337–352.
34 A. Brandt-Talbot, F. J. V. Gschwend, P. S. Fennell, T. M. Lammens, B. Tan, J. Weale and J. P. Hallett, *Green Chem.*, 2017, **19**, 3078–3102.
35 F. Hu, S. Jung and A. Ragauskas, *ACS Sustain. Chem. Eng.*, 2013, **1**, 62–65.
36 P. Bajpai, *Wood and Fiber Fundamentals*, Elsevier, 3rd edn., 2018.
37 P. E. A. Debiagi, C. Pecchi, G. Gentile, A. Frassoldati, A. Cuoci, T. Faravelli and E. Ranzi, *Energy and Fuels*, 2015, **29**, 6544–6555.
38 B. Pecha and M. Garcia-Perez, in *Bioenergy: Biomass to Biofuels*, ed. A. Dahiya, Academic Press, 2015, pp. 413–442.
39 K. Thammasouk, D. Tandjo and M. H. Penner, *J. Agric. Food Chem.*, 1997, **45**, 437–443.
40 P. Bruijnincx, B. Weckhuysen, G.-J. Gruter, A. Westenbroek and E. Engelen-Smeets, *Lignin Valorisation : The Importance of a Full value chain approach*, 2016.
41 L. Weigand, S. Mostame, A. Brandt-Talbot, T. Welton and J. P. Hallett, *Faraday Discuss.*, 2017, **202**, 331–349.
42 D. S. Zijlstra, C. A. Analbers, J. de Korte, E. Wilbers and P. J. Deuss, *Polymers (Basel).*, 2019, **11**, 14–17.
43 M. Chen, F. Malaret, A. E. J. Firth, P. Verdía, A. R. Abouelela, Y. Chen and J. P. Hallett, *Green Chem.*, 2020, **22**, 5161–5178.
44 F. J. V. Gschwend, F. Malaret, S. Shinde, A. Brandt-Talbot and J. P. Hallett, *Green Chem.*, 2018, **20**, 3486–3498.
45 C. Chambon, PhD Thesis, Imperial College London, 2017.
46 Z. Hu, M. Foston and A. J. Ragauskas, *Bioresour. Technol.*, 2011, **102**, 7224–7228.
47 F. J. V. Gschwend, C. L. Chambon, M. Biedka, A. Brandt-Talbot, P. S. Fennell and J. P. Hallett, *Green Chem.*, 2019, **21**, 692–703.
48 L. Weigand, PhD Thesis, Imperial College London, 2018.
49 M. Borrega and H. Sixta, *Cellulose*, 2013, **20**, 2803–2812.
50 M. Borrega, S. Concha-Carrasco, A. Pranovich and H. Sixta, *Cellulose*, 2017, **24**, 5133–5145.
51 V. Köpcke, PhD Thesis, KTH Royal Institute of Technology, 2010.
52 T. Zhang, D. Xu, F. He, Y. Zhang and Z. Wu, *Ecol. Eng.*, 2012, **47**, 189–197.
53 J. Vymazal, L. Kröpfelová, J. Švehla and J. Štíchová, *Ecol. Eng.*, 2010, **36**, 939–945.
54 A. Monti, F. Zanetti, D. Scordia, G. Testa and S. L. Cosentino, *Ind. Crops Prod.*, 2015, **75**, 129–134.

55 M. H. N. Tahir, M. D. Casler, K. J. Moore and E. C. Brummer, *Bioenergy Res.*, 2011, **4**, 111–119.
56 F. Dragoni, N. N. o Di Nasso, C. Tozzini, E. Bonari and G. Ragaglini, *Bioenergy Res.*, 2015, **8**, 1321–1331.
57 T. P. Kandel, S. Sutaryo, H. B. Møller, U. Jørgensen and P. E. Lærke, *Bioresour. Technol.*, 2013, **130**, 659–666.
58 F. Dragoni, V. Giannini, G. Ragaglini, E. Bonari and N. Silvestri, *Bioenergy Res.*, 2017, **10**, 1066–1078.
59 G. Ragaglini, F. Dragoni, M. Simone and E. Bonari, *Bioresour. Technol.*, 2014, **152**, 107–115.
60 X. Ge, N. Zhang, G. C. Phillips and J. Xu, *Bioresour. Technol.*, 2012, **124**, 485–488.
61 F. W. Croon, *Mires Peat*, 2014, **13**, 1–13.
62 D. Mishima, M. Kuniki, K. Sei, S. Soda, M. Ike and M. Fujita, *Bioresour. Technol.*, 2008, **99**, 2495–2500.
63 X. Zhao, G. K. Moates, N. Wellner, S. R. A. Collins, M. J. Coleman and K. W. Waldron, *Carbohydr. Polym.*, 2014, **111**, 410–418.
64 C. Gupta and D. Prakash, *Toxicol. Environ. Chem.*, 2014, **95**, 1256–1266.
65 X. Zhao, G. K. Moates, D. R. Wilson, R. J. Ghogare, M. J. Coleman and K. W. Waldron, *Biomass and Bioenergy*, 2014, **72**, 206–215.
66 Q. Chen, Y. Jin, G. Zhang, Y. Fang, Y. Xiao and H. Zhao, *Energies*, 2012, **5**, 3019–3032.
67 J. J. Cheng and A. M. Stomp, *Clean - Soil, Air, Water*, 2009, **37**, 17–26.
68 C. O. Akinbile and M. S. Yusoff, *Int. J. Phytoremediation*, **14**, 201–211.
69 Q. Lu, Z. L. He, D. A. Graetz, P. J. Stoffella, X. Yang, P. J. Stoffella, D. A. Graetz and X. Yang, *Env. Sci Pollut Res*, 2010, **17**, 84–96.
70 S. Das, S. Goswami and A. Das Talukdar, *Bull. Environ. Contam. Toxicol.*, 2014, **92**, 169–174.
71 Q. Lu, Z. L. He, D. A. Graetz, P. J. Stoffella, X. Yang, P. J. Stoffella, D. A. Graetz and X. Yang, *Env. Sci Pollut Res*, 2011, **18**, 978–986.
72 N. R. Baral and A. Shah, *Biofuels, Bioprod. Biorefining*, 2016, **10**, 70–88.
73 W. Tu, PhD Thesis, Imperial College London, 2018.
74 P. Verdía, A. Brandt, J. P. Hallett, M. J. Ray and T. Welton, *Green Chem.*, 2014, **16**, 1617–1627.
75 A. Pattiya, in *Direct Thermochemical Liquefaction for Energy Applications*, ed. L. Rosendahl, Woodhead Publishing, 2018, pp. 3–28.
76 F. J. Gschwend, L. M. Hennequin, A. Brandt, F. E. Bedoya-Lora, G. H. Kelsall, K. Polizzi, P. Fennell and J. Hallett, *Green Chem.*, 2020, **22**, 5032–5041.
77 A. R. Abouelela, S. Tan, G. H. Kelsall and J. P. Hallett, *ACS Sustain. Chem. Eng.*, 2020, **8**, 14441–14461.
78 L. Chen, M. Sharifzadeh, N. Mac Dowell, T. Welton, N. Shah and J. P. Hallett, *Green Chem.*, 2014, **16**, 3098–3106.
79 P. T. Bobrowsky and B. Marker, Eds., *Encyclopedia of Engineering Geology*, Springer International Publishing, Cham, 2017.
80 J. Nyquist and M. Greger, *Ecol. Eng.*, 2009, **35**, 630–642.
81 M. S. Humphries, T. S. McCarthy and L. Pillay, *S. Afr. J. Sci.*, 2017, **113**, 63–71.
82 US Environmental Protection Agency, *Acid Mine Drainage Prediction, EPA 530-R-94-036*, 1994.
83 F. J. V. Gschwend, L. M. Hennequin, A. Brandt-Talbot, F. Bedoya-Lora, G. H. Kelsall, K. Polizzi, P. S. Fennell and J. P. Hallett, *Green Chem.*, 2020, **22**, 5032–5041.
84 B. J. Cox, S. Jia, Z. C. Zhang and J. G. Ekerdt, *Polym. Degrad. Stab.*, 2011, **96**, 426–431.
85 J. Schellekens, P. Buurman and T. W. Kuyper, *Soil Biol. Biochem.*, 2012, **53**, 32–42.
86 R. Celis, M. Torres, P. Valenzuela, R. Ríos, W. Gacitúa and H. Pesenti, *BioResources*, 2014, **9**, 6968–6980.
87 H. Pesenti, M. Torres, P. Oliveira, W. Gacitua and M. Leoni, *BioResources*, 2017, **12**, 2660–2672.
88 H. Lachowicz, H. Wróblewska, M. Sajdak, M. Komorowicz and R. Wojtan, *Cellulose*, 2019, **26**, 3047–3067.
89 I. Miranda, J. Gominho, I. Mirra and H. Pereira, *Ind. Crops Prod.*, 2013, **41**, 299–305.
90 N. G. Lewis and E. Yamamoto, *Annu. Rev. Plant Physiol. Plant Mol. Biol.*, 1990, **41**, 455–496.
91 V. M. Reznikov and V. F. Novitskii, *Chem. Nat. Compd.*, 1976, **11**, 76–81.
92 B. Lindberg, O. Theander, K. Motzfeldt, E. Finsnes, J. S. Sörensen and N. A. Sörensen, *Acta Chem. Scand.*, 1952, **6**, 311–312.
93 M. A. Wilson, J. Sawyer, P. G. Hatcher and H. E. Lerch, *Phytochemistry*, 1989, **28**, 1395–1400.
94 V. C. Farmer and R. I. Morrison, *Geochim. Cosmochim. Acta*, 1964, **28**, 1537–1546.
95 W. Stumpf and E. E. Conn, Eds., *Secondary Plant Products: A Comprehensive Treatise*, Academic Press, 2016.
96 G. G. Gross, in *Biochemistry of Plant Phenolics*, eds. T. Swain, J. B. Harbone and C. F. Van Sumere, Springer US, Boston, 1979, pp. 177–220.

97 J. T. A. Verhoeven and W. M. Liefveld, *Acta Bot. Neerl.*, 1997, **46**, 117–130.
98 K. Y. Børsheim, B. E. Christensen and T. J. Painter, *Innov. Food Sci. Emerg. Technol.*, 2001, **2**, 63–74.
99 S. Ballance, K. Y. Børsheim, K. Inngjerdingen, B. S. Paulsen and B. E. Christensen, *Carbohydr. Polym.*, 2007, **67**, 104–115.
100 O. Theander, *Acta Chem. Scand.*, 1954, **8**, 989–1000.
101 J. Michels and K. Wagemann, *Biofuels, Bioprod. Biorefining*, 2010, **4**, 263–267.
102 X. Yu, T. Gouyo, N. Grimi, O. Bals and E. Vorobiev, *Comptes Rendus Chim.*, 2016, **19**, 766–777.
103 N. Uppugundla, A. Engelberth, S. V. Ravindranath, E. C. Clausen, J. O. Lay, J. Giddens, D. J. Carrier and R. E. Martin, *J. Agric. Food Chem.*, 2009, **57**, 7763–7770.
104 M. K. Islam, C. Dong, H. Hsu, C. S. K. Lin and S. Leu, in *Waste Valorisation: Waste Streams in a Circular Economy*, eds. C. S. K. Lin, C. L. Guneet Kaur and X. Yang, Wiley, 2020, pp. 87–108.

Chapter 5: Pretreatment of Duckweed

5.1 Introduction

Duckweed's high growth rate and high proportion of starch make it a suitable candidate for bioethanol production.[1] Currently, however, it tends to be used as animal feed due to its high protein content, or as fertiliser due to its high water and nitrogen contents.[2,3] Zhao et al. state that the use of duckweed as a biorefining feedstock is held back by a lack of information on duckweed composition.[4] Several studies have, nevertheless, been carried out on its use as a feedstock for production of bioethanol (see Section 1.5.5). The generally high digestibility of duckweed relative to other bioethanol crops allows lower enzyme costs, which are said to lead to a lower production cost for ethanol than wheat straw.[5] Xu et al. suggest, however, that pretreatment may be required to further increase the enzymatic digestibility and thus reduce enzyme costs and energy inputs for grinding.[1] The high protein content in duckweed has also been mentioned as a possible biorefining co-product, although there have been no studies to date that have investigated this dual potential.[5,6]

As detailed in Section 1.5.4, one of the main attractions of duckweed is its ability to accumulate high levels of starch (up to 75 wt% has been reported[7]). Similarly to cellulose, starch is a biopolymer made up of only glucose monomers. However, the properties of starch are very different to those of cellulose due to structural differences. Cellulose is a linear polymer, with glucose monomers joined by β-1,4 linkages, with this structure allowing extensive hydrogen bonding within and between chains, thus making it crystalline and resistant to breakdown (see Section 1.2.2). Starch, however, is made up of two different polymers that are hydrogen bonded together: amylose and amylopectin (see Fig. 5.1).[8,9] Amylose generally accounts for around 20-35% of starch and is made up of glucose monomers joined by 99% α-1,4 glycosidic bonds and 1% α-1,6 glycosidic bonds, giving it an essentially linear helical structure.[10,11] Amylopectin generally accounts for 65-80% of starch, and is made up of glucose monomers joined by 95% α-1,4 glycosidic bonds and 5% α-1,6 glycosidic bonds, giving it a highly branched structure (see Fig 5.1).[10,11] In addition to these structural differences, amylopectin chains are typically much larger than amylose chains, with a typical molecular weight of around 10^7-10^9 g mol^{-1} compared to around 10^5-10^6 g mol^{-1}.[9,10,12–14] Compared to cellulose, starch is less resistant to chemical attack due to its less extensive hydrogen bonding network. Both components of starch are able to form double helical structures than can associate to form crystalline regions, but this is typically thought to be mainly confined to amylopectin.[10] In biomass, starch serves as energy storage, and is organised in granules with highly complex structures containing both amorphous and crystalline

regions.[11] In order to solubilise starch the network of strong inter and intra-molecular hydrogen bonds within the starch network must be disrupted. This may be achieved using a number of solvents such as DMSO, strong alkali solutions, or imidazole.[8] Unlike cellulose, starch can be solubilised in water to a certain extent with sufficient heating. This irreversible process is termed gelatinisation, and involves the swelling of the starch granule, followed by leaching of the amylose and eventual disruption of the ordered granular structure.[11,13,15,16] This disruption may not be complete, however, leading to granule remnants termed ghost starch.[8,17]

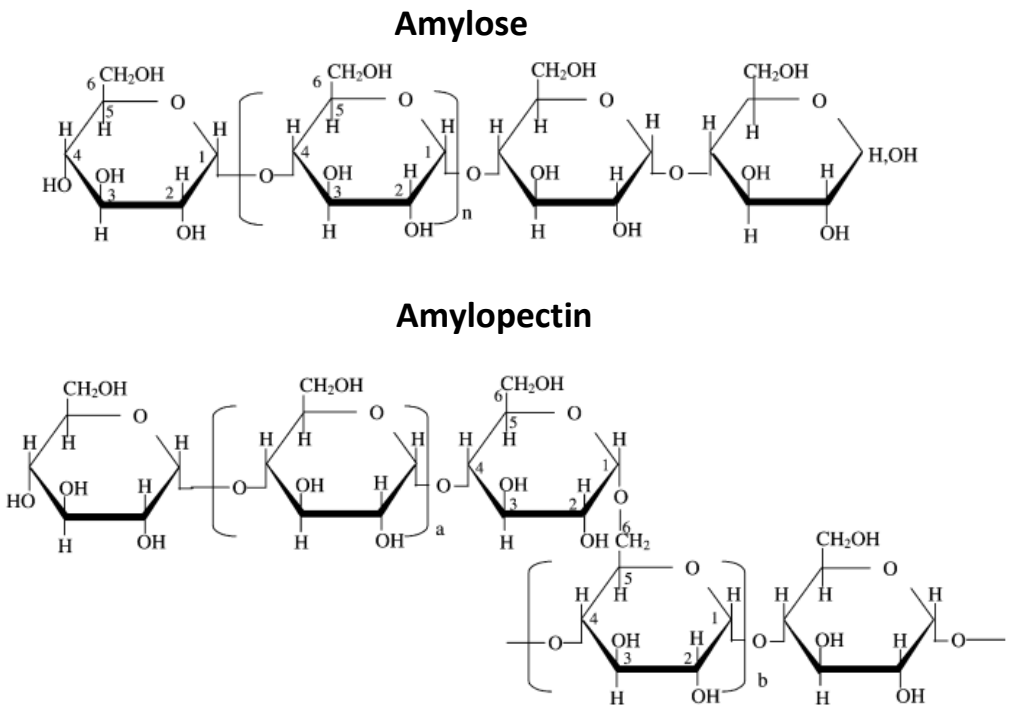


Figure 5.1: Structure of amylose and amylopectin. Adapted from Tester et al.[10]

A number of studies have investigated the interactions between starch and ILs, mainly for the purpose of starch modification. This is the subject of an extensive review by Ren et al. in 2020.[8] The vast majority of studies have focussed on the use of aprotic ILs with a dialkyl-imidazolium cation, paired with a carboxylate or halide anion.[8] These ILs have been repeatedly shown to dissolve starch, extensively disrupting the structure of native starch, with faster dissolution in ILs with more nucleophilic anions such as Br^-.[8,18–20] The dissolution mechanism of cellulose has typically been extended to starch, namely that basic IL anions form hydrogen bonds with hydroxyl groups. In reality, however, the mechanism of starch dissolution in ILs appears more complicated and remains to be fully elucidated.[8] This is exemplified by the strong effect of water content on the dissolution and phase transition of starch in ILs. Whereas cellulose dissolution is strongly inhibited upon addition of water,[21]

adding water has been shown to improve starch dissolution in certain ILs, attributed to several factors including the decreased viscosity of the resulting solutions and complex interactions between all three species.[8,13,15,22–24] The destructuration mechanism of starch in aqueous IL systems would appear to vary with IL/water ratio: it is dominated by gelatinisation at low ratios, while at high ratios it is a mix of depolymerisation and dissolution.[13,23] Upon dissolution in ILs, depolymerisation of the starch has been reported, particularly elevated in acidic ILs such as dialkylimidazolium chlorides, although addition of water has been reported to reduce depolymerisation in certain ILs.[13,14,20,25] There have been no studies investigating the use of ionic liquids for pretreatment of duckweed. Only two investigations (one paper, one patent) have been published involving the use of ionic liquids for duckweed processing; both aiming for the hydrolysis of the glucan through catalysis by an acidic IL (for production of platform chemicals or just direct hydrolysis to sugars).[26,27]

Another promising attribute of duckweed as a biorefinery feedstock is its often high protein content. Proteins are large macromolecules made up of amino acids bonded together by peptide bonds, with complex structures that are crucial to their highly specialised biological functions.[28,29] Protein extraction from biomass is of interest to improve the economic viability of biorefinery, reduce the carbon footprint of nutritional protein, and for use in non-food applications such as coatings and polymers.[29–31] The incorporation of protein as a co-product in a bioethanol plant was found by Laser et al. to reduce the minimum ethanol selling price the most out of all configurations investigated ($0.17/L).[32] There exists a range of methods for protein extraction from biomass, such as dissolution in organic solvents, alkaline solutions (pH ≥ 9), deep eutectic solvents, or the use of enzymes (carbohydrolases and/or peptidases).[30,31,33] Duckweed protein is has been reported to have a favourable amino acid composition for supplementing human diets or to replace costly fish meal in aquaculture.[34–37] Despite this, however, there has been only one process developed for duckweed protein extraction (a 2015 patent), involving crushing and liquefaction of the feedstock, before addition of a coagulating agent, allowing recovery of a high-purity duckweed stream.[38]

There have been a number of studies aiming to combine bioethanol production with protein recovery. The majority have focussed on cascade processing: extracting protein by dissolution into alkali solvents or by proteolysis, prior to subsequent pretreatment of the remaining lignocellulose through established processes such as liquid hot water, dilute acid, or AFEX.[39–42] However, another possible configuration is protein extraction from the pulp (in alkali) following pretreatment but before saccharification, with protein extraction yields found to be improved by the AFEX process and liquid ammonia treatment.[43–45] A third configuration involves the enrichment of protein in the pulp following saccharification, as the carbohydrate content is reduced by enzymatic hydrolysis.[46,47]

Ionic liquids have been extensively studied for protein purification and processing, as covered in a recent review by Schindl et al.[48] There have even been studies looking at the use of ILs for separation of proteins and polysaccharides extracted from biomass, using aqueous two-phase systems to separate the two fractions.[49–53] However, these studies have either used purified proteins and polysaccharides mixed together, or used real biomass fractions pre-extracted by a mechanical pretreatment (bead milling) that disrupted the cellular structure and released its contents into solution (with further processing in certain studies). As a result, the use of ILs for separation of the released fractions may not be considered a pretreatment step. Additionally, the biomass used is generally very low-lignin, generally algae, which may explain the lack of thermophysical/chemical pretreatment requirement for complete cellular disruption.

In this Chapter, the use of ILs for duckweed pretreatment is reported, with the aim of utilising this feedstock's potential for starch accumulation, protein accumulation, and metal uptake. The overall aim was to therefore develop a single pretreatment process producing a highly digestible, starch-rich pulp, as well as a high-purity protein stream, with any heavy metals remaining dissolved in the IL. No previous studies have been carried out on IL pretreatment of duckweed, on IL pretreatments targeting protein extraction, nor on combining bioethanol production with protein production and metal extraction in a single pretreatment process. The impact of IL pretreatment on starch degradation was first evaluated by pretreating pure starch using four ILs, allowing promising pretreatment conditions and ILs to be identified. Using timecourse pretreatments, the performance of two ILs was then investigated for the pretreatment of two duckweed species, in terms of starch recovery, sugar release, and protein recovery. In addition, the metal extraction capabilities of the ILs were evaluated for one batch of duckweed that was contaminated with heavy metals.

5.2 Materials and Methods

5.2.1 General Equipment

Unless stated otherwise, all general equipment used was the same as in Chapter 2.

5.2.2 IL Synthesis

Reagents for [DMBA][HSO_4] were obtained as in Chapter 2, and reagents for [DMEtA][HCOO] and [Hmim]Cl were obtained as in Chapter 4. Ethanolamine (>99%) and acetic acid (>99%) were purchased

from Sigma Aldrich. All the above were used as received for IL synthesis. ILs were synthesised as in Chapter 2. Acid-base ratios of monoprotic ILs were determined by pH (see Appendix). Acid-base ratios are expressed on a molar basis. NMR signals are provided below, with NMR spectra provided in the Appendix.

MonoEthanolAmmonium Acetate [MEA][OAc] (Figs. A1-13 and A1-14):

^{1}H NMR: δ_H (400 MHz, DMSO-d_6)/ppm: 6.37 (s, br, N-*H*, N-CH_2-CH_2-O*H*), 3.45 (m, 2H, N-CH_2-C*H*$_2$), 2.68 (m, 2H, N-C*H*$_2$), 1.70 (m, 3H, C*H*$_3$-COO^-).

^{13}C NMR δ_C (101 MHz, DMSO-d_6)/ppm: 175.33 (CH_3-*C*OO^-), 59.25 (N-*C*H_2), 42.25 (N-CH_2-*C*H_2OH), 24.45 (*C*H_3-COO^-).

[MEA][OAc] was synthesised to a purity of 97%, as determined by NMR. The remaining impurity was found to be N-hydroxyethyl-acetamide acetate, with the following peak assignments:

^{1}H NMR: δ_H (400 MHz, DMSO-d_6)/ppm: 3.33 (t, 2H, N-CH_2-C*H*$_2$), 3.04 (m, 2H, N-C*H*$_2$), 1.75 (s, 3H, C*H*$_3$-CO-N).

5.2.3 Pretreatment of Biomass

The biomass pretreatment protocol of the Hallett group laboratory was followed, as described in Chapter 2. In this case, however, no grinding of the biomass was carried out before pretreatment. Under milder pretreatment conditions, a portion of the pretreated duckweed floated following centrifugation, during the first ethanol washing step. In such cases, the pulp was separated from the ethanol/IL mixture by vacuum filtration through filter paper.

5.2.4 Pretreatment of Starch

Rice, wheat, corn, and potato starch were purchased from Sigma Aldrich, and were used as received. Their moisture content was determined as described in Chapter 2. The starch pretreatment protocol was based on that of the biomass pretreatment protocol, as described in Chapter 2. There were two differences in procedure:

1. Under certain conditions, the starch was found to partially or fully dissolve in the IL. In these cases, a white/colourless precipitate was produced upon addition of ethanol.
2. No Soxhlet washing was performed. Following the fourth ethanol wash, the falcon tube containing the remaining starch was dried in a vacuum oven at 40 ^{o}C overnight. After this, the solid was weighed and its moisture content was determined as described in Chapter 2. The remaining solid was then weighed into a 50 mL falcon tube, and 50 mL of DI water were added.

The falcon tube was vortexed and left to stand for one hour, before being manually shaken and then centrifuged at 3000 rpm for 50 minutes. After decanting the supernatant, the tube was dried in a vacuum oven at 40 °C overnight. After this, the remaining solid was weighed and its moisture content was determined as described in Chapter 2.

5.2.5 Biomass Characterisation

Enzymatic Hydrolysis

Enzymatic hydrolysis assays were carried out on pretreated pulps and untreated biomass, as well as on blank controls. A slightly modified version of the enzymatic hydrolysis protocol of the Hallett group laboratory (as described in Chapter 2) was followed. Instead of 7 days, assays were carried out over 5 days. In addition to cellulase Ctec2 enzymes, α-amylase (>250 U/g) and amyloglucosidase (>260 U/mL) enzymes were added in order to hydrolyse the starch fraction (both purchased from Sigma Aldrich). The resulting enzyme solution was prepared using the following quantities of reagent per sample: 5 mL of 0.1M sodium citrate buffer of pH 4.8, 40 μL of tetracycline hydrochloride antibiotic solution (10 mg/mL in 70% ethanol), 30 μL of cycloheximide antibiotic solution (10 mg/mL in purified water), 4.76 mL of purified water, 20 μL of Ctec2 enzymes, 40 μL of α-amylase, and 2 μL of amyloglucosidase. This led to similar enzymatic loadings to previous studies using duckweed as a feedstock.[5,54–60]

Enzymatic hydrolysis assays were sampled after 8, 24, 48, 72, and 120 hours of incubation. Sampling was carried out by cutting the end off a 1000 μL Eppendorf pipette tip, stirring the sample, and removing 300 μL of the hydrolysis mixture. This aliquot was then transferred into a microcentrifuge tube and centrifuged at 13.3 xG for 10 minutes in a VWR MICRO STAR 17R centrifuge, pre-cooled to 4 °C. The supernatant was then filtered and run through the HPLC, as described in Section 2.2.1 (using a glass insert in the HPLC vial due to the small volume).

For selected samples, the solid residue from the saccharification assay was collected for protein content analysis. This was done by rinsing the assay tube into a 50 mL Falcon tube using purified water, and centrifuging at 3300 rpm for 30 minutes. The supernatant was decanted, and the resulting solid was then washed with 50 mL of water, vortexed, and centrifuged again, in order to remove any remaining enzyme solution which would interfere with the protein content analysis. After decanting the supernatant, the Falcon tube was capped with tissue paper (held in place with Parafilm) and partially immersed in liquid nitrogen for several minutes, before being placed in a freeze-dryer for 48 hours. The resulting dry solid was then transferred onto a piece of tared aluminium foil, had its mass recorded, and was transferred into a glass sample vial.

Compositional Analysis

The compositional analysis protocol followed was that of the National Renewable Energy Laboratory 'Determination of Structural Carbohydrates and Lignin in Biomass', as described in Chapter 2.[61] Unless specified, only ethanol Soxhlet extraction was performed on the pulp beforehand (as part of the pretreatment protocol), while water, ethanol, and hexane Soxhlet extraction were performed on the untreated biomass. All measurements were performed in triplicates on untreated biomass and once for each pulp. In addition to the ash content obtained through the compositional analysis procedure, the ash content of certain samples was verified by directly ashing the samples, using the same heating profile. Cellulose content of the biomass was found by subtracting the starch content from the glucan content of the biomass.

Determination of Protein Content

Biomass protein content was determined using a nitrogen-to-protein conversion factor of 6.25, a commonly used method that has also been shown to be accurate for duckweed.[62] Biomass nitrogen content was measured by Medac Ltd.

Determination of Starch Content

Starch assays were carried out on pretreated pulps and untreated biomass, as well as on blank controls. Starch content was determined using a modified version of the Megazyme Rapid Total Starch Assay procedure (using Note 1),[63] in which released glucose was determined by HPLC rather than spectrophotometry. Out of the several Megazyme procedures, this was found to be most suitable for the feedstocks used (see Appendix). A Megazyme Total Starch Assay kit was purchased, containing the enzymes used in this procedure: thermostable α-amylase (2500 U/m) and amyloglucosidase (3,300 U/mL). In this process, a large excess of both enzymes are added to fully hydrolyse any starch present in the samples. The resulting glucose quantified, allowing the original starch content to be determined.

The moisture content of the feedstock was first determined out as detailed in Section 2.2.6. When analysing untreated material, the feedstock was ground into a fine powder using a coffee grinder. When analysing pulp, the feedstock was ground using a pestle and mortar, due to the more limited quantities of material. Approximately 450 mg of ground biomass on an oven–dry basis were then measured on a piece of tared aluminium foil, with the air-dry mass recorded, and transferred into a 15mL ACE pressure tube. 10 mL of 0.1M sodium acetate buffer (containing 5 mM $CaCl_2$) were added to each tube using an Eppendorf pipette, and the tubes were then vortexed for 5 seconds. 0.1 mL of

thermostable α-amylase were then added to each tube using an Eppendorf pipette, the tubes were vortexed again for 5 seconds, and the caps was loosened.

The tubes were then transferred to a boiling water bath. After 2 minutes, the caps were tightened and the tubes were vortexed for 5 seconds. The tubes were then vortexed every 5 minutes, until they had spent a total of 60 minutes in the boiling water bath. The tubes were then placed in a water bath at 50 °C for 5 minutes to equilibrate. Following this, 0.1 mL of amyloglucosidase were added to each tube using an Eppendorf pipette. The tubes were vortexed for 3 seconds and were then placed back into the 50 °C water bath for 30 minutes without further mixing. The tubes were then removed from the water bath and allowed to cool to room temperature over 10 minutes. The tubes were inverted in order to mix any condensed water on the walls, and were then filtered and run through the HPLC, as described in Section 2.2.1.

Eqs 5.1 and 5.2 were used to calculate starch content and starch recovery:

$$Starch\ (\%) = \frac{\left(c_{sample} - c_{blank}\right) \times V_{sample} \times corr_{anhydro}}{m_{sample} \times \left(1 - mc_{sample}\right)} \times 100 \quad (5.1)$$

$$Starch\ Recovery = \frac{Starch_{pulp} \times Pulp\ Yield}{Starch_{untreated}} \times 100 \quad (5.2)$$

where c_{sample} is the glucose concentration of the hydrolysis sample as determined by HPLC, c_{blank} is the glucose concentration of the blank control as determined by HPLC , V_{sample} is the volume of the hydrolysis sample (10.2 mL), $corr_{anhydrous}$ is a correction factor accounting for the increase in mass of sugars during hydrolysis (0.9 for glucose), *Pulp Yield* is as defined in Eq. 2.5, m_{sample} is the mass of sample hydrolysed, mc_{sample} is the moisture content of the sample hydrolysed, $Starch_{untreated}$ is the starch content of the untreated biomass, and $Starch_{pulp}$ is the starch content of the pulp. It should be noted that, although blank samples were analysed in order to account for any glucose or starch contained in the enzyme and buffer solutions, they were found to contain no glucose during HPLC analysis.

5.2.6 Liquor Analysis

Liquor analysis was carried out on starch pretreatment liquors, as described in Chapter 4, but also analysing for maltose. Following determination of the concentration of each solute in the liquor, the total mass of carbon associated with each solute was determined using Eq. 5.2. Following this, the degree of degradation of the starch was determined using Eq. 5.3.

$$Carbon_{solute} = c_{HPLC} \times \left(m_{liquor} + m_{water}\right) \times \rho_{sample} \times \frac{12 \times nc_{solute}}{MW_{solute}} \quad (5.2)$$

$$Degradation\ (\%) = 100 - \frac{\sum Carbon_{solute}}{\frac{12 \times nc_{starch}}{MW_{starch}} \times m_{starch} \times (1 - mc_{starch})} \times 100 \quad (5.3)$$

where C_{solute} is the mass of carbon associated with each solute, c_{HPLC} is the concentration of the solute in the sample as determined by HPLC, m_{liquor} is the mass of liquor sampled, m_{water} is the mass of water added to the sample, ρ_{sample} is the density of the sample (taken as 1.04), nc_{solute} is the number of carbon atoms in the solute, MW_{solute} is the molecular weight of the solute, nc_{starch} is the number of carbon atoms in a starch monomer, MW_{solute} is the molecular weight of a starch monomer, m_{starch} is the mass of input starch, and mc_{starch} is the moisture content of the input starch.

5.2.7 Biomass Digestion and Metal Quantification

Digestions and metal quantification were performed as in Chapter 4.

5.2.8 Liquor Dialysis

Dialysis was carried out on selected liquors in order to remove the IL and recover any dissolved protein. Dialysis tubing membranes with a 3.5 kDa molecular weight cut-off were purchased from Fisher Scientific and soaked in purified water for 5 minutes before use. A section of approximately 10 cm of membrane was cut, and sealed at one end using a dialysis clip. Approximately 10 g of liquor (of known water content) were weighed into the membrane tube using a serological pipette. The membrane was then sealed using a second dialysis clip, leaving enough air enclosed for the resulting package to float in water. Excess tubing was then cut, leaving around 1cm at either end.

The resulting package was placed in a 5 L beaker full of purified water with magnetic stirring and allowed to dialyse for 48 hours. Over this duration, the dialysis water was changed 7 times. The resulting solution inside the membrane tubing was then drained into a pre-weighted 50 mL Falcon tube, and the package was rinsed twice into this tube with purified water. The Falcon tube was then capped with tissue paper (held in place with Parafilm) and partially immersed in liquid nitrogen for several minutes, before being placed in a freeze-dryer for 72 hours. The resulting solid mass was determined by subtracting the mass of the centrifuge tube from the combined mass of the centrifuge tube and the solid.

5.2.9 Duckweed Sourcing and Metal Contamination

Spirodela polyrhiza was harvested from Regent's Canal, London, in August 2019 (see Fig. 5.2). *Lemna minor* was harvested from Holland Park, London, in September 2020. Both species were identified visually, with additional confirmation by Dr. Fred Rumsey, of the Natural History Museum. Following collection, all samples were rinsed with copious quantities of DI water, and any large fragments of non-duckweed material removed by hand. *S. polyrhiza* samples were then spread out on paper towels and allowed to air dry over one week, before being stored away from sunlight in an airtight bag.

After rinsing with DI water, a small fraction of the *L. minor* samples were air-dried on paper towels before being stored (as detailed above). The remainder of the *L. minor* was transferred to trays containing 10 L of 20% Hoagland nutrient solution, doped with 2 ppm of Cd and 2 ppm of Ni (in the form of $CdCl_2$ and $NiCl_2$, as in previous studies [64–66]), with a depth of 7 cm of water. Sufficient duckweed was added to each tray to just cover the surface of the water. The growth medium was replaced daily, for a total of 3 days. The trays were illuminated by blue-red grow lights suspended 90 cm above the surface of the water, providing 130 µmol/m^2/s of photosynthetically active radiation (400-700 nm), in line with previous studies.[67–70] The light intensity was measured using an Aseq LT1 quantum meter, and analysed using CheckTr software. Using timer sockets, a 16 hour/8 hour light/dark photoperiod was used, as in previous studies.[65,67–72] After harvesting the metal-contaminated *L. minor* samples, a small fraction was directly air-dried and stored. The remaining majority of the duckweed was rinsed with a large quantity of DI water before being air-dried and stored, with this fraction being used for pretreatments.

In addition, strains of *S. polyrhiza* and *L. minor* sourced from Rutgers Duckweed Stock Cooperative were cultivated in the laboratory but were not used in pretreatment experiments due to insufficient growth. Further details on the growth-measuring methods are detailed in the Appendix. Hoagland solution, $CdCl_2$, and $NiCl_2$ were all purchased from Sigma Aldrich.

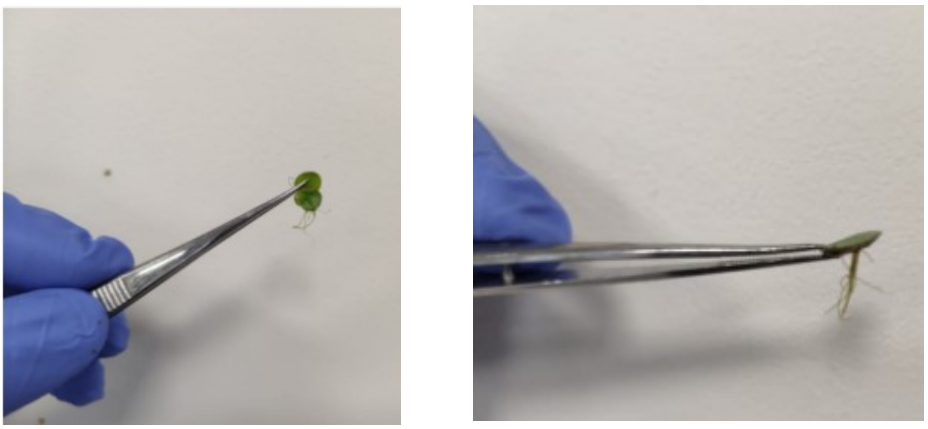


Figure 5-2: Harvested *Spirodela polyrhiza.*

5.2.10 Statistical Analysis

Statistical analysis was performed using the Student's *t*-test for comparison of 2 data points, and using two-tailed ANOVA followed by a post-hoc Tukey test for comparison of three or more data points. Correlations were determined using Pearson's correlation coefficient. When comparing saccharification curves, statistical analysis was applied to each sampling timepoint separately. The significance level used was 0.05, corresponding to a 5% risk of falsely concluding statistical difference exists.

5.3 Results and Discussion

5.3.1 Starch Pretreatment

It was decided to first pretreat pure starch with a range of ILs. This was done for two reasons: firstly, to gain a better understanding of the future interactions between ILs and starch-based biomass; secondly, to identify conditions under which starch significantly degrades in various ILs and thus determine suitable initial duckweed pretreatment conditions. Four different types of starch were pretreated: potato, rice, corn, and wheat. Pretreatments were carried out at 90 °C and 120 °C for 30 minutes, with a water content of 20% and at a solids loading of 10%. A higher water content would have lower IL regeneration costs and IL viscosity, but may also promote starch hydrolysis. The water content of 20% was selected as a compromise between these factors, and to allow easier comparison to results with lignocellulosic biomass.

Four protic ILs were selected for screening: [DMBA][HSO_4], [Hmim]Cl, [DMEtA][HCOO], and [MEA][OAc]. The first two of these are acidic ILs (H_0 of 1.62 and 1.48, respectively), whereas the two latter are neutral/basic ILs (as inferred from their pretreatment behaviours[73,74] and aqueous pH). A mass balance was conducted for each condition tested, consisting of the recovered solid that was ethanol- and water-insoluble (termed the water-insoluble residue), the recovered solid that was ethanol-insoluble and water-soluble (termed the ethanol-insoluble residue), and the degraded solubilised material detected by HPLC (see Fig. 5.3). The purpose of isolating both the water-insoluble and ethanol-insoluble residues was to gain insight into the degree of partial depolymerisation of the starch. Larger starch oligomers were expected to remain insoluble in water and ethanol, whereas smaller oligomers would be insoluble in ethanol but soluble in water.

Four different types of starch were chosen in order to examine whether the effects of IL pretreatment were consistent across starches with different physical properties such as granule size, molecular weight, and amylose/amylopectin ratio. While these properties were not measured for the starches used, trends for these have been reported in the literature. Starch granule size has been shown to decrease in the order potato > wheat > corn > rice.[75,76] The overall molecular weight of several of the different starches has been reported to decrease in the order potato > wheat, corn.[76–78] The amylose/amylopectin trend in these studies decreased in the opposite order, explained by the lower degree of polymerisation of linear amylose compared to highly branched amylopectin. However in some reviews collating starch data, large, overlapping ranges of amylose/amylopectin are reported for the four types of starch used in this study.[75,79,80] It would, therefore, not appear possible to generalise the trends amongst the types of starches used.

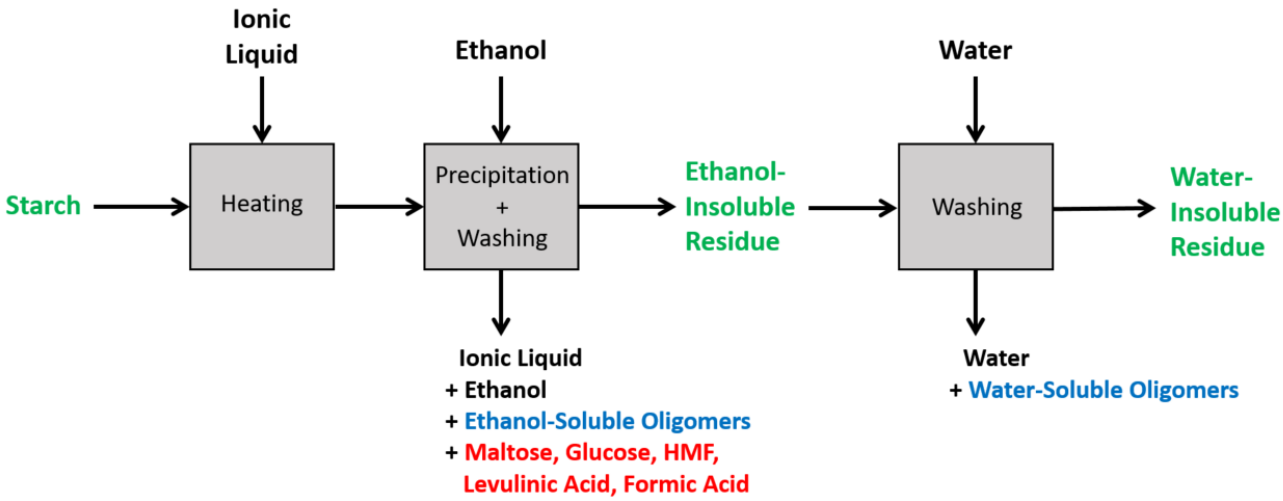


Figure 5.3: Material flow diagram during IL pretreatment of starch. Materials written in green are measured by mass, materials written in red are measurable by HPLC, and materials written in blue are not directly measurable.

[DMBA][HSO_4]

Results using [DMBA][HSO_4] are shown in Fig. 5.4. None of the starches were found to dissolve in [DMBA][HSO_4] at either 90 °C or 120 °C, remaining as powders, and no significant precipitation was observed upon addition of ethanol. It can, therefore, be assumed that there was not total disruption of the starch granule structure. At 90 °C, no degradation was observed by HPLC, and recovered solids were quantitative for all four starches. This was somewhat surprising, considering the elevated temperature and highly acidic nature of this IL. Furthermore, the water-insoluble residue accounted for above 96% of input starch for all types except rice (89%). It would therefore appear as though starch remains fairly stable in [DMBA][HSO_4] at 90 °C, with slow rates of degradation, if any. Mass closures ranged from 100% to 104%, possibly indicating incomplete removal of IL from the starch from ethanol washing.

At 120 °C, degradation products were observed by HPLC (around two thirds of which were glucose, and one third was maltose). Such degradation products were found to account for 1-15% of input starch, increasing in the order potato (1%) < corn (3%) < wheat (11%) < rice (15%). At this elevated temperature, the ethanol-insoluble residue was found to increase substantially, while the water-insoluble residue decreased substantially. This is consistent with partial depolymerisation of the starch, forming oligomers that are ethanol-insoluble but water-soluble. The water-insoluble residue decreases in the order potato (37%) > corn (22%) > wheat (8%) > rice (4%), opposite to that of the degradation rates. Therefore, it would appear as though the starch stability during pretreatment

decreases in the order potato > corn > wheat > rice. As the starches remained undissolved, and thus had their granular structure preserved, it is thought that the decreasing stability order in this acidic IL can be tied to a decreasing overall molecular weight, due in turn to a decreasing proportion of amylopectin.

There is also a significant unaccounted fraction across all four starches at 120 °C (22-51%). It is hypothesised that these are low molecular weight starch oligosaccharides that were soluble in the IL-ethanol mixture during the first ethanol wash. These oligosaccharides, which would not be detectable by HPLC, would have been discarded with the supernatant following this washing step. 120 °C is thus not a suitable temperature for starch preservation using [DMBA][HSO_4]. At this elevated temperature, the acidic nature of the IL leads to rapid starch depolymerisation. It is worth noting, however, that water-soluble, low-molecular weight starch oligomers have been targeted in previous studies due to their potential for modification.[20,81]

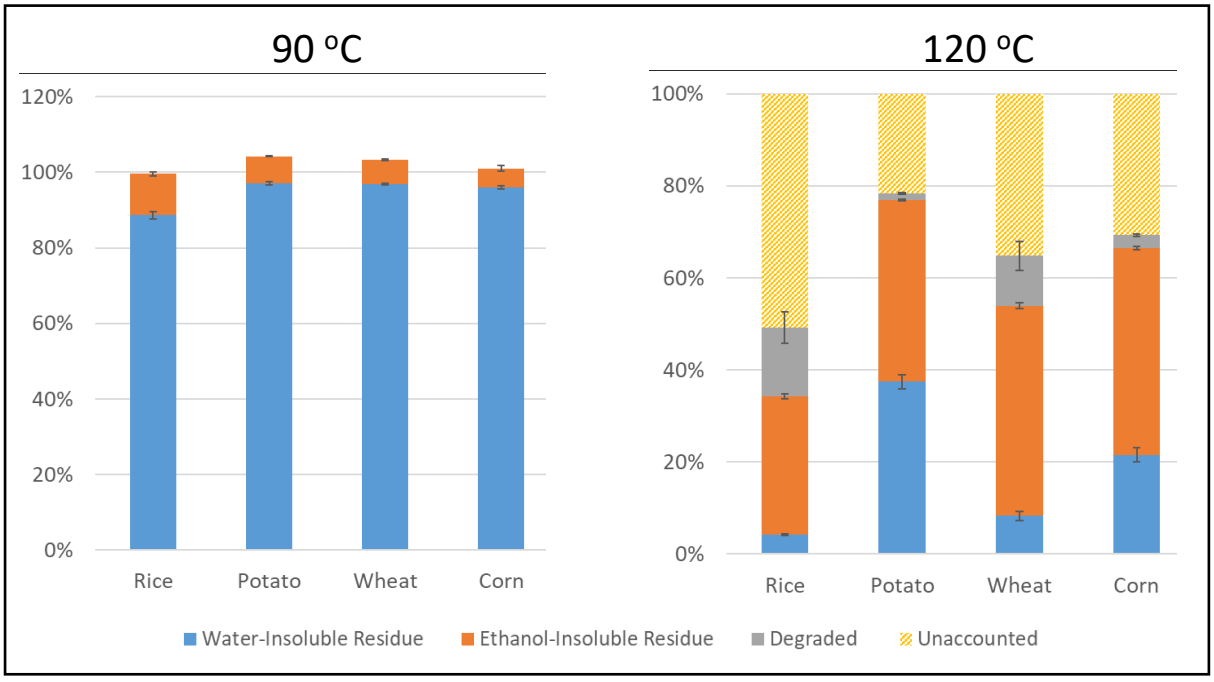


Figure 5.4: Fractionation of different starches following pretreatment with [DMBA][HSO_4]. All pretreatments were carried out at a solids loading of 10% wt/wt, with an IL water content of 20 wt%, for a duration of 30 minutes.

[DMEtA][HCOO] and [MEA][OAc]

Three of the starches were found to fully dissolve in these ILs, all except potato starch which partially dissolved. This is consistent with previous studies, showing that the $[HCOO]^-$ and $[OAc]^-$ anions are fairly effective at dissolving starch.[15,20,82–84] These basic anions break the granule structure of the powdered starch, leading to its dissolution, without extensive depolymerisation.[20] The resulting liquor was a thick gel. The starch was then precipitated upon addition of ethanol, forming a less viscous white-colourless gel that was insoluble in ethanol. Over the course of the ethanol washing procedure, this gel was replaced by a white solid. This was presumed to be an indication of the gel containing both starch and residual IL, with this residual IL being removed by ethanol washing and thus leaving only starch.[20] This fraction was recovered as a fairly hard, crumbly white solid for all starches.

Following the water wash, the appearance of the water-insoluble residue was dramatically different for all except potato starch, as shown in Fig. 5.5. Rice, wheat, and corn starch all produced a very hard, crystalline, white/colourless solid, whereas potato starch did not significantly change in appearance. This was observed at both 90 °C and 120 °C using both ILs. At 120 °C, the residue was completely colourless, whereas at 90 °C there were patches of white within the solid. The abundance of these patches decreased in the order corn > wheat > rice, seemingly correlated inversely with starch stability as determined using $[DMBA][HSO_4]$. CHN analysis was carried out on the water-insoluble residues, and no nitrogen (indicating presence of the cation) was detected, except 0.4 wt% in potato starch. It can therefore be concluded that the appearance of the recovered water-insoluble residues is not attributable to residual IL.

The changed appearance of the water-insoluble residue is thought to be due to starch retrogradation. This process describes the reassociation or recrystallization of the disrupted amylose and amylopectin chains in dissolved starch, which hydrogen bond together and form a crystalline structure.[85,86] Retrogradation is a complex process, dependent on a number of factors including time, water content, amylose/amylopectin ratio, and the molecular weights of the amylose and amylopectin fractions. [9,85–87] As a result, the change in appearance from the ethanol-insoluble residue to the water-insoluble residue (i.e. by washing with water) is more challenging to explain using the available data. Hypotheses include removal of residual IL from the solid structure, removal of any non-retrograded starch sections, or that the ethanol-insoluble residue retrogrades into a more stable conformation in the water. However, determining the mechanisms responsible for this change are beyond the scope of this study, and should be examined further in future.



Figure 5.5: Water-insoluble residue of starches following pretreatment with [DMEtA][HCOO]. Potato starch is shown on the left, while rice starch is displayed on the right. All pretreatments were carried out at a solids loading of 10% wt/wt, with an IL water content of 20 wt%, at 120 °C for a duration of 30 minutes.

Results using [DMEtA][HCOO] and [MEA][OAc] are shown in Figs. 5.6 and 5.7, respectively. Potato starch displayed the lowest yields for the water-insoluble residue, despite appearing to be the most stable starch using [DMBA][HSO_4], and despite having similar ethanol-insoluble residue yields. It was also the only starch to be only partially solubilised, and not to substantially change in appearance following the water wash. This observation is also difficult to explain using the available data. The suggested theory is that the dissolved potato starch did not undergo similar, if any, retrogradation (for example due to its molecular weight or a lower amylose/amylopectin ratio). Amylose retrogrades more rapidly than amylopectin,[86–88] with the latter found to form at least two states: either integrating with the amylose or remaining as clusters of amylopectin.[88] These compounds are both insoluble in ethanol, but amylopectin is soluble in water.[89] The low quantities of water-insoluble residue could thus be due to the solubilisation of such free clusters of amylopectin.

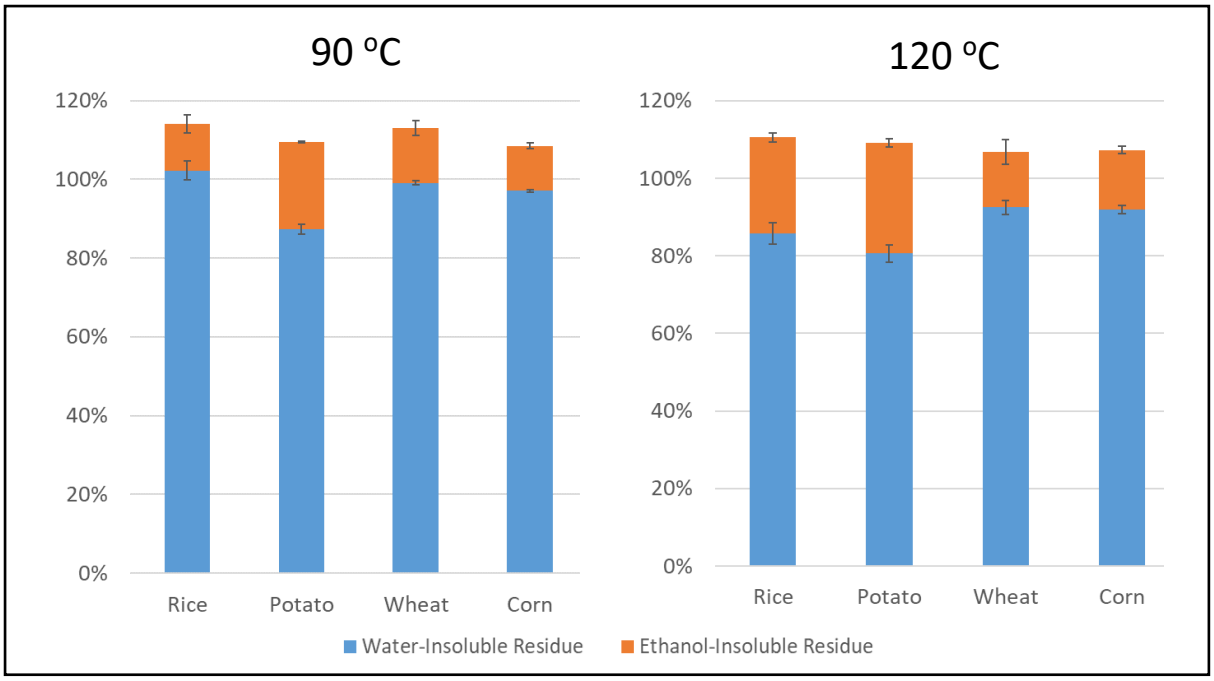


Figure 5.6: Fractionation of different starches following pretreatment with [DMEtA][HCOO]. All pretreatments were carried out at a solids loading of 10% wt/wt, with an IL water content of 20 wt%, for a duration of 30 minutes.

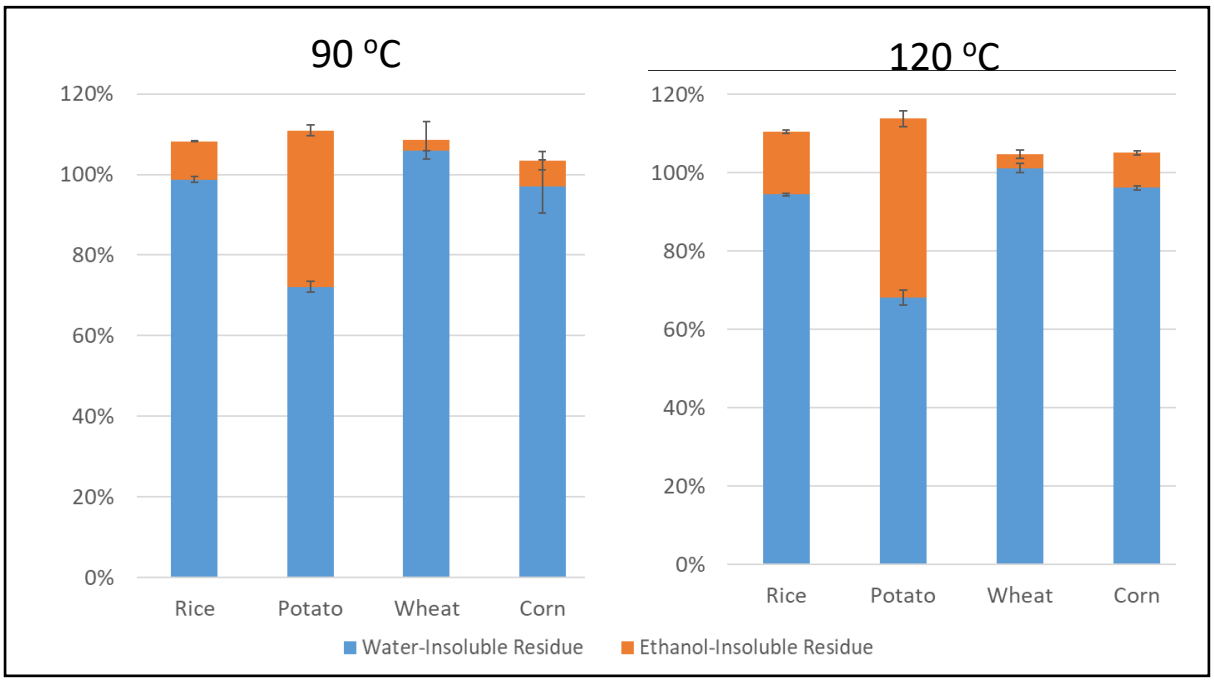


Figure 5.7: Fractionation of different starches following pretreatment with [MEA][OAc]. All pretreatments were carried out at a solids loading of 10% wt/wt, with an IL water content of 20 wt%, for a duration of 30 minutes.

The performance of both carboxylate ILs was very similar. At 90 °C, the water-insoluble residue was found to be near-quantitative for all starches, except potato starch. This was assumed to be due to the low acidity of both ILs leading to little depolymerisation despite dissolution of the starch. At 120 °C, the water-insoluble residue was found to reduce slightly, with larger drops using [DMEtA][HCOO] except for potato starch. This would appear to suggest that [DMEtA][HCOO] is slightly more acidic than [MEA][OAc], which may be expected due to the former having a stronger constituent acid.[90] Conversely, potato starch displayed a lower water-insoluble residue in [MEA][OAc] despite it appearing to be less acidic. This may be due to differences in starch solubility and granule disruption between both ILs.

Over 100% mass balances were observed under all conditions. This was taken to be a sign of residual IL in the recovered solids, in the solid recovered following ethanol washing (due to higher solubility of these PILs in water than in ethanol, and due to the extra washing step). Similar results have been noted in the literature using similar ILs.[20] Additionally, some water may have been trapped within the retrograded, crystalline starch structure.

Both ILs would therefore appear to be promising solvents for pretreating starch-based biomass at elevated temperatures. However, for extended durations at 120 °C degradation may eventually increase to substantial levels.

[Hmim]Cl

Results using [Hmim]Cl are shown in Fig. 5.8. Three of the starches were found to fully dissolve in this IL, all except potato starch which partially dissolved. This is consistent with literature reports, stating that the Cl^- anion is highly effective at dissolving starch,[8,14,20,25] but also describing incomplete disruption of potato starch granules in a similar IL.[14] At 90 °C, recovered starches had the same physical appearance as those pretreated with both neutral ILs. At 120 °C, however, almost no solid was recovered, except using potato starch.

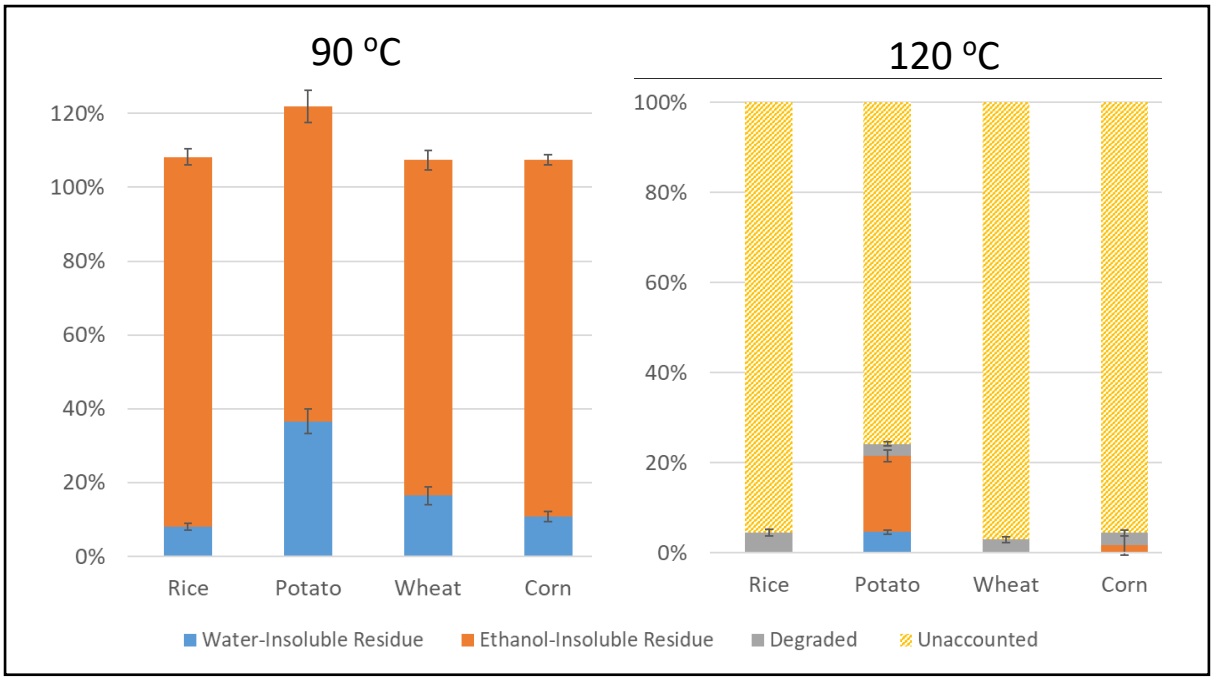


Figure 5.8: Fractionation of different starches following pretreatment with [Hmim]Cl. All pretreatments were carried out at a solids loading of 10% wt/wt, with an IL water content of 20 wt%, for a duration of 30 minutes.

At 90 °C, mass balances were all found to be above 100%, once again attributed to residual IL that was not removed by ethanol washing. [Hmim]Cl displayed the lowest water insoluble residues at both 90 °C and 120 °C, far lower than the similarly acidic [DMBA][HSO_4]. At 90 °C, despite quantitative ethanol-insoluble residues, water-insoluble residues were low (8-37%). These results indicate substantial depolymerisation of the starches in the acidic IL, forming ethanol-insoluble but water-soluble oligomers. The depolymerisation of starch dissolved in ILs containing the Cl^- anion has been reported in several studies.[14,20,91] At 120 °C, only potato starch displayed any significant water-insoluble residue. The extent of starch loss in [Hmim]Cl was assumed to be due to the dissolution of the starch in the IL, with the disruption of the granular structure allowing easier depolymerisation by this acidic IL; whereas all starches were insoluble in [DMBA][HSO_4] and thus did not depolymerise as extensively. This would explain the lower water-insoluble residue at 90 °C. Furthermore, the higher concentration of dissolved starch in the solution may have led to more widespread but less complete degradation of starch. This would explain the lower proportion of starch degradation products detected using [Hmim]Cl than using [DMBA][HSO_4] at 120 °C, and the higher proportion of unaccounted starch (attributed to ethanol-soluble starch oligomers).

Results using [Hmim]Cl generally corroborate the starch stability order determined using [DMBA][HSO_4]. At both temperatures, potato starch displayed the highest water-insoluble residue. At

90 °C, wheat and corn starches showed similar water-insoluble residues, while at 120 °C, only corn starch showed ethanol-insoluble residue. Rice starch had the lowest water-insoluble residue at 90 °C. These observations are in line with the findings of Karkkainen et al, who found that amylopectin in potato starch degraded more slowly in [Bmim]Cl than corn, wheat, and rice starches.[14] This therefore corroborates the previously proposed stability order of potato > corn > wheat > rice being due to decreasing amylopectin content.

[Hmim]Cl is therefore not a suitable pretreatment solvent for starch-based biomass due to its acidity and ability to solubilise starches, leading to degradation and solubilisation of starch oligomers.

5.3.2 Pretreatment of Virgin Duckweed

Spirodela polyrhiza was pretreated using [DMEtA][HCOO] at 120 °C, and [DMBA][HSO_4] at 90 °C, 120 °C, and 150 °C, performing timecourse experiments for all. The aim of these pretreatments was to observe the effect on the duckweed composition and digestibility, as well as on the partitioning of the protein fraction. An optimal pretreatment would both preserve starch in a highly digestible pulp and produce a high-purity protein fraction. However, it was anticipated that achieving both goals simultaneously may not prove feasible. Therefore, while the more prolonged pretreatments at 120 °C and 150 °C were expected to hydrolyse a substantial proportion of the starch, they were included in order to observe the effect of temperature on protein partitioning behaviour. Full pretreatment and compositional analysis data for the pretreated samples are provided in the Appendix.

Duckweed Composition

The composition of the untreated duckweed was first determined using the NREL compositional analysis (CA) protocol.[61] The Megazyme starch assay was then used to differentiate the glucan fraction into starch and cellulose.[63] However, as shown in Table 5.1, this yielded an unsatisfactory overall mass balance of 70%, including a mass closure of 55% when analysing the extractive-free material during the compositional analysis protocol. Several measures were taken to identify the missing mass fractions, allowing a quantitative mass balance to be reached.

Firstly, extraction with hexane was attempted, in order to remove any lipids.[92,93] However, no significant difference was found between two-stage (EtOH and H_2O) and three-stage (EtOH, H_2O, and C_6H_{14}) extractive content.

Secondly, the extractive-free biomass was directly ashed. Similarly to the results in Section 4.3.5, a substantial ash fraction was detected through this method, that was not detected through the standard CA protocol: 22% of the extractive-free biomass, or 14% on an overall basis. As in Section

4.3.5, this ash fraction would appear to be solubilised during the CA protocol and is thus not detectable.

Thirdly, a protein mass balance was carried out on the biomass over the entire process (see Fig. 5.9). According to the NREL CA protocol, protein was expected to be solubilised during the H_2O extraction.[61] The protein balance of the course of the extraction process revealed that only 35% of the original protein was removed during the H_2O extraction, with protein accounting for 35% of the remaining extractive-free biomass. In order for this fraction to be detectable, it would be required to remain within the solid fraction and would be classed as "acid-insoluble lignin" (AIL) in the CA protocol. However, protein analysis on the AIL revealed it only accounted for 19% of the protein in the extractive-free biomass. It was, therefore, concluded that the remaining 81% (accounting for 28% of the extractive-free biomass) must have been solubilised during the CA procedure. This may have been partly due to degradation of the protein as a result of either the first stage hydrolysis (concentrated sulfuric acid at 30 °C for 60 minutes) or the second stage hydrolysis (autoclaved in dilute sulfuric acid at 121 °C for 60 minutes). The presence of dissolved protein and/or oligopeptides in the liquid phase was also concluded to be the reason behind the extremely slow filtration through the filtering crucibles.

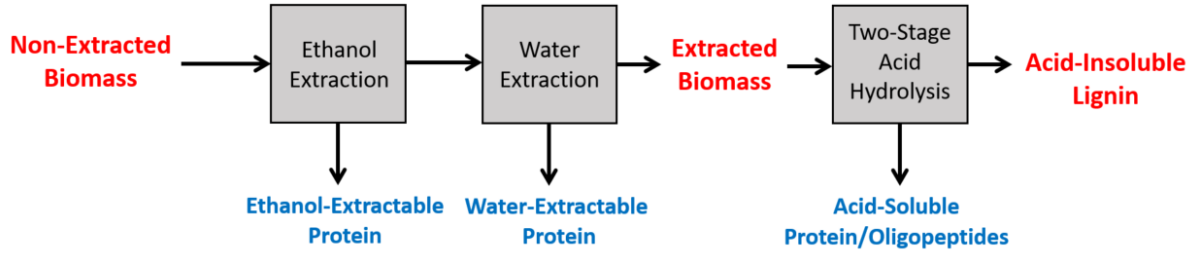


Figure 5.9: Protein material flow during compositional analysis. The protein content of material written in red was measured through CHN analysis. Protein content of the material written in blue was determined by mass balance.

Table 5.1: Effect of extra analysis on determined composition of *Spirodela polyrhiza*.

	Cellulose	Starch	Hemicellulose	Lignin	Protein	Ash	Extractives (H_2O + EtOH)	Acetyl	Mass Balance
CA + Starch	7.3% ±0.3%	3.2% ±0.1%	6.3% ±0.1%	18.5% ±0.3%	-	1.5% ±0.3%	32.9% ±2.9%	0% ±0%	69.7% ±0.6%
CA + Starch + Protein + Direct Ashing	7.3% ±0.3%	3.2% ±0.1%	6.3% ±0.1%	13.9% ±0.3%	35.0% ±0.7%	16.2% ±0.9%	20.5% ±2.9%	0% ±0%	102.4% ±1.1%

According to the literature, duckweed tends to rapidly accumulate starch during periods of stress, rather than periods of rapid growth in favourable conditions.[7,94–96] The duckweed was harvested during a period of high temperatures and consistent sunlight, and was thus growing extensively (covering the canal, see Fig. A5-2 in the Appendix). The glucan content (and particularly starch content) of the feedstock is thus fairly low, while the protein content is high (higher than the large majority of agro-residues considered for protein extraction,[30] but at the top of the reported range for duckweed[37,97,98]).

Starch Recovery

Starch recoveries under all four conditions are displayed in Fig. 5.10. Based on the results in Section 5.3.1, it was expected that high starch recoveries would be observed using [DMEtA][HCOO], as well as [DMBA][HSO_4] at 90 °C. Above 90 °C, the highly acidic [DMBA][HSO_4] was expected to hydrolyse the starch rapidly. The results using duckweed align fairly closely with this predicted behaviour.

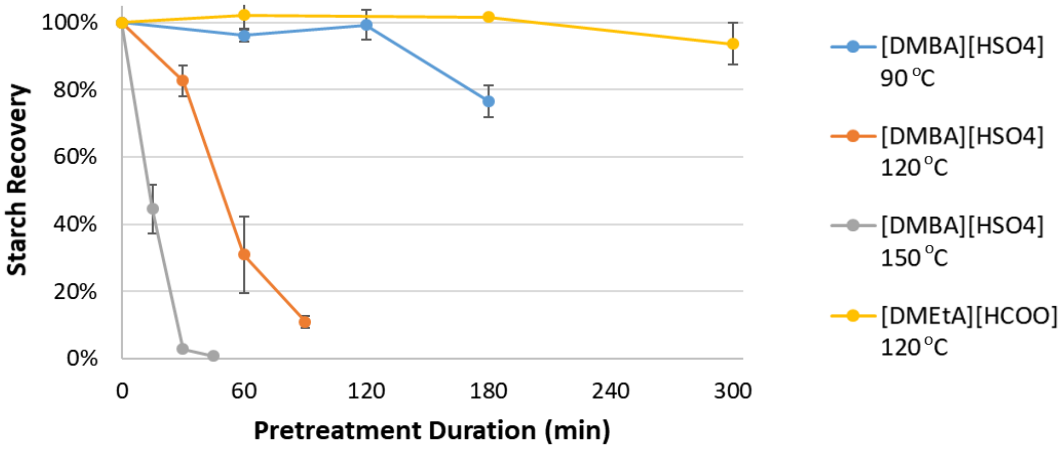


Figure 5.10: Starch recovery in *Spirodela polyrhiza* under several pretreatment conditions. All pretreatments were carried out with 20 wt% water, and at a biomass loading of 10% wt/wt.

Using [DMEtA][HCOO], quantitative starch recovery is observed between 1 and 3 hours, with the slight decrease at 5 hours found not to be statistically significant. This is somewhat in line with observations from Section 5.3.1, in which raising the temperature from 90 °C to 120 °C led to a slight decrease in water-insoluble residue (5-16% depending on starch type), showing that depolymerisation of the starch was occurring, albeit at a slow rate.

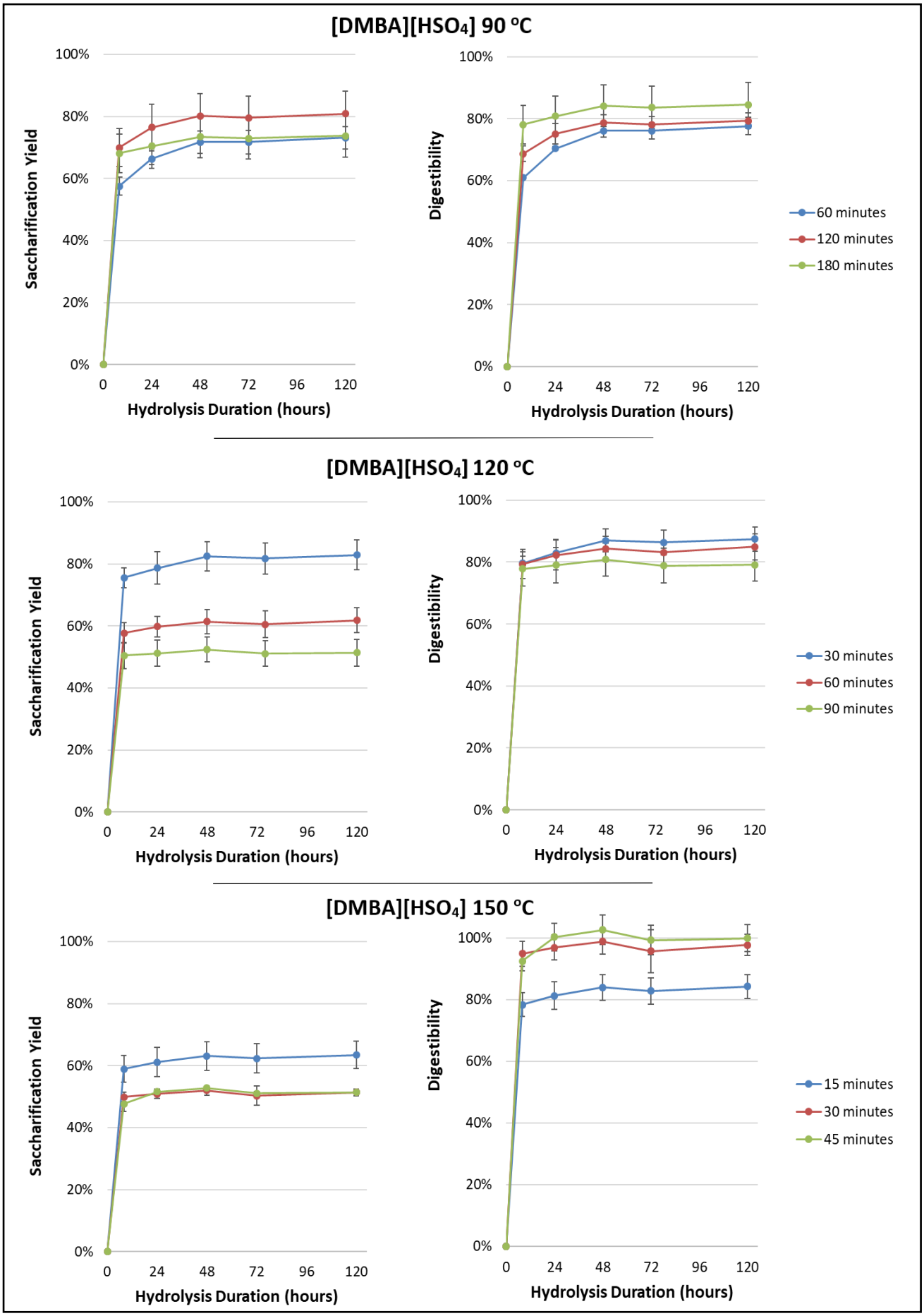
Using [DMBA][HSO_4], results were found to be very dependent on temperature. At 90 °C, near-quantitative recoveries were observed up to 2 hours. However, a significant drop occurred after 3 hours, with recoveries decreasing to 77%. It would, therefore, appear that the starch is depolymerising

at 90 °C, but at a slow rate. Initially, the resulting starch fragments remain insoluble in the IL/ethanol mixture, but begin to solubilise between 2 and 3 hours. Expectedly, increasing the temperature accelerates the kinetics of this depolymerisation, with no quantitative recoveries observed at any of the measured timepoints at either 120 °C or 150 °C. After 30 minutes at 150 °C, near-quantitative removal of the starch has occurred.

Interestingly, starch removal tracks hemicellulose removal differently at different temperatures using [DMBA][HSO_4] (numerical data provided in Table A5-2 in the Appendix). At 150 °C, both values are very similar across all timepoints, with rapid depolymerisation and solubilisation. At 120 °C, the initial increase in hemicellulose removal after 30 minutes (37%) is larger than that of starch removal (17%). However, hemicellulose removal starts to plateau between 60 and 90 minutes (52% and 56%), whereas starch removal continues to increase over the same time period (to 69% and 89%). Results at 90 °C are similar: hemicellulose displays a rapid initial removal with a slow subsequent increase, whereas starch displays very low initial removal that begins to accelerate later on. This is likely because certain parts of the hemicellulose structure are more easily hydrolysable (e.g. the α-glycosidic side branches) while others are more recalcitrant (e.g. the β-glycosidic linked backbone).[99–103] The starch, meanwhile, would appear to be harder to remove initially, possibly due to its organised granular structure, but would not contain a substantial recalcitrant moiety. Similarly, hemicellulose removal using [DMEtA][HCOO] (18-22% over 1-5 hours) was found to be substantially higher than starch removal (which was not observed significantly), and once again showed an initial large increase before rapidly slowing down.

Saccharification

Enzymatic saccharification was performed for every generated pulp as well as the untreated material, with timepoint sampling after 8, 24, 48, 72, and 120 hours of hydrolysis. Results are presented in Fig. 5.11. The relatively large variances displayed were presumed to be due to heterogeneity in the biomass (harvested from a canal). As a result, statistical analysis was used to determine whether differences between samples were statistically significant, and to what degree.


[DMBA][HSO4] 90 °C
Saccharification Yield
Digestibility
Hydrolysis Duration (hours)
60 minutes
120 minutes
180 minutes
[DMBA][HSO4] 120 °C
30 minutes
60 minutes
90 minutes
[DMBA][HSO4] 150 °C
15 minutes
30 minutes
45 minutes

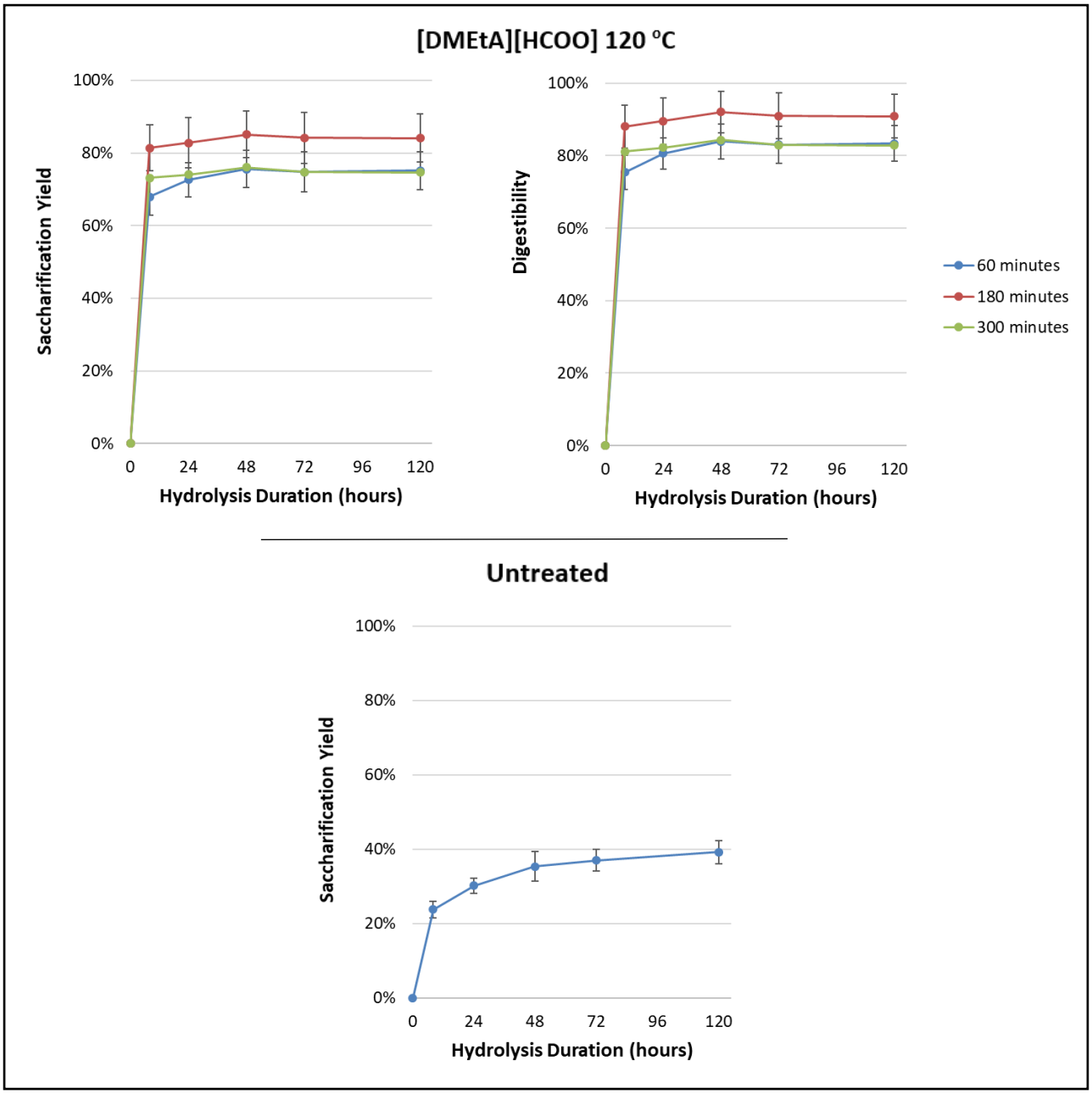


Figure 5.11: Saccharification and digestibility kinetics of pulps pretreated using varying ionic liquids and temperatures. All pretreatments were carried out on *Spirodela polyrhiza*, with 20 wt% water, and at a biomass loading of 10% wt/wt. It should be noted that saccharification yield and digestibility are numerically equivalent in untreated biomass.

For all pulps except those pretreated for 1-2 hours at 90 °C, saccharification was over 90% complete after 8 hours of hydrolysis, substantially faster than observed using more "traditional" lignocellulosic biomass (see Section 2.3.5). Such accelerated rates are extremely important, allowing a potential trade-off between enzyme loading and hydrolysis duration. As pretreatment severity increased, hydrolysis kinetics tended to increase slightly, likely as a result of increased disruption of the biomass

structure and thus higher substrate accessibility. Untreated biomass displayed significantly slower kinetics, taking 48 hours to reach 90% of its final value. The untreated biomass was found to be fairly digestible compared to more traditional lignocellulosic feedstocks (e.g. *Miscanthus* in Chapter 2, or even the more digestible wetland feedstocks in Chapter 4), reaching 39% after 120 hours. This may be due to starch accounting for around one third of the glucan in the feedstock, or to the non-lignocellulosic biomass structure.

Pretreatment using [DMEtA][HCOO], at all conditions, significantly enhanced both saccharification yield and digestibility relative to untreated biomass, as well as the hydrolysis kinetics. This was despite relatively little apparent disruption of the biomass structure or change in composition (examined later). Particularly for 180 and 300 minutes of pretreatment, pulps displayed very rapid hydrolysis kinetics, with 97% and 98% of the final yield reached after 8 hours of hydrolysis. Saccharification yields and corresponding digestibility values were very similar, due to the low levels of glucan degradation in this neutral IL. 180 minutes appeared the best pretreatment duration tested for both saccharification yield and digestibility. However, statistical analysis revealed that the difference between all three conditions was only significant after 8 hours of hydrolysis. At longer hydrolysis durations, all three conditions are not statistically different, as the slower kinetics of the less severely pretreated samples eventually converge.

Saccharification behaviour using [DMBA][HSO_4] was found to be dependent on pretreatment temperature. At 90 ^oC, pulp saccharification and digestibility was found to be substantially better than untreated biomass at all three durations, despite relatively little apparent disruption to the biomass structure. There was little statistical difference between all three conditions, despite 120 minutes and 180 minutes appearing most successful for saccharification yield and digestibility. As with [DMEtA][HCOO], the only statistically significant differences were at short hydrolysis durations. After 8 hours of hydrolysis, the 60 minute pulps had significantly lower saccharification yields and digestibilities than the 120 minute and 180 minute pulps, respectively. However, these differences would appear to be due to the slower kinetics of the less severely pretreated samples, and were eliminated at longer durations.

At 120 ^oC, pulps pretreated using [DMBA][HSO_4] display more variability in results. The shortest pretreatment duration of 30 minutes is the optimal condition for saccharification yield at all hydrolysis timepoints, with similar results to those using [DMEtA][HCOO] and [DMBA][HSO_4] at 90 ^oC. Saccharification yields decrease as pretreatment severity increases, although differences between 60 and 90 minute durations are only significant at the final timepoint. The two longer duration pretreatments have saccharification yields that are more comparable to those of the untreated

biomass after 120 hours of hydrolysis (62% and 51% vs 39%), albeit with much faster kinetics. Despite this, however, there is no statistical difference between the digestibilities of the three sets of pulps, which are all elevated (79-88%). Therefore, the lower saccharification yields of the two longer pretreatment durations are due to glucan degradation rather than enzyme inhibition due to pretreatment severity.

At 150 °C, pulps also display variability in results depending on pretreatment duration. Trends in saccharification yields are similar to those at 120 °C. The shortest pretreatment duration (15 minutes) leads to the highest yields at all timepoints, while results for both 30 minutes and 45 minutes are near-identical. Saccharification yields are generally fairly low at this temperature (51-63% after 120 hours), although the hydrolysis kinetics are much improved relative to untreated biomass. Trends for digestibility, however, are the opposite to those for saccharification yield. Both longer pretreatments generated pulps with near-quantitative digestibilities, significantly higher than the shortest pretreatment, which are still elevated and in line with those of lower temperatures (84%). Therefore, as at 120 °C, the low saccharification yields of more severe pretreatments are due to glucan degradation rather than enzyme inhibition.

At 150 °C, pulp digestibility displayed a strong negative correlation ($r = -1.00$, $p < 0.05$) with starch recovery, while saccharification yield displayed a strong positive correlation ($r = 1.00$, $p < 0.05$) with starch recovery. It would, therefore, appear that at this elevated temperature, the structure of the duckweed is being completely disrupted at 30 and 45 minutes of pretreatment duration, depolymerising the starch into IL-soluble fragments (and thus limiting the maximum yield) but making the remaining glucan highly accessible to the enzymes. This can be seen through a change in appearance of the pulp as pretreatment duration increases, from clearly defined fronds to one single, solid pulp. This clear trade-off between digestibility and yield is not observed at the lower temperatures using [DMBA][HSO_4], nor using [DMEtA][HCOO]. This suggests two "degrees" of disruption of the biomass structure: the first increasing digestibility relative to untreated biomass, leading to digestibilities of around 80-90%; the second increasing digestibility to quantitative levels.

Maximum saccharification yields were compared for each different pretreatment condition. This was at 180 minutes using [DMEtA][HCOO]; using [DMBA][HSO_4], this was at 120 minutes at 90 °C, 30 minutes at 120 °C, and 15 minutes at 150 °C. Yields at 150 °C were significantly lower than all others, while there were no significant differences between the other three conditions. Digestibilities at these conditions were similar: the only significant difference was that of [DMEtA][HCOO] being higher than that of [DMBA][HSO_4] at 90 °C.

Maximum digestibilities were also compared for each different pretreatment condition. This was at 180 minutes using [DMEtA][HCOO]; using [DMBA][HSO_4], this was at 180 minutes at 90 °C, 30 minutes at 120 °C, and 45 minutes at 150 °C. It should be noted that this was the same condition as for maximum saccharification using [DMEtA][HCOO] and [DMBA][HSO_4] at 120 °C. Digestibility using [DMEtA][HCOO] was not found to be significantly different to those using [DMBA][HSO_4]. Statistical differences were found between different temperatures using [DMBA][HSO_4]; digestibilities at 150 °C were significantly higher than those at 90 °C, and higher than those at 120 °C for short hydrolysis durations. Saccharification yields at these conditions were similar: the only significant differences in yields was [DMBA][HSO_4] at 150 °C being significantly lower than all other conditions.

Due to the combination of high saccharification yields and high digestibilities, the optimal operating conditions for sugar release were thus determined to be [DMEtA][HCOO] for 180 minutes and using [DMBA][HSO_4] for 30 minutes at 120 °C. At these conditions, saccharification yields of 76-81% were achieved after 8 hours of hydrolysis, rising to 83-84% after 120 hours. The corresponding digestibilities were 80-88% and 87-91%. This highlights the potential of duckweed for bioethanol production: these yields and digestibilities are similar to, or higher than, traditional lignocellulosic energy crops (such as *Miscanthus*, willow, sugarcane bagasse, or wastewood) pretreated in the ionoSolv process.[74,104–106] This is despite much milder conditions and shorter hydrolysis durations. While it must be noted that the carbohydrate contents of the *S. polyrhiza* strain used is much lower than most feedstocks investigated for bioenergy, enzyme loadings were adjusted correspondingly, and starch recovery results were in line with those obtained using pure starch. Similar trends and results can thus be expected with strains containing higher carbohydrate contents.

Comparison with the (relatively small) number of other duckweed pretreatment studies is challenging for a number of reasons. Many studies focus on bioethanol production, using either simultaneous saccharification and fermentation configurations, or sequentially. In such cases, the hydrolysis performance is often not evaluated in great detail, instead focussing on ethanol yield.[59,107–109] The second main reason why comparison is challenging is the lack of reporting of enzyme loadings, the use of differing loadings, or the use of different classes of enzymes (e.g. pullulanases). This is also not helped by a lack of "control" hydrolysis on completely untreated duckweed which would allow the relative improvements in digestibility to be quantified, missing from almost all investigations except those of Zhao et al (see below).[70,110] Despite this, results obtained here appear in line with those of other such studies.[54,56–58,111,112]

Zhao et al. initially investigated the effect of enzyme loading on the sugar release of a water-, acetone-, and ethanol-extracted duckweed slurry. Maximum glucose release was found to be 85%

after 8 hours of hydrolysis, using a mixture of cellulase and β-glucosidase. This was using 4000 U/g biomass of both enzymes, compared to 230 U/g of cellulase, 120 U/g of α-amylase, and 10 U/g of amyloglucosidase in this study. However, this was reduced to around 60% and 80% glucose after 8 and 24 hours by Zhao, following reduction to 100 U/g of both enzymes. In a follow-up study, following steam explosion of freeze-milled duckweed, sugar release was increased to around 70% after 8 hours, and 80% after 24 hours at an even lower enzyme loading (20 U/g of cellulase and 2 U/g of β-glucosidase), compared to 10% for untreated material.[110] Although comparison would ideally be using the same enzymes and loadings, It would, therefore, appear as though steam explosion renders the biomass more digestible compared to IL pretreatment. This is likely due to the gelatinisation and partial depolymerisation of starch at the steam explosion conditions (210 ^{o}C for 10 minutes). Any dissolved oligomers would still be available for saccharification following the pretreatment process as the entire pretreated slurry was directly saccharified. This is unlike IL pretreatment, in which any ethanol-soluble starch oligomers would remain dissolved in the IL liquor. Additionally, Zhao et al's study used milled duckweed, which was found to release 40% of sugars without any treatment. Thus, the improved performance of the steam exploded slurry may be partially due to the milling of the input material.

Protein Partitioning

A material flow diagram depicting the protein fractionation during pretreatment is provided in Fig. A5-4 in the Appendix. The protein content of the pulp and lignin streams was determined for all conditions and a mass balance thus carried out, with results displayed in Fig. 5.12. Neither the lignin nor the pulp fractions were found to have enriched protein contents relative to the untreated biomass (see Appendix for numerical data). Using both [DMBA][HSO_4] and [MBA][HSO_4], protein content of the pulp decreased with pretreatment duration, while the protein content of the lignin fraction increased. Using [DMEtA][HCOO], protein content stayed constant at around 25% in both the pulp and the lignin fractions.

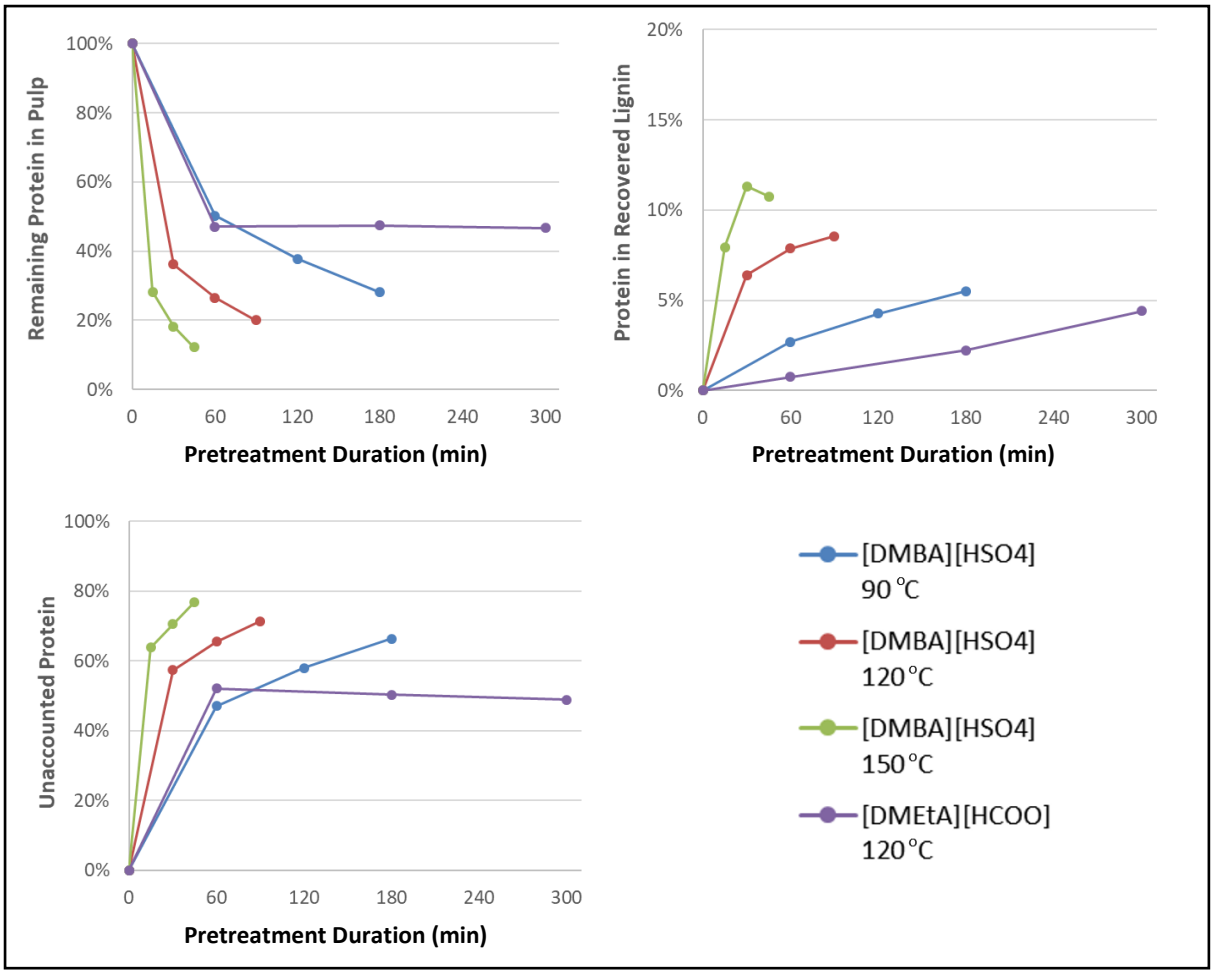


Figure 5.12: Protein partitioning during IL pretreatment of *Spirodela polyrhiza*. Unaccounted protein refers to remaining protein not detected in the pulp or lignin fractions. All pretreatments were carried out with 20 wt% water, and at a biomass loading of 10% wt/wt.

The behaviour of both ILs is fairly distinct regarding protein removal from the pulp. Using [DMBA][HSO_4], protein was selectively removed from the pulp. Trends were very similar across temperatures, with kinetics accelerated at higher temperatures Although the rate of removal was observed to decrease over time at a given temperature, there was no clear sign of a plateau as with [DMEtA][HCOO]. This may be a sign of proteins being broken down into oligopeptides and dissolved into the IL: the peptide bonds linking the amino acids that make up proteins can be hydrolysed, with this reaction strongly catalysed by acidic or basic conditions, as well as temperature.[113–115] The standard method for full hydrolysis of a protein into its constituent amino acids is heating in 6M HCl under vacuum at 110 °C for 18-24 hours.[116] Protein yield in the lignin fraction tended to increase over time, due to both increasing lignin yields and an increasing protein content. However, due to the low quantities of recovered lignin, this yield is fairly low (reaching a maximum of 11% of starting protein). Additionally, protein yield in the lignin fraction would appear to be limited to around 10% based on

trends at 150 °C and 120 °C. This was somewhat surprising, as the extracted proteins were expected to precipitate out with the lignin after addition of water to the acidic IL, as proteins are often recovered following alkaline extraction by addition of acid to lower the pH.[30,117]

Using [DMEtA][HCOO], approximately half the protein was removed from the biomass by 60 minutes of pretreatment, and this value did not change substantially over time. This may be due to the relatively low degree of disruption of the biomass using this IL, as well as its less acidic nature leading to a lower degree of protein hydrolysis. The extracted fraction may also correspond to the water-soluble fraction of leaf protein, which is typically between 40-50%.[118] The amount of protein removed from the pulp using [DMEtA][HCOO] is also comparable to that removed by alkali extraction at pH 8.5 from *S. polyrhiza* in a study by Yu et al.[97] The protein yield in the lignin fraction increased consistently over time due to increasing lignin yields, rather than due to enrichment. As lignin yields were very low during the pretreatment (due to the slower pretreatment kinetics of [DMEtA][HCOO] and the low lignin content in the biomass), protein yields in this fraction were thus below 5%.

Under all conditions, the total mass balance from the pulp and lignin fractions was very low, with 49-77% of the original protein unaccounted. It was presumed that this fraction must be contained within the IL liquor. In order to recover any dissolved protein, dialysis was carried out on selected pretreatment liquors: 60 and 180 minutes using [DMEtA][HCOO], and 30 and 60 minutes using [DMBA][HSO_4] at 120 °C. The resulting solution was then freeze-dried. The recovered solids were paler in appearance (see Fig. 5.13), but were found to only have a moderately increased protein content at most conditions: 23% and 49% for 60 and 180 minutes using [DMEtA][HCOO], and 46% and 53% for 30 and 60 minutes using [DMBA][HSO_4]. However, the recovered solid only accounted for 2-5% of the starting protein, and thus did not significantly affect the overall protein mass balance. Two hypotheses are put forward to explain the large unaccounted protein fraction:

1. Proteins dissolved in the IL are being hydrolysed into oligopeptides that are too small to be recovered by dialysis. If such oligopeptides were recoverable (e.g. by electrophoresis or using a smaller membrane pore size), the purity of the resulting solid fraction would thus be expected to increase substantially.
2. The nitrogen-to-protein conversion factor of 6.25, that has been shown to be suitable for untreated duckweed in the literature,[62] is no longer accurate in the pretreated material.

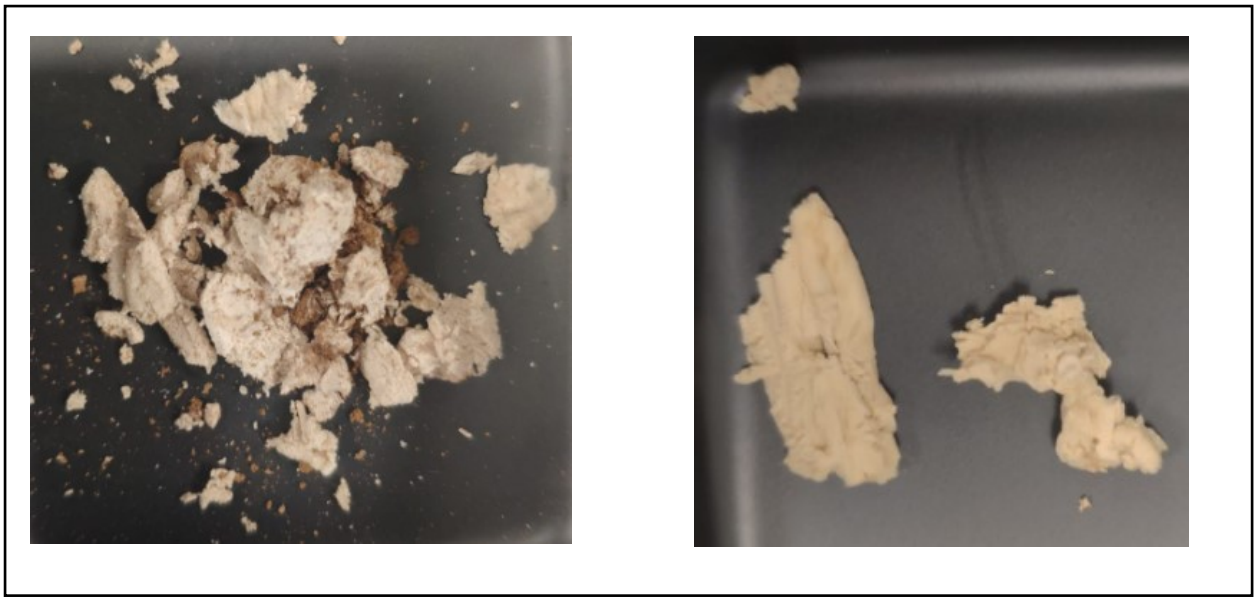


Figure 5.13: Solid recovered following dialysis of IL liquors. Figures are Right: from pretreatment with [DMBA][HSO_4] for 60 minutes at 120 °C, Left: from pretreatment with [DMEtA][HCOO] for 180 minutes at 120 °C. All pretreatments were carried out on *Spirodela polyrhiza*, with 20 wt% water, and at a biomass loading of 10% wt/wt.

Pulps obtained following pretreatment with [DMEtA][HCOO] were found to contain a large fraction of the protein in the starting biomass, albeit at low purity, and demonstrated promising saccharification performance. It was therefore hoped that saccharification would lead to a concentration of protein in the solid fraction. Following saccharification, the solid residue was collected, washed with DI water (in order to remove any enzymes), and freeze-dried. This residue was found to have a moderately increased protein content relative to the pulp: 36, 46%, and 41% in pulps pretreated for 60, 180, and 300 minutes. This was equivalent to a yield of 97%, 71%, and 70% relative to the protein contained within the corresponding pulps, or 46%, 34%, and 33% of the original protein.

While these protein partitioning results may not seem that promising at first glance, comparison with previous studies shows a possible cause for optimism, albeit one that will require further study. Firstly, should the oligopeptides in the IL liquor be recoverable, a high purity protein fraction would be expected, with the reduced molecular weight a desirable property for nutritional applications.[41] This would be the ideal outcome, due to the high purity of such a stream, but depending on the degree of hydrolysis of the protein may not be feasible. It would be similar to the protein extraction process reported by Wahlström et al, who used urea and carboxylate-based using Deep Eutectic Solvents (DES) to extract protein from Brewer's Spent Grain (BSG), a common high-protein waste product from the brewing process.[33] 80% of proteins were extracted after 1 hour at 80 °C, and were recovered by dialysis to a purity of around 50% (containing both polysaccharides and lignin). A 37% loss in was observed

between extraction and solid recovery, attributed to protein fragmentation (to below the molecular weight cut-off of 3.5 kDa) as in this study.

Secondly, compared to a number of other studies attempting to integrate bioethanol production with protein extraction, the final protein concentrations in the post-saccharification residue are relatively elevated; the high starting protein concentrations in the duckweed also mean the absolute yields may still be reasonable, particularly for valorisation as a secondary co-product. For example, Hou et al. increased protein concentration in brown seaweed from 4% to 14% (with a 97% yield) in post-saccharification residue following a simple milling pretreatment.[47] Similarly, Hamley-Bennett et al. reported an increase in protein content from 8% to 15% following steam pretreatment and saccharification of sugar beet (although no yield was provided).[46]

Thirdly, there are a number of bioethanol-protein extraction studies that have investigated the effect of pretreatment on protein extractability. However, these studies have not involved the production of a high-purity protein stream as part of the biomass fractionation process, but have instead involved traditional extraction methods either before or after pretreatment. Kehili et al. found that supercritical CO_2 treatment substantially improved alkaline protein extraction from tomato seeds and peels, allowing purities of 36% and 81% to be reached, from initial contents of 13% and 39% (although no yield was provided).[39] However, CO_2 pretreatment was for carotene extraction, with a liquid hot water pretreatment used after protein removal. A number of studies have found ammonia-based pretreatments to improve protein extractability. De La Rosa et al. found AFEX pretreatment of bermudagrass increased extractability from 55% to 80% (by alkaline extraction), with 90% saccharification yield, although protein recovery was not evaluated.[43] Improvements were also found by Urribarri et al. following liquid NH_3 treatment. Alkaline extractability of elephant-grass increased from 12% to 53%, although recovery was not evaluated,[44] while that of cassava leaves increased from 20% to 29% (with 36% purity).[45] A series of two studies by Kemppainen and Rommi found steam explosion pretreatment to also improve protein extractability and recovery as well as sugar release from BSG, with substantial depolymerisation but little solubilisation (or enrichment) of the protein during the pretreatment.[117,119] Final recovery yields increased from 10% to 25% following steam explosion without protease enzymes, and from 45% to 65% with protease enzymes. There was, however, difficulty in separating the lignin from the protein, with co-precipitation of both after acid addition following alkali extraction, leading to low purities of 30%.

Two studies have also observed the effect of pretreatment following extraction, with both leading to low saccharification yields, which in the work of Bals et al. were explicitly shown to be lower than in non-extracted biomass.[41,42] Further work should, therefore, focus on the studying the extractability of

proteins after pretreatment, both from the pulp and from the protein-enriched post-saccharification residue. Considering duckweed protein extractability was found to be around 40-46% using *Spirodela polyrhiza* and *Lemna minor* by Brouwer and Yu at a moderately alkaline pH of 8, with purities of 67-68%, an improvement upon this by IL pretreatment may allow easy extraction of high-purity protein.[97,118]

Pulp Composition

Full pretreatment and compositional analysis datasets are provided in the Appendix. Pulps pretreated using [DMBA][HSO_4] displayed high hemicellulose removal, moderate delignification, and glucan recoveries that mirrored those of starch recoveries, all typical of pretreatments with this class of IL. The degree of hemicellulose removal and delignification were enhanced at higher temperatures. Pulps pretreated using [DMEtA][HCOO] displayed a slower removal of both hemicellulose and lignin and high glucan recoveries, also typical of this class of IL. Due to the low carbohydrate content of the starting biomass, glucan contents of all pulps were low (11-15%).

In addition, direct ashing was carried out on two sets of pulps, at the previously identified promising conditions: 180 minutes at 120 ^oC using [DMEtA][HCOO], and 30 minutes at 120 ^oC using [DMBA][HSO_4]. As in Section 5.3.2, the ash content of pulps was found to be significantly higher than that determined by compositional analysis: 25% and 40% using [DMBA][HSO_4] respectively. It would thus appear likely that the IL anion is reacting with part of the large inorganic fraction in the starting biomass, and producing insoluble salts that remain in the pulp (as observed in Section 4.3.5), with the higher reactivity of the $[HSO_4]^-$ anion explaining its higher ash content. The low carbohydrate content of these samples means that they are unsuitable for materials applications. In future, however, high-starch pulps from high-starch feedstocks may potentially attract attention for materials applications. In such a case, the very high ash content of the pulps may be problematic and require an extra processing step for removal.

5.3.3 Pretreatment of Metal-Contaminated Duckweed

Metal-contaminated *Lemna minor* was pretreated using [DMEtA][HCOO] at 120 ^oC for 180 minutes, and [DMBA][HSO_4] at 120 ^oC for 30 minutes. These conditions were previously identified as most promising for sugar release. The aim of these experiments was twofold: firstly, to observe whether pretreatment behaviour is similar between different batches of duckweed; and secondly, to determine whether these promising pretreatment conditions are suitable for metal removal.

Duckweed Composition

The composition of the untreated duckweed was determined as for *Spirodela polyrhiza*, shown in Table 5.2. Compared to *S. polyrhiza*, this strain of duckweed was found to have a substantially lower protein content, and higher starch content. This is consistent with literature: duckweed has been reported to increase starch content and reduce protein content when in a stressed environment (such as heavy metal-contaminated water).[96,120,121] The other most notable differences in composition are the lower ash content, possibly a result of being harvested from a small park pond rather than a busy canal in the heart of London. Lignin content in this feedstock was also much lower, which may be due to the difference in species (e.g. due to the much smaller frond size). Using the previously described technique led to a mass balance of 90%. Extraction with hexane was again attempted, as with *S. polyrhiza*, but led to no significant change. The unaccounted 10% of the mass is either due to other extractable materials that solubilise during compositional analysis (e.g. apiose or pectins)[111], or to the assumed nitrogen/protein conversion factor not being appropriate for this feedstock.

Table 5.2: Composition of *Lemna minor*.

Cellulose	Starch	Hemicellulose	Lignin	Protein	Ash	Extractives (H_2O + EtOH)	Acetyl	Mass Balance
10.4% ±0.5%	10.0% ±0.1%	5.7% ±0.1%	6.7% ±0.1%	19.9% ±0.5%	5.5% ±0.0%	32.1% ±0.7%	0% ±0.0%	90.3% ±0.5%

Starch Recovery

The starch recoveries for both conditions are shown in Fig. 5.14, with the corresponding values using *S. polyrhiza* also included for reference. Values for starch recovery in *L. m*inor were in line with those of the previous feedstock, at 77% and 83% using [DMBA][HSO_4] (and not statistically different) and being quantitative in both cases using [DMEtA][HCOO]. This encouraging evidence for these process conditions being somewhat feedstock-independent in terms of starch content. It is interesting to compare starch recoveries in real biomass samples to those obtained when pretreating pure starch in Section 5.3.2. Using [DMEtA][HCOO], quantitative ethanol-insoluble residues were obtained in both the biomass and pure starch. Using [DMBA][HSO_4], ethanol-insoluble residues were around 80% in the biomass samples, which is generally higher than those using pure starch. Only potato starch (77%) gave similar results, with corn and wheat starch moderately similar (66% and 54%), while rice starch was much lower (34%). It would, therefore, appear that duckweed starch is either similar in structure to potato starch, and/or that pretreatment of starch in biomass is slightly less severe than pretreatment of pure starch, possibly due to some degree of protection of the starch offered within plant cell or to the impact of the lignin on the IL acidity. *S. polyrhiza* starch has been previously shown

to have an average degree of polymerisation around 20% higher than corn starch.[122] However, such a trend may not be broadly applicable.

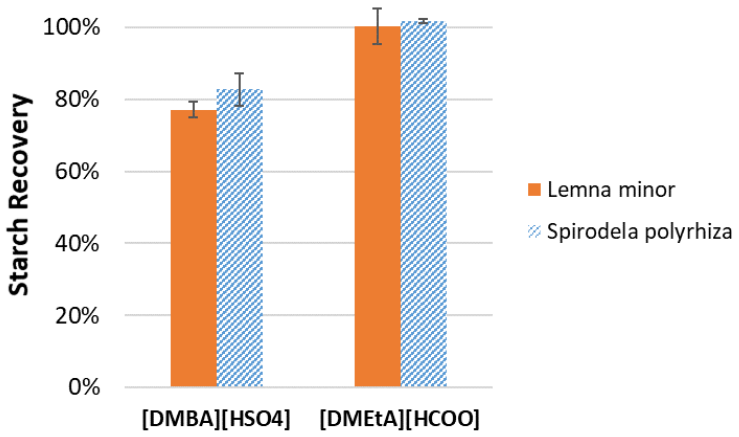


Figure 5.14: Starch recovery in two duckweed species under two pretreatment conditions. All pretreatments were carried out at 120 °C with 20 wt% water, and at a biomass loading of 10% wt/wt. Pretreatment duration was 30 minutes using [DMBA][HSO_4], and 180 minutes using [DMEtA][HCOO].

Saccharification

The enzymatic hydrolysis curves for both conditions and the untreated feedstock are shown in Fig. 5.15, with the corresponding curves using *S. polyrhiza* also included for reference. *L. minor* was found to be a highly digestible feedstock even when untreated, with a saccharification yield of 61% after 120 hours. This is substantially higher than that of *S. polyrhiza* (39%), and appeared to still be increasing slowly after 120 hours of hydrolysis. The reason for this may be this strain's much higher proportion of starch relative to cellulose. The kinetics of the pretreated pulps were much faster than the untreated material, particularly using [DMEtA][HCOO]. After 8 hours of hydrolysis, pulps pretreated using [DMEtA][HCOO] and [DMBA][HSO_4] had reached 98% and 87% of their 120-hour sugar yields. These are in line with the kinetics observed using *S. polyrhiza* at the same conditions (corresponding values of 97% and 91%).

Both conditions led to substantially higher saccharification yields and digestibilities than the untreated material, particularly at short hydrolysis durations. Using [DMEtA][HCOO], near-quantitative yields and digestibilities were obtained after 8 hours of hydrolysis (92% for both), with yields not then increasing significantly. Compared to *S. polyrhiza*, pretreatments using this IL led to significantly higher yields at all points (10-11%), but there were no significant differences in digestibility. This is explained by the higher glucan recoveries using *L. minor* than *S. polyrhiza*. There is thus almost no difference

between yield and digestibility in the former, while in the latter digestibility is slightly higher than yield.

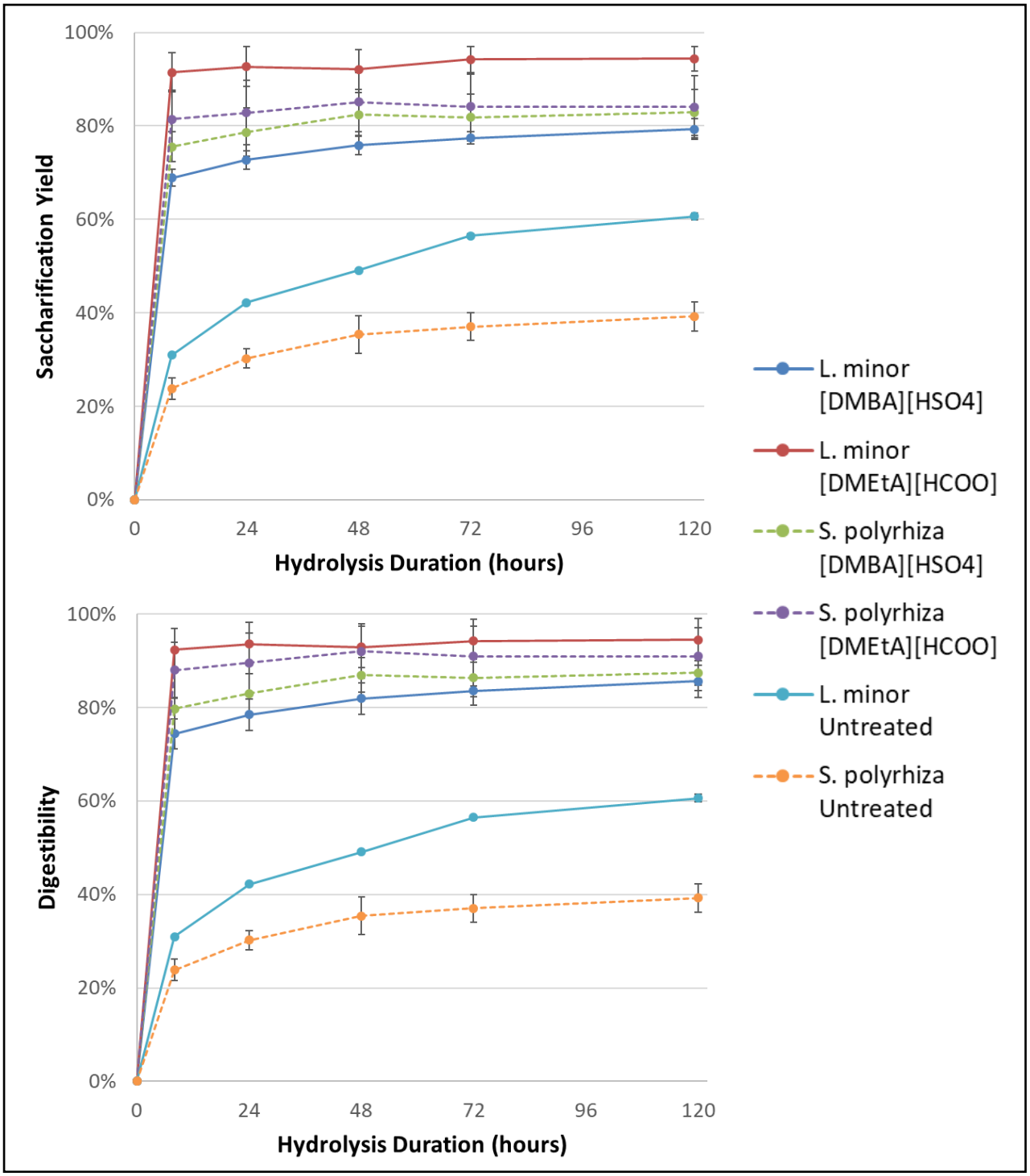


Figure 5.15: Saccharification and digestibility kinetics of duckweed pulps pretreated using varying ionic liquids. All pretreatments were carried out with 20 wt% water, and at a biomass loading of 10% wt/wt.

Using [DMBA][HSO_4] with *L. minor*, both yields and digestibilities were much lower than using [DMEtA][HCOO]. No such differences were observed between ILs when pretreating *S. polyrhiza*. The difference in this case may be due to the higher starch contents of *L. minor*, both in absolute terms (10% vs. 3%) and as a proportion of glucan (49% vs. 30%). As a result, the differences in starch recovery between both ILs leads to a larger difference in glucan composition of pulps, compared to those using *S. polyrhiza*. Pulps pretreated with [DMBA][HSO_4] thus have a lower proportion of (more easily hydrolysable) starch, making them less digestible as well as limiting their yields. No significant differences in either yield or digestibility were observed between both strains of duckweed using [DMBA][HSO_4].

Protein Partitioning

The protein partitioning behaviour was also investigated for this strain of duckweed, encompassing the pulp, lignin, and dialysate fractions, with results displayed in Fig. 5.16. Similarly to *S. polyrhiza*, neither pulp nor lignin fractions displayed any enrichment in protein content relative to the untreated feedstock.

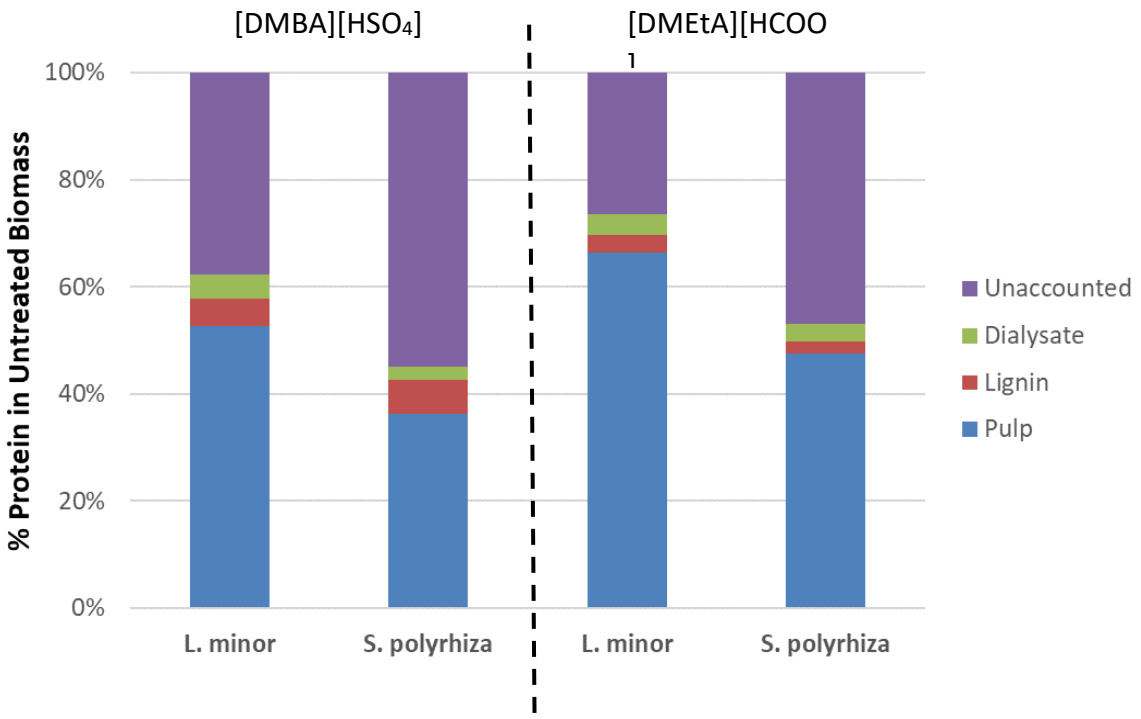


Figure 5.16: Protein partitioning during IL pretreatment of two duckweed species. Unaccounted protein refers to remaining protein not detected in the pulp lignin, or dialysate fractions. All pretreatments were carried out with 20 wt% water, and at a biomass loading of 10% wt/wt.

The same trends between ILs were noted when pretreating *L. minor* as when using *S. polyrhiza*. The main difference between the ILs is that [DMBA][HSO_4] removes a higher proportion of the protein from the pulp, while protein yields in the lignin and dialysate fractions are both very similar due to the low lignin yields using this type of feedstock. As a result, there is a smaller unaccounted protein fraction using [DMEtA][HCOO], as protein removed from the pulp and (presumably) dissolved into the IL would appear to degrade into unrecoverable fragments. Between feedstocks, the only substantial difference is in the proportion of the protein retained within the pulp. This is higher for both ILs, and consequently leads to a smaller unaccounted fraction. This unaccounted fraction is still large, however, and further studies should aim to more conclusively determine its cause and thus reduce this fraction. The amount of protein removed from the pulp using [DMEtA][HCOO] is comparable to that removed by alkali extraction at pH 8 from *L. minor* in a study by Brouwer et al.[118]

The protein content of the post-saccharification residue was again measured, to check for enrichment which may allow subsequent purification/recovery. Moderate enrichment was again observed relative to the pulp fraction: 46% from 17% using [DMBA][HSO_4], and 40% from 18% using [DMEtA][HCOO]. This account for 63-64% of the protein in the pulp, or 34-42% of the protein in the starting biomass.

Metal Uptake and Extraction

L. minor was collected from the wild and then transferred to water containing 2 ppm of Cd and Ni for three days. A small portion of the original duckweed was air-dried before being transferred into the metal-contaminated water, in order to check the "baseline" level of these metals in the biomass. Following 3 days of growth in the contaminated water, the duckweed was harvested, washed with DI water, and air-dried. The washing with DI water was to ensure that any metals detected in the biomass were chemically bound to the biomass (either uptaken or adsorbed to the surface), rather than remaining following evaporation of the metal-contaminated nutrient solution. A small portion of the metal-contaminated duckweed was air-dried without washing with DI water, for comparison of metal contents. Results are displayed in Table 5.3.

The original biomass was found to contain no Cd and only 9 ppm of Ni, expectedly. Following growth in metal-contaminated solution, high levels of both metals were observed in the biomass. The contents are generally lower than those reported in literature for duckweed grown in similar concentrations of Cd (around 2,000-6,000 ppm), maybe partly due to the shorter duration.[65,66,123] For duckweed grown in Ni, mixed values have been reported in previous studies, ranging from no uptake at water concentrations of 0.23-2 ppm in water but tissue concentrations of 800-3000 ppm at 5 ppm water concentrations,[123,124] to 15 ppm tissue concentrations from 0.06 ppm in water.[125] This may be

taken as an example of the strong variability of individual duckweed strains. Rinsing with DI water was found to remove a small proportion of the metals, showing that the metals were either uptaken or chemically bound to the surface of the biomass. Although the effect on growth was not investigated, these results are further evidence of the ability of duckweed to uptake heavy metals in significant quantities, and confirm that it has significant potential for phytoremediation of water

Table 5.3: Metal contents of duckweed before and after growth in metal-contaminated water.

Feedstock	Ni (ppm)	Cd (ppm)
Virgin	9 ±13	0 ±0
Contaminated	453 ±41	681 ±62
Contaminated + DI water rinse	414 ±29	636 ±3

The metal content of the pulp, lignin, and liquor were then determined following pretreatment, allowing the partitioning behaviour to be determined. Results are displayed in Fig. 5.17. Large differences were observed in the partitioning behaviour of both metals, as well as moderate differences between the performance of both ILs. Metals were predominantly concentrated in the pulp and liquor fractions, with the lignin fractions displaying both low absolute quantities as well as concentrations of either metal.

Ni extraction proved more successful out of the two metals, particularly using [DMEtA][HCOO]. This IL achieved 81% removal of Ni from the pulp. As a result, pulp concentrations dropped to under 100 ppm, from over 400 ppm in the starting biomass. Using [DMBA][HSO_4], only 28% of the Ni was extracted from the pulp, with resulting pulp concentrations slightly higher than those of the starting biomass. Cd extraction proved unsuccessful in both ILs, with only 6-7% removal, and with pulps having significantly higher Cd concentrations than the starting biomass. In this case, the pretreatment process essentially concentrated the metal in the remaining solid fraction.

The reasons behind the generally unsuccessful metal extractions are not completely clear. [DMBA][HSO_4] was shown to remove around 75% of the Cd in the metal-contaminated wetland species in Chapter 4, and similar values were obtained in the work of Rafat et al, in which a protic alkylammonium carboxylate IL showed similar extraction capabilities for Cd.[106] However, in both cases the starting material contained only 1 ppm of the metal, and therefore absolute quantities extracted were therefore small. In the same study by Rafat et al, Ni extraction was also measured (with an original concentration of 8 ppm), with both ILs extracting around 50-60% of the Ni present.

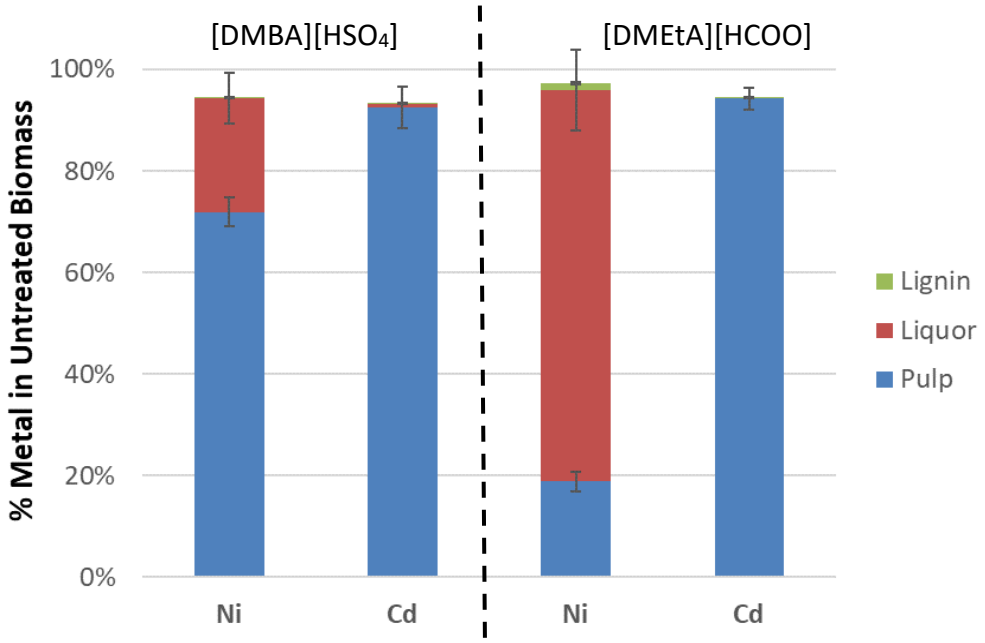


Figure 5.17: Metal partitioning during IL pretreatment of metal-contaminated *Lemna minor*. All pretreatments were carried out at 120 °C, with 20 wt% water, and at a biomass loading of 10% wt/wt. Pretreatments were carried out for a duration of 30 minutes using [DMBA][HSO_4], and 180 minutes using [DMEtA][HCOO].

One possible explanation for the generally low levels of extraction is thus that metal extraction is limited by solubility of the metals in the IL solutions. No data was found regarding solubility limits in such aqueous IL solutions, but due to the low biomass loadings, theoretical metal concentrations would be very low even in the case of full removal (around 40 ppm of Ni and 60 ppm of Cd). The solubility of the metal species would thus have to be very low for solubility to be limiting extraction. Another possible explanation is that the pretreatment conditions employed were too mild to sufficiently disrupt the biomass structure and thus extract the metals, especially if metals were taken up into the biomass structure instead of simply adsorbing to the surface of the fronds. Previous studies investigating metal extraction through IL pretreatment have used temperatures of 150 °C and above, for durations of 30 minutes and above, mostly with acidic ILs.[106,126] However, it would be hard to consolidate this with the relatively high levels of Ni extraction using [DMEtA][HCOO]. The most likely hypothesis is, therefore, that these metal species have a limited affinity for the ILs employed (with the exception being Ni in [DMEtA][HCOO]), and that in order for them to be extracted the biomass structure would needs to be severely disrupted by employing harsher pretreatment conditions. [Hmim]Cl was not considered for duckweed pretreatment in this study due to its poor performance when pretreating pure starch. However, it has been shown to outperform a number of acidic ILs (including [DMBA][HSO_4]) and basic ILs in terms of metal extraction from other types of biomass

(including in Chapter 4).[106,127] Due to the limited degree of metal extraction achieved here using both ILs, further work should include investigating the use of [Hmim]Cl for pretreatment of metal-contaminated duckweed at mild conditions.

Pulp Composition

Similarly to pulps from *S. polyrhiza* pretreated at these conditions, pulps from *L. minor* showed an increase in glucan content of around 50% relative to the starting biomass, reaching 28-30%. It is, therefore, anticipated that pretreatment of high-starch duckweed strains may be capable of producing pulps with very high glucan contents that may be suitable for applications beyond hydrolysis to glucose, or may prove even more highly digestible at lower enzyme loadings. The ash contents of pulps from *L. minor* were also found to be much lower than those from *S. polyrhiza*, in line with the lower ash content of the untreated biomass. Once again, [DMBA][HSO_4] produced pulps with a higher ash content than [DMEtA][HCOO] (23% vs 12%).

Liquor Recovery

When recovering liquor for dialysis, liquor recovery yields were determined for both ILs. Using [DMBA][HSO_4], quantitative recoveries were observed for both feedstocks, as in Chapter 4 and as has been reported in the literature using this class of IL.[104,128] Using [DMEtA][HCOO], however, liquor recoveries were much lower (94-95%). The acid/base ratio of the liquors were analysed and were found to consistently show a 3% excess of acid. However, a 3% loss of base alone would only lead to a 2% loss in IL mass, not the 5-6% observed. Therefore, there may be loss of both acid and base (with the base being lost at a higher rate), or the presence of other solutes in the liquor renders the acid/base determination inaccurate and the loss of base is in fact greater. Nakasu et al. investigated solvent recovery using [MEA][OAc] during pretreatment.[74] Similar values were found at acid/base ratios of 0.1-1.1 (94-97%), attributed to evaporation of the acetic acid during solvent recovery, and much lower recoveries were observed at higher acid excesses. Achivinu et al. also investigated solvent recovery using pyridinium acetate, reporting 98% recovery with no change in acid/base ratio, but using low-pressure distillation as the IL recovery method.[129] Lower recoveries might thus be expected using a formic acid rather than acetic acid-based IL due to formic acid's higher volatility, but the acid/base ratio measurements go against this.

Possible reasons for this loss may thus be thermal degradation during pretreatment at 120 °C, incomplete proton transfer leading to volatilisation of constituent acid and base during vacuum evaporation, or incorporation into pulp or lignin streams. When examined by FTIR, however, the degree of proton transfer in this IL appeared substantial (see Fig. A5-3 in the Appendix). In addition,

no significant nitrogen content was found in either the pulp or lignin streams (as seen during the protein partitioning analysis). A 97% required recovery of IL has been reported a pretreatment IL to be economically viable, with a solvent cost of $2.5/kg.[130] However, Nakasu et al. have estimated the bulk cost of [MEA][OAc] at $1.8/kg and concluded that their recovery values are sufficient.[74] Therefore, although this IL may also still be economically viable, for it to be carried forward the reason for losses should be examined and rectified. In the case of thermal degradation being the issue, lower temperatures may be employed, particularly as duckweed does not require severe pretreatment conditions, although lower temperatures may increase required duration substantially. In the case of incomplete proton transfer being the issue, other carboxylate anions or tertiary amines with a greater pKa difference could be tested to improve ionicity (although this alone is no guarantee of improved ionicity).[131]

5.4 Conclusions

In this chapter, a pretreatment process aimed towards utilising duckweed's many promising features has been proposed and tested. The ultimate goal was to identify a set of IL pretreatment conditions which preserved the easily hydrolysable starch in the pulp and generated a secondary product stream enriched with protein, all while solubilising any metals in the starting biomass.

Due to duckweed's starch-accumulating capabilities, the interaction between starch and IL under pretreatment conditions was first investigated. The wider aim was to identify promising pretreatment conditions for the preservation of starch. Four different ILs were tested for 30 minutes at 90 °C and 120 °C: [DMBA][HSO_4], [Hmim]Cl, [MEA][OAc], and [DMEtA][HCOO]. Four types of starch from different botanical sources were used in order to investigate the effect of different starch structures on results. Despite its highly acidic nature, [DMBA][HSO_4] was not found to significantly degrade the starch at 90 °C. This was attributed to the ILs inability to dissolve the starch, limiting the rate of hydrolysis. At 120 °C, however, significant degradation of the starch occurred among all four varieties. [DMEtA][HCOO] and [MEA][OAc] displayed similar behaviour, both fully dissolving all starches except potato starch, even at 90 °C. Quantitative ethanol-insoluble yields were obtained at both temperatures, but some degree of hydrolysis occurred, evidenced by decreasing water-insoluble yields at higher temperatures. The water-insoluble yield was also observed to undergo retrogradation into a clear, highly crystalline form for all starches except potato starch using these ILs. [Hmim]Cl dissolved all starches fully except potato starch, and was found to rapidly hydrolyse the starch due to its acidic nature.

Based on results using pure starch, [DMBA][HSO_4] and [DMEtA][HCOO] were chosen for pretreatment of duckweed. *Spirodela polyrhiza* was pretreated using [DMEtA][HCOO] at 120 °C, and using [DMBA][HSO_4] at 90 °C, 120 °C, and 150 °C, all in timecourse experiments. Starch recoveries were found to remain quantitative for up to three hours of pretreatment using [DMEtA][HCOO] and up to two hours using [DMBA][HSO_4] at 90 °C, but rapidly decreased at 120 °C and 150 °C. Although the untreated biomass was found to be highly digestible (39% sugar release after 120 hours of enzymatic hydrolysis), IL pretreatment significantly enhanced hydrolysis kinetics, with most pulps reaching over 90% of their final sugar release yield after 8 hours of hydrolysis. In addition, pretreated pulps all displayed highly elevated pulp digestibilities. This was particularly true for those pretreated at 150 °C which appeared to have severely disrupted the biomass structure and displayed near-quantitative digestibilities, but at the cost of reduced sugar yields due to extensive starch degradation. The untreated biomass was found to contain high levels of protein (36%), and the partitioning behaviour of the protein was investigated. [DMBA][HSO_4] was found to remove the protein from the pulp, with the rate of removal increasing at higher temperatures. [DMEtA][HCOO] rapidly removed around half the protein from the pulp, but no further extraction then occurred at longer durations. Neither the pulp nor the lignin fractions demonstrated any increase in protein concentration relative to the starting biomass, although there was significant concentration in the post-saccharification residue. The majority of the protein was concluded to be remaining in the IL, but was not recoverable by dialysis, leaving a large unaccounted fraction that was presumed to be due to protein degradation in the IL. Pretreatments at the two most promising conditions were found to slightly concentrate the glucan in the pulp, but pulps also contained a large fraction of ash (up to 40%).

A different strain of duckweed, *Lemna minor*, was found to accumulate significant quantities of Ni and Cd (around 400 ppm and 600 ppm) from relatively low concentrations in water (2 ppm). When pretreated at the optimal conditions determined using *S. polyrhiza*, however, metal removal from the biomass was found to be very limited, with almost no removal for Cd. Other pretreatment indicators (saccharification, starch recovery, and protein partitioning) were found to be very similar to those of *S. polyrhiza*, despite some differences in composition of the untreated biomass. This would appear to be promising signs of IL pretreatment of duckweed being feedstock-independent, important due to the large variability in duckweed composition by both species and geography. Using [DMEtA][HCOO], near-quantitative saccharification yields and digestibilities were observed after 8 hours of hydrolysis.

Overall, this chapter has provided a foundation for the study of IL pretreatment of duckweed. An ideal IL-based process for duckweed biorefinery would be able to take advantage of this feedstock's three promising abilities: metal removal from dilute concentrations, starch accumulation, and protein accumulation. Such a process would, therefore, lead to recovery of a highly digestible pulp that

preserves much of the starch, of a high-purity protein stream, and would solubilise the extracted metals into the IL phase. This study has demonstrated that the first of these three goals is achievable under a range of conditions and was loosely optimised. Further studies should aim to investigate the other two aims independently, and to then find a single operating point able to meet all three aims simultaneously. This may be done by testing different ILs and acid/base ratios, different temperatures and durations, and different IL water contents. This would require fairly extensive study, but the number of required experiments may be minimised while maintaining statistical significance by careful design of experiments. In order to facilitate this, a high-level study of protein stability in ionoSolv ILs under pretreatment conditions should be carried out, similar to the one used for starch in this Chapter. Should it not prove feasible to optimise for both saccharification yield and protein extraction, other configurations should be investigated, such as alkaline pre-extraction of protein.

References

1 J. Xu, H. Zhao, A. M. Stomp and J. J. Cheng, *Biofuels*, 2012, **3**, 589–601.
2 R. A. Leng, *Duckweed: A tiny aquatic plant with enormous potential for agriculture and environment*, FAO, 1999.
3 S. Iqbal, *Duckweed Aquaculture. Potentials, Possibilities and Limitations for Combined Wastewater Treatment and Animal Feed Production in Developing Countries, SANDEC Report No. 6/99*, 1999.
4 X. Zhao, G. K. Moates, N. Wellner, S. R. A. Collins, M. J. Coleman and K. W. Waldron, *Carbohydr. Polym.*, 2014, **111**, 410–418.
5 X. Zhao, G. K. Moates, A. Elliston, D. R. Wilson, M. J. Coleman and K. W. Waldron, *Bioresour. Technol.*, 2015, **194**, 263–269.
6 W. Cui, J. Xu and J. J. Cheng, in *American Society of Agricultural and Biological Engineers Annual International Meeting*, Louisville, 2011, vol. 7, pp. 5820–5834.
7 M. S. Reid and R. L. Bieleski, *Plant Physiol.*, 1970, **46**, 609–613.
8 F. Ren, J. Wang, F. Xie, K. Zan, S. Wang and S. Wang, *Green Chem.*, 2020, **22**, 2162–2183.
9 Y. Isbeth Cornejo-Ramírez, O. Martínez-Cruz, C. Lizette, D. Toro-Sánchez, F. J. Wong-Corral, J. Borboa-Flores, F. J. Cinco-Moroyoqui and F. J. Cinco, *CyTA-Journal Food*, 2018, **16**, 1003–1017.
10 R. F. Tester, J. Karkalas and X. Qi, *J. Cereal Sci.*, 2004, **39**, 151–165.
11 E. Bertoft, *Agronomy*, 2017, **7**, 1–29.
12 H. F. Zobel, *Starch - Stärke*, 1988, **40**, 44–50.
13 L. S. Sciarini, A. Rolland-Sabaté, S. Guilois, P. Decaen, E. Leroy and P. Le Bail, *Green Chem.*, 2014, **17**, 291–299.
14 J. Kärkkäinen, K. Lappalainen, P. Joensuu and M. Lajunen, *Carbohydr. Polym.*, 2011, **84**, 509–516.
15 S. Mateyawa, D. Fengwei, R. W. Truss, P. J. Halley, T. M. Nicholson, J. L. Shamshina, R. D. Rogers, M. W. Boehm and T. Mcnally, *Carbohydr. Polym.*, 2013, **94**, 520–530.
16 W. S. Ratnayake and D. S. Jackson, *Carbohydr. Polym.*, 2007, **67**, 511–529.
17 M. R. Debet and M. J. Gidley, *J. Agric. Food Chem.*, 2007, **55**, 4752–4760.
18 K. Wilpiszewska and T. Spychaj, *Carbohydr. Polym.*, 2011, **86**, 424–428.
19 F. Ren, J. Wang, H. Luan, J. Yu, L. Copeland, S. Wang and S. Wang, *ACS Omega*, 2019, **4**, 14981–14986.
20 K. Lappalainen, J. Kärkkäinen and M. Lajunen, *Carbohydr. Polym.*, 2013, **93**, 89–94.
21 X. Tan, X. Li, L. Chen and F. Xie, *Phys. Chem. Chem. Phys.*, 2016, **18**, 27584–27593.
22 W. Liu and T. Budtova, *Carbohydr. Polym.*, 2013, **93**, 199–206.
23 F. Ren, F. Xie, H. Luan, S. Wang and S. Wang, *Ind. Crops Prod.*, 2020, **144**, 112043–112049.
24 J. Wang, F. Ren, J. Yu, L. Copeland, S. Wang and S. Wang, *ACS Omega*, 2019, **4**, 11312–11319.
25 D. G. Stevenson, A. Biswas, J. lin Jane and G. E. Inglett, *Carbohydr. Polym.*, 2007, **67**, 21–31.
26 Z. Chen, X. Ma, L. Xu, Y. Wang and J. Long, *Bioresour. Technol.*, 2018, **268**, 488–495.
27 Ch. Pat., CN103409566A, 2015.
28 J. C. Bischof and X. He, *Ann. N. Y. Acad. Sci.*, 2006, **1066**, 12–33.
29 S. Chiesa and E. Gnansounou, *Bioresour. Technol.*, 2011, **102**, 427–436.
30 M. del M. Contreras, A. Lama-Muñoz, J. Manuel Gutiérrez-Pérez, F. Espínola, M. Moya and E. Castro, *Bioresour. Technol.*, 2019, **280**, 459–477.
31 A. Fetzer, T. Herfellner, A. Stäbler, M. Menner and P. Eisner, *Ind. Crops Prod.*, 2018, **112**, 236–246.

32 M. Laser, H. Jin, K. Jayawardhana, B. E. Dale and L. R. Lynd, *Biofuels, Bioprod. Biorefining*, 2009, **3**, 231–246.
33 R. Wahlström, K. Rommi, P. Willberg-Keyriläinen, D. Ercili-Cura, U. Holopainen-Mantila, J. Hiltunen, O. Mäkinen, H. Nygren, A. Mikkelson and L. Kuutti, *ChemistrySelect*, 2017, **2**, 9355–9363.
34 L. L. Rusoff, E. W. Blakeney and D. D. Culley, *J. Agric. Food Chem.*, 1980, **28**, 848–850.
35 R. Chakrabarti, W. D. Clark, J. G. Sharma, R. K. Goswami, A. K. Shrivastav and D. R. Tocher, *Front. Chem.*, 2018, **6**, 479.
36 M. Ismail, *Pertanika J. Sci. Techno!*, 1998, **6**, 7–21.
37 K. J. Appenroth, K. S. Sree, V. Böhm, S. Hammann, W. Vetter, M. Leiterer and G. Jahreis, *Food Chem.*, 2017, **217**, 266–273.
38 Ch. Pat., CN105166318A, 2015.
39 M. Kehili, L. M. Schmidt, W. Reynolds, A. Zammel, C. Zetzl, I. Smirnova, N. Allouche and S. Sayadi, *Biotechnol. Biofuels*, 2016, **9**, 261.
40 M. S. Celiktas, C. Kirsch and I. Smirnova, *Energy Convers. Manag.*, 2014, **84**, 633–639.
41 M. J. Rojas, P. F. Siqueira, L. C. Miranda, P. W. Tardioli and R. L. C. Giordano, *Ind. Crops Prod.*, 2014, **61**, 202–210.
42 B. Bals, V. Balan and B. Dale, *Bioresour. Technol.*, 2009, **100**, 5876–5883.
43 L. B. De La Rosa, S. Reshamwala, V. M. Latimer, B. T. Shawky, B. E. Dale and E. D. Stuart, *Appl. Biochem. Biotechnol.*, 1994, **45–46**, 483–497.
44 L. Urribarrí, A. Ferrer and A. Colina, *Appl. Biochem. Biotechnol.*, 2005, **122**, 0721–0730.
45 L. Urribarrí, D. Chacón, O. González and A. Ferrer, in *Applied Biochemistry and Biotechnology*, Springer, 2009, vol. 153, pp. 94–102.
46 C. Hamley-Bennett, G. J. Lye and D. J. Leak, *Bioresour. Technol.*, 2016, **209**, 259–264.
47 X. Hou, J. H. Hansen and A. B. Bjerre, *Bioresour. Technol.*, 2015, **197**, 310–317.
48 A. Schindl, M. L. Hagen, S. Muzammal, H. A. D. Gunasekera and A. K. Croft, *Front. Chem.*, 2019, **7**, 1–31.
49 E. Suarez Garcia, C. A. Suarez Ruiz, T. Tilaye, M. H. M. Eppink, R. H. Wijffels and C. van den Berg, *Sep. Purif. Technol.*, 2018, **204**, 56–65.
50 Y. Pei, Z. Li, L. Liu, J. Wang and H. Wang, *Sci. China Chem.*, 2010, **53**, 1554–1560.
51 Z. jian Tan, F. fang Li, X. lei Xu and J. min Xing, *Desalination*, 2012, **286**, 389–393.
52 J. K. Yan, H. Le Ma, J. J. Pei, Z. Bin Wang and J. Y. Wu, *Sep. Purif. Technol.*, 2014, **135**, 278–284.
53 C. F. Miranda, MSc Thesis, Tecnico Lisboa, 2017.
54 X. Ge, N. Zhang, G. C. Phillips and J. Xu, *Bioresour. Technol.*, 2012, **124**, 485–488.
55 S. Soda, T. Ohchi, J. Piradee, Y. Takai and M. Ike, *Biomass and Bioenergy*, 2015, **81**, 364–368.
56 J. Xu, W. Cui, J. J. Cheng and A. Stomp, *Biosyst. Eng.*, 2011, **110**, 67–72.
57 O. Calicioglu and R. A. Brennan, *Bioresour. Technol.*, 2018, **257**, 344–348.
58 Q. Chen, Y. Jin, G. Zhang, Y. Fang, Y. Xiao and H. Zhao, *Energies*, 2012, **5**, 3019–3032.
59 L. R. F. Souto, I. F. da Silva, J. L. Ninow, S. R. A. Collins, A. Elliston and K. W. Waldron, *Biomass and Bioenergy*, 2019, **127**, 1–7.
60 X. Zhao, G. K. Moates, D. R. Wilson, R. J. Ghogare, M. J. Coleman and K. W. Waldron, *Biomass and Bioenergy*, 2014, **72**, 206–215.
61 A. Sluiter, B. Hames, R. O. Ruiz, C. Scarlata, J. Sluiter and D. Templeton, *Determination of Structural Carbohydrates and Lignin in Biomass, NREL/TP-510-42618*, 2008.
62 J. A. Casal, J. E. Vermaat and F. Wiegman, *Aquat. Bot.*, 2000, **67**, 61–67.
63 Megazyme, *Total starch assay procedure (amyloglucosidase/ alpha-amylase method), AOAC Method 996.11*, 2020.
64 K. Appenroth, K. Krech, Á. Keresztes, W. Fischer and H. Koloczek, *Chemosphere*, 2010, **78**, 216–223.
65 A. Basile, S. Sorbo, B. Conte, R. Castaldo Cobianchi, F. Trinchella, C. Capasso and V. Carginale, *Int. J. Phytoremediation*, 2012, **14**, 374–387.
66 D. Chaudhuri, A. Majumder, A. K. Misra and K. Bandyopadhyay, *Int. J. Phytoremediation*, 2014, **16**, 1119–1132.
67 Y. Yin, C. Yu, L. Yu, J. Zhao, C. Sun, Y. Ma and G. Zhou, *Bioresour. Technol.*, 2015, **187**, 84–90.
68 Y. Liu, X. Chen, X. Wang, Y. Fang, M. Huang, L. Guo, Y. Zhang and H. Zhao, *Sci. Rep.*, 2018, **8**, 1–9.
69 Z. Zhao, H. Shi, X. Kang, C. Liu, L. Chen, X. Liang and L. Jin, *Aquat. Toxicol.*, 2017, **192**, 216–223.
70 X. Zhao, A. Elliston, S. R. A. Collins, G. K. Moates, M. J. Coleman and K. W. Waldron, *Biomass and Bioenergy*, 2012, **47**, 354–361.
71 Z. A., G. S. and T. N., *J. Environ. Qual.*, 1998, **27**, 715–721.
72 C. B. Sekomo, D. P. L. Rousseau, S. A. Saleh and P. N. L. Lens, *Ecol. Eng.*, 2012, **44**, 102–110.
73 T. C. Pin, P. Y. S. Nakasu, S. Mattedi, S. C. Rabelo and A. C. Costa, *Fuel*, 2019, **235**, 1506–1514.
74 P. Y. S. Nakasu, C. J. Clarke, S. C. Rabelo, A. C. Costa, A. Brandt-Talbot and J. P. Hallett, *ACS Sustain. Chem. Eng.*, 2020, **8**, 7952–7961.
75 N. Singh, J. Singh, L. Kaur, N. S. Sodhi and B. S. Gill, *Food Chem.*, 2003, **81**, 219–231.
76 E. Gregorová, W. Pabst and I. Bohačenko, *J. Eur. Ceram. Soc.*, 2006, **26**, 1301–1309.
77 J. J. M. Swinkels, *Starch - Stärke*, 1985, **37**, 1–5.
78 D. Domene-López, J. J. Delgado-Marín, I. Martin-Gullon, J. C. García-Quesada and M. G. Montalbán, *Int. J. Biol. Macromol.*, 2019, **135**, 845–854.
79 N. H. Zakaria, N. Muhammad and M. M. A. B. Abdullah, in *IOP Conference Series: Materials Science and Engineering*, Institute of Physics Publishing, 2017, vol. 209.

80 B. M. J. Martens, W. J. J. Gerrits, E. M. A. M. Bruininx and H. A. Schols, *J. Anim. Sci. Biotechnol.*, 2018, **9**, 91.
81 P. V. Andreev, *Pharm. Chem. J.*, 2004, **38**, 447–450.
82 S. Mateyawa, D. F. Xie, R. W. Truss, P. J. Halley, T. M. Nicholson, J. L. Shamshina, R. D. Rogers, M. W. Boehm and T. McNally, *Carbohydr. Polym.*, 2013, **94**, 520–530.
83 W. Liu and T. Budtova, *Carbohydr. Polym.*, 2013, **93**, 199–206.
84 Y. Fukaya, A. Sugimoto and H. Ohno, *Biomacromolecules*, 2006, **7**, 3295–3297.
85 F. de A. C. Farias, M. M. de S. Moretti, M. S. Costa, S. E. BordignonJunior, K. S. B. Cavalcante, M. Boscolo, E. Gomes, C. M. L. Franco and R. da Silva, *Ind. Crops Prod.*, 2020, **157**, 112825–112833.
86 S. Wang, C. Li, L. Copeland, Q. Niu and S. Wang, *Compr. Rev. Food Sci. Food Saf.*, 2015, **14**, 568–585.
87 H. Fredriksson, J. Silverio, R. Andersson, A. C. Eliasson and P. Åman, *Carbohydr. Polym.*, 1998, **35**, 119–134.
88 M. R. Jacobson, M. Obanni and J. N. Bemiller, *Cereal Chem. J.*, 1997, **74**, 511–518.
89 M. M. Green, *J. Chem. Educ.*, 1975, **52**, 729–730.
90 Table of Acids with Ka and pKa Values, https://clas.sa.ucsb.edu/staff/Resource Folder/Chem109ABC/Acid, Base Strength/Table of Acids w Kas and pKas.pdf, (accessed 22 July 2020).
91 A. Hernoux-Villière, J.-M. Lévêque, J. Kärkkäinen, N. Papaiconomou, M. Lajunen and U. Lassi, *Catal. Today*, 2014, **223**, 11–17.
92 Y. Shen, Z. Pei, W. Yuan and E. Mao, *Int. J. Agric. Biol. Eng.*, 2009, **2**, 51–57.
93 C. C. Akoh, *Food Lipids: Chemistry, Nutrition, and Biotechnology, Fourth Edition - Google Books*, CRC Press, 4th edn., 2017.
94 K. S. Sree and K. Appenroth, *Albanian J. Agric. Sci.*, 2014, 11–14.
95 H. L. White, *Ann. Bot.*, 1928, **3**, 771–782.
96 W. Cui, J. Xu, J. J. Cheng and A. M. Stomp, *Biol. Eng.*, 2011, **3**, 187–197.
97 G. Yu, H. Liu, K. Venkateshan, S. Yan, J. Cheng, X. S. Sun and D. Wang, *Trans. ASABE*, 2011, **54**, 555–561.
98 J. P. Goopy and P. J. Murray, *Asian-Australasian J. Anim. Sci.*, 2003, **16**, 297–305.
99 L. Negahdar, I. Delidovich and R. Palkovits, *Appl. Catal. B Environ.*, 2016, **184**, 285–298.
100 L. Vilcocq, P. C. Castilho, F. Carvalheiro and L. C. Duarte, *ChemSusChem*, 2014, **7**, 1010–1019.
101 G. González, J. López-Santín, G. Caminal and C. Solà, *Biotechnol. Bioeng.*, 1986, **28**, 288–293.
102 T. Salmi, D. Y. Murzin, P. Mäki-Arvela, B. Kusema, B. Holmbom, S. Willför and J. Wärnå, *AIChE J.*, 2014, **60**, 1066–1077.
103 B. T. Kusema, T. Tönnov, P. Mäki-Arvela, T. Salmi, S. Willför, B. Holmbom and D. Y. Murzin, *Catal. Sci. Technol.*, 2013, **3**, 116–122.
104 F. J. V. Gschwend, F. Malaret, S. Shinde, A. Brandt-Talbot and J. P. Hallett, *Green Chem.*, 2018, **20**, 3486–3498.
105 L. Weigand, S. Mostame, A. Brandt-Talbot, T. Welton and J. P. Hallett, *Faraday Discuss.*, 2017, **202**, 331–349.
106 A. R. Abouelela, S. Tan, G. H. Kelsall and J. P. Hallett, *ACS Sustain. Chem. Eng.*, 2020, **8**, 14441–14461.
107 Y. TAKAI, D. MISHIMA, M. KUNIKI, K. SEI, S. SODA and M. IKE, *Japanese J. Water Treat. Biol.*, 2014, **50**, 133–140.
108 Q. Chen, Y. Jin, G. Zhang, Y. Fang, Y. Xiao and H. Zhao, *Energies*, 2012, **5**, 3019–3032.
109 D. Pagliuso, A. Grandis, E. Lam and M. S. Buckeridge, *Bioenergy Res.*, 2020, 1–11.
110 X. Zhao, G. K. Moates, D. R. Wilson, R. J. Ghogare, M. J. Coleman and K. W. Waldron, *Biomass and Bioenergy*, 2015, **72**, 206–215.
111 S. Soda, T. Ohchi, J. Piradee, Y. Takai and M. Ike, *Biomass and Bioenergy*, 2015, **81**, 364–368.
112 A. Faizal, A. A. Sembada and N. Priharto, *Saudi J. Biol. Sci.*, 2021, **28**, 294–301.
113 R. M. Smith and D. E. Hansen, *J. Am. Chem. Soc.*, 1998, **120**, 8910–8913.
114 M. Sajib, E. Albers, M. Langeland and I. Undeland, *Sci. Rep.*, 2020, **10**, 1–13.
115 J. Csapó, Z. Csapó-Kiss, L. Wágner, T. Tálos, T. G. Martin, S. Folestad, A. Tivesten and S. Némethy, *Anal. Chim. Acta*, 1997, **339**, 99–107.
116 I. Davidson, *Methods Mol. Biol.*, 2003, **211**, 111–122.
117 K. Rommi, P. Niemi, K. Kemppainen and K. Kruus, *J. Cereal Sci.*, 2018, **79**, 168–173.
118 P. Brouwer, K. G. J. Nierop, W. J. J. Huijgen and H. Schluepmann, *Biotechnol. Reports*, 2019, **24**, 1–9.
119 K. Kemppainen, K. Rommi, U. Holopainen and K. Kruus, *Appl. Biochem. Biotechnol.*, 2016, **180**, 94–108.
120 C. Gupta and D. Prakash, *Toxicol. Environ. Chem.*, 2014, **95**, 1256–1266.
121 W. Hou, X. Chen, G. Song, Q. Wang and C. Chi Chang, *Plant Physiol. Biochem.*, 2007, **45**, 62–69.
122 C. J. Lee, H. Yangcheng, J. J. Cheng and J. Jane, *Starch - Stärke*, 2016, **68**, 348–354.
123 A. Zayed, S. Gowthaman and N. Terry, *J. Environ. Qual.*, 1998, **27**, 715–721.
124 S. H. Bokhari, I. Ahmad and M. Mahmood-ul-hassan, *Int. J. Phytoremediation*, 2016, **18**, 25–32.
125 K. J. Appenroth, K. Krech, Á. Keresztes, W. Fischer and H. Koloczek, *Chemosphere*, 2010, **78**, 216–223.
126 F. J. Gschwend, L. M. Hennequin, A. Brandt, F. E. Bedoya-Lora, G. H. Kelsall, K. Polizzi, P. Fennell and J. Hallett, *Green Chem.*, 2020, **22**, 5032–5041.
127 F. Gschwend, PhD Thesis, Imperial College London, 2017.
128 A. Brandt-Talbot, F. J. V. Gschwend, P. S. Fennell, T. M. Lammens, B. Tan, J. Weale and J. P. Hallett, *Green Chem.*, 2017, **19**, 3078–3102.
129 E. C. Achinivu, R. M. Howard, G. Li, H. Gracz and W. A. Henderson, *Green Chem.*, 2014, **16**, 1114–1119.
130 D. Klein-Marcuschamer, B. A. Simmons and H. W. Blanch, *Biofuels, Bioprod. Biorefining*, 2011, **5**, 562–569.
131 J. Stoimenovski, E. I. Izgorodina and D. R. MacFarlane, *Phys. Chem. Chem. Phys.*, 2010, **12**, 10341–10347.

Conclusions

Key Findings

This PhD has explored the potential for integrating ionic liquid biorefinery with constructed wetland remediation of wastewater. Firstly, the current understanding of the ionoSolv process was built upon by investigating the effects of acidity through cation modification The economic and technical feasibility of wetland remediation and subsequent biomass valorisation were then explored computationally, providing a more defined scope for constructed wetland implementation. Lastly, the potential for valorisation of wetland biomass was demonstrated through ionic liquid pretreatment, for both emergent macrophytes and for promising duckweed species.

In Chapter 2, it was shown that the acidity of alkylammonium $[HSO_4]^-$ ILs increases significantly as the degree of substitution of the cation decreases, which was not predicted by aqueous acid theory. The acidity of [MBA][HSO_4], [HA][HSO_4], and [BA][HSO_4] were found to be equivalent to that of [DMBA][HSO_4] containing 11%, 31%, and 32% excess acid respectively. Although addition of butylamine reduced the acidity of [BA][HSO_4], it was still found to be more acidic than [MBA][HSO_4] after addition of 20% excess base. The enhanced acidity of primary and secondary alkylammonium cations was found to be due to increased anion-cation and anion-anion interactions, leading to clusters of concentrated IL with less water intercalation, thus increasing the proton activity of the $[HSO_4]^-$ anion.

The effect of excess acidity on pretreatment of *Miscanthus* was evident with more rapid hemicellulose removal and cellulose degradation, sharper delignification and pulp purity peaks, and earlier re-deposition of pseudolignin and lignin. Despite equal Hammett acidity, solutions of [DMBA][HSO_4] with excess acid clearly displayed higher severity than those using primary and secondary alkylammonium cations, taken to show different “types” of acidity. Besides a general increase in the rate of ether bond cleavage, no high-level trends with acidity were apparent regarding recovered lignin structure. Although reasonable pulp purities (above 80%) were obtained at short durations using primary alkylammonium cations and 11% excess acid, saccharification was severely inhibited. It was not found to be possible to reduce this inhibition by changing process conditions or protocols, which was due to enhanced enzyme deactivation rather than cellulose inaccessibility. No such inhibition occurred using [MBA][HSO_4], however, which appears to be a promising pretreatment solvent, performing as well as [DMBA][HSO_4] but with faster kinetics. [MBA][HSO_4] was found to produce high purity pulps (over

90%) with high digestibilities (around 90%) at temperatures between 120 and 170 °C, even with up to 5% excess base, and was confirmed to be thermally stable at pretreatment conditions.

Chapter 3 saw a high-level economic comparison between constructed wetland remediation and conventional remediation technologies, for BOD and nutrient removal, and for low-pH and circumneutral-pH AMD remediation. Wetland design was found to be important, with optimisation of the number of cells allowing substantial economic and areal savings, as the increased cost from the decrease in cell size was offset by the improved hydraulic performance of the system. Overall, the economic advantages were found to be most pronounced at low flow rates and contaminant levels. Secondary treatment costs were found to be lower for constructed wetlands than using conventional technologies, even at high flow rates. For integrated secondary and tertiary treatment, wetland remediation was found to be economically favourable until stringent effluent standards (0.5 mg/L phosphorus and 1 mg/L ammonia), and was competitive even at flows above 10,000 m^3/d. However, wetland remediation was not more competitive for tertiary treatment of post-secondary treatment wastewater. These findings were robust to variation in costing and removal parameters, and land costs were found to have little effect. AMD remediation was found to always be economically favourable using Free Water Surface wetlands for circumneutral-pH drainage. For low-pH AMD, constructed wetlands were only economically favourable for low flow rate and/or acidity low-pH drainage. However, this range of conditions covers most of the collated real site data. When investigating the valorisation of the wetland biomass, a profit of around $100/t of harvested biomass were required to offset 10% of total treatment costs. However, the area requirement was identified as the major barrier to operate an IL biorefinery using only wetland biomass, which may need to be blended with other feedstocks.

Chapter 4 then investigated the suitability of the ionoSolv process for the pretreatment of constructed wetland species, focussing on emergent macrophytes. Through timecourse experiments, promising pretreatment conditions were determined at 150 °C using virgin *Phragmite australis*: 30 and 45 minutes using [DMBA][HSO_4], and 30 minutes using [MBA][HSO_4]. [DMEtA][HCOO] was found to lead to a much higher total sugar release by preserving hemicellulose, and generated more native-like lignin, but required much longer pretreatment durations (2-3 hours). By testing two more batches of *Phragmites australis*, it became apparent that the high extractives content (over 20%) was enhancing pseudolignin formation and redeposition, leading to lower pulp purities compared to *Miscanthus*. The date of harvest of the feedstock was found to be important, with feedstocks harvested in winter following chlorosis having a much lower extractive content and behaving more similarly to *Miscanthus*. Feedstock independence was then further demonstrated by pretreating a total of 11 wetland feedstocks, covering 7 common species. Pretreatment using [DMBA][HSO_4] improved

digestibilities to over 80% for most feedstocks, corresponding to 20-25 wt% glucose release for the majority of species. Pretreatment also improved pulp purities to around 70%, predicted to rise to around 80% following a water Soxhlet step, to remove calcium and potassium sulfate salts generated by reaction with the anion that otherwise impeded mass closure during compositional analysis.

Nine wetland feedstocks were then combined and pretreated at 150 °C using [DMBA][HSO_4] (30 and 45 minutes) and [MBA][HSO_4] (30 mins). Behaviour closely matched the arithmetic mean of constituent species. However, when recycling the IL solvent for up to 4 cycles, delignification worsened progressively, leading to drops in digestibility and purity. This was accompanied by a drop in acid/base ratio of 6%. Attempts to restore the solution to a stoichiometric acid/base ratio led to a clear excess of acid, however, and performance worsened further. Addition of $^1/_3$ and $^2/_3$ of the calculated amount of missing acid between cycles (as well as a water Soxhlet of the pulp) appeared to stabilise drops in acid/base ratio and delignification, but the water Soxhlet worsened digestibility through presumed formation of degradation products on the pulp from the second cycle onwards. Pre-extraction of the biomass still led to decreasing acid/base ratio and delignification, but maintained high digestibility over 3 cycles. Addition of $^1/_2$ the calculated acid led to an overshoot in severity, however, decreasing digestibility substantially.

When pretreating a mixed metal-contaminated wetland feedstock, containing 6 species from wetlands treating AMD, metal extractions of 75-90% were observed for Fe, Zn, Al, and Cd using [DMBA][HSO_4], [MBA][HSO_4], and [Hmim]Cl. [Hmim]Cl outperformed both [HSO_4] ILs and was the only IL to extract Pb. [MBA][HSO_4] was shown to outperform [DMBA][HSO_4] for metal extraction. Pretreatment performance was similar across all three ILs: limited delignification (56-58%) but very high digestibilities (over 90%), with the low lignin removal attributed to the high feedstock content of non-lignocellulosic *Sphagnum spp*.

Chapter 5 explored the possibility for ionic liquid pretreatment of duckweed, aiming to ultimately separate starch and protein, while simultaneously extracting metals. The interactions of four ILs with pure starch at pretreatment conditions were initially investigated, in order to determine what conditions could be employed without starch degradation. [DMBA][HSO_4] was found to be suitable even at 120 °C for short durations. Starch was stable in [MEA][OAc] and [DMEtA][HCOO] at 120 °C, but its water-insoluble residue was found to change into a crystalline structure. [Hmim]Cl was found to hydrolyse the starch extensively and was not considered suitable.

S. polyrhiza was pretreated at 120 °C using [DMEtA][HCOO] and at 90-150 °C using [DMBA][HSO_4]. IL pretreatment significantly enhanced digestibility, allowing over 90% of final yield to be reached after only 8 hours of hydrolysis. Optimal conditions for starch recovery and pulp digestibility were found to

be [DMBA][HSO_4] at 120 °C for 30 minutes, and [DMEtA][HCOO] at 120 °C for 3 hours. [DMBA][HSO_4] was found to continuously remove the protein from the pulp, whereas [DMEtA][HCOO] rapidly extracted around half of the protein but this did not increase further. There was no protein enrichment in the pulp or the lignin, but a protein content of 46% was reached in the post-saccharification residue. The protein extracted into the liquor was not able to be recovered by dialysis. *L. minor* was found to readily uptake Cd and Ni, up to around 600 and 400 ppm from water concentrations of 2 ppm in only 3 days. Pretreatment behaviour of this different duckweed species was very similar to *S. polyrhiza* despite a much higher starch content and lower protein content. Using [DMEtA][HCOO], near-quantitative saccharification yields and digestibilities were observed after 8 hours of hydrolysis. However, metal removal at these pretreatment conditions was found to be very limited, and Cd was barely extracted from the pulp.

Limitations and Further Work

This body of work represents an initial, and (hopefully) compelling argument for the integration of constructed wetland remediation with ionic liquid biorefinery, and improved understanding of the ionoSolv process. In doing so, however, a number of new questions have been raised, and there remains further work to be done in order to conclusively show that the combination of these processes can function at scale. Furthermore, the limitations of the work carried out in this study must be analysed in order to improve future investigations and analyses.

The acidity trends uncovered in Chapter 2 highlight the tunability of ILs, and can certainly be built upon in both biomass pretreatment and beyond. Further molecular modelling such as QM calculations should be used to validate the hypothesis of enhanced proton activity on the anion. In addition, the effect of further cation modification should be investigated, such as addition of hydroxyl groups, or the effect of alkyl chain length on secondary and tertiary alkylammonium cations. The suitability of primary and secondary alkylammonium $[HSO_4]^-$ ILs for catalysis may be of interest due to their enhanced acidity, and comparison of their behaviour in a process such as Fischer esterification compared to simply adding excess acid to [DMBA][HSO_4] would help enlighten this. Their enhanced acidity could also be used for the production of nanocellulose, as their enhanced levels of cellulose hydrolysis may improve yields, while residual pseudolignin would be easier to remove during oxidation than native lignin. While a number of factors were ruled out for explaining saccharification inhibition, further testing should have been carried out to help elucidate the cause, in particular liquor analysis and SEM of the pretreated pulps. Furthermore, even milder pretreatment conditions (such as below

100°C) should be attempted for primary cations, both for potential improvements in process energy use and to elucidate the reasons behind inhibition.

To replace [DMBA][HSO_4] as first-choice pretreatment solvent, [MBA][HSO_4] should be tested among a wider range of feedstocks, and its corrosion behaviour should be compared, as this may limit its suitability. Additionally, an economic comparison between bulk costs of both ILs would be useful to help choose between the two. In addition, the Hammett acidity of [MBA][HSO_4] using excess base should have been determined, for better comparison to pretreatments using [DMBA][HSO_4].

The methodology employed in Chapter 3 could be improved in a number of ways. Future work should firstly focus on the development of improved wetland design models and parameters. Arguably, the most important of these involves increased removal rate data, with an aim to reduce the uncertainty introduced by the wide range of removal rate estimates or to gain a better understanding of high-level parameters affecting the removal rate. Additionally, this type of study would also benefit from an improvement in the generalised wetland sizing methodology. While the first-order removal rate model for nutrient removal may be regarded as more sophisticated than that of the zero-order rate used for AMD remediation, both clearly have drawbacks. Intrinsically, the former removal rate will eventually lead to overly high estimates for *k* at increasing concentrations, while the latter will provide overly optimistic estimates at low concentrations. This was explored in more detail in Section 3.4. Lastly, the impact of economies of scale on the costs of individual cells within one wetland was estimated using the available wetland cost data, which is likely to slightly overestimate the costs of multiple smaller cells within one larger wetland. However, this is not thought to have a large impact on the results nor on the determined trends.

Aside from the improvement of the underlying contaminant removal models, there exist multiple possible areas for further work on this topic. More careful consideration of the water budget, such as through precipitation and evapotranspiration, could allow identification of geographic regions with the highest potential for wetland remediation. This could be further improved by combination with geographic factors such as the Construction Cost Index to account for variation in capital and O&M costs. Additionally, more detailed modelling of project cash flows such as discounting may improve cost estimates. Other passive technologies used as a pretreatment step for wetland remediation may also be included in the model, such as facultative ponds or anoxic limestone drains. Moreover, the impact of using floating biomass species with high nutrient uptake rates (i.e. duckweed) should be investigated as a way of improving the process economics of tertiary treatment. Lastly, thorough technoeconomic investigation into utilisation of wetland biomass in an IL biorefinery should be carried out in order to determine whether a significant proportion of costs may be offset.

The work carried out in Chapter 4 opens up many avenues for further study. Firstly, valorisation of the extractives content should be investigated, starting with identification of the main types of compounds within wetland species. This is particularly relevant following the findings in Chapter 3, which showed that the area requirements for a biorefinery using only wetland feedstocks are infeasible, and that they will need to be blended with other feedstocks. As a result, pre-extraction to prevent accelerated pseudolignin formation and to reduce sulfate salt formation would be preferable. Secondly, a methodology should be developed for accurately determining the "true" acid/base ratio of pretreatment liquor, which was found to be inaccurate using existing methods. Lastly, pretreatment of pre-extracted feedstocks appears most promising for recycling purposes. The required amount of acid to maintain the acid/base ratio using pre-extracted feedstocks should be investigated, as was done using non-extracted feedstocks.

The work in Chapter 4 could have been improved upon in a number of ways. Firstly, by pre-extracting all feedstocks analysed, following the realisation that high extractives content was enhancing pseudolignin formation. Timecourse pretreatments to determine whether pre-extracted *Phragmites Australis* behaved the same as *Miscanthus* would also have been insightful. Secondly, when performing HSQC NMR of *Phragmites australis* lignin, lignin recovered using [DMBA][HSO_4] should also have been analysed, as an intermediate in severity between [MBA][HSO_4] and [DMEtA][HCOO]. Thirdly, in the second recycling pretreatment, when adding varying amounts of acid the water Soxhlet should not, in hindsight, have been performed as well, as it ended up inhibiting saccharification. There was, however, no basis for anticipating this. Fourthly, the lignin obtained during recycling experiments should have been characterised, which may have provided further insight into the mechanisms underlying the reduction in delignification across cycles. Fifthly, the individual metal-contaminated feedstocks should have been individually pre-treated and characterised. This would have made the strange pretreatment behaviour of the mixed metal-contaminated feedstock easier to explain. Lastly, a higher solids loading should have been employed, as 10% wt/wt is unlikely to be sufficient for any larger-scale process.

There remains significant promise surrounding the use of duckweed for ionic liquid biorefinery, and the possibility to extract both starch and protein should studied further. The interactions between duckweed and protein should be studied, in a manner analogous to that which was used to study interactions with pure starch. This will allow protein partitioning behaviour to be better understood during pretreatment, and will also allow optimal conditions for protein extraction to be determined. The use of a membrane with a smaller molecular weight cut-off should be investigated for protein recovery from the liquor. This could form part of a larger investigation into the use of membranes in the ionoSolv process, for example for water removal between cycles or clean-up of the liquor through

solute removal. If protein recovery from the ionic liquid is not feasible, work should focus on the extractability of protein from the post-saccharification residue, and how to maximise yields and purity within this fraction. Closure of the protein mass balance may also be carried out by analysing the amino acid composition of the duckweed protein, and then analysing the IL liquor for those amino acids. It may also be worthwhile to investigate the use of [Hmim]Cl to pretreat duckweed for its high metal removal abilities, despite its poor performance with pure starch. In future, duckweed feedstocks should be stressed just before harvesting in order to raise starch content, for example by transferring them to tap water and leaving them in the dark. This may, however, have non-trivial additional costs on a large scale. Lastly, as with other wetland feedstocks, investigation into the compounds within the extractives fraction should be carried out.

Regarding the limitations of the work in Chapter 5, the starch employed should have been characterised by GPC, as this would have improved the understanding of the interactions with the ILs. Additionally, some analysis should have been carried out on the clear, crystalline solid obtained, possibly GPC or X-Ray Diffraction, to further understand its structure and reasons behind its formation. In terms of duckweed pretreatments, the composition of *L. minor* should have been determined before metal-contamination to check for any increases in starch content. Lastly, the duckweed strains used both had low starch contents (around 3% and 10%). It would have been preferable to use a strain with a higher starch content, as starch accumulation is one of the key reasons for the interest in duckweed as a biorefinery feedstock. However, the pretreatment behaviour of starch fractions was consistent between feedstocks, and mirrored that of pure starch.

Concluding Remarks

The eventual widespread adoption of constructed wetlands for wastewater remediation may feel like a pipe dream at this point in time. However, this low-maintenance and (now proven) low-cost water remediation technology has the potential to positively affect the lives of millions, for whom there is scant chance of a modern treatment plant being constructed in their back yard. However, technological deployment is often slow, and depends primarily on perceived risk and cost.

Constructed wetland uptake has to date been encouraged through increasing experimental evidence of their efficacy, aiming to assuage fears over their remediation performance. This must now be complemented by economic modelling to showcase their financial advantages, and with valorisation of biomass to show that constructed wetlands fit into the wider sustainable solution of biorefinery.

Through bodies of work such as this PhD, it is hoped that the case for constructed wetlands will eventually become too strong to ignore.

Appendix

Ionic Liquid Synthesis NMRs

Proton and carbon NMRs for the synthesised ILs are provided in Figs. A1-1-14, all carried out in deuterated DMSO.

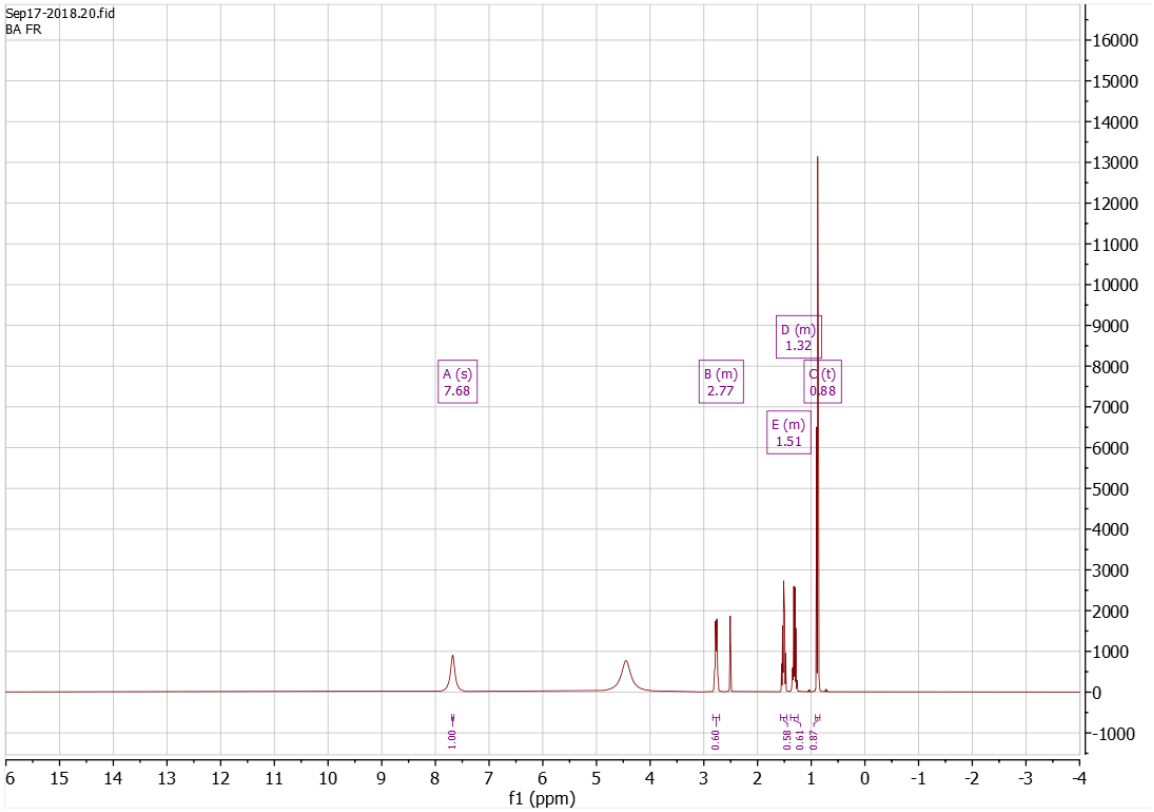


Figure A1-1: Proton NMR of [BA][HSO_4]

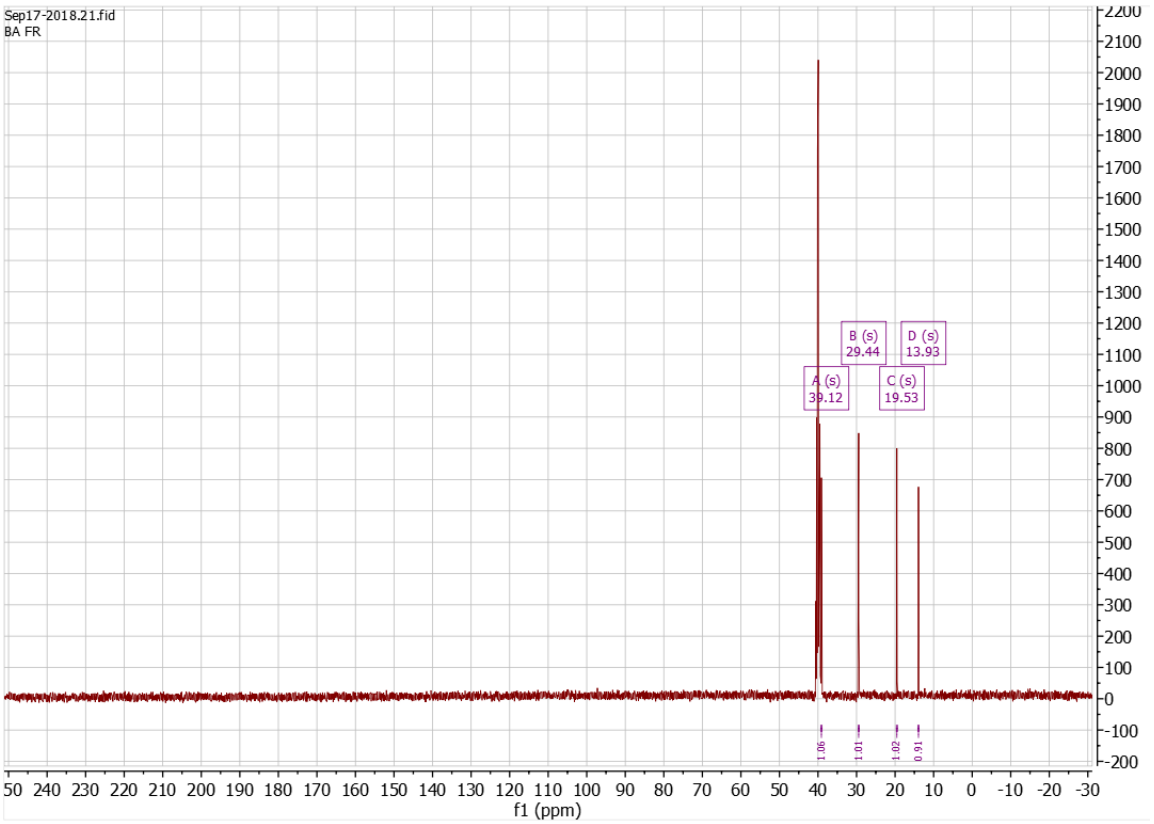


Figure A1-2: Carbon NMR of [BA][HSO_4]

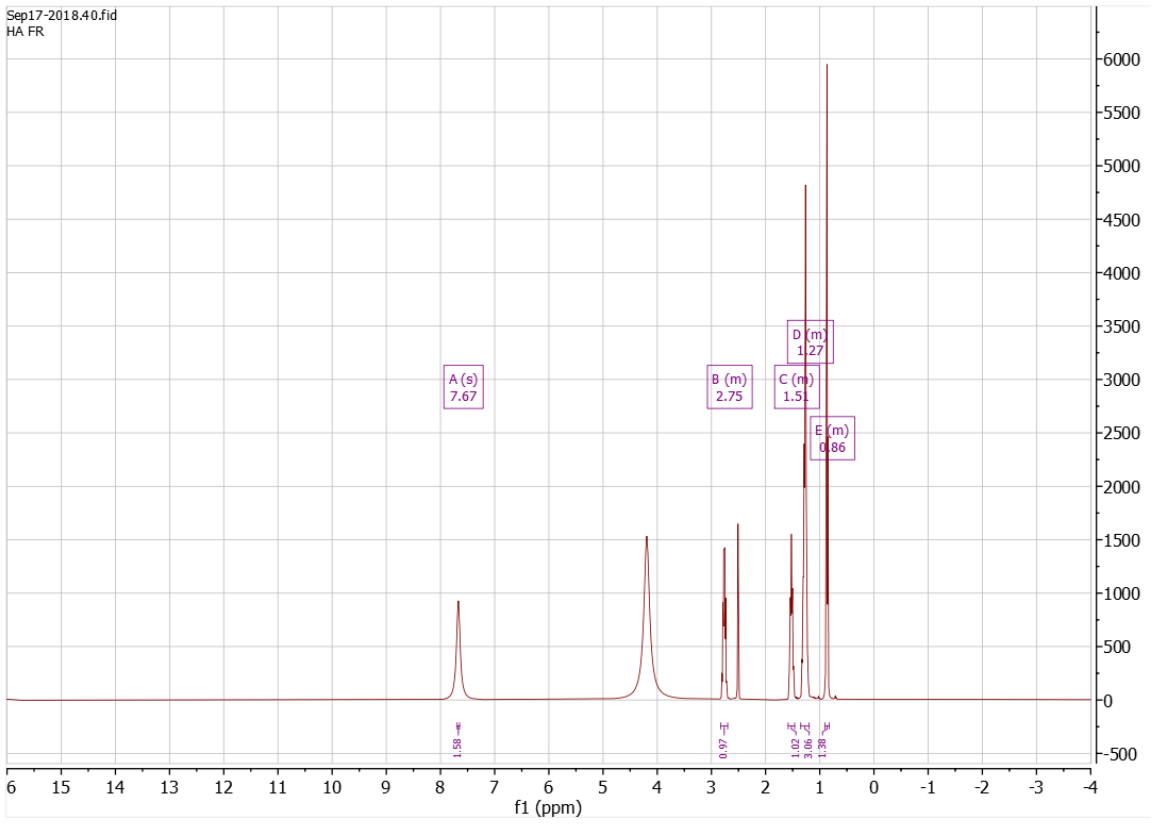


Figure A1-3: Proton NMR of [HA][HSO_4]

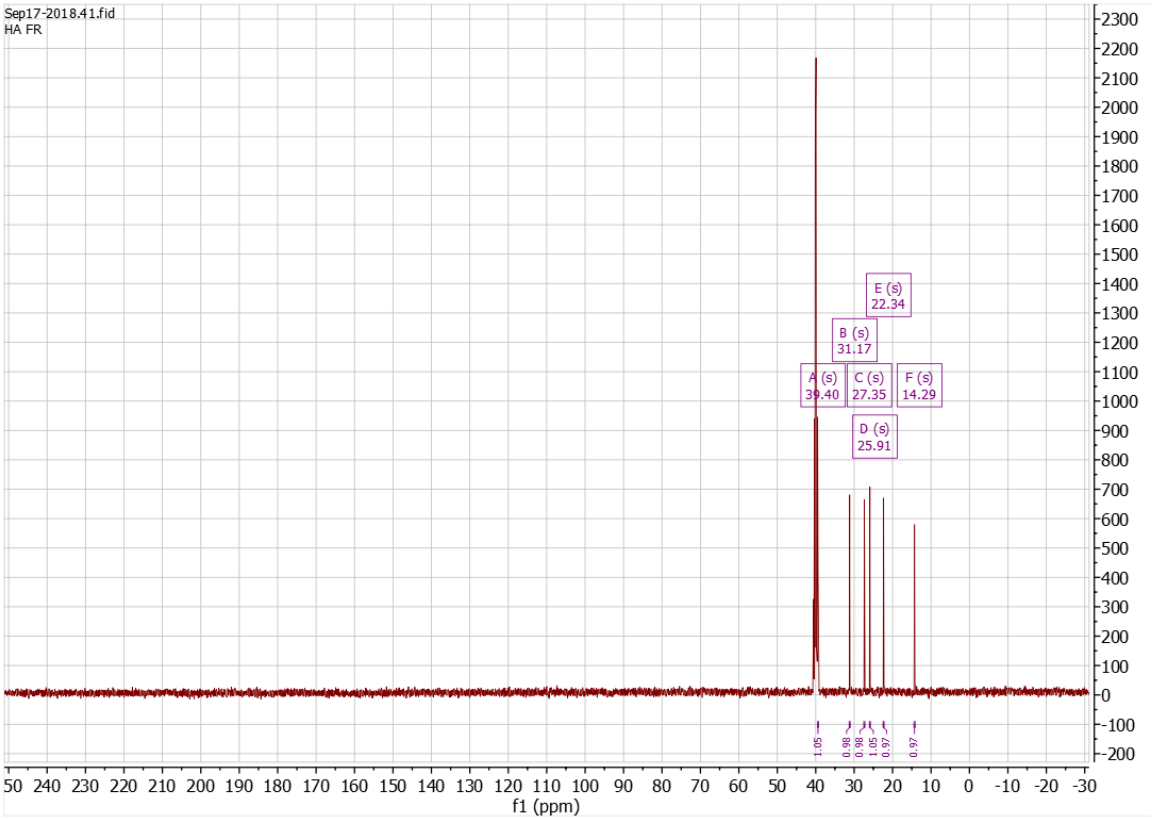


Figure A1-4: Carbon NMR of [HA][HSO_4]

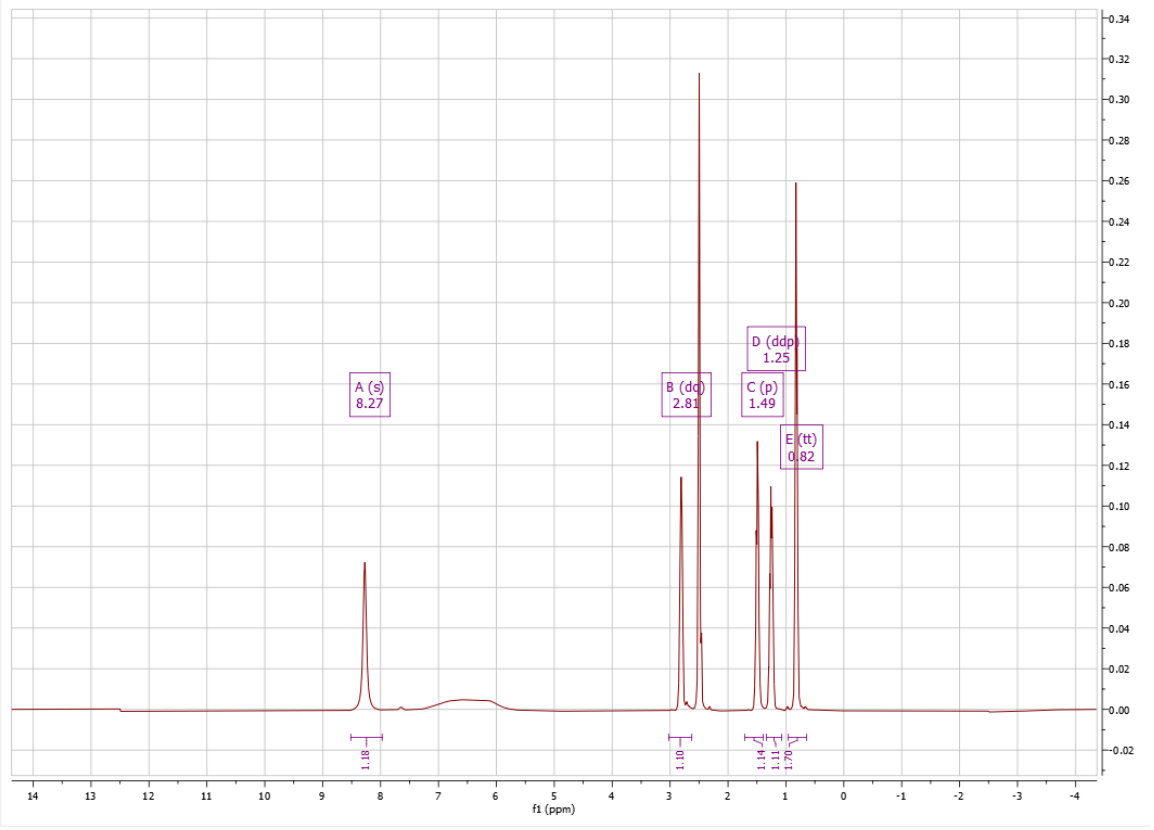


Figure A1-5: Proton NMR of [MBA][HSO_4]

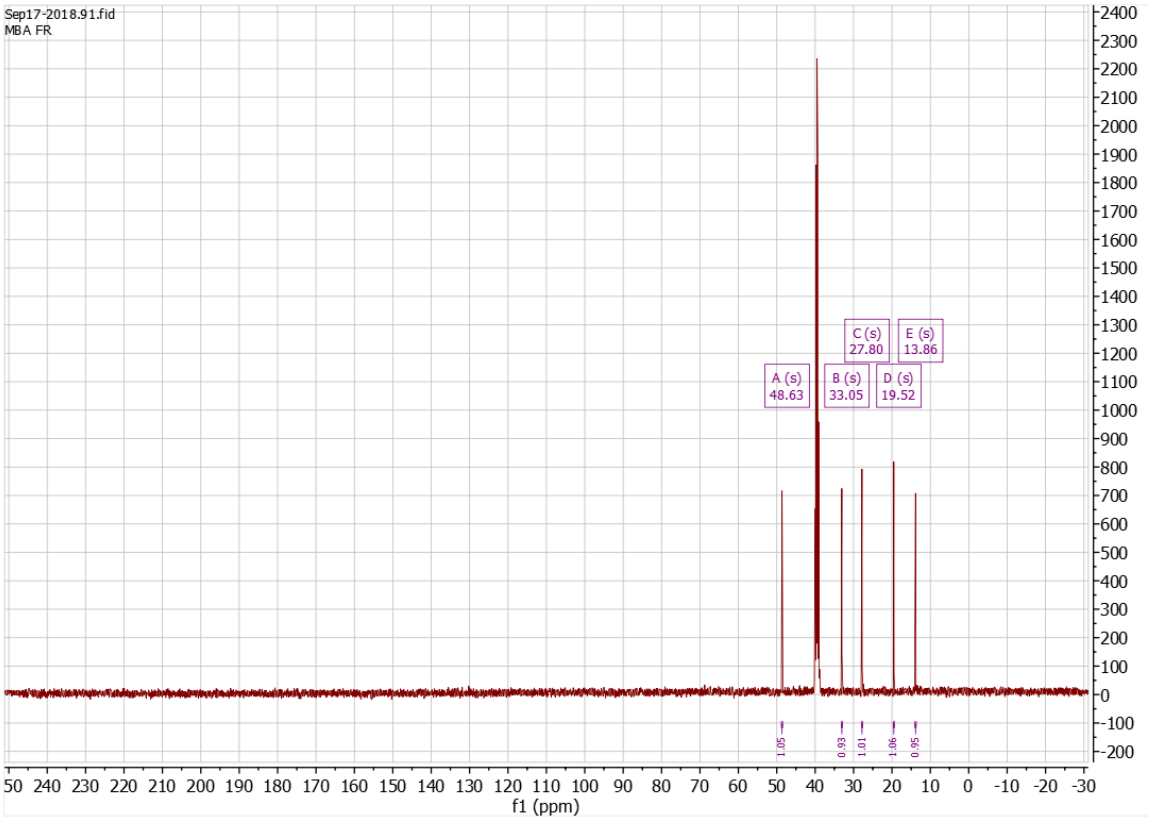


Figure A1-6: Carbon NMR of [MBA][HSO_4]

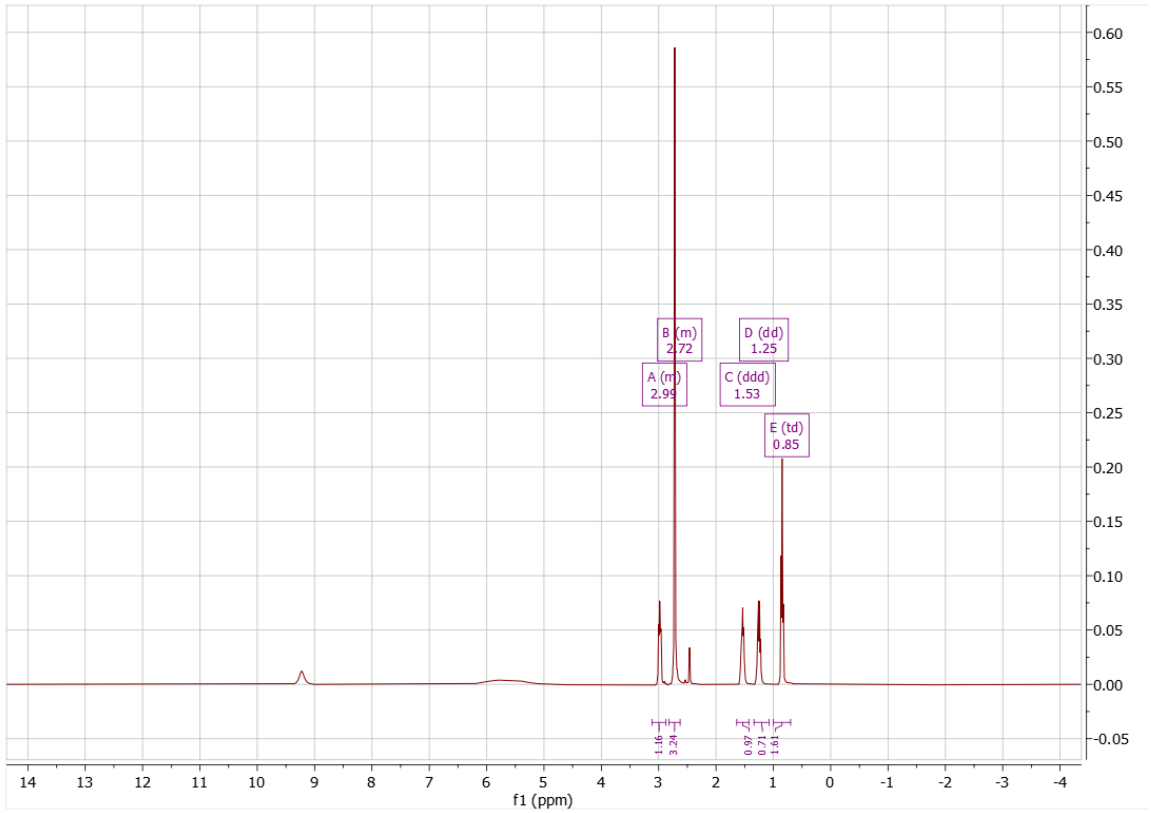


Figure A1-7: Proton NMR of [DMBA][HSO_4]

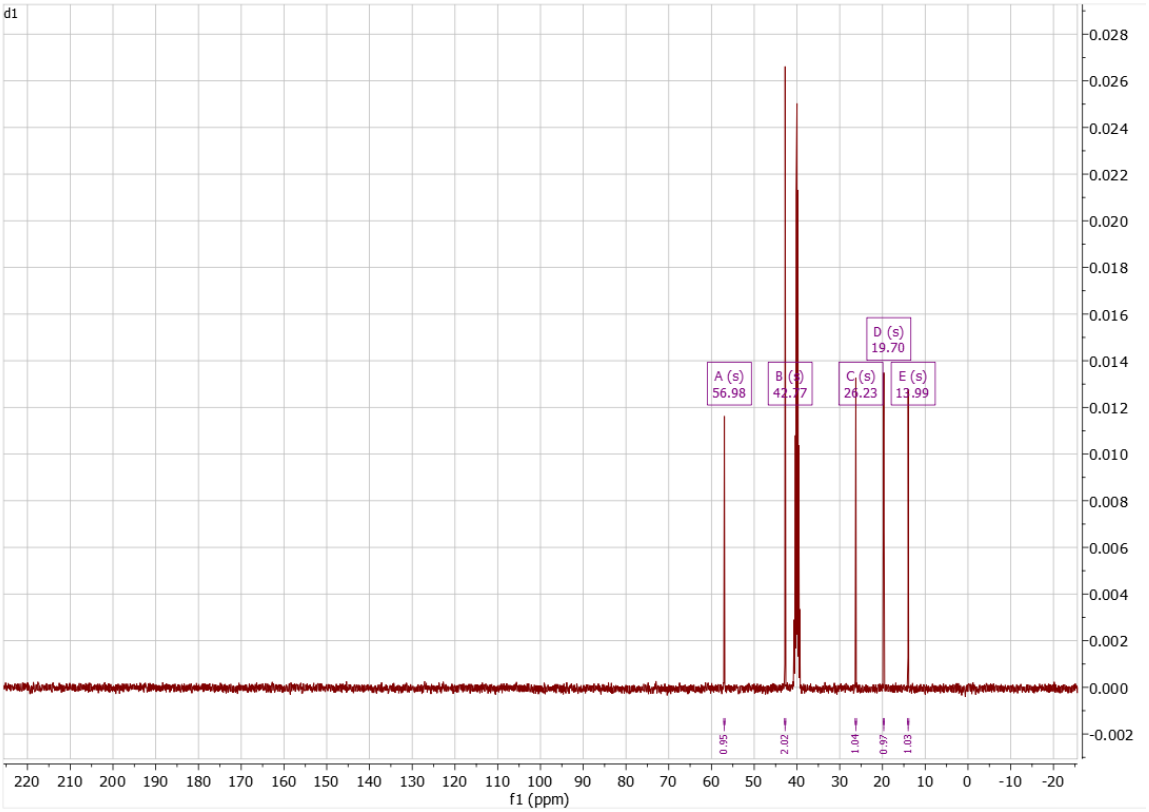


Figure A1-8: Carbon NMR of [DMBA][HSO_4]

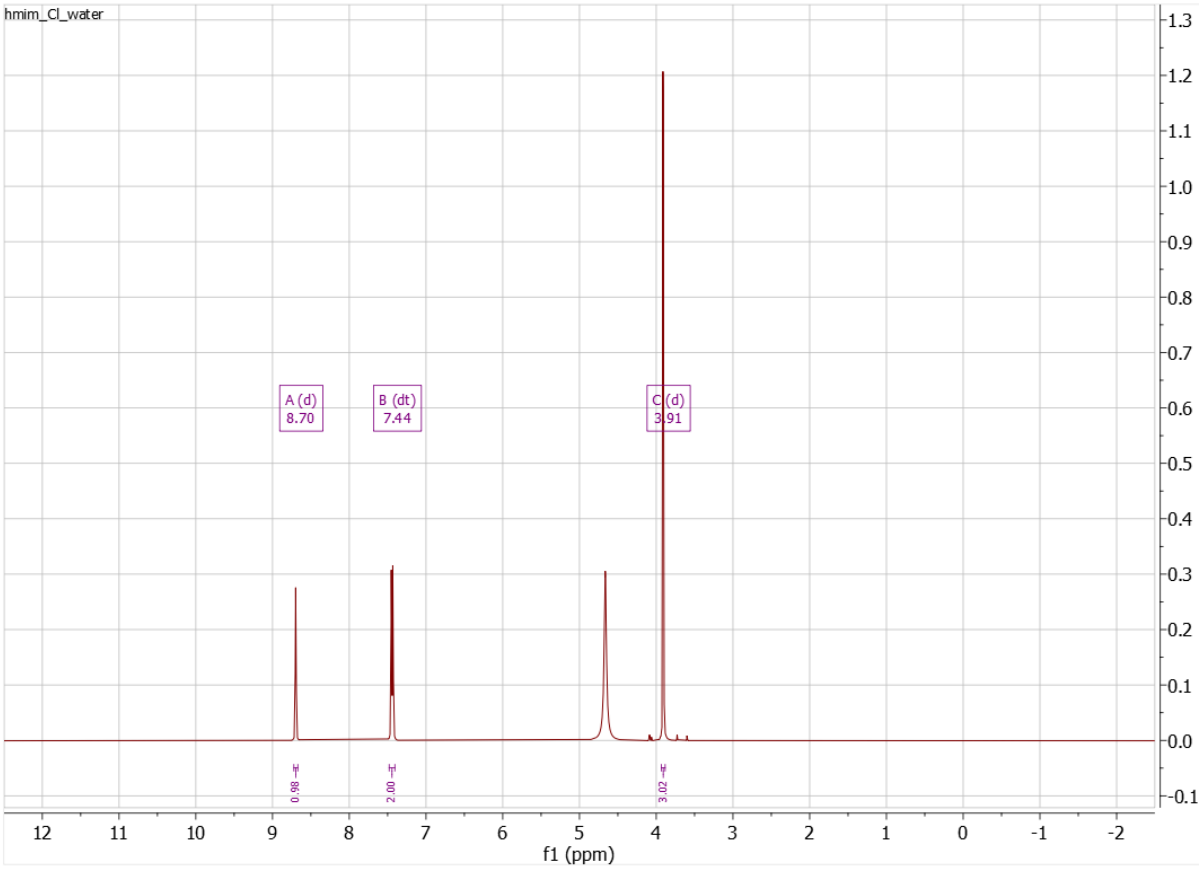


Figure A1-9: Proton NMR of [Hmim][Cl]

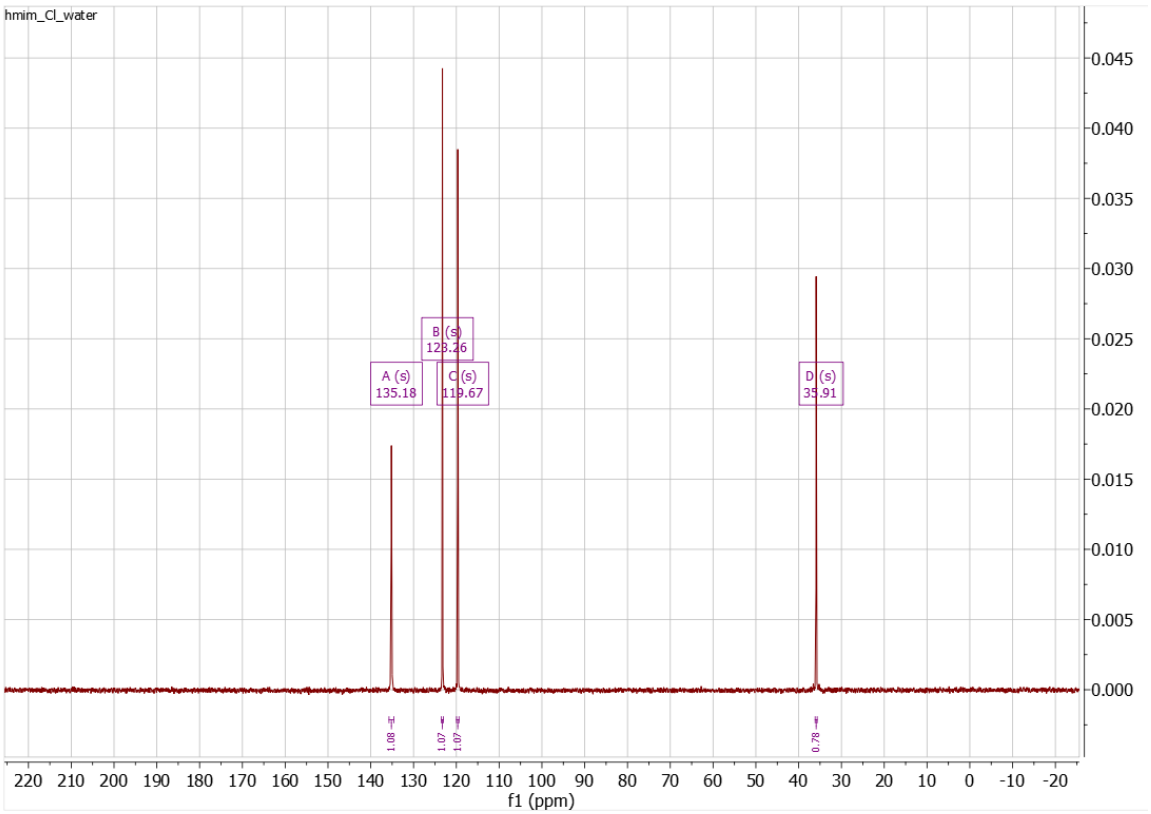


Figure A1-10: Carbon NMR of [Hmim][Cl]

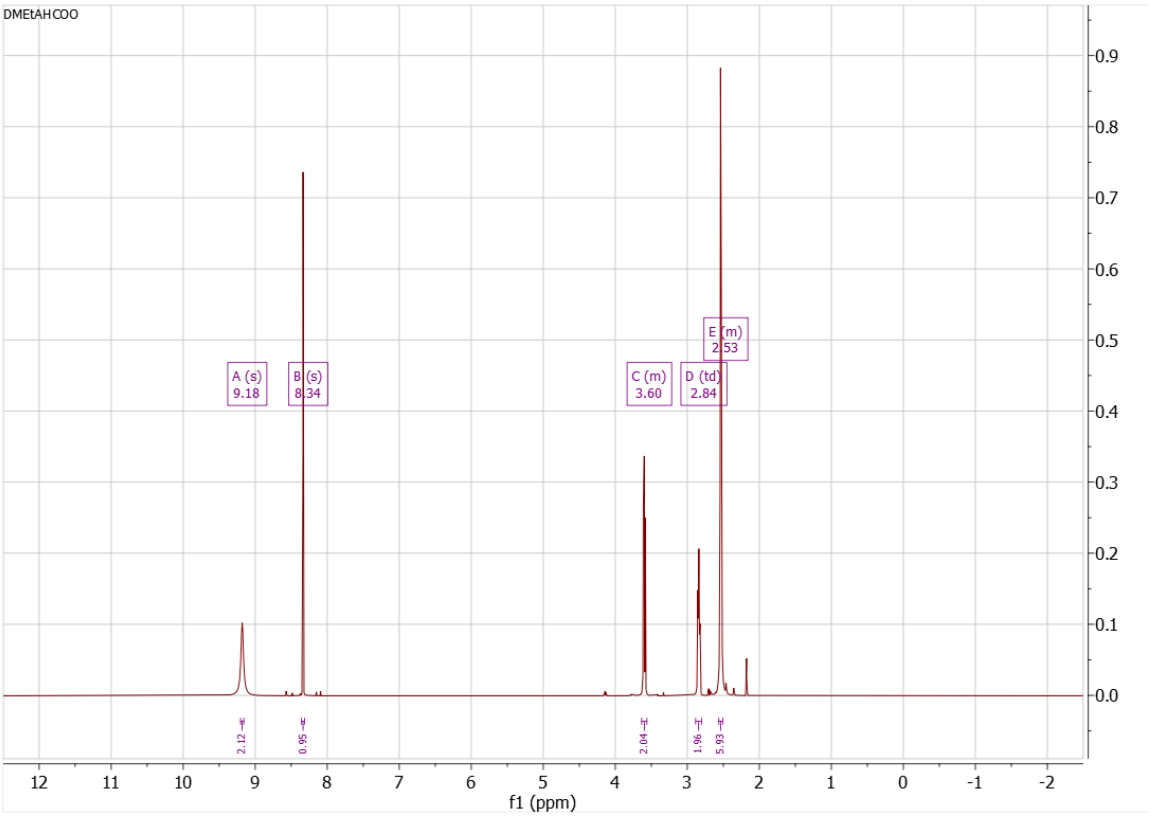


Figure A1-11: Proton NMR of [DMEtA][HCOO]

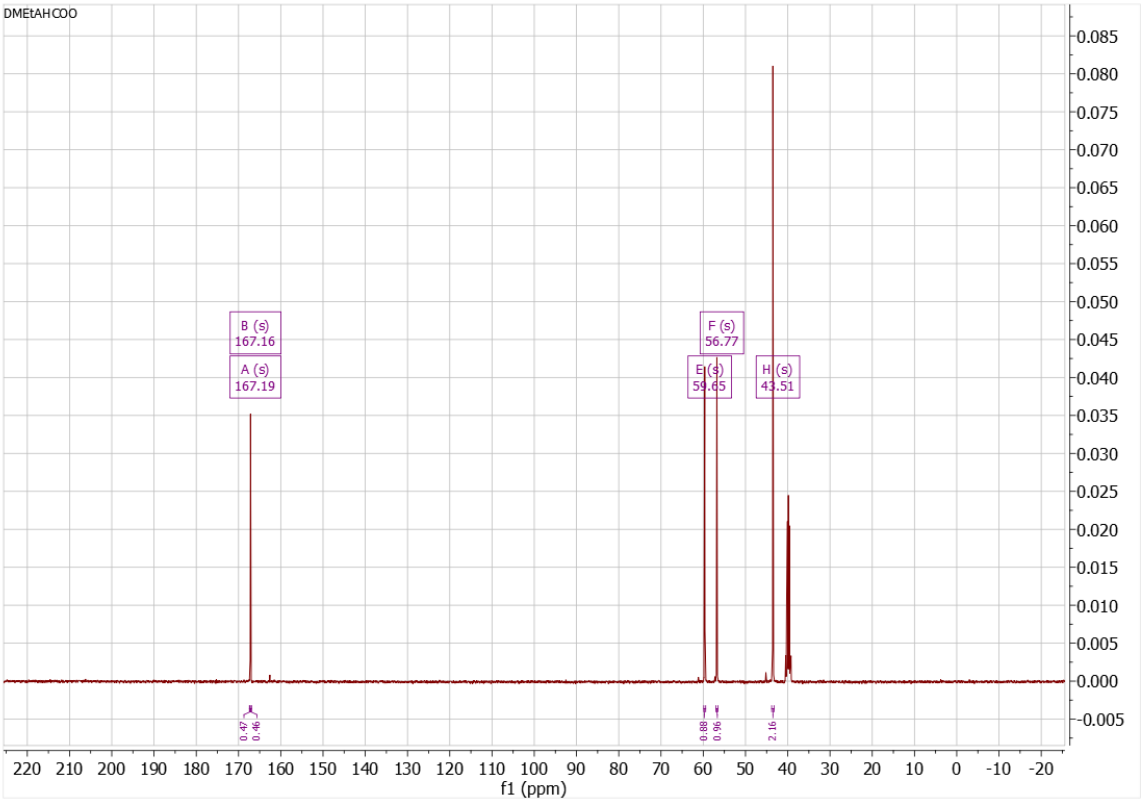


Figure A1-12: Carbon NMR of [DMEtA][HCOO]

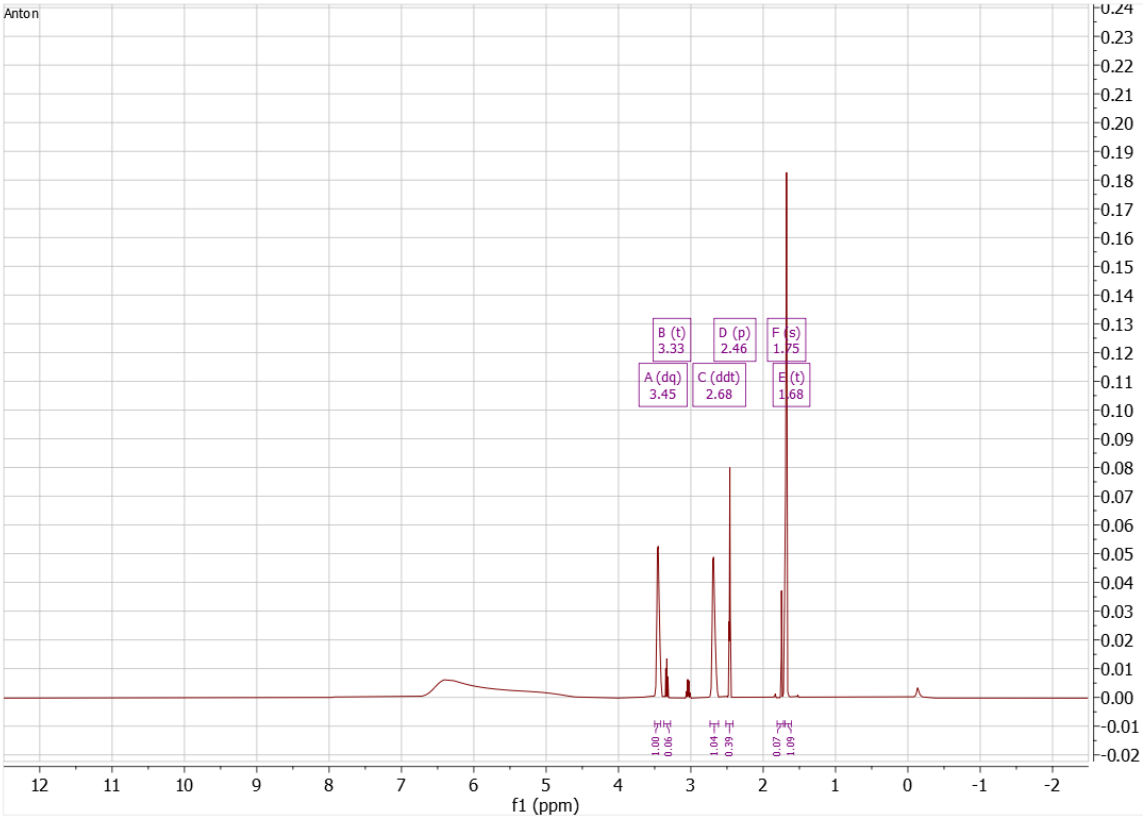


Figure A1-13: Proton NMR of [MEA][OAc]

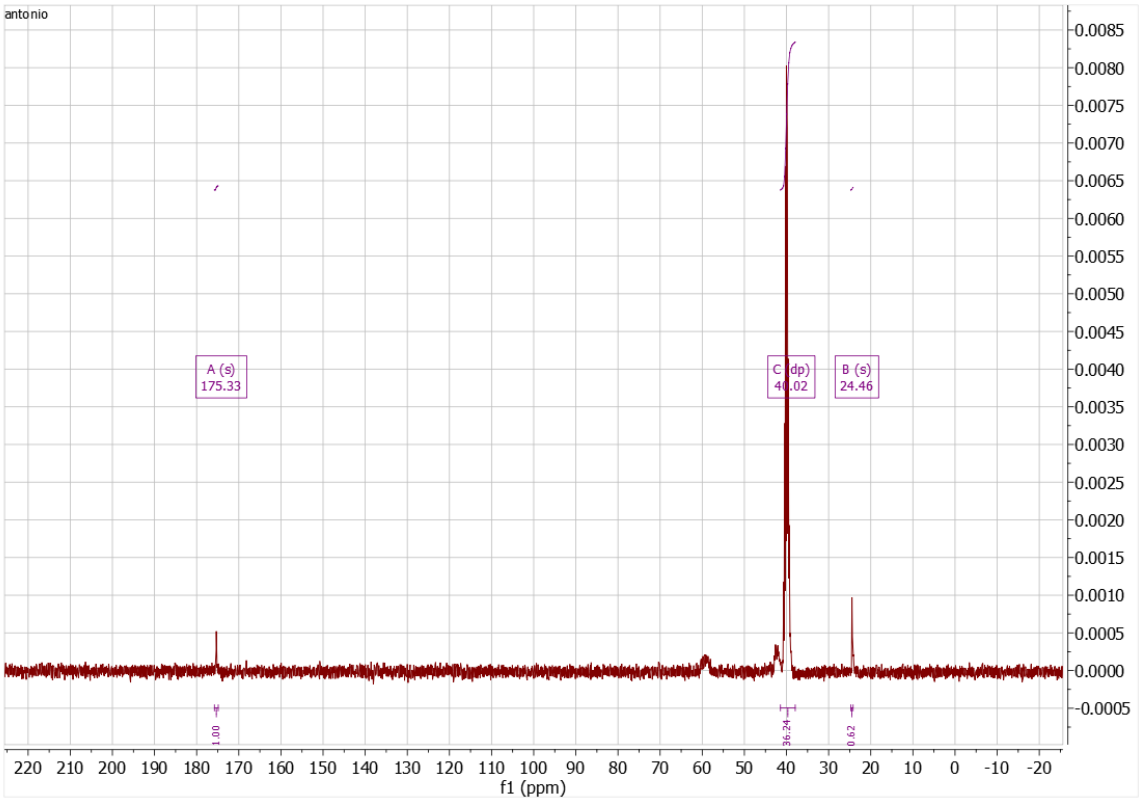


Figure A1-14: Carbon NMR of [MEA][OAc]

Chapter 2

Hammett Acidity Equation Derivation

The dissociation equilibrium of the Hammett base molecule (Scheme A2-S1) is expressed by Eq. A2-1. This can also be expressed through a simple mass balance, in Eq. A2-2. By definition, Hammett acidity is defined as in Eq. A2-3, which can thus be combined with Eq. A2-1 to yield Eq. A2-4.

$$B + H^+ \leftrightarrow BH^+ \quad \text{(A2-S1)}$$

$$pK_{BH^+} = -log_{10}\left(\frac{[BH^+]}{A_{H^+}\,[B]}\right) = log_{10}(A_{H^+}) - log_{10}\left(\frac{[BH^+]}{[B]}\right) \quad \text{(A2-1)}$$

$$[B_0] = [B] + [BH^+] \quad \text{(A2-2)}$$

$$H_0 = -log_{10}(A_{H^+}) \quad \text{(A2-3)}$$

$$H_0 = pK_{BH^+} + log_{10}\left(\frac{[BH^+]}{[B]}\right) \quad \text{(A2-4)}$$

where *B* is the un-protonated Hammett base, *BH⁺* is the protonated Hammett base, B_0 is the total amount of Hammett base (i.e. sum of protonated and un-protonated), pK_{BH^+} is the basicity constant of the Hammett base, and A_{H^+} is proton activity.

The Beer-Lambert law can be expressed in this system as either Eq. A2-5 and Eq. A2-6, which may be combined with Eq. A2-2 to yield Eq. A2-7.

$$A = [B] \times \varepsilon_0 \times l \quad \text{(A2-5)}$$

$$A = [B_0] \times \varepsilon \times l \quad \text{(A2-6)}$$

$$\frac{[BH^+]}{[B]} = \frac{\varepsilon_0 - \varepsilon}{\varepsilon} \quad \text{(A2-7)}$$

where A is the UV-Vis absorbance of the un-protonated Hammett base, ε_0 is the absorptivity of the fully un-protonated Hammett base, ε is the absorptivity of the partially protonated Hammett base, and *l* is path length.

Eq. A2-7 can be combined with Eq. A2-4 to yield Eq. A2-8, which was used to determine the Hammett acidity of the IL systems in Chapter 2, as in the work of Grasvik et al.[1]

$$H_0 = pK_{BH^+} - log\left(\frac{\varepsilon_0 - \varepsilon}{\varepsilon}\right) \quad \text{(A2-8)}$$

Hammett Acidity Measurements

The Hammett acidity was determined by measuring the absorbance of the unprotonated UV-Vis peak of 4-nitroaniline in the IL solutions, for multiple 4-nitroaniline concentrations. Several example spectra are shown in Fig. A2-1, with the corresponding graph of absorbance vs. (concentration * path length) shown in Fig. A2-2.

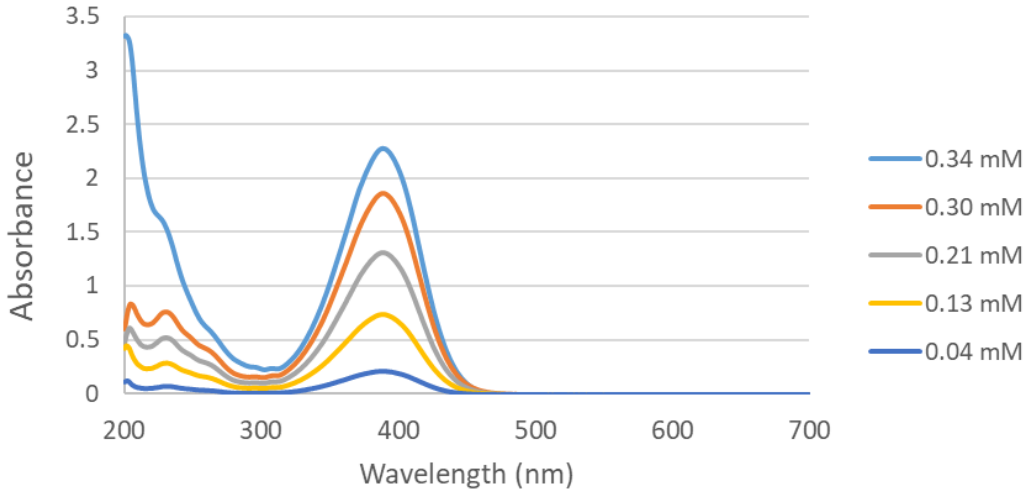


Figure A2-1: Example UV-Vis spectrum, for varying concentrations of 4-nitroaniline in [DMBA][HSO_4] (20 wt% water).

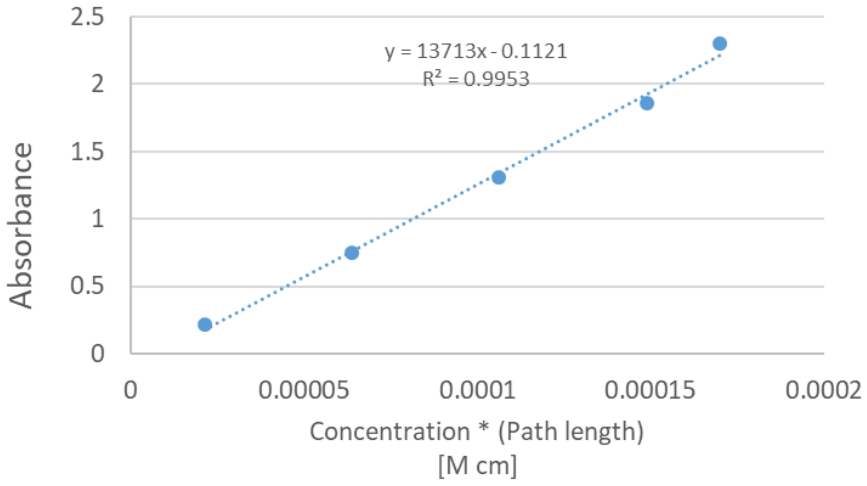


Figure A2-2: Example graph of UV-Vis absorbance vs. (concentration * path length), for a solution of 4-nitroaniline in [DMBA][HSO_4] (20 wt% water).

Molecular Dynamics Simulations

MD simulations were carried out by Dr Richard Matthews, with a brief overview of the methods provided here.

MD simulations were been carried out using the Amber16 program. Structural and dynamical analysis of each trajectory has been performed using the open source program TRAVIS. PILs ([BA][HSO_4], [HA][HSO_4], [MBA][HSO_4] and [DMBA][HSO_4]) have been modelled using the GAFF2 (General Amber force field). Partial atomic charges for PILs have been assigned using the RESP (restrained electrostatic potential) method as implemented in Antechamber. This process fitted ESP (MK) data obtained from quantum chemical calculations, performed on the equilibrium geometry of all individual ions, at the B3LYP/6-311+g(d,p) level using Gaussian16 (version X) to the model ions. No charge scaling has been applied to the PILs. The four-site TIP4P-EW model has been used to describe water.. Each system consisted of 200 cation-anion ion pairs. The number of water molecules added for each system was chosen to correspond to our experimental setup (20 wt% water for each IL). PIL boxes were simulated using periodic boundary conditions and a 2fs time step. The particle mesh Ewald (PME) method was employed for long-range electrostatics interactions and a 1.2 nm cut-off for nonbonded interactions. SHAKE was employed for all bonds containing hydrogen atoms.

The results of the MD calculations may be summarised through Fig. A2-3, which gives a visual representation of the H-bonding network found in the studied systems. The numbers shown corresponding to the average hydrogen bond count of each donor and acceptor. Fig. A2-3 thus demonstrates that the degree of cation-anion and anion-anion interaction decreases in the order [BA][HSO_4] = [HA][HSO_4] > [MBA][HSO_4] > [DMBA][HSO_4], in line with experimentally determined acidity.

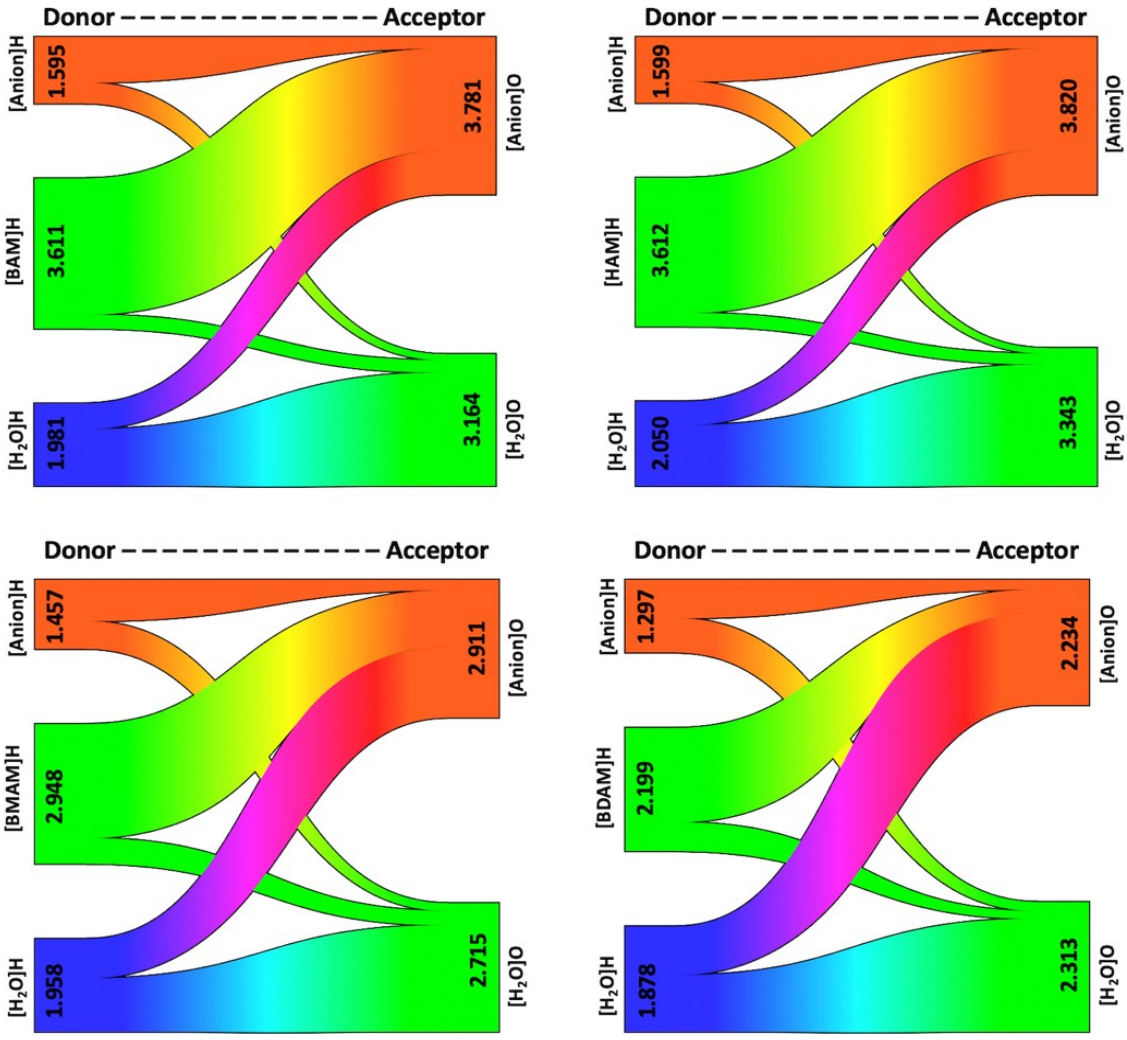
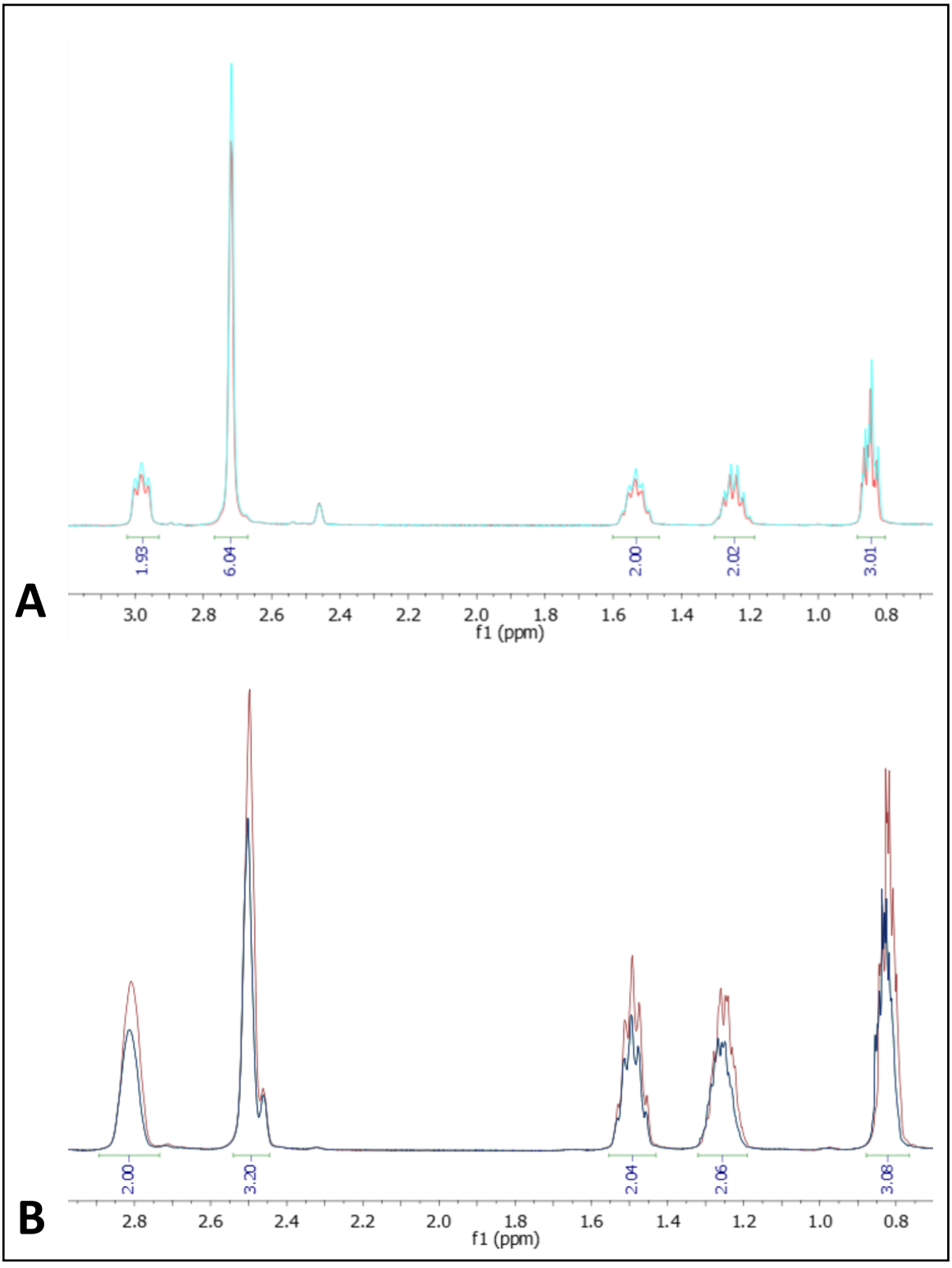


Figure A2-3: Linear Sankey diagrams for H-bond donors and acceptors in aqueous IL systems. Plots are top-left: [BA][HSO_4], top-right: [HA][HSO_4], bottom-left: [MBA][HSO_4], bottom-right: [DMBA][HSO_4]. Figure provided by Dr Richard Matthews.

Thermal Degradation Tests

As described in the main text, thermal degradation tests were conducted to investigate the thermal stability of [DMBA][HSO_4], [MBA][HSO_4], [HA][HSO_4], and [BA][HSO_4] for 72 hours at 170 ^{o}C. The resulting nmr spectra (before and after) are shown in Fig. A2-4.


A
1.93
6.04
2.00
2.02
3.01
3.0
2.8
2.6
2.4
2.2
2.0
1.8
1.6
1.4
1.2
1.0
0.8
f1 (ppm)
B
2.00
3.20
2.04
2.06
3.08
2.8
2.6
2.4
2.2
2.0
1.8
1.6
1.4
1.2
1.0
0.8
f1 (ppm)

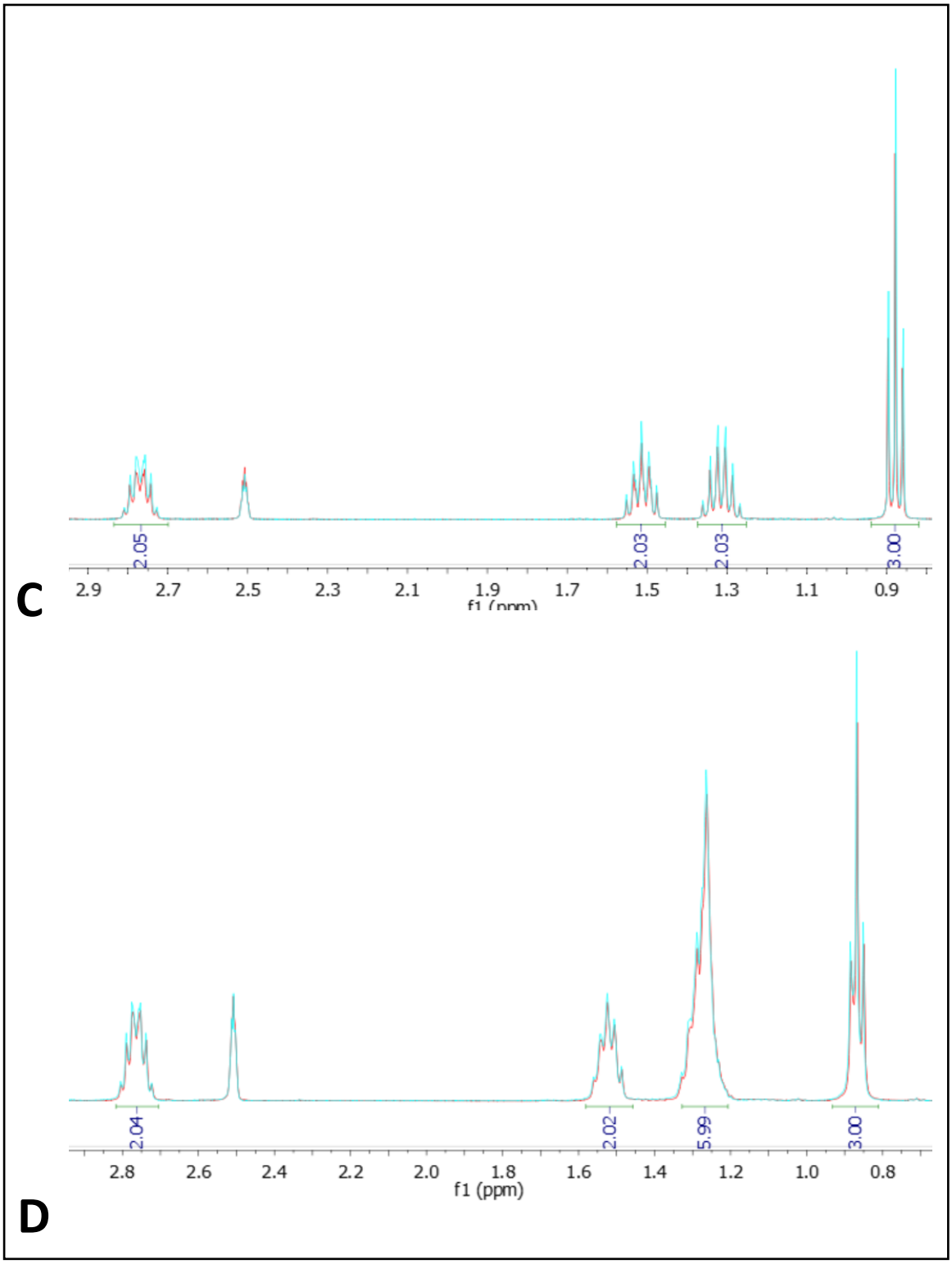


Figure A2-4: ^{1}H NMR (400 MHz; DMSO-d_6) spectra of IL solutions before (red) and after (blue) thermal degradation testing for 72 hours at 170 °C. Plots are A: [DMBA][HSO_4] containing 5 wt% water, B: [MBA][HSO_4] containing 5 wt% water, C: [HA][HSO_4] containing 5 wt% water, D: [BA][HSO_4] containing 5 wt% water.

Effect of Pulp Washing Protocol on Saccharification Inhibition

Four different pulp washing protocols were used on pulps pretreated with [BA][HSO_4] to reduce saccharification inhibition. The protocols are shown in Table A2-1, with saccharification yields shown in Fig. A2-4. Ethanol washes and the ethanol Soxhlet wash are carried out in order to remove IL and dissolved lignin as in the standard protocol, with the latter also used to remove any DMSO present in protocol 4. The purpose of the DMSO wash was to remove any lignin that had re-precipitated onto the pulp surface, as in the work of Chambon.[2] The water wash was carried out after the ethanol Soxhlet in order to remove any IL remaining in the pulp, as well as to remove any water-soluble saccharification-inhibiting compounds. Air-drying of the pulp allows low pulp moisture levels to be reached, but the air-drying process has been shown to cause hornification in certain feedstocks and thus significantly reduce saccharification yields.[3,4] No significant differences were found between any of the washing protocols. Therefore, hornification, residual IL, lignin re-deposition on the pulp surface, and formation of water- and DMSO-soluble saccharification inhibitors are shown not to be the primary reason for the low saccharification yields.

Table A2-1: Varying pulp washing protocols.

Protocol	Four Ethanol Washes	DMSO Wash	Ethanol Soxhlet	Water Wash	Air-drying
1					
2					
3					
4					

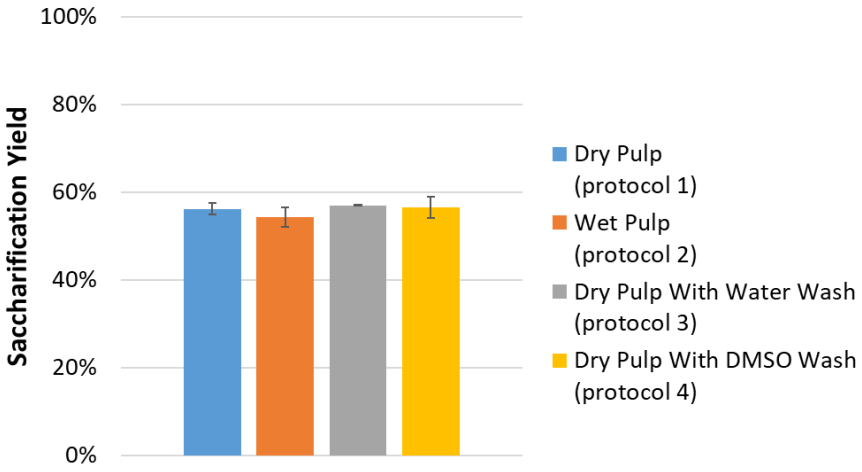


Figure A2-5: Saccharification yield of pulps pretreated using [BA][HSO_4] followed by varying pulp washing protocols. Protocols numbers are defined in Table A2-1. All pretreatments were carried out on *Miscanthus* at 150 °C for 30 minutes, with 20 wt% water, an acid/base ratio of 1.00, and at a biomass loading of 10% wt./wt.

Effect of Increasing Enzyme Loading on Saccharification Inhibition

Enzyme loading was doubled from 24 to 48 FPU/$g_{biomass}$, for the saccharification of pulps obtained by pretreating *Miscanthus* at 150°C for 30 minutes using [HA][HSO_4]. Results are shown in Fig. A2-6.

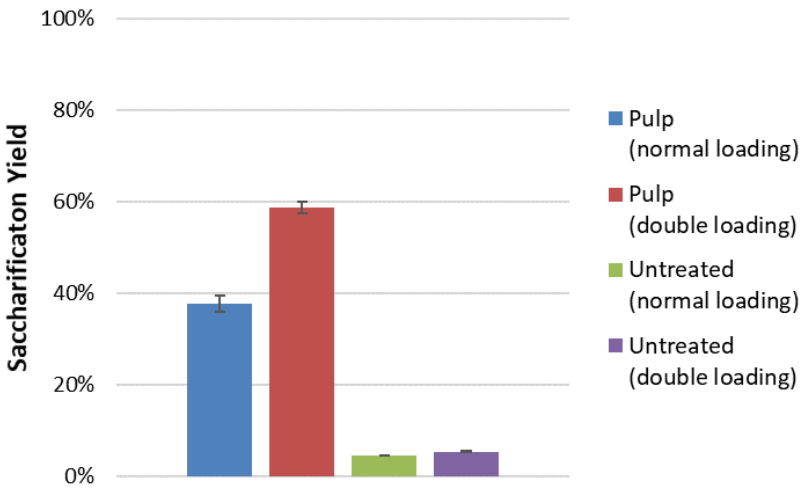


Figure A2-6: Saccharification yield of pulps pretreated using [HA][HSO_4] and of untreated *Miscanthus*, using different cellulase enzyme loadings. Normal loading refers to 24 FPU/$g_{biomass}$, and double loading refers to 48 FPU/$g_{biomass}$. Pretreatments were carried out on *Miscanthus* at 150 °C for 30 minutes, with 20 wt% water, an acid/base ratio of 1.00, and at a biomass loading of 10% wt./wt.

Effect of 100% Excess Base on Pretreatment Using [BA][HSO_4]

A pretreatment timecourse was carried out using [BA][HSO_4] with 100% excess base (i.e. $[BA]_2[SO_4]$) at 150 °C. Results are displayed in Fig. A2-7.

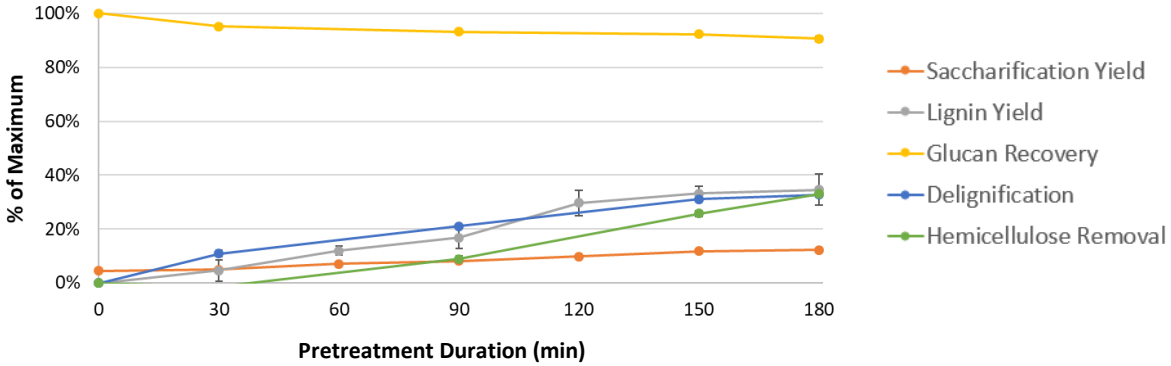


Figure A2-7: Pretreatment performance using [BA][HSO_4] with 100% excess base. All pretreatments were carried out on *Miscanthus* at 150 °C, with 20 wt% water, and at a biomass loading of 10% wt./wt.

Effect of Excess Base on Pretreatment Using [MBA][HSO_4]

Pretreatments were carried out using [MBA][HSO_4] with 2% and 5% excess base at 150 °C, and with 2% excess base at 170 °C. Results are displayed in Fig. A2-8.

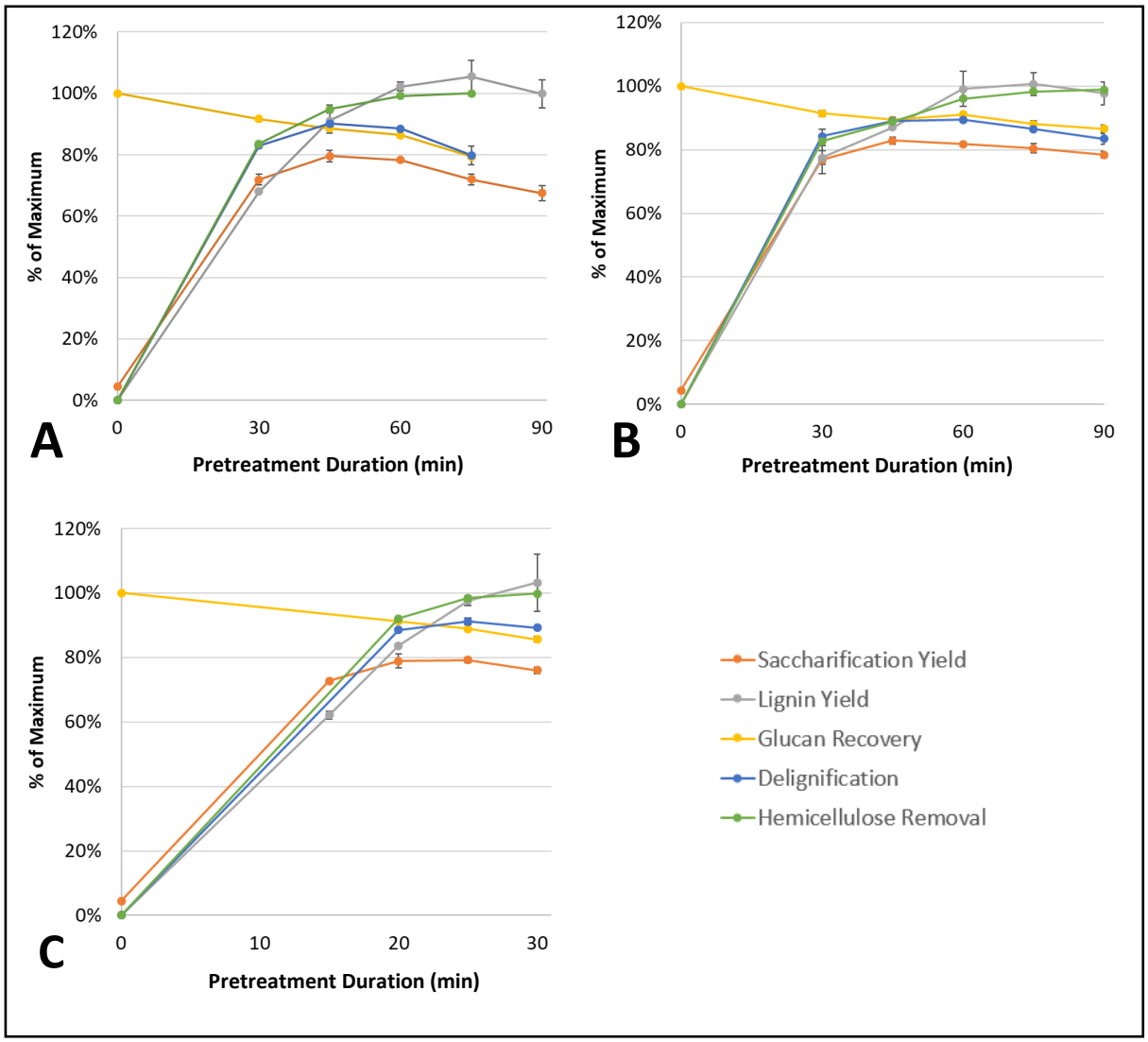


Figure A2-8: Pretreatment performance using [MBA][HSO_4] with excess base. Plots are A: Pretreatment at 150 °C with 2% excess base, B: Pretreatment at 150 °C with 5% excess base, C: Pretreatment at 170 °C with 2% excess base. All pretreatments were carried out on *Miscanthus*, with 20 wt% water, and at a biomass loading of 10% wt./wt.

HSQC Spectra

HSQC-NMR spectroscopy was carried out on lignin recovered after pretreatment for 60 minutes at 150 °C, using [DMBA][HSO_4] with an acid-base ratio of 1.00, 1.11, and 1.31, [MBA][HSO_4], [HA][HSO_4], and [BA][HSO_4] with an acid-base ratio of 1.03. The S/G ratio and degree of condensation of G and S units are shown in Fig. A2-9. Spectra for the side-chain region and aromatic region are provided in Fig. A2-10. Peaks labelled "PL" were assigned to leaching of the plasticiser bis(2-ethylhexyl) phthalate from pressure tube seals as in a previous study[5], while peaks labelled "IL" correspond to residual [DMBA][HSO_4] within the lignin.

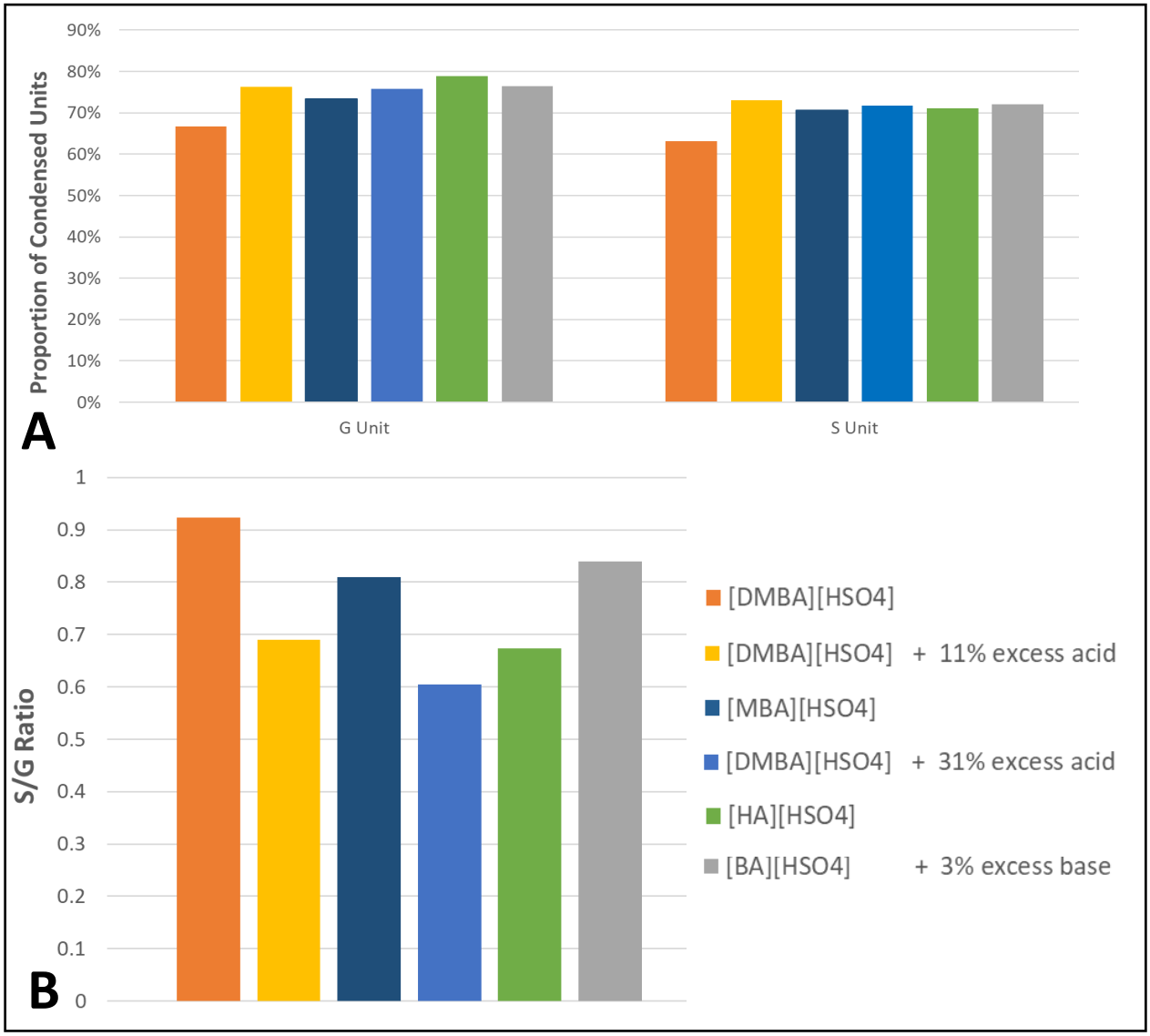
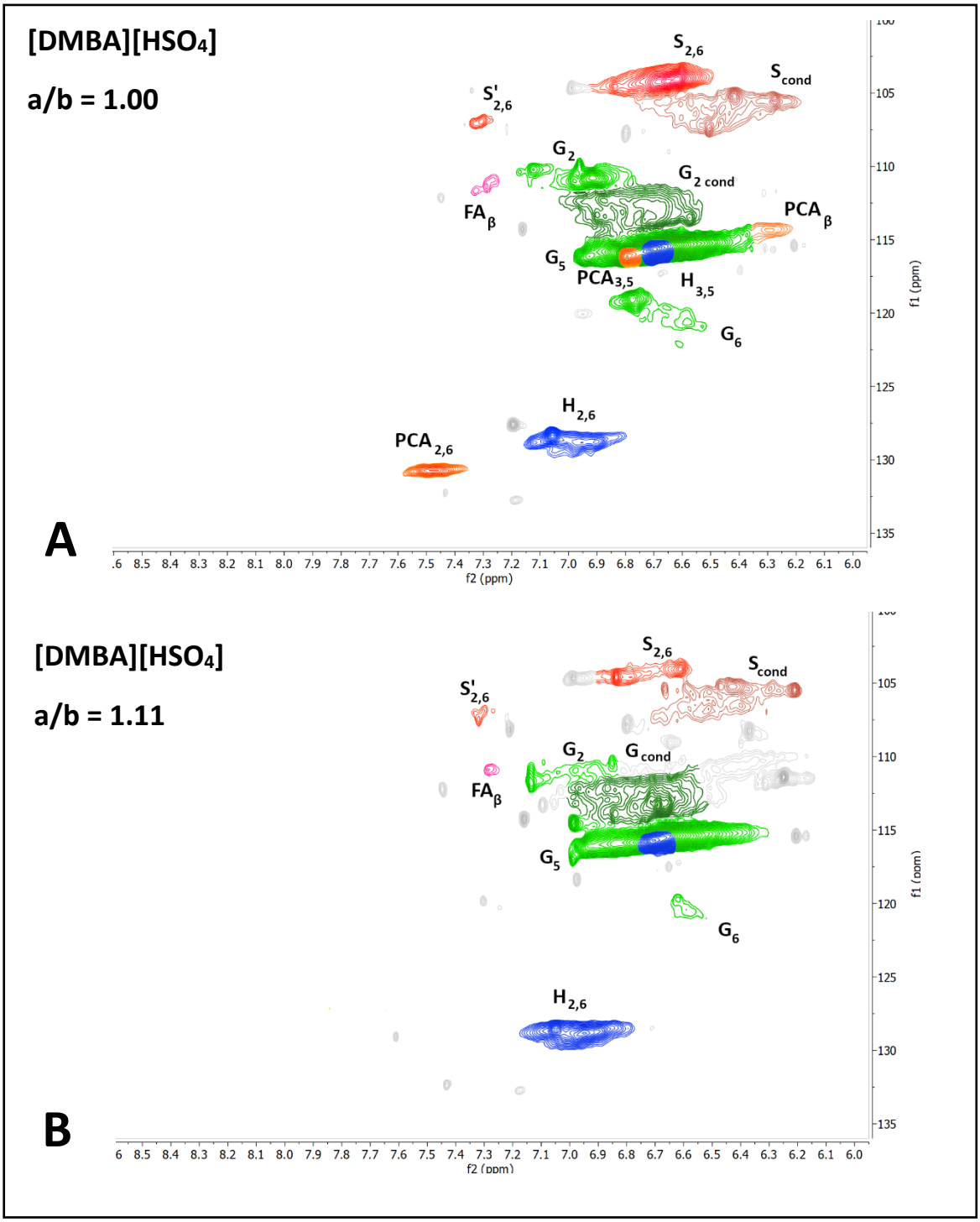
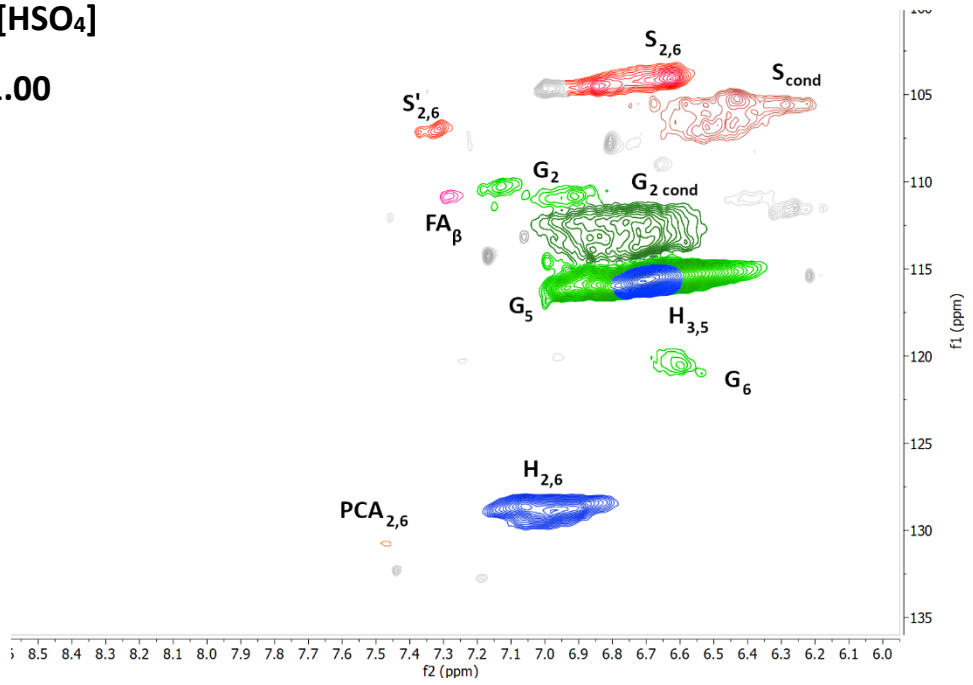


Figure A2-9: Degree of condensation and S/G ratio of lignin recovered following pretreatment with varying ionic liquids, as determined by HSQC NMR. Plots are A: Degree of condensation of G and S units, B: S/G ratio. All pretreatments were carried out on *Miscanthus* at 150 °C for 60 minutes, with 20 wt% water, and at a biomass loading of 10% wt/wt.


[DMBA][HSO4]
a/b = 1.00
S2,6
Scond
S'2,6
G2
G2 cond
FAβ
PCAβ
G5
PCA3,5
H3,5
G6
H2,6
PCA2,6
A
f2 (ppm)
f1 (ppm)
[DMBA][HSO4]
a/b = 1.11
S2,6
Scond
S'2,6
G2
Gcond
FAβ
G5
G6
H2,6
B
f2 (ppm)
f1 (ppm)

[MBA][HSO$_4$]

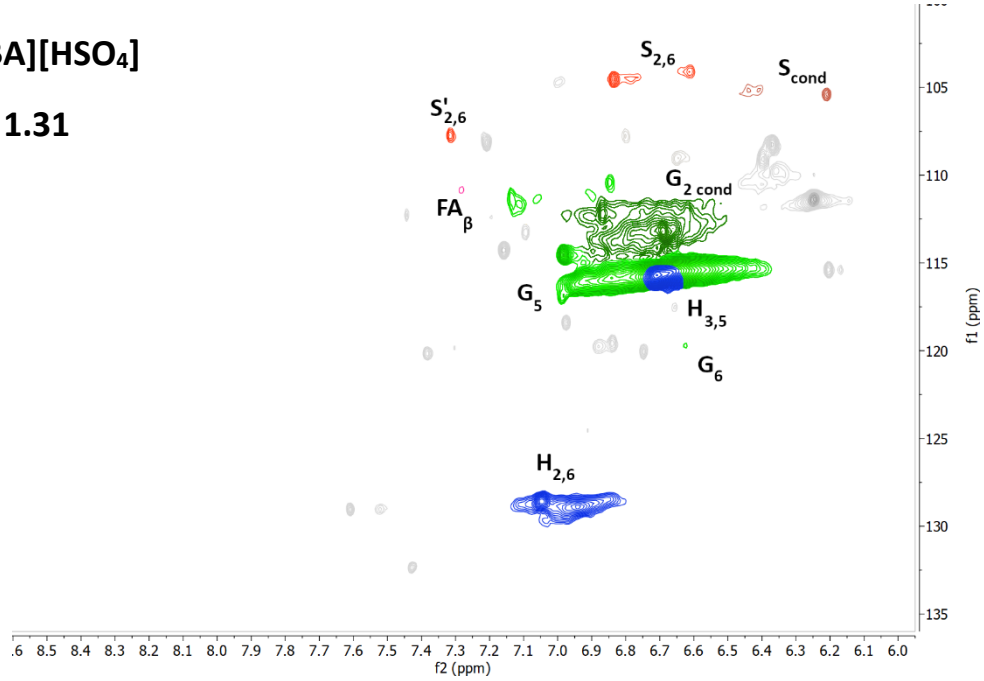
a/b = 1.00



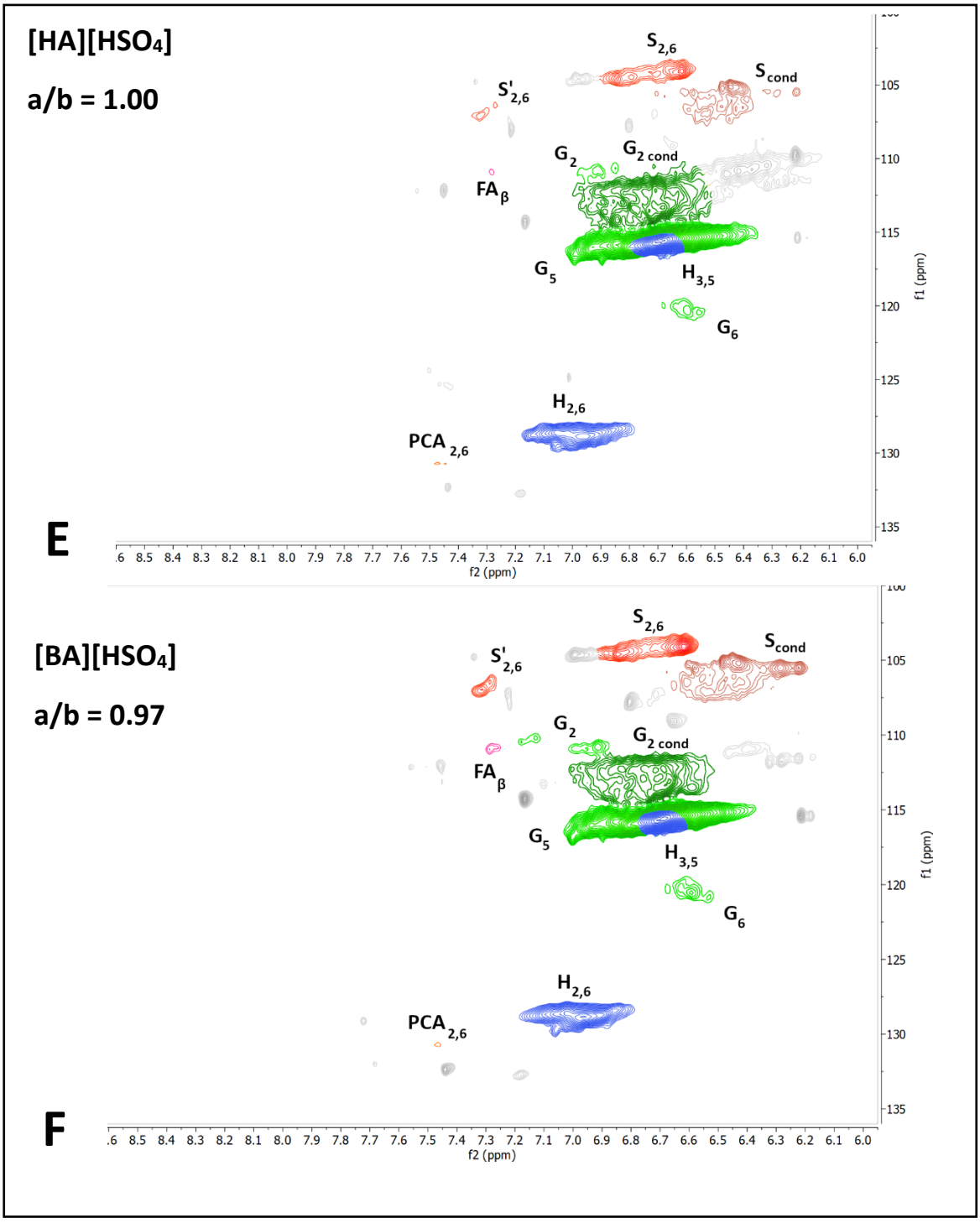
C

[DMBA][HSO$_4$]

a/b = 1.31

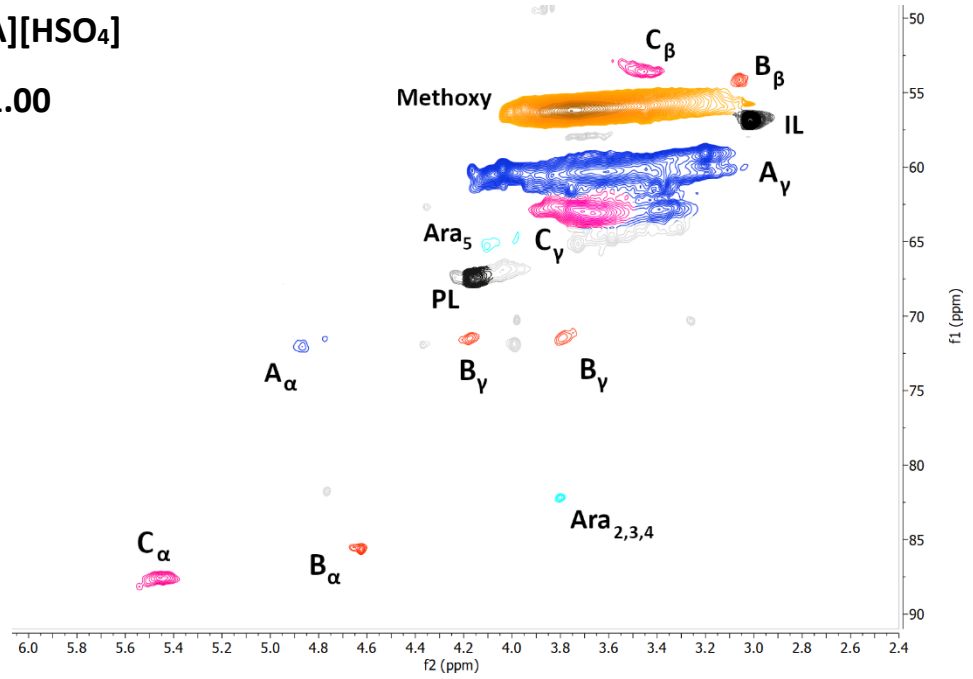


D


[HA][HSO4]
a/b = 1.00
S2,6
Scond
S'2,6
G2
G2 cond
FAβ
G5
H3,5
G6
H2,6
PCA 2,6
E
f2 (ppm)
f1 (ppm)
[BA][HSO4]
a/b = 0.97
S2,6
Scond
S'2,6
G2
G2 cond
FAβ
G5
H3,5
G6
H2,6
PCA 2,6
F
f2 (ppm)
f1 (ppm)

[DMBA][HSO4]

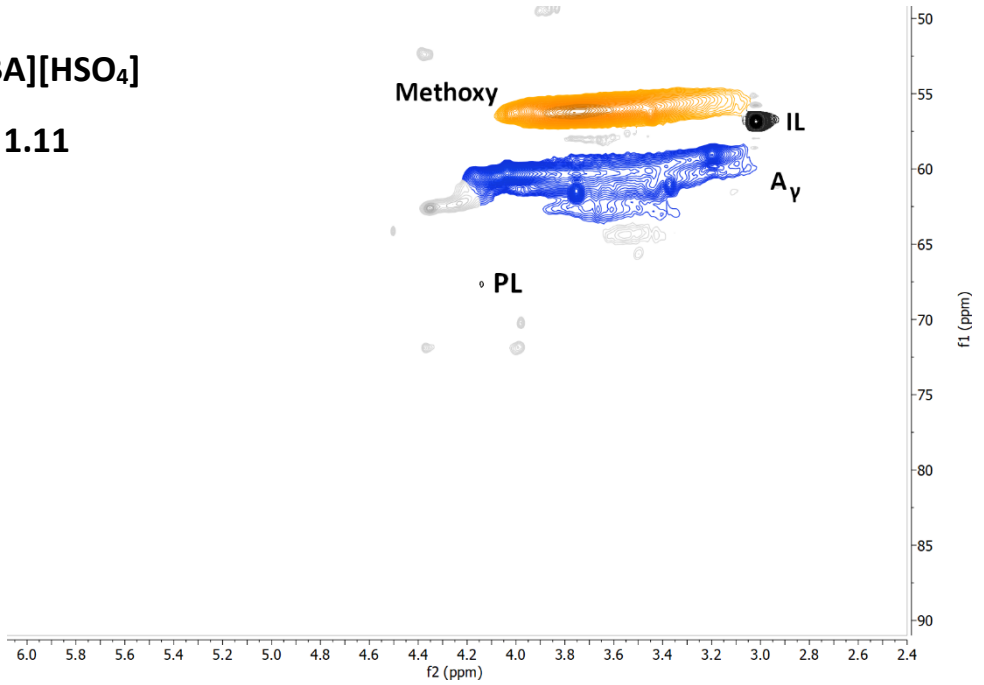
a/b = 1.00



G

[DMBA][HSO4]

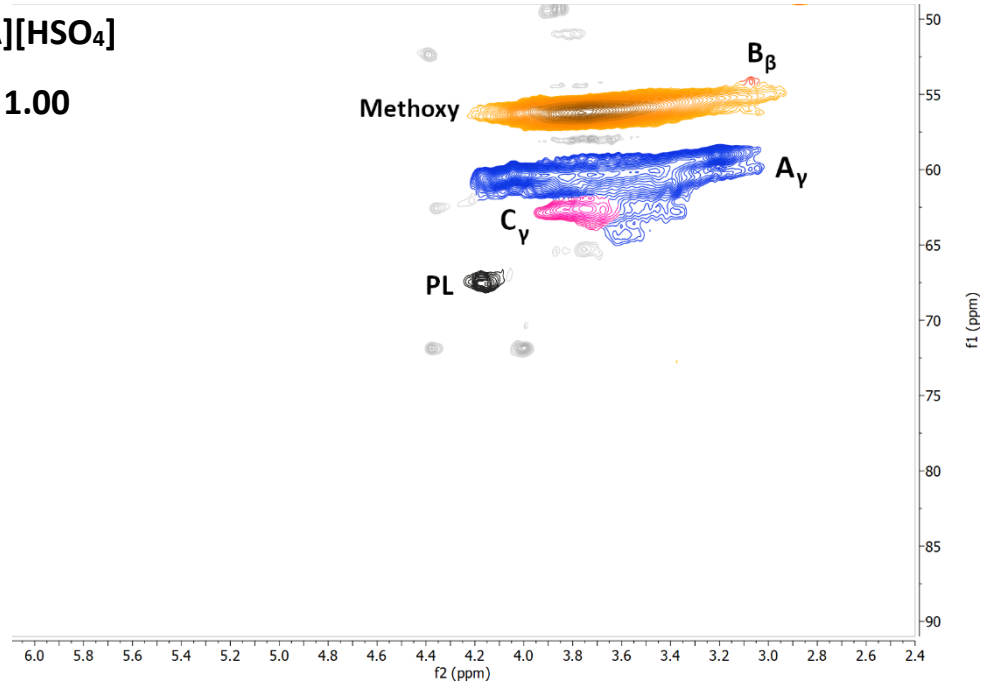
a/b = 1.11



H

[MBA][HSO$_4$]

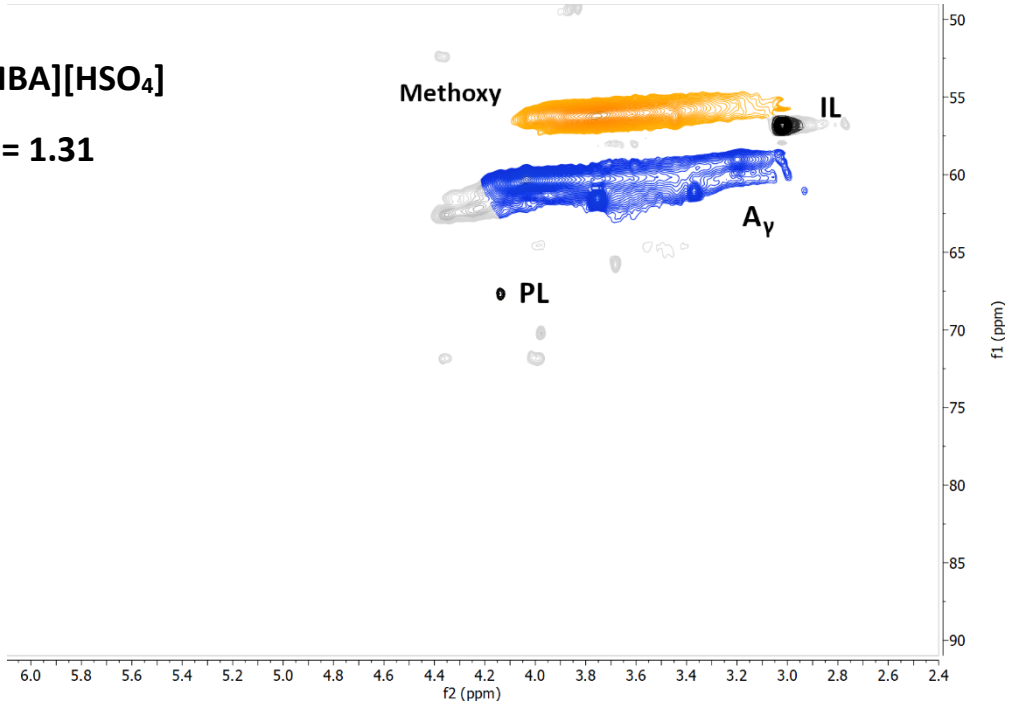
a/b = 1.00



I

[DMBA][HSO$_4$]

a/b = 1.31



J

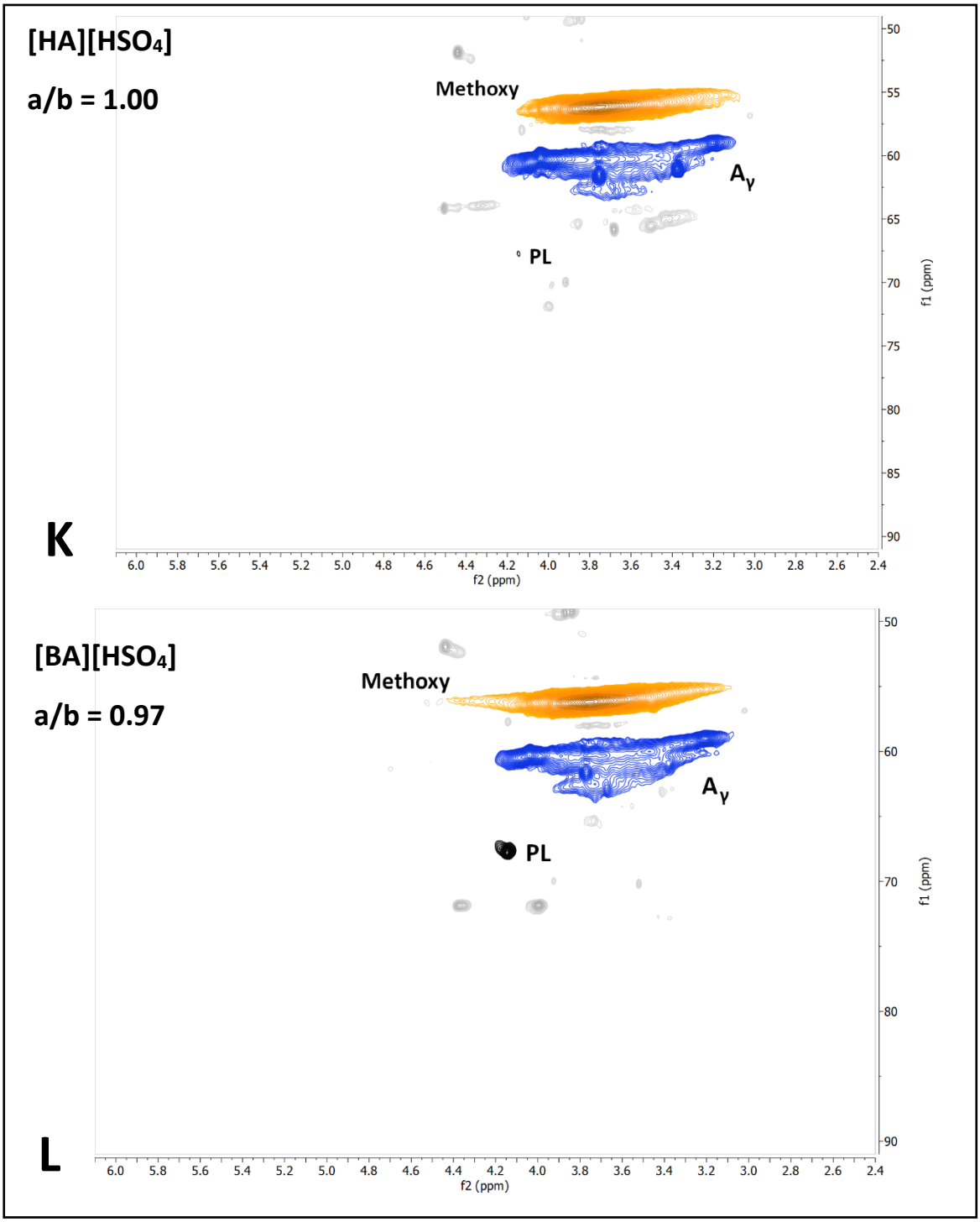


Figure A2-10: HSQC NMR spectra of recovered lignin following pretreatment with varying ionic liquids. Plots A-F show the aromatic region, plots G-L show the side-chain region. The ILs used are displayed on the plots, as well as their acid-base ratios (a/b). Pretreatments were carried out on *Miscanthus* at 150 °C for 60 minutes, with 20 wt% water, and at a biomass loading of 10% wt/wt.

Additional GPC Data

GPC analysis was carried out on lignins recovered using [MBA][HSO_4] with 5% excess base, for 30-90 minutes at 150 °C. Results are shown in Fig. A2-11, and compared to those using [MBA][HSO_4] (acid-base ratio 1.00).

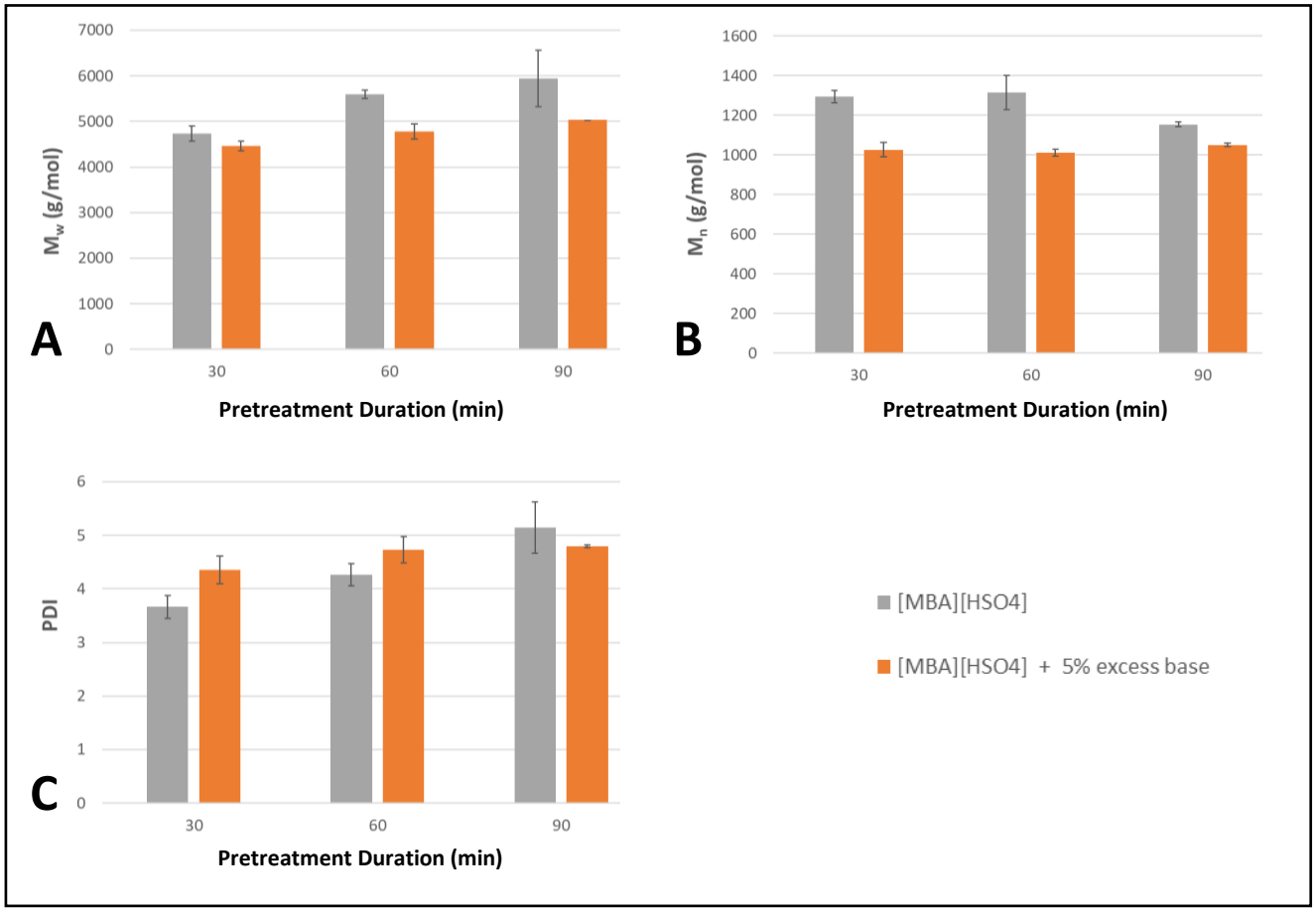


Figure A2-11: GPC analysis of recovered lignin following pretreatment with [MBA][HSO_4] with an acid/base ratio of 1.00 and with 5% excess base. Plots are A: Weight-averaged molecular mass, B: number-averaged molecular mass, C: Polydispersity Index (PDI). All pretreatments were carried out on *Miscanthus* at 150 °C, with 20 wt% water, and at a biomass loading of 10% wt/wt.

Chapter 3

Design

In the nutrient removal *P-k-C** model, each wetland cell is taken to behave hydraulically as a number, *N*, of tanks in series (TIS). A higher *N* value corresponds to a well-designed wetland with a narrower range of residence times, and thus a closer approximation to ideal plug flow, with lower output concentrations. A low *N* value corresponds to a poorly-designed wetland with channelling and/or poor mixing, leading to a larger range of outputs, with a generally higher mean. The value of *N* is determined

in practice using tracer measurements through the wetland. To reflect the weathering of a particular contaminant as it flows through the cell and the subsequent change in removal rates, a value termed the *P*TIS is used as a an effective value for *N*, thus accounting for both hydraulics and contaminant removal. Kadlec and Wallace provide a methodology for estimating *P*TIS for a given wetland.[6]

Values for *k* and *C** for different contaminants in FWS wetlands were taken from the compiled data in the work of Kadlec and Wallace, using median values in the reported frequency distributions for phosphorus and nitrogen removal.[6] No precipitation, evapotranspiration, infiltration or transpiration were included when generating results, making these conservative estimates (i.e. without contaminant removal through transpiration and infiltration, or dilution of contaminants through precipitation). For BOD removal, the mean *k*-value of the super, primary, secondary, and tertiary wetland categories (defined by Kadlec and Wallace[6]) was used. The background concentration, *C**, was linearly scaled with the BOD input concentration for input BOD concentrations above 15 mg/L, using the function: $BOD_{output} = 0.0593*(BOD_{input}-15) + 2$. For input BOD concentrations below 15 mg/L, *C** was set to 2 mg/L.

Comparison of Nutrient Removal Costs With Conventional Costs

Costs of nutrient removal using constructed wetland were compared to those of conventional technologies reported in literature, and used to construct Fig. 3-3. Full data is provided in Table A3-1.

Table A3-1 : Comparison of conventional nutrient removal costs from literature with calculated costs for wetland BOD and nutrient removal.

Inputs/Influent Type	Outputs/Treatment Level	Reported Costs ($/m^3)	This Study ($/m^3)	Wetland Area (ha)	Source
8,000-36,000 m^3/d Municipal Wastewater	Secondary (conventional activated sludge)	0.19-0.25	0.10-0.12	22.8-100	[7]
2,000-15,000 m^3/d Municipal Wastewater	Secondary (extended aeration activated sludge with mechanical dewatering)	0.17-0.28	0.10-0.15	6.00-42.4	[7]
310-15,000 m^3/d Municipal Wastewater	Secondary (extended aeration activated sludge with air drying)	0.13-0.31	0.11-0.21	0.955-42.4	[7]
4800 m^3/d 130 mg/L BOD, 25 mg/L NH_3, 3 mg/L org-N, 8 mg/L P	Secondary extended aeration activated sludge with mechanical dewatering)	0.67	0.10	11.4	[8]
	Secondary (Conventional Activated Sludge)	0.49	0.10	11.4	[8]
	8 mg/L BOD, 10 mg/L TN, 1 mg/L TP	0.61	0.36	52.8	[8]
10,000-50,000 m^3/d Municipal Wastewater	25 mg/L BOD	0.17-0.28	0.10-0.12	30.8-149	[9]
	10 mg/L BOD	0.21-0.24	0.15-0.18	43.7-211	[9]
	10 mg/L BOD, NH_4-N < 5 mg/L	0.23-0.28	0.24-0.27	83.9-413	[9]
400-10,000 m^3/d Municipal Wastewater (assumed)	Secondary (unstated)	0.57-2.97	0.11-0.20	1.36-28.6	[10]
	Tertiary (unstated)	0.57-2.97	0.36-0.53	5.03-114	[10]
10-50 m^3/d Municipal Wastewater	40 mg/L BOD, 15 mg/L NH_4-N, 10 mg/L P	0.62-1.87	0.32-0.45	0.054-0.269	[11]
2,700-59,000 m^3/d Municipal with rare industrial discharge	Secondary	0.16-1.29, mean: 0.47	0.11-0.17	9.81-200	[12]
3,000-10,000 m^3/d Post-activated sludge effluent (post-secondary treatment), 4.09 mg/L phosphorus	0.1 mg/L phosphorus	0.14-0.24	0.55-0.62	53.0-172	[13]
	0.5 mg/L phosphorus	0.08-0.19	0.34-0.39	33.3-108	[13]
	1 mg/L phosphorus	0.01-0.07	0.26-0.29	24.8-81.2	[13]
45,000 m^3/d Post-Secondary Treatment	TN < 3mg/L	0.11	0.43	668	[14]
	TP < 0.1 mg/L	0.15	0.52	823	[14]

	TN < 3mg/L, TP < 0.1 mg/L	0.24	0.52	823	[14]
100-400 m^3/d Domestic Wastewater	BOD < 30 mg/L, NH_4 < 0.5 mg/L, P < 0.5 mg/L, TN < 15 mg/L	1.18-3.04	0.75-0.95	1.70-6.59	[15]
	BOD < 30 mg/L, NH_3 < 1 mg/L, P < 0.5 mg/L	1.15-2.97	0.65-0.82	1.49-5.74	[15]
	BOD < 30 mg/L, NH_3 < 1 mg/L	1.09-2.81	0.65-0.82	1.49-5.74	[15]
	BOD < 30 mg/L	1.04-2.73	0.20-0.26	0.319-1.23	[15]
4,500-45,500 m^3/d 174 mg/L BOD, 7.5 mg/L TP	22 mg/L BOD, 5.86 mg/L TP	0.62-1.29	0.11-0.15	15.2-152	[16]
	10 mg/L BOD, 1 mg/L TP	0.80-1.51	0.29-0.36	48.2-468	[16]
	7.5 mg/L BOD, 0.325 mg/L TP	0.84-1.57	0.42-0.51	67.9-665	[16]
23,000 m^3/d Municipal Wastewater, 239 mg/L BOD, 5.7 mg/L TP, 26.8 mg/L NH_4-N, 15.5 mg/L org-N	1.02 mg/L phosphorus	0.47	0.28	212	[17]
	1.02 mg/L phosphorus, 0.08 mg/L NH_4-N, 0.8 mg/L BOD, 7.01 mg/L NO_x-N	0.47	0.62	469	[17]
	0.05 mg/L phosphorus, 1.04 mg/L NH_4-N, 0.62 mg/L BOD, 7.23 mg/L NO_x-N	0.51	0.63	487	[17]
18-455 m^3/d Municipal Wastewater	12 mg/L TN	1.33-7.75	0.37-0.68	0.163-4.11	[18]
	6 mg/L TN	1.47-11.54	0.52-0.95	0.249-5.43	[18]

Secondary treatment standards were considered to be 30 mg/L BOD. Tertiary treatment standards were considered to be 10 mg/L BOD, 1 mg/L phosphorus and 5 mg/L ammonia. One population equivalent was taken to signify 200 L/d. Municipal and domestic wastewater were taken to contain 200 mg/L BOD and 9.5 mg/L phosphorus, 22.9 mg/L NH_4-N, and 15.6 mg/L org-N. Municipal with rare industrial discharge was taken to contain 350 mg/L BOD, 45 mg/L NH_4-N, 15 mg/L org-N, and 15 mg/L P. Post-secondary treatment influent was taken to contain 30 mg/L BOD, 5.9 mg/L P, and 25 mg/L TN (half org-N and NH_4-N). Treatment plant lifetime was taken to be 20 years.

*BOD not achievable due to minimum background concentrations of 2 mg/L. However, all other levels were achieved, with the focus of the referenced study being phosphorus removal rather than BOD removal.

Cost of Nitrogen Removal As a Function Of Number of Cells

Fig. A3-1 shows the effects of varying the number of cells on overall costs and areas for nitrogen removal, for varying input concentrations and fixed output concentrations, at a flow rate of 5,000 m^3/d.

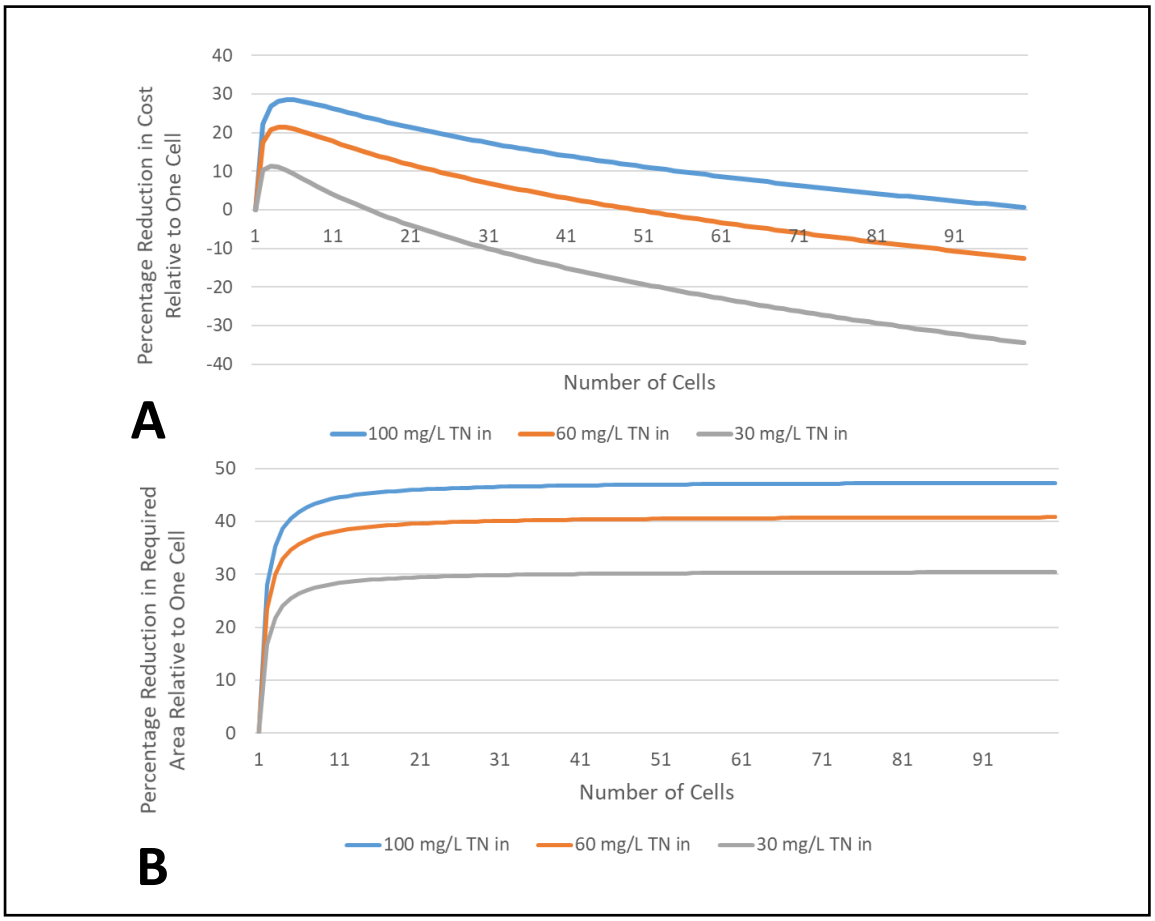


Figure A3-1: Effect of varying the number of wetland cells on required overall area and treatment costs for nitrogen removal. All plots are for 5,000 m^3/d of varying Total Nitrogen (TN) input concentrations, with an output concentration of 5 mg/L. Plots are A: Reduction in total cost, B: Reduction in required area.

Cost of Nutrient Removal Per Unit Mass of Contaminant Removed

Fig. A3-2 shows the costs of nutrient removal using constructed wetlands, per unit mass of contaminant removed.

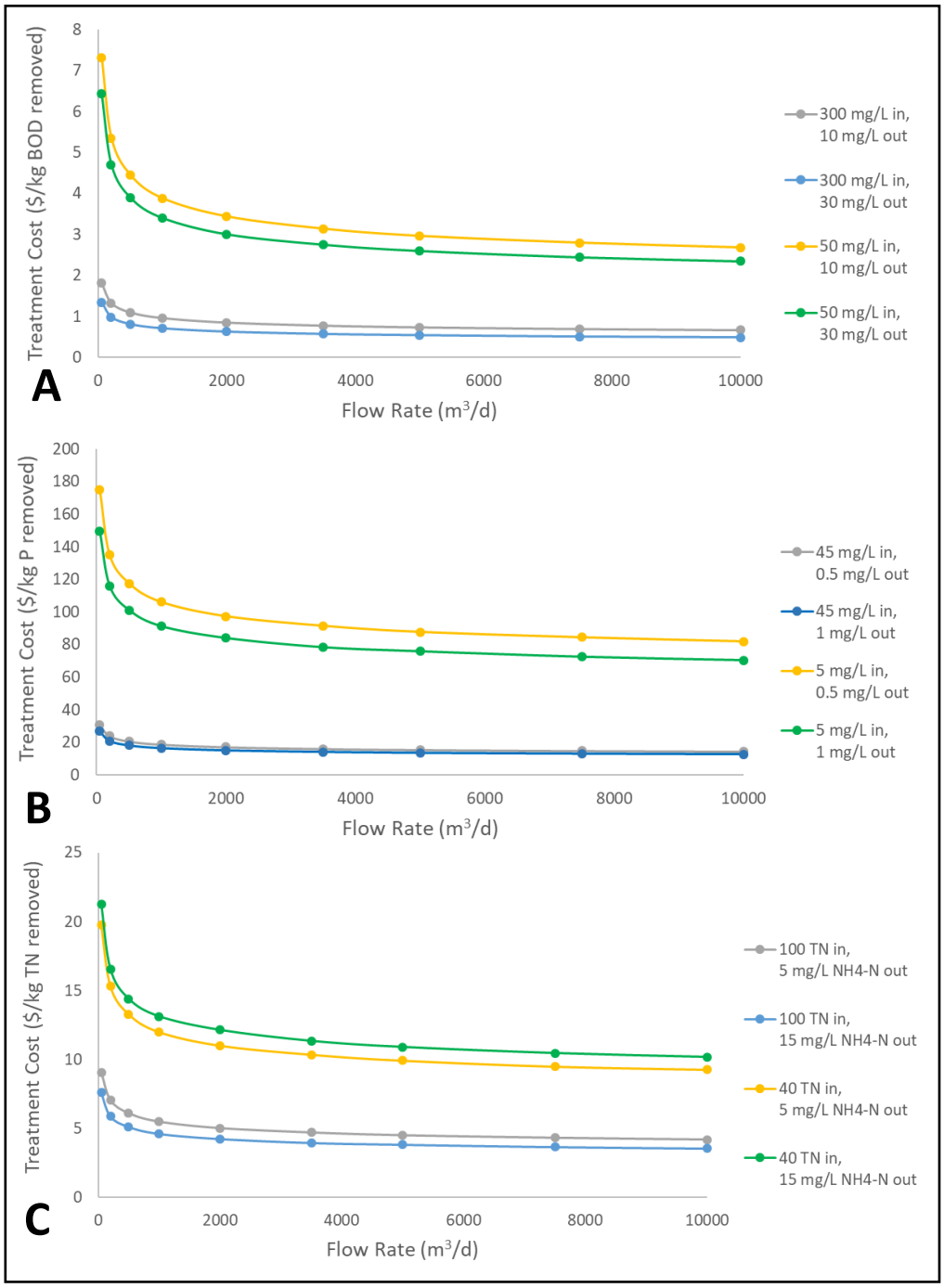


Figure A3-2: Costs of nutrient removal using constructed wetlands per unit mass of contaminant removed, for a range of input and output conditions. Plots are A: biochemical oxygen demand (BOD) removal, B: phosphorus (P) removal, C: total nitrogen (TN) removal, assuming input nitrogen made up of 50% organic nitrogen and 50% ammonia nitrogen (NH_4-N).

Full Contour Plots for Cost of Nutrient Removal

BOD Removal

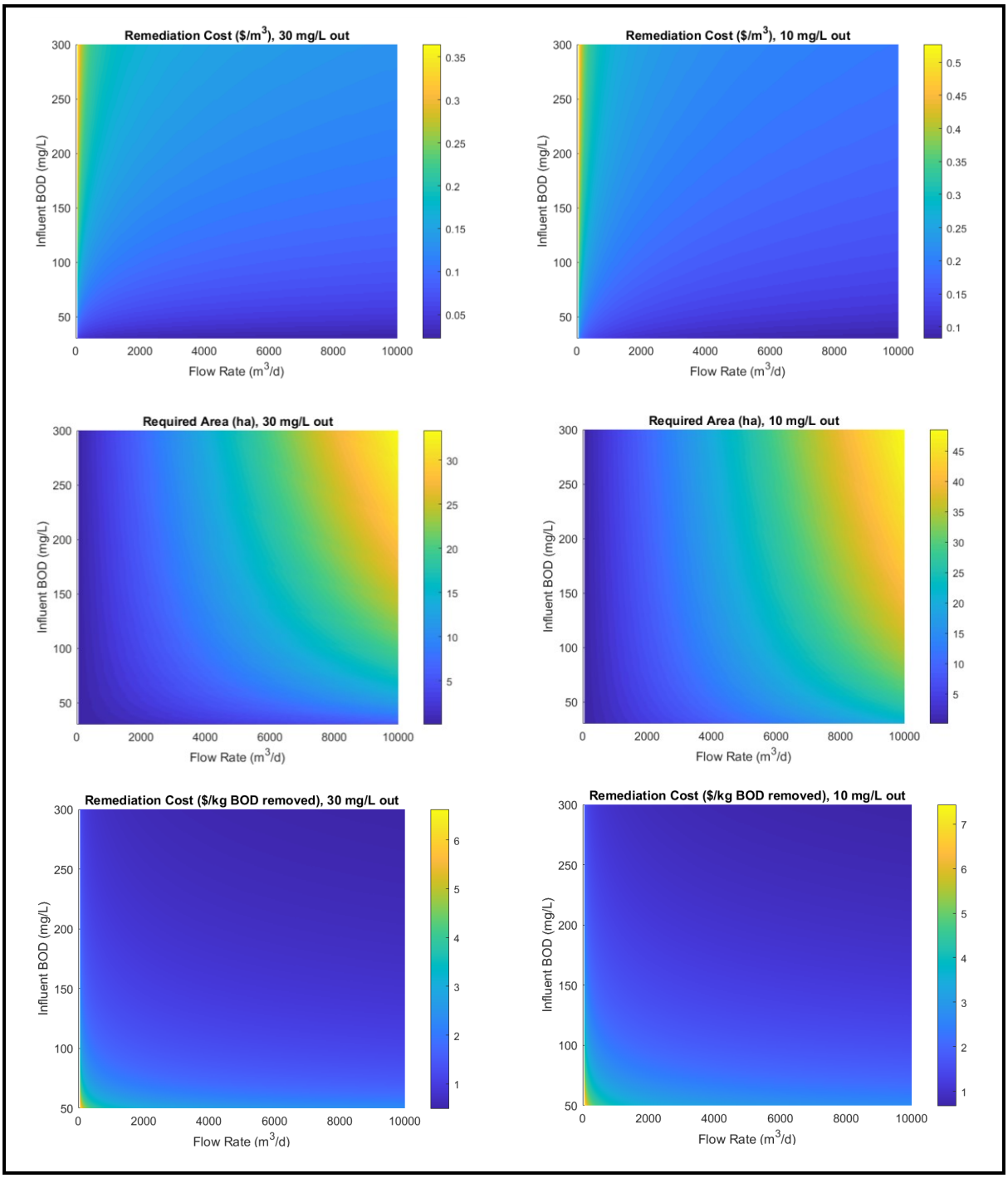


Figure A3-3: Remediation costs and required wetland areas for BOD removal, varying with flow rate and influent concentration, for two different effluent concentrations.

Phosphorus Removal

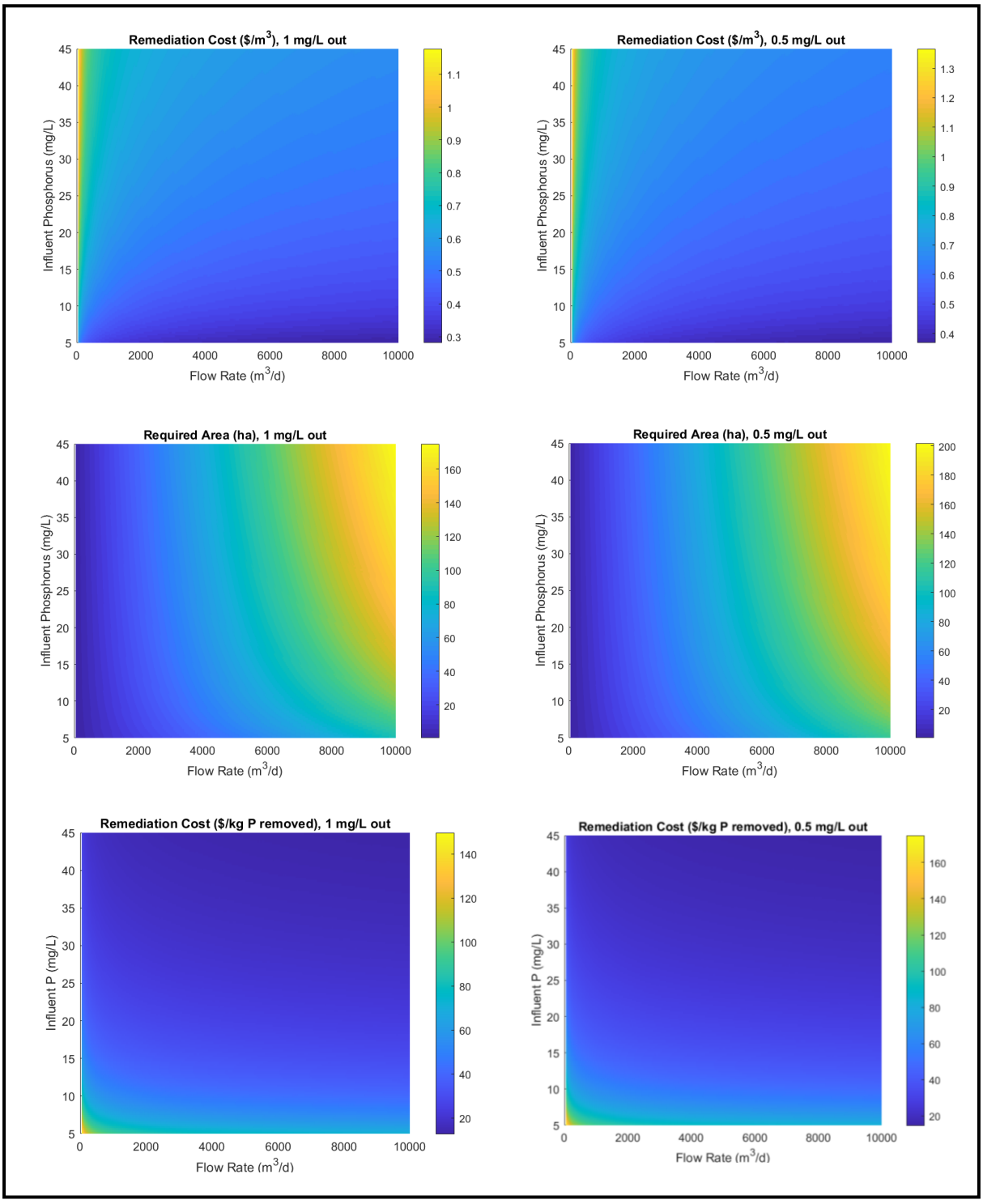


Figure A3-4: Remediation costs and required wetland areas for phosphorus removal, varying with flow rate and influent concentration, for two different effluent concentrations.

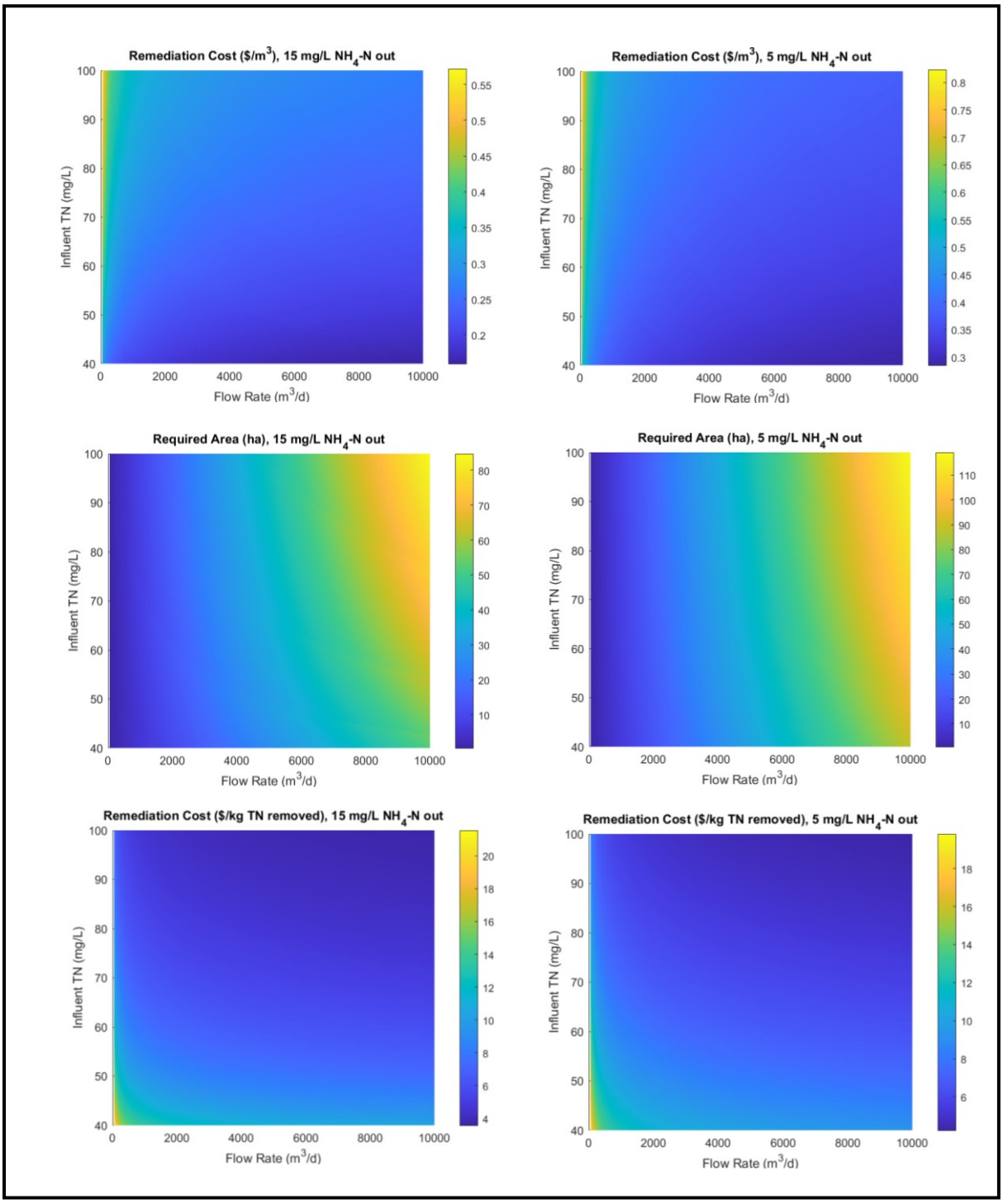


Figure A3-5: Remediation costs and required wetland areas for nitrogen removal, varying with flow rate and influent concentration, for two different ammonia nitrogen effluent concentrations. Input nitrogen assumed to be made up of 50% organic nitrogen and 50% ammonia nitrogen (NH_4-N).

Chapter 4

Composition of Wetland Species Used for Pretreatment

Compositional data of the untreated wetland species studied is shown in Table A4-1.

Table A4-1: Composition of wetland species used for pretreatment.

Species	Composition (% dry wt.)					
	Glucan	Hemicellulose	Lignin	Ash	Extractives (H_2O + EtOH)	Other
Phragmites australis (batch 1)	30.0	21.6	19.9	2.3	21.3	4.9
Phragmites australis (batch 2)	30.6	22.3	19.7	0.5	23.4	3.6
Phragmites australis (batch 3)	40.7	22.4	22.7	2.8	7.7	3.8
Typha latifolia (batch 1)	34.3	25.9	19.4	0	19.4	1.1
Typha latifolia (batch 2)	22.5	20.2	14.0	0.2	36.7	6.6
Typha angustifolia	30.6	19.1	21.7	0.6	18.2	9.8
Cyperus alternifolius	28.8	19.6	20.9	0.6	26.1	4.1
Carex pendula	30.4	23.3	19.3	0.6	23.9	2.6
Scirpus lacustris	31.6	21.9	18.9	0.3	24.2	3.0
Juncus effusus (batch 1)	29.0	23.2	17.4	0.2	24.1	6.1
Pistia stratiotes	33.0	6.5	10.6	0.4	32.3	17.9
Mixed Feedstock	31.9	22.1	20.0	0.9	20.6	4.4
Mixed Metal-Contaminated Feedstock	29.6	19.2	29.8	0.9	15.4	5.3

Determination of Dissolved Lignin Content

Dissolved lignin content was determined by weighing approximately 200 mg of recycled IL solution into a pre-weighed 1.5 mL microcentrifuge tube. Dissolved lignin was then precipitated by adding

around 1 mL of distilled water. The mixture was vortexed and centrifuged at 13.3 xG for 20 minutes at 4 °C. The supernatant was then decanted, and the precipitated lignin was washed twice more with around 1 mL of distilled water, removed each time by decanting the supernatant following centrifugation. Any remaining moisture was then removed by heating the tube at 105 °C for 24 hours. The final mass of the tube and lignin was then measured. By subtracting the initial mass of the tube from the final mass, the mass of dissolved lignin was determined.

HSQC Spectrum of Lignin Extracted From *Phragmites Australis* Batch 1

HSQC analysis was performed on recovered lignin from pretreatments of *Phragmites australis* with [MBA][HSO_4] and [DMEtA][HCOO] at 150 °C for 60 minutes. The spectrum of the side-chain region is shown as Fig. 4-7 in the main text, while the aromatic region is shown in Fig. A4-1.

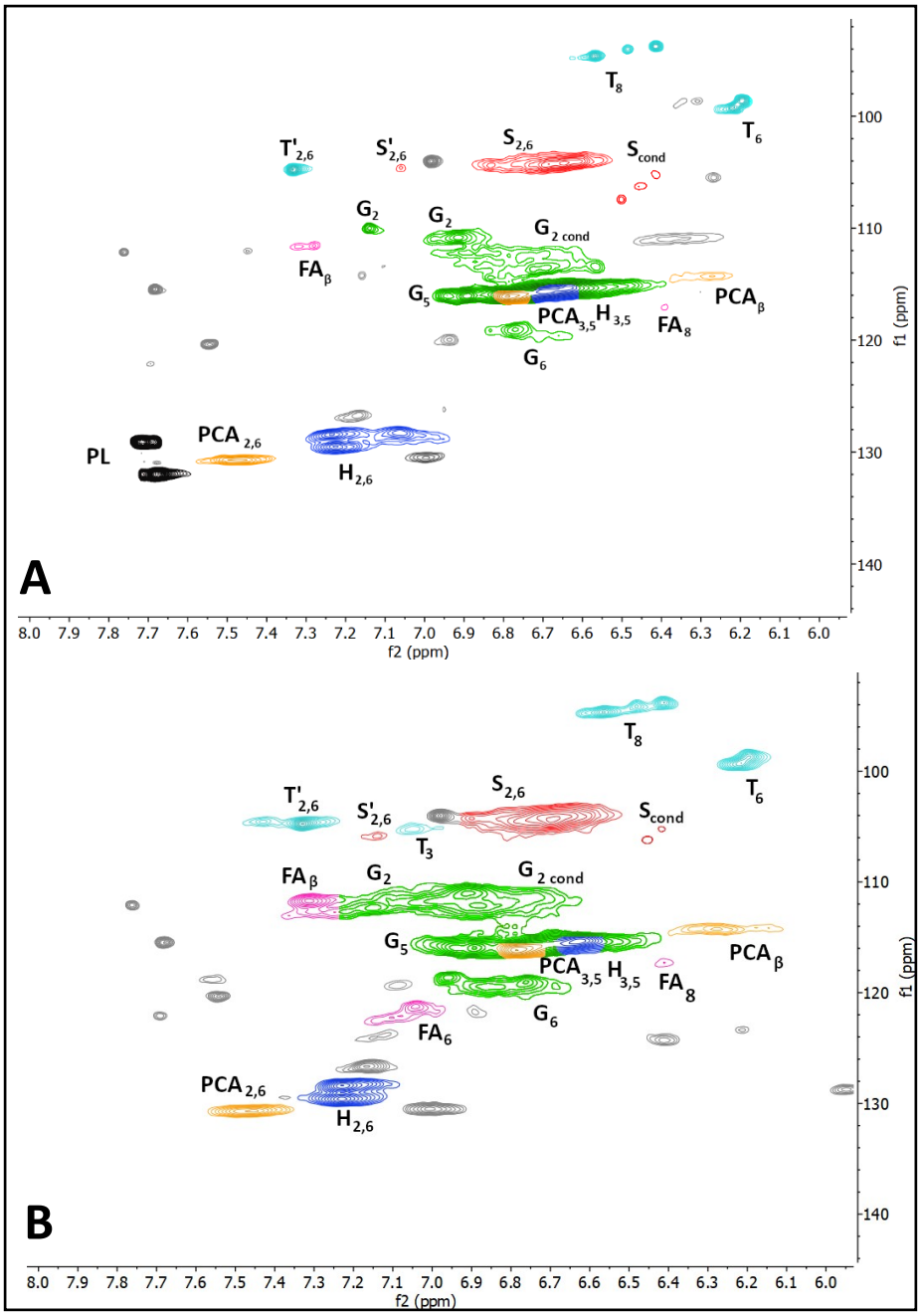


Figure A4-1: HSQC NMR spectra of recovered lignin following pretreatment with varying ionic liquids. Plots are A: Using [MBA][HSO_4], B: Using [DMEtA][HCOO]. Pretreatments were carried out on Batch 1 of *Phragmites australis* (as defined in Table 4.1) at 150 °C for 60 minutes, with 20 wt% water, and at a biomass loading of 10% wt/wt.

Pretreatment Indicators of Multiple Wetland Species

A range of wetland species were pretreated at 150 °C for 30 and 45 minutes using [DMBA][HSO_4], with several pretreatment indicators shown in Fig. 4-12 in the main text. Two further indicators are shown in Fig. A4-2.

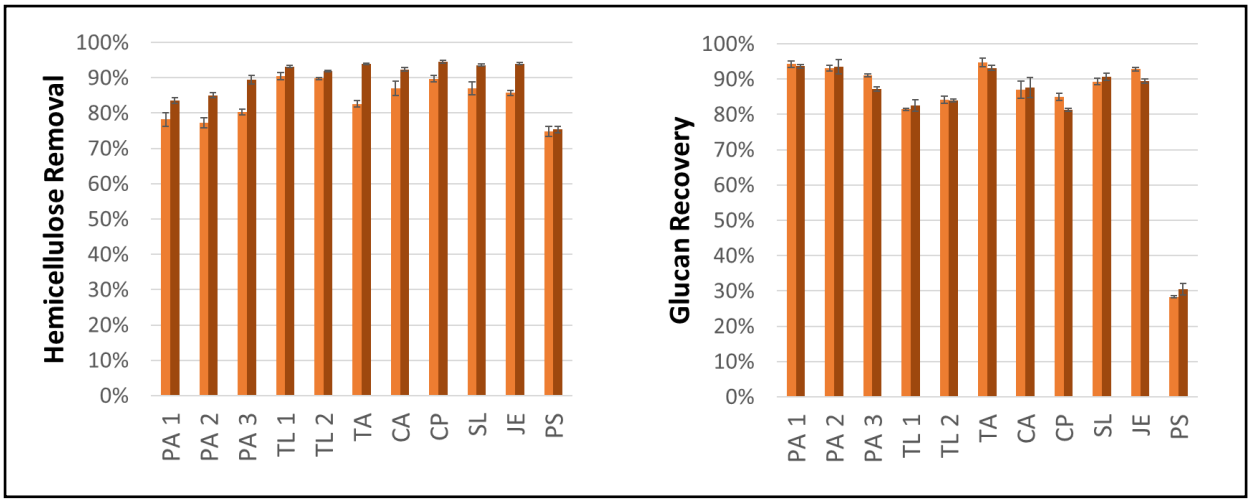


Figure A4-2: Two further pretreatment indicators of 11 wetland feedstocks. Species abbreviations are provided in Table 4.1 in the main text. All pretreatments were carried out using [DMBA][HSO_4] at 150 °C, with 20 wt% water, and at a biomass loading of 10% wt/wt.

Compositional Analysis and Pretreatment of Nut Shells

Walnut and almond shells were pretreated using [DMBA][HSO_4], for 30-75 minutes at 150 °C, at a biomass loading of 10% wt/wt and with an IL water content of 20 wt%. The following compositions were determined for the untreated samples, shown in Table A4-2. Pretreatment and compositional analysis data of pretreated pulps are shown in Table A4-3. Glucan recoveries and saccharification yields of above 100% were observed. This was attributed to physical characteristics of the untreated nut shells, which had been ground to 180-850 µm using a knife mill, but were still very hard. It is thought that during the compositional analysis protocol, acid was not able to fully penetrate and fractionate the nut shells (into polysaccharides and lignin). As a result, substantial polysaccharides were not hydrolysed and stayed as Acid Insoluble Residue, and were thus attributed as lignin. Following pretreatment, however, the nut shells were better able to be penetrated by the acid, explaining the high yields and glucan recoveries.

Table A4-2: Composition of untreated nut shells

Feedstock	Composition (% dry wt.)					
	Glucan	Hemicellulose	Lignin	Ash	EtOH-Extractives	Other
Walnut Shell	16.4	23.7	47.4	0.0	3.4	9.0
Almond Shell	19.9	31.6	41.6	0.1	0.8	6.1

Table A4-3: Pretreatment data of nut shells.

Feedstock	Pretreatmet Duration (min)	Glucan Recovery (%)	Delignification (%)	Hemicellulose Removal (%)	Saccharification Yield (%)
Walnut Shell	30	-	-	-	36.3
	45	-	-	-	102.6
	60	-	-	-	109.9
	75	-	-	-	116.9
Almond Shell	30	125.0	40.4	58.8	53.6
	45	131.4	81.2	88.2	113.0
	60	129.5	79.7	90.0	111.0
	70	127.1	81.5	93.9	116.9

Compositional Analysis of *Pistia Stratiotes*

As detailed in Chapter 4, *Pistia stratiotes* was pretreated using [DMBA][HSO_4]. However, the compositional analysis protocol was found to be unsuitable for both pretreated and untreated samples, with a large unaccounted fraction (as shown in Table A4-4).

Table A4-4: Composition of *Pistia stratiotes* before and after IL pretreatment

Species	Composition (% dry wt.)						
	Glucan	Hemicellulose	Lignin	Ash	Extractives (H_2O + EtOH)	Acetyl	Unaccounted
Untreated	33.0	6.5	10.6	0.4	32.3	0.6	17.3
30 min, 150 °C	23.0	4.0	13.1	1.4	0	0	58.5
45 min, 150 °C	26.2	4.2	11.4	0.6	0	0	57.6

Determination of Acid/Base Ratios of Monoprotic ILs by pH

Protic ILs have attracted attention due to their simple synthesis: a neutralisation reaction between a Bronsted acid and Bronsted base. However, many of the constituent acids and bases used in protic ILs are volatile, which can lead to an imbalance of acid or base in the final product. Even small imbalances of a few percent can have strong impacts in certain applications such as biomass pretreatment or protein manipulation.[19–22] Currently, the acid-base ratio of ILs is often not reported. When it is reported, it typically determined by ^{1}H NMR, or by titration of a diluted sample. However, such measurements are not rapid, and in the latter case require careful calibration of the titrant in order to ensure results are suitably accurate. Additionally, the use of NMR to determine acid-base ratio for only certain classes of protic ILs may A quick, high-throughput characterisation technique is currently lacking. The use of pH to determine the acid-base ratio is appealing due to the ease, simplicity, and rapidity of measurements. For this reason, calibration curves of pH vs. acid-base ratio for diluted IL solutions have been developed, by measuring the pH of aqueous solutions of known acid and base content. However, each curve is IL-specific and only applies at a single dilution ratio.

At high levels of dilution, ILs are effectively weak electrolyte solutions, and can therefore be modelled using aqueous acid-base theory. The dissociation behaviour of the constituent acid and base in an aqueous solution (as in Schemes A4-S1-S3) are modelled by the dissociation constants. In the case of the acid, this is the acid dissociation constant (termed $K_{a,a}$ in this study), as defined in Eq. A4-1. For bases, the dissociation constant of the conjugate acid is often used (termed $K_{a,b}$ in this study), as defined in Eq. A4-2. For the dissociation of water itself, the water dissociation constant K_w is used, as defined in Eq. A4-3.

$$AH + H_2O \leftrightarrow A^- + H_3O^+ \quad \text{(A4-S1)}$$

$$B + H_3O^+ \leftrightarrow BH^+ + H_2O \quad \text{(A4-S2)}$$

$$2\,H_2O \leftrightarrow H_3O^+ + OH^- \quad \text{(A4-S3)}$$

where *AH* represents the undissociated acid, A^- represents the dissociated acid, *B* represents the undissociated base, and BH^+ represents the dissociated base.

$$K_{a,a} = \frac{[A^-] \cdot [H_3O^+] \cdot \gamma_{H_3O^+} \cdot \gamma_{A^-}}{[AH] \cdot \gamma_{AH}} = 10^{-pK_{a,a}} \quad \text{(A4-1)}$$

$$K_{a,b} = \frac{[B] \cdot [H_3O^+] \cdot \gamma_{H_3O^+} \cdot \gamma_{B}}{[BH^+] \cdot \gamma_{BH^+}} = 10^{-pK_{a,b}} \quad \text{(A4-2)}$$

$$K_w = [H_3O^+] \cdot [OH^-] \cdot \gamma_{H_3O^+} \cdot \gamma_{OH^-} = 10^{-14} \quad \text{(A4-3)}$$

$$[H_3O^+] \cdot \gamma_{H_3O^+} = 10^{-pH} \quad \text{(A4-4)}$$

where γ_i represents the activity coefficient of species *i*, K_w represents the dissociation constant of water, $K_{a,a}$ represents the dissociation constant of the constituent acid, and $K_{a,b}$ represents the dissociation constant of the conjugate acid of the constituent base. Chemical species *AH, A^-, BH,* and BH^+ are defined as in Schemes A4-1-S3.

When accurately modelling the dissociation behaviour of acids and bases and the measurement of pH (Eqs. A4-1-4) at non-infinite dilution, non-ideal behaviour must be taken into account through the use of activity coefficients. As the ionic strength (defined in Eq. A4-5) of the solution increases, the impact of activity coefficients becomes increasingly large and challenging to accurately predict. A range of models exist for predicting activity coefficients of ionic species, with increasing levels of complexity for increasing ionic strengths. The extended Debye-Huckel equation (Eq. A4-6) is accurate up to ionic strengths of 0.1 M.[23,24] In order to account for the observed increase in activity at higher ionic strengths due to ion association, the Truesdell-Jones equation was developed (Eq. A4-7), adding an extra term dependent on ionic strength, and is valid up to 1 M ionic strengths.[23–25] However, both the extended Debye-Huckel and the Truesdell-Jones equations require ion-specific parameters that are not widely reported. In the case of the extended Debye-Huckel, this is the ion size parameter, equal to the effective diameter of the hydrated ion that is empirically measured.[26] In the case of the Truesdell-Jones equation, both parameters are completely empirical. The Davies equation (Eq. A4-8) serves as an approximation to the Truesdell-Jones equations that is accurate up to around 0.6 M ionic strengths.[24,27] The Davies equation assumes an average ion size parameter for all ions, while also incorporating a generalised second term to account for higher strength solutions.[27] As a result, it may be applied to all ions in a solution. The Davies equation is therefore useful for solutions with a large number of different ionic species, or for ionic species whose parameters are poorly reported. There exists a number of other activity coefficient models of varying complexity (e.g. the Pitzer, Guntelberg, or SIT models) that may also be used over suitable ionic strength ranges. While often not included (i.e. set to 1), the activity of neutral species is also affected by ionic strength and may be accounted for using the Setschenow equation (Eq. 9).[24,27]

$$I = \frac{1}{2} \sum_i c_i \cdot {z_i}^2 \quad \text{(A4-5)}$$

$$\log_{10}(\gamma_i) = \frac{-\mathrm{A(T)} \cdot {z_i}^2 \cdot \sqrt{I}}{1 + \mathrm{B(T)} \cdot a_i \cdot \sqrt{I}} \quad \text{(A4-6)}$$

$$\mathrm{A(T)} = \frac{1.8246 \cdot 10^{6}}{(\varepsilon(T) \cdot T)^{1.5}} \approx 0.509 \; for \; 25^{o}C \; water$$ [28,29]

$$B(T) = \frac{50.29 \cdot 10^{8}}{(\varepsilon(T) \cdot T)^{0.5}} \approx 0.328 \; for \; 25^{o}C \; water$$ [28,29]

$$\varepsilon(T) = 2727.586 + 0.6224107 \cdot T - 466.9151 \cdot \ln(T) - \frac{5200.87}{T}$$

$$\log_{10}(\gamma_i) = \text{-A(T)} \cdot {z_i}^2 \cdot \left(\frac{\sqrt{I}}{1 + \mathrm{B(T)} \cdot b_i \cdot \sqrt{I}} - d_i \cdot I \right) \quad \text{(A4-7)}$$

$$\log_{10}(\gamma_i) = \text{-A(T)} \cdot {z_i}^2 \cdot \left(\frac{\sqrt{I}}{1 + \mathrm{B(T)} \cdot e \cdot \sqrt{I}} - f \cdot I \right) \quad \text{(A4-8)}$$

$$\log_{10}(\gamma_i) = g_i \cdot \mathrm{I} \quad \text{(A4-9)}$$

where *I* represents the ionic strength of an aqueous electrolyte solution, γ_i represents the activity coefficient of species *i*, z_i represents the charge of species *i*, c_i represents the concentration of species *i*, a_i represents the ion size parameter of species *i* in the extended Debye-Huckel equation, *T* represents temperature, ε represents the permittivity of water, b_i and d_i represent empirical constants of species *i* in the Truesdell-Jones equation, *e* and *f* represent constants in the Davies equation, and g_i represents the Setschenow constant of species *i* in the Setschenow equation.

In this study, a model was developed for predicting the acid-base ratio of a monoprotic ionic liquid from the pH of a diluted sample. This model was validated for two monoprotic ionic liquids: dimethylethanolammonium formate, and 1-methylimidazolium chloride. Calibration solutions of dilute IL were prepared with known acid-base ratios, and their pH was measured. The predicted acid-base ratios obtained from the model were then compared to determine the accuracy of the proposed technique.

Methods

Measurements

Dimethylethanoamine (99.98%), 1-methylimidazole (99.9%) and formic acid (99.7%) were purchased from Sigma Aldrich, and 1M HCl was purchased from Fisher Scientific. All reagents were used as received. Aqueous solutions (approximately 0.5 wt%) of known acid-base ratios were prepared by weighing approximately 85 mg of formic acid and 165 mg of dimethylethanolamine into approximately 50 g of water, or 2 g of 1M HCl and 160 mg of 1-methylimidazole into approximately 45 g of water. Acid-base ratios were calculated, taking into account reagent purities provided in the certificates of analysis from the manufacturers. pH measurements were carried out using a Mettler-Toledo DG 115-SC pH probe, following a 3-point calibration with Mettler-Toledo buffer solutions at pH 4.01, 7, and 9.21. All solutions were stirred for 30 seconds prior to measurements.

Predictions

The acid-base ratio of the ILs was calculated from the pH of the IL-water mixtures using Eq. A4-13, obtained by combining equations for aqueous acid-base equilibria (Eqs. A4-1-4) with equations for mass balance (Eqs. A4-10-11) and charge balance (Eq. A4-12). Samples were prepared as a 0.5 wt%. solution, allowing the sample concentration to be estimated as in Eq. 14. At these levels of dilution, the ionic strength of the solutions was around 0.03-0.05 M. As a result, activity coefficients were determined using either the Davies equation (Eq. A4-8, using values of 1 and 0.2 for *e* and *f*)[25,27] or extended Debye-Huckel equation (Eq. A4-6) for charged species. During optimisation tests of model parameters, activity coefficients were also included for all neutral species using the Setschenow equation (Eq. A4-9). All optimisations were carried out as global optimisations using the FMINCON function in a MultiStart object with 20 trial starting points, implemented using Matlab R2019b.

$$[S] = MW_a \cdot ([A^-] + [AH]) \; + \; MW_b \cdot ([BH^+] + [B]) \tag{A4-10}$$

$$X = \frac{[A^-] + [AH]}{[BH^+] + [B]} \tag{A4-11}$$

$$[BH^+] + [H_3O^+] - [A^-] - [OH^-] = 0 \tag{A4-12}$$

$$\frac{10^{-pH}}{\gamma_{H_3O^+}} + \frac{[S] \cdot 10^{-pH} \cdot \gamma_B}{(X \cdot MW_a + MW_b) \cdot (10^{-pH} \cdot \gamma_B + 10^{-pK_{a,b}} \cdot \gamma_{BH^+})} - \frac{K_w}{10^{-pH} \cdot \gamma_{OH^-}} \tag{A4-13}$$

$$- \frac{[S] \cdot X \cdot 10^{-pK_{a,a}} \cdot \gamma_{AH}}{(X \cdot MW_a + MW_b) \cdot (10^{-pH} \cdot \gamma_{A^-} + 10^{-pK_{a,b}} \cdot \gamma_{AH})} = 0$$

$$[S] = \frac{m_{IL}}{m_{IL}/\rho_{IL} + m_{water}/\rho_{water}} \approx \frac{m_{IL}}{(m_{IL} + m_{water})/\rho_{water}} \tag{A4-14}$$

where [*S*] represents sample concentration, MW_a represents the molecular weight of the acid, MW_b represents the molecular weight of the base, *X* represents the acid/base ratio, and γ_i represents the activity coefficient of species *i*. Chemical species *AH, A⁻, BH,* and BH^+ are defined as in Schemes A4-S1-S3. *pH*, K_w , $K_{a,a}$, and $K_{a.b}$ are defined as in Eqs. A4-1-4.

Results – Dimethylethanolammonium formate ([DMEtA][HCOO])

Predicted acid-base ratios of [DMEtA][HCOO] were carried out using a $pK_{a,a}$ of 3.75 for formic acid,[30–32] and $pK_{a,b}$ of 9.23 for dimethylethanolamine,[33,34] unless stated otherwise. 33 solutions were prepared, with acid-base ratios of 0.91-1.08. Fig. A4-3 shows the error in predicted acid-base ratio across the range investigated, with and without incorporating activity coefficients.

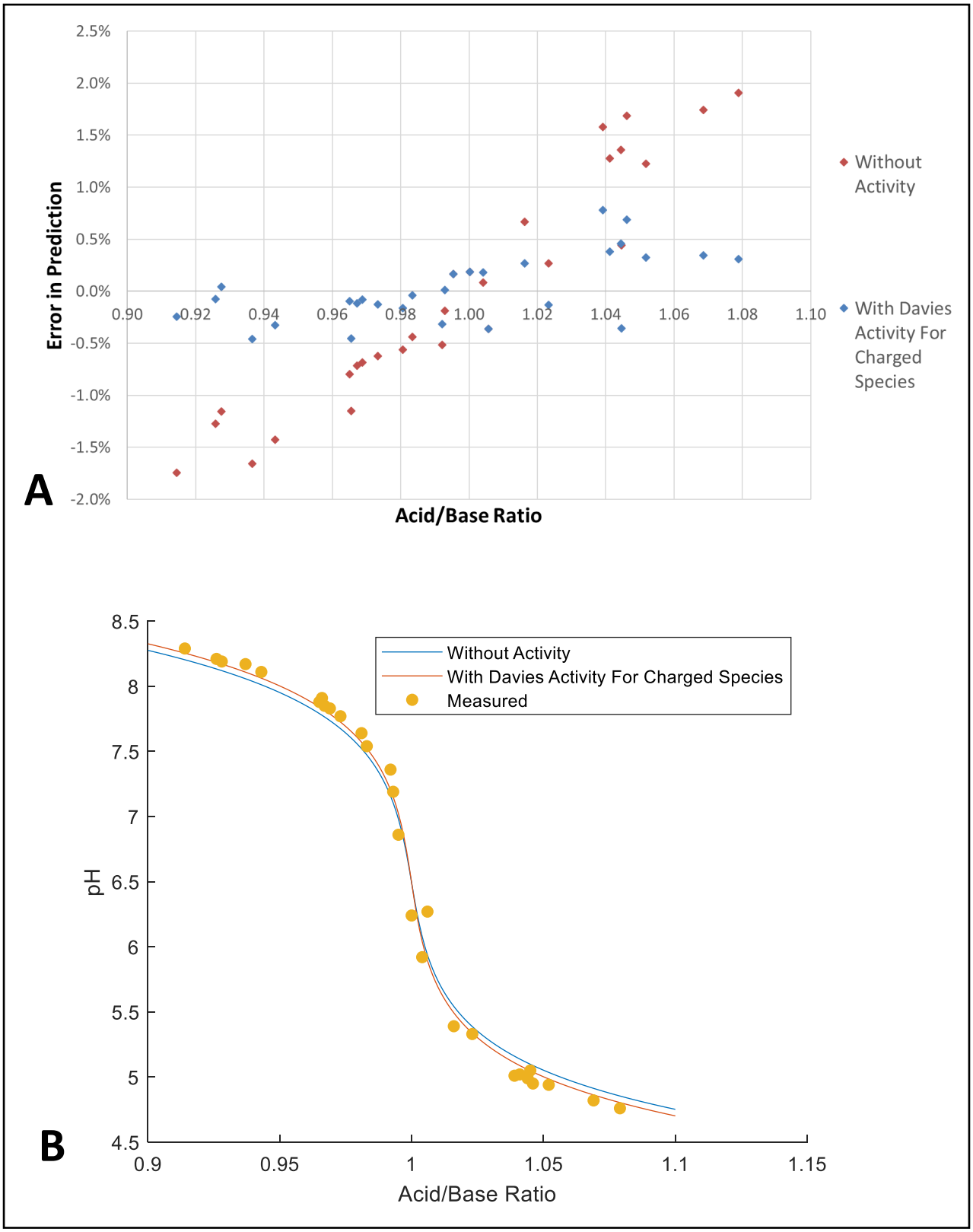


Figure A4-3: Accuracy of model predictions for 0.5 wt%. [DMEtA][HCOO], with and without including Davies activity for charged species. Plots are A: Errors in acid-base ratio prediction, B: Predicted relationship of pH vs. acid-base ratio compared to measured data.

Without activity coefficients, predictions were found to be most accurate at near-stoichiometric ratios, with errors increasing in magnitude at increasing excess acid and base. Across all measurements, the average error magnitude was 0.94%.

When incorporating activity coefficients of charged species (proton, hydroxide, cation, and anion) using the Davies equation (Eq. A4-8) predictions were found to improve significantly at non-stoichiometric ratios. As a result, the average error magnitude fell to 0.27% across all measurements, with the majority of predictions falling within 0.5% of the measured acid-base ratio. Depending on the intended IL application, such accuracy may be considered acceptable. One such example is biomass pretreatment, in which the acid-base ratio has previously been reported to the nearest percent.[19–21] The significant improvement of predictions with activity coefficients is to be somewhat expected at such ionic strengths, with calculated activity coefficients in this range significantly below 1 (see Fig. A4-4).

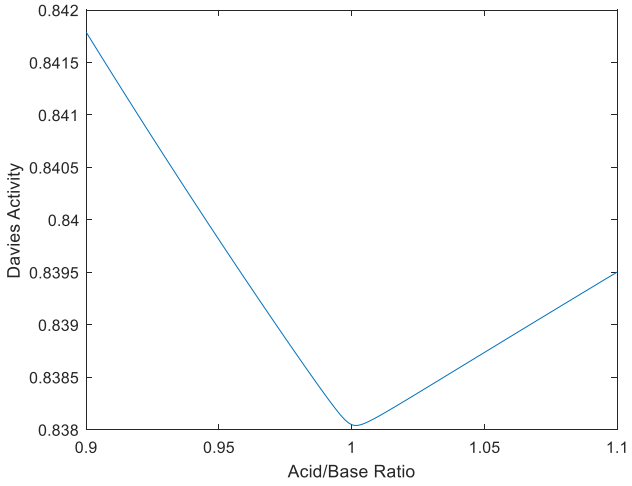


Figure A4-4: Davies activity vs. acid/base ratio for 0.5 wt% [DMEtA][HCOO].

It was possible to further improve accuracy by optimising certain model parameters to reduce the sum of squares error of the predictions. Two sets of optimisation were carried out, one based on the Davies equation (Optimisation 1), and the other on the extended Debye-Huckel equation (Optimisation 2). Prediction errors are displayed in Fig. A4-5.

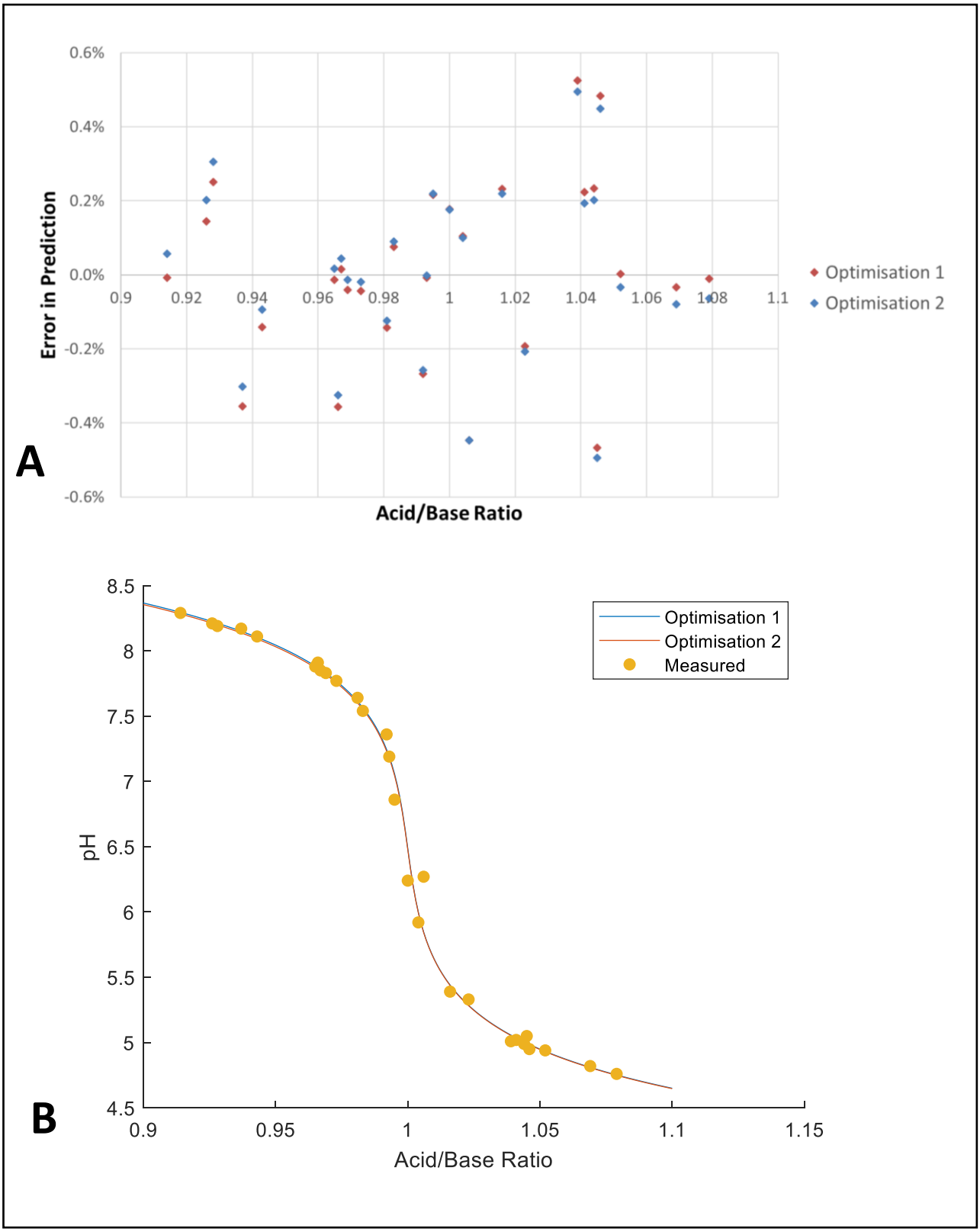


Figure A4-5: Accuracy of optimised model predictions for 0.5 wt% [DMEtA][HCOO]. Plots are A: Errors in acid-base ratio prediction, B: Predicted relationship of pH vs. acid-base ratio compared to measured data.

In optimisation 1, the average error magnitude was reduced to 0.23% by optimising charged species activity terms in the Davies equation (*e* and *f* in Eq. A4-8, between 0.5-3 and 0.2-0.3) and $pK_{a,b}$ (between 8.5-9.5). The $pK_{a,a}$ of formic acid was not optimised, as it is a common chemical that has been well-studied, and its pK_a widely reported as 3.75.[30–32] In contrast, the $pK_{a,b}$ of dimethylethanolamine is less widely reported, and reported values vary slightly. [33–35] By also including and optimising neutral species activity (*g* in Eq. A4-9, between 0 and 0.5),[36,37] the average error magnitude was reduced further, to 0.19%.

In Optimisation 2, the activity coefficients of charged species were determined using the extended Debye-Huckel equation (Eq. A4-6). As described previously, the Davies equation is a generalised approximation of the extended Debye-Huckel and Truesdell-Jones equations, eliminating the need for ion-specific parameters. In this case, the size parameter of each charged species was optimised (between 8.5-9.5 Å for proton, 3-4 Å for hydroxide, 3-4 Å for the anion, 2-10 for the cation), as well as the $pK_{a,b}$ and neutral species activity as in Optimisation 1. For all species except the cation, the ranges of size parameter used were small, as size parameter values had been reported in the literature.[26] The resulting average error magnitude was found to be 0.19%, as in Optimisation 1 using more generalised parameters. A size parameter of 9.0 Å was found for the dimethylethanolammonium cation. This value is larger than those reported by Kielland for a number of tertiary alkylammonium ions (4-7 Å),[26] possibly due to the alkanolammonium structure of the cation. The optimal value of $pK_{a,b}$ was 9.22, very close to the value of 9.23 taken from literature and used in the non-optimised predictions.[33,34]

Although it is thus possible to reduce the prediction errors of a set of calibration solutions through optimisation of parameters, the aim of predicting acid-base ratio from pH is to replace such calibration solutions. Additionally, in order to develop a simple technique that is applicable to a wide range of protic ILs, such a technique should ideally not require the use of ion-specific parameters. Therefore, the fact that the performance of the optimised model using ion-specific parameters was comparable to that of the non-optimised model using generalised parameter values adds credence to the generalised model's validity.

Results – 1-Methylimidazolium Chloride ([Hmim][Cl])

Predicted acid-base ratios of [DMEtA][HCOO] were carried out using a $pK_{a,a}$ of -8.0 for hydrochloric acid[38] and $pK_{a,b}$ of 7.06 for 1-methylimidazole,[39] unless stated otherwise. 36 solutions were prepared, with acid-base ratios of 0.94-1.07. Fig. A4-6 shows the error in predicted acid-base ratio across the range investigated, with and without incorporating activity coefficients. Without activity coefficients, predictions were found to be least accurate at near-stoichiometric ratios, with errors decreasing in magnitude at increasing excess acid and base. Across all measurements, the average error magnitude was 0.34%, but around stoichiometric ratios predicted values were generally around 0.5% too acidic. When incorporating activity coefficients of charged species using the Davies equation, prediction errors were found to increase significantly at all ratios, particularly non-stoichiometric ratios. In all cases, predicted ratios were overly acidic. As a result, the average error magnitude increased to 0.79%.

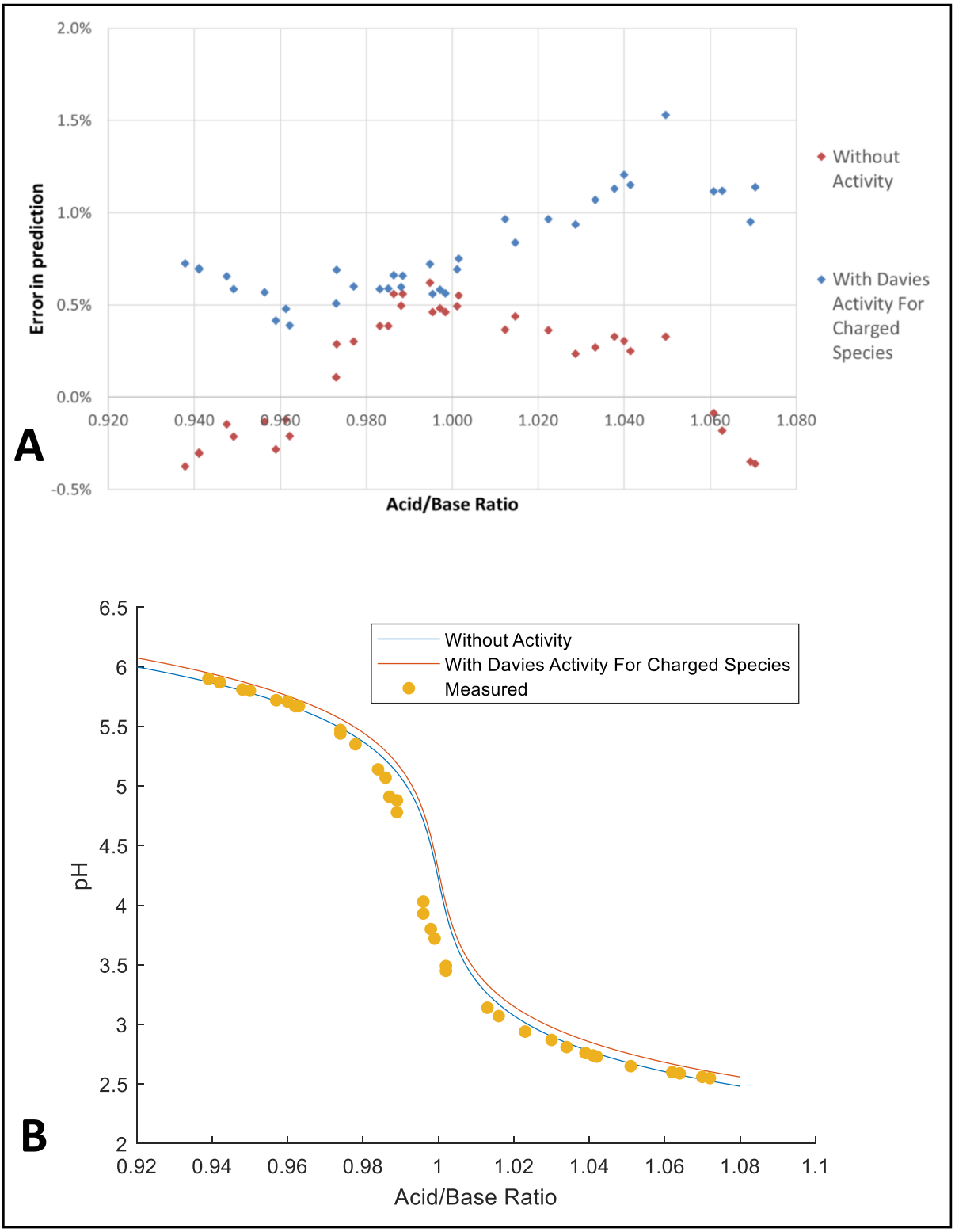


Figure A4-6: Accuracy of model predictions for 0.5 wt% [Hmim][Cl], with and without including Davies activity for charged species. Plots are A: Errors in acid-base ratio prediction, B: Predicted relationship of pH vs. acid-base ratio compared to measured data.

Similarly to the [DMEtA][HCOO] system, a number of different model parameters were optimised over two optimisations in order to improve the accuracy of the predictions. Results are shown in Fig. A4-7. Optimisation 3 varied the Davies equation *e* and f terms (Eq. A4-8) and g term from Eq. A4-9 (using the same ranges as Optimisation 1), and the $pK_{a,b}$ (between 6.5 and 8). Once again, the $pK_{a,a}$ was not optimised as it was well reported in the literature for HCl. Additionally HCl is a strong acid, meaning that at such low concentrations any realistic deviations in $pK_{a,a}$ had a negligible impact on predicted acid dissociation. Optimal $pK_{a,b}$ was found to be 7.01, close to the value used in the non-optimised model, and within the reported range of 6.95-7.3.[39–45] The average error magnitude, while reduced, remained fairly high at 0.49% and generally predicted an excessively acidic solution. Results were found to be most accurate for solutions containing excess base, but deviated up to around 1% for solutions containing excess acid.

Optimisation 4 optimised the extended Debye-Huckel equation ion size parameters (between 8.5-9.5 Å for proton, 3-4 Å for hydroxide, 2.5-3.5 Å for the anion, 2-10 Å for the cation),[26] while varying the neutral activity coefficient and $pK_{a,b}$ across the same ranges as Optimisation 3. However, despite using ion-specific parameters where available and optimising the most uncertain model parameters, average error magnitudes remained high at 0.59%, with a very similar distribution of errors. A size parameter of 7.0 was found for the 1-methylimidazolium cation, within the range of 4.5 -7 Å of most of the organic cations reported by Kielland.[26] The optimal value of $pK_{a,b}$ was 7.00, close to that found in Optimisation 3 and again within the reported range of 6.95-7.3.[39–45]

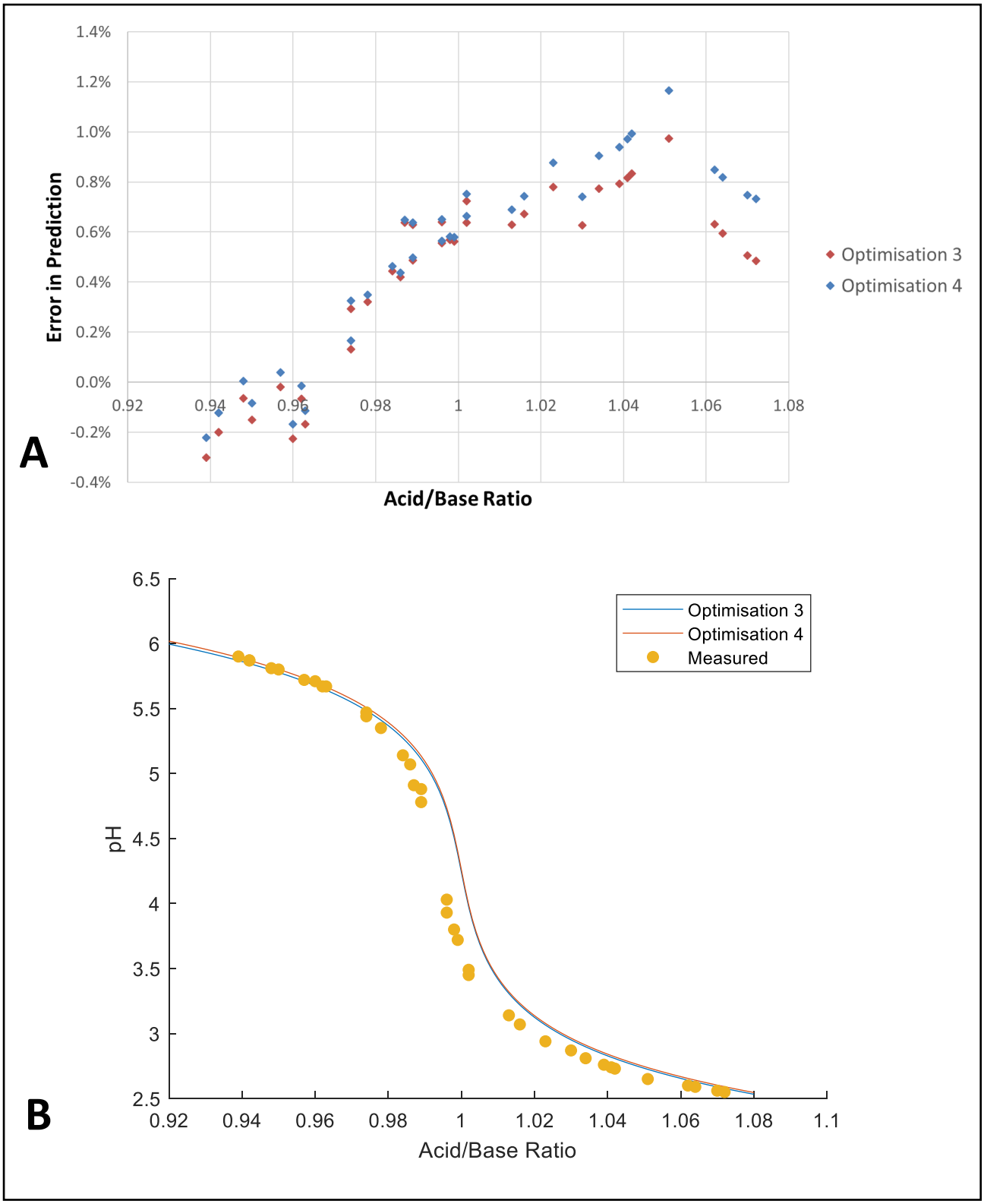


Figure A4-7: Accuracy of optimised model predictions for 0.5 wt% [Hmim][Cl]. Plots are A: Errors in acid-base ratio prediction, B: Predicted relationship of pH vs. acid-base ratio compared to measured data.

Chapter 5

Duckweed Growth Measurement Method

Different batches of duckweed were grown in the laboratory, but eventually were not used for pretreatment or metal uptake purposes. Duckweed growth rates were initially determined by the increase in mass over the course of one week. However, due to the high water-retaining abilities of a thick duckweed mat, such measurements were inaccurate, as well as inconvenient. Instead, an optical method was developed, using the free software ImageJ. In this method, the percentage surface coverage of the duckweed was determined based on its green colour compared to the dark background (see Fig. A5-1). This allowed rapid, accurate determination of growth rates without the need to disturb the duckweed by harvesting.

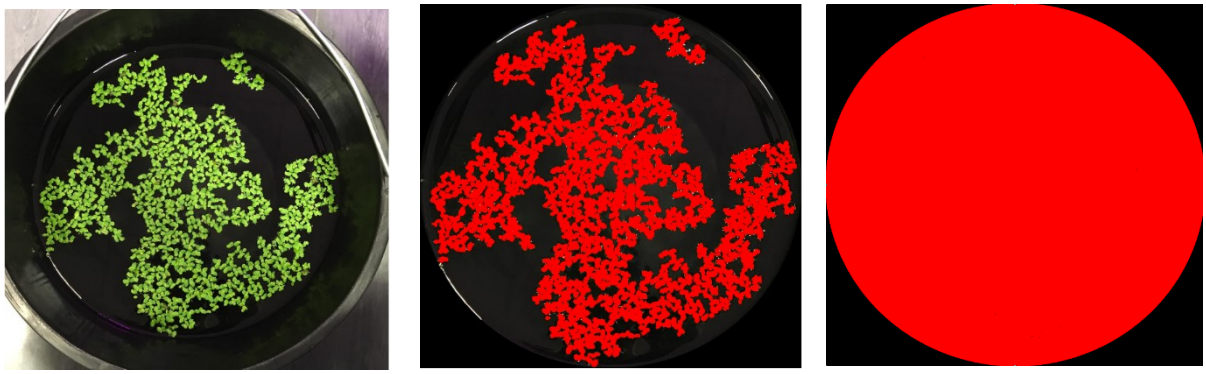


Figure A5-1: Optical determination of duckweed growth rates.

Starch Assay Procedures

The Megazyme Total Starch Assay procedure was used for determination of starch content in biomass samples. However, three different methods were provided. In order to test which method was most suitable, all three were tested on pure starch samples, and on untreated duckweed samples. Results are shown in Table A5-1, and show that the RTS Method (Note 1) is the most suitable for duckweed starch, able to liberate the highest quantity from the starting material. This is likely due to the higher amounts of sample used, as well as the much longer incubation time at 100 °C using thermostable α-amylase, allowing total liquefaction of the duckweed.

Table A5-1: Starch content determined according to different Megazyme protocols. Numbers in brackets are standard deviations of triplicates.

Feedstock	RTS	RTS – NaOH	RTS – Note 1
Rice Starch	99.1% (0.3%)	98.1% (0.2%)	99.1% (0.2%)
Spirodela Polyrhiza	1.9% (0.0%)	2.8% (0.1%)	3.3% (0.1%)
Lemna Minor	5.5% (0.1%)	7.6% (0.3%)	10.0% (0.1%)

Pretreated Duckweed Data

Pretreatment data for *Spirodela Polyrhiza* and *Lemna Minor* are provided in Table A5-2, with protein contents of pulp and lignin provided in Table A5-3. All pretreatments were performed at 150 °C, at a solids loading of 10% wt/wt, and 20 wt% water content.

Table A5-2: Duckweed pretreatment data.

Feedstock	Temp (°C)	Time (min)	IL	Pulp Yield (%)	Lignin Yield (%)	Glucan Recovery (%)	Hemi. Removal (%)	Deligni-Fication (%)	Starch Content (%)	Cellulose Content (%)
Spirodela Polyrrhiza	90	60	[DMBA] [HSO_4]	67.6	36.7	94.2	59.5	30.4	5.0	9.8
		120		66.6	44.6	97.9	62.0	34.4	5.2	11.0
		180		63.9	50.3	87.19	68.5	40.9	4.0	10.4
	120	30		64.8	51.6	94.1	37.2	47.6	3.9	11.4
		60		56.9	61.3	73.0	51.9	54.9	1.8	11.8
		90		51.1	63.2	64.8	55.9	57.0	0.7	12.7
	150	15		60.7	58.2	75.1	77.5	46.5	2.4	10.7
		30		49.3	73.2	52.5	97.8	55.7	0.2	11.1
		45		45.9	80.7	51.5	100.0	64.1	0.1	11.8
	120	60	[DMEtA] [HCOO]	72.1	6.0	90.0	18.2	6.0	4.7	8.5
		180		67.9	18.4	95.1	20.2	19.2	5.0	10.1
		300		65.2	37.8	89.8	21.8	25.4	4.8	10.2
Lemna Minor	120	30	[DMEtA] [HCOO]	65.6	51.1	93.3	31.7	22.8	12.2	17.9
		180	[DMBA] [HSO_4]	70.0	31.6	98.9	7.8	-24.3	13.8	14.0

Table A5-3: Protein content of pulp and lignin from pretreated duckweed.

Feedstock	Temp (°C)	Time (min)	IL	Pulp Protein Content (%)	Lignin Protein Content (%)
Spirodela Polyrhiza	90	60	[DMBA] [HSO_4]	26.9	16.7
		120		20.4	21.5
		180		15.8	25.0
	120	30		19.9	27.6
		60		12.3	29.9
		90		13.9	29.6
	150	15		16.8	29.7
		30		13.1	32.8
		45		9.6	29.4
	120	60	[DMEtA] [HCOO]	23.4	25.1
		180		24.9	25.3
		300		25.7	29.6
Lemna Minor	120	30	[DMBA] [HSO_4]	16.6	18.2
		180	[DMEtA] [HCOO]	18.8	15.4

Harvested Duckweed



Figure A5-2: Harvested *Spirodela polyrhiza* covering canal.

FTIR of [DMEtA][HCOO]

In order to qualitatively evaluate the degree of ionicity of the IL [DMEtA][HCOO], FTIR was carried out on formic acid, dimethylethanolamine, and on the IL itself, with data shown in Fig. A5-3.

Looking at the spectrum of formic acid, the peak around 1655-1704 corresponds to stretching of the C=O bond in the COOH group, while the broad peak around 1140-1180 corresponds to stretching of the C-OH stretching of the COOH group.[46–48] Looking at the spectrum of the IL, the aforementioned C-OH peak disappears due to the deprotonation of the acid, and the C=O group associated with the carboxylic group is substantially reduced. Instead, a peak at 1589 appears, due to stretching of the COO^- group of the deprotonated anion.[46–48] It can, therefore, be concluded that there is a very substantial degree of ionicity in this IL, but not quantitative. For this to be quantified, however, by calibrated FTIR or proton NMR.[49]

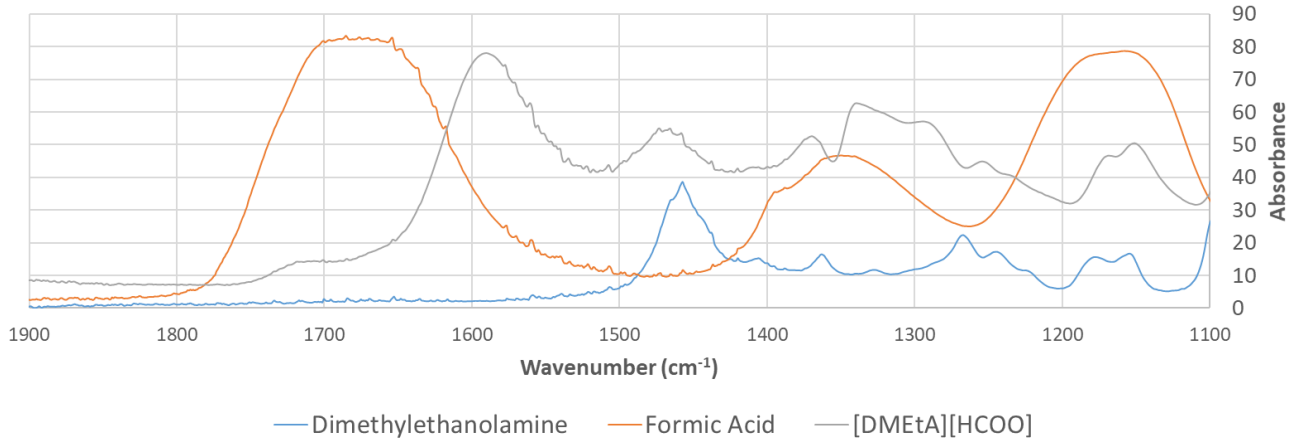


Figure A5-3: FTIR spectra of formic acid, dimethylethanolamine, and [DMEtA][HCOO].

Protein Fractionation During Pretreatment of Duckweed

A material flow diagram illustrating the fractionation behaviour of duckweed protein during IL pretreatment is shown in Fig. A5-4.

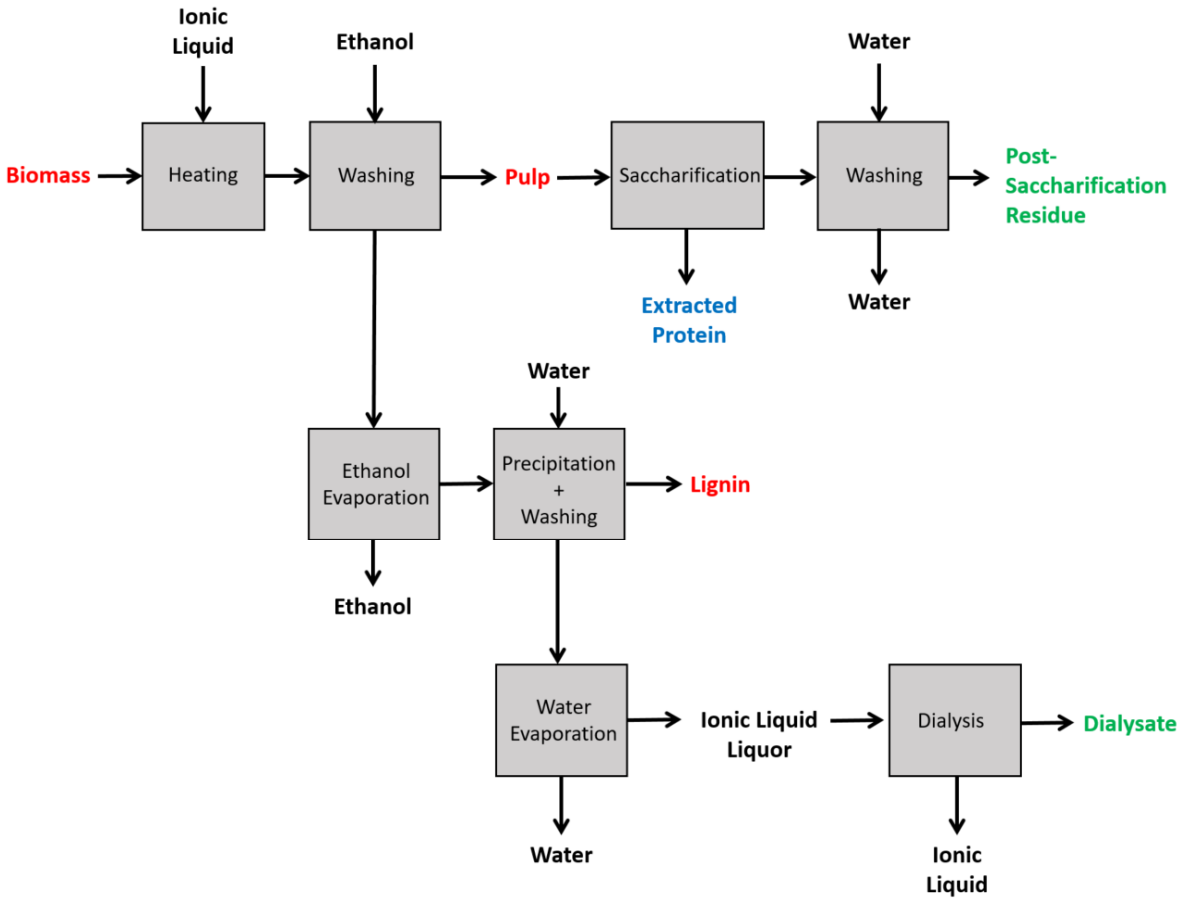


Figure A5-4: Protein fractionation during pretreatment. The protein content of material written in red was measured through CHN analysis for all samples. Protein content of the material written in green was measured through CHN analysis for selected samples. Protein content of the material written in blue was not directly measurable.

References

1 J. Grasvik, J. P. Hallett, T. Q. To and T. Welton, *Chem. Commun.*, 2014, **50**, 7258–7261.
2 C. Chambon, PhD Thesis, Imperial College London, 2017.
3 X. L. Luo, J. Y. Zhu, R. Gleisner and H. Y. Zhan, *Cellulose*, 2011, **18**, 1055–1062.
4 F. J. V. Gschwend, C. L. Chambon, M. Biedka, A. Brandt-Talbot, P. S. Fennell and J. P. Hallett, *Green Chem.*, 2019, **21**, 692–703.
5 A. Brandt-Talbot, F. J. V. Gschwend, P. S. Fennell, T. M. Lammens, B. Tan, J. Weale and J. P. Hallett, *Green Chem.*, 2017, **19**, 3078–3102.
6 R. H. Kadlec and S. D. Wallace, *Treatment wetlands*, CRC Press, Boca Raton, 2nd edn., 2009.

7 B. Papadopoulos, K. P. Tsagarakis and A. Yannopoulos, *J. Environ. Eng.*, 2007, **133**, 581–586.
8 S. Jafarinejad, *Appl. Water Sci.*, 2017, **7**, 2513–2521.
9 E. Friedler and E. Pisanty, *Water Res.*, 2006, **40**, 3751–3758.
10 T. Dogot, Y. Xanthoulis, N. Fonder and D. Xanthoulis, *Water Sci. Technol.*, 2010, **62**, 640–648.
11 R. Nogueira, A. G. Brito, A. P. Machado, P. Janknecht, J. J. Salas, L. Vera and G. Martel, *Desalin. Water Treat.*, 2009, **4**, 16–21.
12 M. Molinos-Senante, F. Hernández-Sancho, M. Mocholí-Arce and R. Sala-Garrido, *Resour. Energy Econ.*, 2014, **38**, 125–140.
13 Bolton & Menk Inc, *Ultra-Low Phosphorus Removal Pilot Study City of Mankato, Minnesota, Project No. M24.109541*, 2016.
14 US Environmental Protection Agency, *Economic Analysis of Final Water Quality Standards for Nutrients for Lakes and Flowing Waters in Florida*, Washington DC, 2010.
15 G. McNamara, PhD Thesis, Dublin City University, 2018.
16 F. Jiang, M. Beck, R. Cummings and K. Rowles, *Estimation of costs of phosphorus removal in wastewater treatment facilities: construction de novo, Water Policy Working Paper #2004-010*, 2004.
17 R. Bashar, K. Gungor, K. G. Karthikeyan and P. Barak, *Chemosphere*, 2018, **197**, 280–290.
18 United States Environmental Protection Agency, *Biological nutrient removal processes and costs, EPA-823-R-07-002*, Washington DC, 2007.
19 L. Weigand, S. Mostame, A. Brandt-Talbot, T. Welton and J. P. Hallett, *Faraday Discuss.*, 2017, **202**, 331–349.
20 P. Y. S. Nakasu, C. J. Clarke, S. C. Rabelo, A. C. Costa, A. Brandt-Talbot and J. P. Hallett, *ACS Sustain. Chem. Eng.*, 2020, **8**, 7952–7961.
21 P. Verdía, A. Brandt, J. P. Hallett, M. J. Ray and T. Welton, *Green Chem.*, 2014, **16**, 1617–1627.
22 E. C. Wijaya, F. Separovic, C. J. Drummond and T. L. Greaves, *J. Chem. Phys.*, 2018, **148**, 193838–193847.
23 J. R. Black, in *Encyclopedia of Geochemistry*, ed. W. M. White, Springer, Cham, 2018th edn., 2018, pp. 345–347.
24 N. Eby, in *Principles of Environmental Geochemistry*, Brooks, 2003.
25 Activity Coefficients (Activity Models), https://www.aqion.de/site/101, (accessed 23 July 2020).
26 J. Kielland, *J. Am. Chem. Soc.*, 1937, **59**, 1675–1678.
27 R. Harrison, Ed., *Principles of Environmental Chemistry*, Royal Society of Chemistry, 2007.
28 D. Langmuir, in *Aqueous Environmental Geochemistry*, Pearson, 1997, pp. 123–149.
29 G. M. Anderson and D. A. Crerar, *Thermodynamics in geochemistry: The equilibrium model*, Oxford University Press, 1993.
30 J. A. Riddick, W. B. Bunger and T. K. Sakano, *Techniques of Chemistry 4th ed., Volume II. Organic Solvents.*, NY: John Wiley and Sons, New York, 1985.
31 Table of Acids with Ka and pKa Values, https://clas.sa.ucsb.edu/staff/Resource Folder/Chem109ABC/Acid, Base Strength/Table of Acids w Kas and pKas.pdf, (accessed 22 July 2020).
32 X. xiang Wang, H. Fu, D. mei Du, Z. yu Zhou, A. guo Zhang, C. fang Su and K. sheng Ma, *Chem. Phys. Lett.*, 2008, **460**, 339–342.
33 R. J. Lttel, M. Bos and G. J. Knoop, *J. Chem. Eng. Data*, 1990, **35**, 276–277.
34 2-dimethylaminoethanol - Registration Dossier - ECHA, https://echa.europa.eu/registration-dossier/-/registered-dossier/14464/4/22#sLinkToRelevantStudyRecord, (accessed 22 July 2020).
35 K. E. Haneke, *Dimethylethanolamine (DMAE) and Selected Salts and Esters Review of Toxicological Literature (Update), N01-ES-65402*, 2002.
36 A. Burant, G. V. Lowry and A. K. Karamalidis, *Acc. Chem. Res.*, 2017, **50**, 1332–1341.
37 N. Ni and S. H. Yalkowsky, *Int. J. Pharm.*, 2003, **254**, 167–172.
38 Evans pKa Table, http://www.mch.estranky.sk/file/40/evans_pka_table.pdf, (accessed 23 July 2020).
39 V. Delcoigne and M. C. Haulait, *J. Solution Chem.*, 1976, **5**, 47–55.
40 B. Lenarcik and P. Ojczenasz, *J. Heterocycl. Chem.*, 2002, **39**, 287–290.
41 M. Alei, W. E. Wageman, T. W. Whaley and L. O. Morgan, *J. Am. Chem. Soc.*, 1980, **102**, 2881–2887.
42 B. E. Boulton and B. A. W. Coller, *Aust. J. Chem.*, 1974, **27**, 2331–2341.
43 K. Naka, S. Masuoka, R. Shinke and M. Yamada, *Polym. J.*, 2012, **44**, 353–359.
44 B. Kraushaar-Czarnetzki, H. Jongkind, R. J. Dogterom and W. H.J. Stork, *Appl. Catal.*, 1991, **75**, L9–L12.
45 J. A. Dean, *LANGE'S HANDBOOK OF CHEMISTRY*, McGraw-Hill, New York, 15th edn., 1999.
46 M. Gadermann, D. Vollmar and R. Signorell, *Phys. Chem. Chem. Phys.*, 2007, **9**, 4535–4544.
47 C. Lucks, A. Rossberg, S. Tsushima, H. Foerstendorf, K. Fahmy and G. Bernhard, *Dalt. Trans.*, 2013, **42**, 13584–13589.
48 F. P. Rotzinger, J. M. Kesselman-Truttmann, S. J. Hug, V. Shklover and M. Grätzel, *J. Phys. Chem. B*, 2004, **108**, 5004–5017.
49 M. Shen, Y. Zhang, K. Chen, S. Che, J. Yao and H. Li, *J. Phys. Chem. B*, 2017, **121**, 1372–1376.